Meteoritics & Planetary Science 42, Nr 8, Supplement, A11–A171 (2007)
http://meteoritics.org

Abstracts

5114

STUDY OF Fe^{2+}-Mg^{2+} ORDER-DISORDER IN PYROXENE FROM THE CACHARI METEORITE

Y. A. Abdu[1], R. B. Scorzelli[2], I. Souza Azevedo[2], and M. E. Varela[3]. [1]Department of Geological Sciences, University of Manitoba, Winnipeg, Manitoba R3T 2N2, Canada. [2]Centro Brasileiro de Pesquisas Físicas, Rua Xavier Sigaud 150, 22290-180 Rio de Janeiro, Brazil. [3]Complejo Astronómico El Leoncito (CASLEO), Av. España 1512 Sur, CP J5402DSP, San Juan, Argentina.

Introduction: The Cachari meteorite, found in 1916 in Argentina, is a monomictic eucrite that belongs to the basaltic achondrites. It is composed mainly of low-Ca pyroxene and plagioclase [1, 2]. Mössbauer spectroscopy indicates that the only Fe-containing mineral present in the Cachari eucrite is pyroxene [3]. The study of intracrystalline distribution of Fe^{2+} and Mg^{2+} between the nonequivalent octahedral sites M1 and M2 in pyroxenes is useful in tracing the thermal history of a rock. In unshocked and slowly cooled pyroxenes, Fe^{2+} orders at the M2 site whereas Mg^{2+} occurs predominately at the M1 site [4].

Here we study the partitioning of Fe^{3+} and Mg^{2+} between the M1 and M2 sites in orthopyroxene from the Cachari eucrite by Mössbauer spectroscopy in the temperature range (300–80 K) and electron microprobe analysis.

Results: The average chemical composition of the Cachari pyroxene determined by electron microprobe analysis is $(Fe^{2+}_{1.16}Mg_{0.75}Ca_{0.04}Mn_{0.04}Al_{0.01})\ Si_{2.00}O_6$.

The room-temperature (300 K) Mössbauer spectrum of bulk Cachari is composed of two overlapping doublets due to Fe^{2+} at the M1 and M2 sites in pyroxene, and very small amounts of Fe^{2+} and an impurity component. The resolution of the M1 and M2 doublets increases with decreasing temperature as a result of the differential dependence of the quadrupole splittings on temperature. Using the normalized Mössbauer relative areas of the doublets at 80 K, the Fe^{2+} fractions at the M1 and M2 sites are found to be 0.36 and 0.64, respectively. The site occupancies $X_{Fe^{2+}(M1)}$ and $X_{Fe^{2+}(M2)}$ are obtained by multiplying the above Fe^{2+} fractions by the total amount of Fe^{2+} given by electron microprobe analysis. This gives $X_{Fe^{2+}(M1)} = 0.42$ and $X_{Fe^{2+}(M2)} = 0.74$. Assuming complete order of Ca and Mn at the M2 site, and Al at the M1 site, Mg^{2+} is then distributed over the M1 and M2 sites as: $X_{Mg^{2+}(M1)} = 0.57$ and $X_{Mg^{2+}(M2)} = 0.18$. The Fe^{2+} and Mg^{2+} site populations can be related to the disordering parameter p, defined by $p = (X_{Fe^{2+}[M1]} \cdot X_{Mg^{2+}[M2]})/(X_{Fe^{2+}[M2]} \cdot X_{Mg^{2+}[M1]})$, and we obtain a disordering parameter $p = 0.18$ for the Cachari pyroxene.

In light of the work done on heated orthopyroxenes [4, 5], the disordering parameter (0.18) obtained for the Cachari pyroxene corresponds to an equilibrium temperature of ~800 °C. This temperature is consistent with the reported equilibration temperatures for eucrites (800–900 °C) estimated using the coexisting ortho- and clinopyroxes geothermometer [6].

References: [1] Fredricsson K. and Kraut F. 1967. *Geochimica et Cosmochimica Acta* 31:1701–1704. [2] Boctor et al. 1987. *Meteoritics* 22: 332. [3] Abdu et al. 2005. *Hyperfine Interactions* 166:543–547. [4] Dundon R. W. and Hafner S. S. 1971. *Science* 174:581–583. [5] Virgo D. and Hafner S. S. 1969. Mineralogical Society of America Special Paper 2. pp. 67–81. [6] Yamaguchi et al. 1996. *Icarus* 124:97–112.

5159

ISOTOPE FRACTIONATION DURING IMPACT: EARTH VERSUS THE MOON

F. Albarede[1], T. E. Bunch[2], F. Moynier[1], and C. Douchet[1]. [1]Ecole Normale Supérieure de Lyon, France. E-mail: albarede@ens-lyon.fr. [2]Northern Arizona University, Flagstaff, AZ 86011, USA.

Introduction: Because the extent of isotope fractionation of many elements, Cu, Zn, and S among them, in lunar soils [1] is very strong (up to 3 per mil per amu) and well beyond what is expected from petrological processes, we investigated the isotopic effects of a large terrestrial impact. The 49,000-year-old Meteor Crater in Arizona is recent and well suited for this particular study because the composition and the geology of the flat-lying sediments in which the impactor formed a kilometer-size crater are particularly simple [2]. Seven classes of shock features were identified [3] from the pristine rocks (0) to shock melts (6). The respective contribution of the impactor and target rocks to the melts is well understood [4].

Results: Cu and Zn isotopes were determined on seven shocked samples of the Coconino sandstone. These two elements behave consistently. Most interestingly, a negative correlation is observed between isotope compositions and shock grades. The samples from intermediate shock grades (3 and 4) are isotopically more fractionated than shock melts (6) and show excesses of heavy isotopes of up to 0.4 per mil for $^{68}Zn/^{66}Zn$ and 0.8 per mil for $^{65}Cu/^{63}Cu$, which is a rather large extent of fractionation for these elements in terrestrial samples. The shock melts are essentially indistinguishable from the pristine samples.

Interpretation: This ongoing study indicates that, even on Earth, shocks fractionate the isotope compositions of rather heavy elements to a measurable extent. We surmise that when the energy of the shock cannot be redistributed fast enough to prevent local melting, isotope fractionation remains minimal. Intermediate shock grades are more susceptible to partial loss of material and isotope fractionation, presumably during impact when vapor may escape through cracks, or later when groundwater leaches impact-altered material. Isotope fractionation at Meteor Crater (MC) is important but nowhere near the spectacular effects observed in the lunar regolith. This difference may be due to either the lack of an atmosphere on the Moon or to a major difference in the physical scale and types of events leading to fractionation. The presence of the terrestrial atmosphere reduces the mean free path between collisions and therefore reduces mass loss and isotope fractionation. In contrast, on the Moon, expansion of small impact clouds in vacuum leads to severe mass loss and mass fractionation in $M^{3/2}$. Alternatively, the events causing isotope fractionation in lunar soils may not be due mainly to large MC-type impactors but to micrometeorite bombardment or to ablation by the solar wind and cosmic rays.

References: [1] Moynier F., Albarede F., and Herzog G. F. 2006. *Geochimica et Cosmochimica Acta* 70:6103–6117. [2] Shoemaker E. M. and Kieffer S. W. 1974. Guidebook to the geology of Meteor Crater. Center for Meteorite Studies Publication 17. [3] Kieffer S. W. 1971. *Journal of Geophysical Research* 90:5449–5473. [4] Hörz F. et al. 2002. *Meteoritics & Planetary Science* 37:501–531.

5134

DID CHONDRULES FORM IN THE NEBULA?

C. M. O'D. Alexander[1], J. N. Grossman[2], and D. Ebel[3]. [1]DTM, Carnegie Institution of Washington, Washington, D.C. 20015, USA. E-mail: alexande@dtm.ciw.edu. [2]U.S. Geological Survey, Reston, VA 20192, USA. E-mail: jgrossman@usgs.gov. [3]Department of Earth and Planet. Sci., American Museum of Natural History, New York, NY 10024, USA. E-mail: debel@amnh.org.

Introduction: Any model for chondrule formation must explain their abundance, range of textures (reflecting cooling rate and peak temperature), size distributions, elemental and O isotopic compositions, and the evidence for chondrules having undergone multiple heating events (e.g., relict grains and igneous rims). While most features of chondrules are consistent with formation in the nebula (i.e., protoplanetary disk) as opposed to on asteroidal surfaces or by collisions between planetesimals, there is no definitive evidence that this is where they formed. The case for a nebular origin is largely indirect, relying as it does on substantial objections to other proposed mechanisms (e.g., [1]).

Non-Nebular Models: Volcanism on asteroids is unlikely to efficiently produce abundant chondrules, and cannot explain the range of O isotopic and elemental compositions or the evidence for multiple formation events. Impacts can produce chondrule-like objects (e.g., lunar spherules), but in cold targets (e.g., a regolith) most of the impact energy goes into fragmentation rather than melting. Hyper-velocity impacts between partially or fully molten planetesimals would probably produce copious amounts of chondrule-like objects. However, such bodies are likely to undergo rapid metal-silicate differentiation, and crystal-liquid fractionation in their mantles; there is no evidence for either process in chondrules. Collisions of such bodies are unable to explain the evidence for multiple heating events preserved in individual chondrules.

Nebular Models: Nebular formation mechanisms are not without their problems. The differences in the physical, textural, and chemical properties of chondrules from different chondrite groups, as well as the range of chondrule cooling rates, point to large but relatively localized formation events [2]. Preservation of these differences in a turbulent nebula requires chondrule formation shortly before accretion of the parent bodies [3]. In this context, and if it is real, the apparent 1–2 Ma range in ages of chondrules from a given meteorite (e.g., [4]) are difficult to understand. The volatile element inventories and the lack of isotopic fractionation are also difficult to understand if chondrules formed under canonical nebular conditions because models and experiments predict substantial evaporation should occur at near-liquidus temperatures. In moderately dust-enriched environments (10^2–10^3 × solar), re-equilibration between gas and chondrules should erase isotopic fractionations on reasonable time scales. The presence of moderately and highly volatile elements in chondrules would require that gas-chondrule exchange continue to low temperatures. However, our recent finding that Na was present in chondrules at current abundances even at near-liquidus temperatures [5] seems to require dust enrichments (order 10^6–10^7 × solar) that are hard to achieve with current nebular models.

References: [1] Taylor et al. 1983. In *Chondrules and their origins*. pp. 262–278. [2] Cuzzi and Alexander. 2006. *Nature* 441:483–485. [3] Alexander. 2005. In *Chondrites and the protoplanetary disk*. pp. 972–1002. [4] Kita et al. 2005. In *Chondrites and the protoplanetary disk*, pp. 558–587. [5] Alexander et al. 2007. Abstract #2012. 38th Lunar and Planetary Science Conference.

5261

ISOTOPIC ANALYSIS OF PRESOLAR GRAPHITE FROM THE MURCHISON KFB1 SEPARATE

S. Amari[1], E. Zinner[1], and R. S. Lewis[2]. [1]Laboratory for Space Sciences and the Physics Department, Washington University, St. Louis, MO 63130, USA. E-mail: sa@wuphys.wustl.edu. [2]Enrico Fermi Institute and Chicago Center for Cosmochemistry, University of Chicago, Chicago, IL 60637, USA.

Introduction: Presolar graphite grains, the carrier of Ne-E(L), show a range of density (1.6–2.2 g/cm^3) and their isotopic features depend on density [1–3]. Low-density graphite grains from the separate KE3 (1.65–1.72 g/cm^3) extracted from Murchison [4] are characterized by ^{18}O excesses, Si isotopic anomalies (mainly in the form of ^{28}Si excesses), high inferred ^{26}Al/^{27}Al ratios (up to 0.1), as well as the initial presence of ^{44}Ti ($T_{1/2}$ = 60 a) [5]. These features indicate that they formed in supernova ejecta. Of the other three graphite separates from Murchison, KFA1 (2.05–2.10 g/cm^3) and KFB1 (2.10–2.15 g/cm^3) also contain grains with ^{18}O excesses, although the fraction of grains with such excesses is smaller than in KE3 [6, 7].

Amari et al. [8] have reported on a search for the initial presence of ^{60}Fe in low-density graphite grains but could not confirm it. ^{22}Ne in low-density graphite grains appears to be due to the decay of ^{22}Na ($T_{1/2}$ = 2.6 a) synthesized in the O/Ne zone [9, 10]. One of the radioactive isotopes that are produced in this zone and are of interest with respect to the early solar system is ^{60}Fe ($T_{1/2}$ = 1.49 Ma). Here we report on our continuing effort in the search for ^{60}Fe in graphite grains.

Results and Discussion: We analyzed isotopic ratios of 15 grains from KFA1 with the NanoSIMS at Washington University. Ten grains have ^{12}C/^{13}C ratios between 74 and 90 (solar: 89). Only one grain has a ^{12}C/^{13}C ratio significantly higher (493) than the solar ratio. Two of the three ^{18}O-rich grains exhibit low ^{12}C/^{13}C ratios (7.7 and 13.9). One grain with a low ^{12}C/^{13}C ratio (14.5) but a normal ^{18}O/^{16}O ratio shows anomalous Ti with a V-shape isotopic pattern when normalized to ^{48}Ti and the solar ratios. The ^{50}Ti/^{48}Ti of the grain was not determined because of a huge ^{50}Cr correction. Grains that belong to this population, characterized by low ^{12}C/^{13}C ratios (~10), are enigmatic: many of them show normal isotopic ratios in trace elements and it is not easy to decipher the stellar sources of these grains. In this study, two such grains, with ^{18}O excesses, undoubtedly originated from supernovae. The grain with the Ti isotopic anomaly shows a signature of neutron capture. However, it is not clear whether it was produced in a supernova, an AGB star, or a yet-unidentified stellar source. ^{57}Fe/^{56}Fe, ^{60}Ni/^{62}Ni, and ^{61}Ni/^{62}Ni ratios of all 15 grains are normal within errors and we still have not obtained any evidence for the initial presence of ^{60}Fe.

References: [1] Amari S. et al. 1995. *Geochimica et Cosmochimica Acta* 59:1411–1426. [2] Hoppe P. et al. 1995. *Geochimica et Cosmochimica Acta* 59:4029–4056. [3] Jadhav M. et al. 2006. *New Astronomy Reviews* 50: 591–595. [4] Amari S. et al. 1995. *The Astrophysical Journal* 447:L147–L150. [5] Travaglio C. et al. 1999. *The Astrophysical Journal* 510:325–354. [6] Amari S. et al. 2004. Abstract #2103. Lunar Planet. Sci. XXXV. [7] Amari S. et al. 2005. *Meteoritics & Planetary Science* 40:A15. [8] Amari S. et al. 2007. Abstract #2024. Lunar. Planet. Sci. XXXVIII. [9] Amari S. et al. 2005. Abstract #1867. Lunar Planet. Sci. XXXVI. [10] Amari S. 2006. *New Astronomy Reviews* 50:578–581.

5097

THE INFLUENCE OF MINERAL INCLUSIONS ON THE PRODUCTION RATES OF COSMOGENIC NUCLIDES IN GRANT (IIIAB) AND CARBO (IID)

K. Ammon and I. Leya. University of Bern, Sidlerstrasse 5, 3012 Bern, Switzerland. E-mail: katja.ammon@space.unibe.ch.

Introduction: Beside the major elements iron (Fe) and nickel (Ni), iron meteorites also contain other elements like sulfur (S), phosphorous (P), and carbon (C), which affect production rates of cosmogenic nuclides. The most common mineral inclusions are troilite (FeS), schreibersite (Fe,Ni_3P), and graphite (C) [1]. Related to this, the production of cosmogenic Ne, which is of major importance for exposure-age studies, is very sensitive to contributions from S- and/or P-rich inclusions. For example, since the production rates of cosmogenic Ne from S and/or P are about ten times higher compared to production from Fe and Ni [2–4], only about 1% of S and/or P increase the cosmogenic Ne concentration by about 10%. Iron meteorites contain between 0.1–2% P and 0.03–17% S [1 and references therein]; therefore such effects have to be considered for detailed exposure ages studies.

Experimental: SEM images of Grant and Carbo clearly demonstrate that there are many troilite and schreibersite inclusions with sizes of a few hundred microns only, which makes the separation of a pure metal sample, i.e., without any inclusions, impossible. Such small inclusions, however, are nevertheless sufficient to substantially increase the production rates and a reliable quantification is therefore necessary. The finding that ^{21}Ne in Grant and Carbo is affected by such inclusions is confirmed by the extensive data set measured by us for both meteorites. The data clearly demonstrate that the scatter for ^{21}Ne is larger than for, e.g., ^{4}He and ^{38}Ar and is also larger than expected considering the external reproducibility.

Quantifying Contributions from S and P: The procedure performed by us to quantify contributions from S and P to cosmogenic ^{21}Ne is based on the observation that, for outliers in our Grant and Carbo database, the ^{22}Ne/^{21}Ne ratios correlate with ^{21}Ne concentrations. Furthermore, most of the ^{22}Ne/^{21}Ne ratios measured by us are higher than expected from nuclear reaction mechanism. We basically assume simple mixing of two components. Component one is a typical meteoritic mixture for Fe and Ni having a ^{22}Ne/^{21}Ne ratio of about 1.02 and the second component is pure S and P having a ^{22}Ne/^{21}Ne ratio of about 1.28. Note that our procedure does not allow distinguishing between S and P contributions. Assuming that the production rates for ^{21}Ne from S and P are about ten times higher than for Fe and Ni, we calculate that about 20% of total ^{21}Ne measured in Grant and Carbo is due to reactions on S and P.

Exposure Ages and Model Calculations: The finding that a significant part of the measured ^{21}Ne is not from Fe and Ni but from S and P has also a major impact for the ^{41}K-^{40}K dating technique (e.g., [5]). We therefore present a re-evaluated version of the ^{41}K-^{40}K dating technique, which, beside the aforementioned results, also based on new sophisticated model calculations.

References: [1] Mittlefehldt D. W. et al. 1998. Reviews in Mineralogy 36. pp. 4-1–4-4. [2] Begemann F. 1965. *Zeitschrift für Naturforschung* 20A: 950–960. [3] Levsky L. and Komarov A. N. 1974. *Geochimica et Cosmochimica Acta* 39:275–284. [4] Leya I. et al. 2004. *Meteoritics & Planetary Science* 39:367–386. [5] Voshage H. and Feldmann H. 1979. *Earth and Planetary Science Letters* 242:1–15.

5098

CROSS SECTIONS OF THE PRODUCTION OF He, Ne, AND Ar ISOTOPES BY PROTON-INDUCED REACTIONS ON IRON AND NICKEL

K. Ammon[1], I. Leya[1], B. Lavielle[2], E. Gilabert[2], J.-C. David[3], and R. Michel[4]. [1]University of Bern, Sidlerstrasse 5, Switzerland. E-mail: katja.ammon@space.unibe.ch. [2]Laboratoire de Chimie Nucléaire Analytique et Bio-environnementale (CNAB). Universités Bordeaux, France. [3]DSM DAPNIA/Sphn, CEA-Saclay, France. [4]Center for Radiation Protection and Radioecology, University of Hannover, Germany.

Introduction: For proper modeling of cosmogenic production rates in terrestrial and extraterrestrial matter, the differential particle spectra and the excitation functions for all relevant nuclear reactions have to be known. While calculating differential particle spectra using state-of-the-art Monte Carlo codes is now very reliable, the thus-calculated cross sections are accurate within a factor of 2 at best, which is far from sufficient for astrophysical and cosmochemical applications. Therefore, experimental cross sections are still essential for the study of cosmogenic nuclides in meteorites and planetary surfaces. While the cross section database for most of the target elements relevant for stony meteorites and lunar surface rocks is fairly complete by now, which directly translates into reliable model calculations [1, 2], the database for Fe and Ni, which are the major elements for the study of iron meteorites, is rather scarce and scattering. In our systematic study of iron meteorites we therefore measured the excitation functions for the production of He, Ne, and Ar isotopes from Fe and Ni from the respective reaction thresholds up to 1.6 GeV. These data are currently used to establish the first set of purely physical model calculations for cosmogenic nuclides in iron meteorites.

Experimental: The cross section database is obtained from 30 irradiation experiments performed between 1993 and 1997 using either the stacked foil-technique or the mini-stack approach. The noble gas isotopic concentrations were measured either in Bern or Bordeaux using static noble gas mass spectrometry. Tritium diffusive losses during irradiation and/or storage have been corrected and new data for the ^{3}H/^{3}He branching ratios have been considered [3].

Results: We present consistent excitation functions for the proton-induced production of ^{3,4}He, ^{21,22}Ne, and ^{36,38}Ar from Fe and Ni from the respective reaction thresholds up to 1.6 GeV. In general our cross sections, where overlapping, reasonably agree with earlier data (e.g., [4, 5]). For the production of ^{4}He our data fit well into the systematic expected for evaporation processes. Some of the ^{21}Ne data, however, are compromised by recoil effects from directly neighbored Al monitor foils. For the production of ^{38}Ar from Fe and Ni precise and consistent excitation functions are obtained. For ^{36}Ar, however, the database still (slightly) scatters, because the cross sections are rather low as most of the production on isobar 36 stops at ^{36}Cl. With our new measurements the cross section database for Fe and Ni is fairly complete by now, which enables for the first time detailed studies of cosmogenic production rates in iron meteorites.

References: [1] Leya I. et al. 2000. *Meteoritics & Planetary Science* 35:259–286. [2] Leya I. et al. 2001. *Meteoritics & Planetary Science* 36: 1547–1561. [3] Herbach C.-M. et al. 2006. *Nuclear Physics A* 765:426–463. [4] Michel R. et al. 1997. NIMB, 153–193. [5] Bieri R. H. and Rutsch W. 1962. *Compte Rendu de la Réunion de la Society Suisse de Physique* 35:553–554.

5180

DUST SETTLING AND DUST PROCESSING IN PROTOPLANETARY DISKS AROUND COOL STARS

D. Apai and I. Pascucci. The University of Arizona. Steward Observatory, Tucson, AZ, USA. E-mail: apai@as.arizona.edu.

Introduction: Disks around cool stars and brown dwarfs offer a unique laboratory to study how the early phases of planet formation are affected by disk mass, stellar luminosity, and orbital period. Infrared excess measurements demonstrate that dust disks around cool stars live longer (e.g., [1]) and may be more flat [2, 3] than those around Sun-like stars. We present here results from ongoing Spitzer Space Telescope infrared spectroscopic (IRS) campaigns to characterize dust composition and disk flaring in large sets of co-eval brown dwarf disks in the Rho Oph, Cha I, and Taurus star-forming regions. Using semi-analytical disk structure, dust composition, and dust settling models, we seek to explain the prolonged lifetime of the disks and establish its connection to the flatter disk structure.

Results: The mid-infrared continuum slopes of brown dwarf disks reveal a dominantly flattened disk structure, with only a few objects consistent with the spectral energy distributions expected from classical flared disks [4]. Different analytical methods of the fine structure of the 10-micron silicate emission feature consistently demonstrate a widespread dust processing in these disks. In particular, we find evidence for both silicate grain growth (from submicron to ~2 micron sizes) and significant contribution from crystalline silicates [4, 5].

Discussion: Our observations are consistent with an evolutionary sequence of dust processing from small (submicron-size) amorphous grains toward larger amorphous grains with increased crystalline silicate content. These large grains quicken dust settling leading to flatter disk structures. The presence of these processes in disks around cool stars and brown dwarfs demonstrates that neither low disk masses, low stellar luminosity, nor long orbital periods slow widespread dust processing, the earliest steps of planet formation. Interestingly, several questions remain open. May the presence of crystals around such cool objects be explained via thermal annealing in the inner disk and subsequent outward mixing, or are other processes, such as shock-heating, required? What is the casual relation, if any, between the flatter disk structures around cool stars and the prolonged disk lifetimes? What is the impact of this different dust disk evolution on the emerging planetary systems?

References: [1] Carpenter J. et al. 2006. *The Astrophysical Journal* 651:L49. [2] Apai D. et al. 2002. *The Astrophysical Journal* 573:L115. [3] Apai D. 2004. *Astronomy & Astrophysics* 426:L53. [4] Apai D. et al. 2005. *Science* 310:834. [5] Pascucci I. et al. *The Astrophysical Journal*. Forthcoming.

5167

LITHOLOGY OF LUNAR FARSIDE CRUST

T. Arai[1], H. Takeda[2], A. Yamaguchi[1], and M. Ohtake[3]. [1]Antarctic Meteorite Research Center, National Institute of Polar Research, Kaga, Itabashi, Tokyo 173-8515, Japan. E-mail: tomoko@nipr.ac.jp. [2]Department of Earth and Planetary Science, The University of Tokyo, Hongo, Tokyo 113-0033, Japan. [3]Planetary Science Department, Japan Aerospace Exploration Agency (JAXA), 3-1-1 Yoshinodai, Sagamihara, 229-8510, Japan.

Introduction: Dhofar 489 and 14 paired meteorites are originated from the lunar farside crust [1, 2]. They are crystalline matrix anorthositic breccias, consisting of clasts of magnesian anorthosite (MAN), a spinel troctolite (ST), impact melt, and granulitic clasts. Preliminary study of Dhofar 309 showed a wide range of variations in texture, mineral composition, and modal abundance relative to those in Dhofar 489 [3]. In this study, we present further results of mineralogical and petrologic studies of Dhofar 489 and others (Dhofar 307, 309, 908), to understand the compositional/textural diversity of the impact-melt suite and to discuss the lithologies of the farside crust.

Diversity of the Impact-Melt Suite: While Dhofar 489 includes the clasts of probably pristine MAN and ST, others predominantly consist of angular clasts of crystalline impact melt (IM). Some of the IM clasts include angular plagioclase up to 1 mm across. While fine-grained (10–50 μm across) olivines in the IM clasts are subrounded, plagioclases are lath-shaped. A few MAN clasts are present in Dhofar 309. The modal abundance of the IM clasts in Dhofar 309 is roughly similar to that of the ST clast in Dhofar 489 (plagioclase ~70%, olivine ~25%), suggesting the precursor of the IM have a similar composition to the ST. Yet, the pyroxene abundance in the IM clast (10.7%) is greater than that of ST clast (2.7%). The pyroxene of >10 vol% in the IM clast should be originated from neither the MAN nor ST, but from some other rock type bearing pyroxene, although clasts of norite have not been found. Olivine compositions in Dhofar 309 show bimodal distribution for the MAN and IM, as well as the MAN and ST in Dhofar 489. The olivine composition of the MAN in Dhofar 309 ($Fo_{77–79}$ at peak composition) is slightly more Mg-rich than those of Dhofar 489 ($Fo_{75–77}$). The difference in Fo value may reflect distinct crystallization timing from the trapped liquid among the plagioclase cumulates.

Lithology of the Farside Crust: The highly anorthositic compositions, relatively coarse grain sizes, and extremely low abundances in incompatible trace elements of the MAN and ST [1] imply that they formed as cumulates from a common differentiation magma body. If the ST is a primary product of the magma ocean, it was generated at a depth of a few tens of kilometers [1]. The bimodal mg# distribution of MAN and ST/IM and higher modal pyroxene in the IM indicate that at least three distinct rock types (MAN, ST, norite) exist in the farside crust. However, the pyroxene may not be a dominant phase in the farside highland as suggested by the global mineral maps [4]. Norites distributed in and around the South Pole-Aitken basin of the farside [4] might be associated with the missing norite in the impact-melt suite sampled by Dhofar 489 et al.

References: [1] Takeda H. et al. 2006. *Earth and Planetary Science Letters* 247:171–184. [2] Korotev R. L. et al. 2006. *Geochimica et Cosmochimica Acta* 70:5935–5956. [3] Takeda H. et al. 2007. Abstract #1607. 38th Lunar and Planetary Science Conference. [4] Lucey P. G. 2004. *Geophysical Research Letters* 31:L08701.

5028

PARENTAL MAGMAS OF LUNAR TROCTOLITES: TEMPERATURE, COMPOSITION, AND ORIGIN

A. A. Ariskin. Vernadsky Institute of Geochemistry and Analytical Chemistry, Kosygin Str. 19, Moscow, 119991, Russia.

Introduction: To identify the most primitive magmas of the lunar highland crust, a set of low pressure calculations simulating equilibrium crystallization of troctolites and dunite fragments has been carried out [1]. The results of these calculations allowed us to estimate a range of probable temperatures and melt compositions corresponding to the parental magmas of the magnesian suite (Table 1).

Sample Selection and Modeling: Seven troctolites of a high pristinity of 6–9 were selected, ranging in mass from 0.1 to 155 g [2]. These samples were composed of Ol containing 87–90% Fo and included 30–70% modal Pl. In addition, the composition of dunite 72415, which is thought to be genetically linked with troctolite 76535, was utilized. Modeling of the crystallization trajectories was conducted at 1 atm pressure using an updated version of the METEOMOD model [3] adjusted to simulate the Ol-Pl cotectic more correctly [1]. The modeled average temperatures and parental melt compositions in equilibrium with olivine Fo_{88} and Fo_{91} are listed in Table 1.

Interpretation: The compositional data are interpreted in the context of a hybrid origin of the troctolitic magmas generated via assimilation of a primary anorthosite crust by high-temperature melts of a subchondritic lunar mantle [4, 5]. These processes are thought to have proceeded simultaneously with the consolidation of the highland crust and resulted in high-Mg magmas, which gave rise to the HMS suite of troctolites, norites, and gabbronorites. The modeled characteristics may be used for the development of a thermochemical model of the early lunar contamination including variations in the temperature and composition of the initial mantle melts that assimilated compositionally similar feldspathic material.

Table 1. Compositions of Ol-Pl cotectics approximating the most primitive (T = 1288 °C) and more evolved (T = 1254 °C) troctolitic magmas of the early lunar highland crust.

wt%	1254 ± 10 °C	1288 ± 10 °C
SiO_2	47.91 (2.15)	45.14 (0.94)
TiO_2	0.59 (0.13)	0.36 (0.22)
Al_2O_3	17.91 (0.97)	22.73 (0.94)
FeO	8.18 (0.42)	6.76 (0.28)
MnO	0.13 (0.02)	0.10 (0.01)
MgO	11.18 (0.10)	11.58 (0.23)
CaO	12.95 (0.73)	12.37 (0.56)
Na_2O	0.64 (0.18)	0.72 (0.18)
K_2O	0.24 (0.09)	0.20 (0.10)
P_2O_5	0.26 (0.11)	0.05 (0.03)
Fo (mol%)	88	91
An (mol%)	95.4 ± 1.0	95.8 ± 1.0

References: [1] Ariskin A. A. *Geochemistry International*. Forthcoming. [2] Warren P. H. 1993. *American Mineralogist*. pp. 360–376. [3] Ariskin A. A. et al. 1997. *Meteoritics & Planetary Science* 32:123–133. [4] Warren P. H. 1986. *Journal of Geophysical Research* 91:D331–343. [5] Hess P. C. 1994. *Journal of Geophysical Research* 99:E19,083–19,093.

5145

THE CANYON DIABLO IMPACT EVENT: THE PROJECTILE FATE

N. Artemieva[1, 2] and E. Pierazzo[2]. [1]Institute for Dynamics of Geospheres, Moscow, Russia. [2]Planetary Science Institute, Tucson, AZ, USA. E-mails: artemeva@psi.edu; betty@psi.edu.

Introduction: Mass and impact velocity estimates of the Meteor Crater projectile varied widely, starting from the historical Barringer's hypothesis of a huge body comparable to the crater size buried beneath the crater floor [1] to modern scaling law values [2] giving a rather modest diameter of ~40 m for an 18 km/s impact velocity. Our recent study of the projectile disruption and deceleration in atmosphere [3] suggests that the most probable pre-atmospheric mass was 10^9 kg, corresponding to 68-meter-diameter spherical iron projectile (and 18 km/s impact velocity). Approximately 50% of this mass was lost during atmospheric entry because of ablation and disruption into small fragments (the Canyon Diablo meteorites) dispersed over the impact region. While these fragments landed with low velocities (and survived as meteorites), the main cloud impacted the surface with velocity of ~15 km/s. The possibility of lower impact velocities cannot be totally excluded, as some NEOs have low pre-atmospheric velocities [4].

Projectile Inventory: Meteorites, Spheroids, and Shale Balls: By the early 1900s, thousands of iron meteorites, ranging from less than 25 g to more than 500 kg in weight, were collected within a radius of 5.5 miles from the crater [5]. Meteorites on the plains show clear Widmanstätten figures. Irons recovered near the crater rim show evidence of strong heating, up to partial melting and recrystallization. Tiny spheroids (<1 mm) are abundantly distributed within ~8 km from the crater mainly in the northeast direction and are sorted with distance, with the largest spheroids located on the crater rim [5, 6]. They may be the condensation product of the partially vaporized part of the projectile.

Model: To model the cratering process we use the 3-D SOVA hydrocode with particles [7]. Material strength is taken into account using the rigid-plastic approximation. A moderately dispersed projectile strikes the target with lithology similar to the Meteor Crater region (from top to bottom: Moenkopi, Kaibab, Coconino). The water table at a depth of 150 m can be taken into account to describe additional ejecta dispersion by a water vapor [8]. SOVA is coupled to tabular equations of state for iron (projectile), quartzite and calcite (sedimentary rocks), and water.

Results: Our results on shock compression of the projectile confirm previous results [9]: little vaporization, some melting, while over 50% of the impactor remains solid, although strongly compressed and heated, and is ejected from the crater. We can connect the projectile shock compressions and ejection velocities with the distribution of irons around Meteor Crater. The mass inventory shows that a lot of the projectile material was removed from the crater area before its scientific study began.

References: [1] Barringer D. M. 1909. Paper read before the National Academy of Sciences. [2] Schmidt R. M. and Housen K. R. 1987. *International Journal of Impact Engineering* 5:543–560. [3] Artemieva N. and Pierazzo E. *Meteoritics & Planetary Science*. Forthcoming. [4] Bottke W. 2002. *Icarus* 156:399–433. [5] Nininger H. 1973. *Find a falling star*. 254 p. [6] Rinehart J. S. 1958. *Smithsonian Contribution to Astrophysics* 2:145–159. [7] Shuvalov V. 1999. *Shock Waves* 9:381–390. [8] Artemieva N. 2007. *Meteoritics & Planetary Science* 42:883–894. [9] Schnabel C. et al. 1999. *Science* 285:85–88.

5192

PASSIVATION OF METAL OXIDATION BY IRON OXIDE PRODUCTION IN ORDINARY CHONDRITES WEATHERED IN A MARS ANALOG ENVIRONMENT

J. W. Ashley[1, 2] and M. A. Velbel[3]. [1]School of Earth and Space Exploration, Arizona State University, Mars Space Flight Facility, Box 871404, Tempe, AZ 85287, USA. [2]Minor Planet Research, Inc., Box 19964, Fountain Hills, AZ 85269–9964, USA. E-mail: james.ashley@asu.edu. [3]Department of Geological Sciences, Michigan State University, 206 Natural Science Building, East Lansing, MI 48824–1115, USA.

Introduction: The degree of reduced iron-nickel (kamacite and taenite) alteration in meteorites found by current and future rovers on Mars can serve as a marker for the assessment of paleoclimatic trends on the planet [1, 2]. A similar method of climatic assessment has been applied to terrestrial meteorite weathering [3]. Metal alteration will be "passivated" in a hot desert environment when the production of iron oxides and oxyhydroxides becomes arrested by the tensile strength of the surrounding rock mass as void spaces are filled [4]. We report evidence of similar behavior in OC from Mars-analogous Antarctica [5], suggesting that the magnitude of metal alteration on Mars may be asymptotic to "plateau" values specific for each meteorite type.

Methods: Two separate modal analyses were performed on each of 19 weathering category C OC from Allan Hills and Lewis Cliff, Antarctica. The first utilized a petrographic count of 500 points per sample to differentiate opaques (consisting mainly of reduced metal grains) from stained and unstained phase abundances. In this count, stained areas included all types of secondary oxide visible in thin section. The second count used 500 points per sample to differentiate opaques from crystalline, opaque-pseudomorphic limonites (OPL), and volumetrically less significant non-OPL oxide stain phases. All point counts used medium-power objectives and the condenser apparatus. The first modal count was performed by making manual adjustments of the mechanical stage, while the second employed an automatic stage-advancing unit.

Results: In an attempt to identify any trends in the production of secondary minerals (particularly OPL), the stain component of the iron oxides was separated from the total oxide fraction and included with the unstained silicates fraction. This held constant the sum of all formerly transparent areas, whether stained or unstained, and regardless of the stain intensity. With little or no void space for OPL products to grow into, OPL replacement of reduced metal primary phases is isovolumetric (e.g., [6]). Ternary plots of volumetric modal abundances with OPL, opaques, and silicates (stained and unstained) as endmembers, show a clear, linear trend for 18 of the samples. We interpret this trend to indicate a state of pressure equilibrium (passivation) within each meteorite where the stress produced by the growing minerals is in balance with the tensile strength of the rock itself. Nonisovolumetric metal alteration can occur only if fractures and void spaces are enlarged, or new fractures are created to expose unweathered surfaces to the environment. Therefore, this metastable state of affairs is adjusted each time the meteorite is broken until equilibrium can be re-established.

References: [1] Ashley J. A. and Wright S. P. 2004. Abstract #1750. 35th LPSC. [2] Ashley et al. 2007. Abstract #2264.38th LPSC. [3] Bland P. A. et al. 1996. *Geochimica et Cosmochimica Acta* 60:2053–2059. [4] Bland P. A. et al. 1998. *Meteoritics & Planetary Science* 33:127–129. [5] Wentworth et al. 2005. *Icarus* 174:382–395. [6] Buchwald V. F. and Clarke R. S., Jr. 1989. *American Mineralogist* 74:656–667.

5120

CENTRAL PIT CRATERS ON MARS AND GANYMEDE

N. G. Barlow. Department of Physics and Astronomy, Northern Arizona University, Flagstaff, AZ 86011–6010, USA. E-mail: Nadine.Barlow@nau.edu.

Introduction: Craters containing a central pit are common on Mars and icy moons such as Ganymede and Europa, but are rare on volatile-poor bodies such as the Moon. This observation led Wood et al. [1] to propose that explosive release of vapor produced during crater formation in ice-rich targets produced the central pit. Alternately, Croft [2] proposed that central pits are produced during cometary impacts. Recent numerical simulations of impacts into ice-soil mixtures reveal that vaporization temperatures are surpassed near the center of the transient cavity [3], providing a mechanism for the explosive release of volatile as proposed by [1]. Our study is comparing the characteristics and distributions of central pit craters on Mars and Ganymede to better understand how target volatiles and other environmental factors contribute to central pit formation.

Data: Catalogs of impact craters are being compiled for Mars [4] and Ganymede [5]. The Mars Catalog utilizes image, mineralogic, topographic, and thermophysical data obtained by MGS and Odyssey. The Ganymede data are acquired from Galileo SSI data, with Voyager data used when Galileo data are unavailable. Ejecta and interior morphologies are classified and crater preservational state is denoted. Central pit craters are classified based on whether they occur directly on the crater floor (floor pits) or occur atop a central dome or rise (summit pits). We also determine the ratio of pit-to-crater diameters (D_p/D_c).

Results: To date we have identified ~1600 central pit craters on Mars and ~400 on Ganymede. While floor pits dominate for Mars, pits atop central domes are more common on Ganymede. Ganymede craters containing central pits tend to be larger on Ganymede (29–93 km diameter) than on Mars (5–57 km diameter). Martian floor pits tend to be larger relative to their parent craters than summit pits (average D_p/D_c = 0.15 versus 0.11). Ganymede pits are generally larger relative to their parent crater than Martian pits (average D_p/D_c = 0.19). No strong correlation of central pits with terrain or latitude is seen for either body. Pits are seen in craters with a wide range of preservational states, indicating that the conditions producing central pits have existed on both bodies for much of their histories.

Discussion: While catalog compilation is not yet complete for either body, the current results indicate that there are some differences between central pit craters on Mars and Ganymede. Ganymede's gravity is 2.6× smaller than that for Mars and could be one contributor to observed variations. However, the variations in crater diameters and D_p/D_c between the bodies are not exactly 2.6, suggesting that other contributors, such as the purity of the ice target, play a role in central pit formation.

Acknowledgements: This research is supported by NASA MFRP award #NNG05GM14G and NASA OPRP award #NNG05G116G.

References: [1] Wood C. A. et al. 1978. Proceedings, 9th LPSC. pp. 3691–3709. [2] Croft S. K. 1983. Proceedings, 14th LPSC. pp. B71–B89. [3] Pierazzo E. et al. 2005. *Large meteorite impacts III*. GSA Special Paper #384. pp. 443–457. [4] Barlow N. G. 2006. Abstract #1337. 37th LPSC. [5] Katz-Wigmore J. and Barlow N. G. 2006. Abstract #1387. 37th LPSC.

5123

ARE STANNERN-TREND EUCRITES ORDINARY EUCRITES CONTAMINATED BY CRUSTAL PARTIAL MELTS?

J. A. Barrat[1], A. Yamaguchi[2], R. C. Greenwood[3], M. Bohn[1], J. Cotten[1], M. Benoit[1], and I. A. Franchi[3]. [1]UBO-IUEM, CNRS-UMR 6538, Place Nicolas Copernic, F-29280 Plouzané Cedex, France. E-mail: barrat@univ-brest.fr. [2]Antarctic Meteorite Research Center, National Institute of Polar Research, 1-9-10 Kaga, Itabashi, Tokyo 173-8515, Japan. [3]PSSRI, Open University, Walton Hall, Milton Keynes MK7 6AA, UK.

Introduction: Stannern-trend eucrites are not only richer in incompatible trace element than the other eucrites, but their trace-element patterns are clearly distinctive, with pronounced negative Be, Sr, and Eu anomalies. Many authors have proposed that the diversity of the eucritic melts could simply reflect part of the diversity of the primary melts from the parent body mantle (e.g., [1–3]). Alternatively, to explain the decoupling of major elements from incompatible trace elements requires a complex scenario involving interaction between eucritic and highly residual melts [4, 5]. As an alternative to previous hypotheses for the origin of Stannern-trend eucrites, we propose a model of contamination of ordinary eucrites by melts produced by melting of the asteroidal crust. The composition of melts generated by the partial melting of eucritic crust can be calculated theoretically. The first partial melts would certainly not be acidic, but rather intermediate to basic in composition. We have calculated the trace element abundances of melts produced by partial melting of an equilibrated eucrite using literature partition coefficients, and the composition of our reference eucrite Juvinas. The calculated magmas produced by partial melting of a eucritic crust are rich in incompatible trace elements and display pronounced negative anomalies in K, Ba, Be, Sr, Eu, and Ti relative to ordinary eucrites. Contamination of a normal eucrite by a crustal partial melt should have little effect on its major element concentration, but a huge impact on the incompatible trace element abundance, which is exactly the variation displayed by Stannern-trend eucrites. We have calculated the melts obtained by simple mixing between a eucrite and a crustal partial melt produced by 10% melting. The trace element abundances are strikingly well reproduced by this model. The trace element concentrations of Stannern and Bouvante are explained by a combination of about 85% Juvinas and 15% crustal partial melt. The calculated proportions are obviously dependent to the compositions of the endmembers. For example, very different proportions are obtained using the partial melts calculated for 5% or 15% of melting of the eucritic crust.

References: [1] Consolmagno G. J. and Drake M. J. 1977. *Geochimica et Cosmochimica Acta* 41:1271–1282. [2] Stolper E. 1977. *Geochimica et Cosmochimica Acta* 41:587–611. [3] Mittlefehldt D. W. and Lindstrom M. M. 2003. *Geochimica et Cosmochimica Acta* 67:1911–1935. [4] Barrat J. A. et al. 2000. *Meteoritics & Planetary Science* 35:1087–1100. [5] Warren P. H. and Kallemeyn G. W. 2001. Abstract #2114. 32nd Lunar and Planetary Science Conference.

5050

A SCALE OF HETEROGENEITY FOR THE REGOLITH OF VESTA SEEN THROUGH A SUITE OF PAIRED HOWARDITES

A. W. Beck, C. E. Viviano, and K. K. Cheung. Earth and Planetary Sciences, University of Tennessee, Knoxville, TN 37996, USA. E-mail: abeck3@utk.edu.

Introduction: HED (howardite, eucrite, and diogenite) meteorites are a unique suite of achondrites thought to originate from asteroid 4 Vesta [1]. Howardites, impact-generated polymict breccias of eucrite and diogenite clasts (e.g., [2]), represent samples of the regolith [3]. In this study, analyses of three, likely paired howardite meteorites, Pecora Escarpment (PCA) 02009, 02013, and 02015 [4], indicate centimeter-scale lithologic variability on the surface of Vesta.

Results: Although the composition and texture of diogenite and eucrite clasts in PCA 02009, 02013, and 02015 fall within previously defined ranges, significant differences exist between the three meteorites. Orthopyroxene compositions in the three meteorites are typical for the HED suite, $Wo_{3 \pm 2}En_{73 \pm 4}Fs_{24 \pm 3}$ [5]. Clinopyroxene in PCA 02013 is generally more Fe-rich than that in 02015, whereas 02009 clinopyroxene contains a range of Mg and Fe-rich compositions. Ratios of minor elements, such as Ti and Al, differ between PCA 02015 and 02013 pyroxenes. All three meteorites have plagioclase compositions of An_{96}-An_{63}. Lathe-shaped plagioclase only appears in PCA 02015. Zoned olivine grains (~$Fo_{92–50}$) occur in PCA 02015 and 02009. In PCA 02013, homogenous olivine grains have compositions of ~Fo_{67}. The largest variability exists in FeNi metal. PCA 02013 and 02009 contain predominantly HED-like FeNi metal compositions [6], along with some tetrataenite. However, all FeNi grains in PCA 02015 (and one in 02009) lie within a Co/Ni range defined for iron meteorites [7] and have distinct textures.

Discussion and Conclusion: A 2002 collection map of the Pecora Escarpment ice field shows these three howardites were found within 4 km of six other howardites [4]. Given the chance of finding nine howardites in one location, they are likely paired. Major and minor elements in clinopyroxene in PCA 02015 and 02009 suggest they may be sampling two different types of eucrite. In contrast, PCA 02013 appears to sample only one. These differences, coupled with contrasting olivine characteristics, suggest sampling of a variety of eucrite and diogenite sources. The wide range of FeNi metal compositions also indicates variable lithologic sources from Vesta, and potential contamination via an impactor.

The centimeter-scale variation of lithologic components within this suite helps define a scale of heterogeneity for the regolith. Determining the extent of regolith variability is essential in preparation for future mapping missions to Vesta (e.g., Dawn) and handling the spatial resolution of the GRaND and VISNIR spectrometers [8].

References: [1] McCord T. B. et al. 1970. *Science* 168:1445–1447. [2] Wahl W. 1952. *Geochimica et Cosmochimica Acta* 2:91–117. [3] Gaffey M. J. 1997. *Icarus* 127:130–157. [4] Russell S. S. et al. 2004. *Meteoritics & Planetary Science* 8:A215–A272. [5] Mittlefehldt D. et al. 1998. In *Planetary materials*. pp. 102–131. [6] Gooley R. and Moore C. 1976. *American Mineralogist* 61:373–378. [7] Moore C. E. et al. 1969. In *Meteorite research*. pp. 738–748. [8] Russell C. T. et al. 2004. *Planetary and Space Science* 52: 465–489.

5241

IRON-60 ACTIVITIES OF CANYON DIABLO, GRANT, AND DOROFEEVKA

E. L. Berger[1], T. Faestermann[2], G. F. Herzog[1], K. Knie[2], G. Korschinek[2], I. Leya[3], and F. Serefiddin[1]. [1]Department of Chemistry, Rutgers University, Piscataway, NJ 08854–8087, USA. E-mail: herzog@rutchem.rutgers.edu. [2]Fakultät für Physik, Technische Universität München, D-85748, Garching, Germany. [3]Physikalisches Inst., CH 3012 Bern, Switzerland.

Introduction: In meteoroids, cosmic rays produce the β^- emitter ^{60}Fe ($t_{1/2}$ = 1.5 Ma) mainly through nuclear reactions with the minor isotopes of nickel. Even in nickel-rich iron meteorites, however, ^{60}Fe production rates are low and only a few measurements of ^{60}Fe activities have been reported to date [1]. The utility of ^{60}Fe in interpreting cosmic-ray exposure histories depends on understanding its production rate systematics. To contribute toward such an understanding, we have measured the activities of ^{60}Fe in six samples representing a large range of shielding conditions in three iron meteorites.

Experimental Methods: Samples with masses of ~100 mg were dissolved in HCl. Iron was separated by ion exchange and precipitated as the hydroxide. Ratios (atom/atom) of ^{60}Fe to Fe were measured by accelerator mass spectrometry (AMS) [1].

Results and Discussion: Table 1 shows measured ^{60}Fe activities; Ni contents are from the literature. Published activities (dpm/[kg Ni]) range from ~0.7 for metal from chondrites to 2.0 ± 0.6 for a 2.5 kg (!) sample of Odessa [see 1, 2].

Production rates of spallogenic nuclides such as ^{3}He, ^{10}Be, ^{21}Ne, and ^{36}Cl generally decrease with increasing depth in large iron meteorites (e.g., [3]), as we also find for ^{60}Fe in Canyon Diablo. With sample depths based on [4], we obtain a half thickness of 11.5 ± 5.0 cm for ^{60}Fe. In contrast, modeling calculations for iron meteoroids with radii <40 cm [1] predict an increase with depth of ~30% in the production of ^{53}Mn and ^{60}Fe. If we use for Grant the size and the depth scale proposed in [5], our ^{60}Fe activities for O +10 and K –47 (distances from center 28.6 cm and 19.0 cm, respectively) confirm an increase of ^{60}Fe with depth, although uncertainties are appreciable. Dorofeevka's small recovered mass (12.6 kg) and rather high ^{10}Be and ^{26}Al activities [6] indicate relatively light shielding. Its ^{60}Fe activity is consistent with these observations.

Table 1. Activities of ^{60}Fe (dpm/[kg Ni]) in iron meteorites.

Sample	Counts	Ni	Activity
Canyon Diablo			
266	9	6.91	0.84 ± 0.36
4340	3	6.98	0.11 ± 0.09
4367	7	6.98	0.41 ± 0.20
Grant 836			
O +10	30	9.29	1.01 ± 0.20
K –47	28	9.29	1.21 ± 0.25
Dorofeevka	50	11.3	0.99 ± 0.15

References: [1] Knie K. et al. 1999. *Meteoritics & Planetary Science* 32:729–734. [2] Goel P. S. and Honda M. 1965. *Journal of Geophysical Research* 70:747–748. [3] Kohman T. P. and Bender M. L. 1967. In *High-energy nuclear reactions in astrophysics*. pp. 169–245. [4] Michlovich E. S. et al. 1994. *Journal of Geophysical Research* 99:23,187–23,194. [5] Ammon K. and Leya I. 2006. Abstract #1556. 37th LPSC. [6] Xue S. et al. 1995. *Earth and Planetary Science Letters* 136:397–406.

5272

A COMMON ORIGIN FOR FeO-RICH SILICATES IN KAKANGARI AND ENSTATITE CHONDRITE CHONDRULES?

J. Berlin, R. H. Jones, and A. J. Brearley. Department of Earth and Planetary Sciences, University of New Mexico, Albuquerque, NM 87131, USA. E-mail: jberlin@unm.edu.

Introduction: Chemical and oxygen isotopic evidence shows that chondritic components in different chondrite groups (e.g., CAIs, refractory forsterites) could have originated from common reservoirs in the solar nebula [1–3]. To assess if this concept also applies to chondrules, we are comparing the mineralogical, petrographic, and chemical characteristics of chondrules in Kakangari (K) and primitive enstatite chondrites (EC), because their oxygen isotopic compositions are indistinguishable [4]. We studied a suite of Kakangari chondrules by EPMA [5]. Data for EC chondrules include literature data [6–10] and our data for the EH3 chondrite Sahara 97096.

Results: Kakangari chondrules are similar to EC3 chondrules in the following aspects: a) no typical FeO-rich type II chondrules are present, b) most chondrules are pyroxene-rich, and c) many chondrules contain SiO_2. These characteristics make K and EC chondrules more similar to each other than to OC and CC chondrules. However, there are also major differences (e.g., [11]) which imply that EC chondrules formed in a more reducing environment. For example, most chondrule silicates are more Mg-rich in EC (Fs < 2 and Fa < 1, e.g., [6]) than in Kakangari (histograms peak at Fs ~6 and Fa ~3 [4, 5]).

Even though no typical FeO-rich type II chondrules are present, ubiquitous FeO-rich silicates ($Fs_{5–35}$, $Fa_{3–14}$) have been observed in EC chondrules (e.g., [8–10]). FeO-rich pyroxenes and olivines with similar characteristics and chemical compositions are observed in K chondrules [5]. In both EC and K chondrules, FeO-rich silicates show evidence that they have undergone solid-state reduction (e.g., Ni-poor metal blebs, presence of SiO_2, reverse zoning [5, 8–10]), which must postdate chondrule formation. Some of the metal blebs (in both K and EC) have subsequently been sulfidized, forming troilites. Troilites in FeO-rich EC silicates have high Cr (1.5–3 wt%) and Ti (0.15–0.25 wt%) contents, similar to troilites in the EC matrix [10]. Troilites in K chondrules have Cr contents between 0.15 and 0.4 wt% and Ti below EMP detection limits, similar to Kakangari matrix. This is consistent with a less reducing environment for Kakangari.

Discussion: We suggest that chondrules in Kakangari and EC that contain FeO-rich silicates could have originated from similar FeO-rich precursor material. Both underwent a reduction event, but for Kakangari chondrules the environment was less reducing. Sulfidization of metal blebs probably followed, after reduction, via the reaction $Fe + H_2S \rightarrow FeS + H_2$. Then the evolutionary paths of FeO-rich K and EC chondrule silicates diverged: FeO-rich objects in EC record a more complex history, including formation of rims, brecciation, and remelting [9].

References: [1] Zanda B. et al. 2006. *Earth and Planetary Science Letters* 248:650–660. [2] Guan Y. et al. 2000. *Earth and Planetary Science Letters* 181:271–277. [3] Pack A. et al. 2004. *Geochimica et Cosmochimica Acta* 68:1135–1157. [4] Weisberg M. K. et al. 1996. *Geochimica et Cosmochimica Acta* 60:4253–4263. [5] Berlin J. et al. 2007. Abstract #2395. 38th LPSC. [6] Grossman J. N. et al. 1985. *Geochimica et Cosmochimica Acta* 49:1781–1795. [7] Schneider D. M. et al. 2002. *Meteoritics & Planetary Science* 37:1401–1416. [8] Lusby D. et al. 1987. *Journal of Geophysical Research* 92:E679–695. [9] Weisberg M. K. et al. 1994. *Meteoritics* 29:362–373. [10] Kimura M. et al. 2003. *Meteoritics & Planetary Science* 38:389–398. [11] Prinz M. et al. 1989. 20th LPSC. pp. 870–871.

5251

SURVIVAL OF ASTEROIDAL IMPACTOR MATERIAL ON THE MOON

P. A. Bland[1, 2], N. A. Artemieva[3], D. B. J. Bussey[4], G. S. Collins[1], and K. H. Joy[2, 5]. [1]Impacts and Astromaterials Research Centre (IARC), Department of Earth Sci. and Eng., Imperial College London, SW7 2AZ, UK. E-mail: p.a.bland@imperial.ac.uk. [2]IARC, Department of Mineralogy, Natural History Museum, London SW7 5BD, UK. [3]Institute for Dynamics of Geospheres, Russian Academy of Sciences, Leninsky Prospect 38/6, Moscow, Russia 117939. [4]The Johns Hopkins University Applied Physics Laboratory, 11100 Johns Hopkins Road, MP3-E180, Laurel, MD 20723, USA. [5]UCL/Birkbeck Research School of Earth Sciences, UCL, Gower Street, London, WC1E 6BT, UK.

Introduction: The lower limit for pre-atmospheric impacts at Earth is 11.2 km/s (Earth escape velocity). Although our atmosphere is effective at significantly reducing surface impact velocities for smaller (less than 100s of meters) asteroids (e.g., [1]), larger objects strike the surface at close to their cosmic velocity. Principally due to these high velocities, solid projectile material is rare at terrestrial craters >1–2 km. However, in addition to velocity, impact angle can have a profound effect on projectile survival [2]. In high-velocity impacts, only at low angles does a significant proportion of the projectile remain in the solid phase, but even at 15° shock pressures are high, with 90% of material at >50 GPa [2].

Lacking an atmosphere, there is no mechanism to decelerate impactors on the Moon. But minimum impact velocity (related to its escape velocity and the gravitational effect of the Earth at lunar distance) is much lower: 2.78 km/s. Projectiles of all sizes are therefore capable of striking the lunar surface at velocities far lower than is possible on Earth. We chose to explore the effect of these (comparatively) low-velocity impacts on projectile survival.

Results and Discussion: We modeled impacts at 3 km/s and 7 km/s, and 15° and 45°. In all scenarios >90% of the projectile remained in the solid phase (although fragmented to varying degrees). At 3 km/s, at both angles, >60% of the impactor experienced shock pressures <10 GPa—essentially unaltered. Does this material remain close to the source crater, or is it widely dispersed? Preliminary results for projectile dispersion after a 45° impact at 3 km/s show that the amount of material deposited within or near the crater is substantially greater than that which escapes the Moon or is widely dispersed (>5 crater diameters).

How common are these events? Only 0.18% of all lunar impacts occur at 2–4 km/s [3, 4] (6.7% of all impacts will be at <15°, and 50% at <45°). Scaling lunar mare and highland crater size frequency distributions [5] to the overall proportion of mare and highland (16% and 84%, respectively), and scaling this value to the proportion of projectiles striking at 2–4 km/s and <45°, we find that of the current population of lunar craters >10 km in size, >15 were formed under conditions which should have seen only a small fraction of the projectile shocked to high pressure.

Conclusions: Our preliminary analysis suggests: 1) that low-velocity impact events should be recorded on the Moon, 2) that the projectile experienced low shock, and 3) that fragment dispersion would not be great. We are exploring whether craters (and possibly impactors) are detectable by remote sensing.

References: [1] Bland P. A. and Artemieva N. A. 2006. *Meteoritics & Planetary Science* 41:607–631. [2] Pierazzo E. and Melosh H. J. 2000. *Meteoritics & Planetary Science* 35:117–130. [3] Bottke W. F. et al. 2002. *Icarus* 156:399–433. [4] Bottke W. F. et al. 1994. *Icarus* 107:255–268. [5] Neukum G. et al. 2001. *Space Science Reviews* 96:55–86.

5309

SHOCK METAMORPHISM OF LATE CRYSTALLIZATION PRODUCTS IN SHERGOTTY

U. Bläss and F. Langenhorst. Institute for Geosciences, Friedrich-Schiller-Universität Jena, Germany. E-mail: Ulrich.Blaess@uni-jena.de.

Introduction: Shergotty is a basaltic type meteorite of the SNC achondrite group, which is widely accepted to be of Martian origin. It originated from a highly evolved melt fraction and consists predominantly of large zoned clinopyroxene crystals and original plagioclase. The latter has been converted into maskelynite by a shock event that ejected Shergotty from Mars. Stöffler et al. concluded that all shock features in minerals can be attributed to a single shock with an equilibrium pressure of 29 GPa [1]. Local peak temperatures reached up to 1600–2000 °C and resulted in the formation of melt pockets that may contain submicron crystallization products. In addition, other fine-grained crystallization products originated from a late-stage crystallization of the parent melt, which phases may have transformed to high-pressure phases during the shock event. In this study, we attempt to distinguish the various fine-grained crystallization products and try to understand their origin and thermal histories.

Results: To address these issues, we have studied the mineralogy of fine-grained fractions in Shergotty using optical microscopy, scanning electron microscopy, and transmission electron microscopy (TEM). The results show that these micrometer-size crystallites can be split into two groups: 1) mafic symplectites composed of either fayalite plus hedenbergite or fayalite plus a SiO_2 polymorph, and 2) felsic areas consisting of potassium-rich maskelynite and SiO_2 phases, which show a similar lamellar microstructure as those described recently as post-stishovite phases [2]. These felsic areas also contain minor fractions of a new residual zirconium- and titanium-bearing iron-silicate, Ca phosphates, and Fe sulfides. Under the TEM all these phases show deformation microstructures characteristic of strong shock metamorphism.

Discussion: The first group of mafic symplectites are similar to symplectites described recently in shergottites and are break-down products of former pyroxferroite and ferrosilite rather than primary crystallization products [3]. In contrast, the second group represents late crystallization products of a magmatic melt which differs significantly from shock-induced melt pockets with respect to their chemical composition, grain sizes, and shock-induced microstructures. TEM analyses will be further applied to distinguish between late magmatic differentiation processes on Mars and to obtain more information on shock-induced phase transformation of high-pressure minerals occurring frequently in such late crystallization products as the example of the post-stishovite polymorph.

References: [1] Stöffler D. et al. 1986. *Geochimica et Cosmochimica Acta* 50:889–903. [2] El Goresy A. et al. 2004. *Journal of Physics and Chemistry of Solids* 65:1597–1608. [3] Aramovich C. J. et al. 2002. *American Mineralogist* 87:1351–1359.

5229

OLD SHERGOTTITES AND YOUNG IMPACT AGES

J. Blichert-Toft[1], A. Bouvier[2], J. D. Vervoort[3], P. Gillet[1], and F. Albarède[1]. [1]Ecole Normale Supérieure de Lyon, France. E-mail: jblicher@ens-lyon.fr. [2]The University of Arizona, Tucson, AZ, USA. [3]Washington State University, Pullman, USA.

Abundant isotopic data obtained on basaltic shergottites for different long-lived radiogenic systems (^{87}Rb-^{87}Sr, ^{147}Sm-^{143}Nd, ^{176}Lu-^{176}Hf, U-Pb) give internal isochron ages that cluster around 180 and 330–475 Ma [1]. The general view that these ages represent the time of shergottite crystallization was questioned by Blichert-Toft et al. [2] and more recently by Bouvier et al. [3]. We argue that i) regardless of the uncertainties, cratering chronology [4] and stratigraphy [5] assign to most of the Martian surface an age >2 Ga; ii) evidence of old Pb-Pb ages in basaltic shergottites, for which the labile component (dominated by apatite) has been removed by acid leaching, is overwhelming; iii) the preservation of ^{142}Nd and ^{182}W anomalies [6, 7] in shergottites is at odds with young ages; and iv) other indications of old ages for Martian meteorites exist, such as 2.5–4.0 Ga old fission tracks in phosphate grains [8] and ^{39}Ar-^{40}Ar ages in excess of emplacement ages [9, 10].

New Pb isotopic compositions of leached whole-rock fragments and maskelynite separates of Shergotty and Los Angeles fall on the ~4.1 Ga Zagami isochron of [3], which we interpret as dating the crystallization of the basaltic shergottite suite. In contrast, Sm-Nd and Lu-Hf internal isochrons give, as expected, young ages, namely respectively, 170 ± 41 Ma (MSDW = 6.3) and 187 ± 89 Ma (MSDW = 5.1) for Shergotty and 178.8 ± 4.6 Ma (MSDW = 0.95) and 158 ± 14 Ma (MSDW = 0.97) for Los Angeles. Both the ~180 and ~450 Ma cluster ages are observed by Ar-Ar chronometry in Martian meteorites, as well as in ordinary chondrites [11], and recently also by U-Pb chronology of shocked [12] baddeleyite in shergottites [13]. We surmise that these isotopic systems were reset by strong impacts on the Martian surface, which in turn raised global rock temperatures to 200–400 °C [14], thereby creating the conditions for permafrost to melt and induce aqueous circulation and alteration near the surface. Such a scenario is supported by the atmospheric-like δD values measured in shergottite apatites [15, 16]. Consequently, the young ages of shergottites date the last re-equilibration of phosphate (the main carrier of U, Sr, and REE) with Martian groundwater before the last dry-out of these water bodies.

References: [1] Nyquist L. E. et al. 2001. *Space Science Reviews* 96: 105–164. [2] Blichert-Toft J. et al. 1999. *Earth and Planetary Science Letters* 173:25–39. [3] Bouvier A. et al. 2005. *Earth and Planetary Science Letters* 240:221–233. [4] Hartmann W. K. and Neukum G. 2001. *Space Science Reviews* 96:165–194. [5] Tanaka K. L. et al. 1992. *Mars* 345–382. [6] Kleine T. et al. 2004. *Geochimica et Cosmochimica Acta* 68:2935–2946. [7] Foley C. N. et al. 2005. *Geochimica et Cosmochimica Acta* 69:4557–4571. [8] Rajan R. S. et al. 1986. *Geochimica et Cosmochimica Acta* 50: 1039–1042. [9] Bogard D. D. and Garrison D. H. 1999. *Meteoritics & Planetary Science* 34:451–473. [10] Walton E. L. et al. 2007. *Geochimica et Cosmochimica Acta* 71:497–520. [11] Bogard D. D. 1995. *Meteoritics* 30: 244–268. [12] El Goresy A. 1965. *Journal of Geophysical Research* 70: 3454–3465. [13] Herd C. D. K. et al. 2007. Abstract #1664. 38th LPSC. [14] Stöffler D. et al. 1986. *Geochimica et Cosmochimica Acta* 50:889–903. [15] Leshin L. A. 2000. *Geophysical Research Letters* 27:2017–2020. [16] Greenwood J. P. et al. 2007. Abstract #1338. 38th LPSC.

5191

THE DRIEST GLASS IN THE SOLAR SYSTEM: GLASS SPHERULES IN HOWARDITES

J. S. Boesenberg and C. W. Mandeville. Earth and Planetary Sciences, American Museum of Natural History, Central Park West, New York, NY 10024, USA. E-mail: bosenbrg@amnh.org; cmandy@amnh.org.

Introduction: Howardites are polymict breccias composed of mineral and lithic fragments from both eucrites and diogenites. In some howardites and polymict eucrites, glass spherules ranging in size from a few hundred microns to over a centimeter in diameter occasionally have been found [1–3]. The spherules, much like the lunar glasses, have been interpreted as resulting from either impact [1, 4–6] or fire-fountaining [1, 3] on the parent body. To distinguish between these formational processes, the volatile (water, CO, and CO_2) and chemical compositions of three glass spherules (two from the howardite Northwest Africa 1664 and one from howardite Kapoeta) have been determined.

Results: Analysis using a Thermo Nicolet Nexus 670 Fourier transform infra-red spectrometer (FTIR) in transmission mode, and using 85–95-micron-thick, doubly polished samples, shows that all three glass spherules contain NO evidence of water or carbon monoxide. Absolutely flat spectra were obtained at wavenumber positions for total water (3570 cm^{-1}), molecular water (1630 and 5200 cm^{-1}), OH (4500 cm^{-1}), and CO (2140 cm^{-1}). Detection limits for water at wavenumber 3570 cm^{-1} are ~100 ppm, while limits for CO at 2140 cm^{-1} are ~50 ppm. Very low abundances (less than 50 ppm) of both CO_2 (2330 cm^{-1}) and CO_3 (1450 and 1550 cm^{-1}) though were measured. There were minor variations in CO_2 content observed within single glass spherules, however with the abundances present at such low levels, small amounts of terrestrial atmospheric contamination likely account for the slight variation.

Cameca SX-100 microprobe analysis of major and minor elements shows that the chemical compositions within each glass are only mildly variable. However, interspherule comparison shows large variations in bulk composition, particularly in CaO, FeO, and K_2O, similar to those analyzed by [2, 3].

Discussion: The determination over whether howardite spherules are the product of fire-fountaining or impact has, in the past, been ambiguous. If fire-fountaining is the source, volatile abundances should be moderately high and spherule chemical compositions should be quite uniform, as the spherules would all be expected to derive from a relatively homogeneous mantle source. However, just the reverse is seen in the howardite spherules analyzed. Very low volatiles are observed and the bulk compositions of the spherules vary widely. Impacts appear to be the definitive source of the spherules. Impacts would substantially lower any volatiles present in the source rocks as well as produce variable spherule bulk compositions by partial melting of the local regolith.

References: [1] Delaney J. S., Prinz M., and Takeda H. 1984. Proceedings, 15th Lunar Planet. Sci. Conf. pp. C251–C288. [2] Kurat G., Varela M. E., Zinner E., Maruoka T., and Brandstatter F. 2003. Abstract #1733. 34th Lunar Planet. Sci. Conf. [3] Delaney J. S., Prinz M., and Nehru C. E. 1982. *Meteoritics* 17:204. [4] Desnoyers C. and Jerome D. Y. 1977. *Geochimica et Cosmochimica Acta* 41:81–86. [5] Hewins R. H. and Klein L. C. 1978. Proceedings, 9th Lunar Planet. Sci. Conf. pp. 1137–1156. [6] Noonan A. F. 1974. *Meteoritics* 9:233–242.

5014

EXCESS ^{40}Ar IN THE ZAGAMI SHERGOTTITE: DOES IT REVEAL CRYSTALLIZATION HISTORY?

Donald D. Bogard and Jisun Park. ARES code KR, NASA-JSC, Houston, TX 77058, USA.

The Zagami basaltic shergottite has fine- and coarse-grained (FG and CG) areas, which may reflect partial crystallization in a deep, slowly cooled magma chamber to form Mg-rich pyroxene cores, followed by entrainment of these crystals into a magma that rose and crystallized near the surface [1–3]. Late-stage melt pockets formed mesostasis and feldspar (maskelynite) having a range of compositions, but low water abundance [2]. Higher I_{Sr} in the FG portion may result from the second stage having incorporated old crustal rocks that failed to reach isotopic equilibrium [4, 5]. Zagami, like other shergottites, contains excess $^{40}Ar_{xs}$ beyond that expected from internal decay of ^{40}K during its Sm-Nd age of 177 Myr. We suggest that at least a portion of this $^{40}Ar_{xs}$ in Zagami and some other shergottites was inherited from the magma, much as is the case of MORBs on Earth. We made ^{39}Ar-^{40}Ar age determinations on feldspar and pyroxene separates from both the FG and CG portions of Zagami. If Zagami experienced an evolving fractional crystallization history, including possible crustal contamination of the magma, that might be indicated in differing amounts of $^{40}Ar_{xs}$ between mineral phases and between FG and CG portions.

Surprisingly, the concentration of $^{40}Ar_{xs}$ is similar for all Zagami FG and CG separates at ~10^{-6} cm^3/g (~2 ppb), in spite of differences between feld. and pyx. crystallization temperature and Ar diffusivity. $^{40}Ar_{xs}$ is not proportional to the K concentration, which argues against the $^{40}Ar_{xs}$ being residual from diffusion loss of ^{40}Ar formed by in situ K decay. These data indicate that neither the FG nor CG portions of Zagami are the major carrier of $^{40}Ar_{xs}$, but rather that $^{40}Ar_{xs}$ is present in similar amounts in all phases. If different Zagami textures originated from progressive fractionation at different time and depths in the magma [1, 2], the magmas must have contained similar ^{40}Ar concentrations. The concentration of $^{40}Ar_{xs}$ in Zagami falls within the broad range of ~10^{-8}–10^{-5} cm^3/g seen in terrestrial MORBs and deep oceanic samples. Because the mineral-melt distribution coefficient for Ar in basaltic material is ~10^{-3} [6], if Zagami formed by fractional crystallization from a melt, the melt would have contained ~10^{-3} cm^3/g of ^{40}Ar. As the solubility of Ar in magma is ~5 × 10^{-5} cm^3/g-bar, this would imply rather high partial Ar pressures (~20 bar). The initial estimated lithostatic pressure on Zagami and Shergotty magma is ~5–7 kbar [2, 7]. If such a melt fully crystallized to form Zagami, we might expect the last feldspathic phases to crystallize would contain much larger $^{40}Ar_{xs}$. Alternatively, if assimilation of crustal rocks contributed $^{40}Ar_{xs}$, this must have occurred prior to significant crystallization. Possibly Zagami fractional crystallization occurred as the magma ascended, releasing pressure so as to maintain nearly constant ^{40}Ar concentration in the magma before allowing most of the ^{40}Ar to ultimately escape. This was suggested by [7] for water loss from Shergotty. Whether rich in water or not, the source of $^{40}Ar_{xs}$ must have been relatively rich in K. If the magma, like bulk Zagami, had K = 0.1%, ~10^{-3} cm^3/g of ^{40}Ar would require >5 Gyr to accumulate, whereas 4 Gyr old crustal rock with K = 2% would accumulate ~10^{-3} cm^3/g of ^{40}Ar in <4 Gyr. Clearly the full implications of excess ^{40}Ar in Zagami for its petrogenesis deserve additional study.

References: [1] McCoy et al. 1992. *Geochimica et Cosmochimica Acta* 56:3571. [2] McCoy et al. 1999. *Geochimica et Cosmochimica Acta* 63:1249. [3] Lentz and McSween. 2000. *Meteoritics & Planetary Science* 35:919. [4] Nyquist. Planet. Chron. Workshop, LPI, May 2006. [5] Jones. 1989. Proceedings, 19th LPSC. p. 465. [6] Heber et al. 2007. *Geochimica et Cosmochimica Acta* 71:1041. [7] McSween et al. 2001. *Nature* 409:487.

5287

RAMAN SPECTROSCOPIC STUDY OF ORGANIC MATTER IN MATRIX LUMPS FROM THE CH/CB CHONDRITE ISHEYEVO

L. Bonal, G. R. Huss, and A. N. Krot. HIGP/SOEST, University of Hawai'i at Manoa, Honolulu, HI 96822, USA. E-mail:bonal@higp.hawaii.edu.

Introduction: The metal-rich CB and CH chondrites are characterized by the presence of the mineralogically primitive high-temperature components (Fe-Ni metal grains, chondrules, CAIs) co-existing with the heavily hydrated matrix lumps and by the large positive anomalies in δ^{15}N [1]. Although the carrier phase of ^{15}N is likely to be organic, its origin is unknown [2]. It has been recently suggested that some of the chondrules and metal grains in CH chondrites formed in a gas-melt plume produced during large scale asteroidal collision and that these components subsequently accreted together with the matrix clasts and nebular chondrules, metal grains and CAIs into the CH parent asteroid [3]. In this scenario, the matrix lumps experienced aqueous alteration on the pre-existing parent body(ies) that could be largely unsampled by known hydrated chondrite groups (CM, CI, CR). To understand the origin, thermal and alteration history of matrix lumps in the metal-rich carbonaceous chondrites, and identify a possible carrier of ^{15}N anomaly, we initiated detail mineralogical (SEM), chemical (EPMA), structural (Raman), and isotopic (SIMS) studies of matrix lumps in the CH/CB chondrite Isheyevo. Here we present preliminary results on in situ structural characterization of the organic matter (OM) in the matrix lumps from the metal-rich and metal-poor lithologies of Isheyevo.

Results and Discussion: We used a confocal Raman microscope (WITec) equipped with a Nd-YAG laser (λ_{exc} = 532 nm; P_{sample} = 400 μW) to measure 11 matrix lumps composed of magnetite, sulfides, carbonates, and phyllosilicates; 100 analyses per lump were acquired. All Raman spectra exhibit the *D* and *G* carbon bands, indicative of aromatic OM. Based on the structural ordering of the OM, two groups of matrix lumps can be recognized; both groups are found in both lithologies of Isheyevo. Eight lumps of group 1 have Raman spectra characterized by the presence of a significant fluorescence background. These spectra reveal poorly organized OM, similar to that in type 1 or 2 carbonaceous chondrites. A degree of structural ordering of the OM is rather homogeneous within each lump, with the exception of a few micron-size areas, where the OM is even less organized than the surrounding matrix. Three lumps of group 2 show no fluorescence background and their Raman spectra are comparable with those from OM of the slightly metamorphosed type 3 chondrites. These clasts have very homogeneous structural ordering of the OM. There are also some petrographic differences between the matrix lumps of group 1 and 2: the latter are characterized by the presence of metal associated with sulfides, whereas metal grains are absent in matrix lumps of group 1.

The observed differences in the degree of structural ordering of the OM, which is largely insensitive to aqueous alteration but highly sensitive to thermal metamorphism [4], suggest two groups of matrix lumps experienced different thermal history. All matrix lumps in Isheyevo experienced aqueous alteration before incorporation into their host meteorite parent body. The analysis of the structural ordering of the OM coupled to the mineralogy of the lumps will allow to determine if some of them also experienced thermal metamorphism, or if the difference between the both groups of clasts is due to shock metamorphism after incorporation.

References: [1] Krot et al. 2002. *Meteoritics & Planetary Science* 37: 1451. [2] Sugiura and Zashu. 2001. *Meteoritics & Planetary Science* 36:515. [3] Krot et al. 2005. *Nature* 436:989. [4] Bonal et al. 2007. *Geochimica et Cosmochimica Acta* 71:1605.

5245

CHEMICAL AND DYNAMICAL MODELING OF TERRESTRIAL PLANET FORMATION

J. C. Bond[1], D. S. Lauretta[1], and D. P. O'Brien[2]. [1]Lunar and Planetary Laboratory, The University of Arizona, Tucson, AZ, USA. E-mail: jbond@lpl.arizona.edu. [2]Planetary Science Institute, Tucson AZ, USA.

Introduction: The formation of the terrestrial planets is a long-standing question in the geological, planetary, and astronomical sciences. While is it well accepted that the terrestrial planets formed from material originally located within the solar nebula, numerical models have not yet been able to reproduce the dynamics of the terrestrial planets. Additionally, most chemical models focus on determining the origin of the Earth's water and the origin of the observed siderophile enrichment present in the Earth's mantle. To date, very little has been done on combining detailed chemical abundance and distribution models with specific planetary formation simulations. Here we present a theoretical model to explain the bulk compositions of the terrestrial planets and planetesimals in the solar system using n-body accretion simulations. The dynamical simulations of [1] were combined with a chemical model produced with the HSC Chemistry (v 5.1) software package and the disk model of [2] to produce expected bulk abundances of the simulated planetesimals.

Preliminary Results: Using our combined chemical-dynamical model, we have determined the composition of a 0.78 M_{Earth} planet located at 1.69 AU in our solar system. This planet should ideally have a composition analogous to Mars based on its size and orbital parameters. We determined that the final planet is predominantly composed of enstatite (26.9 wt%), iron (23.9 wt%), and forsterite (23.3 wt%) with minor amounts of feldspar, pyroxene, and iron sulfate. This basic description conceptually agrees with the general description of Mars as given in [3]—an enstatite-dominated planet with a basaltic crust (possibly composed of Mg-rich minerals), an olivine and pyroxene mantle, and an iron-rich core. For the main elements in the simulated planet, we obtain weight percent values of 27.7 wt% Fe, 15.1 wt% Si, 14.6 wt% Mg, and 1.3 wt% Al. With the exception of Si (which is within 2 wt%), these values are within 0.5 wt% of the average weight percents estimated for Mars by [3] and [4].

Discussion: The agreement between the bulk chemistry of the simulated planet and Mars implies that these dynamical models are producing simulated terrestrial planets that are similar to our own in terms of both orbital parameters and chemical composition. This will allow us to expand this work out to examine several chemical formation models such as the late veneer model.

References: [1] O'Brien D. P., Morbidelli A., and Levison H. F. 2006. *Icarus* 184:39–58. [2] Hersant F., Gautier D., and Huré J. 2001. *The Astrophysical Journal* 554:391–407. [3] Burbine T. H. and O'Brien K. M. 2004. *Meteoritics & Planetary Science* 39:667–681. [4] Lodders K. and Fegley B. 1997. *Icarus* 126:373–394.

5232

Rb-Sr AND Sm-Nd ISOTOPIC SYSTEMATICS OF NWA 032

L. Borg[1], A. Gaffney[1], and D. DePaolo[2]. [1]Lawrence Livermore National Laboratory, CA, USA. E-mail: borg5@llnl.gov. [2]University of California, Berkeley, CA, USA.

Introduction: The lunar meteorite NWA 032 is an unusual low-Ti mare basalt that is characterized by high incompatible element abundances, elevated LREE/HREE and Th/REE ratios, and a young Ar-Ar age of 2779 ± 14 Ma [1–2]. Fagan et al. [1] speculated that NWA 032 either 1) underwent an unusual, and unidentified, petrogenetic mechanism that fractionated Th from REE; or 2) was derived from a unique, possibly KREEP-like, source region that has not been identified in other lunar samples. We have completed Rb-Sr and Sm-Nd isotopic analyses on NWA 032 in order to unambiguously determine its crystallization age and to constrain the composition of its source region.

Analytical Procedures: NWA 032 contains 15–20% phenocrysts of olivine and pyroxene in an extremely fine groundmass consisting primarily of these phases and calcic plagioclase. The fine-grained nature of NWA 032 prohibited hand-picking the mineral fractions. Consequently, the sample was crushed and sieved at 44–75 μm and then run through a Frantz isodynamic separator. The magnetic fractions were washed in water, leached at ~25 °C in 2N HCl for 15 minutes, and finally leached in 4N HCl at ~65 °C for 30 minutes. The initial wash and 2N HCl leachate primarily removed terrestrial contamination, whereas the 4N HCl leachate primarily dissolved plagioclase, producing a greater spread in parent/daughter ratios on isochron plots. Sm-Nd and Rb-Sr were separated from the residues and leachates at LLNL, and analyzed with VG Sector 54 and Triton TI mass spectrometers at UCB. Preliminary results are presented here.

Results: Rb-Sr analyses yield a crystallization age of 2852 ± 65 Ma and initial Sr isotopic composition of 0.700337 ± 98, whereas Sm-Nd analyses yield an age of 2692 ± 160 Ma and an initial ε_{Nd} of +11.9 ± 1.4. Several fractions on both isochrons demonstrate evidence for terrestrial contamination. In addition, very limited variation in Sm/Nd ratios in the residue fractions result in large uncertainty on the Sm-Nd age. Nevertheless, these ages are concordant with the Ar-Ar age and indicate the Ar-Ar data have not been reset by a metamorphic event [2]. The initial Sr and Nd isotopic compositions indicate that NWA 032 was derived from a strongly incompatible-element-depleted source region. This feature is not consistent with its relatively high bulk rock incompatible-element abundances and elevated Th/REE and LREE/HREE ratios that are typically interpreted to imply that KREEP was involved in its petrogenesis (e.g., [3]). Instead, these data require a mechanism to produce incompatible-element-enriched magmas from incompatible-element-depleted sources without the addition of KREEP. This implies that there may be several mechanisms to impart KREEP-like geochemical signatures on lunar rocks. One possibility is that NWA 032 is produced by a much smaller degree of partial melting than other lunar samples. Alternatively, the source region of NWA 032 might have been enriched in incompatible elements by a metasomatic event near the time of eruption. This mechanism might also account for the unusually high Th/REE ratio of NWA 032. In any case, the apparent discordance between the incompatible-element-geochemistry of the bulk rock and the Sr-Nd isotopic systematics of its source region suggests that this sample has had a petrogenetic history that is different from other lunar basalts.

References: [1] Fagan et al. 2002. *Meteoritics & Planetary Science* 37: 371–394. [2] Fernandez et al. 2003. *Meteoritics & Planetary Science* 38: 555–564. [3] Neal and Taylor 1992. *Geochimica et Cosmochimica Acta* 56: 2177–2211.

5063

ACFER 094 PRESOLAR SILICATES CHARACTERIZED USING NANOSIMS AND AUGER NANOPROBE

M. Bose, C. Floss, and F. J. Stadermann. Laboratory for Space Sciences and Physics Department, Washington University, St. Louis, MO 63130, USA. E-mail: mbose@physics.wustl.edu.

Introduction: The discovery of presolar silicates in meteorites was initially achieved by NanoSIMS raster ion imaging of size-separated grains from the primitive meteorite Acfer 094 (e.g., [1]). Here we report further searches for presolar silicate and oxide grains in Acfer 094 using the NanoSIMS; we also report elemental compositions acquired with the Auger Nanoprobe (e.g., [2]) in order to better understand grain formation in stellar environments.

Experimental: Presolar grains are identified by NanoSIMS C and O isotopic imaging of grain size separates. They are subsequently characterized in the Auger Nanoprobe by elemental mapping and spot measurements to determine their elemental compositions. We are currently developing analytical routines and calibrating powdered standards (e.g., olivine and pyroxene), which will allow us to quantitatively determine the compositions of these presolar grains.

Results and Discussion: Our current round of NanoSIMS analyses led to the identification of 14 presolar silicate/oxide grains. Ten grains have enrichments in ^{17}O and are normal in their $^{18}O/^{16}O$ indicating an origin from a low-mass red giant or asymptotic giant branch star [3]. The other 4 grains show enrichments in ^{18}O and are consistent with a group 4 classification. Elemental characterization shows that 8 grains are silicate grains, 3 are Al-rich oxide grains, and 1 is an exceptionally Fe-rich oxide grain [4]. Based on preliminary calibrations of the standards, 2 silicate grains have pyroxene-like compositions (e.g., Mg + Fe + Ca/Si ratios close to 1) with one of these containing a small amount of Ca. The other silicates appear to have nonstoichiometric compositions. Two silicate grains are Mg-rich, 4 are Fe-rich, and 2 have similar Fe and Mg contents. Condensation under nonequilibrium conditions produces substantially higher Fe contents in silicate grains than equilibrium condensation [5]. Thus, the high abundance of Fe in many of our grains suggests that they may have formed under nonequilibrium conditions (e.g., [6]), although we cannot rule out parent body alteration.

We also identified 4 grains with carbon anomalies; $^{12}C/^{13}C$ ratios range from 18 to 48, similar to the compositions of mainstream SiC grains [7]. Although accurate abundances are difficult to determine on grain size separates, a relative comparison of the abundances of silicates/oxides with those determined by [1] suggests an abundance of presolar carbonaceous phases of ~85 ppm. This is significantly higher than the estimated abundances of SiC and graphite in primitive meteorites and, if corroborated, may require substantial revision of presolar grain abundance estimates.

Acknowledgements: We thank A. Nguyen for preparation of the Acfer 094 silicate grain separates.

References: [1] Nguyen A. N. et al. 2007. *The Astrophysical Journal* 656:1223–1240. [2] Stadermann F. J. et al. 2006. Abstract #1663. 37th Lunar and Planet. Sci. Conf. [3] Nittler L. et al. 1997. *The Astrophysical Journal* 483:475–495. [4] Stadermann F. J. et al. 2007. This issue. [5] Ferrarotti A. S. and Gail H.-P. 2001. *Astronomy & Astrophysics* 371:133–151. [6] Floss C. et al. 2005. *Meteoritics & Planetary Science* 40:A49. [7] Zinner E. 2004. In Treatise on Geochemistry, vol. 1, edited by Davis A. M. pp. 17–39.

5011

TRIGGERING PRESOLAR CLOUD COLLAPSE AND INJECTION OF SHORT-LIVED RADIOISOTOPES BY A SUPERNOVA SHOCK WAVE

A. P. Boss[1], S. I. Ipatov[1], and E. A. Myhill[1, 2]. [1]DTM, Carnegie Institution of Washington, 5241 Broad Branch Road NW, Washington, D.C. 20015–1305, USA. E-mail: boss@dtm.ciw.edu. [2]Marymount University, Arlington, Virginia, USA.

The short-lived radioisotope (SLRI) ^{60}Fe must have been synthesized in a supernova [1, 2] and then either injected into the presolar cloud [3, 4] or onto the surface of the solar nebula [5]. A similar nucleosynthetic event is likely to be the source of the bulk of the solar nebula's ^{26}Al [6, 7] and of other SLRIs. Here we reconsider the problem of triggering the collapse of the presolar cloud and of simultaneously injecting SLRI with a supernova shock wave. Previous work on this problem [3, 4, 8–10] used either fixed grid or smoothed particle hydrodynamics (SPH) codes with a limited ability to resolve fine-scale structure in the Rayleigh-Taylor fingers that form at the shock/cloud interface and are responsible for SLRI injection into the collapsing presolar cloud [9]. Here we study the same problem with an adaptive mesh refinement hydrodynamics code, FLASH, which provides a superior ability to resolve small-scale structures. We have verified the accuracy of FLASH on three test cases relevant to the problem of triggering cloud collapse, namely the Sod shock tube problem, the collapse of a pressureless sphere, and the long-term stability of the target cloud. We have reproduced the main results of [8, 9] in 2-D cylindrical coordinates with isothermal thermodynamics and a range of shock speeds (2–40 km/s), finding that shocks with speeds in the range of 5–30 km/s are able to both trigger collapse and inject shock wave material. We are extending these isothermal runs to 3-D Cartesian coordinates to learn what happens in a fully 3-D cloud. We then intend to study nonisothermal shocks. [10] found that when nonisothermal shocks were employed in SPH calculations, it was not possible for a shock wave to simultaneously trigger collapse and inject SLRIs, a potentially fatal flaw for the triggering and injection scenario. However, [11] found that improvements in the dust grain cooling model led to rapid postshock cooling, closer to the isothermal assumptions used in [3, 4, 8, 9]. Our ultimate goal is to use FLASH to determine if the triggering and injection scenario [12] is consistent with post-shock cooling processes. The software used in this work was in part developed by the DOE-supported ASCI/Alliances Center for Astrophysical Thermonuclear Flashes at the University of Chicago.

References: [1] Mostefaoui S., Lugmair G., and Hoppe P. 2005. *The Astrophysical Journal* 625:271. [2] Tachibana S. et al. 2006. *The Astrophysical Journal* 639:L87. [3] Vanhala H. A. T. and Boss A. P. 2000. *The Astrophysical Journal* 538:911. [4] Vanhala H. A. T. and Boss A. P. 2002. *The Astrophysical Journal* 575:1144. [5] Ouellette N., Desch S. J., and Hester J. J. *The Astrophysical Journal*. Forthcoming. [6] Limongi M. and Chieffi A. 2006. *The Astrophysical Journal* 647:483. [7] Sahijpal S. and Soni P. 2006. *Meteoritics & Planetary Science* 41:953. [8] Foster P. N. and Boss A. P. 1996. *The Astrophysical Journal* 468:784. [9] Foster P. N. and Boss A. P. 1997. *The Astrophysical Journal* 489:346. [10] Vanhala H. A. T. and Cameron A. G. W. 1998. *The Astrophysical Journal* 508:291. [11] Vanhala H. A. T. and Boss A. P. 1999. Abstract #1433. 30th Lunar and Planetary Science Conference. [12] Boss A. P. 1995. *The Astrophysical Journal* 439:224.

5268

RESOLVING Lu-Hf IN CHONDRITES AND THE BULK EARTH COMPOSITION

A. Bouvier[1], J. D. Vervoort[2], and P. J. Patchett[1]. [1]The University of Arizona, Tucson, USA. E-mail: abouvier@email.arizona.edu. [2]Washington State University, Pullman, USA.

Introduction: Interpretation of Hf isotope data for planetary material evolution is highly dependent on the ^{176}Lu-^{176}Hf system parameters employed. Beyond the ^{176}Lu decay constant discrepancy (e.g., [1]), Lu-Hf chondritic uniform reservoir (CHUR) and bulk silicate earth (BSE) compositions need to be clarified. The Lu-Hf CHUR determination is hampered by a variation in Lu/Hf of ~20% (2σ SD) among the ordinary (OC) and carbonaceous chondrites (CC) analyzed previously [2–4]. This contrasts with Sm/Nd which varies by only ~3% [5, 6] and has prevented an unambiguous choice for the Lu-Hf BSE composition from the chondrite data. The BSE value should correspond to CHUR as both Lu-Hf and Sm-Nd isotopic systems involve refractory and lithophile elements.

Results: We analyzed twenty new chondrites for Lu-Hf and Sm-Nd isotope systematics. While most OC used in previous studies were petrologic types 4 to 6 [2–4], we investigated thirteen of the least-metamorphosed H, LL, and L chondrites available (types 3.0 to 3.8) which limits the growth of phosphate (main carrier of REE). We also analyzed seven CC of types 1 to 3 from the CI, CV, CO, and CK groups. Including four CC data previously analyzed [4], we obtained mean values of ^{176}Lu/^{177}Hf = 0.0337 ± 3 and ^{176}Hf/^{177}Hf = 0.282802 ± 23 (2σ SE, n = 22), which we consider to be our best estimate of CHUR. These two values are respectively higher by 0.0005 and 0.000030 (~1 epsilon unit) than the values currently in use [2] which were determined from twenty-one OC and two CC data. For the Sm-Nd system, the values for these same chondrites yield ^{147}Sm/^{144}Nd = 0.1961 ± 6 and ^{143}Nd/^{144}Nd = 0.512629 ± 16, within the lower limits of [5, 6].

Discussion: The ^{176}Lu/^{177}Hf range obtained from all the types 1 to 3 CC and OC is now constrained to ~4%, which is similar to Sm/Nd. Our new Lu-Hf CHUR estimate places the chondrite composition within the Hf-Nd isotope correlation of the Earth's mantle and continental crust [7]. It consequently involves a chondritic evolution of the BSE and removes the need for a hidden reservoir to explain the Lu-Hf systematics. The ~20% range of Lu/Hf, mostly due to the equilibrated OC, must reflect partly the sample heterogenities and also the open behavior of the Lu-Hf system during thermal metamorphism of the chondrite parent bodies. Both are related to the heterogeneous phosphate growth effects as these minerals are characterized by extremely fractionated ^{176}Lu/^{177}Hf of 0.3–100 [8] and only slightly lower ^{147}Sm/^{144}Nd of 0.18–0.19 [6] compared to the respective whole-rock isotopic ratio.

References: [1] Albarède F. et al. 2006. *Geochimica et Cosmochimica Acta* 70:1261–1270. [2] Blichert-Toft J. and Albarède F. 1997. *Earth and Planetary Science Letters* 148:243–258. [3] Bizzarro M. et al. 2003. *Nature* 421:931–933. [4] Patchett P. J. et al. 2004. *Earth and Planetary Science Letters* 222:29–41. [5] Jacobsen S. B. and Wasserburg G. J. 1980. *Earth and Planetary Science Letters* 50:139–155. [6] Amelin Y. and Rotenberg E. 2004. *Earth and Planetary Science Letters* 223:267–282. [7] Vervoort J. D. et al. 1999. *Earth and Planetary Science Letters* 168:79–99. [8] Amelin Y. 2005. *Science* 310:839–841.

5233

ON THE OCCURRENCE OF A DIOPSIDE-RICH CAI IN THE CV3 CHONDRITE NORTHWEST AFRICA 4669

F. Brandstätter. Naturhistorisches Museum, Burgring 7, A-1010, Vienna, Austria. E-mail: franz.brandstaetter@nhm-wien.ac.at.

Introduction: In general, diopside is not an especially abundant phase in CAIs in CV chondrites where it most commonly occurs within the Wark-Lovering rim sequences on inclusions [1]. However, aluminous diopside has been mainly described from fine-grained, spinel-rich inclusions from the oxidized CV chondrites Allende, Kaba, and Mokoia (e.g., [2–4]), and from the reduced CVs Efremovka and Leoville (e.g., [5]).

Here I report on the mineralogy of an unusual CAI from the recently described CV3 chondrite NWA 4669. A detailed study by analytical SEM and EMPA revealed that the entire inclusion consists mainly of Al-diopside and (Mg, Al)-spinel.

Results: The inclusion is an irregularly shaped fine-grained aggregate that stretches out over 4 mm with expanses of intervening matrix of the host meteorite. The overall texture can be described as consisting of multiple, closely packed micro-aggregates (< 50 to >100 μm in size), each of which contains spinal "cores" surrounded by a thick layer of Al-diopside (comprising >50 vol%). The spinels typically are surrounded by an in places >10 μm wide zone exhibiting a mottled appearance in backscattered electron images. This zone, which occurs throughout the whole inclusion, is interpreted as chemical reaction zone at the contact between spinel and diopside.

Compositionally, the spinels are close to pure $MgAl_2O_4$ with contents of 0.1–0.3 wt% TiO_2, 0.4–0.8 wt% FeO, 0.4–0.7 wt% Cr_2O_3, and 0.1–0.3 wt% V_2O_3. Al-diopsides commonly have Al_2O_3 contents that range from ~2–5 wt%, a few analyses gave contents up to ~9–10 wt%. TiO_2 contents of Al-diopside are low (0.1–0.5 wt%) as are the contents of other minor elements with 0.2–0.6 wt% FeO, <0.1 wt% Cr_2O_3, <0.1 wt% MnO, <0.1 wt% V_2O_3. The reaction zone around the spinel nodules is a heterogeneous mixture of a fine-grained intergrowth with individual grain sizes below the analytical resolution of the electron microprobe. Therefore, EMP analyses show some compositional variation in the range of 29–32 wt% SiO_2, 33–36 wt% Al_2O_3, 14–16 wt% CaO, 0.4–0.8 wt% FeO, and 0.1–0.3 wt% TiO_2.

Conclusions: The fine-grained and irregularly shaped inclusion exhibits a nonigneous texture. Therefore, it is very likely that it formed from minerals that condensed in the solar nebula. The modal composition (mainly Al-diopside + spinel), the absence of other major phases, and the presence of an apparent reaction zone between spinel and diopside suggest that the inclusion was altered by a gas-solid reaction in the final stage of its formation. The (Mg,Al)-spinel appears to be a relict from a precursor mineral association whereas the abundant Al-diopside was formed by the final gas-solid nebular reaction.

References: [1] Brearley A. J. and Jones R. H. 1998. In *Planetary materials*, edited by Papike J. J. Rev. Mineral. #36. pp. 3-1–3-398. [2] McGuire A. V. and Hashimoto A. 1989. *Geochimica et Cosmochimica Acta* 53:1123–1133. [3] Fegley B., Jr. and Post J. E. 1985. *Earth and Planetary Science Letters* 75:297–310. [4] Cohen R. E. et al. 1983. *Geochimica et Cosmochimica Acta* 47:1739–1757. [5] Krot A. N. et al. 2004. *Meteoritics & Planetary Science* 39:1517–1553.

5239

DISTRIBUTION OF TRACE ELEMENTS IN SULFIDE AND METAL IN REDUCED AND OXIDIZED CV3 CARBONACEOUS CHONDRITES DETERMINED BY EPMA AND SXRF

Adrian J. Brearley. Department of Earth and Planetary Sciences, University of New Mexico, Albuquerque, NM 87131, USA. E-mail: brearley@unm.edu.

Introduction: Sulfide minerals are a common and ubiquitous phase in all chondrite groups, but almost nothing is known about the trace element compositions of these phases. The sulfides are of special importance for understanding the behavior of a number of moderately volatile elements that have chalcophile affinities and may be sensitive to thermal processing either in the nebular or on asteroidal parent bodies. We have commenced a study to gain new insights into the trace element chemistry of sulfides and metal phases in the CV carbonaceous chondrites at the microscale using electron microprobe and SXRF analyses.

We have analyzed trace elements in sulfides and metals in a range of different textural occurrences in the CV3 chondrites Leoville, Vigarano, and Allende. Our goal is understand how sulfides and metals in the reduced and oxidized CV chondrites differ and what these differences may tell us about the cosmochemical evolution of the two subgroups. Initial analyses were carried out by electron microprobe and selected grains were analyzed by SXRF microprobe at Brookhaven National Laboratory. Here we report SXRF data for Cr, Co, Ni, Cu, Zn, As, Ge, Se, and Ga. As expected, siderophile elements such as Co, Ni, and Ge are preferentially incorporated into metal, but the behavior of other elements is quite variable. In all three chondrites, troilites contain <5 ppm As, but can contain elevated Se abundances ranging from 5–100 ppm. Troilite in Vigarano and Leoville have quite similar concentrations, between 50–100 ppm, but Allende is different. Se is preferentially partitioned into pentlandite (60–120 ppm), whereas troilite contains <30 ppm. Surprisingly, As is incorporated preferentially into the metal phase in Leoville and Vigarano. Essentially all the metal grains in these meteorites have higher concentrations of As than the sulfides (5–50 ppm), but Se concentrations <5 ppm. Zn concentrations in troilite are very similar in all three meteorites, ranging from 2–30 ppm, and metal contains similar concentrations of Zn. The Zn data for Allende pentlandites indicate that Zn is quite heterogeneously distributed and has evidently not fully equilibrated during metamorphism.

The different metal and sulfide phases in the three meteorites are clearly differentiated in a plot of Co versus Se. In Allende, troilite and pentlandite plot in two distinct groups that lie along a positive correlation line with elevated Co and Se in the pentlandite. Vigarano and Leoville troilite plot in a distinct field and two distinct groups of metal grains (high Co, low As) and low Co, high As are well defined. High Se contents occur in metal nodules in the matrix in Vigarano and are distinct from chondrule metal.

Discussion: These data show that the behavior of the moderately volatile elements is quite different in the reduced and oxidized CV chondrites. The volatile trace elements clearly underwent extensive redistribution during oxidation and sulfidization. In particular, Cu, Zn, and Se, which are present in low concentrations in metal and troilite in the reduced CVs, are concentrated in pentlandite in Allende. Zn is also probably hosted by magnetite in Allende. In addition, Co released by oxidation of kamacite is partially incorporated into pentlandite, in addition to Ni-rich taenite. Although our data are limited, it appears that the spread in trace element concentrations in troilite in Leoville and Vigarano is quite small. It seems probable that this is due to metamorphic equilibration, rather than a reflection of primary processes.

5148

COORDINATED MINERALOGICAL AUTOPSY OF A FRAGMENT-RICH COMET PARTICLE COLLECTED BY STARDUST

D. E. Brownlee[1], D. Joswiak[1], G. Matrajt[1], Z. Gainsforth[2], A. Butterworth[3], A. S. Fakra[3], M. A. Marcus[3], C. Snead[2], and A. J. Westphal[2]. [1]Department of Astronomy, University of Washington, Seattle, WA 98195, USA. E-mail: brownlee@astro.washington.edu. [2]Space Sciences Laboratory, University of California at Berkeley, Berkeley, CA 94720, USA. [3]Advanced Light Source, Lawrence Berkeley National Laboratory, Berkeley, CA 94720–8225, USA.

Introduction: Some of the comet samples collected by Stardust separated into 1–25 μm solid fragments that came to rest either at the ends of multirooted tracks or along track walls. Other than erosional rounding, and formation of submicron crusts of melted aerogel, these relatively "coarse" fragments are usually captured in excellent condition. Fragmentation was presumably initiated by the ~0.2 GPa ram pressure from 6 km/s impact into aerogel. A comet particle that produces a fragment-rich track could have either been a) similar to common IDPs and composed of an aggregate of unrelated fine and coarse components, or b) an entity like a chondrule, AOA, or CAI where the individual components have a stronger genetic association.

Of the limited studies of the richly fragmented tracks that we have examined, most or all fragments >1 μm appear to be mineralogically related within a given track. To better understand these tracks we are doing a very detailed study of all of the large fragments of T77, a track that contains more than 22 fragments >3 μm. In a collaborative effort, the components of this track have been studied by a coordinated program of synchrotron XRF, XANES, and XRD, and by electron microscopy.

Methods: The track was cut out in a keystone [1], mapped by XRF, and many of the major fragments were analyzed by combinations of Fe, Ca, or Ca XANES. The keystone was then compressed and impregnated to form a 100 μm thick acrylic sheet and individual 2–10 μm fragments were cut from the sheet and microtomed to produce thin sections and potted butts for TEM and SEM studies. The synchrotron and TEM data are being correlated for each fragment but this paper concentrates on mineralogical results from TEM studies.

Results: The TEM studies suggest that all fragments of T77 are related to each and that the original particle was not a random aggregate of random components. As is common with particles from comet Wild-2, the original impactor was a remarkable collection of minerals. For the six large fragments studied so far, all contained olivine and it is clear that Fe-rich olivine was the dominant phase in the impactor. Olivine occurs in two composition populations; most are in the $Fo_{52–67}$ range and a second population exists at Fo_{99}. Two fragments contained kamacite with associated schreibersite, two contained a Ca rich pyroxene with moderate Cr and Na, one contained an Na,Al-bearing glass, two contained Al-rich chromite, and two contained sulfides.

Conclusions: The fragments of Track 77 indicate that impacting particle was not a random aggregate. Its mineral inventory is quite different from materials commonly seen in IDPs and possible relationships to chondrite components such as type II chondrules are being evaluated as more of the fragments are investigated.

References: [1] Westphal A. J. et al. 2004. *Meteoritics & Planetary Science* 39:1375–1386.

5265

FORSTERITE-BEARING TYPE B CAIs: BULK COMPOSITION EVIDENCE FOR A HYBRID ORIGIN

E. S. Bullock[1], G. J. MacPherson[1], and A. N. Krot[2]. [1]Department of Mineral Sciences, Smithsonian Institution, Washington, D.C. 20560, USA. [2]Hawai'i Institute of Geophysics and Planetology, University of Hawai'i at Manoa, Honolulu, HI 96822, USA.

Introduction: Forsterite-bearing type B refractory inclusions (FoBs) are unusual because a disproportionate fraction of the known examples possess mass-dependent isotopic fractionation in magnesium, silicon, and oxygen [1–3] that correlates with petrological evidence for melt distillation. All have textures broadly consistent with solidification of a silicate melt, but their outer aluminium-rich mantles have mineral assemblages that are petrologically incompatible with their interiors [2–4]. Many have an extreme patchiness of mineral distribution ("islands") that cannot be explained by melt solidification alone. We previously [4] interpreted these textures as evidence that melt evaporation and hybridization both played a role in the formation of these objects. Here we give new bulk compositional data that relate directly to the nature of the hybridization process.

Analytical Techniques: We made full-spectrum elemental maps of polished thin sections of five each of FoBs: Vigarano USNM 3137-2 [5], Allende "ALVIN" and TS-35F1 [6, 7], and Efremovka E60 [8] and E64. The maps were collected using the FEI NanoSEM field emission scanning electron microscope at the Smithsonian, which is equipped with a THERMO-NORAN energy dispersive (EDS) X-ray analytical system. Each CAI was mapped as a multiframe mosaic, with a spatial resolution sufficient to resolve features >5 μm in these approximately centimeter-size objects. This technique differs from conventional X-ray mapping in that a complete spectrum is collected for each pixel, background subtracted, and quantified using a conventional EDS algorithm. The CAIs were quantified independent of the enclosing matrix.

Results: The bulk compositions of the FoBs are distinct from those of Al-rich chondrules and from those of any other known CAIs, and are broadly intermediate between type B CAIs and Al-rich chondrules. Unlike chondrules and other CAIs, the data do not define smooth trends, and scatter far more than can be explained by analytical uncertainty. Analyses of olivine-free, spinel-rich islands within several FoBs give compositions that extend in the direction of type B CAIs.

Discussion: Although the magnesium-poor mantles are clearly the result of melt distillation, the spinel-rich islands are not. The observations that the FoB bulk compositions are intermediate between Al-rich or ferromagnesian chondrules and type B CAIs, and that the spinel-rich islands are closer in composition to type B CAIs than are the FoBs themselves, are consistent with the interpretation that FoBs are hybrids of type B CAI and olivine-rich material that melted and incompletely homogenized prior to final solidification.

References: [1] Wark D. A. 1987. *Geochimica et Cosmochimica Acta* 51:607. [2] Clayton R. N. et al. 1984. *Geochimica et Cosmochimica Acta* 48: 535. [3] Davis A. M. et al. 1991. *Geochimica et Cosmochimica Acta* 55:621. [4] MacPherson G. J. et al. 2005. *Meteoritics & Planetary Science* 40:A94. [5] MacPherson G. J. and Davis A. M. 1992. *Meteoritics* 27:253. [6] Clayton R. N. et al. 1977. *Earth and Planetary Science Letters* 34:209–224. [7] MacPherson G. J. et al. 1985. *Geochimica et Cosmochimica Acta* 49: 2267– 2279. [8] Krot A. N. et al. 2000. *Meteoritics & Planetary Science* 35: A93.

5132

PETROLOGY AND BULK COMPOSITION OF CH3 CHONDRITE NORTHWEST AFRICA 2210

T. E. Bunch[1], A. J. Irving[2], J. H. Wittke[1], S. M Kuehner[2], M. Gellissen[3], H. Palme[3], D. Rumble III[4], and D. A. Gregory. [1]Department of Geology. Northern Arizona University, Flagstaff, AZ, USA. E-mail: tbear1@cableone.net. [2]Earth and Space Sciences, University of Washington, Seattle, WA, USA. [3]Inst. Geologie/Mineralogie, Univ. Köln, Germany. [4]Geophysical Laboratory, Washington, D.C., USA.

Petrology: This relatively fine-grained and fresh (W1/2) black magnetic stone (74 grams) is composed mainly of rounded glass spheres and chondrules (together with broken fragments of the same) and metal (~15 vol%) in a sparse matrix (see Fig. 1a). Chondrules contain zoned, euhedral olivine ($Fa_{1–50}$) and/or orthopyroxene ($Fs_{1–50}$) in a matrix of glass. Some cryptocrystalline chondrule fragments are composed of "eutectoid" intergrowths of low-Ca and high-Ca enstatite, and homogeneous glass spheres have various compositions intermediate between almost pure forsterite and enstatite. Other phases include Cr-Al-rich diopside, troilite, feldspathic glass, Al-rich chromite, and a large grain of opx ($Fs_{6.5}Wo_{1.5}$) with exsolved aluminous cpx ($Fs_{14}Wo_{33}$, 18.5 wt% Al_2O_3; see Fig. 1b). No CAIs were found, and this specimen evidently differs from and is not paired with NWA 470, NWA 739, or NWA 770 [1, 2].

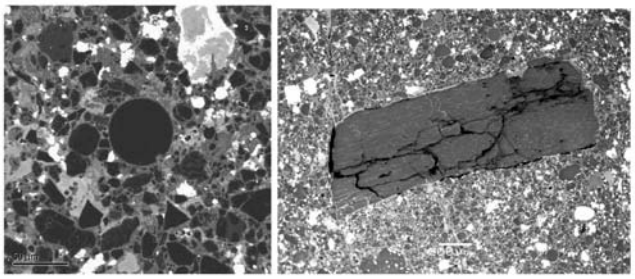

Fig. 1. BSE images. a) Complete and broken glassy spheres (~Fa_1Fs_1; blue) and altered metal (white, orange). b) Large 1.6 mm long opx grain with Al-rich cpx exsolution lamellae.

Oxygen Isotopes: Analyses of acid-washed, metal-free material by laser fluorination gave $\delta^{17}O$ = 1.07, 1.05; $\delta^{18}O$ = 3.95, 4.11; $\Delta^{17}O$ = –1.008, –1.112 per mil. These values are like those for other CH chondrites, except NWA 739 [1, 3].

Bulk Composition: X-ray fluorescence analyses gave in wt%: Mg 10.2, Si 12.1, Al 0.86, Ca 0.88, Ti 0.058, Fe 36.1, Cr 0.31, Mn 0.10, P 0.12, V 57 ppm. These abundances are similar to those found for other CH chondrites [4], except for somewhat lower refractory element contents.

References: [1] Ivanova M. et al. 2001. Abstract #1817. 32nd LPSC; Lawrence S. et al. 2004. Abstract #1451. 35th LPSC; Krot A. et al. 2004. Abstract #1394. 35th LPSC; Jones R. et al. 2005. Abstract #1813. 35th LPSC. [2] The Meteoritical Bulletin, Nos. 85, 86. [3] Clayton R. and Mayeda T. 1999. *Geochimica et Cosmochimica Acta* 63:2089–2104. [4] Lodders K. and Fegley B. 1998. *The planetary scientist's companion*. Oxford U. Press.

5133

DISTINCTIVE MAGNESIAN, PROTOGRANULAR, AND POLYMICT DIOGENITES FROM NORTHWEST AFRICA, OMAN, AND UNITED ARAB EMIRATES

T. E. Bunch[1], A. J. Irving[2], J. H. Wittke[1], S. M. Kuehner[2], and D. Rumble III[3]. [1]Department of Geology, Northern Arizona University, Flagstaff, AZ, USA. E-mail: tbear1@cableone.net. [2]Department of Earth and Space Sciences, University of Washington, Seattle, WA, USA. [3]Geophysical Laboratory, Washington, D.C., USA.

Our studies of diogenites collected recently from hot deserts (24 from Northwest Africa, 2 from Oman, and 3 from UAE) have revealed new compositional and textural types not previously represented in collections, which have important implications for magmatic and impact-mixing processes on 4 Vesta. The majority of the specimens resemble classic falls and finds in that they are crushed or cataclastic monomict orthopyroxenites composed predominantly of orthopyroxene ($Fs_{22–31}Wo_{1.3–3.6}$, FeO/MnO = 25–35) with accessory chromite, troilite, and Ni-poor metal. Several examples contain minor olivine ($Fa_{25–39}$), calcic plagioclase ($An_{78–96}$), and/or clinopyroxene; NWA 3329 contains minor silica and merrillite. NWA 1461 (composed mostly of $Fs_{13.6}Wo_{0.8}$ orthopyroxene) is the most magnesian diogenite known, and attests to the existence of some very primitive Vestan parent magmas (as also inferred from dunite NWA 2968 [1]). NWA 1821 and AP 004 have distinctive protogranular textures, similar to that of GRO 95555 [2]. "Necklace" textures of various phases within chromite (as reported [3] in NWA 4215) occur in NWA 2997, AP 003, and unique vesicular diogenite Dhofar 700. NWA 4473 is a polymict breccia with clasts from at least three different diogenite precursors (mean opx compositions: $Fs_{17.2}Wo_{1.0}$, $Fs_{21.6}Wo_{2.1}$, and $Fs_{37.2}Wo_{3.5}$, FeO/MnO = 29.3–34.4).

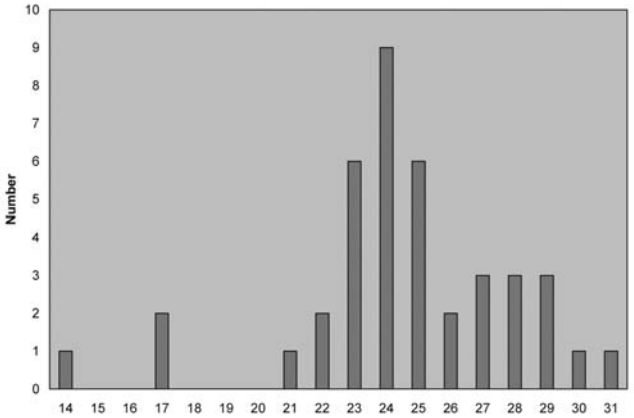

Fig. 1. Fs values in orthopyroxene for 40 diogenites (this work, [2–4]).

Oxygen Isotopes: Results of laser fluorination analyses on acid-washed samples. NWA 1461: $\delta^{17}O = 1.410, 1.634$; $\delta^{18}O = 3.177, 3.584$; $\Delta^{17}O = -0.261, -0.251$ per mil. NWA 1821: $\delta^{17}O = 1.43$; $\delta^{18}O = 3.23$; $\Delta^{17}O = -0.269$ per mil.

References: [1] Bunch T. et al. 2006. Abstract #5252. *Meteoritics & Planetary Science* 41:A31. [2] Papike J. et al. 2000. Abstract #1009. 31st LPSC. [3] Barrat J. A. et al. 2006. *Meteoritics & Planetary Science* 41:1045–1057. [4] Fowler G. 1994. *Geochimica et Cosmochimica Acta* 58:3921–3929; The Meteoritical Bulletin, Nos. 87–91.

5189

^{182}Hf-^{182}W CHRONOMETRY OF CAIs AND THE AGE OF THE SOLAR SYSTEM

C. Burkhardt[1, 2], T. Kleine[1], H. Palme[2], B. Bourdon[1], J. Zipfel[3], J. Friedrich[4], and D. Ebel[5]. [1]Institute for Isotope Geology and Mineral Resources, ETH Zürich, Switzerland. E-mail: burkhardt@erdw.ethz.ch. [2]Inst. Geol. Min., Univ. Cologne, Germany. [3]Forschungsinst. Senckenberg, Frankfurt, Germany. [4]Chem. Department, Fordham University, NY, USA. [5]Am. Mus. Nat. Hist., NY, USA.

Determining the initial $^{182}Hf/^{180}Hf$ and $^{182}W/^{184}W$ of the solar system is essential for establishing a precise Hf-W chronology for the accretion and differentiation of asteroids. Ca-Al-rich inclusions (CAIs) are the first solid objects that formed in the cooling solar nebula and as such are ideally suited for determining the initial Hf-W systematics of the solar system. Combined with Hf-W data and precise Pb-Pb ages of angrites, the Hf-W systematics of CAIs can also be used to determine the age of the solar system. This is important because age estimates for the formation of the solar system range from ~4567 [1] to ~4570 Ma [2]. Here we report new Hf-W data for four bulk CAIs and mineral separates from two CAIs from the Allende CV3 chondrite.

CAIs were separated from Allende slices using steel-free tools, then cleaned with abrasive paper and in an ultrasonic bath. Fassasite- and melilite-rich separates were obtained using heavy liquids and hand-picking. Samples were dissolved and processed using anion exchange chromatography as described in [3]. Measurements were performed using the Nu Plasma MC-ICP-MS at ETH Zürich.

All bulk CAIs have Hf/W and $^{182}W/^{184}W$ slightly higher than average carbonaceous chondrites [4], but the limited spread in Hf/W precludes determining a precise Hf/W isochron for bulk CAIs. In contrast, fassaites exhibit high Hf/W and radiogenic $^{182}W/^{184}W$, whereas melilites have low Hf/W and $^{182}W/^{184}W$. This permits determination of precise internal isochrons. Our new data combined with earlier reported data define an isochron (MSWD = 0.65) with initial $^{182}Hf/^{180}Hf = (1.01 \pm 0.05) \times 10^{-4}$ and initial $\varepsilon_W = -3.32 \pm 0.14$ (ε_W is the deviation of $^{182}W/^{184}W$ from the terrestrial value in parts per 10^4). All uncertainties are 2σ. These new values are identical to but a factor of ~2 more precise than an earlier estimate [4].

Relative to the angrite D'Orbigny with an initial $^{182}Hf/^{180}Hf = (7.4 \pm 0.2) \times 10^{-5}$ [5] and a Pb-Pb age of 4564.48 ± 0.24 Ma [6], the initial $^{182}Hf/^{180}Hf$ for CAIs reported here corresponds to an absolute age of 4568.5 ± 0.8 Ma. A similar result of 4568.8 ± 1.0 Ma is obtained relative to the angrite Sahara 99555. The absolute age of 4568.5 ± 0.8 Ma is our best estimate for the age of the solar system and agrees with Pb-Pb ages reported for CAIs [1, 7], indicating that the Hf-W isochron for CAIs dates their formation but not a later event.

The initial ε_W of CAIs is indistinguishable from values for iron meteorites with $^{182}W/^{184}W$ unaffected by cosmic rays. This indicates that accretion, melting, and core formation in the parent bodies of magmatic iron meteorites occurred in less than ~0.5 Myr after formation of CAIs.

References: [1] Amelin Y. et al. 2002. *Science* 297:1678–1683. [2] Baker J. et al. 2005. *Nature* 436:1127–1131. [3] Kleine T. et al. 2004. *Geochimica et Cosmochimica Acta* 68:2935–2946. [4] Kleine T. et al. 2005. *Geochimica et Cosmochimica Acta* 69:5805–5818. [5] Markowski A. et al. *Earth and Planetary Science Letters*. Forthcoming. [6] Amelin Y. 2007. Abstract #1669. 38th LPSC. [7] Bouvier A. et al. 2007. *Geochimica et Cosmochimica Acta* 71:1583–1604.

5070

CHONDRULE THERMOMETRY FROM NUEVO MERCURIO H5 ORDINARY CHONDRITE

K. Cervantes-de la Cruz[1, 4], F. Ortega-Gutiérrez[2, 4], M. Reyes-Salas[2, 4], and C. Linares-López[3, 4]. [1]Posgrado en Ciencias de la Tierra. E-mail: kecervan@hotmail.com. [2]Instituto de Geología. [3]Instituto de Geofísica. [4]Universidad Nacional Autónoma de México.

Introduction: We studied chondrule mineral chemistry of Nuevo Mercurio H5 (S1) ordinary chondrite in order to understand its thermal history. Chondrules were melted at high temperatures and later subjected to thermal metamorphism in parental bodies (e.g., [1]).

Analytical Procedures: We selected pyroxene-rich chondrules of different textural groups showing diopsidic rims and exsolution textures (RP, C, and PP). We obtained 187 WDS microprobe chemical analyses. To calculate the temperature, we used the QUILF program for two-pyroxene thermometry by [2, 3] (at 40 bar), and as [1] we only determined minimum values because Ca-poor pyroxene crystallized prior to Ca-rich pyroxene.

Textural Description and Geothermometry: Radial pyroxene chondrule shows orthoenstatite crystals that are as large as the entire chondrule. Diopside forms exsolution lamellae and blebs, while pigeonite lamellae show a composition of $En_{69.8}Wo_{17.8}$. All temperatures and compositions are show in the table.

Cryptocrystalline chondrule contains enstatite crystals whereas diopside occurs as lamellar and bleb exsolutions.

A poikilitic chondrule has coarse-grained orthoenstatite showing resorption textures and contraction cracks suggesting precursor protoenstatite. Anhedral olivine is enclosed by enstatite phenocrysts, and diopside formed rims around enstatite crystals.

Table 1.

Sample	Enstatite core	Enstatite near rim	Diopside rim	Diopside exsolution	Diopside grain
C	915–1051 °C $En_{79.5–81.1}$ $Wo_{1.6–3.5}$	969– 1118 °C $En_{79.5–81.1}$ $Wo_{1.6–3.5}$		926–933 °C $En_{48.7–49.1}$ $Wo_{45.7–46.1}$	
R	909–960 °C $En_{80.3–81.6}$ $Wo_{1.4–3.3}$	938– 1080 °C $En_{80.3–81.6}$ $Wo_{1.4–3.3}$		869 °C $En_{47.0}$ $Wo_{45.7–50.8}$	1065 °C $En4_{7.0}$ $Wo_{45.7–50.8}$
PP	890–936 °C $En_{80–82}$ $Wo_{1–4}$	956–1093 °C $En_{80–82}$ $Wo_{1–4}$	877– 993 °C $En_{46.7–51.9}$ $Wo_{43–46.8}$		817– 1087 °C $En_{46.7–51.9}$ $Wo_{43.5–46.8}$

Discussion and Conclusion: Enstatite composition is homogeneous according to [4] (<1 mean deviation). Rich-Ca pyroxene temperatures are similar to those obtained by [3]. On the other hand, we think that enstatite range of 890–1118 °C represents temperatures when monoclinic was inverted to orthorhombic state. Although petrologic type 5 is only partly supported texturally, temperatures obtained are not a product of progressive thermal metamorphism; they probably reflect cooling stages after crystallization of chondrules.

Acknowledgements: This work was supported by CONACyT Grant #43227. We thank Dr. Hugo Delgado for access to LUP, and Diego Aparicio who made the polished thin sections.

References: [1] Folco L. and Mellini M. 2000. *Meteoritics & Planetary Science* 35:733–742. [2] Lindsley D. 1980. *American Mineralogist* 68:477–493. [3] Ferraris et al. 2002. *Meteoritics & Planetary Science* 37: 1299–1321. [4] Van Schmus W. and Wood J. *Geochimica et Cosmochimica Acta* 31:747–765.

5025

THE EFFECT OF Ni ON ELEMENT PARTITIONING DURING IRON METEORITE CRYSTALLIZATION

N. L. Chabot[1], S. A. Saslow[2], W. F. McDonough[3], and T. J. McCoy[4]. [1]Applied Physics Laboratory, 11100 Johns Hopkins Road, Laurel, MD 20723, USA. E-mail: Nancy.Chabot@jhuapl.edu. [2]University of Maryland, College Park, MD 20742, USA. [3]Department of Geology. [4]Department of Mineral Sciences, National Museum of Natural History, Smithsonian Institution, Washington, D.C. 20560, USA.

Iron meteorites exhibit a large range of Ni concentrations, from only 4% to nearly 60% (e.g., [1]). Most previous experiments aimed at understanding the crystallization of iron meteorites have been conducted in systems with about 10% Ni or less (e.g., [2]). It has not been demonstrated whether the crystallization models and the experimental data on which they are based are appropriate for understanding systems over such a large range of Ni contents. With this motivation, we have conducted experiments to investigate the effect of different Ni concentrations on the solid metal/liquid metal partitioning behavior of 20 trace elements pertinent to iron meteorites.

Experiments were conducted at 1 atm in evacuated silica glass tubes. Starting compositions in the Fe-Ni-S system varied from the Ni-free Fe-S endmember system to the other extreme endmember composition of the Fe-free Ni-S system. A systematic set of experiments was specifically conducted with about equal parts of Fe and Ni, a composition applicable to the most Ni-rich iron meteorites. Experiments produced equilibrium run products that contained both solid metal and a S-bearing metallic liquid. The major elements of Fe, Ni, and S were analyzed by electron microprobe analysis. Trace elements were present at a level of about 100 ppm each and were measured by laser ablation ICP-MS microanalysis [3].

Our experimental results indicate that the Ni content of the system does affect solid metal/liquid metal partitioning behavior. For a given S concentration, partitioning values can be up to an order of magnitude larger in the Ni-S system than in the Fe-S system. The observed partitioning behavior for siderophile elements is consistent with being due to the different speciation of Fe and Ni in the S-bearing metallic liquid; while Fe will form FeS "domains" in the metallic liquid [4, 5], Ni appears to form Ni_3S_2 "domains."

However, for compositions relevant to even the most Ni-rich iron meteorites, the effect of Ni on partitioning behavior is minor, amounting to less than a factor of two for the majority of trace elements studied. This effect especially appears minor in comparison to the significant effect of S on elemental partitioning behavior, (e.g., [2]). Thus, for iron meteorites crystallizing in the presence of an evolving S-bearing metallic liquid, we conclude that the effect of Ni can safely be neglected when modeling crystallization over the entire range of Ni contents found in iron meteorites.

Acknowledgements: Supported by NASA grants NNG06GI13G, NNG04GG17G, and NNG06GF56G.

References: [1] Chabot N. L. and Haack H. 2006. In *Meteorites and the early solar system II*. pp. 747–771. [2] Chabot N. L. et al. 2003. *Meteoritics & Planetary Science* 38:181–196. [3] McDonough W. F. et al. 1999. Abstract #2062. 30th Lunar and Planetary Science Conference. [4] Jones J. H. and Malvin D. J. 1990. *Metallurgical Transactions* 21B:697–706. [5] Chabot N. L. and Jones J. H. 2003. *Meteoritics & Planetary Science* 38:1425–1436.

5165

THE ABSENCE OF NICKEL ISOTOPIC ANOMALY IN IRON METEORITE METAL AND SULFIDE

J. H. Chen[1], D. A. Papanastassiou[2], and G. J. Wasserburg[3]. [1]Science Division, M/S 183-601, Jet Propulsion Laboratory, Pasadena, CA 91109–8099, USA. [2]Science Division, M/S 183-335, Jet Propulsion Laboratory, Pasadena, CA 91109–8099, USA. [3]The Lunatic Asylum, GPS Div., 170-25, Caltech, Pasadena, CA 91125, USA.

Introduction: Evidence for ^{60}Fe ($\tau^{1/2}$ = 1.5 Ma) has been reported in eucrites and chondrites [1–4], consisting of excesses in ^{60}Ni, in phases with high Fe/Ni. Recent work on iron meteorites, using MC-ICP-MS, indicates a complex picture. Quitté et al. [5] analyzed FeNi and sulfide from iron meteorites and found no ^{60}Ni effects in the FeNi at ±0.3 εu. However, in some sulfides, they found large and correlated effects in ε^{60}Ni and ε^{61}Ni. In irons, Bizzarro et al. [6] claimed small shifts in ^{60}Ni and ^{62}Ni. Cook et al. [7] showed shifts of –0.5 εu in ^{60}Ni in several sulfides and up to –2.4 εu in Mundrabilla sulfide.

In this study, using TIMS, we determined that, for samples of FeNi from 6 iron meteorites of different groups (Bennett County, Bella Roca, Gibeon, Piñon, Odessa, and Mundrabilla), the ε^{60}Ni are the same as terrestrial normal to within ±0.1 εu and ε^{61}Ni are normal to ±0.5 εu. For the observed ^{56}Fe/^{58}Ni in FeNi as low as 7 and $(^{60}Fe/^{56}Fe)_0 < 2.4 \times 10^{-7}$, we would expect a deficit in ^{60}Ni of –0.1 εu, which is not resolvable. The preliminary Ni data [8] on sulfide samples have larger uncertainties, due to low Ni concentrations and possibly some residual mass interference problems (CaF ions). After further purification, the Ni data on sulfide samples from Odessa, Toluca, and Mundrabilla (Fig. 1) show normal Ni isotopic ratios within limits of errors. We do not confirm deficits in ^{60}Ni in sulfides in Mundrabilla or other iron meteorites. The data show no evidence for ^{60}Ni excesses and yield limits on ^{60}Fe/^{56}Fe of $<2 \times 10^{-9}$.

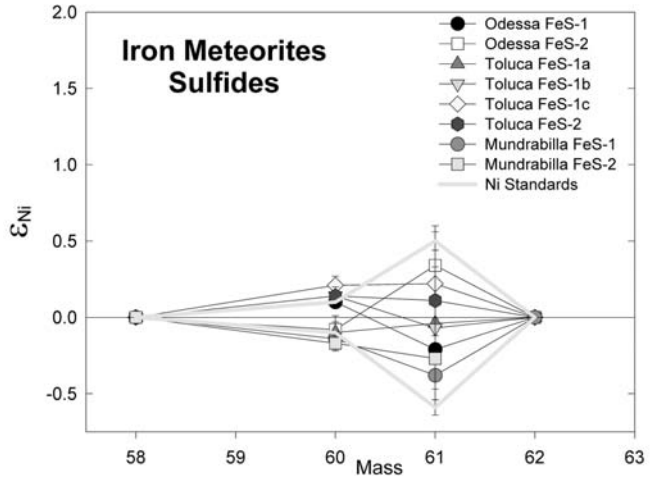

Fig. 1.

Acknowledgements: This work was supported by NASA Cosmochemistry (RTOP 344-31-55-01). The chemical separation techniques were developed under JPL R&TD (Task R.03.019.006).

References: [1] Shukolyukov A. and Lugmair G. W. 1993a. *Earth and Planetary Science Letters* 119:159. [2] Shukolyukov A. and Lugmair G. W. 1993b. *Science* 259:1138. [3] Tachibana S. and Huss G. R. 2003. *The Astrophysical Journal* 588:L41. [4] Mostefaoui S. et al. 2004. *New Astronomy Reviews* 48:155. [5] Quitté G. et al. 2006. *Earth and Planetary Science Letters* 242:16. [6] Bizzarro M., Ulfbeck D., and Thrane K. 2006. Abstract #2020. 37th LPSC. [7] Cook et al. 2007. Abstract #2287. 38th LPSC. [8] Chen J. H., Papanastassiou D. A., and Wasserburg G. J. 2007. Abstract #1753. 38th LPSC.

5031

THE ASSEMBLAGE NATIVE COPPER, COBALTIAN KAMACITE, AND TROILITE IN ORDINARY CHONDRITES: DISSOCIATION PRODUCTS NOT RELATED TO A SHOCK EVENT

H. Chennaoui Aoudjehane[1], A. El Goresy[2], and A. Jambon[3]. [1]Université Hassan II Aïn Chock, Laboratoire Géosciences, BP 5366 Maârif Casablanca, Morocco. E-mail: h.chennaoui@fsac.ac.ma. [2]Bayerisches Geoinstitut, Universität Bayreuth, 95447 Bayreuth, Germany. [3]Université Pierre et Marie Curie-Paris6 Laboratoire MAGIE, Case 110, France. [4]Place Jussieu, 75252 Paris, France.

Introduction: Native Cu in chondritic meteorites is an abundant accessory phase associated with troilite and metal. Ramdohr [1, 2] interpreted its occurrence is the result of exsolution from taenite during cooling. In a recent report, [3] claimed metallic Cu to have formed by shock. No evidence was presented supporting the shock origin nor a chemical mass balance to explain the association of metallic copper with troilite symplectites. We investigated this assemblage in the LL6 chondrite Benguerir to clarify the origin of the assemblage.

Results: SEM and quantitative electron microprobe analyses conducted on the four-phase assemblage, native Cu + troilite + kamacite + taenite, revealed chemical compositions that cannot be produced by exsolution from taenite during a shock event. The native copper grains enclosed in FeNi are usually surrounded by a Ni-poor but Co-rich kamacite. In Usti Nad Orlici the Ni-poor kamacite contains up to 1.77 wt% Co. No depletion in the adjacent taenite was detected in profiles across taenite-kamacite-copper thus negating formation of both native Cu and cobaltian kamacite by exsolution from taenite. In the LL6 chondrite Benguerir a similar assemblage was encountered. The cobaltian kamacite surrounding the Cu grains were found to be enormously enriched in Co (up to 14.3 wt%) and depleted in Ni. This cannot be explained by exsolution from taenite during cooling nor by a shock-induced heat event. The symplectitic texture of FeS, the unusual enrichment of the kamacite engulfing the native Cu specks in Co, and the lack of Ni diffusion profiles in the neighboring taenite strongly suggests formation of the assemblage through breakdown of a meta-stable complex sulfide species containing Fe, Cu, and Co as major constituents. We envisage a pentlandite-type mineral as a precursor that broke down to this assemblage according to the idealized reaction:

$$(Fe_{0.833}Co_{0.33}Cu_{0.33})_9S_8 \rightarrow 8FeS + 0.33Cu + 0.66(FeCo)$$

Both meteorites belong to the shock stage S2 [4] and no evidence for melting veins or pockets, no recrystallization of troilite and no maskelynite. Furthermore, both troilite and ilmenite grains encountered depict twin lamellae // (10-21) and (10-11) respectively, indicating formation at P < 2 GPa and low post-shock temperature (<200 °C).

Conclusions: This assemblage did not form by exsolution from taenite by shock but rather through decomposition of a meta-stable complex sulfide during low-temperature cooling in the parent body.

References: [1] Ramdohr P. 1963. *Journal of Geophysical Research* 68:2011–2036. [2] Ramdohr P. 1973. *The opaque minerals in stony meteorites*. Elsevier. p. 244. [3] Rubin A. E. 1994. *Meteoritics & Planetary Science* 29:93–98. [4] El Goresy A. 2006. *Meteoritics & Planetary Science* 41:A204.

5329

AL HAGGOUNIA (MOROCCO) STREWN FIELD

H. Chennaoui Aoudjehane[1], A. Jambon[2], and E. Rjimati[3]. [1]Université Hassan II Aïn Chock, Laboratoire Géosciences, BP 5366 Maârif Casablanca, Morocco. E-mail: h.chennaoui@fsac.ac.ma. [2]Université Pierre et Marie Curie-Paris 6 Laboratoire MAGIE, Case 110, 4 place Jussieu, 75252 Paris, France. [3]Ministère de l'Energie et des Mines, Rabat Morocco.

Since the fall of 2006, several finds of primitive aubrite or EL chondrite from NWA countries were reported in The Meteoritical Bulletin. According to their descriptions, all look quite similar. Aubrites belong to a rare type of achondrites, therefore getting similar samples on a short term suggests that they could be paired, i.e., belong to the same event, especially considering their weathered state. The origin of the material was obviously poorly known as it was reported from Morocco, from Algeria, or was of doubtful origin. We could learn that the place of find was in the south of Morocco, near the village of Al Haggounia. We conducted field work to document the field relations of the stones with the geological environment in order to state whether this was a recent fall or meteorites found in a geological layer, as claimed by some collectors, or eventually transported as exceptionally observed.

Geological Relationships: The average size of the meteorite stones varies from centimetric to the south, where numerous stones are still visible on the floor, to nearly 50 cm to the NE where stones are recovered by digging the soil, a number of them exceeding 50 kg. Stones of various sizes are found on the soil of various geological strata, from Quaternary lacustrine limestone (dalle à Helix) in the south to Cretaceous limestones to the NE. Therefore the meteorites are clearly discordant and cannot belong to any of the strata presently cropping out.

Topographic Relationship: The area of find is carved by a Quaternary topography with depression of up to 15 m below the flat surface of the region. In particular, Al Haggounia River (presently dry) exhibits two levels of terraces and a wide riverbed. Meteorites are found independently of the elevation and clearly the fall postdates the Quaternary topography.

Conclusions: Positioning of the meteorite stones on top of, or in, the soil above either Quaternary strata (dalle à Helix) or Cretaceous limestones clearly indicates that they are not included in any of the geological strata. They are found at their very place of fall.

The position of the stones on a topography dating from the quaternary indicates that the fall postdates the topography.

As of today, the stones occur over an area of nearly 40 km. This corresponds to a typical strewn field of significant size corresponding to a mass of several tons of extraterrestrial material. At present, no accurate dating of the fall can be done except that it is late Quaternary.

The strongly weathered state of the meteorites is expected due to the very unstable mineralogy, a feature shared by both enstatite chondrites and aubrites. Water is necessary for weathering but according to the vegetal coverage, precipitations are presently on the order of 60 mm/year on average. It is known that during cold recent climatic episodes precipitation was more important and that it was the rule before 12,000 B.P.

The strewn field near Al Haggounia is the most important one reported so far for this kind of meteorite.

5173

ANTARCTIC METEORITES RECOVERED FROM THIEL MOUNTAINS, WEST ANTARCTICA, BY THE FIRST KOREA EXPEDITION FOR ANTARCTIC METEORITES

B.-G. Choi[1], J. I. Lee[2], I. Ahn[1, 2], J. M. Han[1], and M. Kusakabe[2]. [1]Department of Earth Science Education, Seoul National University, Seoul, Korea 151-748. E-mail: bchoi@snu.ac.kr. [2]Korea Polar Research Institute, Incheon, Korea.

Introduction: In January 2007, the first Korea Expedition for Antarctic Meteorites (KOREAMET) conducted a search for meteorites on the blue ice fields at Martin/Nash/Pirrit Hills and Thiel Mountains, West Antarctica [1]. No meteorite was found in Martin/Nash/Pirrit Hills after 2 weeks of survey. Five meteorites were recovered on the blue ice field at Moulton Escarpment, Thiel Mountains (85°10′S, 94°33′W) during 7 hours. The meteorites were put into Teflon bags and then vacuum-sealed with plastic bags. They were transported to the lab under freezing temperature, and the bags were opened in a Globe box filled with high purity N_2 gas. Small amounts of samples were taken for petrological study and oxygen isotopic measurements.

Petrological Characteristics: Masses of five meteorites vary from 193 to 432 grams. Surface textures and magnetic susceptibility (64–217 × 10^{-3} SI unit) measured at the field show that they are ordinary chondrites according to [2]. Petrological characteristics of five meteorites are those of typical equilibrated ordinary chondrites. Three of them have no clear boundaries between chondrules and matrix, indicating that they are type 6. Olivine and pyroxene in these meteorites are highly equilibrated. The others show clear chondrule textures, however minerals are chemically equilibrated, thus classified as type 5. According to fayalite contents, two of them (Fa ~20) belong to H group, and the others (Fa ~30) belong to the LL group. At least near surfaces of them show moderate degree of weathering, e.g., having iron oxide veins.

Oxygen Isotopic Compositions: Oxygen isotopic compositions were measured with a CO_2 laser fluorination system at Korea Polar Research Institute. About 2 mg of samples were used for each run. The results agree with previously measured Antarctic ordinary chondrites [3] that show contamination by Antarctic ice, i.e., shifted to lighter isotopic composition. However, data of samples after HCl treatment (2 min in 6 N HCl) in order to remove terrestrial weathering products fall in the ranges of unweathered ordinary chondrites [3]. Classification based on oxygen isotopic compositions ($\Delta^{18}O$ values are 0.7–1.1‰) well agrees with those of petrological study.

Summary and Conclusions: Five new Antarctic meteorites were recovered at Thiel Mountains, West Antarctica, by KOREAMET. Based on magnetic susceptibility, petrological characteristics, and oxygen isotopic compositions, two of them are H6, two are LL5, and one is LL6.

References: [1] B.-G. Choi et al. 2007. The 31st Symposium on Antarctic Meteorites. [2] Folco L. et al. 2006. *Meteoritics & Planetary Science* 41:343–353. [3] Clayton et al. 1991. *Geochimica et Cosmochimica Acta* 55:2317–2337.

5122

TWO-DIMENSIONAL DYNAMICS OF CAIs IN THE SOLAR NEBULA

F. J. Ciesla. Carnegie Institution of Washington, Department of Terrestrial Magnetism, USA. E-mail: fciesla@ciw.edu.

Introduction: Among the challenges in reconciling our physical models for the evolution of the solar nebula with the meteoritic record is understanding how calcium-aluminum-rich inclusions were preserved for >1 million years prior to their incorporation into chondritic meteorite parent bodies [1, 2]. Due to gas drag, these 0.1–1-centimeter-size objects are expected to spiral into the Sun on time scales of ~10^5 years [3]. Yet CAIs are intimately mixed with much younger chondrules and matrix in chondritic meteorites, and appear to have experienced very little alteration since their formation via condensation and evaporation processes in the nebula.

Previous Models: Cuzzi et al. [4] showed that turbulence in the nebula would not only counteract the inward migration of small particles via gas drag, but also lead them to migrate outwards with time, by allowing them to diffuse outwards along concentrations gradients. This provides a way that CAIs could have formed in the very hot inner regions of the solar nebula (<1 AU) and then be delivered to the chondrite formation region (2–4 AU). However, in order for the proper mass of CAIs to be preserved for over 10^6 years, the CAI formation region had to be enhanced in rocky material by factors of 100 or more so that large amounts of CAIs could have been formed. Recent modeling [5] has shown that such large enhancements would be difficult to achieve. Additionally, Cuzzi et al. predict that CAIs will be evenly distributed throughout the solar nebula, whereas the meteoritic record points to CAIs being sorted by size prior to formation of the chondrite parent bodies.

New Model: Recently I have been developing a model to examine the combined radial and vertical dynamics of solids in a turbulent-viscous solar nebula. Outward transport is encouraged in such disks because large-scale flows carry materials away from the Sun around the disk midplane [6–8] and diffusion occurs much more rapidly in this region than one-dimensional models had realized. As a result, outward transport through the solar nebula can be fairly efficient, explaining the presence of high-temperature materials in comets [9]. This increased efficiency may thus reduce the need for large enhancements of rock in the CAI formation region.

I am now investigating how the dynamics of outward transport in such disks varies as a function of particle size. Larger dust particles will migrate inwards due to gas drag more rapidly [3], but they would also concentrate around the midplane more efficiently (due to their higher settling velocities) where flows are directed outwards. These flows will help to counteract the inward migration due to gas drag, allowing those CAIs at the midplane to be pushed outwards, the distance being dependent on the size of the particles, and thus resulting in size-sorting.

References: [1] Amelin Y. et al. 2002. *Science* 297:1678–1683. [2] Bizzarro M. et al. 2004. *Nature* 431:275–278. [3] Weidenschilling S. J. 1977. *Monthly Notices of the Royal Astronomical Society* 180:57–70. [4] Cuzzi J. N. et al. 2003. *Icarus* 166:385–402. [5] Ciesla F. J. and Cuzzi J. N. 2006. *Icarus* 181:178–204. [6] Urpin V. A. 1984. *Soviet Astronomy* 28:50–53. [7] Takeuchi T. and Lin D. N. C. 2002. *The Astrophysical Journal* 5281:1344–1355. [8] Keller Ch. and Gail H.-P. 2004. *Astronomy & Astrophysics* 415: 1177–1185. [9] Ciesla F. C. Forthcoming.

5212

CATACLYSMIC BOMBARDMENT RECORDED IN ^{40}Ar-^{39}Ar AGES OF IMPACT-MELT CLASTS IN HOWARDITES

B. A. Cohen. Institute of Meteoritics, University of New Mexico, Albuquerque, NM 87131, USA. E-mail: bcohen@unm.edu.

Introduction: Lunar impact-melt rock ages suggest an extraordinary bombardment event ("cataclysm") in the Earth-Moon system at ~3.9 Ga. Dynamical models implicate subequal numbers of main-belt asteroids and icy trans-Neptunian planetesimals in the bombardment. If these models are correct, the collisional history within the main asteroid belt should resemble that of the Earth-Moon system, though perhaps modified to reflect the lower interbody velocities within the main belt. For instance, ordinary chondrites show a wider range of impact resetting ages than the lunar impact-melt rocks but statistically peak at ~3.8 Ga [1].

Of particular interest for understanding bombardment history are surficial products from very large asteroids. In particular, HED meteorites (from 4 Vesta) record impact resetting in multiple chronometers. Igneous clasts in eucrites show that the ^{40}Ar-^{39}Ar system was significantly disturbed within 1 Gyr after crystallization [2]. This work investigates impact-melt clasts in howardites, polymict regolith breccias containing impact-melt clasts that record Vesta's bombardment history.

Meteorites: QUE 94200, QUE 97001, EET 87513, and GRO 95574 are Antarctic howardites. Impact-melt clasts were identified in thin sections of these meteorites on the basis of their textures (glassy to microporphyritic) and characterized using the electron microprobe. Their bulk compositions are a mixture between typical eucritic and diogenitic compositions and unable to be derived by igneous fractionation of eucrite parent melts, indicating their probable impact origin [3].

Impact-Melt Ages: Eleven impact-melt clasts were extracted using a Medenbach microcorer and irradiated at the University of Oregon TRIGA reactor. Laser step-heat experiments were conducted at the New Mexico Geochronology Research Laboratory at the New Mexico Institute of Mining and Technology using a continuous Ar-ion laser heating system. Data were corrected for system blanks, decay time, reactor-induced interferences, decay time, and cosmic-ray spallation. After these corrections, the trapped ^{40}Ar/^{36}Ar ratios were all 0 within uncertainty and ages are reported without further corrections at this time.

The age distribution among these clasts has a bimodal distribution (Fig. 1). Two clasts have well-constrained apparent ages ~4.3 Ga. The remaining clasts are spread between 3.9 and 3.4 Ga (though the four youngest clasts have very large [1 Ga] uncertainties). These ages reinforce the distribution compiled by [1], in which a high number of reset ages occurs very early, tails off, and resumes ~3.9 Ga. This distribution is consistent with an early chaotic main belt where collisions are frequent, followed by a period of stability and few impacts, punctuated by a cataclysmic event at around 3.9 Ga.

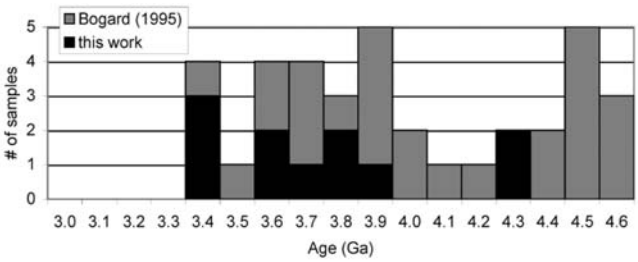

Fig. 1. Impact-reset ages in howardite clasts.

References: [1] Bogard D. D. 1995. *Meteoritics* 30:244. [2] Bogard D. D. and D. H. Garrison. 1993. *Meteoritics* 28:325. [3] Cohen B. A. 2004. *Meteoritics & Planetary Science* 39:A24.

5183

THE CONTINENTAL PERMIAN-TRIASSIC BOUNDARY IN THE KAROO BASIN, SOUTH AFRICA: NO EVIDENCE FOR METEORITE IMPACT

L. Coney[1], W. U. Reimold[2], C. Koeberl[3], P. J. Hancox[1], D. Mader[3], I. McDonald[4], U. Struck[2], V. Vadja[5], and S. L. Kamo[6]. [1]University of the Witwatersrand, Private Bag 3, P.O. WITS, 2050, Johannesburg, South Africa. E-mail: louiseconey@yahoo.com. [2]Museum for Natural History, Humboldt University in Berlin, Germany. [3]Department of Geological Sciences, University of Vienna, Austria. [4]School of Earth, Ocean and Planetary Sciences, Cardiff University, UK. [5]Department of Geology, Lund University, Sweden. [6]Department of Geology, University of Toronto, Canada.

A multidisciplinary investigation of three different continental sections across the Permian-Triassic boundary in the Karoo Basin, South Africa, has been conducted by our group since 2003. In particular, complete geochemical profiles (major, trace, PGE elements, carbon isotopes) across the boundary have been measured, and a search for evidence of meteorite impact at the boundary has been undertaken.

All three sections (located in both the southern and eastern Karoo Basin) studied here comprise mudstones, siltstones, sandstones, and varying numbers of carbonate nodular horizons, and a laminated mudrock layer (referred to as the "event bed") was encountered at the position of the paleontological boundary (PB). At the Commando Drift Dam (CDD) section, the boundary is also constrained paleomagnetically (~5.3 m above the PB; [1]). Variations in the major and trace element abundance profiles are mostly limited to the carbonate nodular horizons, besides the overall effects of weathering. Bulk carbon isotopic studies of the CDD section revealed a negative $\delta^{13}C_{bulk}$ excursion 2 cm below the PB, followed by a gradual recovery and then another decrease in values leading towards the paleomagnetic boundary (PMB). Above the PMB recovery to less negative $\delta^{13}C_{bulk}$ values (approximately −18‰) occurs. The organic carbon record is comparable to the results of previous studies of different sections in the southern Karoo Basin [1]. The variations of the carbon isotopic ratios can be interpreted to indicate a variety of different sources of organic carbon.

Several Late Permian key-species are present in the CDD section, and are traces of the surviving plants enduring after the major extinction pulse. A lack of pollen/spores related to photosynthetic plants is observed, together with the presence of fungal polymorphs. This is similar in pattern to that observed at the Cretaceous-Paleogene boundary [2].

The timing of vertebrate extinctions in the Karoo Basin has so far not been determined, but a 252.5 ± 0.7 Ma age, which was determined for a single zircon crystal from the PB at CDD, gives a maximum constraint on the age of the event bed, which is in agreement with the accepted age of the boundary [3].

No evidence for impact-produced microdeformation features were found in quartz grains from the southern Karoo sections. Also, siderophile element data (including platinum-group element concentrations) do not support the possible presence of a meteoritic component at the boundary. Thus, a link between impact and P-Tr extinction is not indicated by the results of this study.

References: [1] Ward P. D. et al. 2005. *Science* 307:709–714. [2] Vajda V. and McLoughlin S. 2004. *Science* 303:1489. [3] Kamo S. L. et al. 2006. *Geochimica et Cosmochimica Acta* 70:A303.

5163

CARBONATE CRYSTALLOGRAPHY IN THE CARBONACEOUS CHONDRITES—A NEW INDICATOR OF IMPACT SHOCK?

S. Conolly[1, 2], C. L. Smith[2], M. R. Lee[3], and G. K. Benedix[2]. [1]IARC, Department of Earth Science and Engineering, South Kensington Campus, Imperial College London, SW7 2AZ, UK. [2]IARC, Department of Mineralogy, The Natural History Museum, London, SW7 5BD, UK. E-mail: C.L.Smith@nhm.ac.uk. [3]Department of Geographical and Earth Sciences, The University of Glasgow, Glasgow, G12 8QQ, UK.

Introduction: Carbonates are an important constituent of the fine-grained matrix of carbonaceous chondrites and were formed during aqueous alteration within their asteroidal parent body(ies) (e.g., [1, 2]). We have characterized the morphology, chemical compositions, and crystallographic orientations of carbonate grains within three CM chondrites using a combination of analytical SEM, EPMA, and electron backscattered diffraction (EBSD). Our results reveal that the carbonate (calcite) grains display complex morphologies and crystallographies which, we suggest, may in part reflect late-stage shock processing on the parent asteroid(s).

Background: Calcite grains from Mighei, Pollen (both shock stage S1), and Murchison (shock stage S1–2) were initially located and imaged using a JEOL 5900 analytical SEM. Selected grains were then characterized using a FEI Quanta 200F SEM equipped with an EDAX-TSL EBSD system. EBSD is a powerful technique for determining the crystallographic orientations of polished surfaces of minerals at submicrometer spatial resolutions. This technique has been used to study calcite in terrestrial metamorphic rocks (e.g., [3]) but the crystallography of meteoritic carbonates has been studied by TEM [4]. The advantages of EBSD mapping are that it is nondestructive, can be used to rapidly characterize large areas of mineral grains (relative to TEM), and results can be readily integrated with SEM images.

Results and Interpretation: All of the carbonate grains studied were calcite, although a small aragonite inclusion was found in a single Murchison grain. Four types of calcite grains were found.

1. *Single Crystals*: These grains are uniform in BSE images (although may display fractures and cracks). All the calcite is in a single crystallographic orientation.
2. *Twinned Single Crystals*: Twins, each a few microns in width, are present throughout the crystal.
3. *Polycrystalline Grains*: Individual grains (sometimes fractured) are composed of a number of differently oriented crystals.
4. *Twinned Polycrystalline Grains*: In this type each of the individual subgrains is finely twinned.

Some of the polycrystalline grains may have formed by growth of crystals from several nucleation sites into open pores. The planar compromise boundaries between constituent crystals of some grains supports this model, but compositional zoning has not been identified by monochromatic CL imaging on the SEM or by EPMA. The majority of grains in Murchison and Pollen are twinned whereas twinning is very rare in Mighei calcite. Such significant differences in the abundance of twinned grains between the three CMs studied suggests that the crystallography of meteoritic carbonates could be a new way of quantifying impact shock within S1 and S2 meteorites.

References: [1] Fredriksson K. and Kerridge J. F. 1988. *Meteoritics* 23: 33–44. [2] Johnson C. A. and Prinz M. 1993. *Geochimica et Cosmochimica Acta* 57:2843–2852. [3] Bestmann M. et al. 2006. *Tectonophysics* 413:185–200. [4] Barber D. J. 1981. *Geochimica et Cosmochimica Acta* 45:945–970.

5118

BULK DENSITIES OF ASSORTED CK CHONDRITES, PRIMITIVE ACHONDRITES, AND BENCUBBIN

G. Consolmagno[1, 2], D. P. Wignarajah[1], and D. T. Britt[3]. [1]Fordham University, Bronx, NY 10458, USA, and The American Museum of Natural History, New York, NY 10024, USA. E-mail: gjc@specola.va. [2]Specola Vaticana, Vatican City. [3]University of Central Florida, Orlando, FL 32816, USA.

Introduction: Density and porosity are indicators of a meteorite's physical fabric, and meteorite bulk densities can be compared against potential parent body asteroids to infer their internal structure. As a part of our ongoing project to determine the densities and porosities of meteorites, we measured the bulk densities of 45 samples of 29 different meteorites from the collection of the American Museum of Natural History using the glass bead method [1, 2]. Along with samples for which a few densities had previously been reported [3], these include some of the first bulk densities to be reported for the CK class of carbonaceous chondrites, the brachionite and winonaite class of primitive achondrites, and Bencubbin.

In addition, we have begun measuring grain densities of these samples using helium pycnometry, from the difference between grain and bulk densities, porosities can be computed.

Some of the highlights of our results to date:

CK Chondrites: The average bulk density for ten pieces of Karoonda [CK4], total mass 244 g, is 2.84 ± 0.1 g/cm^3; similarly, the density of a 71 g Ningqiang [CK3] sample is 2.80 g/cm^3. However, a 25 g piece of Maralinga [CK5] had a bulk density of only 2.54 g/cm^3. Previously, grain densities of Karoonda and Maralinga of 3.49 g/cm^3 and 3.46 g/cm^3, respectively, have been reported [3]. These are lower than our measured grain density of 3.64 g/cm^3 for a 37 g piece of Karoonda, and 3.74 g/cm^3 for Ningqiang. We derive a porosity of 24 ± 4% for Ningqiang and 22 ± 4% for Karoonda. Using the previously published grain density of Maralinga, it would have a porosity of 27%. Though essentially metal-free, CKs have been linked petrographically to CVs [4]. We find both classes have similar grain densities, and porosities in excess of 20%. This porosity is double that of ordinary chondrites, implying a distinctive lithification history.

Primitive Achondrites: We measured bulk densities of two pieces of Winona (95.9 g and 16.8 g) and the winonaite Tierra Blanca (33 g) as 3.22, 3.4, and 2.92 g/cm^3, respectively. (The smaller Winona piece has a large uncertainty.) A grain density measurement of Tierra Blanca of 3.38 g/cm^3 yields a porosity of 14 ± 4%. Three brachinites, Eagles Nest, Hughes 026, and Nova 003 (all less than 20 g), have an average bulk density of 3.3 ± 0.15 g/cm^3. Primitive achondrites and ordinary chondrites both have compositions consistent with S asteroid spectra; but since their bulk densities and porosities are similar, density alone cannot distinguish between them as possible S-asteroid analogues.

Bencubbin: The grain density of a 183 g sample of the unusual meteorite Bencubbin was measured at 4.9 ± 0.1 g/cm^3. Bulk density provides a fast estimate the metal content; assuming rock at 3 g/cm^3 and metal at 7.8 g/cm^3, this sample is 63% metal.

References: [1] Consolmagno G. J. and Britt D. T. 1998. *Meteoritics & Planetary Science* 33:1231–1240. [2] Wilkison S. L. and Robinson M. S. 2000. *Meteoritics & Planetary Science* 35:1203–1213. [3] Britt D. T. and Consolmagno G. J. 2003. *Meteoritics & Planetary Science* 38:1161–1180. [4] Greenwood R. C. et al. 2004. Abstract #1664. 35th Lunar and Planetary Science Conference.

5298

IN SITU LASER DESORPTION MASS SPECTROMETRY OF METEORITIC SAMPLES AS PLANETARY ANALOGS

C. M. Corrigan, W. B. Brinckerhoff, T. Cornish, and S. Ecelberger. Johns Hopkins University Applied Physics Laboratory, 11100 Johns Hopkins Road, Laurel, MD 20723, USA. E-mail: cari.corrigan@jhuapl.edu.

Introduction: Near-future planetary missions will call for high-fidelity geochemical sample analysis, including landed missions to a number of planetary bodies, including asteroids. While emphasizing distinct science goals, all share certain categories of high-priority in situ measurement objectives, including analyses of the elemental, mineralogical, and organic composition of solid samples from a variety of source regions, in order to learn more about the origin, evolution, and current state of the body. There is a strong need to develop methods to improve analytical accuracy, to extend the range of species detected, to significantly lower the detection limits to trace levels, and to provide compositional data on a local, mineral-grain spatial scale. Laser desorption mass spectrometry (LDMS) may contribute to the realization of such ambitious capabilities. The development of LDMS instruments has been ongoing at JHU/APL for a number of years [1–6], in an effort to construct instruments geared toward planetary missions and astrobiology research. Analyses of terrestrial analog and meteoritic material are part of the program we have undertaken to ensure that results from this new instrument are consistent with measurements obtained in proven commercial mass spectrometers [7].

Analog Analyses: In addition to a set of crushed Mars analogs obtained from R. Morris and D. Ming, NASA/JSC, a suite of well-characterized, powdered meteorite samples from the national collection have been obtained from T. McCoy, SI/NMNH. These samples cover a range of terrestrial basaltic compositions as well as a variety of meteorite types (L, LL, H, CO, CK, CV, EC). Powdered samples have been analyzed in a commercial Bruker Autoflex TOF/TOF LDMS available at JHU/APL as well as in the miniature LDMS under development. Additionally, chipped meteorite samples with resolvable features (mineral grains, chondrules, CAIs, matrix) are in hand to test the ability of the LDMS to resolve the chemistry of individual features.

A key objective of this research is to determine the sensitivity to organic compounds in these minimally prepared samples. Organics were predominantly found in a thin surface layer as evidenced by the loss of signal after several initial laser pulses. These compounds were likely introduced prior to collection. The "bulk" organic concentration in Mauna Kea jarositic tephra and Columbia River basalts was very low. However, specific points on the surfaces of individual mineral grains yielded persistent signatures of low to moderate molecular weight, nonvolatile organics. As mineral grains might be capable of preserving water-borne organics in such features over long time scales (e.g., on Mars and/or asteroids), the need for microanalysis of intact sample surfaces in situ warrants further attention and investigation.

Acknowledgements: We appreciate the collaboration and assistance of E. Vicenzi, T. McCoy, P. Mahaffy, D. Stepp, N. Hagen, and P. Demirev. Funding provided by NASA PIDD and MSL programs.

References: [1] Brinckerhoff W. B. et al. 2000. *Review of Scientific Instruments* 71:536. [2] Cornish T. et al. 2000. *Rapid Communications in Mass Spectrometry* 14:2408. [3] Brinckerhoff W. B. 2004. *Applied Physics A* 79:953. [4] Brinckerhoff W. B. et al. 2005. *Planetary and Space Science* 53: 817. [5] Brinckerhoff W. B. et al. 2005. Proceedings, 6th IAA Conf. Low Cost Plan. Missions. [6] Brinckerhoff W. B. et al. 2006. Abstract #2015. 37th LPSC. [7] Corrigan C. M. et al. 2007. Abstract #1475. 38th LPSC.

5217

RUTILE FOUND WITHIN PRESOLAR GRAPHITES FROM MURCHISON

T. K. Croat. Laboratory for Space Sciences and Physics Department, Washington University, St. Louis, MO 63130, USA. E-mail: tkc@wustl.edu.

Introduction: We report the identification of rutile grains found within four different graphite slices from the Murchison KFC1 fraction. It is unexpected for an oxide to condense in circumstellar outflows and then be captured by a growing carbonaceous presolar grain, so a complex formation history is suggested. However, the evidence thus far (diverse chemical compositions of rutiles and other minerals found in the same graphites) does not suggest formation via exsolution or later oxidation of pre-existing grains on the parent body or in the laboratory.

Procedure: Graphites from the Murchison KFC1 density and size separate 2.15–2.20 g cm^{-3}, >1 μm) [1] were ultramicrotomed and examined in a JEOL 2000FX TEM equipped with a NORAN Energy Dispersive X-ray Spectrometer [2].

Results: The properties of the internal rutile grains found within onion graphites are summarized in Table 1 (4a and 4b from the same slice). Although meteoritic rutile has been reported in ordinary chondrites and mesosiderites [3], this is a new (and unexpected phase) within graphite, so thorough indexing of the crystal structures was done. Four to 9 patterns were collected from each grain, including diffraction patterns from the [110], [011], [100], and [111] zone axes. Rutiles 2 and 3 contained twinned domains, whereas the others were single crystals. As seen in Table 1, the rutile compositions were quite variable among the graphites, and can often be distinguished from TiCs on the basis of higher Nb and/or Cr content. No s-process elements (common in TiCs) or Ta (common in terrestrial rutile) were seen. Rutiles 1 and 2 were found along with s-process enriched carbides, with Mo/Ti ratios 137× and 150× the solar values. These strongly suggest an origin in AGB outflows for these rutile-containing graphites. Rutiles 4a and 4b were found along with three metallic Al grains (α-Al, 4.2Å FCC) and an unidentified $Ti_{85}Fe_{15}$ phase (not rutile or TiC).

Discussion: A different oxide (chromite) was previously found within several graphites, but these had normal O isotopes and were hypothesized to form due to laboratory oxidation of existing iron grains by dichromate solution (used during separation). Formation of rutile by oxidation of pre-existing TiCs seems unlikely though, due to the survival of TiC in the same slices and due to the odd compositions (e.g., Nb never detected in TiCs). NanoSIMS investigations of the O and Ti isotopic composition of the rutiles are planned to clarify their likely origin.

Table 1. Properties of internal rutile grains.

#	Size (in nm)	Composition (at%, excluding O)	Associated phases
1	387 × 150	$Ti_{90}V_7Fe_2Ca_1Cr_1$	TiC
2	55 × 29	$Ti_{77}V_{15}Cr_4Fe_3$	TiC
3	39 × 36	$Ti_{53}Cr_{26}Nb_{12}Fe_4Ca_3V_2$	None
4a	26 × 22	$Ti_{85}S_{15}$	α-Al and $Ti_{85}Fe_{15}$
4b	42 × 19	$Ti_{93}S_7$	α-Al and $Ti_{85}Fe_{15}$

References: [1] Amari S. et al. 1994. *Geochimica et Cosmochimica Acta* 58:459–470. [2] Croat T. K. et al. 2005. *The Astrophysical Journal* 631: 976–987. [3] Buseck P. R. and Keil K. 1966. *American Mineralogist* 51: 1506–1515.

5128

EARLY FORMATION OF Fe METEORITES—A CASE STUDY

A. Das and G. Srinivasan. Department of Geology, University of Toronto, Toronto, ON M5S 3B1, Canada. E-mail: srini@geology.utoronto.ca.

The presence of highly nonradiogenic ^{182}W in Fe meteorites has been used to estimate that rapid formation of Fe meteorites took place in <1.5 Ma of formation of the solar system [1]. The formation time of the solar system as determined from $^{207}Pb/^{206}Pb$ ages of constituents of primitive meteorites the Ca-Al-rich inclusions (CAIs) (e.g., [2]) is nearly ~4567 Ma. The CAIs are the first solid objects to form in the solar system and have some of the highest observed abundance of short-lived radionuclide Al^{26} (half-life ~0.7 Ma) which decays to Mg^{26}, with $^{26}Al/^{27}Al \sim 5 \times 10^{-5}$ [3]. The early melting and differentiation of planetary bodies is attributed to the decay of heat generating ^{26}Al [4, 5]. The ability of ^{26}Al to melt a planetary body is determined by its abundance and the size of the latter [6]. Bodies with radii <20 km will not undergo complete melting, however, a part of the inner core may exceed the solidus (~1200 °C) when radius >5 km [6].

The radii of parent bodies of Fe meteorites range from 3–165 km [7]. There is no obvious explanation for melting of a small planetary body with ~3 km radius and chondritic composition. Furthermore, based on ^{26}Al abundance a time interval of ~2 Ma is estimated between formation of CAIs and chondrules (e.g., [8]). If CAIs formed at a rapid rate they would have experienced gas drag resulting in their spiralling into the early Sun [9]. The two possible mechanisms suggested to preserve CAIs are turbulent flow or rapid accretion of CAIs into small bodies. We report preliminary results of thermal evolution of small planetary bodies with CAI abundance greater than chondritic bodies resulting in Al abundance greater than chondritic values. This will result in collateral increase in concentration of ^{26}Al resulting in higher energy generation due its radioactive decay. In our calculations we observe that for bodies with CAI content of ~25% and 50% in a 3 km (radius) body, ~66% and 76% of the inner core of the body will respectively exceed solidus resulting in large-scale differentiation and formation of Fe cores. Bodies with very high CAI were recently reported [10]. The early sequestration of CAIs may be responsible for early formation of Fe meteorites and angrites [1, 11].

References: [1] Kleine T. et al. 2005. *Geochimica et Cosmochimica Acta* 69:5805–5818. [2] Amelin Y. et al. 2002. *Science* 297:1678–1683. [3] MacPherson G. J. et al. 1995. *Meteoritics* 30:365–386. [4] Urey H. C. 1955. *Proceedings of the National Academy of Sciences* 41:127. [5] Srinivasan et al. 1999. *Science* 284:1348–1350. [6] LaTourette T. and Wasserburg G. J. 1998. *Earth and Planetary Science Letters* 158:91–108. [7] Mittlefehldt D. et al. 1998. In Reviews in Mineralogy, vol. 36, edited by Papike J. J. [8] Srinivasan G. et al. 2000. *Meteoritics & Planetary Science* 35:1333–1354. [9] Cameron A. 1995. *Meteoritics* 30:133–161. [10] Sunshine J. et al. 2007. Abstract #1613. 38th LPSC. [11] Baker J. et al. 2005. *Nature* 436:1127–1131.

5250

Fe-Mn-Mg VARIATIONS AS INDICATORS OF PLANETARY MAGMATISM ON 4 VESTA

J. S. Delaney. Department of Earth and Planetary Sciences, Rutgers University, 610 Taylor Rd., Piscataway, NJ 08854, USA. E-mail: jsd@rci.rutgers.edu.

Introduction: Planetary magmatism is ubiquitous, and mineralogical composition ratios provide monitors of crystal-liquid-vapor fractionation. The Fe/Mg ratio commonly has been used as an indicator, but can be extended by the use of Mn. Either Fe and Mg, or Mn and Mg, may be used as a measure of the degree of crystal-liquid partitioning. The three elements together provide an added dimension. Fe and Mn have fairly similar partition coefficients under relatively reducing conditions and are partitioned together between crystal and liquid. In detail, the partitioning of Fe and Mn differs slightly and is sensitive to changes in redox conditions. FeO reduces to metal under many circumstances relevant to planetary magmatism ($0.5 < \log fO_2 < -1.5$) while MnO does not reduce in most meteoritic systems. In contrast, Mn is often viewed as being more volatile than Fe and can be lost by evaporation. Traditionally, Fe/Mn ratios have been used to identify planetary bodies (Laul et al. 1972) but when considered in the context of the Fe-Mn-Mg system which permits distinguishing crystal-liquid fractionation, Fe metal addition or loss, and moderately volatile element phenomena, greater detail can be extracted [6].

Sampling Vesta: The "planetoid" 4 Vesta clearly experienced planetary differentiation and is the putative source for a very large number of achondritic meteorites. The polymict breccias provide a wealth of lithic clasts that sample the surface of Vesta and presumably reflect the magmatism in both endogenous Vestan volcanism and impact processing of the body. [2, 3]. The diversity of lithologies available as lithic clasts in breccias far exceeds the number of monolithologic achondrites (eucrites and diogenites). These clasts are the most representative samples of the surface of 4 Vesta. Fe-Mn-Mg systematics provide the potential for distinguishing individual magmatic complexes. Detailed study of olivine clasts in howardites [4, 5] demonstrated significant heterogeneity of Fe/Mn that reflect magmatic heterogeneity on the parent body. Similar variations of Fe-Mn-Mg in mafic clasts are seen in the scatter of the Fe-Mn-Mg systematics of lithic clast pyroxene and mineral clast pyroxene and in experimental studies of basaltic achondrites [1]. Scatter in these data result from three causes: a) imprecision of the analyses, b) pyroxene polymorphism, and c) source heterogeneity. Recognition of source heterogeneity is a primary goal for identification of provincial variations in the crust of Vesta. Fe-Mn-Mg systematics of Vestan lithic clasts potentially constrain not only magmatic fractionation but also metal separation processes including redox reactions in the crust. More problematically, volatile phenomena in the near surface regime of Vesta may also be revealed by Fe-Mn-Mg systematics.

References: [1] Boesenberg and Delaney. 1997. *Geochimica et Cosmochimica Acta* 61:3205. [2] Delaney J. S. 1981a. Lunar Planet Sci. XII. pp. 14–17. [3] Delaney J. S. et al. 1981b. Lunar Planet Sci XII. pp. 211–213. [4] Désnoyers C. and Jerome D. Y. 1973. *Meteoritics* 8:344–345. [5] Désnoyers C. 1982. *Geochimica et Cosmochimica Acta* 46:667–680. [6] Goodrich C. A. and Delaney J. S. 2000. *Geochimica et Cosmochimica Acta* 64:149–160. [7] Laul J. C. et al. 1972. Proceedings, 3rd Lunar Sci Conf. pp. 1181–1200.

5038

CARBONATES IN THE CM CHONDRITE QUE 93005: MINERAL CHEMISTRY AND Mn-Cr SYSTEMATICS

Simone de Leuw[1], Alan E. Rubin[1], Axel K. Schmitt[1] and John T. Wasson[1, 2]. [1]Department of Earth and Space Sciences, University of California, Los Angeles, CA 90095–1567, USA. E-mail: sdeleuw@ucla.edu. [2]Institute of Geophysics and Planetary Physics, University of California, Los Angeles, CA 90095–1567, USA.

Introduction: Secondary carbonates in CM chondrites provide evidence of aqueous alteration that occurred in the CM parent body. In this study, we focus on Mn-rich calcite ($CaCO_3$) and dolomite ($CaMg[CO_3]_2$) grains that are widespread throughout the fine-grained matrix. Alteration products such as carbonates can potentially provide a record of the timing of aqueous alteration on the parent body. Here we describe chemical characteristics of the carbonates in the highly altered QUE 93005 CM chondrite and initial results of ^{53}Mn-^{53}Cr dating of these carbonates using the high-resolution IMS 1270 ion microprobe.

Observations: QUE 93005 contains both calcite and dolomite in the fine-grained matrix. The abundance of these secondary carbonates in the thin section is about 2–3 vol%. Calcite occurs mainly as irregularly shaped aggregates ranging between 50 and 100 μm. In general, dolomite occurs as single crystals in the matrix and in some cases as single grains within larger calcite crystals. Dolomite grains are smaller than calcite grains and range between 10 and 30 μm. All of the single dolomite crystals are surrounded by an Fe-Ni-S rim (EDX analyses) that does not occur around calcite grains.

Results: Electron probe analyses showed high Mn contents in several carbonate grains, indicating their suitability for Mn-Cr isotopic studies. Mn contents range from 0.05 to 1.1 wt% in calcite and 1.8 to 5.0 wt% in dolomite. Cr contents in the secondary carbonates are below the detection limit of the electron probe.

For Mn-Cr isotopic analysis using the UCLA CAMECA IMS 1270 ion microprobe, we selected a subset of 11 out of >60 characterized carbonates for Mn-Cr isotopic compositions based on grain sizes larger than the O-primary ion beam diameter (~10 μm). We obtained replicate analyses on nine carbonate grains; this amounts to a total of 22 spots analyzed. Ten of the 22 measurements show excesses in δ^{53}Cr, whereas the other analyses show normal or near-normal isotopic compositions within 2σ uncertainty. Mn/Cr relative sensitivity factors were calibrated on San Carlos olivine (Mn/Cr = 10.93 [1]). The ^{53}Cr excesses are linearly correlated with the ^{55}Mn/^{52}Cr ratios, indicating the in situ decay of ^{53}Mn at the time of carbonate formation. The highest δ^{53}Cr excess (~1100‰) has a ^{55}Mn/^{52}Cr ratio of more than 30,000. The slope of the correlation line, determined by a weighted least-squares fit, corresponds to an initial ^{53}Mn/^{55}Mn ratio of $(4.1 \pm 0.3) \times 10^{-6}$, which is in agreement with previous studies by [2]. In comparison, less altered CM2 [3] and highly altered CI1 [4] chondrites are reported to have higher and lower initial ^{53}Mn/^{55}Mn ratios, respectively. This implies that the degree of aqueous alteration is correlated with the age of carbonate formation and that alteration processes occurred for an extended period of time on carbonaceous chondrite parent bodies.

References: [1] Hoppe et al. 2004. Abstract #1313. 25th Lunar Planet. Sci. Conf. [2] Brearley A. J. and Hutcheon I. D. 2000. Abstract #1407. 31st Lunar Planet. Sci. Conf. [3] Brearley et al. 2001. Abstract #1458. 32nd Lunar Planet. Sci. Conf. [4] Endress et al. 1996. *Nature* 379:701–703.

5073

INTI DID NOT FORM IN AN X WIND (AND NEITHER DID MOST CAIs)

S. J. Desch and Connolly H. C., Jr. School of Earth and Space Exploration, Arizona State University, AZ, USA. E-mail: steve.desch@asu.edu.

Introduction: Among the samples returned from comet 81P/Wild-2 by the STARDUST sample return mission was a CAI-like grain from track 25, known as "Inti" [1]. This object contains several refractory minerals such as anorthite, Ca- Al- Ti-rich clinopyroxene, gehlenite, spinel, corundum, FeS, osbornite, and probably perovskite, in an object roughly 10 microns in size [1]. This mineralogy very closely resembles that of CAIs (Ca-Al-rich inclusions) in CV3 and CM2 chondrites [2]. The discovery of CAIs in comets was famously predicted by Shu et al. in 1996 [3], within the context of their "X wind" model for the formation of chondrules and CAIs. The presence of this CAI-like object in the comet Wild-2 is taken as evidence for radial mixing within the solar nebula generally (perhaps by turbulent diffusion [4]), and for the X wind model in particular [5]. Here we argue that in fact the X wind model predicts conditions that are incompatible with the formation of CAIs in general, and Inti in particular.

Oxygen Fugacity during CAI Formation: In the context of the X wind model [5, 6], CAIs form when small rocky particles spiral through the solar nebula disk to the X point, where the stellar magnetosphere truncates the disk, at about 0.05 AU from the Sun. Inside this radius nebular gas (mostly hydrogen) is ionized and magnetically funneled onto the Sun, and the rocky particles orbit in the "reconnection ring," naked of gas and directly exposed to stellar radiation and stellar flares. [6] specifically predict that CAIs form and grow in this region when flares evaporate solids, which then recondense via vapor-phase deposition. They estimate a density of rock vapor during recondensation $>10^{-12}$ g cm^{-3} [6, p. 1041], far exceeding the density of coronal gas in the same region, $\sim 2 \times 10^{-16}$ g cm^{-3} [6, p. 1033]. As coronal gas is the only source of hydrogen to buffer the oxygen-rich rock vapor, we estimate an H_2O/H_2 ratio $\sim 10^4$, which is 6 orders of magnitude more oxidizing than a solar-composition gas. Simply put, [6] predict that CAIs condense from rock vapor, and not a solar-composition gas. This contrasts sharply with the prevailing view that CAIs formed in a gas of solar composition [7]. Ti^{3+}/Ti^{4+} ratios in fassaite and rhonite argue strongly for crystallization of CAIs in a solar composition gas [8], but the distinction between formation (condensation) and melting has precluded ruling out CAI formation at the X point.

In the last year, osbornite ([Ti,V]N) has been discovered in two CAIs: Inti [1], and a CAI in the CH/CB-like chondrite Isheyevo [9]. This nitride only condenses in gas with C/O ~0.8–1.0 [10], a factor of 2 less oxidizing than a solar composition gas. The presence of osbornite in Inti and the Isheyevo CAI means that these two CAIs did not form in the X point. Inti in particular must have formed in the solar nebula and then been transported to the region where Wild-2 formed, probably by turbulent diffusion [4], and probably not by the X wind [3].

References: [1] Zolensky M. et al. 2006. *Science* 314:1735. [2] Hörz et al. 2006. *Science* 314:1716. [3] Shu F. H., Shang H., and Lee T. 1996. *Science* 271:1545. [4] Bockelee-Morvan et al. 2002. *Astronomy & Astrophysics* 384:1107. [5] Brownlee et al. 2006. *Science* 314:1711. [6] Shu F. H., Shang H., Gounelle M., Glassgold A., and Lee T. 2001. *The Astrophysical Journal* 548:1029. [7] Krot A. N., Fegley B., Jr., Lodders K., and Palme H. 2000. In *Protostars and planets V.* 1024 p. [8] Beckett J. R. and Grossman L. 1986. 17th LPSC. p. 36. [9] Meibom A. et al. 2007. Abstract #1256. 38th LPSC. [10] Ebel D. In *Meteorites and the early solar system II*. pp. 253–278.

5085

OIL-BEARING MICROMETEORITES FOR AN OILY-DUSTY PANTHALASSA

F. Dias[1] and M. Maurette[2]. [1]ENS-Cachan, 61 Av. Président Wilson, 94235 Cachan, France. E-mail: dias@cmla.ens-cachan.fr. [2]CSNSM, Bat. 104, 91405 Orsay Campus, France. E-mail: maurette@csnsm.in2p3.fr.

Introduction: We already argued that kerogen-rich Antarctic micrometeorites (AMMs) can be considered as "source rocks" for the formation of petroleum [1, 2], which are defined as fine clays with at least 0.5 wt% of kerogen [3]. Indeed, 99% of the AMMs are related to the volatile-rich hydrous-carbonaceous chondrites. They contain about 50% of hydrous silicates (i.e., "clays") and kerogen is their dominant organics (about 2.5 wt%). We next argued that micrometeoritic oil would accumulate on the top surface of Panthalassa (i.e., the early ocean), so as to form a new type of viscous-oily-dusty prebiotic soup looking like a gigantic black tide. As petroleum is the richest source of organics (about 100,000 distinct molecules) we thus wondered whether this micrometeoritic oil could behave as both a prebiotic soup and a catcher medium to trap fine-grained material and molecules "falling from the sky." Then hopefully this new soup could assist the synthesis of the giant macromolecules of pre-cellular life, i.e., proteins and the nucleic acids. After this conjecture, our next priority was to tackle the complex "dynamic" evolution of particles in Panthalassa coated with oil. Was the oily soup frequently dispersed or not by breaking waves and impacts produced during the period of the early massive bombardment? Indeed, it is likely that a quiet soup and a frequently "agitated" soup would not lead to the same prebiotic chemistry.

Fluid Motion Induced by Surface Waves: The calming effect of oil on water waves has been discussed by many authors, including Benjamin Franklin [4]. However, observations of this effect are relevant to small oily surfaces. Can they be extended to the unexplored situation where the whole surface of Panthalassa was an oily-dusty "skin"? No study has been reported yet about the effects of either a worldwide coverage of oil on Panthalassa or an oil thickness, $\Delta \sim 1$ m. We decided to perform simulations for fluid particle trajectories on several models consisting of two fluid layers that were described in [5]. In the case of moderate waves with height ≤3 m, the results show a strong influence of the oily layer in some cases but no influence in other cases. The critical parameters are the density of the oil and the thickness of the oily layer. When it comes to large-amplitude waves that can break, the computations are much harder and have not yet been performed. One expects the oil to disappear from the sea surface because it is washed down by breaking waves.

Challenges Ahead: There are at least two other important parameters that have not been considered here, i.e., surface elasticity and viscosity, which are unrelated. But the choice of their values is still very uncertain and requires further works. Even for water waves, using in the equations the molecular viscosity for oil-free water does not reproduce the proper damping of observed waves!

References: [1] Maurette M. 2006. *Micrometeorites and the mysteries of our origins*. Springer-Verlag. pp. 1–330. [2] Maurette M. et al. 2006. Abstract #1583. 37th LPSC. [3] Rondeel H. D. 2002. See www.geol.vu.nl. [4] Franklin B. 1774. *Philosophical Transactions of the Royal Society of London* 64:445–460. [5] Dias F. et al. 2003. Water-waves as a spatial dynamical system. In *Handbook of mathematical fluid dynamics*. North-Holland. pp. 443–499.

5235

ANALYSIS OF FACTORS CONTRIBUTING TO BULBOUS CAPTURE TRACKS FROM COMETARY DUST PARTICLES IN STARDUST AEROGEL COLLECTOR

Gerardo Dominguez[1], Josep M. Trigo-Rodríguez[2, 3], Mark J. Burchell[4], Fred Hörz[5], Jordi Llorca[6], Peter Tsou[7], and Bill Anderson[8]. [1]UC San Diego, Department of Chem. and Biochem., San Diego, CA 92093–0356, USA. E-mail:gdominguez@ucsd.edu. [2]Institute Space Sciences-CSIC, Campus UAB, Facultat de Ciències, Torre C5-parell-2ª, 08193 Bellaterra, Barcelona, Spain. [3]Institut d'Estudis Espacials de Catalunya (IEEC), Edif. Nexus, c/ Gran Capità, 2-4, 08034 Barcelona, Spain. [4]Centre for Astrophysics and Planetary Sciences, University of Kent, Canterbury, Kent CT2 7NH, UK. [5]Astromaterials Research and Exploration Science, NASA Johnson Space Center, Houston, TX 77058, USA. [6]Institut de Tècniques Energètiques. Universitat Politècnica de Catalunya. Diagonal 647, ed. ETSEIB. 08028 Barcelona, Spain. [7]Jet Propulsion Laboratory, California Institute of Technology, Pasadena, CA 91109–8099, USA. [8]Dynamic and Energetic Material Division, Los Alamos National Laboratory, MS P952, P.O. Box 1663, Los Alamos, NM 87545, USA.

Introduction: The capture of cometary dust grains in aerogel at the well-defined impact velocity of 6.1 km/s resulted in the production of a range of impact cavity morphologies. These tracks range from the classical carrot-shaped tracks (type A) seen in laboratory experiments with refractory-solid projectiles, to bulbous tracks with "turnip"-like properties and a stylus (type B), to bulbous stubby tracks (type C) [1, 2]. These morphologies must reflect the underlying variation in the structure and strength of cometary dust grains. The capture of cometary dust grains also presents the possibility that the chemical content of projectiles, in the form of volatiles that are released during capture, also contributed to bulbous track features, and analyses of the terminal particles and track residues suggest that the volatile content of the projectiles, released preferentially during capture, would have contributed to the range of morphologies seen in the Stardust cometary dust tracks. An additional contributor to track bulb production could come from particle fragmentation during capture and here we present a quantitative analysis of the factors that contribute to the production of bulbous impact cavities in aerogel.

Methods: We reviewed models of the energetics of capture and track formation in aerogel [3, 4]. The two track formation models that we examined were 1) the snowplow model presented in [4] and 2) an adiabatic vapor expansion model [5]. Both models predict track scaling characteristics in which the pressure (kinetic or thermal) decay strongly as a function of radius ($P \sim r^{-\alpha}$, where $\alpha \sim[3.3–4]$) but linearly as a function of the shock front or projectile size.

Conclusions: Based on entrance hole diameters, measured and catalogued in [2], we examined the departure of the ratio of apparent projectile diameter as inferred by the entrance diameter versus the maximum track diameter and the implied projectile size. Detailed analysis of the energetic requirements needed to explain the observed departures (bulbiness) of tracks indicates that a significant fraction of the original projectile would be vaporized. On the other hand, projectile fragmentation and spreading requires modest increases in the size of the shock front (which established the boundary conditions for the track) to explain the observed departures from conventional aspect ratios seen in carrot-shaped tracks. Thus we find that bulbous feature production is likely to be dominated by projectile fragmentation.

References: [1] Hörz et al. 2006. *Science* 234:1716–1719. [2] Burchell et al. *Meteoritics & Planetary Science*. Forthcoming. [3] Anderson and Ahrens. 1994. *Journal of Geophysical Research* 99:2063–2071. [4] Dominguez et al. 2004. *Icarus* 172:613–624. [5] Trigo-Rodríguez et al. *Meteoritics & Planetary Science*. Forthcoming.

5087

REVISITING THE QUESTION OF REDOX CHANGES IN ORDINARY CHONDRITES USING XRD-DERIVED MINERAL ABUNDANCES

T. L. Dunn and H. Y. McSween, Jr. Department of Earth and Planetary Sciences, University of Tennessee, Knoxville, TN 37920, USA. E-mail: tdunn@utk.edu.

Introduction: Early studies on redox state in ordinary chondrites suggested that chondrites became progressively reduced as metamorphism occurred (e.g., [1, 2]). This was later modified by [3], who proposed that equilibrated chondrites became progressively oxidized with increasing metamorphism, resulting in the formation of olivine at the expense of pyroxene [3]. Consequently, ratios of olivine to pyroxene modal abundances should increase with increasing petrologic type if oxidation occurred. Studies by [4, 5] observed this trend in a limited number of ordinary chondrite samples. However, a larger data set of chondrite modal abundances is necessary to confirm this hypothesis.

Few credible determinations of phase abundances in ordinary chondrites exist because of the difficulty associated with measuring accurate modes in fine-grained samples. Recently [5, 6] successfully applied a new X-ray diffraction technique for determining modal abundances of multiphase samples [7, 8] to a few carbonaceous and unequilibrated ordinary chondrites. This technique differs from traditional XRD in that it uses a position-sensitive detector (PSD), which allows for rapid and accurate collection of XRD patterns. Here, we use this technique to determine the modal abundances of equilibrated (types 4–6) L chondrites, and we apply these data to the question redox changes in ordinary chondrites.

Methodology: The PSD-XRD method for phase quantification uses a whole-pattern fitting procedure, which requires considerable data processing [8]. The amounts of individual phases are estimated by comparing peak intensities of a standard to those in the mixture [7]. Each standard pattern is decreased by the appropriate factor and subtracted from the mixture pattern. Provided well-matched standards are available, mineral abundances can be determined with a relative accuracy of ~1% for each phase [6].

Results: We determined modal abundance of nine L-type chondrites (three from each petrologic type) using the whole pattern fitting procedure described above. Modal mineralogies consist of olivine, low- and high-Ca pyroxene, plagioclase, troilite, and Fe-Ni metal. Average olivine abundances increase from 37.7 wt% in type 4 to 43.6 wt% in type 6, with type 5 abundances averaging 40.9 wt%. Low-Ca pyroxene abundances follow a comparable decreasing trend, with 21.2 wt% in type 4, 19.6 wt% in type 5, and 16.9 wt% in type 6. Ratios of Ol/Px vary slightly within each petrologic type but show an overall increase with increasing petrologic type. Ol/Px ratios range from 1.66–1.99 in type 4, 1.82–2.25 in type 5, and 2.36–2.69 in type 6. This systematic increase in Ol/Px suggests that oxidation, not reduction, occurred with progressive metamorphism in L-type ordinary chondrites. We expect forthcoming data from type LL and type H chondrites to yield comparable results.

References: [1] Brett R. and Sato M. 1984. *Geochimica et Cosmochimica Acta* 48:111–120. [2] Sears D. G. and Weeks K. S. 1983. *Journal of Geophysical Research* 88:B301–B311. [3] McSween H. Y., Jr. and Labotka T. C. 1993. *Geochimica et Cosmochimica Acta* 37:1105–1114. [4] Gastineau-Lyons H. K. et al. 2002. *Meteoritics & Planetary Science* 37:75–89. [5] Menzies O. N. et al. 2005. *Meteoritics & Planetary Science* 40:1023–1042. [6] Bland P. A. et al. 2004. *Meteoritics & Planetary Science* 39:3–16. [7] Cressey G. and Schofield P. F. 1996. *Powder Diffraction* 11:35–39. [8] Batchelder M. and Cressey G. 1998. *Clays and Clay Minerals* 46:183–194.

5150

IDENTIFICATION OF SILICATE AND CARBONACEOUS PRESOLAR GRAINS IN THE TYPE 3 ENSTATITE CHONDRITE ALHA81189

S. Ebata[1], T. J. Fagan[2], and H. Yurimoto[1]. [1]Department of Natural History Sciences, Hokkaido University, Sapporo 060-0810, Japan. E-mail: ebashin@ep.sci.hokudai.ac.jp. [2]Department of Earth Sciences, School of Education, Waseda University, Tokyo, Japan.

Introduction: Primitive meteorites contain presolar silicate grains that predate the formation of our solar system [1–6]. In 2006, Ebata et al. discovered the first evidence of presolar silicate grains from two type 3 enstatite chondrites [7]. The abundance of presolar silicates is higher in the ALHA81189. Because the sizes of presolar grains are small (~0.3 μm for silicate grains (e.g., [1–3]), presolar grains in situ determined isotopic composition and chemical composition have been limited. Here we report further in situ studies of presolar silicate and carbonaceous presolar grains in the primitive enstatite chondrite ALHA81189.

Experimental: The samples used in this study are polished thin sections of the ALHA81189. We surveyed presolar grains by isotopography using a Hokudai isotope microscope system (Cameca IMS-1270 + SCAPS [8]). For presolar grain identification, mineralogical and petrographical characterization of matrix areas containing isotopic anomalous grains has been conducted using a field emission type scanning electron microscope (JEOL JSM-7000F) equipped with energy dispersive X-ray spectrometer (Oxford INCA).

Results: The total analyzed areas of O-isotopography are ~41,000 μm^2. From the analyzed area, 10 presolar silicates were identified (volume abundance, ~22.0 ppm). Presolar carbonaceous grains were identified by C-isotopography: 7 grains in the analyzed area of ~36,600 μm^2 (volume abundance, ~17.2 ppm).

The size of presolar silicates is 0.2–0.5 μm (average, ~0.33 μm) and of carbonaceous grains is 0.2–1.2 μm (average, ~0.55 μm). Six of presolar silicates were determined the chemical compositions (enstatite, 2; Fe-rich pyroxene [En_{50}], 1; Fe-rich olivine [Fo_{30}], 1; SiO_2, 1; aggregates of pyroxene-like compositions, 1). The SiO_2 and aggregates may be amorphous. In the case of carbonaceous grains, three grains were determined the chemical compositions (graphite, 1; SiC, 2).

Discussion: The abundances of presolar silicate and carbonaceous grains in this study are ~60, 90% larger than the previous study [7], respectively. This is probably because of improvement of special resolution of isotopography using of smaller contrast aperture. The abundance is smaller than those of primitive carbonaceous chondrite and IDPs (e.g., [1, 5]).

The average size of presolar silicate grains of the enstatite chondrite is comparable with carbonaceous chondrites and IDPs (e.g., [1–3]). In the case of presolar carbonaceous grains, the average size is smaller than those from carbonaceous chondrites [9]. Presolar grains of pyroxene compositions are dominant in the enstatite chondrite, whereas olivine, pyroxene, and GEMS are equally distributed carbonaceous (e.g., [2, 3]), IDPs (e.g., [1]), and AMMs [10]. This suggests presolar silicates of enstatite composition were selectively survived in the enstatite parent body.

References: [1] Messenger et al. 2003. *Science* 300:105–108. [2] Nguyen and Zinner. 2004. *Science* 303:1496–1499. [3] Nagashima et al. 2004. *Nature* 428:921–924. [4] Mostefaoui and Hoppe. 2004. *The Astrophysical Journal* 613:L149–L152. [5] Kobayashi et al. 2005. *Antarctic Meteorites* 29. pp. 30–31. [6] Tonotani et al. 2006. Abstract #1539. 37th LPSC. [7] Ebata et al. 2006. Abstract #1619. 37th LPSC. [8] Yurimoto et al. 2003. *Applied Surface Science* 203-204:793. [9] Amari. 1994. *Geochimica et Cosmochimica Acta* 58:459–470. [10] Yada et al. 2006. Abstract #1470. 37th LPSC.

5326

PALEOMAGNETIC EVIDENCE FOR LOCALIZED CHONDRULE FORMATION AND RAPID PARENT BODY ACCRETION IN THE PROTOPLANETARY DISK

D. S. Ebel. Department of Earth and Planetary Sciences, American Museum of Natural History, New York, NY 10024, USA. E-mail: debel@amnh.org.

Introduction: Macroscopic chondrules and the microscopic matrix between them are the main components of chondritic meteorites, with bulk chemical compositions of most elements within a factor of two of the canonical solar composition. But various chondrites have different chondrule/matrix ratios, different dominant chondrule types, and different mean chondrule and matrix compositions [1]. Chondrules and matrix are chemically complementary, because when normalized to relative abundance, they sum to chondritic (i.e., solar) regardless of meteorite type.

"Complementarity" [2, 3] makes compelling the hypothesis that chondrules formed from the local heating of mineral dust aggregates, and that surrounding dust combined (without mixing with extra-local materials) with those chondrules to form parent bodies of ~solar composition. Thus chondrule formation is variably effective, highly localized, and subsequent accretion is rapid.

Other evidence supports this scenario. Observed differences in the physical, textural, and chemical properties of chondrules from different chondrite groups, and different chondrule cooling rates indicate relatively localized formation events [4]. Recent simulations indicate very rapid accretion rates of boulder-sized objects into planetesimals in disks [5]. Recent paleomagnetic data on individual chondrules also supports this scenario.

Results: Chondrules in Bjurböle (L/LL4) [6] and Allende (CV3) [7] have relatively stable natural remanent magnetization directions randomly oriented with respect to one another, and therefore were magnetized before accretion. Recent high-precision magnetic studies [8, 9] of ~10 chondrules separated from each of the Karoonda (CK4), Bjurböle, and Allende meteorites yield paleointensities that bear on the magnitude and spatial-temporal extent of magnetic fields in the early disk, the extent of magnetorotational instabilities promoting momentum and mass transport [10], and whether current sheets produced by MRI could heat chondrule precursors [11]. Allende and Karoonda give statistically significant paleointensity estimates, suggesting that a different field was experienced, in common, by the chondrules in each meteorite. Bjurbole chondrule paleointensities are also statistically distinct but are probably more a result of the intrinsic magnetic properties of the chondrules than ancient magnetic fields. These data support the hypothesis of localized chondrule formation and rapid accretion, consistent with "complementarity" [1–3].

References: [1] Hezel D. C. and Palme H. 2007. Abstract #1667. 38th Lunar and Planetary Science Conference. [2] Palme H. et al. 1992. 23rd Lunar and Planetary Science Conference. p. 1021. [3] Bland P. A. et al. 2005. *Proceedings of the National Academy of Sciences* 102:13,755–13,760. [4] Cuzzi J. N. and Alexander C. M. O'D. 2006. *Nature* 441:483–485. [5] Johansen A. et al. Forthcoming. [6] Kohout T. et al. 2006. Abstract #1601. 37th Lunar and Planetary Science Conference. [7] Sugiura N. et al. 1979. *Physics of the Earth and Planetary Interiors* 20:342–349. [8] Acton G. et al. 2007. Abstract #1711. LPSC. [9] Acton G. et al. 2007. 38th Lunar and Planetary Science Conference; *Journal of Geophysical Research* 102:1–19. [10] Balbus S. 2003. *Reviews in Astronomy & Astrophysics* 41:555–597. [11] Joung M. K. R. et al. 2004. *The Astrophysical Journal* 606:532–541.

5004

MATHEMATICAL MODELS AND NUMERICAL ESTIMATIONS FOR TSUNAMI GENERATED AT CHICXULUB, MEXICO

J. C. Echaurren. Codelco Chile Chuquicamata, North Division. E-mail: jecha001@codelco.cl.

Introduction: Chicxulub [1] is among the largest impact craters on Earth. This exceptionally well-preserved crater is located in the peninsula of Yucatan in Mexico. Research has identified at least 3 concentric structural rings which comprise a complex ~200 km diameter impact basin. The aim of this work is to realize numerical estimations for the tsunami generated at Chicxulub after the impact of an asteroid (or comet). These estimations are realized according to the models used by Ward and Asphaug [2] for asteroid impact tsunami. Velocity, period, wavelength, energy, diameter of the cavity, and maximum tsunami height for a peak amplitude will be estimated.

Analytical Method and Results: Considering $R_D = 2^{0.5} R_C$ and $k_{max} = 2\pi/2.11\ R_C$, where R_C and R_D are the inner and outer radii of the cavities in the impact, is possible to estimate the velocity for the peak amplitude tsunami as [2],

$$u(k_{max},h) = c(k_{max})[0.5 + k_{max}h/\sin h(2k_{max}h)] \sim 374.03 \text{ km/h},$$

where $c(k_{max}) = v_t[\tan h(k_{max}h)/k_{max}h]0.5$, $v_t = (gh)^{0.5}$ and h = ocean depth ~1.1 km. The frequency associated to this peak amplitude tsunami is expressed as [2],

$$\omega_{max} = [gk_{max}\tan h(k_{max}h)]^{0.5} \sim 3.09E - 3 \text{ Hz}.$$

According these results, the period t_{max} and wavelength λ_{max} associated with this peak amplitude are estimated in ~323.11 s and ~33.56 km, respectively. The tsunami energy is estimated as [2],

$$E_T = (1/3)\pi\rho_W g(D_C R_C)^2 \sim 1.81E20 \text{ J} \sim 43.2 \text{ gigatons of TNT},$$

where ρ_W ~1027 kg/m^3 and D_C is the initial cavity depth. The transient diameter of the cavity [2] is expressed according, $d_c = 2R_I(2\varepsilon V_I^2/gR_I)^{\delta}(\rho_I/\rho_W)^{1/3}(\rho_W/\rho_I)^{1/3-\delta}(1/qR_I^{\alpha-1})^{2\delta} \sim 42.7$ km, R_I, V_I, and ρ_I being impactor radius, impactor velocity, and impactor density, respectively. Besides, laboratory adjustments [2] are realized for the parameters α, $\delta = 1/2(1 + \alpha)$ and q as 1.27, 0.22, and 0.0077 respectively. The maximum tsunami height [2] is

$$u_z^{max}(r, R_I) = D_C[1/(1 + r/R_C)]^{0.5 + [(\chi 1) - 0.5]e^{-[(\chi 2)Rc/h]}}$$

where $\chi 1$ ~1.075 and $\chi 2$ ~0.035. In this formula $u_z^{max}(r;R_C) \to 1.3$ km as $r \to 0$, $u_z^{max}(r;R_C)$ ~911.11 m if $r = R_C$, $u_z^{max}(r;R_C)$ ~825.56 m if $r = 2^{0.5}R_C$ and $u_z^{max}(r;R_C)$ ~748.04 m if $r = (2^{0.5}R_C) + 50$ km. Is possible too, to work with the models used by Shuvalov [3], where the wave amplitude for the tsunami is calculated as $h = 45(H/L)Y^{0.25}$, h being (in this case) the wave amplitude in meters, H being the water basin depth, L being the distance from the source, and Y being the released energy in kilotons TNT equivalent. Though the results are different, both cases are interesting for the numerical estimations realized in the tsunami generated on Chicxulub.

References: [1] Pope K. O., Ocampo A. C., Kinsland G. L., and Smith R. 1996. *Geology* 24:527–530. [2] Ward S. N. and Asphaug E. 1999. *Icarus* 145:64–78. [3] Shuvalov V. V. 2003. Abstract #4131. Large Meteorite Impacts Conference.

5003

NUMERICAL ESTIMATIONS FOR IMPACT CONDITIONS ON CAMPO DEL CIELO, CRATER FIELD, SOUTH AMERICA

J. C. Echaurren. Codelco Chile Chuquicamata, North Division. E-mail: jecha001@codelco.cl.

Introduction: The aim of this work is to estimate the impact conditions for Campo del Cielo's crater 3. The Campo del Cielo crater field is located in Argentina (S27°35′, W61°40′). It contains at least 20 small craters, the largest of them being crater 3, which has a diameter of ~103 m [1]. The crater field covers a 19 × 3 km area. The craters were formed about 4000 years ago by fragments of an IA-type meteorite. The mathematical model used here is applied in quantum formalism, polynomial elements, and Korteweg-DeVries (KDV) soliton theory [2]; also included are mass distributions for the calculation of ejected fragments using a HP 49 g, which is a Scientific Programmable Graphing Calculator with 1.5 Mb in RAM memory. Other craters in this field will be studied in future works. Then, for both, the impact event and estimations are used the diameter of crater 3, elliptical shape, and basement composition ~ clay.

Analytical Method and Results: According this model [2], the diameter of this piece of asteroid is ~3.34 m, with velocity and impact angle on the terrestrial surface of ~3.41 km/s and 11.07°, respectively. The number of rings on the crater are calculated as ~0.1, with a initial crater profundity of ~12.99 m; this quantity could be altered across the passage of time to ~3.28 m. The melt volume is ~18,156.68 m^3, or ~0.000018 km^3. The number of ejected fragments is estimated to be ~321.07, with average sizes of ~0.49 m and a cloud of dust with a diameter of ~1.06 km. The total energy of the impact is estimated to be from ~1.07E21 Erg (~25.4 kiloton) to 1.25E21 Erg (~29.81 kiloton). Before the erosion effects the transient crater is estimated as ~20.11 m; the possible hydrothermal zone (hydrothermal systems) is ~2.11–10.06 m from the nucleus of impact. The lifetimes estimated for this possible hydrothermal zone are ~502 to ~784 years with uncertainties of ~±1.74% to ±4.56%, i.e., from ±8.76 years to ±35.74 years. Possible hydrothermal temperatures from 0.25 to 1400 years are estimated as ~257.06 to 7.68 °C, respectively. The fragments are ejected ~307.85 m from the impact center, with an ejection velocity of ~298.8 m/s. The density of this piece of asteroid is estimated as ~7.25 g/cm^3, i.e., approximately 92.15% Fe. Using linear interpretation, the seismic shock wave magnitude is estimated from ~4.88 to ~4.96 in the Richter scale. The maximum time of permanency for the cloud of dust and acid in the atmosphere is ~9.02 hours and 1.88 days, respectively. The pressure in the final crater rim is estimated as ~0.98 GPa, and the creation time of the final crater is carried out from ~3.24 to ~31.89 s. These results are estimations based exclusively in empirical information, mathematical models, and previous works in this area. More complete results with better precision will be presented in future works.

References: [1] Paillou P., Barkooky A. E., Barakat A., Malezieux J., Reynard B., Dejax J., and Heggy E. 2004. *Comptes Rendus Geosciences* 336: 1491–1500. [2] Echaurren J. C. and Ocampo A. C. 2003. *Geophysical Research Abstracts*, vol. 5, 04450. EGS-AGU-EUG Joint Assembly.

5220

EVIDENCE FOR A NON-CHUR INITIAL Nd ISOTOPIC COMPOSITION FOR THE MOON

J. Edmunson[1] and L. E. Nyquist[2]. [1]Institute of Meteoritics, University of New Mexico, NM, USA. E-mail: Edmunson@unm.edu. [2]NASA Johnson Space Center, USA.

Introduction: Samarium-Nd dating of Mg-suite troctolites 76335 [1] and 76535 [2] indicate relatively young ages and initial epsilon Nd values within error of the Chondritic Uniform Reservoir (CHUR). The difficulty in this lies in the interpretation of the formation of KREEP as well as the established petrologic relationships between the Mg-suite rocks (e.g., [3]). According to [4, 5], the lunar KREEP component, found in Mg-suite norites and some younger KREEP-rich samples with negative epsilon Nd values relative to CHUR, formed from a CHUR-like reservoir at 4492 ± 61 Ma ago. In contrast, KREEP in the troctolites had to form either from a CHUR source at about 4278 Ma ago, or as a mixture of KREEP with a different magma than is responsible for the norites, or KREEP formed from a source with an initially positive epsilon Nd value relative to CHUR.

Observations: Given the petrologic relationship between Mg-suite rocks, it is expected that their sources should be isotopically related. In an age versus initial epsilon Nd diagram, the sources of the norites and troctolites of the Mg-suite share an evolution line with a $^{147}Sm/^{144}Nd$ ratio of 0.165 ± 0.017. This is in agreement with the $^{147}Sm/^{144}Nd$ ratio of 0.163 estimated for KREEP from [6]. The Mg-suite trend intersects the CHUR evolution line at 4318 ± 85 Ma. However, the fact that norites 78238, 78236, and 15445,17 are older than 4318 Ma; that 78236 and 15445,17 have positive epsilon Nd values relative to CHUR; and that Apollo 16 FANs have positive epsilon Nd values, indicates that the CHUR Nd isotopic composition [7] may be inappropriate for lunar data. The calculated formation age of KREEP for an HED Nd isotopic composition of the bulk Moon [8], +0.83 epsilon units relative to CHUR, using the same Mg-suite source evolution line indicates KREEP formed at 4518 ± 85 Ma.

Implications: A HED bulk Moon Nd isotopic composition may indicate a lunar magma ocean origin for most, but not all, Apollo 16 FANs and accounts for the isotopic composition of norite 15445,17. This isotopic composition is also in agreement with Archean rocks on Earth (e.g., [9]). The KREEP model age is concordant with estimates by [10, 11]. The approach used in determining the model age implies that none of the source region lithology REE signature of the Mg-suite rocks remains after its interaction with KREEP. Although the KREEP evolution line overlaps some of the older non-Mg-suite KREEP-rich samples, it does not overlap younger KREEP-rich samples (i.e., NWA 773). Therefore, either the geochemical signature of NWA 773 is not indicative of primary KREEP formation, or this model does not accurately reflect the relationship between old Mg-suite samples and young KREEP-rich rocks.

References: [1] Edmunson J. et al. 2007. Abstract #1962. 38th Lunar and Planet. Sci. Conference. [2] Lugmair G. W. et al. 1976. 7th Lunar Sci. Conference. pp. 2009–2033. [3] Dymek R. F. et al. 1975. 6th Lunar Sci. Conference. pp. 301–341. [4] Borg L. E. et al. 2005. Abstract #1026. 36th Lunar and Planet. Sci. Conference. [5] Edmunson J. and Borg L. E. 2006. Abstract #4034. Workshop on Early Planetary Differentiation. [6] Warren P. H. 1989. LPI Technical Report #89-03. pp. 106–110. [7] Jacobsen S. B. and Wasserburg G. J. 1984. *Earth and Planetary Science Letters* 67:137–150. [8] Nyquist L. E. et al. 2006. *Geochimica et Cosmochimica Acta* 70:5990–6015. [9] Nägler Th. F. and Kramers J. D. 1998. *Precambrian Research* 91: 233–252. [10] Nyquist L. E. and Shih C.-Y. 1992. *Geochimica et Cosmochimica Acta* 56:2213–2234. [11] Taylor D. J. et al. 2007. Abstract #2130. 38th Lunar and Planet. Sci. Conference.

5024

TWO CONTRASTING NUCLEATION AND GROWTH SETTINGS INDUCED BY DYNAMIC HIGH-PRESSURE PHASE TRANSITIONS OF OLIVINE TO RINGWOODITE AND WADSLEYITE IN SHOCKED L6 CHONDRITES

A. El Goresy[1], N. Miyajima[1], M. Miyahara[2], E. Ohtani[2], T. Ferroir[3], Ph. Gillet[3], and M. Chen[4]. [1]Bayerisches Geoinstitut, Universität Bayreuth, 95447 Bayreuth, Germany. E-mail: ahmed.elgoresy@uni-bayreuth.de. [2]Tohoku University, Sendai 980-8578, Japan. [3]ENS-Lyon, 69364 Lyon, France. [4]Guangzhou Institute of Geochemistry, CAS, Guangzhou 510640, China.

Introduction: We conducted detailed investigations on the textures and compositions of olivine to ringwoodite and wadsleyite phase transitions in shocked L chondrites using reflected light microscopy, SEM-BSE, electron microprobe, laser microRaman mapping, and FIB-TEM techniques. We recognize two co-existing but contrasting settings in two different lithologies entrained in and adjacent to shock-melt veins: 1) intracrystalline lamellae of ringwoodite or both ringwoodite and wadsleyite in large individual olivine crystals [1–3], and 2) unique concentric to semi-concentric arrangements of both dense polymorphs in porphyritic olivine chondrules. The porphyritic olivine crystals entrained in the melt vein transformed to concentric intergrowths of Fa-rich ringwoodite shells (10–25 μm wide) enclosing Fa-poor wadsleyite-rich cores.

Results: 1) Intracrystalline ringwoodite lamellae are encountered in olivines in shock-melt veins both in the Sixiangkou and Peace River chondrites [3]. Textures, orientation, and structure reported here and before [1–3] are distinct from the ambiguous features in Tenham L6 chondrite claimed by [4] to be lamellar ringwoodite. The straight lamellae in the Sixiangkou olivines are polycrystalline with crystallite sizes <250 nm. Few ringwoodite crystallites at the interface between ringwoodite lamellae and parental olivine display a novel topotaxial intergrowth: (400) ringwoodite // (131) olivine. This intergrowth was not reported previously from naturally shocked samples nor produced experimentally. There is considerable lattice mismatch between ringwoodite and olivine: d_{400} ringwoodite = 0.21 nm, d_{131} olivine = 0.25 nm. The topotaxial intergrowth is inferred to be the remnant of the original coherent growth texture that commenced at the olivine-ringwoodite interface but was considerably consumed by the growing ringwoodite in the lamellae interiors. 2) TEM studies of FIB cuts of ringwoodite-wadsleyite concentric intergrowths in former olivines in porphyritic olivine chondrules in Peace River revealed coarse-grained (<600 nm) granoblastic ringwoodite-wadsleyite crystallite fabric with triple junctions and contrasting compositions: Fo-poor ringwoodite ($Fa_{30–39}$) with stacking faults along (110) and Fa-poor wadsleyite ($Fa_{07–09}$), latter barren of any stacking faults. Both the Mg*-rich wadsleyite in the cores of original olivines and the Mg*-poor ringwoodite at the outer rims of the original olivines are interpreted to have crystallized from the chondritic melt. The formation of the olivine high-pressure polymorphs was hence not strictly a solid-state transformation process but also involved interaction with the chondritic liquid at high pressures and temperatures.

References: [1] Chen M. et al. 2004. *Proceedings of the National Academy of Sciences* 101:15,033–15,037. [2] El Goresy A. et al. 2005. *Meteoritics & Planetary Science* 40:A43. [3] El Goresy A. et al. 2006. *Meteoritics & Planetary Science* 41:A50. [4] Xie Z. and Sharp T. G. 2007. *Earth and Planetary Science Letters* 3-4:433–445.

5222

MAGNETIC PROPERTIES OF THE BOSUMTWI IMPACT STRUCTURE, GHANA

T. Elbra[1], S. Danuor[2], and L. J. Pesonen[1]. [1]Division of Geophysics, University of Helsinki, Helsinki, Finland. E-mail: tiiu.elbra@helsinki.fi. [2]Department of Physics, Kwame Nkrumah University of Science and Technology, Kumasi, Ghana.

Introduction: The rock magnetic properties, including hysteresis measurements, of impactites and target rocks from two hard-rock drill cores obtained by the Bosumtwi Crater Drilling Project, and exposed surface samples near the inner rim, have been investigated and compared to understand the formation mechanism and magnetic signature of the 1.09 Ma old Bosumtwi impact structure in Ghana.

Results: Core samples and exposed rocks from northern rim area indicate similarities in magnetic susceptibility and remanence data. In both cases the magnetic susceptibility (below 500 E^{-6} SI) and natural remanent magnetization (NRM; 0.1–100 mA/m) are relatively weak. Only a very small, inhomogeneously distributed ferrimagnetic component with higher susceptibility and remanence values is present within target lithologies of the cores. However, the large-scale differences between core samples and surface rocks appear in magneto-mineralogy. In all core sample lithologies the magnetic properties are carried by pyrrhotite. Instead, the surface samples indicate that the main carrier is titanomagnetite and not pyrrhotite. To get further insights the new target-rock samples from previously unstudied areas of southern rim were collected. These new samples are currently analyzed to understand the differences existing in core and surface samples (e.g., surface-near alteration of pyrrhotite), and to provide new input data for modeling and interpreting the aeromagnetic and shipborn anomaly patterns.

5121

A CORE-COLLAPSE SUPERNOVA AS THE SOURCE OF SHORT-LIVED RADIONUCLIDES IN THE SOLAR SYSTEM

C. I. Ellinger[1], S. J. Desch[2], and N. Ouellette[1]. [1]Department of Physics, Arizona State University, Tempe, AZ, USA. E-mail: carola.ellinger@asu.edu. [2]School of Earth and Space Explorations, Arizona State University, Tempe, AZ, USA.

A type II supernova seems to be the likely source of the short-lived radionuclides (SLRs) in the solar system (^{26}Al, ^{36}Cl, ^{41}Ca, ^{53}Mn, ^{60}Fe, ^{107}Pd, ^{129}I, ^{182}Hf) [1]. In this scenario a massive star is believed to have gone supernova within a few tenths of a parsec, injecting some of its ejecta into the forming solar system. Preliminary to extensive calculations have been done using computed supernova ejecta to reproduce the abundances of SLRs in meteorites [2–4]. The progenitor star is usually divided in two using a mass cut, such that all the ejecta outside of this mass cut (or at least a fraction thereof) is included and everything inside of it is not. This way the abundances of some (usually 4–5), but not all, SLRs can be more or less accurately reproduced [2–4].

Here we carry the idea of a mass cut further and divide computed supernova ejecta into 4 zones (an excluded remnant, an outer envelope, and two intermediate zones) to calculate the resulting abundances of SLRs. Isotopic abundances were taken from [5]. The contributions from each zone were optimized using χ^2 fitting to the meteoritic abundances of SLRs. The distance d to the supernova and the time delay Δt before the formation of solids were considered free parameters. Results for a 21 $M_\odot$ progenitor are shown below. The figure shows that $\chi^2 = 1$ for d ~0.1–0.3 pc and t ~0.4–0.7 Myr. Progenitor stars a little bit more and less massive that 21 $M_\odot$ also yield good agreements. We will present further results of our calculations and discuss some of their possible implications.

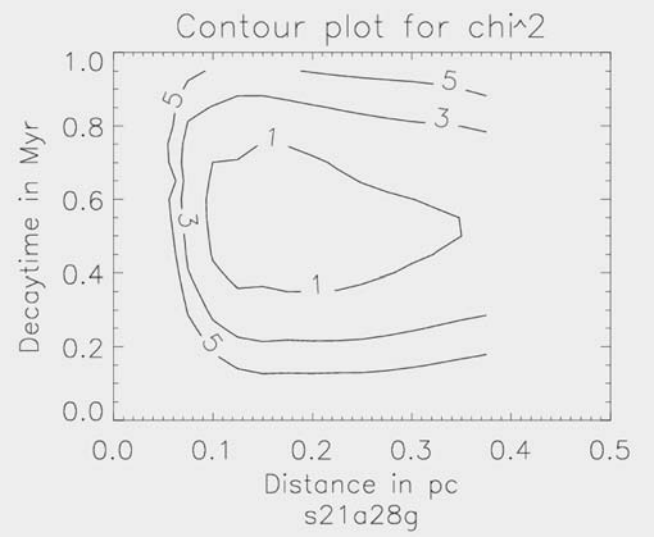

Fig. 1.

References: [1] Wadhwa M. et al. 2007. *Protostars and planets V.* pp. 835–848. [2] Meyer B. S. and Clayton D. D. 2000. *Space Science Reviews* 92:133–152. [3] Takigawa A. et al. 2007. Abstract #1720. 38th Lunar and Planetary Science. [4] Looney L. W. et al. 2006. *The Astrophysical Journal* 652:1755–1762. [5] Rauscher T. et al. 2002. *The Astrophysical Journal* 576:323–348.

5263

SIGNIFICANCE OF BUSHVELD INLIERS: EVIDENCE FOR IMPACT AND FOR CRATER MODIFICATION BY COLLAPSE OF CENTRAL UPLIFT AND PEAK RING

W. E. Elston. Department of Earth and Planetary Sciences, MSC03 2040, University of New Mexico, Albuquerque, NM 87131–0001, USA. E-mail: welston@unm.edu.

The 2.06 Ga Bushveld impact cluster created a nearly 200 km lobate transient multi-ring crater, followed by collapse of its central uplift(s). Subsequently, overflows from a Sudbury-type meltpool, mixed with sedimentary material, overtopped the collapsing peak ring and collected in the ~300 km first outer ring as the basal ~200 m of the Dullstroom Formation (Rooiberg Group), earliest member of the Bushveld Complex. Its basal contact was later invaded by massive sills of mafic cumulates (Rustenburg Layered Suite [RLS]) and granite (Lebowa Granite Suite [LGS]), generated at the head of an impact-induced mantle upwelling. Floods of LGS also obscured most of the meltpool. Rheomorphism and metamorphism destroyed the basal Dullstroom zones, and thereby most of the direct evidence for impact, in all but three places: a) in three paleochannels at the type section, preserved beneath RLS [1], and (b, c) in paired deformed and undeformed inliers of pre-Bushveld rocks, tens of kilometers across, which survived LGS flooding at the margins of the eastern and western lobes of the transient crater [2].

The rocks of the inliers belong to the Proterozoic Pretoria Group, but their most conspicuous formation, the ~500 m Magaliesberg Quartzite, is missing. In the deformed inliers, pre-Magaliesberg formations are metamorphosed to pyroxene facies, isoclinally folded, and complexly faulted. They are interpreted as segments of the collapsed central uplift. In the undeformed inliers, brecciated but undeformed post-Magaliesberg formations, topped by basal Dullstroom zones (proximal facies), are interpreted as segments of the collapsed peak ring.

In the strike-slip fault zone that juxtaposes the eastern deformed and undeformed inliers, chaotic slabs of post-Magaliesberg quartzite, meters to hundreds of meters long, broke off the undeformed inlier and became engulfed by hot inflated explosive overflows from the meltpool. These became the basal zones of the Dullstroom Formation. Overflow deposits are mixtures, in varying proportions, of superheated upper and lower crust and quartz and argillic material of sedimentary provenance, in every stage of recrystallization and melting. Heat and cataclasis obliterated evidence of shock. The time of the Bushveld impact is bracketed between the end of sedimentation of the Pretoria Group and the coming-to-rest of the basal zones of the Dullstroom Formation.

It is proposed that Magaliesberg and post-Magaliesberg formations, detached from the collapsing central uplift, caused overflows from the meltpool and became the source of the dominant sedimentary components in basal zones of the Dullstroom Formation.

The above interpretations explain three of the most enigmatic Bushveld problems: a) the juxtaposition of intensely deformed and relatively undeformed units of the Pretoria Group in the inliers, b) the absence of the Magaliesberg Formation in the inliers, and c) the source of the dominant sedimentary components of the basal zones of the Dullstroom Formation.

References: [1] Schweitzer J. K. et al. 1995. *South African Journal of Geology* 98:245–255. [2] Hartzer F. J. 2000. Geological Survey of South Africa Memoir #88. 222 p.

5252

A CONCORDIA ANTARCTIC MICROMETEORITE USED AS A COMETARY PROXY FOR THE ANALYSES OF COSIMA ONBOARD ROSETTA

C. Engrand[1], C. Briois[2], L. Thirkell[2], and H. Cottin[3]. [1]CSNSM, 91405 Orsay Campus, France. E-mail: Cecile.Engrand@csnsm.in2p3.fr. [2]LPCE - UMR CNRS 6115, 3A Av. de la Recherche Scientifique, 45071 Orléans Cedex, France. [3]LISA Univ. Paris 12 and Paris 7, 61 Ave. Gal de Gaulle, 94010 Créteil Cedex, France.

Introduction: The Rosetta spacecraft was launched in 2004 and aims at comet 67P/Churyumov-Gerasimenko in 2014. A time-of-flight secondary ion mass spectrometer (TOF-SIMS) instrument, COSIMA (COmetary Secondary Ion Mass Analyzer), is on board Rosetta and is dedicated to the in situ analysis of cometary dust grains [1]. Cometary grains will be collected on a variety of metallic targets (silver, gold, palladium, and platinum) and an optical system (COSISCOPE) will identify the cometary grains to be further analyzed by COSIMA. To help the interpretation of the cometary data in 2014, calibration laboratory work has started using the reference model of COSIMA in Lindau (Germany) and the prototype of COSIMA in Orléans (France). This work includes the construction of a database of spectra for common inorganic (olivines, pyroxenes, iron sulfides, etc.) and organic (amino acids, kerogens, etc.) compounds. Here we report the analysis with the COSIMA prototype in Orléans of a fragment of Concordia micrometeorite #03-31-Y that was previously used for consortium studies in France in the frame of the Stardust sample return [2, 3].

Methods and Results: COSIMA has a mass resolving power ($M/\Delta M$) of about 2000 at $M = 100$ amu, and the size of the primary ion beam is around 50 µm. The TOF-SIMS technique is very sensitive to surface contamination as it only analyzes the first mono-layers of the sample. TOF-SIMS spectra are difficult to interpret as they contain a very large amount of information, showing both elemental and molecular masses up to masses ~1000 amu. A first step in extracting information on the nature of minerals analyzed by COSIMA required the use of a statistical treatment of the spectra [4, 5]. In this work, we have used the COSIMA prototype based in Orléans to analyze a 30 µm fragment of a Concordia micrometeorite (#03-31-Y) used as a proxy for a cometary grain. The sample was pressed in a silver foil in clean conditions, yielding a ~50 µm crushed sample. Contamination control spectra were taken on the silver foil outside of the sample area. COSIMA positive spectra mainly show significant Mg^+, Si^+, Ca^+, and Fe^+ peaks associated with silicate minerals present in the micrometeorite, and the H_3O^+ peak at mass 19. The H_3O^+ signal is correlated with the micrometeorite signal, suggesting that hydrogen ions coming from the micrometeorite's hydrated silicates or from its organic matter are measured. Because of the large size of the primary beam, the signal/background ratio (defined as the ratio of the largest sample peak to the highest target peak) reaches only 0.05. Negative spectra taken on the same grain mainly show signatures of sulfur-bearing compounds (S^-, SO_2^-, SO_3^-, and SO_4^-) probably related to the presence of Fe-Ni sulfides, and organic compounds possibly indigenous to the micrometeorite (e.g., C_2H^-, CN^-). Higher statistics spectra will have to be acquired in order to possibly detect minor elements and organics.

References: [1] Kissel J. et al. *Space Science Reviews.* Forthcoming. [2] Duprat J. et al. *Advances in Space Research.* Forthcoming. [3] Gounelle M. et al. 2006. Abstract #1613. Lunar Planet. Sci. XXXVII. [4] Engrand C. et al. 2004. *Applied Surface Science* 231:883–887. [5] Engrand C. et al. 2006. *Rapid Communications in Mass Spectrometry* 20:1361–1368.

5331

A MARINE MAGNETIC STUDY OF THE ILE ROULEAU IMPACT STRUCTURE, LAKE MISTASSINI, QUEBEC, CANADA

J. Evangelatos[1, 2], K. E. Butler[2], and J. G. Spray[1, 2]. [1]Planetary and Space Science Centre. E-mail: j.evan@unb.ca. [2]Department of Geology, University of New Brunswick, Fredericton, NB, E3B 5A3, Canada.

Introduction: Ile Rouleau (also known as Mintunikus Island) was categorized as an impact structure following the discovery of shatter cones on the subcircular, 1 km diameter island located in Lake Mistassini, Canada [1]. The structure is hosted in the Paleoproterozoic dolomite-rich Lower Albanel Formation and has an uncertain age predating the Pleistocene. Geological mapping suggests that Ile Rouleau is a central peak structure characteristic of complex craters with a diameter limited to 5 km. This size coincides with the boundary between simple and complex crater forms, and thus provides a rare opportunity to study the magnetic signature of an impact crater in this transitional size.

Acquisition: In late June of 2006, we acquired 288 line-km of bathymetric and marine magnetic data in a 6.5 × 10 km area surrounding Ile Rouleau using an acoustic depth sounder and an Overhauser-type proton precession magnetometer. The magnetometer was towed at surface 30 m behind a 5 m aluminum boat. For positioning and navigation, we used a DGPS receiver providing submeter accuracy with the aid of CDGPS differential corrections. Magnetic field measurements were obtained at intervals of 1 second or approximately 4–5 m along each line. Survey lines, oriented both perpendicular and parallel to the regional geological structure, were spaced 100 m apart within 2.5 km of the island and 300 m apart at greater distances to sample the regional signal.

Results and Discussion: Water depths were typically 5–80 m but reached up to 140 m in a narrow trench striking NNE to the west of Ile Rouleau. Our map of the residual total magnetic field shows several coherent anomalies with amplitudes in the range of 10–50 nT. The most prominent feature is a high-amplitude anomaly that wraps around the western side of Ile Rouleau and correlates with an abrupt change in bathymetry. To the east, an arc-like anomaly that may be impact-related parallels the island 100 m from shore. This feature is locally transected by faulting. NNE-SSW trending anomalies, resolvable throughout the survey area, parallel the glacially shaped long axis of Lake Mistassini and thus may be related to glacial landforms on the lake bed. Measurements of the magnetic susceptibility of bedrock samples collected on site are practically negligible ($<10^{-6}$ SI units). Therefore, we argue that magnetic till, which overlays much of North America, is responsible for the regional short-wavelength features in our area of study [2].

Future Work: We are currently working to differentiate impact-related anomalies from the overprinting effects of glacial landforms, bathymetry, and the underlying Archean basement. Forward modeling of impact-related anomalies will follow with the intent of resolving faults and other magnetic sources at the Ile Rouleau impact site.

References: [1] Caty J. L., Chown E. H., and Roy D. W. 1976. *Canadian Journal of Earth Sciences* 13:824–831. [2] Gay S. P., Jr. 2004. *The Leading Edge* 23:542–547.

5204

FORMATION OF SYMPLECTITE-LIKE INCLUSIONS BY DIRECT QUENCHING FROM IGNEOUS LIQUID IN LUNAR METEORITE NWA 773

T. J. Fagan. Department of Earth Sciences, Waseda University, Tokyo, Japan, 169-8050. E-mail: fagan@waseda.jp.

Introduction: Symplectites are finely intergrown minerals with curved surfaces which formed by rapid breakdown of a pre-existing phase. Fayalite+hedenbergite+silica symplectites have been observed in lunar and Martian meteorites and in returned samples from the Moon, and are commonly attributed to breakdown of pyroxferroite [1–4]. Pyroxferroite is a pyroxenoid that forms metastably during rapid cooling of a liquid that has evolved to very low Mg/(Mg + Fe); subsequently the pyroxferroite breaks down to form fayalite+hedenbergite+silica symplectite (see [1–4]; but also see [5]). Key observations for the pyroxferroite breakdown petrogenesis are the uniform modal distribution and stoichiometry of fayalite, hedenbergite, and silica, such that modal recombination of these phases yields a pyroxferroite composition [4].

Symplectite clasts have been identified in the breccia of lunar meteorite Northwest Africa (NWA) 773 and paired meteorites [6, 7]. Many of the NWA 773 symplectites apparently formed by pyroxferroite breakdown as described above. However, deviations from silica stoichiometry in some silica-rich blebs associated with the symplectite suggest a different origin—namely, direct quenching from silicate liquid.

Analytical Methods: One polished thin section (on loan from M. Killgore of the University of Arizona) was studied by petrographic microscope, backscattered electron and elemental imaging, and quantitative elemental analyses. Imaging and analyses were collected using a JEOL JXA-8900 electron microprobe at Waseda University.

Results and Discussion: Several symplectite clasts with uniform distributions of hedenbergite, fayalite, and silica are present in the NWA 773 breccia. One large clast has a texturally distinct core composed of a fayalite (Fa_{98}) crystal with abundant, blebby inclusions. Elemental mapping shows that the symplectite surrounding the fayalite core is essentially free of K and Al, whereas K and Al are concentrated in the blebby inclusions. The blebby inclusions do not have feldspar stoichiometry (~3.4 Si, 0.6 Al, and 0.5 K atoms per 8 oxygen, respectively). Detailed mapping shows elongate SiO_2 crystals present within some inclusions. The lobate shape of the inclusions, deviations from stoichiometry, and presence of silica microphenocrysts suggest an origin by direct quenching from liquid, without an intervening pyroxferroite stage.

Other lithic clasts with low Mg/(Mg + Fe) in the NWA 773 breccia are characterized by high-Ba K-feldspar [6]. This variety of evolved clasts reflects a diversity of processes during late-stage solidification of evolved lunar magma. The variety of clasts in NWA 773 may have resulted from more than one magmatic system, or from immiscibility of late-stage liquids, among other processes.

References: [1] Burnham C. W. 1971. Proceedings, 2nd Lunar Sci. Conf. pp. 47–57. [2] Rubin A. E. et al. 2000. *Geology* 28:1011–1014. [3] Aramovich C. J. et al. 2002. *American Mineralogist* 87:1351–1359. [4] Warren P. H. et al. 2004. *Meteoritics & Planetary Science* 39:137–156. [5] Xirouchakis D. et al. 2002. *Geochimica et Cosmochimica Acta* 66:1867–1880. [6] Fagan T. J. et al. 2003. *Meteoritics & Planetary Science* 38:529–554. [7] Zeigler R. A. et al. 2007. Abstract #2109. Lunar Planet. Sci. Conf. XXXVIII.

5205

ROLES OF CHONDRULE FORMATION AND PARENT BODY METAMORPHISM DURING EQUILIBRATION OF EH CHONDRITES

T. J. Fagan[1], S. Kataoka[1], Y. Takahashi[1], and K. Matsui[2]. [1]Department of Earth Sciences, Waseda University, Tokyo, Japan, 169-8050. E-mail: fagan@waseda.jp.

Introduction: Mild variations in extent of equilibration—generally considered metamorphic grade—have been identified in ordinary [1–3] and carbonaceous chondrites [4, 5]. In contrast, subtle variations in equilibration of enstatite chondrites have been difficult to characterize [6–8]. In this study, we combine chondrule type with abundance of SiO_2-rich rims, Fe/(Mg + Fe) of mafic silicates, and speciation of silica to characterize equilibration in EH chondrites. Some of our observations are best explained by variations during chondrule formation—not parent body metamorphism.

Analytical Methods: Chondrule types were identified in polished thin sections of four EH3 chondrites (ALHA81189, MET 01018, ALH 84170, and PCA 82518) and one EH5 chondrite (St. Marks). Elemental maps collected by electron microprobe (JEOL JXA-8900 at Waseda University) were combined with petrographic microscope observations to identify classical chondrule type (PP, POP, RP, etc.), presence or absence of a SiO_2-rich rim, and fragmented versus whole chondrules. Silica polymorphs were identified (same samples except for MET 01018) by Raman spectroscopy (Jobin Yvon LabRam300 Raman microspectrometer). EPMA was used to determine Fe/(Mg + Fe) of pyroxene on a grid pattern in ALHA81189, ALH 84170, and St. Marks.

Results and Discussion: St. Marks is distinguished from the EH3s by its 1) hazy, indistinct chondrule outlines, 2) absence of olivine, and 3) low Fe/(Fe + Mg) pyroxene. The only SiO_2 polymorph identified is quartz (also see [7]), consistent with slow cooling rates of parent body metamorphism.

ALHA81189 is distinguished from the other EH3s by its abundance of 1) POP chondrules, 2) SiO_2-rich rims, and 3) whole chondrules. Cristobalite is abundant, but quartz has not been identified. Furthermore, ALHA81189 is characterized by low progress on the olivine + silica = pyroxene reaction [9]. Lack of equilibration on this reaction combined with the distinct set of chondrules suggests that the unequilibrated condition of this meteorite is due in part to incomplete reaction of olivine and SiO_2 (or $SiO_{[g]}$) during chondrule formation. The predominance of cristobalite indicates rapid cooling from high temperatures—suggestive of chondrule formation and minimal reheating. The abundance of Fe-rich pyroxene in ALHA81189, while higher than in several other EH3s [10], is comparable to that in ALH 84170, suggesting that the reaction of olivine + Si-phase was decoupled from the reduction of Fe in pyroxene.

References: [1] Huss G. R. et al. 1981. *Geochimica et Cosmochimica Acta* 45:33–51. [2] Sears D. W. G. et al. 1982. *Geochimica et Cosmochimica Acta* 46:2471–2481. [3] Grossman J. N. and Brearley A. J. 2005. *Meteoritics & Planetary Science* 40:87–122. [4] Scott E. R. D. and Jones R. H. 1990. *Geochimica et Cosmochimica Acta* 54:2485–2502. [5] Bonal L. et al. 2006. *Geochimica et Cosmochimica Acta* 70:1849–1863. [6] Zhang Y. et al. 1996. *Journal of Geophysical Research* 100:9417–9438. [7] Kimura M. et al. 2005. *Meteoritics & Planetary Science* 40:855–868. [8] Weisberg M. K. et al. 2005. Abstract #1420. 36th Lunar Planet. Sci. Conf. [9] Hicks T. L. et al. 2000. Abstract #1491. 31st Lunar Planet. Sci. Conf. [10] Lusby D. et al. 1987. Proceedings, 17th LPSC. pp. E679–E695.

5091

SECONDARY MELT CHARACTERISTICS EXHIBITED BY 200–425 μm DIAMETER MICROSPHERULES: EVIDENCE SUPPORTING AN EXTRATERRESTRIAL PROVENANCE FOR WESTWATER, UTAH, PARTICLES

Joe W. Fandrich.

Where cosmic objects smaller than 200 μm are essentially unaffected, particles greater than 200 μm and less than about 600 μm will survive and experience secondary partial melting when passing through the Earth's atmosphere. Secondary melt characteristics observed on these particles often include ablation rings, melt material migration tracks, annealed tails, partial melting of the crystalline body, and projectile reshape and partial melt transformation of the primary particle.

More than 250 microspherules ranging in size from 1 to 425 μm were discovered at Westwater, Utah, in 2001. Several of the particles greater than 200 μm exhibit varying degrees of secondary melting. The sediments in which these particles are found appear to be related to deltaic deposits in the immediate area, and have been ^{14}C-dated to 9560 YBP. The age of the primary particles has not been determined.

The Westwater particles are spherical to spheroidal, commonly metallic, magnetic, crystalline to amorphous, and primarily iron in composition. Trace amounts of calcium, silicon, manganese, titanium, potassium, copper, and chromium are commonly present. These particles were first located using a 0.7× by 30× stereozoom microscope, isolated by magnetized needle from the unconsolidated sediments, placed upon carbon discs on aluminum stubs and then studied by an Amray 1000 scanning electron microscope (SEM). Qualitative chemistry was determined by employing energy dispersive spectrometry (EDS).

SEM/EDS research has produced numerous images and graphs that describe and define the secondary melt characteristics and chemistry exhibited by the Westwater microspherules. I suggest that these particles are cosmic in origin and were modified by frictional heating as they passed through Earth's atmosphere.

References: [1] Holmes H. 2001. *The secret life of dust.* pp.14–42. [2] Dao-Yi Xu et al. 1989. *Astrogeological events in China* pp. 96–111. [3] Fandrich J. W. *Microscopy Today* #01-8:24–25. [4] Fandrich J. W. *Microscopy Today* 11–1:37.

5243

FORMATION CONSTRAINTS FOR TYPE IIA CHONDRULES

A. V. Fedkin[1], L. Grossman[1, 2], and S. B. Simon[1]. [1]Department of Geophysical Sciences, University of Chicago, Chicago, IL, USA. E-mail: avf@uchicago.edu. [2]Enrico Fermi Institute, University of Chicago, Chicago, IL, USA.

In [1], calculations were presented of the mineralogical, chemical and isotopic evolution of a C-, S-, H_2O-free chondrule precursor through nonequilibrium melting, evaporation, fractional crystallization, and recondensation, during passage of a 7 km s^{-1} nebular shock [2] in a closed system of solar composition except for enrichments of 300× in dust and of enough H_2O to yield initial ambient log fO_2 = IW-2.1. This thermal history leads to formation of PO chondrules, as the peak T of 1859 K is too low for dissolution of all olivine, even for equilibrium melting. Here, we explore the sensitivity of computed histograms of X_{Fa} and $\delta^{56}Fe$ (rel. to ^{54}Fe) of type IIA chondrule olivine in such models to: evaporation coefficient of oxygen (α_o); fO_2 of ambient gas and precursor; fraction of the total metal (S) on the droplet surface; fraction of original olivine (R) that does not equilibrate with melt; fraction of crystallizing olivine that is isolated from the liquid (F); and quench T. The standard case is defined as α_o = 0.3, initial log fO_2 of the precursor and ambient gas of IW-3.1 and IW-2.1, respectively, S = 0.02 (corresponding to metal covering 12% of the surface area at the initial T = 1398 K), R = 0.05, F varying from .05 at peak T to 0.5 at 1400 K, and quench T = 1050 K. α_{Na} and α_K were derived from experiments in air at 1723 K [3] and were assumed to fall by <50% by 1000 K in order for Na and K to fully recondense in the standard case. In this case, 14% of the total olivine has $X_{Fa} \leq 0.06$ and falls from 14 at X_{Fa} = 0.07 to 2 at X_{Fa} = 0.27, 18% has X_{Fa} = 0.29, and mean X_{Fa} = 0.15. The mean $\delta^{56}Fe$ of olivine is –0.6‰ but 15% of the olivine has $\delta^{56}Fe \geq 6$‰, while the bulk droplet has $\delta^{56}Fe$ = –1.2‰. At α_o = 0.4 and 0.5, oxidation of metal and redox equilibration of droplet and ambient gas are faster but the Fa and $\delta^{56}Fe$ histograms are virtually unchanged. When the quench T is 75 K lower, more olivine fractionally crystallizes, the tail of the histogram extends to X_{Fa} = 0.47, the high-Fa peak (representing olivine still in equilibrium with melt at the quench T) falls to <10% of the olivine, mean X_{Fa} = 0.18, and mean $\delta^{56}Fe$ of olivine drops to –0.8‰ because more crystallizes from the melt whose $\delta^{56}Fe$ is becoming more negative. All else being equal, when S is lower, 0.005, or higher, 0.04, than the standard case, corresponding to initial metal surface areas of 3 and 24%, respectively, mean X_{Fa} varies by <0.01, and mean $\delta^{56}Fe$ of olivine rises to –0.2‰ at S = 0.04, due to more oxidation of more highly evaporated metal. At initial ambient log fO_2=IW-1.9, the high-Fa tail of the histogram extends to X_{Fa} = 0.35, mean X_{Fa} increases to 0.18 and mean $\delta^{56}Fe$ of olivine is –1.0‰. In this case, increasing the degree of fractional crystallization of olivine by raising F from 0.5 to 0.7 at 1400 K eliminates the high-Fa peak by producing more olivine with $X_{Fa} \leq 0.15$, reduces mean X_{Fa} to 0.13 and yields $\delta^{56}Fe$ of olivine = –0.3‰. The best match to actual type IIA chondrules is obtained for F varying from 0.1 at peak T to 1.0 at 1600 K; and initial precursor and ambient log fO_2 of IW-2.6 and IW-1.0, respectively, for which 49% of total olivine has X_{Fa} = 0.08–0.16, 32% has X_{Fa} = 0.17–0.28, mean X_{Fa} = 0.21 and mean $\delta^{56}Fe$ of olivine = 0.1‰. At 300× dust enrichment, this ambient fO_2 requires enormous H_2O enrichment, ~700×solar.

References: [1] Fedkin A. V. and Grossman L. 2007. Abstract #2014. 38th LPSC. [2] Desch S. J. and Connolly H. C., Jr. 2002. *Meteoritics & Planetary Science* 37:183–207. [3] Fedkin et al. 2005. *Geochimica et Cosmochimica Acta* 70:206–223.

5152

ASSEMBLAGES OF OLIVINE POLYMORPHS IN GROVE MOUNTAINS (GRV) 052049: CONSTRAINTS ON PRESSURE-TEMPERATURE CONDITION OF SHOCK METAMORPHISM

L. Feng[1], Y. Lin[1], S. Hu[1], L. Xu[2], and B. Miao[1]. [1]State Key Laboratory of Lithospheric Revolution, Institute of Geology and Geophysics, Chinese Academy of Sciences, Beijing, China. E-mail: LinYT@mail.igcas.ac.cn. [2]National Astronomical Observatory, Chinese Academy of Sciences, Beijing, China.

Introduction: Grove Mountains (GRV) 052049 (96.7 g) is a new L5 chondrite found in the Grove Mountains area, Antarctica, by the 22nd Chinese Antarctic Research Expedition. It was severely shocked, with melt veins up to >3 mm in width. The host-rock silicates have homogeneous compositions, with the Fa content of olivine from 23.5 to 25.0 mol% and the Fs content of low-Ca pyroxene from 20.3 to 22.0 mol%. The melt veins and the entraining host-rock clasts contain various assemblages of high-pressure polymorphs of silicates, which have constraints on the pressure-temperature condition during shock metamorphism.

Observation: The melt veins consist of numerous host-rock fragments (up to 700 μm), fine-grained silicate matrix, and metal-sulfide spheres. Majorite-pyrope is predominant in the matrix, with sizes up to 3 μm. The fragments entrained in the veins are rounded or ovoid. Olivine in most of the fragments has been partially transformed to ringwoodite along its grain boundaries and/or cracks as polycrystalline rims (up to 10 μm in width). Patch-like assemblages (up to 30 μm) of polycrystalline ringwoodite commonly occur inside large olivine grains. Ringwoodite shows a wide range of Fa content (36–75 mol%) among clasts and within individual grains of the host olivine. The boundaries adjacent to ringwoodite are Fe-poor ($Fa_{8–14}$), and Raman spectrums show they are olivine. Concentric exsolution was found in several large grains of olivine, and both Fe-poor ($Fa_{13–17}$) and Fe-rich ($Fa_{26–28}$) zones are olivine based on Raman spectrums. It is noticed that the wall of host rock in contact with the melt veins has only a very thin rim (<2 μm) of polycrystalline ringwoodite. The olivine layer (<6 μm) adjacent to the ringwoodite rim is also Fe-poor. The interior of host rock >10 μm from the veins shows little evidence for high-pressure polymorph transformation.

Discussion: The existence of majorite-pyrope of the veins is similar to those reported in other meteorites [1–3], suggestive of crystallization at ~21–25 GPa. After the peak pressure, olivine-ringwoodite equilibrium probably retained down to a low pressure <10 GPa according to the very Fa-rich ringwoodite and the phase diagram at temperature of 1473 K [4]. The concentric exsolution of olivine probably formed through solid-state transformation of olivine to wadsleyite and ringwoodite as reported in other meteorites [5], but both have retrograded back to olivine with different compositions retained.

Acknowledgements: The sample was supplied by the Polar Research Institute of China. This study was supported by the One-Hundred-Talent Program and the Knowledge Innovation Program (Grant no. kzcx2-yw-110) of the Chinese Academy of Sciences.

References: [1] Chen M. et al. 1996. *Science* 271:1570–1573. [2] Ohtani E. et al. 2004. *Earth and Planetary Science Letters* 227:505–515. [3] Xie Z. et al. 2006. *Geochimica et Cosmochimica Acta* 70:504–515. [4] Akaogi M. et al. 1989. *Journal of Geophysical Research* 94:15,671–15,685. [5] Chen M. et al. 1995. *Meteoritics* 30:497.

5170

UV/VIS SPECTROSCOPY OF METEORITES AND ASTEROIDS

C. D. Fernandes[1], M. C. Towner[1], and M. M. Grady[1, 2]. [1]Open University, PSSRI, MK7 6AA, UK. E-mail: c.d.fernandes@open.ac.uk. [2]Natural History Museum, Department of Mineralogy, London SW7 5BD, UK.

Introduction: Asteroids are classified into different groups on the basis of their optical reflectance spectra [1]. Meteorites are fragments of asteroids and are subclassified according to their composition. Reflectance spectroscopy has been used to link classes of meteorites to groups of asteroids as a means of identifying parent bodies. However, there are many discrepancies mainly because asteroids are subject to space weathering by cosmic-ray irradiation and collisions. Work has been done simulating the effects of space weathering on asteroids by modification of meteorites [2], mostly using laser pulse heating to simulate the space weathering. However, this is probably not a true analogue of space weathering, as it causes modification by heat rather than shock [3].

We are undertaking experiments in order to identify the effects of shock weathering on the UV/Vis spectra of meteorites using a different technique. The purpose is to refine the asteroid-meteorite link.

Method: *UV/Vis Microspectrophotometer:* UV/Vis spectroscopy is a technique that utilizes the excitation of valence electrons within an atom as a tracer of atomic or molecular bonds. We use a Craic optical microspectrophotometer system fitted with xenon lamps (wavelength range 200–800 nm). The instrument can acquire data by transmission and reflectance, and is able to measure spectra from powders, discrete grains, or polished mounts. The technique is nondestructive and the samples can be as small as 2 μm.

Van de Graaff Accelerator: The accelerator develops a DC voltage of up to 2 MV. It accelerates dust particles less than 1 μm in diameter to velocities up to 50 km s^{-1} by generating a charge on the particle and accelerating it across a potential difference [4]. The target can be bombarded for long periods, up to one week at a time. The criteria for selection of the particles lie on the capacity to charge their surfaces. Initial experiments will use copper particles rather than iron, which are routinely used in accelerators. Iron is one of the alteration products of asteroids and would provide contamination. Copper will not interfere with the results.

Results: We have selected a range of suitable meteorites: stony meteorites believed to derive from S, C, D, and V class asteroids and also metal-rich meteorites. They are cut into small ~1 cm^3 wide pieces and at least one of the surfaces is broken (not cut) to better represent the rough surface of an asteroid. UV/Vis spectra are being taken of these samples. The meteorites are then bombarded with copper projectiles on the Van de Graaff accelerator and analyzed again on the UV/Vis microspectrophotometer.

References: [1] Bus S. J. et al. 2002. *Asteroids III*. pp. 169–182. [2] Johnson J. R. and Hörz F. 2003. *Journal of Geophysical Research* E108:6–1. [3] Sasaki et al. 2001. *Nature* 410:555–557. [4] Burchell M. J. et al. 1999. *Measurement Science and Technology* 10:41–50.

5079

BALLEN QUARTZ, AN IMPACT SIGNATURE: NEW OCURRENCE IN IMPACT-MELT BRECCIA AT ROCHECHOUART-CHASSENON IMPACT STRUCTURE, FRANCE

L. Ferrière and C. Koeberl. Department of Geological Sciences, University of Vienna, Althanstrasse 14, A-1090 Vienna, Austria. E-mail: ludovic.ferriere@univie.ac.at.

The 214 ± 8 Ma old Rochechouart-Chassenon impact structure [1], about 25 km in diameter, has been known for about forty years. Rocks there display a wide variety of shock-metamorphic effects, including shatter cones, planar features in quartz grains, isotropization of feldspar, kink-banding in muscovite and biotite, melt particles, diaplectic quartz glass, and impact-melt unit (e.g., [2]). The presence of ballen quartz in impact breccia samples from the Rochechouart-Chassenon structure has not been mentioned in earlier publications. Here, we note the presence of ballen quartz (Fig. 1) in impact-melt breccia from Babaudus and discuss implications for pressure and temperature of the breccia formation. The formation mechanism of ballen quartz is still unresolved [3, 4] and this new discovery can be added to the other impact structures for which ballen quartz is known.

Babaudus breccia is a vesicular impact-melt rock, which consists of feldspar and pyroxene laths in a matrix of devitrified glass. Rare clasts of shocked quartz and feldspar occur and a few recrystallized quartz show the ballen texture (Fig. 1). Ballen frequently display different optical orientation and also some ballen with intragranular polycrystallinity occur (heterogeneous extinction within single ballens). Most of the ballen are oval in shape and are ~15–90 μm in long dimension.

The identification of ballen quartz with different optical orientation and intragranular polycrystallinity provide some constraints on the pressure (>50 GPa) and temperature (>1200 °C) conditions for the formation of the Babaudus breccia and/or post-impact alteration processes that have affected the breccia.

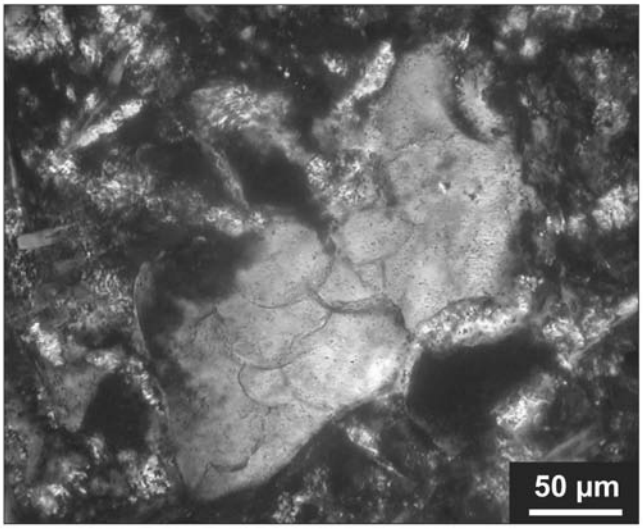

Fig. 1. Thin section microphotograph (plane-polarized light) of ballen quartz in Babaudus breccia from Rochechouart-Chassenon impact crater.

Acknowledgements: This work was supported by the Austrian Science Foundation (FWF).

References: [1] Kelley S. P. and Spray J. G. 1997. *Meteoritics & Planetary Science* 32:629–636. [2] Kraut F. and French B. V. 1971. *Journal of Geophysical Research* 76:5407–5413. [3] Carstens H. 1975. *Contributions to Mineralogy and Petrology* 50:145–155. [4] Bischoff A. and Stöffler D. 1984. *Journal of Geophysical Research* 89:645–656.

5078

DISTRIBUTION OF SHOCKED QUARTZ GRAINS WITH DEPTH IN CENTRAL UPLIFT OF THE BOSUMTWI IMPACT CRATER, GHANA

L. Ferrière[1], C. Koeberl[1], and W. U. Reimold[2]. [1]Department of Geological Sciences, University of Vienna, Althanstrasse 14, A-1090 Vienna, Austria. E-mail: ludovic.ferriere@univie.ac.at. [2]Mineralogy, Museum of Natural History, Humboldt University, Invalidenstrasse 43, D-10115 Berlin, Germany.

Introduction: During the 2004 ICDP drilling project at the 1.07 Ma Bosumtwi impact structure, Ghana, the LB-08A borehole with a final depth of 451 m below lake level was drilled into the central uplift [1, 2]. This drill core consists of approximately 25 m of polymict, clast-supported lithic breccia intercalated with suevite, which overlies fractured/brecciated basement composed of metasediment (mainly meta-graywacke) [2]. Here, we report the results of a study of the distribution of shocked quartz grains (with planar fractures [PFs] and planar deformation features [PDFs]) in meta-graywacke samples. For this study, systematic analysis of ~9000 quartz grains in eighteen different samples (of comparable grain size) from the basement was carried out using an optical microscope and a 4-axis universal stage.

Results: Shocked quartz grains observed in meta-graywacke samples display PFs and PDFs (1, 2, or rarely 3 to 4 sets), some of which are decorated with numerous small fluid inclusions; some of the shocked grains show a "toasted appearance." This study revealed an obvious decrease of the abundance of shocked quartz grains with increasing depth, from ~60 rel% shocked grains at 270 m, to ~20 rel% at 380 m, and just a few shocked quartz grains at around 450 m depth. Surprisingly, the relative abundance of quartz grains with 1 and 2 sets of PDFs is relatively constant with depth, averaging about 68 and 32 rel%, respectively. The relative abundances of toasted quartz grains and of those with decorated planar features show a moderate, but significant correlation ($R = 0.64$).

Discussion: The observed distribution of the shocked quartz grains reflects the variation of shock pressure in the uppermost part of the central uplift. Estimation of shock levels by measuring the PDF orientations in quartz grains is currently in progress and will be used to estimate the amount of shock-wave attenuation in the uplifted target rocks.

Acknowledgments: This work was supported by the Austrian Science Foundation (FWF) and the Austrian Academy of Sciences.

References: [1] Koeberl C. et al. 2007. *Meteoritics & Planetary Science* 42:483–511. [2] Ferrière L. et al. 2007. *Meteoritics & Planetary Science* 42:611–633.

5116

SPINEL-BEARING ASTEROIDS: THE MOST ANCIENT ASTEROIDS IN THE SOLAR SYSTEM

S. K. Fieber-Beyer[1, 2, 3], M. J. Gaffey[1, 3], and P. S. Hardersen[1, 3]. [1]Department of Space Studies, University Stop 9008, University of North Dakota, Grand Forks, ND 58202, USA. E-mail: sherryfieb@hotmail.com. [2]Department of Earth System Science and Policy, University Stop 9007, University of North Dakota, Grand Forks, ND 58202, USA. [3]Visiting astronomer at the Infrared Telescope Facility under contract from the National Aeronautics and Space Administration, which is operated by the University of Hawai'i. Mauna Kea, HI 96720, USA.

Introduction: Five spinel-bearing asteroids have been identified in the Main Belt. These asteroids are distributed across the asteroid belt, implying they are not fragments of a common disrupted parent body. The spinel contained within these asteroids appears to be embedded in calcium-aluminum-rich inclusions (CAIs) much like that of the CV3 chondrite Allende [1]. Their preservation implies a lack of igneous processing and places further constraints on the heating that occurred within the early solar system. This study analyzes the five known spinel-bearing asteroids: 980 Anacostia [1], 387 Aquitania [1], 755 Quintilla [2, 3], 347 Pariana [4], and 234 Barbara [5].

Conclusions: The sine i versus semi-major axis graph indicates that the distribution of spinel-bearing asteroids within the Main Belt is not consistent with these bodies being derived from a single parent body. We propose these asteroids come from four different parent bodies with the exception of 980 Anacostia and 387 Aquitania, which have been previously proposed as having been derived from the same parent body [1]. The spinel within the asteroids is most likely refractory spinel grains embedded in CAIs. In order to be spectroscopically detected, the spinel-bearing CAIs must make a significant fraction of the asteroid surface material, indicating CAI concentrations several times that found in CV3 chondrites such as Allende. In order to achieve this concentration, the parent bodies must have formed at an early time when CAIs still represented of substantial fraction of the grains that had formed in the cooling solar nebula. Alternately, parent body accretion may have occurred somewhat later in regions where dynamical processes had concentrated CAIs. We propose these spinel-bearing asteroids are the most ancient asteroids in the solar system and that they were the first large bodies to accrete out of the cooling nebula. Investigation is still ongoing concerning 234 Barbara as a potential candidate supplying the ν_6 resonance with asteroidal fragments.

Acknowledgments: Various portions of this research were supported by NASA Planetary Geology and Geophysics Grant NNG04GJ86G (M. J. G.) and NASA Planetary Astronomy Grant NNG05GH01G (P. S. H.).

References: [1] Burbine T. H., Gaffey M. J., and Bell J. F. 1992. *Meteoritics* 27:424–434. [2] Fieber-Beyer S. K. 2006. MS thesis, University of North Dakota. pp. 1–92. [3] Fieber-Beyer S. K., Gaffey M. J., and Harderson P. S. 2006. Abstract #1315. 37th Lunar and Planetary Science Conference. [4] Hardersen P. S. 2007. Personal communication. [5] Sunshine J. M., Connolly H. C., Jr., McCoy T. J., Bus S. J., and La Croix L. 2007. Abstract #1613. 38th Lunar and Planetary Science Conference.

5266

AN EXPERIMENTAL INVESTIGATION INTO THE EFFECT OF CHLORINE ON CRYSTALLIZATION OF A GUSEV BASALT

J. Filiberto and A. H. Treiman. Lunar and Planetary Institute, 3600 Bay Area Blvd., Houston, TX 77058, USA. E-mail: filiberto@lpi.usra.edu.

Introduction: High chlorine abundances have been reported on the Martian surface, suggesting that Cl is widespread on Mars. GRS elemental mapping has shown that Cl is not compositionally uniform across the surface of Mars and has a range from 0.2–1 wt% [1]. The MER rovers have confirmed the high Cl concentrations with soil analysis up to 1 wt% Cl [2]. The SNC meteorites also contain numerous alteration products (e.g., siderite, anhydrite, iddingsite, gypsum, carbonate, clay, epsomite, and halite [3–5]). This data suggests that chlorine may be important during Martian magmatic and alteration processes. Therefore, we are conducting an ongoing study to investigate the effects of Cl during crystallization of a Martian magma.

While little is known about the effects of Cl in Martian magmatic systems, much is known about the effects of Cl in terrestrial systems. Chlorine is soluble in terrestrial basalts with a maximum solubility around 3 wt% [6]. Cl is known to form complexes with Ca, Mg, Fe, Al, and P in terrestrial systems, and thus can affect phase relations [7]. However, these relations are highly dependent on melt composition [8] and all current experimental work is on terrestrial compositions. Since no experimental work has been done to investigate the effect of Cl on Martian magmatic compositions, we are conducting high pressure experiments (3–16 kb) on a synthetic Gusev basalt composition with Cl added to investigate the effect of Cl on liquidus and near-liquidus phase relations.

Experimental Strategy: Previous experiments on a synthetic anhydrous [9] and hydrous [10] Humphrey composition are the basis for this study. The same synthetic powder and experimental technique from [9] are being used for this study; however, Cl is added as AgCl which decomposes at temperature to an Ag metal nugget and Cl in the melt.

The ongoing experiments will elucidate the effects of Cl in Martian magmatic systems and help place constraints on the availability of Cl for acidic alteration models.

References: [1] Keller J. M. et al. 2007. *Journal of Geophysical Research* 111:E03S08. [2] Gellert R. et al. 2006. *Journal of Geophysical Research* 111(E2). [3] Bridges J. C. et al. 2001. *Chronology and evolution of Mars*. pp. 365–392. [4] Treiman A. H. 2005. *Chemie der Erde—Geochemistry* 65:203–270. [5] Treiman A. H. et al. 2002. *Earth and Planetary Science Letters* 204:323–332. [6] Webster J. D. et al. 1999. *Geochimica et Cosmochimica Acta* 63:729–738. [7] Webster J. D. and De Vivo B. 2002. *American Mineralogist* 1046–1061. [8] Webster J. D. and Rebbert C. R. 1998. *Contributions to Mineralogy and Petrology* 132:198–207. [9] Filiberto J. and Treiman A. H. 2007. Abstract #1341. Lunar and Planetary Science Conference XXXVIII. [10] Monders A. G. et al. 2007. *Meteoritics & Planetary Science* 42:131–148.

5060

VERY HIGH PRESOLAR GRAIN ABUNDANCES IN THE CR CHONDRITE QUE 99177

C. Floss and F. J. Stadermann. Laboratory for Space Sciences and Physics Department, Washington University, St. Louis, MO 63130, USA. E-mail: floss@wustl.edu.

Introduction: CR chondrites represent one of the most primitive chondrite groups and have often been compared with IDPs because both types of materials contain abundant H and N isotopic anomalies (e.g., [1, 2]). However, whereas IDPs contain abundant presolar silicates [3], such grains are very rare in CR chondrites measured to date [4, 5]. In order to explore whether aqueous alteration accounts for the lack of presolar silicates in these meteorites, we are investigating the presolar grain abundances in the CR chondrite QUE 99177, which is less altered than most members of this group [6].

Experimental and Results: We used the NanoSIMS to carry out isotopic (C and O) imaging on 8500 μm^2 of matrix material in a thin section of QUE 99177 and found 33 O-anomalous grains and 16 C-anomalous grains.

Thirty-two of the O-anomalous grains are ^{17}O-enriched and belong to group 1, with likely origins in low-mass AGB stars [7]. The remaining grain belongs to group 4 and is ^{18}O-rich. Eleven of the 16 C-anomalous grains have $^{12}C/^{13}C$ ratios between 20 and 80, similar to the ratios observed in mainstream SiC grains (e.g., [8]). The remaining 5 grains are enriched in ^{12}C, with $^{12}C/^{13}C$ ratios up to 135. Carbon isotopic compositions enriched in ^{12}C are seen in SiC Y grains but also in low-density graphite grains [8]. All of the C-anomalous grains have normal O isotopic compositions and/or are O-poor. Planned elemental (and additional isotopic) measurements will allow us to identify the carrier phases of these anomalies more accurately.

Discussion: Calculations show that QUE 99177 contains very high abundances of presolar silicate/oxide grains (~220 ppm; matrix-normalized, uncorrected for instrumental detection efficiencies). Previously the highest presolar silicate/oxide abundances have been found in Acfer 094 and ALHA77307, with (uncorrected) abundances of ~145 ppm and ~125 ppm, respectively [9]. These results indicate that the lower abundances of presolar silicates/oxides in other CR chondrites are, indeed, the result of more extensive aqueous alteration, and emphasize the primitive nature of QUE 99177.

More surprising are extremely high abundances of C-anomalous grains (~145 ppm) in this meteorite. Estimated meteoritic abundances of SiC and graphite are generally an order of magnitude or more lower [8, 10]. We note, however, that NanoSIMS C and O isotopic imaging of Acfer 094 also suggests elevated abundances of presolar carbonaceous phases [11].

References: [1] Messenger S. et al. 2003. *Space Science Reviews* 106: 155–172. [2] Busemann H. et al. 2006. *Science* 312:727–730. [3] Floss C. et al. 2006. *Geochimica et Cosmochimica Acta* 70:2371–2399. [4] Nagashima K. et al. 2004. *Nature* 428:921–924. [5] Floss C. and Stadermann F. J. 2005. Abstract #1390. 36th Lunar and Planetary Science Conference. [6] Abreu N. and Brearley A. 2006. Abstract # 2395. 37th Lunar and Planetary Science Conference. [7] Nittler L. et al. 1997. *The Astrophysical Journal* 483: 475–495. [8] Zinner E. 2004. In Treatise on Geochemistry, vol. 1. pp. 17–39. [9] Nguyen A. et al. 2007. *The Astrophysical Journal* 656:1223–1240. [10] Huss G. et al. 2003. *Geochimica et Cosmochimica Acta* 67:4823–4848. [11] Bose M. et al. 2007. This issue.

5182

ELEMENT HETEROGENEITY IN THE WILD-2 SAMPLES COLLECTED BY STARDUST

G. J. Flynn, Department of Physics, SUNY–Plattsburgh, 101 Broad St., Plattsburgh NY 12901, USA. E-mail: george.flynn@plattsburgh.edu.

Introduction: The Stardust Bulk Composition Preliminary Examination Team reported the elemental compositions of material deposited along 23 entry tracks in aerogel and as residue in seven craters in Al-foil collected from the coma of comet 81P/Wild-2 [1]. The mean composition is CI-like, but Fe and S were depleted and several moderately volatile elements were enriched compared to CI in the Wild-2 material. However, the most striking observation is the heterogeneity in elemental composition from track to track or crater to crater.

Since no mineral has the CI composition, a CI-like composition demonstrates that a sample is composed of several phases of different composition. The size at which the composition of individual particles begins to approach the mean composition provides an indication of the mean grain size in the material.

Typical ~10 μm fine-grained anhydrous interplanetary dust particles (IDPs), having masses of ~1 ng, show approximately factor of two variations in major-element abundances and factor of five variations in trace-element abundances. However, preliminary data indicate that ~100 ng cluster IDPs show considerably less variation in their compositions [2], suggesting the most grains in anhydrous IDPs are significantly smaller than 100 ng.

The Fe-masses of the 23 Wild-2 particles analyzed in aerogel spanned the range from 180 to 4×10^6 femtograms. Figure 1 shows the Ni/Fe, S/Fe, and Ca/Fe ratios for the 23 particles. Although the particle with the largest Fe mass agrees well with the 23-particle mean composition, order-of-magnitude variation is seen for each of these major element ratios even among the most massive particles. This indicates that the mineral hosts of Ni, S, and Ca are not homogeneously distributed in Wild-2 particles having Fe masses $>10^5$ femtograms, suggesting the mineral hosts of these elements are relatively large in size.

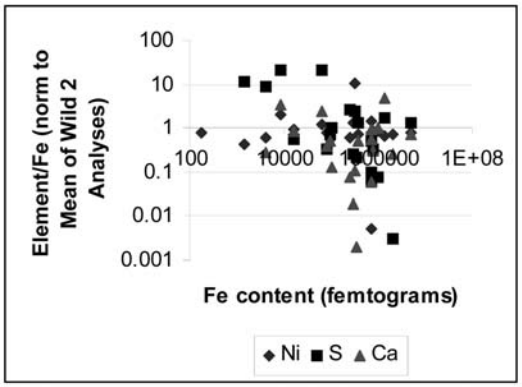

Fig. 1. Element/Fe ratios for 23 "whole tracks," each normalized to the 23 track mean composition plotted as a function of the Fe mass of the particle.

References: [1] Flynn. G. J. et al. 2006. *Science* 314:1731–1735. [2] Flynn G. J. et al. 2007. Abstract #1338. Lunar and Planetary Science Conference XXXVIII.

5185

THE AGE OF THE ICE AT THE FRONTIER MOUNTAIN BLUE ICE FIELD (ANTARCTICA) CONSTRAINED BY $^{40}Ar/^{39}Ar$ CHRONOLOGY OF ENGLACIAL TEPHRA

L. Folco[1], P. Curzio[1], M. A. Laurenzi[2], M. Mellini[3], and A. Zeoli[1]. [1]Museo Nazionale dell'Antartide, Università di Siena, Italy. E-mail: folco@unisi.it. [2]Istituto di Geoscienze e Georisorse, CNR–Area della Ricerca di Pisa, Via G. Moruzzi 1, 56124 Pisa, Italy. [3]Dipartimento di Scienze della Terra, Università di Siena, Via Laterina 8, 53100 Siena, Italy.

Englacial tephra are chronostratigraphic markers of the Antarctic ice sheet. Structural, mineralogical, geochemical, and geochronological data on selected samples collected during the 1995, 1997, 1999, and 2001 PNRA expeditions allowed the reconstruction of a chronostratigraphic framework for the Frontier Mountain blue ice field—an important meteorite trap on the southeastern flank of Talos Dome in northern Victoria Land. The stratigraphic thickness of the blue ice succession is ~1150 m. The $^{40}Ar/^{39}Ar$ age of one layer close to the stratigraphic bottom of the ice succession is 100 ± 5 ka and constrains the maximum age of the bulk of Frontier Mountain blue ice. The 49 ± 11 ka age of a second layer at a depth of ~950 m in the stratigraphic succession indicates that >90% of the ice is younger than this value. These ages agree well with terrestrial ages of meteorites found on this ice (up to 140 ± 30 ka; [1–3]), suggesting that a mechanism of exhumation of meteorites in the blue ice field by ablation after englacial transport is at work at Frontier Mountain.

Acknowledgements: This work was supported by the Italian Programma Nazionale delle Ricerche in Antartide (PNRA).

References: [1] Welten K. C. et al. 2001. *Meteoritics & Planetary Science* 36:301–317. [2] Welten K. C. 2006. *Meteoritics & Planetary Science* 41:1081–1094. [3] Folco L. et al. 2006. *Earth and Planetary Science Letters* 248:209–216.

5095

MICROTEKTITES FROM THE TRANSANTARCTIC MOUNTAINS

L. Folco[1], P. Rochette[2], N. Perchiazzi[3], M. D'Orazio[3], M. A. Laurenzi[4], and M. Tiepolo[5]. [1]Museo Nazionale dell'Antartide, Università di Siena, Italy. E-mail: folco@unisi.it. [2]CEREGE, Université d'Aix-Marseille III, France. [3]Dip. di Scienze della Terra, Università di Pisa, Italy. [4]IGG-CNR Pisa, Italy. [5]IGG-CNR Pavia, Italy.

Microtektites were discovered on top of Frontier Mountain during the 2003 PNRA expedition. They were found in the micrometeorite traps described by [1] and [2]. These are joints and decimetric-sized pot-hole cavities of flat, glacially eroded granitic surfaces filled with fine-grained bedrock detritus. During the 2006 PNRA expedition, microtektites were also found in two other glacially eroded granitic summits of the Transantarctic Mountains in northern Victoria Land: Miller Butte and an unnamed nunatak in the Timber Peak area, ~30 km and ~100 km due north and south of Frontier Mountain, respectively. A total of ~130 microtektites have been so far separated from the host detritus (along with thousands of micrometeorites) in the 400–800 μm size fraction. Their concentration is in the order of 1 particle per 100 g of detritus. Preliminary observations revealed microtektites also in the 200–400 μm size fraction.

Description: Microtektites are pale yellow, transparent glass spheres. Rare exceptions have oblate to button shapes. Rare particles contain one or two microbubbles. The external surface is typically smooth and clean, although some particles are partially covered by Fe,K- and Ca sulfate deposits. Eleven particles analyzed by synchrotron X-ray diffraction at the BM8 GILDA beamline (ES RF Grenoble) resulted completely amorphous.

Bulk Composition: EMP major element composition of 37 particles defines a single coherent population of microtektites. The silica content varies from 64.4 to 77.7 wt%. All major element oxides, except K_2O, show negative correlation with SiO_2. The total alkalies ($Na_2O + K_2O$) are very low (0.90–1.85 wt%) and the K_2O/Na_2O is always >1 (2.7–4.4). The trace element composition of 6 particles by LA-ICP-MS appears to be homogeneous, and most elements match the average Upper Continental Crust composition defined by [3].

Age: Preliminary laser fusion ^{40}Ar-^{39}Ar analyses of the largest particles define a peak in the age distribution of 8.8 ± 0.4 Ma (weighed mean age, 6 particles). This age is distinct from those of the other known microtektite strewn fields, i.e., the North American (35 Ma), Ivory Coast (1.1 Ma), and Australasian (0.8 Ma) strewn fields (e.g., [4, 5]).

Conclusions: Microtektites from the Transantarctic Mountains in northern Victoria Land identify a new microtektite strewn field associated with an impact on Earth's continental crust in the Late Miocene. The impact crater is yet to be located, but future studies of size distribution (and concentration) along the ~3500 km long Transantarctic Mountain range may help to predict the source crater location. In addition, the age of microtektites constrains the minimum age of the collection surfaces, with important implications on the Antarctic bedrock denudation history and the age of the micrometeorite traps in which they were found.

References: [1] Rochette et al. 2005. Abstract #1315. 36th LPSC. [2] Folco et al. 2006. *Meteoritics & Planetary Science* 41:A56. [3] Taylor and McLennan. *Reviews in Geophysics* 33:241–265. [4] Glass et al. 2004. *Geochimica et Cosmochimica Acta* 68:3971–4006. [5] Montanari and Koeberl. 2002. *Impact stratigraphy*. Springer. 364 p.

5125

ALTERATION AND BRECCIATION OF A CALCIUM-ALUMINUM-RICH INCLUSION IN THE ALLENDE METEORITE

R. L. Ford and A. J. Brearley. Department of Earth and Planetary Sciences. University of New Mexico, Albuquerque, NM 87131, USA. E-mail: rford@unm.edu.

Introduction: The timing and location of alteration of CAIs within the Allende meteorite has been a subject of controversy. Both pre-accretionary and parent body alteration arguments have been made [1–4]. One issue that has not been addressed in detail is the possible effects and timing of brecciation on the textural relationships between CAIs and the surrounding matrix, which add further complexity in assessing the environment of alteration for CAIs in Allende. Here, we present new observations from a highly brecciated, altered, compact type A CAI from Allende.

Results: Within the brecciated region, CAI clasts, mineral fragments, and chondrules are present. The brecciated region is a distinct, linear feature that extends across the thin section for 6.5 mm and is defined by a highly disrupted array of CAI fragments that range in size from 20 to 700 μm. The mineralogy and textures of these fragments indicates that they are pieces of a single, compact, type A CAI. The primary mineralogy of the CAI fragments consists of melilite, Al,-Ti pyroxene, perovskite, spinel, and diopside. Asymmetrical rims of spinel, diopside, and Al,-Ti pyroxene enclosed the original CAI before brecciation, and are now present as partial rims around some of the fragments. Nepheline, andradite, secondary melilite, a platy phase with similar chemistry to margarite, and minor amounts of sodalite comprise the secondary mineralogy of the CAI clasts.

Textural relationships between the mineral phases within the CAI clasts indicate that the primary melilite altered sequentially to the secondary melilite, the platy phase, nepheline, and sodalite. Spinel grains appear to be unaltered except for some minor Fe enrichment. Cross-cutting relationships indicate that the platy phase formed before brecciation of the CAI occurred.

Element maps record elevated Na concentrations in the CAI fragments and adjacent matrix, compared to the matrix outside the brecciated region. Calcium X-ray maps show that the abundance of Ca-pyx-andradite nodules are slightly higher in the matrix directly adjacent to the CAI clasts, compared to typical matrix regions in the same thin section. In addition, distinct regions of matrix with little or no Na or Ca are present within the brecciated region. These regions may represent matrix clasts with a different history from matrix material directly associated with brecciated CAI fragments.

Conclusion and Discussion: DIs studied by [5] clearly show evidence of post-brecciation interaction with Allende host. In the case of this CAI, we observed no evidence of such a process. Cross-cutting relationships indicate that the alteration of the CAI happened prior to brecciation. Although the CAI-matrix relationships have been disturbed by brecciation, some CAI fragments still appear to have original matrix attached to them. This matrix is characterized by elevated Na and Ca signatures.

References: [1] Krot A. N. et al. 1995. *Meteoritics* 30:748. [2] Keller L. P. and Buseck P. R. 1991. *Science* 425:946–948. [3] Meeker G. P. et al. 1983. *Geochimica et Cosmochimica Acta* 47:707. [4] MacPherson G. J. et al. 2005. ASP Conference Series 341:225. [5] Krot A. N. et al. 2000. *Geochemistry International* 38:351.

5186

IDENTIFICATION BY RAMAN SPECTROSCOPY OF PROCESSING EFFECTS IN FORSTERITE-FAYALITE SAMPLES DURING HYPERVELOCITY IMPACTS ON FOILS AND CAPTURE IN AEROGEL

N. J. Foster[1], P. J. Wozniakiewicz[2], M. J. Burchell[1], A. T. Kearsley[2], A. J. Creighton[1], and M. J. Cole[1]. [1]Centre for Astrophysics and Planetary Science, School of Physical Sciences, University of Kent, Canterbury, Kent, CT2 7NH, UK. E-mail: nf40@kent.ac.uk. [2]IARC, Department of Mineralogy, The Natural History Museum, London, SW7 5BD, UK.

Introduction: The return of NASA's Stardust spacecraft has given us an opportunity to study relatively pristine materials from the outer regions of early solar system [1]. Grains from comet 81P/Wild-2 were captured as they impacted into the Stardust collector surface, composed of aerogel cells and aluminium foils, at 6.1 km s^{-1} [2]. Such an impact velocity generates pressures and temperatures that could cause modification to collected grains in both media. Olivines, of which a wide variety of compositions have been found as common components of the cometary grains so far analyzed [3], have a distinctive Raman response depending on their Fe-Mg content [4]. It has been shown in previous studies that Fe-Mg olivines can been effected by heating [5] causing a shift in the characteristic Raman peaks at 820 and 850 cm^{-1}. We are investigating whether the capture process involved in the sample return mission can alter the Raman signal from olivines.

Experimental Method: Samples of a suite of olivines from forsterite to fayalite composition (Fo_{100}, Fo_{80}, Fo_{60}, Fo_{40}, Fo_{20}, and Fo_0) were fired using a two-stage light-gas gun at both Stardust grade foils and aerogels (density of ≈30 kg m^{-3}), at a speed of ≈6.1 km s^{-1}. After firing, the foils were imaged and analyzed at the Natural History Museum, using SEM EDX to identify craters bearing sufficient residue for Raman spectroscopy. Raw grains, impacted foils, and aerogel samples were analyzed at the University of Kent using a microRaman module illuminated with a HeNe laser of wavelength 632.8 nm. Peak maximum positions associated with olivine, around 820 and 850 cm^{-1}, were recorded and plotted to highlight any changes before and after firing.

Results and Discussion: For the raw grains the position of the "820" cm^{-1} peak varied from ≈812 cm^{-1} for Fo_{00} to ≈826 cm^{-1} for Fo_{100}, and the "850" cm^{-1} peak varied from ≈837–858 cm^{-1} for the same sample range. Preliminary analysis of impact residue in foil craters of diameter ≈50 μm has revealed Raman signals with a shift of ≈2 cm^{-1} relative to that of the equivalent raw sample. Further work is needed to quantify the extent of peak shape and position change for both the foils and the aerogel samples. Our Raman study has already shown that although recognizable olivine survives it is altered due to shock effects associated with the impact/capture event.

Acknowledgements: N. J. F. would like to thank University of Kent Alumni. P. J. W. thanks NHM for provision of projectile samples. M. J. B. thanks PPARC (UK).

References: [1] Brownlee D. E. et al. 2006. *Science* 314:1711–1716. [2] Brownlee D. E. et al. 2003. *Journal of Geophysical Research* 108:8111–8125. [3] Zolensky M. et al. 2006. *Science* 314:1735–1739. [4] Kuebler K. et al. 2005. Abstract #2086. 36th Annual Lunar and Planetary Science Conference. [5] Kolesov B. A. and Geiger C. A. 2004. *Physics and Chemistry of Minerals* 31:142–154.

5271

QUANTITATIVE PETROGRAPHY OF L CHONDRITES: 3-D MORPHOLOGIC VARIATIONS WITH DEGREE OF EQUILIBRATION AND SHOCK LOADING

J. M. Friedrich[1, 2], M. L. Rivers[3], C. E. Nehru[2, 4], and D. S. Ebel[2]. [1]Department of Chemistry, Fordham University, Bronx, NY 10458, USA. E-mail: friedrich@fordham.edu. [2]Department of Earth and Planetary Sciences, American Museum of Natural History, New York, NY 10024, USA. [3]Consortium for Advanced Radiation Sources, The University of Chicago, Argonne, IL 60439, USA. [4]Department of Geology, Brooklyn College, CUNY, Brooklyn, NY 11210, USA.

The petrographic study of two-dimensional (2-D) thin sections of chondrites has given us extensive insights into the post-accretionary processes that changed chondritic materials due to heating, aqueous activity, and impact-related processes [1]. Although thin section–derived (2-D) information such as chemical makeup or exactingly precise mineralogical composition can not be rigorously extended to three dimensional (3-D) analytical methods, X-ray computed microtomography (XRCMT) does allow for an approximate 3-D compositional examination of chondritic meteorites [2]. Combined with computer-aided 3-D visualizations, XRCMT can be a useful technique for examining the physical metal dispersion in metamorphosed chondrites [3, 4]. Here, we are examining and comparing the effect of thermal metamorphism and shock loading on the morphology and distribution of metal and sulfide in a large suite (n = 47) of L chondrites.

We have analyzed our suite of unequilibrated and equilibrated L chondrites by XRCMT at resolutions of at least 17 μm/voxel at the GSECARS 13-BM beamline with the methods outlined in [2]. Sample sizes are between 1–3 cm^3. One of the challenges of using L chondrites as analogues for incipient planetary differentiation is quantifying the descriptive language used in petrographic studies: in this work, we augment typical XRCMT volumetric data analysis techniques (e.g., [3]) with several in-house methods for the quantitative 3-D structural analysis of chondrites. These quantative descriptors were created to help us quantify the lumpiness of a component (metal and sulfide) or extent of a component's resemblance to a vein-like structure [5]. The metrics we calculated include textural metrics for classification [6], model-dependent structural parameters [7], and algebraic topological descriptors for 3-D structures [8].

To date, we have verified statistical differences between the textures of 29 equilibrated (n = 18) and unequilibrated (n = 11) L chondrites in our current suite. Our work will increase knowledge of metal/silicate distribution and segregation in primitive solar system bodies and identify the extent to which possible mechanisms are responsible for their current distribution.

References: [1] Stöffler et. al. 1991. *Geochimica et Cosmochimica Acta* 55:3845–3867. [2] Ebel D. S. et al. *Meteoritics & Planetary Science.* Forthcoming. [3] Benedix G. K. et al. 2003. Abstract #1947. 34th Lunar and Planetary Science Conference. [4] Nettles and McSween. 2006. Abstract #1996. 37th Lunar and Planetary Science Conference. [5] Friedrich J. M. *Meteoritics & Planetary Science.* Forthcoming. [6] Haralick R. M. et al. 1973. *IEEE Transactions on Systems, Man, and Cybernetics* SMC-3:610–621. [7] Parfitt A. M. et al. 1983. *The Journal of Clinical Investigation* 72: 1396–1409. [8] Odgaard A. 1997. *Bone* 20:315–328.

5181

CHEMISTRY AND PETROGRAPHY OF A HIGH-PRESSURE SHOCK VEIN IN THE Y-75100 CHONDRITE

J. M. Friedrich[1, 2], S. F. Wolf[3], and M. Kimura[4]. [1]Department of Chemistry, Fordham University, Bronx, NY 10458, USA. [2]Department of Earth and Planetary Sciences, American Museum of Natural History, New York, NY 10024, USA. E-mail: friedrich@fordham.edu. [3]Department of Chemistry, Indiana State University, Terre Haute, IN 47809, USA. E-mail: wolf@indstate.edu. [4]Faculty of Science, Ibaraki University, Mito 310-8512, Japan. E-mail: makotoki@mx.ibaraki.ac.jp.

Introduction: Heavily shocked chondrites, products of hypervelocity impacts, can give us insight into the metamorphic processes that have processed chondritic parent bodies. We have also seen that major- and trace-elemental patterns are useful for the investigation of shock-related processes [1–3]. For example, we can investigate if the shock-process occurred within a chemical system open or closed to material transfer. Additionally, the detection and analysis of high-pressure mineral polymorphs within heavily shocked chondrites can be used to constrain local pressure, temperature, pressure pulse duration, and even parent body size [4–6]. Here, we use these methods to investigate the nature of a shock-induced vein within Yamato-75100, a heavily shocked H6 chondrite. We compare the chemistry and mineralogy of the H chondrite host rock with that of the vein material.

Methods: We used EMPA for the observation of Y-75100 in thin section and ICPOES and ICPMS for the analysis of major, minor, and trace elements within physically separated Y-75100 host and vein materials.

Results and Discussion: Detailed mineralogical analysis combined with bulk chemical data provide unique insight into the effects of shock-induced transformations on the trace elemental chemistry.

Mineralogy: The shock-induced vein comprises the same phases as the host, such as olivine, low-Ca pyroxene, and plagioclase in composition, with minor amounts of chromite and phosphate. Fine-grained (submicron) metal and troilite seem highly abundant in the vein. Silicate phases were abundantly transformed into high-pressure phases, such as wadsleyite and ringwoodite from olivine, majorite, and trace amount of akimotoite from low-Ca pyroxene, and lingunite and jadeite from plagioclase. We also found breakdown products (perovskite and majorite) from high-pressure Ca-rich pyroxene [5].

Chemical Analysis: We found several differences between vein and host compositions. Results show depletions of up to 50% in the thermally labile elements Zn, Bi, and Cd; however, we found little difference between vein and host In and Tl contents. Rb and Cs show substantial enrichments of ~20%, while K and Na demonstrate only slight enrichments in vein material. Na, K, Rb, and Cs enrichment in the vein may indicate the addition of a plagioclase component during the shock event. Se and Te display vein material enrichments of about 20% possibly due to sulfide mobilization.

References: [1] Friedrich et al. 2004. *Geochimica et Cosmochimica Acta* 68:2889–2904. [2] Friedrich J. M. 2006. *Geochemical Journal* 40:501–512. [3] Wang M.-S. et al. 1999. *Meteoritics & Planetary Science* 34:713–716. [4] Ohtani E. et al. 2004. *Earth and Planetary Science Letters* 277:505–515. [5] Tomioka N. and Kimura M. *Earth and Planetary Science Letters* 208:271–278. [6] Chen M. et al. *Science* 271:1570–1573.

5103

DUST SIZE AND CRYSTALLINITY AROUND HERBIG AE/BE STARS

H. Fujiwara[1], T. Onaka[1], H. Kataza[2], Y. K. Okamoto[3], M. Honda[4], and T. Yamashita[5]. [1]Department of Astronomy, School of Science, University of Tokyo, Bunkyo-ku, Tokyo 113-0033, Japan. E-mail: fujiwara@astron.s.u-tokyo.ac.jp. [2]Institute of Space and Astronautical Science, JAXA, 3-1-1 Yoshinodai, Sagamihara, Kanagawa 229-8510, Japan. [3]Institute of Astrophysics and Planetary Sciences, Ibaraki University, Bunkyo 2-1-1, Mito, Ibaraki 310-8512, Japan. [4]Department of Information Science, Faculty of Science, Kanagawa University, 2946 Tsuchiya, Hiratsuka, Kanagawa 259-1293, Japan. [5]Astrophysical Science Center, Hiroshima University, 1-3-1 Kagamiyama, Higashi-Hiroshima, Hiroshima 739-8526, Japan.

Introduction: Recent infrared spectroscopic observations have revealed a large variety in the properties of silicate dust around young stars [1, 2]. However, the precise process of the evolution of dust grains in protoplanetary disks is still unknown. In particular, the process of crystallization and grain growth of silicate dust provides key information linking protoplanetary disks with the present-day solar system. Here, we present N-band (8–13 μm) spectra of 58 Herbig Ae/Be stars and the results of spectral decomposition analysis.

Observations and Analysis: We have carried out mid-infrared N-band spectroscopic observations of 11 Herbig Ae/Be stars with the Cooled Mid-Infrared Camera and Spectrometer on the 8.2 m Subaru Telescope [3]. We also extracted spectra of 17 Herbig Ae/Be stars obtained with the Infrared Spectrograph on board Spitzer Space Telescope and 30 Herbig Ae/Be stars obtained with the Short Wavelength Spectrometer on board Infrared Space Observatory, and made systematic analysis on N-band spectra of 58 Herbig Ae/Be stars. We made compositional model fitting to the spectra of Herbig Ae/Be stars. In the analysis, we considered five dust species (amorphous olivine, amorphous pyroxene, crystalline forsterite, crystalline enstatite, and silica) and two dust sizes (0.1 and 1.5 μm) for each of them. We derived the contributions of each component for each star.

Results and Discussion: We derived the fraction of large grains (1.5 μm grains) and the fraction of crystalline silicate grains as indicators of dust evolution, and compared them with the stellar parameters [4]. We found that massive, young, or luminous stars with the small value of the large grain fraction do not exist while less massive, old, or less luminous stars with the small value of the large grain fraction do. This trend is explained by the difference in the strength of turbulence in the disk and the radiation pressure on grains, which controls the removal and supply of large grains at the disk surface. We also found that most sample stars show the crystallinity of circumstellar silicate of larger than 5%. On the other hand, no dependence of the crystallinity on the stellar parameters was found. This suggests that dust crystallization has already started in a very early stage of the pre-main sequence before the Herbig Ae/Be phases.

References: [1] Van Boekel R. et al. 2005. *Astronomy & Astrophysics* 437:189–208. [2] Honda M. et al. 2006. *The Astrophysical Journal* 646: 1024–1037. [3] Kataza H. et al. 2000. *Proceedings of SPIE* 4008:1144–1152. [4] Manoj P. et al. 2006. *The Astrophysical Journal* 653:657–674.

5296

WHERE ARE ALL THE PARTIALLY MELTED METEORITES?

M. J. Gaffey. Department of Space Studies, University of North Dakota, Box 9008, Grand Forks, ND 58202–9008, USA. E-mail: gaffey@space.edu.

Introduction: There are a number of apparent contradictions between the thermal histories of the meteorites and the asteroids and the proposed heating mechanism(s) for the meteorite parent bodies. Of the 135 distinct parent bodies represented in the meteorite collections, 80% experienced temperatures sufficient to produce at least partial melting (i.e., igneous processes) while most of the remaining 20% experienced heating sufficient to produce significant metamorphism [1]. Most meteorite investigators have concluded that the short-lived radioisotope ^{26}Al was the primary heat source that caused the metamorphism and melting of the meteorite parent bodies.

Puzzlements: The canonical value derived from the Ca-Al inclusions in the CV3 chondrite, Allende, for the early solar system ^{26}Al/^{27}Al ratio is ~5×10^{-5} [2]. Thermal models using the canonical value produce melting even in small (tens of kilometers) bodies. However, the parent body of Allende did not undergo any significant heating indicating that the ^{26}Al had decayed prior to formation of the parent body. The actual content of "live" ^{26}Al in the meteorite parent bodies at the time that they accreted is poorly constrained. Models typically invoke a time delay between formation of the CAIs and formation of the chondritic meteorite parent bodies to allow some of the ^{26}Al to decay (e.g., [3, 4]).

If ^{26}Al is the heat source, the large number of igneous parent bodies indicates that many bodies accreted early with a nearly canonical ^{26}Al abundance. The issue is complicated by the variation of ^{26}Al abundance among the various chondrite types. If the ^{26}Al in the ordinary and enstatite chondrite parent bodies was "live" they would have contained sufficient ^{26}Al to produce partial melting but not complete melting [5].

The Issue: Telescopic spectra indicate the presence of a significant number of partially melted bodies in the asteroid belt [5]. Unless one invokes two distinct accretion epochs—an early episode producing the ^{26}Al-rich parent bodies of the igneous meteorites and a later episode producing the ^{26}Al-poor chondrite parent bodies—there should be a significant number of parent bodies with intermediate ^{26}Al contents that attained limited partial melting rather than complete or nearly complete melting. The co-existence of E-, S-, and C-type asteroids at the same heliocentric distances indicates that asteroids accreted on short time scales throughout the cooling (or mixing) history of the nebula. The telescopic studies of asteroids indicate the presence of such partially melted asteroids, but the meteorite collections do not contain the expected diversity of partially melted meteorites.

Since apparent paradoxes are due to either incomplete knowledge or inaccurate models, this discord must be telling us something interesting if we are clever enough to solve the problem.

Acknowledgements: Various portions of this research were supported by NASA Planetary Geology and Geophysics Grant NNG04GJ86G.

References: [1] Keil K. 2000. *Planetary and Space Science* 48:887–903. [2] Lee T. et al. 1976. *Geophysical Research Letters* 3:109–112. [3] Amelin Y. et al. 2005. *Geochimica et Cosmochimica Acta* 69:505–518. [4] Hevey P. J. and Sanders I. S. 2006. *Meteoritics & Planetary Science* 41:95–106. [5] Gaffey M. J. 2006. Abstract #1223. 37th Lunar and Planetary Science Conference.

5135

Mn-Cr DECAY SYSTEM: DIFFUSION KINETICS IN PYROXENES AND THERMOCHRONOLOGY OF EARLY SOLAR SYSTEM PROCESSES IN METEORITES

J. Ganguly[1], M. Ito[2], and X.-Y. Zhang[1]. [1]Department of Geosciences, The University of Arizona, Tucson, AZ 85721, USA. E-mail: ganguly@email.arizona.edu. [2]NASA, Johnson Space Center ARES, Mail Code KR, 2101 NASA Parkway, Houston, TX 77058, USA.

Introduction: The ^{53}Mn-^{53}Cr decay system ($t(1/2)$ = 3.7 Myr) has emerged as an important tool to explore the chronology of early solar system processes, and cooling rates and parent body structures of meteorites [1]. Interpretation and thermochronological application of the Mn-Cr age, however, require an understanding of the closure temperature of the system, which in turn depends on the diffusion kinetics of Cr in the minerals that are used for dating. Thus, we have undertaken a systematic study of Cr diffusion in major meteoritic minerals, namely olivine [1], orthopyroxene (Opx), and clinopyroxene (Cpx), which have been reported to show radiogenic ^{53}Cr (^{53}Cr*).

Experimental Studies: We have determined the diffusion of Cr in Opx parallel to the three crystallographic directions. Likewise olivine [1], Cr diffusion in orthopyroxene is anisotropic with D(//c) > D(//b) > D(//a), having activation energies of ~260 kJ/mol and D_o(//c) = 3.10 (±3.99)10^{-10}, D_o(//b) = 1.78 (±3.19)10^{-10} and D_o(//a) = 7.41 (±6.66)10^{-11} m^2s^{-1} at $f(O_2)$ condition of wüstite-iron buffer. Work on diffusion kinetics in Cpx is currently in progress.

Applications: The diffusion data have been used to calculate the closure temperatures (T_c) of Mn-Cr decay system in Opx, assuming a homogeneous infinite reservoir (HIR), and to formulate thermochronological relations [2] that permit retrieval of cooling rate from knowledge of the resetting of Mn-Cr mineral age during cooling. Application of these results to the Mn-Cr age data of Opx in the cumulate eucrite Serra de Magé yields a T_c of 830–980 °C, and cooling rates (CR) of 2–27 °C/Myr at T_c and ~1–13 °C/Myr at 500 °C, implying a burial depth of ~30 km within the basaltic lower crust of the parent asteroid, Vesta. Such a thickness of the lower crust is greater than that in most models of the internal structure of Vesta, but is compatible with a proposed model [3] of relatively olivine-poor bulk mineralogy in which olivine constitutes 19.7% of the total asteroidal mass.

For HIR, T_c(Cr) in Opx is significantly greater than that in olivine [1]. On the other hand, T_c(Pb) in Cpx, as calculated from Pb diffusion data [4], is intermediate between the two for CR >4 °C/Myr. An Mn-Cr mineral isochron involving Opx closes at the T_c that is at least as high as that of Opx in an HIR, and thus provides a more robust chronometer for dating early solar system processes than the Pb-Pb age of Cpx for CR >4 °C/Myr.

Work in progress on the Cr diffusion in Cpx will be used to the interpretation of the available Mn-Cr and Pb-Pb ages of Cpx in the angrite D'Orbigny, which represents the most primitive basaltic rock in the solar system, and reported in the meeting.

References: [1] Ito M. and Ganguly J. 2006. *Geochimica et Cosmochimica Acta* 70:799–806. [2] Ganguly J. and Tirone M. 1999. *Earth and Planetary Science Letters* 170:131–140. [3] Ruzicka A. et al. 1997. *Meteoritics & Planetary Science* 32:825–840. [4] Cherniak D. J. 2001. *Chemical Geology* 150:105–107.

5327

METEOROID STREAMS OF ASTEROIDAL ORIGIN AS EVIDENCE OF RECENT IMPACTS ON NEAs

J. J. García-Martínez[1] and F. Ortega-Gutiérrez[2]. [1]Posgrado en Ciencias de la Tierra, UNAM. E-mail: pepeluis@correo.unam.mx. [2]Instituto de Geología, UNAM.

Introduction: The probable existence of meteor streams of asteroidal origin was first suggested in 1937 by Hoffmeister. Since then, several authors have reported persistent evidence of streams on asteroidal orbits. A summary of the most outstanding authors, up to 1998, is presented by [1]. Among the works on the subject, the most notable have been the ones presented by [4] and [6] in which they report the observation with two camera networks of two meteorite falls following nearly the same orbit in each case, i.e., the cases of Innisfree-Ridgedale and Příbram-Neuschwanstein pairs.

Interpretation: From the above observations and the discovery of several meteoroid streams on NEA orbits containing substream of two or three meteoroids on nearly the same orbit in the IAU_MDC Database of Photographic Meteors [3], a plausible interpretation is that we are observing asteroidal fragments from NEAs due to the most recent impacts received. Since meteoroid streams are expected to last as such for at most a few thousands of years [2], probably some of the most recent impacts, responsible for the substreams, took place no more than one hundred years ago. The latter in agreement with the expected impact frequency on typical NEAs of more than 5 impacts per millennium by objects with $d = 1$ m or larger, as deduced from the observed impact rate on the Moon by this kind of impactor.

References: [1] Hoffmeister C. 1937. *Die meteore.* Leipzig: Akademische Verlagsgesellschaft. [2] Jopek T. J. et al. 2002. *Asteroids III*: 645–652. [3] García-Martínez J. L. and Ortega-Gutiérrez F. 2007. Abstract #2038. 38th Lunar and Planetary Science Conference. [4] Halliday I. 1987. *Icarus* 69:550–553. [5] Kostolansky E. 1998. *Contributions of the Astronomical Observatory* 29:22–30. [6] Oberst J. et al. 2004. *Meteoritics & Planetary Science* 39:1627–1641.

5285

PETROLOGY OF THE METAL-RICH LL6 NWA 1396

K. G. Gardner[1], D. S. Lauretta[1], D. H. Hill[1], and M. Killgore[2]. [1]Lunar and Planetary Laboratory, The University of Arizona, Tucson, AZ, USA. E-mail: kgardner@lpl.arizona.edu. [2]Southwest Meteorite Center.

Introduction: Northwest Africa 1396 is an unusual LL6 ordinary chondrite; while containing silicate clasts of LL composition, it contains millimeter-wide taenite veins and has textural similarities to the H6 ordinary chondrite Portales Valley, an impact-melt breccia [1–3]. We perform a comprehensive study of the petrology and geochemistry of NWA 1396 in order to better constrain its origin and genetic relationship to other ordinary chondrites and possibly the primitive achondrites.

Initial Results: Electron microprobe (Cameca SX-50) analyses of one thin section of NWA 1396 reveal homogeneous olivine ($Fa_{30.7 \pm 0.3}$), both low- and high-Ca pyroxene ($Wo_{1.6 \pm 0.4}En_{73.5 \pm 0.3}Fs_{24.8 \pm 0.2}$ and $Wo_{43.8 \pm 0.7}En_{46.3 \pm 0.3}Fs_{9.9 \pm 0.6}$), and inhomogeneous secondary plagioclase (averaging $Ab_{80.2 \pm 18}An_{9.6 \pm 2.3}Or_{10.2 \pm 20.2}$). Two pyroxene thermometry yields an equilibration temperature of 866 ± 6 °C. Iron alloys occurs rarely as kamacite (~4.4 wt% Ni) and frequently as millimeter-wide taenite (40–52 wt% Ni) veins, which extend up to ~7.5 mm in length, and taenite blebs in the matrix. Minor troilite and chromite are also present. Relict chondrules exist that are 0.5–1 mm in diameter. Based on the methods of [4] and [5], NWA 1396 is a shocked (S2) monomict LL6 ordinary chondrite breccia with a weathering grade of W2.

Discussion: The texture of NWA 1396 is very similar to that of Portales Valley; it contains metal with a sinuous, wormy texture indicative of shock processing. Thus, NWA 1396 likely formed as an impact-melt breccia on the LL-chondrite parent body. It is curious, however, that the metal veins in NWA 1396 are Ni-rich, indicating they did not result from the melting of LL chondrite material during the impact. It is possible that the metal veins in NWA 1396 are melt products of the impactor, perhaps an iron meteorite.

The silicate portion of NWA 1396 shares compositional similarities to the primitive achondrites Tafassasset and RBT 04239 [6]. However, the two-pyroxene equilibration temperatures are different for these three. It is noteworthy that Fa and Fs values of NWA 1396 silicates are at the Fe-rich end of the LL range and are similar to Tafassasset and the brachinites. Likewise, NWA 1396 plots near Tafassasset and the brachinites on a mol% Fa versus Fe/Mn plot. Oxygen-isotopic analysis is needed to determine whether a genetic link exists between NWA 1396 and these primitive achondrites. However, it is possible that these samples equilibrated in a similar oxidation environment.

Acknowledgements: This work was supported by NASA Grant NNX07AF96G.

References: [1] Kring D. A. et al. 1999. *Meteoritics & Planetary Science* 34:663–669. [2] Rubin A. E. et al. 2001. *Geochimica et Cosmochimica Acta* 65:323–342. [3] Ruzicka A. et al. 2005. *Meteoritics & Planetary Science* 40:261–295. [4] Kallemeyn G. W. et al. 1989. *Geochimica et Cosmochimica Acta* 53:2747–2767. [5] Wlotzka F. 1993. *Meteoritics & Planetary Science* 28:A460. [6] Gardner K. G. et al. 2007. Abstract #2086. 38th Lunar and Planetary Science Conference.

5007

EVIDENCE FOR SHOCK IN MICROMETEORITES

M. J. Genge. Impact and Astromaterials Research Centre, Department of Earth Science and Engineering, Imperial College London, UK. E-mail: m.genge@imperial.ac.uk.

Introduction: Micrometeorites (MMs) are that fraction of the extraterrestrial dust flux that survives atmospheric entry to be recovered from the Earth's surface. The majority of MMs have textures, mineralogies, and compositions similar to chondrules and matrix of chondrites and are, therefore, asteroidal dust liberated from its parent bodies during collision events. An appreciable proportion of particles might therefore be expected to exhibit shock features. To date, however, there have been no studies of the shock state of MMs.

This work evaluates whether shock features within MMs can be identified in backscattered electron images since the small size of particles precludes standard optical techniques. This result suggests that shock features are present but most relate to impact events prior to dust generation.

Results: Three textural features are identified in MMs that potentially represent shock indicators: 1) metal-sulfide veins, 2) olivine grains with numerous subdomains, and 3) highly vesicular glasses. Metal-sulfide melt veins are the most common putative shock feature and are similar to those observed within chondrites [1]. They occur mainly in coarse-grained MMs (cgMMs) dominated by pyroxene and olivine, are usually <5 μm in width, and consist of trails of disconnected subspherical droplets and thus imply post-shock annealing. Olivine grains with subdomains were identified in several particles and are broadly similar to shock-induced mosaicism [1]. Highly vesicular glass was observed in two particles and may represent shock melt [1]. In one, a cgMM, partially melted olivines are present within the glass. In the second particle, a fine-grained MM (fgMM), the glass is pure SiO_2 and is a microclast contained in CI-like matrix. Owing to its highly unusual composition, this microclast represents the most convincing evidence for shock yet in MMs.

Implications: Both metal-sulfide veins, which appear to have undergone an extended period of annealing, and the vesicular microclast in the CI-like particle evidently originate from shock events that predate liberation of the particles from their parent bodies. Among fgMMs, dehydration of matrix is predicted by shock experiments [2], however, a significant fraction of MMs exhibit igneous rims generated during atmospheric entry that are supported by dehydration reactions [3] and thus indicate that the majority of particles were still hydrous when they entered the Earth's atmosphere.

The paucity of identifiable shock features may simply relate to the detection technique, which needs to be calibrated by studies of shocked meteorites; however, the results of this preliminary study imply that the shock state of the majority of MMs is lower than might be expected for particles liberated from their parent bodies by collisions. This could suggest that small erosive collisions dominate dust production or alternatively that radiative cooling from dust sized ejecta inhibits the formation of features dependent on post-shock heating such as dehydration of phyllosilicates.

References: [1] Stöffler D. *Geochimica et Cosmochimica Acta* 55: 3845–3867. [2] Tomeoka K. et al. 2003. *Nature* 423:60–62. [3] Genge M. J. 2006. *Geochimica et Cosmochimica Acta* 70:2603–2621.

5045

IDENTIFICATION AND ANALYSIS OF IN SITU CARBON-BEARING PHASES IN NAKHLA

E. K. Gibson[1], D. S. McKay[1], S. J. Clemett[2], K. L. Thomas-Keprta[2], S. J. Wentworth[2], F. Robert[3], A. B. Verchovsky[4], I. P. Wright[4], C. T. Pillinger[4], T. Rice[5], B. Van Leer[5], A. Meibom[3], S. M. Mostefaoui[3], R.Socki[2], and L. Le[2]. [1]KR, ARES, NASA-JSC, Houston, TX 77058, USA. E-mail: everett.k.gibson@nasa.gov. [2]Jacobs Engr., Bay Area Blvd., Houston, TX, USA. [3]LEME, CNRS-Museum d'Histoire Naturelle, Paris, France. [4]PSSRI, The Open University, Milton Keynes, UK. [5]FEI Co., Hillsboro, OR 97124, USA.

Nakhla is a relatively young igneous olivine clinopyroxenite Martian meteorite with a crystallization age of 1.3 Gy [1] which underwent pre-terrestrial aqueous alteration [2] ~600–700 Ma ago [3]. Within the Nakhla alteration products there is evidence of indigenous reduced carbon phases. In situ analysis of the carbon phases has been carried out to identify and characterize the reduced carbonaceous matter. Optical analysis of several Nakhla petrographic thin sections reveal the existence of a dark brown/red vein-filling material appearing as a series of bifurcating intrusions into a fine (<300 nm width) crack/fissure system within an olivine/augite groundmass. Microanalysis utilizing focus ion beam (FIB) extraction techniques, FESEM/EDX, STEM/EDX, nanoSIMS ion microprobe, laser Raman spectroscopy, and stepped-combustion isotopic mass spectrometry have been used to characterize the carbon phases. STEM/EDX shows the carbon phases are amorphous. Stepped-combustion isotopic analysis indicates the reduced carbon components have a carbon isotopic composition of −15 to −20‰. NanoSIMS analysis of the reduced carbon phases indicates the $^{12}C/^{12}C^{14}N$ ratios are not associated with potential epoxy contaminants. The close association of the carbonaceous matter to a region of secondary mineralization suggests that it was formed contemporaneously with the iddingsite. This carbonaceous material has similarities to macromolecular carbonaceous matter and yet possesses a complex structural and textural morphology that is not observed in carbonaceous or ordinary chondrite meteoritic kerogen.

Comparison of the pre-terrestrial aqueous alteration textural features in Nakhla SNC meteorite with bacterial alteration features in submarine basaltic glass, as reported by [4], is striking because of the similarities in size and appearance of the large and small tunnels and galleries in both materials. DNA has been found within the submarine glass corrosion features. One of the possible origins for the reduced carbon components which cannot be ruled out is that the carbonaceous matter within Nakhla may be from biogenic processes operating on Mars.

References: [1] Meyer C. 2006. *Compendium of Martian meteorites*. JSC Curatorial Office, NASA, Houston, TX. [2] Gooding J. L. et al. 1991. *Meteoritics* 26:135–143. [3] Swindle T. D. and E. K. Olson 2004. *Meteoritics & Planetary Science* 39:755–766. [4] Fisk M. R. et al. 2006. *Astrobiology* 6: 48–68.

5161

IRON OXIDATION STATE IN MICROTEKTITES BY HIGH-RESOLUTION XANES SPECTROSCOPY

Gabriele Giuli[1], Sigrid Griet Eeckhout[2], Christian Koeberl[3], Maria Rita Cicconi[1], and Eleonora Paris[1]. [1]Dip. Scienze della Terra, Università di Camerino, Italy. E-mail: gabriele.giuli@unicam.it. [2]European Synchrotron Radiation Facility (ESRF), Grenoble, France. [3]Department of Geological Sciences, University of Vienna, Austria.

Introduction: We examined the iron oxidation state and coordination number in a number of microtektites from all three known strewn fields for which microtektites have been reported (namely, the North American, Ivory Coast, and Australasian strewn fields). Also, also a few microscopic glass spherules from the immediate post-impact fallback layer retrieved from a core drilled at the Bosumtwi impact crater (Ghana) were also analyzed.

These samples were studied by Fe K-edge high-resolution X-ray absorption near edge structure (XANES) spectroscopy, and Kα- or Kβ-detected XANES spectroscopy.

Despite the availability of geochemical studies on microtektites, very few studies exist of the Fe coordination number and oxidation state in such materials. As microtektites constitute a large fraction of the mass of the glass produced by a tektite-generating impact event, such studies are of great importance for a more complete study of impact-generated glasses and, in particular, to try to reconstruct the oxygen fugacity conditions prevailing during impact melt formation.

The XAS data have been collected at the ID26 beamline of the ESRF storage ring (Grenoble, F) using a Si (311) monochromator and with a beam size at the sample of 55 × 300 μm. The pre-edge peaks of our XANES spectra display well discernible variations in intensity and energy, which are indicative of significant changes in the Fe oxidation state.

In the Australasian and Ivory Coast microtektites all Fe is divalent. Small components in the pre-edge peak are detected related to Fe^{3+} in amounts at well below 10 mol% level. North American microtektites display varying $Fe^{3+}/(Fe^{2+} + Fe^{3+})$ ratio ranging from 0 to 0.5. All data plot along a trend, falling between two mixing lines joining a point calculated as the mean of a group of the tektites studied so far (consisting of 4- and 5- coordinated Fe^{2+}) to $^{[4]}Fe^{3+}$ and $^{[5]}Fe^{3+}$, respectively. Thus, the XANES spectra can be interpreted as a mixture of $^{[4]}Fe^{2+}$, $^{[5]}Fe^{2+}$, $^{[4]}Fe^{3+}$, and $^{[5]}Fe^{3+}$. There is no evidence for six-fold coordinated Fe; however, its presence in small amounts cannot be excluded from XANES data alone.

Bosumtwi glass microspherules display small variations in the pre-edge peak shape but contain essentially only divalent Fe. It is somewhat surprising that the Bosumtwi glasses are relatively reduced, because proximal impact glasses often are not as reduced as distal ones.

The relatively high $Fe^{3+}/(Fe^{2+} + Fe^{3+})$ ratio in North American microtektites poses a problem regarding the mechanism of impact melt reduction. No obvious relationship is evident between Fe oxidation state and glass composition. Possibly several parameters affect Fe oxidation state, including target-rock type, marine versus continental target, amount of energy released, and mass of produced glass.

5162

IRON REDUCTION IN SILICATE GLASS PRODUCED DURING THE 1945 NUCLEAR TEST AT THE TRINITY SITE (ALAMOGORDO, NEW MEXICO, USA)

Gabriele Giuli[1], Giovanni Pratesi[2], Sigrid Griet Eeckhout[3], and Eleonora Paris[1]. [1]Dip. Scienze della Terra, Università di Camerino, Italy. E-mail: gabriele.giuli@unicam.it. [2]Dipartimento di Scienze della Terra, Universita di Firenze, Italia. [3]European Synchrotron Radiation Facility (ESRF), Grenoble, France.

The oxidation state of Fe in silicate glasses produced during the first atomic bomb blast at the trinity test site (New Mexico) has been studied by high-resolution XANES (X-ray absorption near edge spectroscopy). The samples consist of green glass resulting from the melting of the quartz bearing sand at the test site; some relict sand is still present at the bottom of the sample. Comparison of the pre-edge peak data with model compounds with known Fe oxidation state and coordination number show that in the trinity glass sample Fe is in the divalent state and, on average, in a mixture of 4- and 5-fold coordinated sites.

XANES spectra collected at various heights of the glass sample from the bottom up to exposed surface, show no variation of the pre-edge peak, meaning that Fe oxidation state does not vary with the distance from the sand/glass interface. However, XANES analysis of a portion of the sand at the bottom of the sample show Fe to be in a mixture of Fe^{2+} and Fe^{3+}, with an $Fe^{3+}/(Fe^{2+} + Fe^{3+})$ ratio close to 52%. This demonstrates that during the nuclear explosion the molten ground rock was instantaneously reduced, transforming all the iron from mostly trivalent state to almost purely divalent.

5047

POSSIBLE SHOCK-METAMORPHOSED GRAINS FROM THE PRECAMBRIAN CARAWINE SPHERULE LAYER, RIPON HILLS, WESTERN AUSTRALIA

B. P. Glass[1], F. C. Smith[1], J. B. Zullo[1], and B. M. Simonson[2]. [1]Department of Geological Sciences, University of Delaware, Newark, Delaware 19716, USA. E-mail: bglass@udel.edu. [2]Oberlin College, Oberlin, Ohio 44074, USA.

Introduction: Over a dozen Precambrian spherule layers, believed to be of impact origin, have been found in South Africa, Western Australia, and Greenland (see, e.g., [1]). Geochemical evidence (e.g., Ir, Cr isotopic ratios) supports an impact origin for many of these spherule layers. However, except for a single quartz grain containing at least two sets of planar deformation features (PDFs) observed [2] in a sample from the Jeerinah spherule layer in Western Australia, no shock-metamorphosed mineral grains have been found in any of these Precambrian spherule layers [3]. The Jeerinah spherule layer may correlate with a spherule layer in the Carawine Dolomite, and both may correlate with the Monteville spherule layer in South Africa [4–6].

Method: As part of a larger study to search for shocked mineral grains in Precambrian spherule layers and to determine the heavy mineral assemblages associated with these layers, we dissolved an ~10.7 kg sample of the carbonate-rich Carawine spherule layer from the Ripon Hills area. The insoluble fractions from six subsamples, which originally weighed a total of 6.44 kg, were sieved into five size fractions. The 63–125 μm size fractions of these six subsamples were put through heavy liquid separations. A portion of each light fraction (<2.96 g/cm^3) was used to make a total of 13 grain mounts which were searched for PDFs.

Results: An estimated 18,200 grains were observed on the 13 slides. Most of the grains are finely crystalline chert fragments. Approximately 4.8% (~880) are quartz grains. Close to 20% of the quartz grains are transparent, fresh-looking with euhedral to anhedral shapes, and may be authigenic grains. None of these quartz grains exhibited planar microstructures. Most of the quartz grains (>80%) are subrounded to angular with cloudy to "dirty" appearances. Fourteen (~2%) of these grains contain planar microstructures. The number of sets in a single grain varies between 1 and 3. The planar features are all fairly faint and only traverse a portion of each grain. They are <1 μm in width with a spacing of ~2–8 μm. The planar features may be PDFs, but their orientations need to be determined.

X-ray diffraction (XRD) data, obtained using Gandolfi and Debye-Scherrer (D-S) cameras, indicate that most of the heavy minerals recovered from the 63–125 μm size fractions are rutile and anatase (over 90%) and zircon (~6%), with a trace of spinel. Twenty-five zircons were recovered. Six are translucent to opaque. D-S XRD patterns were obtained for three of these and all three patterns showed X-ray asterism, but none showed any evidence of baddeleyite or reidite.

Acknowledgements: This research was partly supported by NASA grant NAG5-11522 to B. P. G. and a Barringer Family Fund for Meteorite Research grant to F. C. S.

References: [1] Simonson B. M. and Glass B. P. 2004. *Annual Review of Earth and Planetary Science* 32:329–361. [2] Rasmussen B. and Koeberl C. 2004. *Geology* 32:1029–1032. [3] Simonson B. M. et al. 1998. *Geology* 26:195–198. [4] Rasmussen B. et al. 2005. *Geology* 33:725–728. [5] Kohl I. et al. 2006. GSA Special Paper #405. pp. 57–73. [6] Jones-Zimberlin S. et al. 2006. *South African Journal of Geology* 109:245–261.

5069

THERMAL RADIATION FROM DISTAL CHICXULUB EJECTA

T. J. Goldin[1] and H. J. Melosh[2]. [1]Department of Geosciences, The University of Arizona, Tucson, Arizona 85721, USA. E-mail: tgoldin@email.arizona.edu. [2]Lunar and Planetary Laboratory, The University of Arizona, Tucson, Arizona 85721, USA.

Introduction: An accurate model of the heat exchange between ejecta and the atmosphere is essential to understanding the environmental effects of large impacts. Found worldwide, the distal Chicxulub ejecta layer at the K/T boundary is ~2–3 mm thick and contains mainly 250 μm spherules. The presence of soot within the boundary layer [1] and calculations of thermal energy radiated from falling ejecta [2] suggest atmospheric re-entry of Chicxulub ejecta triggered global wildfires. Previous models [3] employing a simple blackbody radiation model also suggest the delivery of significant thermal radiation to the Earth's surface, but do not consider the optical opacity of spherules in the atmosphere. Incorporating a complex treatment of thermal radiation into our model allows us to accurately compute the radiation energy density, both throughout the atmosphere and through time.

Modeling: We model the interactions between distal Chicxulub ejecta and the atmosphere using the two-dimensional, two-phase fluid flow code KFIX-LPL (modified from KFIX [4]). The initial mesh approximates the Earth's atmosphere and 250 μm spherules are injected into the top of mesh at 8 km/s. The spherules fall through the thin upper atmosphere, compressing the air. The spherules slow and accumulate at ~100 km altitude. This deceleration heats the spherules.

We have implemented in KFIX-LPL a complete treatment of thermal radiation, which takes into account optical opacity variations across the mesh in both air and spherule phases. In the dense band of spherules, as well as below (where the atmosphere is densest), optical opacity must be considered. However, the mean free paths in the relatively clear upper atmosphere greatly exceed the mesh height, so here we assume simple blackbody radiation. The top (space) and bottom (ground) boundaries of the mesh are 100% absorptive.

Our model results for the distal Chicxulub scenario suggest maximum atmospheric temperatures of ~400–800 K over the period of spherule atmospheric reentry. During this time, the ground receives a radiation flux of ~200–300 W/m^2.

Discussion: Maximum temperatures calculated from the complex radiation model are similar to those from our previous models employing purely blackbody thermal radiation [3]. Thus the spherules are able to efficiently radiate their heat while they fall through the thin upper atmosphere. Although temperatures in the lower atmosphere are elevated due to atmospheric re-entry, 800 K is not hot enough to destroy shocked quartz or melt spherules and this efficient removal of heat from the atmosphere supports the observed preservation of impact materials on the ground. However, the elevated radiation density in the lower atmosphere would have had severe environmental consequences, possibly triggering both global wildfires [1, 2] and extinctions [5].

References: [1] Wolbach W. S. et al. 1988. *Nature* 334:665–669. [2] Melosh H. J. et al. 1990. *Nature* 343:251–253. [3] Goldin T. J. and Melosh H. J. 2007. Abstract #2114. 38th Lunar and Planetary Science Conference. [4] Rivard W. C. and Torrey M. D. 1977. Los Alamos National Laboratory Report #LA-NUREG-6623. [5] Robertson D. S. et al. *GSA Bulletin* 116:760–768.

5088

Fe-Ni ISOTOPE SYSTEMATICS IN SILICATE PHASES OF UOC CHONDRULES

J. N. Goswami and R. Mishra. Physical Research Laboratory, Ahmedabad-380009, India. E-mail: goswami@prl.res.in.

Introduction: The solar system initial $^{60}Fe/^{56}Fe$ ratio is not well constrained at present [1–4]. An accurate estimation of this ratio will allow us to pinpoint the exact nature of the stellar source of this nuclide and to evaluate the role of ^{60}Fe as a heat source during the late evolution of meteorite parent bodies. We have initiated a study of ^{60}Fe records in silicate phases of chondrules from unequilibrated ordinary chondrites (UOCs) belonging to low petrologic grades (3.0–3.3). Even though troilite is a suitable phase for hosting ^{60}Fe [1, 2], the possibility of diffusion of Ni, particularly when troilite is in association with metal [2], makes silicates a better phase [3] that also facilitates the study of Al-Mg isotope system.

Samples: UOC samples Semarkona and Y-793596, both LL3.0, Y-791324 (LL3.1), ALHA76004 (LL3.3), LEW 86134 (L3.0), and QUE 97008 (L3.05), are included in this work. Al-rich phases in chondrules from these samples have been analyzed earlier for ^{26}Al records [5, 6]. Fe-Ni isotope systematics in chondrules hosting radiogenic ^{26}Mg are studied using an ion microprobe following procedures described previously [7].

Results and Discussion: The initial $^{26}Al/^{27}Al$ values in chondrules from the above UOCs range from 0.5×10^{-5} to 1.9×10^{-5} [5, 6]. The chondrules are mostly porphyritic olivine or porphyritic olivine-pyroxene in nature along with a few porphyritic pyroxene and one bar-chondrule. The study of Fe-Ni isotope systematics was hampered by low Fe/Ni ratios (a few times 10^3) in most of the chondrule olivines. A few pyroxenes in Semarkona chondrules have reasonable Fe/Ni ratio that allowed us to look for excess ^{60}Ni in them and we reported an initial $^{60}Fe/^{56}Fe$ value of $(2.31 \pm 1.8) \times 10^{-6}$ (2σ error) for a Semarkona chondrule [7]. New results obtained from several chondrules in QUE 97008, LEW 86134, and ALH 76004 yielded ×initial $^{60}Fe/^{56}Fe$ values with low precision due to the low count rates of ^{61}Ni (1–10 cps) and ^{62}Ni as well as moderate $^{56}Fe/^{61}Ni$ ratios of $\leq 5 \times 10^5$. Our present data do not allow us to choose between the two sets of initial $^{60}Fe/^{56}Fe$ values, $(2.2–3.7) \times 10^{-7}$ and $(9.2 \pm 2.4) \times 10^{-7}$, reported previously [2, 3]. New results with improved precision, based on studies currently in progress, will be reported.

References: [1] Tachibana S. and Huss G. R. 2003. *The Astrophysical Journal Letters* 588:41–44. [2] Mostefaoui S. et al. 2005. *The Astrophysical Journal* 625:271–277. [3] Tachibana S. et al. 2006. *The Astrophysical Journal Letters* 639:87–90. [4] Quitté G. et al. 2006. *Meteoritics & Planetary Science* 41:A144. [5] Rudraswami N. G. et al. 2006. *Meteoritics & Planetary Science* 41:A155. [6] Rudraswami N. G. and Goswami J. N. 2007. *Earth and Planetary Science Letters* 257:231–244. [7] Goswami J. N. et al. 2007. Abstract #1943. 38th LPSC.

5089

TIME OF ONSET AND DURATION OF CHONDRULE FORMATION

J. N. Goswami and N. G. Rudraswami. Physical Research Laboratory, Ahmedabad 380009, India. E-mail: goswami@prl.res.in.

Formation of Ca-Al-rich inclusions (CAIs) and chondrules, which are considered to be products of high-temperature nebular processes, effectively defines the lifetime of the active solar nebula. Studies of short-lived nuclide records in these objects as well as their absolute ages based on Pb-Pb dating led to a general consensus at present that formation of chondrules started about a million years after the formation of the CAIs [1, 2]. Formation of CAIs hosting radiogenic isotopic anomalies took place within a time scale of a few times 10^5 years [1], although there are also suggestions for a much shorter time scale [3]. On the other hand, the inferred duration of chondrule formation, based primarily on the study of ^{26}Al records in chondrules, varies from less than a million years to more than three million years [1, 2 and references therein]. We have conducted a detailed study of chondrules from nine unequilibrated ordinary chondrites (UOCs) belonging to the L and LL groups with petrologic grades 3.0–3.3 in an attempt to firmly establish the time of onset and duration of chondrule formation. Our data support the view that onset of chondrule formation took place about a million years after CAI formation; however, an intense epoch of large-scale chondrule formation started another ~0.5 Ma afterwards and lasted for <1 Ma [4, 5]. The longer duration of ≥3 Ma for formation for UOC chondrules, inferred in earlier studies (see, e.g., [1]), appears to be an artifact caused by thermal metamorphism affecting some of the individual chondrules during their residence in meteorite parent bodies. In contrast to UOC chondrules, data for chondrules from carbonaceous chondrites, obtained by us [6] and others (see, e.g., [1]), suggest that chondrule formation in the outer region of the inner solar system persisted for a much longer duration of ~3 Ma. Plausible scenarios that may accommodate these observations relevant to the early evolution of the solar system, lifetime of an active solar nebula, and formation of chondrules will be presented.

References: [1] Kita N. T. et al. 2005. In *Chondrites and the protoplanetary disk*, ASP 341:558–587. [2] Russell S. S. et al. 2005. In *Meteorites and the early solar system II*. pp. 233–251. [3] Bizzarro M. et al. 2004. *Nature* 431:275–278. [4] Rudraswami N. G. et al. 2006. *Meteoritics & Planetary Science* 41:A155. [5] Rudraswami N. G. and Goswami J. N. 2007. *Earth and Planetary Science Letters* 257:231–244. [6] Hutcheon I. D. et al. Forthcoming.

5171

CONTINUING INVESTIGATION OF THE NAKHLITE MAGMA PILE

M. M. Grady[1, 2], M. Anand[1, 2], M. A. Gilmour[1], J. Watson[1], and I. P. Wright[1]. [1]PSSRI, The Open University, Milton Keynes MK7 6AA, UK. E-mail: m.m.grady@open.ac.uk. [2]Department of Mineralogy, The Natural History Museum, London SW7 5BD, UK.

Introduction: The nakhlites are a group of 1300-million-year-old mafic cumulates that appear to emanate from a single magma body, as either a single flow or series of related flows [1]. On the basis of variations in olivine composition, it has been suggested that the individual nakhlites might derive from different depths within a cumulate pile [2, 3]. The most recent find, MIL 03346, is thought to be from the outermost edge, and might be a chill margin [4]. Chassigny, which has the same crystallization age as the nakhlites, might come from a related, deeper, magma body. The nakhlites have been altered by water, leading to two populations of Martian weathering products: i) clay minerals produced by alteration of the primary silicate minerals, and ii) evaporates (carbonates and sulfates) deposited from the fluid. When there were only three nakhlites for study, it was inferred that the secondary minerals were a sequence formed by progressive deposition from an evaporating brine [5]. Now that there are more than double that number of nakhlites, we are revisiting this theory, first by re-analyzing the carbonates.

Method: Whole rock powders were dissolved in 100% H_3PO_4 at 72 °C, the product gases were passed through a GC to separate CO_2 from other species. The minimum amount of CO_2 analyzed was ~20 nmole; at this level, errors on $\delta^{13}C$ ~±1‰. Yields were calculated from calibration using NIST19.

Table 1. Results.

Sample	wt (mg)	[C] (ppm)	$\delta^{13}C$ (‰)
GV	26.9	102.0	28.2
GV	30.6	53.3	25.3
Lafayette	13.3	24.8	25.4
Lafayette	36.1	87.4	23.5
MIL 03346	44.3	1.9	9.0
MIL 03346	35.6	26.5	38.2
MIL 03346	30.8	23.7	38.3
Nakhla	27.1	51.3	51.3
Nakhla	49.5	53.1	52.2
Nakhla	54.6	95.0	48.6
Nakhla	73.1	74.3	47.7
Y593	37.2	117.1	42.3
Y593	48.3	221.1	42.2
Y593	72.0	116.9	42.3
Chassigny	68.2	3.2	–8.6
Chassigny	103.7	4.2	–7.6

Conclusions: Carbonates in nakhlites are ^{13}C-enriched; those in Chassigny are not, confirming previous findings [6]. Carbonate abundances are very variable, indicating great heterogeneity in their distribution. Carbonates in MIL 03346 are intermediate in composition between (Nakhla and Y-000593) and (Lafayette and Governador Valadares). This does not necessarily support locating MIL 03346 at the upper margin of a lava flow.

References: [1] Lentz R. et al. 1999. *Meteoritics & Planetary Science* 34:919–932. [2] Harvey R. P. and McSween H. Y., Jr. 1992. *Earth and Planetary Science Letters* 111:467–482. [3] Mikouchi T. et al. 2003. *Antarctic Meteorite Research* 16:34–57. [4] Day J. M. D. et al. 2006. *Meteoritics & Planetary Science* 41:581–608. [5] Bridges J. C. and Grady M. M. 2000. *Earth and Planetary Science Letters* 176:267–279. [6] Wright I. P. et al. 1992. *Geochimica et Cosmochimica Acta* 56:817–826.

5325

A NEW METHOD FOR THE DETERMINATION OF THE DENSITY OF STARDUST AEROGEL WITH SCANNING TRANSMISSION ION MICROSCOPY

P. G. Grant, H. Ishii, P. Tsou, and J. P. Bradley. Lawrence Livermore National Laboratory, Livermore, CA 94550, USA.

In 2006, the Stardust spacecraft returned to Earth with cometary and perhaps interstellar dust particles embedded in silica aerogel collectors for analysis [1]. These particles are the first sample-return from a solid body since the Apollo missions. To understand the capture processes and the in situ analysis of the particles it is necessary to characterize the density of the aerogel after being in space for an extended period. This can be done through the use of scanning transmission ion microscopy (STIM), which was demonstrated on analogue particles that were implanted into a keystone of silica aerogel that had been extracted from bulk silica aerogel as previously described [2, 3].

This new application of STIM to document the density of the aerogel as a function of depth is nondestructive and could enable the calculation of attenuation factors for the quantitation of low Z elements by X-ray fluorescence. Flight grade aerogel retained from the mission and aerogel that flew on the Stardust mission was sliced along the path that particles would impact. The slices were a few millimeters thick and had some variation. The energy of accelerated particles (3 MeV) is measured as a function of position in a 1 mm wide path down the 20 mm depth of the aerogel at 40 micron resolution to determine the mass of the aerogel. The thickness of the aerogel is determined by capturing images of a 200-micron-diameter green laser beam (532 nm) passing through the same region of aerogel imaged by STIM. Simulations utilizing Stopping Range in Matter (SRIM) [3], the energy loss and the thickness give the density of the aerogel at 500 micron steps along the depth.

References: [1] Brownlee D. et al. 2006. *Science* 314:1711–1716. [2] Graham G. A. et al. 2004. *Meteoritics & Planetary Science* 39:1461–1473. [3] Ziegler J. F., Biersack J. P., and Littmark U. *The stopping and range of ions in solids*. 1985. New York: Pergamon Press (new edition in 2009).

5275

EROS' RAHE DORSUM PLANE: IMPLICATIONS FOR INTERNAL STRUCTURE AND PARTIAL DIFFERENTIATION

R. Greenberg. Lunar and Planetary Laboratory, The University of Arizona, Tucson, AZ, USA. E-mail: greenberg@lpl.arizona.edu.

An intriguing discovery of the NEAR imaging and laser-ranging experiments was the ridge system known as Rahe Dorsum and its possible relationship with global-scale internal structure. The curved path of the ridge over the surface roughly defines a plane cutting through Eros. Another lineament on the other side of Eros, Calisto Fossae, seems to lie nearly on the same plane. The NEAR teams (e.g., [1, 2]) interpret Rahe as the expression of a compressive fault (a plane of weakness), because portions of it form a scarp, which on Earth would be indicative of horizontal compression, where shear displacement along a dipping fault has thrust the portion of the lithosphere on one side of the fault up relative to the other side. However, given the different geometry of Eros, a scarp may not have the same relationship to underlying structure as it does on Earth. The plane through Eros runs nearly parallel to, and just below, the surface facet adjacent to Rahe Dorsum. The plane then continues lengthwise through the elongated body, a surprising geometry for a plane of weakness on a battered body. Moreover, an assessment of the topography of Rahe Dorsum indicates that it is not consistent with displacement on the Rahe plane. Rather, the topography suggests that Rahe Dorsum results from resistance of the Rahe plane to impact erosion. Such a plane of strength might have formed in Eros' parent body by a fluid intrusion (e.g., a dike of partial melt) through undifferentiated material, creating a vein of stronger rock. Albedo, color, and near-infrared spectra suggest a distinct material composition consistent with such a history. However the plane of strength formed, it would have interesting implications for the thermal history of the body. Moreover, such structural reinforcing might have enabled and controlled the elongated irregular shape of Eros, as well as Rahe Dorsum.

References: [1] Veverka J. et al. 2000. *Science* 289:2088–2097. [2] Robinson M. S. et al. 2002. *Meteoritics & Planetary Science* 37:1651–1684.

5267

SEARCH FOR EXTINCT ^{36}Cl IN Ca-Al-RICH INCLUSIONS IN PRIMITIVE ORDINARY CHONDRITES

Y. Guan[1], T. Ushikubo[2], J. M. Eiler[1], and M. Kimura[3]. [1]Division of Geological and Planetary Sciences, MC170-25, California Institute of Technology, Pasadena, CA 91125, USA. E-mail: yunbin@gps.caltech.edu. [2]Department of Geology and Geophysics, University of Wisconsin-Madison, Madison, WI 53706, USA. [3]Faculty of Science, Ibaraki University, Mito 310-8512, Japan.

Introduction: The short-lived radionuclide ^{36}Cl decays to either ^{36}Ar (98.1%, β^-) or ^{36}S (1.9%, ε and β^+), with a half life of 3.01×10^5 yr [1]. Recent study has shown that ^{36}S anomalies from the decay of ^{36}Cl exist in sodalite ($Na_8Al_6Si_6O_{24}Cl_2$) of some Ningqiang CAIs and Allende CAIs and chondrule [2–5], but not in sodalite in other CAIs from Allende or Vigarano [6, 7]. In this study, we have expanded the search for ^{36}S anomalies in primitive ordinary chondrites.

Samples and Experimental: The samples used in this study are LEW 88121 (H3) and Y-792947 (H3). Sulfur isotopes (^{33}S, ^{34}S, and ^{36}S) and ^{37}Cl of sodalite grains in CAIs from these two meteorites were measured with the Cameca NanoSIMS 50L ion microprobe at Caltech. A primary Cs^+ beam of 20–30 pA was used to raster areas of 2–3 μm on the sample surface. Negative ions of the selected masses were simultaneously detected with electron multipliers of the multicollection system. Background was monitored periodically at 15 mil-masses from the ^{36}S peak during measurements. Terrestrial sodalite, Canyon Diablo troilite, and troilite texturally close to the analyzed CAIs were used as standards. Terrestrial hauyne ($Na_4Ca_{1.6}K_{0.1}Al_6Si_6O_{30}S_{1.8}Cl_{0.07}$) was measured to determine the Cl/S relative sensitivity factor.

Results and Discussion: The Cl/S ratios in most CAI sodalite grains examined so far in these two H3 chondrites are too low to detect ^{36}S anomalies from the decay of ^{36}Cl. Only one CAI from LEW 88121 contains sodalite that yields resolvable ^{36}S excesses that correlate with Cl/S ratios. The inferred initial $^{36}Cl/^{35}Cl$ ratio from the regression line is $(1.0 \pm 0.8) \times 10^{-7}$, which is significantly lower than the previously reported initial $^{36}Cl/^{35}Cl$ ratios ($\sim 1–5 \times 10^{-6}$) in sodalite from Ningqiang or Allende CAIs [2–5]. The high initial ratios of $^{36}Cl/^{35}Cl$ in sodalite from Ningqiang or Allende CAIs indicate a spallation origin of ^{36}Cl [3]. The substantially lower initial $^{36}Cl/^{35}Cl$ ratio we observed in ordinary chondrites sodalite implies that either a) the ^{36}Cl production in the early solar system was highly localized, b) the ^{36}Cl-^{36}S systematics were disturbed by later alteration and metamorphism, or c) ^{36}Cl had decayed before the formation of the sodalite in ordinary chondrites.

References: [1] Endt P. M. 1990. *Nuclear Physics A* 521:1. [2] Lin Y. et al. 2005. *Proceedings of the National Academy of Sciences* 102:1306–1311. [3] Hsu W. et al. 2006. *The Astrophysical Journal* 640:525–529. [4] Nakashima D. et al. 2006. *Meteoritics & Planetary Science* 41:A129. [5] Ushikubo T. et al. *Meteoritics & Planetary Science.* Forthcoming. [6] Plagge M. et al. 2006. Abstract #1287. 37th Lunar and Planetary Science Conference. [7] Nakashima D. et al. 2007. Abstract #1109. 38th Lunar and Planetary Science Conference.

5276

TEMPERATURES OF AQUEOUS ALTERATION ON CARBONACEOUS CHONDRITE PARENT BODIES

W. Guo[1], M. Perronnet[2], M. E. Zolensky[2], and J. M. Eiler[1]. [1]Division of Geological and Planetary Sciences, California Institute of Technology, Pasadena, CA 91125, USA. E-mail: wfguo@gps.caltech.edu. [2]NASA Johnson Space Center, Houston, TX 77058, USA.

Introduction: Aqueous alteration of primitive meteorites is among the earliest and the most widespread geological processes in the solar system [1]. A better understanding of these processes would help us constrain the early evolution condition of the solar system and test models of thermal and chemical evolution of planetesimals. In this study, we extended our previous work on CM chondrites [2, 3] by further applying carbonate clumped isotope thermometry [4, 5] to other types of carbonaceous chondrites (GRO 95577, CR1; Orgueil, CI; and Tagish Lake, ungrouped type 2) to determine the conditions of their aqueous alteration. Carbonate in GRO 95577 is almost exclusively calcite; both Orgueil and Tagish Lake contain complex mixtures of several carbonates, which necessitated stepped phosphoric acid digestion to separately analyze calcite, dolomite/ankerite and breunnerite. CO_2 gases derived from these acid digestions are exceptionally rich in sulfur and organic contaminants. While so far no consistent evidence suggests their influences on Δ_{47} after extensive purification, we are continuing working on this issue.

Results and Discussion: $\delta^{13}C_{PDB}$ and $\delta^{18}O_{VSMOW}$ values of carbonates we observe are consistent with previous studies [6–8]. Temperatures of carbonate formation (±10 °C, 1σ) are: 6–40 °C for calcite in GRO 95577; 26 °C for dolomite and −6 °C for breunnerite in Orgueil; 50 °C for calcite, 34 °C for dolomite and −26 °C for breunnerite in Tagish Lake. These estimated alteration temperatures are within or below those estimated for CM chondrites (20–71 °C) [2, 3], and thus preclude alteration temperature variations as the principle cause of differences in the degrees of alteration between the CM versus CI and Tagish Lake. Given previous evidences for the sequence of carbonate formation in carbonaceous chondrites (calcite before dolomite before breunnerite) [9, 10], our results suggest carbonate formation (and aqueous alteration) occurred while the parent bodies were cooling.

Based on the known temperature-dependent carbonate-water oxygen isotope fractionations, we estimated $\delta^{18}O_{VSMOW}$ of the water from which these carbonates grew (±2‰, 1σ): −12.3‰ to −7.1‰ for calcite in GRO 95577; −2.1‰ for dolomite and −25.2‰ for breunnerite in Orgueil; 10.3‰ for calcite, 5.1‰ for dolomite, and −15.9‰ for breunnerite in Tagish Lake. These large variations in $\delta^{18}O$ of formation water were accompanied by relatively small variations in $\Delta^{17}O$ [8] (e.g., ~23‰ variation in $\delta^{18}O$ versus <0.2‰ variation in $\Delta^{17}O$ in Orgueil); this result contrasts with previous models of aqueous alteration of the carbonaceous chondrites [11, 12], suggesting that our understanding of the hydrology of their parent bodies must be revised.

References: [1] Brearley A. J. 2006. In *Meteorites and the early solar system II.* pp. 587–624. [2] Guo W. and Eiler J. M. 2006. Abstract #2288. 37th LPSC. [3] Guo W. and Eiler J. M. *Geochimica et Cosmochimica Acta*. Forthcoming. [4] Ghosh P. et al. 2006. *Geochimica et Cosmochimica Acta* 70: 1439–1456. [5] Schauble E. A. et al. *Geochimica et Cosmochimica Acta* 70: 2510–2529. [6] Grady M. M. et al. 1988. *Geochimica et Cosmochimica Acta* 52:2855–2866. [7] Zito K. L. et al. 1998. *Meteoritics & Planetary Science* 33: A171–A172. [8] Leshin L. A. et al. 2001. Abstract #1843. 32nd LPSC. [9] Riciputi L. R. et al. 1994. *Geochimica et Cosmochimica Acta* 58:1343–1351. [10] Hoppe P. et al. 2004. Abstract #1313. 35th LPSC. [11] Clayton R. N. and Mayeda T. K. 1999. *Geochimica et Cosmochimica Acta* 63:2089–2104. [12] Young E. D. et al. 1999. *Science* 286:1331–1335.

5068

AGES OF LARGE SiC GRAINS FROM MURCHISON

F. Gyngard[1], S. Amari[1], E. Zinner[1], and R. S. Lewis[2]. [1]Laboratory for Space Sciences and Department of Physics, Washington University, St. Louis, MO 63130, USA. E-mail: fmgyngar@wustl.edu. [2]Enrico Fermi Institute and Chicago Center for Cosmochemistry, University of Chicago, Chicago, IL 60637, USA.

Introduction: Estimating the presolar residence time of SiC grains in the interstellar medium (ISM) has been a long-standing problem. Previous studies, on bulk samples, have focused on cosmogenic production of ^{21}Ne [1, 2] and ^{126}Xe [3] in estimating cosmic-ray exposure ages. Ott et al. [3] found no clear evidence for cosmogenic ^{126}Xe, implying very short cosmic-ray exposure histories, while ages inferred from ^{21}Ne production have largely been invalidated because of spallation recoil loss [4]. We measured Li isotopes in large presolar grains and found ^{6}Li enrichments of up to ~300‰ [5]. Assuming that these excesses are from cosmic-ray spallation in the ISM, we can infer lower limits on the length of time individual presolar SiC grains spent in the ISM.

Experimental: Grains from Murchison separates LS and LU [6] were placed on a clean gold foil with a micromanipulator and pressed with a quartz disk. SEM-EDX analysis identified forty grains as SiC, ranging in size from 5 to 60 μm. With the Washington University NanoSIMS, Li, B, C, Si, and S isotopic ratios were determined on nine of the largest grains.

Results: Eight out of 9 grains show ^{6}Li enrichments, likely due to spallation from C by cosmic rays. Using Li production rates calculated for grains with radii less than 1 cm by Reedy [7], we infer cosmic-ray exposure ages of the eight grains with ^{6}Li excesses from 24 to 1.2 Gy. Two grains have irradiation ages less than 40 My, four grains are between 100 and 500 My, and two grains have ages greater than 500 My. The dominant source of error in these age determinations is uncertainty in the production rate, as it depends critically on the cross sections of the responsible spallation reactions for realistic targets, and in the interstellar flux of galactic cosmic rays, both poorly constrained quantities. Resulting errors are ~30–40%. These age determinations do not account for any spallation recoil loss or self-shielding; however, these effects would only increase the ages reported here.

Long interstellar exposure ages are not necessarily inconsistent with previous results indicating young SiC exposure ages [3], as the large L-series SiC measured here are morphologically and isotopically distinct from other presolar SiC [5]. Jones et al. [8] estimated SiC grain lifetimes in the ISM to range up to 1.5 Gy, consistent with the ages we have calculated. These results may suggest that some large LS+LU SiC grains come from stars that ejected grains into the ISM before the parent stars of most smaller SiC grains found in meteorites. The large size of these LS+LU grains likely allows them to better survive destruction by SN shock waves and nebular processing in the ISM.

References: [1] Tang M. and Anders E. 1988. *The Astrophysical Journal* 335:L31–L34. [2] Lewis R. S. et al. 1994. *Geochimica et Cosmochimica Acta* 58:471–494. [3] Ott U. et al. 2005. *Meteoritics & Planetary Science* 40:1635–1652. [4] Ott U. and Begemann F. 2000. *Meteoritics & Planetary Science* 35:53–63. [5] Gyngard F. et al. 2007. Abstract #1338. Lunar Planet. Sci. XXXVIII. [6] Amari S. et al. 1994. *Geochimica et Cosmochimica Acta* 58:459–470. [7] Reedy R. C. 1989. Lunar Planet. Sci. XX. pp. 888–889. [8] Jones A. et al. 1997. *Astrophysical Implications of the Laboratory Study of Presolar Materials.* pp. 595–613.

5157

LIFE ON THE EDGE—FORMATION OF CAIs AND CHONDRULES AT THE INNER EDGE OF THE DUST DISK

H. Haack[1] and G. Wurm[2]. [1]Natural History Museum of Denmark, Øster Voldgade 5-7, DK-1350 Copenhagen K, Denmark. E-mail: hh@snm.ku.dk. [2]Institut für Planetologie, Wilhelm-Klemm-Str. 10, D-48149 Münster, Germany.

Introduction: CAIs and chondrules formed during transient heating events in the early solar system while gas and dust co-existed. CAIs probably formed close to the Sun at a very early stage and within a very limited period of time. Chondrules formed further out from the Sun over an extended period of time. The heat source responsible for the transient heating events remains unknown although several possible mechanisms have been suggested. The difference in age between chondrules and CAIs require that the CAIs can remain in the nebula for long periods of time despite predictions that they would quickly spiral into the Sun. A previously overlooked effect, photophoresis, has been shown to be able to prevent millimeter-size particles from spiraling into the Sun [1–3]. Photophoresis exerts a force on particles, embedded in a thin gas, that are exposed to sunlight.

Concentration of Dust at the Inner Edge: A significant consequence of photophoresis on the evolution of the disk is a strong concentration of dust and particles along the inner edge of the dust disk. Particles inside the edge will be pushed toward the edge due to photophoresis, whereas particles outside the edge will be shielded from the Sun and therefore spiral inward due to classical gas drag. This leads to the formation of a sharp inner edge of the dust disk. An enhanced dust density results in more rapid accretion, and since accretion is the only process that can remove dust from the edge, we infer that the dust density at the edge will be controlled by accretion of planetesimals.

Transient Heating Events at the Edge: Isotopic differences between chondrules from different groups of chondrites imply that chondrule formation was local to the environment where size sorting and accretion took place. The rapid change in dust-gas ratio, opacity, and gas temperature across the edge makes it a highly turbulent and very energetic environment. A high dust density would enhance lightning activity and is also consistent with chondrule heating through nebula shocks.

Size Sorting and Source Regions: The combination of turbulence, which tends to lift small particles above the midplane, and photophoresis, which provides a size-dependent force pushing the particles away from the Sun, results in a size variation of particles close to the edge. Also, the transition from the optical thin front side of the edge to the optical thick part of the dust disk results in size sorting, with smaller particles being closest to the Sun.

Conclusions: Photophoresis results in a concentration of solids at the inner edge of the dust disk. The enhanced concentration of solids facilitated very early growth of achondrite parent bodies close to the Sun. As dust and particles accreted to planetesimals, the edge moved outward from the Sun. We suggest that chondrule heating, size sorting, and accretion took place along the inner edge of the outward migrating dust disk.

References: [1] Wurm G. et al. 2006. *Meteoritics & Planetary Science* 41:A191. [2] Haack et al. 2006. *Meteoritics & Planetary Science* 41:A72. [3] Krauss O. and Wurm G. 2005. *The Astrophysical Journal* 630:1088–1092.

5253

REVIEWING TRACE ELEMENT CHARACTERISTICS FOR A SUITE OF CARBONACEOUS CHONDRITES

S. J. Hammond[1, 2], P. A. Bland[1, 3], S. H. Gordon[1], and N. W. Rogers[2]. [1]Impacts and Astromaterials Research Centre (IARC), Department of Earth Science and Engineering, Imperial College London, South Kensington Campus, London, SW7 2AZ, UK. E-mail: s.hammond@imperial.ac.uk. [2]Department of Earth Sciences, The Open University, Walton Hall, Milton Keynes, MK7 6AA, UK. [3]IARC, Department of Mineralogy, Natural History Museum, London, SW7 5BD, UK.

Introduction: Carbonaceous chondrites are among the most primitive materials available to us, and provide an insight into early solar system formation processes. While several studies have focused on the analysis of the various components that make up carbonaceous chondrites (e.g., [1–3]), and the average compositions of chondrite groups are well constrained [1], the data set of bulk rock analyses remains limited, both in terms of the numbers of individual meteorites for which analyses exist, and the range of elements covered. Here we present absolute abundance data for 45 trace elements from a suite of carbonaceous chondrites (including CV, CO, and CM groups), analyzed by inductively coupled plasma mass spectrometry (ICP-MS). The aim of this study is two-fold: to expand the compositional data set for meteorites over a large elemental range, and to provide an internally consistent data set in order to compare bulk rock analyses with milled separate components from the same samples [1].

Methods: Approximately 10 mg of sample powder (from a larger aliquot) was accurately weighed into pre-cleaned Savillex beakers. Samples were digested using a standard HF:HNO_3 digestion technique. Following complete dissolution, samples were analyzed by ICP-MS. Reproducibility (assessed as the relative standard deviation of 10 repeat analyses of Allende) is better than 5% for all elements.

Results and Discussion: Samples analyzed include Vigarano (CV), Allende (CV), Kaba (CV), Arch (CV), Acfer 272 (CV), Ornans (CO), ALH 88045 (CM), and Acfer 094 (ungrouped). Bulk compositions of analyzed CV and CO chondrites are in line with expectations [4]. ALH 88045 is a CM1; our data confirm the compositional similarity to CM2 chondrites [5]. It has been suggested that Acfer 094 is intermediate between CO and CM, or that it is a CM3 chondrite. We observe a composition which, in terms of depletion in moderately volatile elements, is most similar to average CM chondrite. A similar observation was made following matrix analyses of these two meteorites [3]. However, although the difference is not great, Acfer 094 does appear to be consistently enriched in a number of moderately volatile elements relative to CM, justifying its status as a unique meteorite. Additional observations will be discussed at the meeting.

Acknowledgements: The Natural History Museum is acknowledged for providing the samples analyzed in this study.

References: [1] Gordon S. H. et al. 2007. Abstract #1819. 28th Lunar and Planetary Science Conference. [2] Rubin A. E. and Wasson J. T. 1987. *Geochimica et Cosmochimica Acta* 51:1923–1937. [3] Bland P. A. et al. 2005. *Proceedings of the National Academy of Sciences* 102:13,755–13,760. [4] Kallemeyn G. W. and Wasson J. T. 1981. *Geochimica et Cosmochimica Acta* 45: 1217–1230. [5] Zolensky M. E. et al. 1997. *Geochimica et Cosmochimica Acta* 61:5099–5115.

5008

CRATER RETENTION AGES OF PLANETARY SURFACE PROCESSES: NEW PROGRESS

W. K. Hartmann. Planetary Science Institute, Tucson, AZ 85719, USA. E-mail: hartmann@psi.edu.

Introduction: Impact crater densities (craters/km^2) have allowed successful estimate of planetary surface ages and survival times of topography on modified surfaces [1–3]. Malin et al. recently reported a breakthrough observation: formation rate of small (~20 m) Martian craters [4]. If correct, this will allow even more direct age measurement.

History of Technique: The technique was introduced in the 1960s when Canadian impact craters were used to predict the ~3.6 Ga age of lunar lava plains [5], and an "early intense bombardment" prior to 3.6 Ga [6], confirmed by Apollo. In the 1970s, cratering rates were extended to Mars by scaling arguments [1]. This led to age estimates of a few hundred Ma for Mars' broad lava plains [1], supported in the 1980s by ages of Martian basaltic meteorites [7, 8]. My 2005 "isochron" plot [2] shows expected crater densities on Martian surfaces of different age, in the absence of erosion. The new Malin et al. data [4] agree with the isochrons within a factor 3 [9]. This opens the door to direct Martian age measurements without scaling arguments. It also negates most recent critiques of the technique [10].

Example: Debris Aprons, Ice Flow, and Climate/Obliquity Cycles: A striking application illustrates the power of the method. Martian features attributed to ice deposition include debris aprons, mantles, and possible glaciers [2, 11, 12]. Measurements of ages of decameter-scale structure on these surfaces repeatedly give ages in the range ~3–50 Ma, measured either by my isochrons, Neukum's isochrons, or the new Malin et al. measurement [2–4, 9]. These ages are in the range of the last few high-obliquity episodes, and support suggestions that Mars is undergoing ~10 Ma cycles of climate change in which ice deposition occurs [2, 12–14].

Conclusions: The technique offers great promise for further work on Mars and extension to other planetary bodies.

References: [1] Hartmann W. 1973. *Journal of Geophysical Research* 78:4096–4116. [2] Hartmann W. 2005. *Icarus* 174:294–320. [3] Hartmann W. and Neukum G. 2001. *Space Science Reviews* 96:165–194. [4] Malin M. et al. 2006. *Science* 314:1573–1557. [5] Hartmann W. 1965. *Icarus* 4:157–165. [6] Hartmann W. 1966. *Icarus* 5:406–418. [7] Hartmann W. et al. 1981. In *Report of Basaltic Volcanism Study Project.* Elmsford: Pergamon. [8] Nyquist L. et al. 2001. *Space Science Reviews* 96:105–164. [9] Hartmann W. *Icarus*. Forthcoming. [10] McEwen A. et al. 2005. *Icarus* 176:351–381. [11] Arfstrom J. and Hartman W. 2005. *Icarus* 174:321–335. [12] Head J. et al. 2003. *Icarus* 426:797–801. [13] Mustard J. et al. 2001. *Nature* 412: 411–413. [14] Costard F. et al. 2001. *Science* 295: 110–113.

5104

LIGHT NOBLE GAS COMPOSITION OF DIFFERENT SOLAR WIND REGIMES: RESULTS FROM GENESIS

V. S. Heber[1], H. Baur[1], D. S. Burnett[2], D. B. Reisenfeld[3], R. Wieler[1], and R. C. Wiens[4]. [1]Isotope Geology and Mineral Resources, NW C, ETH, 8092 Zurich, Switzerland. E-mail: heber@erdw.ethz.ch. [2]CalTech, JPL, Pasadena, CA 91109, USA. [3]Physics and Astronomy, University of Montana, Missoula, MT 59812, USA. [4]LANL, Space & Atmospheric Science, Los Alamos, NM, 87544, USA.

Introduction: The Genesis mission provided samples of solar wind (SW) from different regions on the Sun. These SW regime samples are important in understanding fractionation processes upon formation and acceleration of the SW to ultimately deduce solar composition from SW values. We present He and Ne isotopic and elemental compositions of the bulk SW (SW of entire collection period) and the 3 major SW regimes: slow (from the ecliptic plane, emanating from above streamers), fast (emanating from coronal holes), and coronal mass ejections (CME). At the conference we will also present Ar data.

Experimental: Noble gases were analyzed in targets composed of amorphous, diamond-like C on Si. The low atomic mass of C minimized backscatter losses and thus isotope fractionation. Backscatter loss was corrected for He and was negligible for Ne based on SRIM [1]. Gases were extracted by UV laser ablation (213 nm). The main focus of this work is to detect differences between SW regimes. Therefore, He and Ne isotopes and ^{4}He/^{20}Ne were analyzed in 3 separate runs, using standard-sample bracketing. The bulk SW target served as "standard" and the other regime targets as "samples." Experimental details are given in [2].

Results: The preliminary ^{4}He/^{3}He of the bulk SW is 2081 ± 17. He isotopes are fractionated between slow and fast SW by 6%, ^{3}He being enriched in the former. The ^{20}Ne/^{22}Ne and ^{21}Ne/^{22}Ne of the bulk SW are 13.80 ± 0.03 and 0.0328 ± 0.0001, respectively, in excellent agreement with reported SW values [3, 4]. In contrast to He, fractionation of the ^{20}Ne/^{22}Ne between slow and fast SW is only marginally significant (≤1%), ^{20}Ne tending to be enriched in the slow SW. The enrichment of light isotopes in the slow SW is in accordance to the Coulomb drag theory, postulating isotope fractionation upon acceleration of SW species in the lower corona [5]. The preliminary ^{4}He/^{20}Ne of the bulk SW is 669 ± 6. The slow SW is depleted by 1% in He relative to Ne and fast SW either due to inefficient Coulomb drag [6] or fractionation upon ionization in the chromosphere (although first ionization potentials of He and Ne are similar, ionization times are very different [7]). In contrast to the quasi-stationary slow and fast SW, transient CME events are known to vary in composition. The Genesis CME targets collected many events, providing an average CME composition. He isotopic composition is similar to bulk SW, thus an enrichment of ^{3}He over ^{4}He as observed in many single events could not be detected. Most prominent is, however, the ^{4}He enrichment over ^{20}Ne of ~10% in CMEs relative to quasi-stationary SW, in accordance with the He over O enrichment detected with the ACE spacecraft [8].

References: [1] Ziegler J. F. 2004. *Nuclear Instruments and Methods in Physics Research* 219/220:1027–1036. [2] Heber V. S. et al. 2007. Abstract #1894. 38th LPSC. [3] Benkert J.-P. et al. 1993. *Journal of Geophysical Research* 98:13147–13162. [4] Geiss J. et al. 2004. *Space Science Reviews* 110:307–335. [5] Bodmer R. and Bochsler P. 1998. *Physics and Chemistry of the Earth* 23:683–688. [6] Bochsler P. 2007. *Astronomy & Astrophysics* 14:1–40. [7] Geiss J. 1998. *Space Science Reviews* 85:241–252. [8] Reisenfeld D. B. et al. *Space Science Reviews*. Forthcoming.

5019

THE SULFUR ISOTOPIC COMPOSITION OF WILD-2 DUST COLLECTED BY STARDUST ANALYZED WITH THE NANOSIMS

P. R. Heck[1], P. Hoppe[1], and J. Huth[1]. [1]Max Planck Institute for Chemistry, 55128 Mainz, Germany. E-mail: prheck@gmail.com.

Introduction: The NASA mission Stardust collected coma dust of comet 81P/Wild-2 using aerogel and Al foil targets [1] and successfully returned it to Earth in 2006 [2]. Preliminary examination (PE) revealed that the dust consists of an unequilibrated, heterogeneous mixture of material with mainly solar system isotopic composition [3]. During PE the H, C, N, O and Ne isotopic compositions of selected samples were analyzed [3]. Only one presolar ^{17}O-rich circumstellar grain was found. A few residues in impact craters are moderately enriched in ^{15}N, consistent with observations in IDPs [4] and insoluble organic matter from primitive meteorites [5]. Sulfur in Wild-2 dust is associated with organic matter [6] but also occurs in sulfides [7]. Here, we present first results of the S isotopic composition of Wild-2 dust in impact crater residues on Stardust Al-foil targets.

Samples and Experimental: We studied impact residues in a large crater (ø 140 µm; foil C013N) and in 13 small craters (ø 430–1860 nm; foil C037N). The latter were found in an SEM high-resolution survey. EDX spectra of the impact residues were obtained to select craters with moderate to high S content. In the NanoSIMS 50 a primary Cs^+ beam (ø ~100 nm) was rastered over the sample area and negative secondary ions of ^{16}O or ^{28}Si and all S isotopes were counted in multicollection. Reproducibility was evaluated by analyzing a thin section of Mundrabilla troilite standard and crater residues on a Stardust-type Al foil, which had been artificially bombarded with pyrrhotite.

Results and Discussion: S isotopic ratios of residues in large impact craters were found to depend noticeably on surface geometry. Topographic correction factors were determined for each analyzed raster area and average from 0.5 to 1.5% on the crater floor, and from 1.4 to 4.4% on the crater rim. In the 15 areas of 10 × 10 µm^2 analyzed on the large Stardust crater, we identified 629 S-rich sub-areas. All of the sub-areas are isotopically normal within 4σ. Topographic effects were less pronounced in small craters and isotope ratios were determined by integrating the secondary ion signals over the whole crater surface. Six out of 13 craters display small to moderate bulk crater anomalies (>2σ and >10‰) in at least one S-value. One crater (#12) has negative anomalies in all δS-values ($\delta^{33}S = -51 \pm 28$‰; $\delta^{34}S = -37 \pm 12$‰; $\delta^{36}S = -177 \pm 154$‰); errors are 2σ. Nucleosynthetic isotope anomalies are expected to be particularly prominent in $\delta^{36}S$ (depending on the stellar source, up to several hundred ‰ [8]). At the meeting we will discuss possible stellar, nebular and solar system sources for the S isotopic anomalies.

Acknowledgements: We thank F. Hörz/NASA for providing Stardust samples, A. Kearsley and M. Burchell for preparing calibration samples, and E. Gröner for NanoSIMS support.

References: [1] Brownlee D. et al. 2004. *Science* 304:1764–1769. [2] Brownlee D. et al. 2006. *Science* 314:1711–1716. [3] McKeegan K. et al. 2006. *Science* 314:1724–1728. [4] Floss C. et al. 2006. *Geochimica et Cosmochimica Acta* 70:2371–2399. [5] Busemann H. et al. 2006 *Science* 312:727–730. [6] Sandford S. A. et al. 2006. *Science* 314:1720–1724. [7] Zolensky M. E. 2006. *Science* 314:1735–1739. [8] Mauersberger et al. 2003. *Astronomy & Astrophysics* 426:219–227.

5027

COSMOGENIC AND SOLAR NOBLE GASES IN 470 Ma FOSSIL METEORITES AND MICROMETEORITES FROM THE L CHONDRITE PARENT BODY BREAKUP

P. R. Heck[1], B. Schmitz[2], H. Baur[3], and R. Wieler[3]. [1]MPI for Chemistry, J. J. Becherweg 27, D-55128 Mainz, Germany. [2]University of Lund, Geology, Sölvegatan 12, SE-22362 Lund, Sweden. [3]ETH Zurich, Isotope Geology, CH-8092 Zurich, Switzerland. E-mail: wieler@erdw.ethz.ch.

Introduction: Schmitz et al. [1] discovered about 50 fossilized meteorites in the Thorsberg quarry of mid-Ordovician marine limestone in southern Sweden, reflecting about two orders of magnitude enhanced flux of extraterrestrial material ~470 Ma ago, caused by the L chondrite parent body breakup. The meteorites are accompanied by abundant extraterrestrial chromite grains (~80–100 microns) dispersed in the same and adjacent limestone strata as the meteorites throughout southern Sweden [2]. Chromite grains from the sediments and the fossil meteorites preserve their original chemical [1, 2] and oxygen isotope [3] composition, allowing classification as L chondrites.

Cosmic-Ray Exposure Ages: Chromites extracted from a suite of fossil meteorites in a stratigraphic sequence from Thorsberg extending over 1–2 Ma yield ^{21}Ne cosmic-ray exposure ages of ~0.1–1.1 Ma, increasing with decreasing stratigraphic age [4]. This is additional evidence that the fossil meteorites were created in a single, very large collision in the asteroid belt and shows that some meteorites from this event arrived on Earth very quickly, by direct injection into a strong resonance in the main belt. A fossil meteorite from the mid-Ordovician Gullhögen quarry in southern Sweden (Gullhögen 001) also has a low exposure age of 0.9 Ma, in agreement with the ages of Thorsberg meteorites from the corresponding sediment beds Tredje Karten and Sextummen. Exposure ages were calculated with a ^{21}Ne production rate of $(7.04 \pm 0.65)^{*}10^{-10}$ cc/g determined with chromites from five modern meteorite falls with long exposure ages.

Solar He and Ne in Dispersed Chromite Grains: Each one of eight batches of 4–6 chromites dispersed in sediment beds contains He and Ne with ~solar isotopic composition. This means that a sizeable fraction—if not most—of the grains were brought to Earth as sub-millimeter-size interplanetary dust particles, being irradiated by the solar wind in space. The alternative, that at least one grain in each batch was irradiated on a L-chondritic regolith (3% of all L chondrites), is highly unlikely. The solar noble gases inhibited detection of cosmogenic ^{3}He or ^{21}Ne and hence exposure ages. This goal will require analysis of strongly etched chromites.

Transfer Times of Dispersed Chromites: The concentration of dispersed chromites increases in the same layer (Arkeologen) where the oldest meteorites were found [2]. These grains were brought to Earth probably by the same fast track as the meteorites, through an orbital resonance. Dispersed chromites are also found in sediments at least 2 Ma younger than Arkeologen, however. This is longer than estimated Poynting-Robertson lifetimes of 0.6–1 Ma for 100 micron-size particles. Such chromites may have been parts of slightly larger IDPs in space or may stem from second- or higher generation collisions some time after the main event leading to the L chondrite parent body breakup.

References: [1] Schmitz B. et al. 2001. *Earth and Planetary Science Letters* 194:1. [2] Schmitz B. and Häggström T. 2006. *Meteoritics & Planetary Science* 41:455. [3] Greenwood R. C. et al. *Earth and Planetary Science Letters*. Forthcoming. [4] Heck P. R. et al. 2004. *Nature* 430:323.

5101

Mg- AND Si-BUDGETS OF CHONDRULES, MATRIX, AND BULK CARBONACEOUS CHONDRITES

D. C. Hezel[1] and H. Palme[2]. [1]Natural History Museum, Cromwell Road, SW7 5BD, London, UK. E-mail: d.hezel@nhm.ac.uk. [2]Universität zu Köln, Institut für Geologie und Mineralogie, Zülpicherstr. 49b, 50674 Köln, Germany.

The bulk chemical composition of chondrules in each carbonaceous chondrite (CC) group is rather variable, with Mg and Si contents plotting along mixing lines between olivine and SiO_2 [1]. The average chondrule Mg/Si ratios are, however, remarkably similar (CV: 0.99, CR: 0.96, CH: 0.94, CB: 0.98, CK: 0.88). CKs are lower as they experienced mild thermal metamorphism on their parent body with Mg-Fe exchange between chondrules and matrix on their parent body. Other CC did not experience extensive metamorphic redistribution of Mg and Si. The constant average Mg/Si of chondrules may indicate that all chondrules formed in a single nebula compartment, in apparent disagreement with different bulk chondrule oxygen isotopic compositions observed in individual chondrite groups. All CC have the CI Mg/Si-ratio of ~0.91, significantly lower than the average chondrule ratios (except for CK). Both elements, Mg and Si, are quantitatively contained in chondrules and matrix. As the mean Mg/Si of chondrules is different from the bulk chondrite, matrix must balance the chondrule Mg/Si to achieve the bulk chondrite composition. Different chondrite groups have highly variable matrix Mg/Si (CV: 0.74, CR: 0.64, CK: 0.95, CM: 0.77; [own data and from 2]). This is a consequence of variations in modal abundances of chondrules and matrix among chondrite groups [3]. If CC matrices had identical Mg/Si, and the average chondrule Mg/Si were also constant bulk CC should have variable Mg/Si. It has been suggested that chondrules and matrix formed in separate nebular environments and chondrules were transported later to the matrix formation locations (e.g., [4]). In this case, the right amount of matrix with the appropriate Mg/Si must have mixed with chondrules to achieve the CI chondritic Mg/Si. It is hard to believe that this was the case. Some authors have suggested that chondrules and matrix formed in the same chemical reservoir [5–8] and our new chondrule data support these findings.

A constant mean chondrule composition in the various CC groups would have important consequences for chondrite formation models. Clearly more data are needed to better define average chondrule compositions. Similar mean chondrule compositions in CC would further support a common formation mechanism of all chondrules, despite the highly variable petrographic appearances of chondrules from different CC groups. Chondrule formation would have preferentially consumed chondrule precursors with elevated Mg/Si. If chondrule precursors formed in a nebula compartment of CI-chondritic composition, their formation must have been accompanied by the simultaneous formation of Mg/Si depleted matrix. Precursor formation led to chondrules of a similar mean composition. The degree to which matrix was depleted in Mg/Si depended on the amount of precursors formed. Then, chondrule formation preferentially consumed precursors with high Mg/Si, maybe only grains of a certain size [9].

References: [1] Hezel et al. 2006. *Geochimica et Cosmochimica Acta* 70:1548. [2] Huss et al. 2005. In *Chondrules and the protoplanetary disk* 341: 701. [3] Brearley and Jones. 1996. In *Planetary materials.* Reviews in Mineralogy 36. [4] Shu et al. 1996 *Science* 271:1545. [5] Palme et al. 1992. 23rd LPSC. p. 1021. [6] Klerner S. and Palme H. 1999. 30th LPSC. p. 1272. [7] Bland et al. 2005. *Proceedings of the National Academy of Sciences* 102: 13,755. [8] Hezel D. C. and Palme H. Forthcoming. [9] Hezel D. C. and Palme H. Forthcoming.

5102

MINOR OCCURRENCE OF CAIs IN CHONDRITIC METEORITES

D. C. Hezel and S. S. Russell. Natural History Museum, Cromwell Road, SW7 5BD, London, UK. E-mail: d.hezel@nhm.ac.uk.

Introduction: The abundance of Ca-Al-rich inclusions (CAIs) in chondritic meteorites (chondrites) is not simple to accurately measure and is sometimes overestimated. Here we perform a simple calculation to show that there is a natural upper limit for the modal abundances of CAIs. We will show that CAIs can only be a minor component and their occurrence should therefore follow a Poisson distribution. We explore to what extent such a distribution introduces a bias when obtaining CAI modal abundances from thin sections.

Results: Chondrites have Al concentrations of (wt%, in increasing order): EH: 0.82, EL: 1.00, CH: 1.05, H: 1.06, R: 1.06, CM: 1.13, CR: 1.15, L: 1.16, LL: 1.18, K: 1.30, CO: 1.40, CK: 1.47, CV: 1.68 [1]. The addition of CAIs to chondrites would increase their bulk Al concentration. The slope of such an increase in a plot with the vol% of CAIs on the x- and Al in wt% of bulk chondrites on the y-axis depends on the abundances and densities of the accompanying components, especially on the amount of metal, as this has a distinct density from all other silicates and oxides. Assuming a mean CAI Al concentration of 17.36 wt% [2] and a density of 3.1 g/cm^3 for CAIs as well as for chondrules and matrix and a density of 8.0 g/cm^3 for metal, the slope varies between 0.14 and 0.17 if 0 and 15 vol% metal, respectively, was present. That is, without metal, each single vol% of CAI added to a chondrite increases its Al budget by 0.17 wt% and with 15 vol% metal present by 0.14 wt%. CV chondrites contain the highest Al concentration (1.68 wt%) among all chondrites. If all Al were contributed by CAIs, 12.0 vol% of CAIs were needed in case of 15 vol% metal was present and 9.9 vol% of CAIs were needed in case metal was absent. Reported metal abundances in CV chondrites do not exceed 5 vol%. This means that if CAIs account for the entire Al budget, the CVs have 10.5 vol% of CAIs. It is clear that Al is not contained entirely within CAIs, however. A significant proportion of the Al budget resides in chondrules and matrix. CI chondrites, which have a composition similar to the Sun [3], contain 0.86 wt% Al [1]. A plausible approach may be to assume that the material that makes up the chondrite groups was initially CI-like, and CAIs were added into this region in such a way as to increase the total Al budget. In this case, in CV3 chondrites only 4.8 vol% of CAIs are sufficient to top up the missing Al.

A Poisson distribution has the characteristic that there might be a lot of CAIs in one place, but only few in another. It is therefore crucial to perform a proper statistical interpretation of obtained CAI modal abundances. We set up a computer model to apply this statistical treatment. Inputs are the modal abundance and size-distribution of CAIs and the studied area in mm^2. First results indicate that too small areas may introduce a large bias in obtained modal abundances.

Conclusions: The most Al-rich chondrite class are CV chondrites, and we calculate that this class likely has a maximum CAI abundance of 4.8 vol%, and other chondrite classes will have less than this.

References: [1] Lodders K. and Fegley B., Jr. 1998. *The planetary scientist's companion.* Oxford University Press. 371 p. [2] Simon S. B. and Grossman L. 2004. *Geochimica et Cosmochimica Acta* 68:4237–4248. [3] Palme H. and Jones A. 2003. In Treatise on Geochemistry, vol. 1. Oxford: Elsevier-Pergamon. pp. 41–62.

5105

IRRADIATION RECORDS OF GAS-RICH OR BRECCIATED METEORITES STUDIED FROM Sm AND Gd ISOTOPIC SHIFTS BY NEUTRON CAPTURE REACTIONS

H. Hidaka[1], R. Bartoschewitz[2], and S. Yoneda[3]. [1]Department of Earth and Planetary Systems Science, Hiroshima University, Higashi-Hiroshima 739-8526, Japan. E-mail: hidaka@hiroshima-u.ac.jp. [2]Bartoschewitz Meteorite Laboratory, Lehmweg 53, D-38518 Gifhorn, Germany. [3]Department of Engineering and Science, National Science Museum, Tokyo 169-0073, Japan.

Introduction: Noble gas studies show that some of regolith brecciated meteorites like Pesyanoe contain significant amount of solar gas component [1]. This suggests near surface irradiation history of such meteorites on the parent bodies. Recent neutron capture study on the Sm and Gd isotopes of Pesyanoe also shows the early irradiation and regolith processes in the parent body [2]. In this study, Sm and Gd isotopic analyses of gas-rich or regolith brecciated meteorites other than aubrites were performed to find a possibility of the early irradiation on the parent bodies.

Samples and Experiments: Four samples of gas-rich or brecciated meteorites, Cook 011 (L3–5), NWA 801 (CR2), SaU 290 (CH3), and Zag (H3–5) were used in this study. Each sample weighing about 200 mg was decomposed by HF+$HClO_4$. After evaporation to dryness, the sample was redissolved in 2M HCl. Conventional ion exchange techniques using two column procedures were carried out to chemically separate Sm and Gd [2]. A Micro-mass VG 54-30 thermal ionization mass spectrometer equipped with seven Faraday cup collectors was used for the isotopic measurements of Sm and Gd.

Results and Discussions: Figure 1 shows a correlation diagram between $^{149}Sm/^{152}Sm$ and $^{150}Sm/^{152}Sm$. Sm isotopic shifts can be clearly identified in NWA 801 and Cook 011, which correspond to the neutron fluences of $(3.6 \pm 0.3) \times 10^{15}$ and $(1.7 \pm 0.3) \times 10^{15}$ n cm^{-2}, respectively. No correlation between the calculated neutron fluences and CRE ages suggest the early irradiation of their meteorite parent bodies.

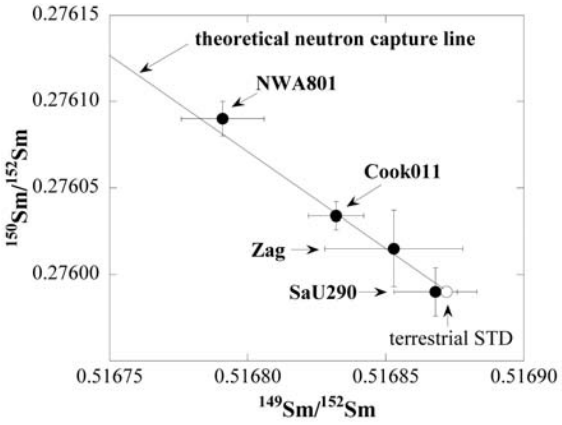

Fig. 1. A correlation diagram between $^{149}Sm/^{152}Sm$ and $^{150}Sm/^{152}Sm$ for NWA 801, Cook 011, Zag, and SaU 290. Error bars are 2σ of the means.

References: [1] Lorenzetti S. et al. 2003. *Geochimica et Cosmochimica Acta* 67:557–571. [2] Hidaka H. et al. 2006. *Geochimica et Cosmochimica Acta* 70:3449–3456.

5140

METAL/OLIVINE PARTITIONING EXPERIMENTS AND THE COOLING RATES OF PALLASITES

E. Hill, M. J. Drake, and K. Domanik. Lunar and Planetary Laboratory, The University of Arizona, Tucson, AZ 85721, USA. E-mail: eddy@lpl.arizona.edu.

Experimentally determined metal/olivine partition coefficients (D) vary with temperature, indicating that use of a constant boundary condition in the calculation of the cooling rates of pallasites will produce erroneous results. We believe use of our experimentally determined D values will help better constrain said cooling rates and thus provide a better understanding of the formation of the parent asteroid body.

Pallasites are intimate mixtures of olivine and metal, thought to be samples of the core-mantle boundaries of disrupted asteroids. As these phases attempted to re-equilibrate, during the slow cooling experienced deep within the asteroids, zoning profiles developed in olivine and metal. Tomiyama and Huss [1] have obtained zoning profiles in olivine for a series of elements including Cr, Ca, and Co. Applying these profiles to a one-dimensional cooling model, they obtain cooling rates four orders of magnitude faster than metallographic cooling rates [2]. Calculations based on zoning profiles in pallasites assume a constant boundary condition between metal and olivine, which cannot be correct. The boundary condition is set by the relevant metal/olivine partition coefficient, which is dependent on intensive variables; primarily temperature in this situation as pressure is fixed. Thus, metal/olivine Ds are required to establish reliable, evolving boundary conditions. To date, only two direct measurements of metal/olivine Ds, both for Ni, appear in the literature [3].

In view of the lack of suitable data, we are performing experiments to determine the metal/olivine partition coefficient of a range of elements including REE, HFSE, Cr, and Mn. Our first efforts have been focused on Ni and Co, elements whose concentrations we are able to measure in both metal and silicate by electron microprobe analysis. Measurement of the other proposed elements in these same experiments will require the use of SIMS in order to resolve the low concentrations encountered in metal, silicate, or both.

Experiments are being performed at decreasing temperatures and under appropriate fO_2 conditions. Our highest experimental temperature, 1550 °C, is above the melting point of Fe but below that of forsterite. Even so, we have found that over a reasonable time period (24 hours) olivines are homogenized for major elements, suggesting the system has fully equilibrated. Between this initial temperature at which diffusion is uniform throughout the system and the temperature at which diffusion becomes so sluggish as to make the experiments impractical, we expect to find a progression of boundary conditions. Our initial results show that between 1550 °C and 1350 °C, D_{Ni} and D_{Co} decrease by a factor of approximately 1.5 and 1.3, respectively, illustrating that a constant boundary condition is unphysical even over this small range in *T*. The different rate of decrease of D_{Ni} and D_{Co} may also explain the discrepancy in cooling rates calculated for different elements by [1].

References: [1] Tomiyama and Huss. 2006. Abstract #2137. 37th LPSC. [2] Buseck and Goldstein. 1969. *Geological Society of America Bulletin* 80:2141–2158. [3] Ehlers, Grove, Sisson, Recca, and Zervas. 1992. *Geochimica et Cosmochimica Acta* 56:3733–3743.

5323

AQUEOUS ALTERATION IN A HUMID CHAMBER OF SYNTHETIC Fe-SILICATE SMOKES

E. J. Hoffman. Physics Department, Morgan State University, Baltimore, MD 21251, USA. E-mail: ehoffman@jewel.morgan.edu.

Introduction: Synthetic iron-silicate smoke models material observed in the dusty circumstellar envelope of asymptotic giant branch (AGB) stars [1], presumably a raw material for planet formation in protosolar disks. Mg-silicate smokes react with liquid water to form silicates of complexity increasing with time and resulting within a few days in well-ordered layer silicates [2, 3]. Incubation in a humid chamber is a milder treatment than immersion in liquid water, but provides the ability to follow water uptake by measurement of mass increase and to hold that water content steady. Surprisingly, however, this approach has turned up some indication of reaction in Fe-silicates, which, as described above, has been difficult to detect in immersed samples. Hoffman et al. [4–6] held Nuth's Fe-silicate smokes in a humid chamber at 10–20 °C for up to several weeks and observed an increase in mass as well as a sharpening of peaks in Fe-Mössbauer spectroscopic patterns.

Under the microscope the Fe in these Fe smokes appears to be both in oxides and silicates [7]. This study has used mass increase and Mössbauer spectroscopy to examine the fate of these components after incubation in a humid chamber.

Results: For Mössbauer spectra displaying evidence of ferric ion a run at low temperature can often determine whether the ions are in oxides or silicates. For example, for a sample incubated in a humid chamber at 26 °C for 17 days, a ferric doublet merely broadened somewhat at 20 K, without appreciable formation of a magnetic sextet ("superparamagnetism"). This is evidence that much of the Fe^{3+} has remained in silicate crystallites, rather than changing to ferric oxides.

References: [1] Nuth J. A. III et al. 2000. *Journal of Geophysical Research* 105:10,387. [2] Rietmeijer et al. 2004. *Meteoritics & Planetary Science* 39:723. [3] Chizmadia L. J. 2007. Abstract #1005. 38th LPSC. [4] Hoffman E. J. et al. 2002. *Hyperfine Interactions C*:419. [5] Hoffman E. J. et al. 2002. *Meteoritics & Planetary Science* 37:A64. [6] Hoffman E. J. et al. 2004. *Hyperfine Interactions* 153:143. [7] Rietmeijer et al. 1999. *The Astrophysical Journal* 527:395.

5174

NEW PERSPECTIVES FROM THE NAKHLITES MAGNETIC SIGNATURE

V. Hoffmann[1, 2], M. Funaki[3], M. Torii[4], and E. Appel[1]. [1]Institute for Geosciences, University of Tübingen, Germany. [2]Faculty of Geosciences, University of München, Germany. E-mail: viktor.hoffmann@uni-tuebingen.de. [3]National Institute of Polar Research, Tokyo, Japan. [4]Department of Geosphere-Biosphere System Science, Okayama University of Science, Okayama, Japan.

Introduction: During the last years, a systematic investigation of the magnetic signature of stony meteorites has been started [1]. Detailed studies of the Martian meteorites (SNC) by magnetic methods deepened significantly our knowledge about their magnetic record and magneto-mineralogy [2–4]. New light was shed in this way on the formation of the SNC as well on surface forming processes such as impacts on Mars.

Investigations and Results: The aim of our project is a systematic study of the magnetic signature of all Martian meteorites (SNC). Preliminary data obtained on the SNC from the NIPR collection have been reported recently [5–7]. The nakhlites are igneous cumulate rocks that formed in flows or shallow intrusions from basaltic magma about 1.3 Gyr ago on Mars [8]. Seven nahklites are identified presently, all with typical ejection ages of ≈11 Ma and terrestrial ages ranging from around 50 ± 20 ka (Y-000593) to recent (observed falls) [8]. Generally, the nakhlites are characterized by minor shock effects (<20 GPa).

The paired nakhlites Y-000593/749/802 have the longest residence time of all nakhlites and are therefore well suited for a detailed study of the influence of terrestrial weathering effects under Antarctic conditions on the magnetic record. For example, a significant trend of decreasing values of magnetic susceptibility (MS) from the large Y593 (13.5 kg) and Y749 (1.28 kg) stones to the small Y802 (22 g) is evident and most likely reflects terrestrial weathering. A more substantiated test for the influence of terrestrial weathering and its discrimination from Martian alteration effects can be proposed based on the magnetic signature.

A new schematic model for the likely petrogenesis of the nakhlites on Mars was recently published [9]. Taking into account MS (log of mass spec. MS in 10^{-9} m^3/kg) and M_{rs} (M_{rs}: saturation magnetic remanence in 10^{-3} Am^2/kg) of all nakhlites (between 2 and 10 samples per nakhlite included in the database), there is clear evidence for a link between magnetic signature and the petrogenesis model: highest MS (3.71–3.77) and M_{rs} values (133–398) for MIL 03346 and NWA 817, respectively, followed by a group of low/moderate MS (3.63, 3.20, 3.30, 3.23)/low M_{rs} (73, 77.4, 89.7, 69.0) nakhlites (Y-000593, Nakhla, Governador Valadares, Lafayette) and again higher MS (3.60)/M_{rs} (427) values for NWA 998. Additional magnetic parameters (and magneto-mineralogy) will be included in our approach to further test and substantiate these findings.

References: [1] Rochette P. et al. 2001. *Quad. Geophys.* 18:31. [2] Rochette P. et al. 2001. *Earth and Planetary Science Letters* 190:1–12. [3] Rochette P., Funaki M., Hoffmann V. et al. 2005. *Meteoritics & Planetary Science* 40:529–540. [4] Rochette P., Hoffmann V., and Funaki M. 2005. Abstract #1614. 36th LPSC. [5] Hoffmann V. and Funaki M. 2006. *Antarctic Meteorites* 30. pp. 22–23. [6] Funaki M., Hoffmann V., and Torii M. 2007. AGU. [7] Hoffmann V., Torii M., and Funaki M. 2007. *Antarctic Meteorites* 31. [8] The Mars Meteorite Compendium. 2007. Compiled by C. Meyer, ARES, NASA, JSC. [9] Day J. M. D. et al. 2006. *Meteoritics & Planetary Science* 41:581–606.

5330

IRRADIATION RECORDS OF GIBEON METEORITE

M. Honda[1], H. Nagai[1], K. Nagao[2], N. Takaoka[3], and Y. Oura[4]. [1]Department of Chemistry, Nihon University, Tokyo, Japan. E-mail: m-honda@p07.itscom.net. [2]Laboratory for Earthquake Chemistry, University of Tokyo, Tokyo, Japan. [3]Department of Earth and Planetary Sciences, Kyushu University, Fukuoka, Japan. [4]Department of Chemistry, Tokyo Metropolitan University, Tokyo, Japan.

Introduction: Gibeon iron, IVA, is a popular large-size iron meteorite. The fall was in a strewn field extending more than 400 km north to south in Namibia. The fall has been known since 1838. The recovery is measured to be 21 tons composed of 80 pieces weighing an average of 280 kg per fragment [1]. The contents of Ni, Ge, and Ga are low. The content of phosphorus is very low at 0.04%. The ductility is high and can sustain for 180 degrees of bending.

Cosmogenic Nuclides: Cosmic ray–produced radioactive nuclides, ^{10}Be, ^{36}Cl, and others, were determined by AMS methods [2]. Stable light noble gases were measured by a sensitive gas mass-spectrometer [3]. Based on the contents of radionuclides and noble gases determined in the fragments, we achieved complex records of the meteorite. The data were obtained with about 100 specimens of the meteorite as a mixture of two subgroups showing different records. Among the available samples, more than 50% have records equivalent to about 10^7 years, which are only 5% of the 3×10^8 years of the older group. A nonvolatile stable cosmogenic nuclide, ^{45}Sc, has also been determined independently by RNAA [4].

Results and Discussion: A reasonable irradiation history of Gibeon can be obtained by assuming the extensive escape of the volatile products and by counting the stable non-volatile products. In this experiment, we selected the number of ^{45}Sc atoms as the stable products staying in the meteorite. The blank level of the natural scandium atoms can be estimated to be negligible in the one of the deepest iron fragments. Among the samples of Campo del Cielo, the deepest sample, El Taco 2/5, was useful, supplying 0.002 ± 0.001 ppb Sc (and 0.09×10^{-8} cc/g ^{3}He; also 0.001 dpm/kg ^{10}Be).

On the whole, the violent breakup in the atmosphere of the Gibeon meteorite, which created one of the longest strewn fields in the world, might be responsible for the meteorite's current status.

References: [1] Buchwald V. 1975. *Handbook of iron meteorites,* vol. 2. pp. 584–593. [2] Noguchi M. et al. 2004. 28th Symposium on Antarctic Meteorites. pp. 64–65. [3] Nord R. and Zaehringer J. 1972. Geochimii I Analiticeskoy Chimii, Acad. Nauk 59. [4] Honda M. et al. 1988. Proceedings of the NIPR Symposium on Antarctic Meteorites 1. pp. 197–205.

5064

1-D SHOCK WAVE SIMULATIONS OF CHONDRULE THERMAL HISTORIES FOR HIGH CHONDRULE NUMBER DENSITIES

L. L. Hood[1] and F. J. Ciesla[2]. [1]LPL, The University of Arizona, Tucson, AZ 85721. E-mail: lon@lpl.arizona.edu. [2]DTM, Carnegie Inst. of Washington, Washington, D.C., USA.

Introduction: Previous detailed 1-D simulations of chondrule thermal and dynamical histories in nebular shock waves have so far demonstrated that cooling rates compatible with furnace experiment results (100–1000 K/h) are possible only for solids-to-gas mass ratios near or below the solar value of ~0.005 [1–3]. In these simulations, the nebular gas density was assumed to be $\leq 10^{-9}$ g cm^{-3}, implying millimeter-diameter chondrule number densities of ≤ 0.01 m^{-3}. However, analyses of the frequency of compound chondrules together with theoretical considerations indicate that chondrules formed in regions with chondrule number densities >6 m^{-3} [4]. Also, one recent model to explain the depletion of volatile elements in chondrules requires that the precursor number density was >10 m^{-3} [5].

Approach: In this paper, we report new simulations using the 1-D shock model of [1] (as modified in [6]) to investigate whether cooling rates in the 100–1000 K/h range can be obtained for chondrule number densities exceeding 10 m^{-3}. For this purpose, we have carried out a series of large-scale shock model runs for such chondrule number densities while simultaneously varying other model parameters (nebular gas density, shock velocity, chondrule/dust mass ratio, solids/gas mass ratio, etc.).

Results: Runs completed so far indicate that cooling rates in the range suggested by furnace experiments are very difficult to achieve for chondrule number densities >10 m^{-3}, even for higher nebular gas densities and for low micron-size dust densities. The high chondrule number densities increase the opacity, which causes chondrules to be exposed to radiation from hot particles immediately behind the shock front for shorter time periods. This effectively increases the cooling rate above the 1000 K/h limit. The addition of a significant fraction of micron-size dust, which is needed to explain the formation of fine-grained rims around chondrules [7, 8], further increases the opacity and, therefore, the cooling rates.

References: [1] Ciesla F. J. and Hood L. L. 2002. *Icarus* 158:281–293. [2] Desch S. and Connolly H. C., Jr. 2002. *Meteoritics & Planetary Science* 37:183–207. [3] Iida A. et al. 2001. *Icarus* 153:430–450. [4] Ciesla F. J. et al. 2004b. *Meteoritics & Planetary Science* 39:531–544. [5] Cuzzi J. N. and Alexander C. 2006. *Nature* 441:483–485. [6] Ciesla F. J. et al. 2004b. *Meteoritics & Planetary Science* 39:1809–1821. [7] Connolly H. C., Jr. and S. G. Love. 1998. *Science* 280:62–67. [8] Liffman K. and M. Toscano. 2000. *Icarus* 143:106–125.

5010

SEARCH FOR S-BEARING PRESOLAR GRAINS IN THE ACFER 094 METEORITE

P. Hoppe[1] and C. Vollmer[1]. [1]Max Planck Institute for Chemistry, 55128 Mainz, Germany. E-mail: hoppe@mpch-mainz.mpg.de.

Introduction: The Acfer 094 meteorite is exceptionally rich in presolar silicate and refractory oxide grains [1–4]. It thus represents a good target to search for other yet unidentified presolar grain types, such as S-bearing minerals. S-bearing minerals, e.g., MgS, are observed in stellar spectra [5] and have been predicted to condense in the atmospheres of C-rich AGB stars [6]. Circumstellar S-bearing condensates are expected to exhibit large S isotope anomalies, specifically in the $^{36}S/^{32}S$ ratio [7]. Here, we report on the search for S-bearing presolar grains in the Acfer 094 meteorite by NanoSIMS ion imaging.

Experimental: The NanoSIMS ion imaging was done on 21 areas (10 × 10 μm^2) in the matrix of Acfer 094 that have been previously screened for O-isotopic anomalies to search for presolar silicates and oxides [4]. Negative secondary ions of all S isotopes together with ^{16}O were measured in multi-collection with a spatial resolution of ~100 nm and primary ion current of ~1 pA. With the integration time of ~1.5 h per image counting statistical errors of $^{33}S/^{32}S$, $^{34}S/^{32}S$, and $^{36}S/^{32}S$ ratios of 300 nm-size S-rich particles are typically 20, 10, and 150‰, respectively.

Results and Discussion: About 1000 S-bearing grains were recognized by an automated particle recognition routine. These grains make up some 18% of the scanned matrix area. Most grains have S-isotopic compositions compatible with solar; two grains with sizes of ~300 nm, however, show small but noticeable enrichments in ^{33}S and/or ^{34}S, with $\delta^{33}S = 68 \pm 26$‰, $\delta^{34}S = 48 \pm 11$‰, and $\delta^{36}S = 144 \pm 203$‰ (#81-4), and $\delta^{33}S = 67 \pm 15$‰, $\delta^{34}S = 31 \pm 6$‰, and $\delta^{36}S = 111 \pm 111$‰ (#84-14), respectively. These data can be compared with expectations for grains from AGB stars, the most prolific suppliers of circumstellar dust. For a 1.5 $M_\odot$ AGB star of solar metallicity, enrichments of tens of ‰ in ^{33}S and ^{34}S and of ~400‰ in ^{36}S are predicted [7]. This is qualitatively in agreement with our grain data, although the observed ^{36}S enrichments tend to be lower than predicted.

If we divide the area occupied by grains #81-4 and #84-14 in the ion images by the total analyzed area (including our previous measurements [8]) we obtain an abundance of 50 ppm for these two grains, clearly less than the inferred abundance of ~200 ppm for presolar silicates [4] but compatible with the abundance of presolar refractory oxides in Acfer 094. Whether the S isotope anomalies seen in these two grains are in fact the signature of stellar nucleosynthesis carried by presolar grains or just statistical outliers remains to be seen. More work is clearly needed to resolve this question. Specifically, finding grains with pronounced ^{36}S enrichments will be important.

References: [1] Nguyen A. and Zinner E. 2004. *Science* 303:1496–1499. [2] Mostefaoui S. and Hoppe P. 2004. *The Astrophysical Journal* 613: L149–L152. [3] Nguyen A. et al. 2007. *The Astrophysical Journal* 656:1223–1240. [4] Vollmer C. et al. 2007. Abstract #1262. 38th LPSC. [5] Molster F. 2002. In *Astromineralogy*, edited by Henning Th. New York: Springer. pp. 121–170. [6] Lodders K. and Fegley B. 1995. *Meteoritics* 30:661–678. [7] Mauersberger R. et al. 2001. *Astronomy & Astrophysics* 426:219–227. [8] Hoppe P. et al. 2005. Abstract #1301. 36th LPSC.

5207

INSIGHTS INTO THE THERMAL HISTORY OF AOAs IN CARBONACEOUS CHONDRITES

L. E. Howard[1], P. A. Bland[1, 2], D. J. Prior[3], and S. S. Russell[1]. [1]Impacts & Astromaterials Research Centre (IARC), Department of Mineralogy, Natural History Museum, London SW7 5BD, UK. E-mail: l.howard@nhm.ac.uk. [2]IARC, Department of Earth Science & Engineering, Imperial College, London SW7 2AZ, UK. [3]Department of Earth & Ocean Sciences, University of Liverpool, 4 Brownlow Street, Liverpool L69 3GP, UK.

Introduction: Amoeboid olivine aggregates (AOAs) are generally regarded as aggregates of solar nebular condensates (e.g., [1, 2]). However, equilibrium (triple junction) textures have occasionally been observed, either in AOA rims [3, 4], or (more rarely) in AOAs themselves [5]. This texture has been attributed to both thermal annealing in the nebular [3–5] and hydrothermal alteration on the parent asteroid [6]. Electron backscattered diffraction (EBSD) offers an excellent mean of visualizing textures in fine-grained materials with similar atomic number. Here we use EBSD in a detailed study of the crystallography and texture of AOAs in a number of carbonaceous chondrites [7].

Methodology: In this study, several AOAs were mapped using EBSD in a variety of carbonaceous chondrites, including the highly unequilibrated meteorites Acfer 094 and ALHA77307. Orientation contrast maps were constructed, and grain-size statistics and degree of crystallinity were calculated to provide textural information on the AOAs in these primitive meteorites.

Results: EBSD analysis reveals that comparatively coarse-grained, equilibrium textures are a common feature of AOAs in these chondrites (e.g., Fig. 1). We observe no systematic correlation between grain size and crystallinity and metamorphic sub-type in the CO3s; different AOAs within the same chondrite display a large range of grain sizes and degrees of textural equilibration; and AOAs in unmetamorphosed chondrites also show equilibrium textures.

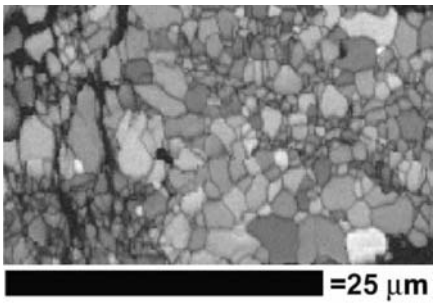

Fig. 1. Pattern quality map of AOA in Acfer 094.

Conclusions: Equilibrium textures and coarse grain sizes are commonly observed in AOAs, suggesting extensive annealing. This is unlikely to be a parent body process: 1) no correlation is observed between AOA textures and metamorphic grade in CO3s; 2) Acfer 094 and ALHA77307 experienced minimal thermal metamorphism; 3) there is a large variation in grain size and textural equilibration between AOAs in the same chondrite. The implication is that annealing was a nebula process.

References: [1] Krot A. N. et al. 2003. *Meteoritics & Planetary Science* 38:A5133. [2] Krot A. N. et al. 2002. Abstract #1412. 23rd LPSC. [3] Kornacki A. S. and Wood J. A. 1984a. *Journal of Geophysical Research* 89: B573–587. [4] Kornacki A. S. and Wood J. A. 1984b. *Geochimica et Cosmochimica Acta* 48:1663–1676. [5] Komatsu M. et al. 2001. *Meteoritics & Planetary Science* 36:629–641. [6] Rubin A. E. 1998. *Meteoritics & Planetary Science* 33:385–391. [7] Watt L. E. 2006. Ph.D. thesis.

5016

LUNAR GRANULITIC IMPACITES: CONSTRAINTS ON THEIR MINERALOGY, PETROLOGY, AND CHRONOLOGY

J. A. Hudgins[1], J. G. Spray[1], S. C. Sherlock[2], and S. P. Kelley[2]. [1]Planetary and Space Science Centre, University of New Brunswick, Fredericton, N.B., Canada. E-mail: jillian.hudgins@unb.ca. [2]Department of Earth Sciences, The Open University, Milton Keynes, UK.

Introduction: Lunar granulitic impactites are complex rocks that are poorly understood. These coherent crystalline rocks were derived by the recrystallization of previously brecciated material. They contain clasts from both the ferroan anorthosite and Mg suites. They are characterized by 70–80% modal plagioclase, are enriched in trace siderophile elements (indicative of meteoritic contamination), and contain virtually no KREEP component. Minerals lack zoning and their compositions are homogeneous. All minerals are assumed to have been re-equilibrated by a major thermal event, or events [1].

Few ages have been conclusively determined for this suite. These rocks are thought to have formed after the initial differentiation of the early lunar crust, yet before the final bombardment period that began around 4.0 Ga. We have performed ultraviolet and infrared laser single shots and step-heating ^{40}Ar-^{39}Ar chronology on plagioclase grains from four Apollo samples (67955, 77017, 78155, and 79215). Although the ^{39}Ar-^{40}Ar systematics of the samples are highly disturbed, we interpret the ages obtained to date the age of the latest dominant metamorphic event [2].

An improved knowledge of the pressure and temperature at a certain depth within the Moon would help place valuable constraints on its thermal gradient and evolution. To this end, we have calculated equilibration pressures and temperatures for nine granulitic impactite samples on loan from NASA using equations based on the exchange of elements between co-existing minerals. Our results represent the suite's last episode of re-equilibration, which corresponds to depths of burial of ~10–30 km (mid-crust of the Moon) [3]. This suggests that metamorphism was due to burial, rather than by juxtaposition at shallower levels with hot impact melt sheets. However, the applied thermobarometric equations were calibrated for terrestrial rocks and may not be appropriate for the lower pressure conditions of the lunar crust. In order to more accurately constrain equilibration conditions, low pressure piston cylinder experiments are being performed with the aim of simulating the formation conditions of the granulitic impactites. The information obtained from these experiments combined with other analyses will provide an understanding of how, when, and where these samples formed and evolved. By determining the age and composition of these samples, in addition to the temperature, pressure, and depth at which they formed, we hope to gain insight into the evolution of the thermal gradient of the Moon during pre-Nectarian times. In this work we report on the mineralogy, petrology, recent Ar-Ar research, and P-T constraints.

References: [1] Warner J. L. et al. 1977. 8th Lunar Science Conference. pp. 2051–2066. [2] Cohen B. 2004. Abstract #1009. 35th LPSC. [3] Hudgins J. A. and Spray J. G. 2006. *Meteoritics & Planetary Science* 41: A81.

5005

^{26}Al AND ^{60}Fe IN CHONDRULES FROM UNEQUILIBRATED ORDINARY CHONDRITES

G. R. Huss[1], S. Tachibana[2], and K. Nagashima[1]. [1]Hawai'i Institute of Geophysics and Planetology, University of Hawai'i at Manoa, 1680 East-West Road, Honolulu, HI 96822, USA. E-mail: ghuss@higp.hawaii.edu. [2]Department of Earth and Planetary Science, University of Tokyo, 7-3-1 Hongo, Tokyo 113-0033, Japan.

Introduction: We recently reported data for the ^{60}Fe-^{60}Ni system in eleven chondrules from Semarkona (LL3.0) and Bishunpur (LL3.1) [1, 2]. Eight of the eleven show resolved excesses of ^{60}Ni that correlate with the Fe/Ni ratio indicating that ^{60}Fe ($t_{1/2}$ = 1.5 My) was present in the chondrules when they formed. Based on these data and an assumption about when the chondrules formed, we inferred an initial ^{60}Fe/^{56}Fe ratio for the early solar system of (0.5–1.0) × 10^{-6} [1]. The assumption about when the chondrules formed is based on ^{26}Al-^{26}Mg data for other chondrules in Semarkona and Bishunpur (e.g., [3]). We could remove the assumption about the chondrule formation time and tie two isotope systems together by measuring ^{26}Al-^{26}Mg systematics in the same chondrules that we have measured for ^{60}Fe-^{60}Ni. Here we report the first such measurements.

Experimental: Six of the eleven chondrules we have measured for ^{60}Fe-^{60}Ni contain Al-rich glass suitable for ^{26}Al-^{26}Mg measurements. Two of these six chondrules were measured with the UH Cameca IMS 1280 ion microprobe. Al-rich glass was measured using a 0.1 nA focused O^- beam. Magnesium isotopes were collected on the monocollector electron multiplier and ^{27}Al was measured on the monocollector Faraday cup (FC2). Olivine was measured to secure the intercept of the isochron using a 3 nA beam; magnesium isotopes were measured on FC2. Data were corrected for deadtime (EM) and baseline (FC2). Standards were Miyake-jima plagioclase and San Carlos olivine.

Results: Chondrules BIS-1 and BIS-32 were measured for ^{26}Al-^{26}Mg systematics. BIS-1 does not show resolved excesses of ^{60}Ni, while BIS-32 has correlated excesses implying and initial ^{60}Fe/^{56}Fe when the chondrule formed of (1.9 ± 1.1) × 10^{-7} [2]. Neither chondrule gave clear evidence of having formed with live ^{26}Al, and the upper limits for their initial ^{26}Al/^{27}Al ratios were essentially identical, <6.3 × 10^{-6} (2σ confidence level). This is a surprising result because it places these chondrules at the low end of the range exhibited by other chondrules in Semarkona and Bishunpur [4]. We cannot tell at this point whether these chondrules did in fact have lower ^{26}Al/^{27}Al initial ratios than most chondrules, or whether we just need better data. If the chondrules we have measured for ^{60}Fe-^{60}Ni systematics are younger than the majority of UOC chondrules, we may have to recalculate the initial ^{60}Fe/^{56}Fe abundance for the early solar system. More measurements are clearly required. We must also measure more chondrules to evaluate whether or not the ^{26}Al-^{26}Mg and ^{60}Fe-^{60}Ni systems can be linked. We anticipate being able to report more data in Tucson.

Acknowledgements: Supported by NASA grant NNG05GG48G (G. R. H.).

References: [1] Tachibana S. et al. 2006. *The Astrophysical Journal* 639:L87–L90. [2] Tachibana S., Huss G. R., and Nagashima K. 2007. Abstract #1709. 38th Lunar and Planetary Science Conference. [3] Kita N. T. et al. 2006. *Geochimica et Cosmochimica Acta* 64:3913–3922. [4] Kita N. T. et al. 2005. In *Chondrites and the protoplanetary disk*, edited by Krot A. N., Scott E. R. D., and Reipurth B. ASP Conference Series 341. pp. 317–350.

5072

ANNEALING AFTER SHOCK: EVIDENCE FROM OLIVINE MICROSTRUCTURES IN PORTALES VALLEY

M. Hutson[1], R. Hugo[1], A. Ruzicka[1], and M. Killgore[2]. [1]Cascadia Meteorite Laboratory, Department of Geology, Portland State University, 17 Cramer Hall, 1721 SW Broadway, Portland, OR 97207, USA. E-mail: mhutson@pdx.edu. [2]Southwest Meteorite Center, The University of Arizona, 1415 N. 6th Ave., Tucson, AZ 85705, USA.

Introduction: TEM dislocation analysis of olivine grains in the Portales Valley (PV) metallic-melt breccia [1] provides an opportunity to test whether post-shock annealing could have lowered optically determined shock stages and contributed significantly to the thermal metamorphism of chondrites (e.g., [2]). Various pre-annealing peak shock pressures have been proposed for PV ranging from S2 [1] to S3 [3] to S6 [2], followed by annealing to the current shock stage of S1 [1–3].

Results and Discussion: Twelve olivine grains were examined from an area of typical PV matrix. The coarsest olivine grain in this region is ~100 μ across. Dislocation densities range from no dislocations to 7.9×10^9 cm^{-2}, with an area-weighted average of 1.1×10^8 cm^{-2}. The character of the dislocations varies from region to region, with straight dislocations predominant. Most dislocations are straight b = [001] screws, sometimes connected with short edge segments, consistent with high strain rate deformation at relatively low temperatures (roughly ≤1000 °C [4]). Curved or jogged dislocations and those located at subgrain boundaries are interpreted as having formed by recovery as a result of annealing.

In PV, the ratio of dislocations that are not part of a subgrain boundary to those in a subgrain boundary (free to bound ratio) varies from region to region and inversely with dislocation density, consistent with annealing. Some dislocations evidently were removed by annihilation during recovery. Thus we interpret the range of dislocation densities to be partly the result of annealing, with a decrease in dislocation densities in a few areas by 1 to 2 orders of magnitude from the maximum value.

The dislocation densities in PV are clearly lower than those observed in heavily shocked (S6) chondrites [5] and higher than those reported for weakly shocked (S1) chondrites [6]. Our observations support the idea that optical evidence for shock in PV is low in part due to annealing effects. However, many regions have few or no dislocations, with no dislocations in subgrain boundaries, suggesting that shock effects were nonuniform from grain to grain and that the maximum shock intensity experienced by PV as a whole was low, possibly S2 to S3 based on comparison to other chondrites [5–7]. It appears that annealing in PV was only moderately effective at lowering its apparent shock stage.

References: [1] Ruzicka A. et al. 2005. *Meteoritics & Planetary Science* 40:261–295. [2] Rubin A. E. et al. 2001. *Geochimica et Cosmochimica Acta* 65:323–342. [3] Kring D. A. et al. 1999. *Meteoritics & Planetary Science* 34:663–669. [4] Phakey P. et al. 1972. In *Flow and fracture of rocks,* edited by Heard H. C. pp. 117–138. [5] Langenhorst F. et al. 1995. *Geochimica et Cosmochimica Acta* 59:1835–1845. [6] Töpel-Schadt J. and Müller W. F. 1985. *Earth and Planetary Science Letters* 74:1–12. [7] Ashworth J. R. and Barber D. J. 1975. *Earth and Planetary Science Letters* 27:43–50.

5238

THE CASE AGAINST MERCURY AS THE ANGRITE PARENT BODY (APB)

M. L. Hutson[1], A. M. Ruzicka[1], and D. W. Mittlefehldt[2]. [1]Cascadia Meteorite Laboratory, Department of Geology, Portland State University, 17 Cramer Hall, 1721 SW Broadway, Portland, OR 97207, USA. E-mail: mhutson@pdx.edu. [2]Mail Code KR, NASA Johnson Space Center, 2101 NASA Parkway, Houston, TX 77058, USA.

Introduction: Angrites are not plausibly from Mercury based on their high FeO contents and ancient ages (e.g., [1]). Rather, the early crystallization ages of angrites argues for a small asteroidal-size parent body for these meteorites (e.g., [2]). Despite this, recently it has been proposed that Mercury is the APB [3–6]. Preserved corona and symplectite textures and the presence of 120° triple junctions in NWA 2999 have been cited as requiring a planetary origin [3, 4], with the symplectites in NWA 2999 resulting from rapid decompression during uplift via thrust faults on Mercury [4], and the coronas during subsequent cooling at low pressure. Glasses along grain boundaries and exsolution lamellae possibly indicative of rapid melting and cooling in NWA 4590 are cited as evidence of rapid decompression [6]. To explain the discrepancy between spectral observations of the Mercurian surface and the high FeO contents in angrites, an early (~4.5 Ga), collisionally stripped FeO-rich basaltic surface has been suggested for Mercury [5, 6].

Discussion: There is no compelling evidence that angrites are derived from a planet-size parent body. The observed corona and symplectite textures in NWA 2999 are not consistent with the metamorphic reactions described [4], but rather with cooling during crystallization from an angrite-like melt [7]. 120° triple junctions do not require a large parent body as they have been observed in brachinites, acapulcoites, lodranites, ureilites, and winonaites (e.g., [2, 8]). It is implausible that Mercury ever had an early FeO-rich basaltic crust and mantle. With this model, Mercury would have had to differentiate under reducing conditions to produce the observed planet, after early differentiation under oxidizing conditions to produce the FeO-rich angrites, for which there is no evidence or apparent mechanism. Additionally, there is no viable mechanism for rapid uplift of ancient Mercurian crust over the depths required. The lobate scarps on Mercury formed relatively late (e.g., [9]), not early as required.

References: [1] Love S. G. and Keil K. 1995. *Meteoritics* 30:269–278. [2] Hutchison R. 2004. *Meteorites: A petrologic, chemical and isotopic synthesis.* Cambridge University Press. [3] Irving A. J., Kuehner S. M., Rumble D., Bunch T. E., Wittke J. H., Hupe G. M., and Hupe A. C. 2005. Abstract #P51A-0898. AGU Fall Meeting. [4] Kuehner S. M., Irving A. J., Bunch T. E., Wittke J. H., Hupe G. M., and Hupe A. C. 2006. Abstract #1344. 37th Lunar and Planetary Science Conference. [5] Irving A. J., Kuehner S. M., and Rumble D. 2006. Abstract #P51E-1245. AGU Fall Meeting. [6] Kuehner S. M. and Irving A. J. 2007. Abstract #1522. 38th Lunar and Planetary Science Conference. [7] Ruzicka A. and Hutson M. 2007. Abstract #5080. *Meteoritics & Planetary Science* 41:A155. [8] Mittlefehldt D. W., McCoy T. J., Goodrich C. A., and Kracher A. 1998. In *Planetary materials,* edited by Papike J. J. Mineralogical Society of America. [9] Chapman C. R. 1988. In *Mercury*, edited by Vilas F., Chapman C. R., and Matthews M. S. Tucson, Arizona: The University of Arizona Press.

5305

QUANTITATIVE ANALYSIS OF NATURAL ABLATION DEBRIS

K. A. Huwig[1] and R. P. Harvey[2]. [1]Department of Geol. and Env. Sci., Stanford University, Stanford, CA 94305, USA. E-mail: khuwig@stanford.edu. [2]Department of Geol. Sci., Case Western Reserve University, Cleveland, OH 44106, USA.

Introduction: The study of ablation debris has been slowed by the difficulty in finding and correctly identifying them in the micrometeorite collections, and the study has so far been mainly focused on the nature and composition of fusion crusts as analogs of ablation spherules [1, 2]. Others have attempted to create artificial ablation debris by taking a known natural mineral and an arc-heated plasma stream of air and then examining the ablated debris [3].

In 1994 the BIT-58 meteorite ablation debris was discovered in a layer near the Allan Hills in the East Antarctic ice sheet. It was determined by [4] to be extraterrestrial due to a number of factors including cosmic ray exposure ages, the layer's homogeneous composition, its strong resemblance to the bulk composition of H-ordinary chondrites and the presence of olivine with Mg-rich cores surrounded by more fayalitic rims. Additional samples of the BIT-58 layer gathered in 2003 revealed some intriguing mineralogy that is important for the understanding of how ablation of a large (several meters or larger) body occurs.

BIT-58 Morphology and Mineralogy: While many of the spherules exhibit high degrees of melting, others consist entirely of zoned euhedral olivine grains that appear unmelted although the outside of the particle is nearly perfectly rounded.

More than 80% of the ablation debris is not rounded at all, and most have shard morphology. Many of the shard-shaped particles have features that indicate that the olivines within them are relict, such as euhedral shapes with distinct grain boundaries or even oscillatory zoning. However some of the shards have mineralogies consistent with melting and recrystallization, i.e., skeletal olivines with indistinct, unzoned grain boundaries. Interestingly the olivine grains are broken at the edge of the particles, indicating that the fracturing most likely occurred after recrystallization.

Another oddity of the ablation debris is that, to date, no other minerals besides olivines, magnetite, and Ni- and Cr-rich spinels have been identified in BIT-58, despite indications that a significant portion seems to have undergone little to no melting.

Methods: We will use microprobe analyses to determine major and trace element compositions of the olivine and spinel grains as well as to look for the presence of other minerals to determine the level of heterogeneity between particles, with particular attention to zoning profiles and inclusions within olivines to determine whether they are relict grains. These analyses will be performed on previously sampled particles as well as a larger representative sample of both spherules and shards. Further investigation of the proportion of relict grains, composition of spinels and morphology of individual particles with respect to mineralogy will lead to a better understanding of the ablation process.

References: [1] Rietmeijer F. J. M. and Mackinnon I. D. R. 1984. *Journal of Geophysical Research* 89:B597–B604. [2] Genge M. J. and Grady M. M. 1999. *Meteoritics & Planetary Science* 34:341–356. [3] Blanchard M. B. 1972. *Journal of Geophysical Research* 77:2442–2455. [4] Harvey R. P. et al. 1998. *Geology* 26:607–610.

5247

SILICON CARBIDE SUBGRAINS IN PRESOLAR GRAPHITE FROM MURCHISON

K. M. Hynes and T. K. Croat. Laboratory for Space Sciences and Department of Physics, Washington University, St. Louis, MO 63130, USA. E-mail: khynes@hbar.wustl.edu.

Introduction: Equilibrium condensation models for AGB stars predict that refractory carbides, like TiC, should condense at higher temperatures than graphite, while SiC condenses at lower temperatures than graphite [1]. Transmission electron microscopy (TEM) observations generally support these predictions, with refractory carbides often observed as internal subgrains within graphite, whereas SiC is only rarely observed inside of graphite [2, 3]. Here we present results from TEM studies of the only graphite grains known to have internal SiC subgrains, including one graphite that also contains an internal TiC subgrain.

Experimental: Graphite grains from the KFC1 density and size separate (2.15–2.20 g cm^{-3}, >1 μm) of the Murchison meteorite [4] were deposited from suspension onto a glass slide. The grains were then embedded in resin and sliced into ~70 nm sections with a diamond ultramicrotome and subsequently studied in a JEOL 2000FX TEM equipped with a NORAN energy dispersive X-ray spectrometer (EDXS).

Results: Out of ~1500 graphite slices examined in the TEM for internal subgrains, only 4 have been found that contain internal SiC grains. Preliminary results for one of these graphites was presented in [5]. Three graphites contain multiple SiC subgrains, with as many as 23 SiCs in a single graphite. The SiC subgrains ranged in size from ~13–83 nm. All of the internal SiC grains were identified by diffraction patterns as FCC 3C-SiC, 2H-SiC, or an intergrowth between the two polytypes. This is consistent with the polytypes observed in both mainstream SiC [6] and SiC X-grains [7]. Although most KFC1 graphites have an AGB origin, the stellar origin of SiC-containing graphites is uncertain. These graphites lack clear indicators of an AGB origin, such as additional subgrains with s-process enrichments commonly observed in other KFC1 graphites [3]. The multiply twinned TiC observed in one of the SiC-containing graphites, as well as the Fe subgrain found in [5], have compositions similar to the subgrains found in KE3 SN graphites [8]. However, EDXS analysis of the graphites with SiC subgrains reveals no radiogenic isotopes, such as ^{26}Mg, which would be a clear indicator of a SN origin. NanoSIMS analysis of two of the SiC-containing graphites gives $^{12}C/^{13}C$ ratios of 110 ± 2 and 782 ± 18 (solar ratio = 89), which confirms their presolar origin. However, because the $^{16}O/^{18}O$ ratios are normal within errors, the stellar sources of these grains remain uncertain. Additional NanoSIMS measurements of the Si isotopic composition of these grains are planned to clearly distinguish between an AGB and a SN origin.

References: [1] Lodders K. and Fegley B., Jr. 1995. *Meteoritics* 30: 661–678. [2] Bernatowicz T. J. et al. 1996. *The Astrophysical Journal* 472: 760–782. [3] Croat T. K. et al. 2005. *The Astrophysical Journal* 631:976–987. [4] Amari S. et al. 1994. *Geochimica et Cosmochimica Acta* 58:459–470. [5] Croat T. K. and Stadermann F. J. 2006. Abstract #2048. 37th Lunar and Planetary Science Conference. [6] Daulton T. L. et al. 2003. *Geochimica et Cosmochimica Acta* 67:4743–4767. [7] Hynes K. M. et al. 2006. Abstract #2202. 37th Lunar and Planetary Science Conference. [8] Croat T. K. et al. 2003. *Geochimica et Cosmochimica Acta* 67:4705–4725.

5029

PETROLOGICAL AND MINERALOGICAL CLASSIFICATION OF THE ISTIFANE CHONDRITES (MOROCCO)

A. Ibhi[1], H. Chennaoui Aoudjehane[2], H. Nachit[1], and El H. Abia[1]. [1]Laboratory of Petrology, Mineralogy and Materials (LPMM), Faculty of Sciences, Agadir, Morocco. E-mail: ibhiabderrahmane@yahoo.fr. [2]Hassan II University, Faculty of Sciences, Casablanca, Morocco. E-mail: h.chennaoui@fsac.ac.ma.

Introduction: The first Istifane meteorite (Istifane 001a) was found in April 2005 about 20 km west of Tinghir, in southeast Morocco [1]. The other five samples were recovered during geological field work in Tinghir areas of Ouarzazate Department in July 2005 (Istifane 001b and 001c), August 2005 (Istifane 002 and Istifane 003), and May 2006 (Istifane 004).

Analytical Methods: Macroscopic and microscopic observations, scanning electron microscope (SEM) equipped with a pentafet-detector for energy dispersive analysis (EDS), and X-ray diffraction data show that these meteorites are composed of olivine, clino- and orthopyroxene, wollastonite, feldspar, and opaque minerals (Fe-Ni alloy and sulfide).

Result and Discussion: All six meteorites show chemical and petrographic features that are characteristic of ordinary chondrites. The olivine compositions of Istifane 001a, 001b, 001c, 002, and 004 are well into the range of typical H-group chondrites, with average of $Fa_{18.4}$, $Fa_{18.8}$, $Fa_{19.2}$, $Fa_{15.5}$, and $Fa_{19.1}$, respectively. Olivine in Istifane 003 has an average of $Fa_{24.9}$, typical for L-group chondrites. Low-Ca pyroxene in Istifane 001a, 001b, 001c, 002, and 004 have average ferrosilite contents of $Fs_{16.2}$, $Fs_{16.4}$, $Fs_{17.5}$, $Fs_{16.8}$, and $Fs_{15.4}$, respectively, typical of H-group chondrites, whereas low-Ca pyroxene in Istifane 003 has a higher average of $Fs_{21.4}$, well within the L-group chondrites.

Istifane 001a, 001b, and 001c are a weakly shocked (shock stage S3) H-group chondrites of petrologic type 4 and weathering grade W4, whereas Istifane AM 005 is a very weakly shocked (S2) H-group chondrite of petrologic type 5 and weathering category W2. Istifane 002 is a strongly shocked (S5) H-group chondrite of petrologic type 5 and weathering category W3 and Istifane 003 as a weakly shocked (S3) L-group chondrite of petrologic type 5 and weathering category W2. Istifane 001a, 001b, and 001c belong to the same chemical class and petrologic type. They exhibit the same composition of olivine and pyroxene and show almost identical degrees of shock metamorphism and weathering. For these reasons and due to optical similarities in hand specimen and thin section, pairing of these samples is probable. They are approved by the Meteoritical Society under the same name of Istifane 001.

Istifane area (Tinghir, Morocco) has not been well prospected, and probably many individual meteorites are still in place. However, the discovery of these meteorites in Istifane area makes us think that the area is a potential search area.

Polished thin sections and a type specimen of each meteorite are preserved in the collection of the Petrology, Mineralogy and Materials Laboratory (LPMM) at the Ibn Zohr University Agadir of Morocco.

References: [1] El Mansouri M., Ibhi A., Nachit H., and Ait Touchent A. 2006. Discovery of a group of meteorites in the Istifane area (Tinghir, Morocco): Potential search area (abstract). *Meteoritics & Planetary Science* 41:A205.

5127

BABY BASALTIC SHERGOTTITE NWA 4480: AN Eu-ANOMALOUS MARTIAN MAGMA RELATED TO "LHERZOLITIC" SHERGOTTITES

A. J. Irving[1], S. M. Kuehner[1], R. L. Korotev[2], and G. M. Hupé. [1]Earth & Space Sciences, University of Washington, Seattle, WA, USA. E-mail: irving@ess.washington.edu. [2]Earth & Planetary Sciences, Washington University, St. Louis, MO, USA.

A 13 gram, almost fully fusion-crusted, ellipsoidal stone found in Algeria is an unusual type of basaltic shergottite.

Petrography: The dominant matrix (mean grain size 0.15 mm) consists of plagioclase laths (maskelynite, $An_{58.4–61.0}$ $Or_{1.6}$) showing some preferred flow (?) alignment of long axes (Fig. 1), olivine ($Fa_{67.9–79.2}$, FeO/MnO = 49–52), and complexly zoned clinopyroxene with accessory Ti-chromite, ilmenite, Mg-Fe-bearing merrillite, and rare Si-rich glass or silica polymorph. Clinopyroxene is patchily zoned from augite cores ($Fs_{24.9–31.2}Wo_{35.3–31.1}$, FeO/MnO = 30–32) to pigeonite rims ($Fs_{55.4–56.4}$ $Wo_{17.5–15.4}$, FeO/MnO = 36). Glomerocryst regions are composed of coarser (0.5–0.8 mm) plagioclase (maskelynite, $An_{66.3–68.5}Or_{0.3}$, more calcic than in the matrix) and olivine with interstitial pigeonite and ilmenite.

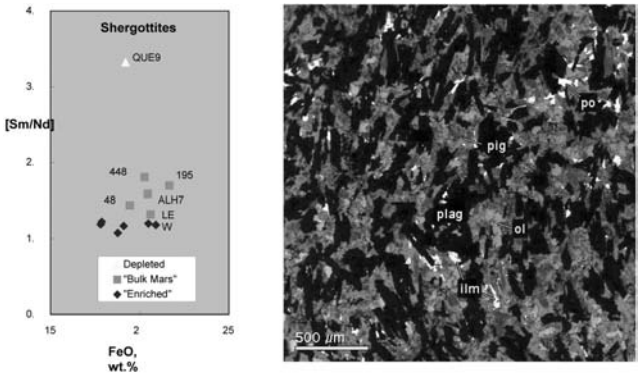

Fig. 1.

Bulk Composition: INAA of two ~37 mg whole fragments of matrix material + fusion crust gave (in wt%) Na 1.40, Fe 15.8, and (in ppm) Sc 39.7, Cr 1027, Ni <60, La 1.85, Sm 2.69, Eu 0.86, Tb 1.05, Yb 4.16, Hf 3.16, Th 0.24.

Magmatic Affinities: NWA 4480 is moderately LREE-depleted with elevated HREE abundances and a negative Eu anomaly. The chondrite-normalized Sm/Nd ratio is similar to values (1.4–1.7) for "lherzolitic" shergottites and basaltic shergottites NWA 480/1460 [1], and intermediate between those for "enriched" and depleted basaltic shergottites (Fig. 1). The abundance of Fe-rich olivine in NWA 4480 and its absence in NWA 480/1460 imply that different types of mafic liquids were derived from the "Bulk Mars" mantle source. Removal of plagioclase-rich glomerocrysts from the NWA 4480 parental magma may explain the matrix Eu anomaly.

References: [1] Barrat J. A. et al. 2002. *Meteoritics & Planetary Science* 37:487–499. [2] Irving A. and Kuehner S. 2003. Abstract #1503. 34th LPSC. [3] Nyquist L. et al. 2006. Abstract #1723. 37th LPSC.

5129

SILICATE+CHROMITE+METAL+PENTLANDITE INCLUSIONS IN LODRANITE BRECCIA NWA 4478: EVIDENCE FOR A REDUCED REGOLITH ON THE LODRANITE/ACAPULCOITE PARENT BODY

A. J. Irving[1], S. M. Kuehner[1], D. Rumble III[2], and G. M. Hupé. [1]Earth & Space Sciences, University of Washington, Seattle, WA, USA. E-mail: irving@ess.washington.edu. [2]Geophysical Laboratory, Carnegie Institution, Washington, D.C., USA.

Two dense brown stones lacking fusion crust found in Algeria represent the first known breccia related to the acapulcoite/lodranite parent body, and contain reduced mineral assemblages similar to those observed in QUE 93148.

Petrography: The specimens are composed of mineral and polycrystalline clasts (up to 8 mm across) with interstitial comminuted debris of the same phases. Large mineral clasts consist of either olivine or orthopyroxene (with clinopyroxene exsolution lamellae associated with blebs of Ni-free iron metal). The lithic clasts consist mainly of coarse interlocking olivine grains ($Fa_{10.6–10.9}$, FeO/MnO = 22.1–23.9, up to 3 mm across) and sparse large chromite grains (Cr/(Cr + Al) = 0.822–0.825, Mg/(Mg + Fe) = 0.506–0.520, TiO_2 = 0.31–0.37 wt%) with interstitial (apparently intercumulus) clinopyroxene ($Fs_{3.9}Wo_{41.9}$, FeO/MnO = 10.2, some with exsolution lamellae of orthopyroxene $Fs_{9.1}Wo_{1.3}$, FeO/MnO = 11.9), orthopyroxene, kamacite, pyrrhotite, pentlandite and troilite. The modal abundance of metal (+limonite after primary metal) measured by BSE imaging on a large polished slice is 5 vol%. Plagioclase is absent. Olivine grains contain numerous blebby to worm-like polycrystalline inclusions of clinopyroxene+chromite+orthopyroxene+pentlandite, and clinopyroxene grains contain similar inclusions composed of orthopyroxene+chromite+kamacite; some examples exhibit symplectitic intergrowths of these various phases. Some olivine grains contain multiple blade-like lamellae of another olivine phase with different composition ($Fa_{9.8}$). Narrow elongate zones or discontinuous veinlets of metal are present within clinopyroxene, and adjacent to such metal the pyroxene has a more magnesian composition.

Oxygen Isotopes: Acid-washed silicate material analyzed by laser fluorination gave, respectively, $\delta^{18}O$ = 2.23, 2.43, 2.23, 2.40; $\delta^{17}O$ = 0.14, 0.30, 0.07, 0.11; $\Delta^{17}O$ = –1.034, –0.984, –1.107, –1.147 per mil: values typical of lodranites [2].

Conclusions: Primary clast textures, grain sizes, mineral compositions and oxygen isotopic compositions indicate that this specimen is a lodranite breccia, and implies that there is a regolith on the ALPB. The polyphase inclusions within mafic minerals are similar to those described in lodranite-like achondrite QUE 93148 by [1], and along with the lamellae in olivine imply an episode of reduction after the formation of the primary magmatic cumulate assemblage.

References: [1] Goodrich C. and Righter K. 2000. *Meteoritics & Planetary Science* 35:521–536. [2] Clayton R. and Mayeda T. 1996. *Geochimica et Cosmochimica Acta* 60:1999–2018. Irving A. et al. 2007. Abstract #2254. 38th LPSC.

5113

HETEROGENEOUS ^{26}Mg MICRODISTRIBUTIONS IN A TYPE A CAI: CONSTRAINTS ON ITS FORMATION PROCESS AND CHRONOLOGY

Motoo Ito and Scott Messenger. ARES, NASA Johnson Space Center, 2101 NASA Parkway, Houston, TX 77573, USA. E-mails: motoo.ito-1@nasa.gov; scott.r.messenger@nasa.gov.

Introduction: The in situ decay of short-lived ^{26}Al in refractory inclusions, such as Ca, Al-rich inclusions (CAIs), and chondrules, results in ^{26}Mg isotopic heterogeneity among co-existing mineral phases. The ^{26}Al-^{26}Mg system has been used to establish the relative ages of the CAIs and chondrules [1]. This chronometer is also able to resolve the time elapsed between multiple metamorphic/heating processes in CAI constituent minerals (e.g., [2]). In this study, we report new data of ^{26}Al-^{26}Mg systematics in fassaite, melilite and anorthite in type-A CAI, EK-1-6-3 whose O isotopic distributions have been reported in previous work [3].

Experimental: EK1-6-3 is a rectangular CAI ~400 × 500 μm in size, mainly consisting of melilite (Ak_{20}, 80 × 70 μm), euhedral anorthite (An_{99}, 100 × 120 μm) and euhedral fassaites (200 × 100 μm). Al-Mg isotopic measurements were made with the JSC NanoSIMS 50L. A focused O^- ion beam was rastered over 5 × 5 μm. $^{24}Mg^+$, $^{25}Mg^+$, $^{26}Mg^+$, and $^{27}Al^+$ were measured in peak-jumping mode with an electron multiplier (EM) at a mass resolving power of ~9000 that is sufficient to resolve Mg hydride interferences at mass 25 and 26. The integration time for each measurement was set depending on Mg and Al contents of the mineral phase. Data were corrected for EM dead time and QSA effect [4]. The instrumental mass fractionation and Al/Mg sensitivity factors were calibrated by terrestrial hibonite, labradorite and melilite glass standards.

Results and Discussions: We found clear evidence for extinct ^{26}Al in fassaite, melilite and anorthite in EK1-6-3. Melilite and fassaite had ^{26}Mg excesses corresponding to $(^{26}Al/^{27}Al)_0 = (5.8 \pm 0.8)\ (2\delta) \times 10^{-5}$, equal the canonical value within error. We also observed two distinct resolvable isochrons in the anorthite crystal having high $^{27}Al/^{24}Mg$ ratio >800; $(^{26}Al/^{27}Al)_0 = (1.9 \pm 0.2) \times 10^{-5}$ for core and $(3.3 \pm 2.2) \times 10^{-6}$ for rim. These might be three different well-behaved isochrons in EK1-6-3. In a chronological interpretation, assuming a homogeneous distribution of ^{26}Al in the early solar system, the Al-Mg data within and/or among mineral phases reflect difference in age. The difference in $(^{26}Al/^{27}Al)_0$ inferred from two separate isochrons of melilite and anorthite implies a relative time interval of ~1–3 Ma. The $(^{26}Al/^{27}Al)_0$ variation found in anorthite crystal is probably a trend from core to rim. Because Mg diffusivity in anorthite is 10 times higher than that in melilite [5, 6], the original ^{26}Mg distributions in the anorthite crystal may have been partially homogenized during its crystallization or subsequent parent body processes. The Mg isotopic compositions of this inclusion will be investigated by isotopic imaging, and will potentially resolve whether the Mg isotopic heterogeneity reflects 1–3 Ma time intervals or has resulted from subsequent alteration processes.

References: [1] MacPherson G. J. et al. 1995. *Meteoritics* 30:365–377. [2] Ito M. et al. 2006. *Meteoritics & Planetary Science* 41:1871–1882. [3] Ito M. and Messenger S. 2007. Abstract #1794. 38th LPSC. [4] Slodzian G. et al. 2004. *Applied Surface Science* 231/232:874–877. [5] LaTourrette T. and Hutcheon I. D. 1999. Abstract #2003. 30th LPSC. [6] Ito M. et al. 2001. Abstract #1518. 32nd LPSC.

5279

CRYSTALLIZATION SEQUENCE OF THE 7R-19-1 TYPE A CAI DETERMINED BY ^{26}Al-^{26}Mg DATING

S. Itoh, K. Makide, and H. Yurimoto. Department of Nat. Hist. Sci., Hokudai, Japan.

Introduction: Compact type A CAIs are believed to be due primarily to be crystallized from a Ca-Al-rich melt in the solar nebula [1]. The crystallization sequence determined by experiment from CAI liquid [2] is the order of spinel, melilite, fassaite, and anorthite. On the other hands spinel and fassaite are normally enriched in ^{16}O, but melilite and anorthite are depleted in ^{16}O [3]. To explain the heterogeneous oxygen isotopic distribution among the minerals, isotopic exchange between ^{16}O-rich CAI liquid and ^{16}O-poor gas occurring in a single crystallization sequence during cooling stage has been proposed [3]. However, it cannot be applicable for the CAI crystallization because crystallization of ^{16}O-poor melilite precedes that of ^{16}O-rich fassaite; that is, fassaite must be also depleted in ^{16}O. Recently, the following crystallization sequence has been proposed by the results of O isotopic petrography in type A 7R19-1 (a) CAI from Allende CV3 chondrite with the evidence of co-existence among ^{16}O-rich and ^{16}O-poor melilite crystals [4, 5]. Initially, this CAI crystallized from ^{16}O-rich CAI liquid, which the crystallization sequence of the CAI minerals is the order of spinel, melilite, and fassaite. Secondly, this CAI experienced partial melting in ^{16}O-poor gas. Following O isotopic exchange reaction between ^{16}O-rich liquid and ^{16}O-poor gas, melilite and fassaite recrystallized from the ^{16}O-poor liquid. However, such O isotopic petrography has not been evaluated by chronology. In this study, we report a high-precision Al-Mg isotopic study of 7R19-1 (a) CAI to evaluate the chronological sequence of crystallization and crystal growth of each phase having ^{16}O-rich and ^{16}O-poor compositions using ^{26}Al-^{26}Mg dating.

Results: Al-Mg isotopic analysis was performed by the Cameca IMS 1270 SIMS instrument using four faraday cups of the multi-collection system. The constituent CAI minerals in 7R-19-1 (a) type A CAI considering O isotopic compositions are divided into ^{16}O-rich spinel, ^{16}O-rich melilite, ^{16}O-rich fassaite, ^{16}O-poor melilite, and ^{16}O-poor fassaite. All of these minerals in a CAI were measured Al-Mg isotope system. The ^{16}O-rich minerals seem to be plotted to the straight line in the Al-Mg isotope diagram. The ^{16}O-poor minerals also seem to be plotted to the other straight line. We calculate an initial ^{26}Al/^{27}Al ratio as: ^{16}O-rich spinel, fassaite and melilite; $(6.44 \pm 0.27) \times 10^{-5}$ (2σ), and that of ^{16}O-poor melilite and fassaite; $(4.96 \pm 0.02) \times 10^{-5}$ (2σ) (forced through origin). Al-Mg isotopic distribution in each phase of 7R-19-1 CAI indicates that the chronological sequence of crystallization is consistent with that of O isotopic petrography [4, 5].

References: [1] Simon et al. 1999. *Geochimica et Cosmochimica Acta* 63:1233–1248. [2] Stolper. 1982. *Geochimica et Cosmochimica Acta* 46: 2159–2180. [3] Clayton. 1993. *Annual Review of Earth and Planetary Science* 21:115–149. [4] Yurimoto et al. 1998. *Science* 182:1874–1877. [5] Ito et al. 2004. *Geochimica et Cosmochimica Acta* 68:2905–2923.

5164

ISHEYEVO: NITROGEN AND CARBON ISOTOPIC COMPOSITIONS OF THE MAGNETIC AND NON-MAGNETIC FRACTIONS

M. A. Ivanova[1], A. B. Verchovsky[2], and I. A. Franchi[2]. [1]Vernadsky Institute of Geochemistry, Kosygin St. 19, Moscow 119991, Russia. E-mail: venus2@online.ru. [2]PSRI Open University, Milton Keynes, MK7 6AA, UK.

Introduction: Isheyevo is a CH/CBb-like chondrite contains the metal-rich and metal-poor lithologies consisting of FeNi metal, chondrules, CAIs and heavily hydrated matrix lumps [1]. N isotopic composition of the whole-rock sample of Isheyevo is highly enriched in ^{15}N [1]. We separated the magnetic and nonmagnetic fractions from Isheyevo and have analyzed C and N isotopic compositions in them to compare the results with the bulk N and C isotopic compositions in order to understand the origin of the heavy N carrier.

Results: The magnetic fraction is very similar to the bulk sample in terms of both N release pattern and isotope profile, and contains a similar concentration of N (113 ppm) with a comparable δ^{15}N value (1056‰). The non-magnetic fraction, largely free of Fe,Ni metal, contains more N (189 ppm) than the whole-rock or magnetic fraction. However, almost all of this N is liberated at low temperatures (<600 °C) and is associated with a large C peak and has a much lower bulk ^{15}N value (214‰). This component is clearly associated with the silicate portion, possibly the hydrated lithic fragments, although this would suggest that they are particularly C-rich, as the non-magnetic fraction contains 1.1 wt% C. The same component is apparent, at reduced levels, in the whole-rock and magnetic fraction. In all the fractions analyzed the heavy N is essentially decoupled from the C release. The vast bulk of the C is released at low temperatures. At high temperatures there is no evidence for a significant C release associated with the large release of isotopically heavy N, although the C isotope signature does peak around 1000 °C in the whole-rock and magnetic fractions with δ^{13}C ~7‰.

Discussion: Isheyevo appears to contain a very similar, or possibly the same carrier of the heavy N as found in Bencubbin [2]. The nature of the heavy N carrier in Isheyevo has not been established, although in Bencubbin it has been argued that the main N component resides in carbides or taenite associated with Cr-rich sulfides [3] as identified with SIMS. However, the stepped combustion data argue against such phases being the major hosts. The very low C/N ratio observed in acid residues strongly argues against carbide being the host phase while the fact that essentially all the nitrogen is retained in a 6M HCl residue [2] argues against taenite as a possible host. Sugiura et al. (2000) argued that N in Bencubbin had been remobilized during the shock melting event, which may also account for the lack of any associated primordial gases in the acid residues [4]. Isheyevo has also experienced a high level of shock metamorphism (S4). Therefore this explanation seems to be suitable for Isheyevo as well, given the strong similarity in the N isotopic systematics and release profile with Bencubbin.

References: [1] Ivanova M. A. et al. 2006. Abstract #1100. 37th Lunar and Planetary Science Conference. [2] Franchi I. A. et al. 1986. *Meteoritics & Planetary Science* 36:401–418. [3] Sugiura N. et al. 2000. *Meteoritics & Planetary Science* 36:401–418. [4] Rooke G. P. et al. 1998. Abstract #1744. 29th Lunar and Planetary Science Conference.

5310

NANOSIMS AND RIMS ISOTOPIC STUDIES OF HIGH-DENSITY GRAPHITE GRAINS FROM ORGUEIL

M. Jadhav[1], M. R. Savina[2], K. B. Knight[3], J. Levine[3], M. J. Pellin[2], S. Amari[1], K. K. Marhas[1], E. Zinner[1], T. Maruoka[1*], and R. Gallino[4]. [1]Laboratory for Space Sciences and the Physics Department, Washington University in St. Louis, One Brookings Dr., St. Louis, MO 63130, USA. E-mail: manavijadhav@wustl.edu. [2]Materials Science Division, Argonne National Laboratory, Argonne, IL 60439, USA. [3]Chicago Center for Cosmochemistry, University of Chicago, Chicago, IL 60637, USA. [4]Dipartimento di Fisica Generale, Università di Torino, Via P. Giuria 1, I-10125 Torino, Italy. [*]Present address: Graduate School of Life and Environmental Sciences, University of Tsukuba, Ibaraki 305-8572, Japan.

Introduction: We report on continuing correlated isotopic studies of light and heavy elements of high-density graphite grains from Orgueil. Previous NanoSIMS isotopic analyses of C, N, O, and Si [1, 2] of high-density graphite grains have suggested that these grains originate from low-metallicity, asymptotic giant branch (AGB) stars. Recently [3], we extended NanoSIMS isotopic analyses to Al-Mg, K, Ca, and Ti, and have also undertaken resonant ionization mass spectrometry (RIMS) analyses of Mo and Ba with CHARISMA at Argonne National Laboratory.

Experimental: Large (average size, ~5 μm) high-density graphite grains from the ORG1f(ρ ~ 2.02–2.04 g cm^{-3}) fraction were picked with a micromanipulator and transferred to a gold-foil mount. C, N, O, and Si isotopic analyses in the NanoSIMS were carried out with negative secondary ions, those of Al-Mg, K, Ca, and Ti with positive secondary ions [3]. We made sure that enough grain material was preserved to allow measurements of heavy-element isotopes with RIMS. The RIMS method has been discussed in detail elsewhere [4]. This technique was modified for our analyses in that the two elements measured, Mo and Ba, were resonantly ionized simultaneously, thus increasing efficiency.

Results and Discussion: A subset of the 44 high-density graphite grains analyzed in the NanoSIMS shows extremely interesting isotopic compositions. The presence of ^{44}Ti in 4 grains indicates an origin in type II supernovae (SNe). Fifteen grains exhibit extremely large Ca and Ti anomalies. The ^{42,43,44}Ca and ^{46,47,49,50}Ti excesses in several of the grains are much higher than predicted for AGB star envelopes and approach those predicted for O-rich supernova zones and pure He-shell material in AGB stars. These measurements lead us to consider type II SNe as a source for some high-density graphite grains. Three of the grains that seem to contain pure He-shell material have ^{12}C/^{13}C < 20. Born-again AGB stars, such as Sakurai's object (V4334Sgr), exhibit enhanced s-process elemental abundances and very low ^{12}C/^{13}C ratios (~4). We consider such stellar objects another possible source for high-density graphite grains. Thus, contrary to our previous conclusions, high-density graphite grains seem to have multiple stellar sources. Two out of the 5 grains measured by the RIMS technique, show depletions in ^{92,94,95,97,98,100}Mo (normalized to s-only ^{96}Mo) by several hundred per mil, indicating an s-process signature. The ^{134}Ba signal is contaminated by a large tail from the ^{133}Cs signal making the ^{134}Ba abundances unreliable. Cs was implanted in the grains during the NanoSIMS measurements. We expect to obtain Mo and Ba data on additional grains in the near future, and to report them at the meeting. These analyses will provide better constraints on the stellar sources of high-density graphite grains.

References: [1] Jadhav M. et al. 2006. *New Astronomy Reviews* 50: 591–595. [2] Zinner E. et al. 2006. Proceedings of Science (Nuclei in the Cosmos IX) 019. [3] Jadhav M. et al. 2007. Abstract # 2256. 38th Lunar and Planetary Science Conference. [4] Savina M. R. et al. 2003. *Geochimica et Cosmochimica Acta* 67:3215–3225.

5106

IMPLICATIONS OF SULFIDE DISTRIBUTIONS IN THE MAIN GROUP PALLASITES

D. Johnson[1], R. Hutchison[2], and M. M. Grady[1, 2]. [1]Open University, Walton Hall, Milton Keynes, MK6AA, UK. E-mail: D.Johnson@open.ac.uk. [2]Natural History Museum, London, UK.

Introduction: Main group pallasites are generally considered to have formed by intrusion of an evolved liquid metal into olivine. It has been suggested that an 80% crystallized melt from the core of the IIIAB irons would produce metal compositions of those found in the main group pallasites [1]. High FeS contents should be present according to this model [2, 3]. Thus far only two FeS rich pallasites are known, Phillips County and Hambleton [4]. Here we give an indication of the distribution of FeS throughout the parent body particularly with respect to olivine rich areas and chromite. We also give a discussion of these data with respect to Hambleton formation and relevance to other angular olivine main group pallasites.

Discussion: Slabs of Hambleton were examined using optical microscopy to characterize olivine, sulfide, metal and chromite distributions. Sections of olivine rich materials spanning 15 cm exist intersected almost exclusively by FeS. Unfortunately, these areas are situated towards the weathered edges of the sample hence making their study particularly difficult. It was noted that the majority of chromites were found within these areas or along the boundary between olivine rich and metal regions. A small number of chromite grains were extracted and underwent microprobe analysis. These results indicated two processes were strongly involved in their crystallization. Chromite crystals from within the olivine regions generally appeared to be in a well defined form, whereas those within the metal or in metal-olivine interface appeared to have been torn apart, probably by a crushing event. This is also apparent by the olivine chips present within the FeS veinlets. These typically are also present along the metal-olivine interface. It is suggested that Hambleton is direct evidence of a crushing event or events on the main group pallasite parent body. A possible model includes a parent body with sulfide segregated within an olivine mantle which underwent intrusion by a metal-olivine mush. Subsequent events took place heating and crushing the mantle olivine which then expelled a liquid FeS partially out of the olivine regions and into the surrounding metal-olivine areas. Small fragments of olivine are contained within the FeS, which appear to be broken from the large crystals due to the forceful extrusion of FeS.

Conclusion: Main group pallasites have a very varied history. Some appear to be rich in FeS particularly in the vicinity to large areas of olivine. It may be that a sub-group is required with in the main group classification scheme for these pallasites. The formation history is complex, but even with sample variation considered the different formation textures can easily be observed, it maybe that oxygen isotope data alone is insufficient for the classification grouping of such samples.

References: [1] Scott E. R. D. 1977. *Geochimica et Cosmochimica Acta* 41. [2] Ulff-Møller F. 1998. *Meteoritics & Planetary Science* 33:207–220. [3] Ulff-Møller F. 1998. *Meteoritics & Planetary Science* 33:221–227. [4] Johnson et al. 2006. *Meteoritics & Planetary Science* 41:A89.

5311

LUNAR METEORITE DHOFAR 961, MAFIC IMPACT-MELT BRECCIA: PETROGRAPHIC COMPONENTS AND POSSIBLE PROVENANCE

B. L. Jolliff, R. A. Zeigler, R. L. Korotev, and P. K. Carpenter. Washington University, Saint Louis, MO 63130, USA. E-mail: blj@wustl.edu.

In a companion abstract [1], a case is made on the basis of geochemistry for possible origin of the Dhofar 961 lunar meteorite in the South Pole–Aitken (SPA) basin. The bulk composition is appropriately mafic and Th-rich for this region of the Moon, and the lithophile trace-element signature differs from that of well-known materials from the Moon's Procellarum KREEP Terrane [2]. Other relatively mafic, brecciated lunar meteorites have been shown to be mixtures of highlands (nonmare) materials and mare basalt [3]. In this abstract, we describe clasts in this complex meteorite to determine 1) the composition of impact-melt and other lithic clast components, 2) if a mare origin for mafic components is indicated, and 3) if the components could reasonably come from the compositionally distinctive SPA basin.

In our polished section of Dhofar 961, large (up to centimeter-size) lithic clasts of fine-grained, subophitic impact-melt breccia (IMB) containing olivine phenocrysts dominate the section (~60 vol%). Other texturally distinctive lithic clasts account for ~8%, and smaller mineral and lithic clasts welded together by minute amounts of glass comprise the remaining ~32%. Thin (5–20 μm) impact-glass veins occur along contacts between breccia matrix and the large lithic clasts. Small lithic clasts in the matrix are subrounded. The matrix contains several subrounded lithic clasts of basaltic-textured lithologies and several of a feldspathic granulite lithology. We have not observed KREEP-rich or granitic components in this section (cf. [4]). FeNi-metal is common and several large grains (~5.5% Ni; ~300 μm) occur in the mafic melt breccia.

The composition of the IMB clasts average ~12.5% FeO and 17% Al_2O_3, with very low TiO_2 (0.5%). Although a few small lithic clasts in the section appear to be basaltic (aluminous and very low Ti), it is not clear that the IMBs have a basaltic precursor component; if they do, it is unlike the main Apollo and Luna basalt groups. Values of Mg′ among lithic clasts range from ~48 to 77, but the prominent IMB clasts have Mg′ of 56–64. Dhofar 961 is dominantly, but not exclusively, composed of ferroan components. Exceptions are feldspathic magnesian granulites.

Compositionally, SPA basin is a potential source for Dhofar 961. The mafic components and ferroan composition compare well with Lunar Prospector gamma-ray data for the interior of SPA basin [5, 6]. Although a noritic mafic mineralogy was advocated by [7], mineral models of [8] indicate abundant high-Ca pyroxene and minor olivine. Pigeonite is common in Dhofar 961 and could be an important part of the solution to the mafic mineralogy of SPA basin, as also concluded by [8].

References: [1] Korotev R. et al. 2007. This issue. [2] Jolliff B. et al. 2000. *Journal of Geophysical Research* 105:4197–4216. [3] Korotev R. 2005. *Chemie der Erde* 65:297–346. [4] The Meteoritical Bulletin No. 89. *Meteoritics & Planetary Science* 40:A201–A263. [5] Jolliff B. and Gillis J. 2005. Abstract #5330. *Meteoritics & Planetary Science* 40:A77. [6] Prettyman T. et al. 2006. *Journal of Geophysical Research* 111:E002656. [7] Pieters C. et al. 2001. *Journal of Geophysical Research* 106:28,001–28,022. [8] Lucey P. et al. 2005. Abstract #1520. 36th Lunar and Planetary Science Conference.

5194

THE SHERGOTTITES ARE YOUNG

J. H. Jones. KR, NASA/JSC, Houston, TX 77058, USA. E-mail: john.h.jones@nasa.gov.

Introduction: Recently, Bouvier et al. (2006), interpreting their Pb isotopic data, have inferred that the shergottite suite of the SNC (Martian) meteorites have ancient ages of ~4–4.5 b.y. But conventional wisdom has it that the shergottites are much younger (~500–150 m.y.) Are the shergottites young or are they ancient rocks whose ages have been reset by metamorphism or alteration?

Are the Shergottites Metamorphic Rocks? No. They are igneous rocks whose constituent minerals retain their igneous zoning. Even olivine, which equilibrates quickly, may be zoned.

Have the Shergottite Ages Been Reset by Shock? No. Jones (1986) gave arguments against shock equilibration in excruciating detail. A synopsis of this issue can be given by consideration of the shergottite EET 79001: i) EET 79001 has a young Sm-Nd age but the olivines and pyroxenes in EET retain igneous zoning. If chemical equilibration of divalent ions was not achieved during shock (or metamorphism), it is nearly impossible to have achieved isotopic equilibration of trivalent ions (i.e., REE). Isotopic equilibration is achieved by diffusion, and trivalent ions diffuse more slowly in mafic silicates than divalent ions do. This is because local charge balance must be maintained. ii) EET 79001 contains two lithologies (A and B) with very different compositions. These lithologies define two distinct Rb-Sr isochrons. The first analyses of impact-melt glasses produced from these two lithologies plotted on their respective isochrons. However, these very different glasses were extracted from a single lithology—lithology A. Therefore, the B impact melts did not have time to isotopically equilibrate with their A surroundings.

Have Shergottite Ages Been Reset by Low-Temperature Alteration? No. Bouvier et al. postulate that the Rb-Sr and Sm-Nd systems have been disturbed because of low-temperature alteration/exchange. However, there is no evidence for this. Using Shergotty and Zagami as examples: i) low-T alteration products are rare to nonexistent (McCoy et al. 1992); ii) if exchange occurred with a hydrous fluid, it did not affect oxygen-oxygen isotopic equilibration temperatures for several mineral pairs in Shergotty yield an equilibration temperature of 1100 ± 100 °C (Clayton and Mayeda 1986) (cf. the solidus temperature for Zagami is 1000–1050 °C [McCoy and Lofgren 1999]); iii) acid-leached residues from Zagami define a Sm-Nd isochron of 157 m.y. (Borg et al. 2005).

This latter observation goes directly to the heart of the issue. The whole-rocks and mineral separates are chemically (i.e., normally) and isotopically zoned. They were cleansed of possibly altered impurities such as phosphates both by meticulous hand-picking and subsequent acid leaching. For Bouvier et al. to be correct, this isochron should have yielded a very old age, and it did not.

Have Young Shergottite Ages Been Confirmed by Multiple Chronometer Systems? Yes. Recent work on Zagami yielded Rb-Sr, Sm-Nd, and ^{238}U-^{206}Pb ages of 166 ± 16, 166 ± 12, and 156 ± 18 m.y., respectively (Borg et al. 2005). Although it is desirable to have multiple chronometers applied to the same aliquot of sample, the Borg et al. results are in good agreement with previous workers, who used other samples of Zagami.

These accumulated observations are inconsistent with an ancient age for the shergottites.

5213

A METAMORPHOSED IGNEOUS INCLUSION IN THE ORO GRANDE H5 ORDINARY CHONDRITE

Rhian H. Jones. Department of Earth and Planetary Sciences, University of New Mexico, Albuquerque, NM 87131, USA. E-mail: rjones@unm.edu.

Introduction: Robert Hutchison was a persistent proponent of the idea that chondrules are the result of disruption of partially molten planetesimals [1]. He argued that the existence of young igneous inclusions in ordinary chondrites (e.g., [2]) supports this model. A lithic inclusion in the Oro Grande H5 chondrite was originally described by [3], who interpreted it as an impact melt clast. I have revisited this inclusion to see what insights it offers into the discussion of chondrule formation by planetary melting.

Petrographic Description: [3] described the 5 mm Oro Grande inclusion as a microcrystalline mixture of olivine and plagioclase, with minor orthopyroxene, clinopyroxene and metal. This description belies an extremely complex texture. The inclusion is indeed dominated by a fine-grained mixture of barred olivine and plagioclase, with olivine bar widths <10 μm. However, throughout the inclusion there are also numerous objects (~50 vol%) that appear to be relicts of euhedral phenocrysts, 100 to 500 μm in length. These relict phenocrysts have complex internal textures. Some are dominated by diopside, with minor low-Ca pyroxene and plagioclase. Some of these regions have ~20 μm wide rims of apatite. Other relict phenocrysts consist of fine-grained intergrowths of low-Ca pyroxene, diopside, olivine, plagioclase, pigeonite, and minor chromite. These regions have thin rims of diopside overgrown with plagioclase. Throughout the inclusion, iron metal and troilite are minor phases, and chromite is present as finely dispersed sub-micrometer crystals. Compositions of all phases are essentially identical to those in the host chondrite [3], and typical of equilibrated ordinary chondrites [4]: olivine is Fa_{18}; low-Ca pyroxene is $En_{82}Fs_{17}Wo_1$; diopside is $En_{48}Fs_6Wo_{46}$; feldspar is $An_{12}Ab_{82}Or_6$; apatite has 0.75 wt% F and 5.1 wt% Cl. Our SIMS analyses of plagioclase show comparable REE abundance patterns in inclusion and host chondrite.

Origin of the Inclusion: Fodor et al. [3] concluded that the lithic inclusion is an impact melt formed from the silicate portion of equilibrated H5 material. However, the relict phenocryst texture rules out such an origin. The inclusion appears to have originated as a porphyritic igneous rock. The original rock was likely subjected to a significant shock event, during which pyroxene phenocrysts, possibly diopside and pigeonite, broke down into multi-phase assemblages. An olivine/plagioclase impact melt was generated, which quenched into a barred olivine texture. Essentially complete chemical equilibration of the inclusion with the Oro Grande host chondrite indicates that formation of the original porphyry, as well as the impact event, occurred prior to parent body metamorphism. Although the groundmass texture of the inclusion is comparable to barred olivine chondrules, no features like the relict phenocrysts are ever observed in chondrules. Hence, one cannot argue that this inclusion is simply a large version of a chondrule. It extends the known range of igneous rock types that were present in the early stages of accretion.

References: [1] Hutchison R. et al. 2005. *Chondrites and the protoplanetary disk*. APS Conference Series 341. pp. 933–950. [2] Hutchison R. et al. 1988. *Earth and Planetary Science Letters* 90:105–118 [3] Fodor R. V. et al. 1972. *Meteoritics* 7:495–507. [4] Brearley A. J. and Jones R. H. 1998. *Planetary materials*, Reviews in Mineralogy, vol. 36, ch. 3.

5256

MINERALOGY OF TERMINAL PARTICLES AND OTHER LARGE MINERAL FRAGMENTS OBTAINED FROM STARDUST TRACKS

D. J. Joswiak, D. E. Brownlee, and G. Matrajt. Department of Astronomy, University of Washington, Seattle, Washington, USA. E-mail: joswiak@astro.washington.edu.

Introduction: We examined the mineralogy, textures, and phase relationships of terminal particles (TP) and other large mineral fragments from 16 Stardust (SD) tracks. Within individual tracks, all fragments are believed to have been attached to the main track TP prior to impact. Here we provide a summary of the important minerals observed focusing on only those that are likely to have originated in comet Wild-2 and were not severely modified during capture. It is hoped that these mineralogical data can provide a useful database for future researchers who can use the prepared samples for complementary studies.

Methods: Each track was keystoned [1], followed by flattening and embedding in acrylic resin [2]. Microtomed sections of each large mineral fragment were then examined with a Tecnai F20 STEM using standard TEM methods including BF and DF imaging, electron diffraction (ED), HRTEM, EDX, and occasionally EELS. Some of the potted butts were also examined with backscattered electrons using a JEOL 7000 FESEM.

Results: The individual particles observed in the 16 tracks showed highly variable mineralogy ranging from monomineralic grains to complete Wild-2 "rocks" which were composed of various silicates, oxides, sulfides, FeNi metal, glass, and a number of unusual phases including the amphibole richterite, roedderite, and probable majorite. One track (Track 25) contains CAI minerals, including highly refractory sub-10 nm osbornite inclusions, while a number of other tracks contain mineralogy analogous to some chondrules. Some of these samples were also discussed during the preliminary examination period [3].

Four tracks are dominated by large monomineralic grains including clinoenstatite (Track 20), pentlandite (Track 59), a 2 μm kamacite grain (Track 38) and two discrete widely separated particles in Track 10, one composed of Fo_{99} and the other composed of pyrrhotite.

Most of the SD particles are composed of multiple phases with pyroxene the most common mineral followed by olivine. Enstatite was observed in Tracks 17, 20, 27, 41, 56, 57, and 80 while high-Ca pyroxenes were observed in Tracks 17, 25, 27, 58, and 77. Ferrosilite may be present in Track 26. Olivines—ranging from Fo_2 to Fo_{99}—varied from minor to modally dominant and were found in 8 tracks (10, 17, 22, 26, 57, 58, 71, and 77).

Large pyrrhotite fragments were present in Tracks 10, 57, and 77 and appear to have been associated with olivines or pyroxenes while resident in Wild-2. A >1 μm FeNi grain with a schreibersite inclusion and associated with Fo_{60} was present in Track 77. Six tracks contain Na+Cr-bearing silicates some of which have ED patterns consistent with high Ca-pyroxenes.

Conclusions: The large variety of minerals observed in SD fragments clearly show that comet Wild-2 is composed of a rich and diverse assemblage of "rocks" many of which have mineralogical similarities to known meteoritic materials including CAIs and chondrules.

References: [1] Westphal A. J. et al. 2004. *Meteoritics & Planetary Science* 39:1375–1386. [2] Matrajt G. and Brownlee D. E. 2006. *Meteoritics & Planetary Science* 41:1715–1720. [3] Zolensky M. E. et al. 2006. *Science* 314:1735–1739.

5223

THE CLAST INVENTORY OF KREEPY LUNAR METEORITE NORTHWEST AFRICA 4472

K. H. Joy[1, 2], V. A. Fernandes[3, 4], R. Burgess[4], I. A. Crawford[1], A. J. Irving[5], and A. T. Kearsley[2]. [1]UCL/Birkbeck Research School of Earth Sciences, UK. E-mail: K.Joy@ucl.ac.uk. [2]IARC, Department of Mineralogy, Natural History Museum, London, UK. [3]Univ. Coimbra, Portugal. [4]Univ. Manchester, UK. [5]University of Washington, Seattle, WA, USA.

Introduction: NWA 4472 is a 64.6 gram lunar KREEP-rich breccia that was found in Algeria in 2006 [1]. It is reportedly paired with the larger (188 g) NWA 4485 stone, on the basis of bulk composition and petrography [1, 2]. Bulk chemistry investigations [2, 3] have concluded that the breccia is rich in incompatible trace elements (ITE) and is compositionally similar to KREEP lithologies collected by Apollo 14 (e.g., [4, 5]). As it is so enriched in KREEP, it is likely to have been launched from the lunar near-side, from a location within the Th-rich [6] (proxy for ITE) Procellarum KREEP Terrane [7].

We present here an initial investigation of a large (31.6 × 24.3 × 4 mm) slab of the breccia. Backscatter electron and elemental mapping have been performed to assess the heterogeneity of the meteorite. From this early analysis, we have identified specific polymineralic and monomineralic clasts that we intend to investigate using a variety of analytical and dating techniques.

Sample Description: NWA 4472 is composed of a wide range (<7 mm) of pale cream, gray, brown, black, and orange clasts consolidated in a dark matrix. The sample is cross-cut with fractures, most of which have been infilled with terrestrially deposited calcium carbonate and have a rusty-red appearance in the hand specimen. Small glass beads (<150 μm) are present within the matrix, suggesting that the sample was fused in a regolith environment. Therefore, the stone is classified as a regolith breccia.

Clast Inventory: Clast source provenance appears to be diverse. There is a small mare basalt lithic component (<4 mm, <10% of the sample), with a range of textures from plumose to sub-ophitic (e.g., basalt 1 pyx: $Fs_{18–59}$ $Wo_{11–31}$ $En_{16–63}$, basalt 2 olivine: $Fo_{46–50}$, pyx: $Fs_{34–46}$ $Wo_{10–30}$ $En_{34–58}$). Most basaltic clasts appear to have been derived from a low-Ti to VLT source region, as they have a relatively low (although variable) abundance of ilmenite. Shock metamorphosed granulized basaltic clasts are quite common, suggesting that included lithic material has experienced a range of thermal metamorphic conditions.

As noted by [2] granophyric KREEP-associated silica-K-feldspar intergrowth clasts occur throughout the NWA 4472 groundmass (<5%). They are often affiliated with small Zr-rich and phosphate (apatite) accessory phases. Additional lithic clast components include a diverse range of impact melt and fragmental breccias, and feldspathic polymineralic lithic clasts, suggesting a minor highland FAN component.

Ongoing and Future Research: We are currently conducting mineral chemistry investigations from the wide range of lithic components in NWA 4472 that will be presented at the conference. Chronologic work will follow.

References: [1] Connolly et al. 2007. The Meteoritical Bulletin, No. 91. *Meteoritics & Planetary Science* 42:A413–A466. [2] Kuehner et al. 2007. Abstract #1516. 38th LPSC. [3] Korotev and Zeigler 2007. Abstract #1340. 38th LPSC. [4] Jolliff et al. 1991. Proceedings, 21st LPSC. pp. 193–219. [5] Warren P. 1989. LPI Tech. Report 89-03. pp. 149–153. [6] Lawrence et al. 2006. *Geophysical Research Letters* 34, Issue 3. [7] Jolliff et al. 2000. *Journal of Geophysical Research* 105:4197–4216.

5315

STUDIES OF ^{14}C AND ^{10}Be IN IRON METEORITES AND ^{129}I IN CHONDRITES

A. J. T. Jull[1], D. Biddulph[1], D. Zahn[1], L. Cheng[1], G. S. Burr[1], and L. McHargue[1, 2]. [1]NSF Arizona AMS Facility, The University of Arizona, Tucson, AZ 85721, USA. E-mail: jull@email.arizona.edu. [2]Scottish Universities Environmental Research Centre, East Kilbride, G75 0QF, UK.

Introduction: The radionuclides produced by galactic cosmic radiation are useful for understanding the exposure age [1] and terrestrial residence age [2] of meteorites. In the past, some ^{14}C measurements of iron meteorites, both falls and finds, have been made [3].

Experimental: We have extracted ^{14}C and ^{10}Be using previously published methods at the Arizona laboratory [4]. We have also developed ^{129}I extractions from meteorites.

Terrestrial Ages: We have studied the ^{14}C and in some cases ^{10}Be composition of a series of iron meteorites of different expected terrestrial ages. Initial ^{14}C results for both Odessa and Canyon Diablo give 1.92 ± 0.02 and 0.60 ± 0.03 dpm/kg, respectively. The terrestrial ages derived from reasonable assumptions about the production rates give much more recent than estimated ages of the craters of >50 ka [4, 5]. Schnabel et al. [6] also estimated the terrestrial age of Canyon Diablo between 44 ± 32 and 154 ± 28 ka. Our estimate of the terrestrial age of Canyon Diablo from ^{14}C is about 17 ± 1 ka. However, this may also indicate that our understanding of ^{14}C production in iron meteorites needs further study. We hope to be able to present more detailed information at the conference.

^{129}I: ^{129}I has been a little-studied nuclide in extraterrestrial material [7, 8]. It is produced mainly from neutron reactions on Te, mainly $^{128}Te(n,\gamma)$ ^{129}I and $^{130}Te(n,2n)$ ^{129}I spallation of Ba and adjacent isotopes. We have extracted ^{129}I from several meteorites collected from the Omani desert, including Shişr 033. Results appear to be consistent with earlier estimates [7, 8].

Summary: The use of ^{14}C and $^{14}C/^{10}Be$ for terrestrial-age measurements can be extended to iron meteorites. Initial studies of ^{129}I in chondrites indicates that this radionuclide may be useful for estimates of exposure ages, when coupled with accurate measurements of Te. These measurements also raise the possibility for live ^{129}I-^{129}Xe dating [9] of irons.

References: [1] Jull A. J. T. 2006. Terrestrial ages of meteorites. In *Meteorites and the early solar system II,* edited by Lauretta D. and McSween H. Tucson: The University of Arizona Press. pp. 889–905. [2] Eugster O. et al. 2006. Irradiation records, cosmic-ray exposure ages and transfer times of meteorites. In *Meteorites and the early solar system II,* edited by Lauretta D. and McSween H. Tucson: The University of Arizona Press. pp. 829–851. [3] Goel P. S. and Kohman T. P. 1962. *Science* 136:875–876. [4] Holliday V. T. et al. *Geology* 33:945–048. [5] Nishiizumi K. et al. *Geochimica et Cosmochimica Acta* 55:2699–2703. [6] Schnabel C. et al. 2001. *Meteoritics & Planetary Science* 36. Abstract #5132. [7] Nishiizumi K. et al. 1983 *Meteoritics & Planetary Science* 18:363. [8] Schnabel C. et al. 2004. *Meteoritics & Planetary Science* 39:453–466. [9] Marti K. et al. Abstract. *Meteoritics & Planetary Science* 39:A63.

5299

SIMS RESULTS FOR SOLAR WIND ELEMENTAL ABUNDANCES FROM GENESIS COLLECTORS

A. J. G. Jurewicz[1], D. S. Burnett[2], D. S. Woolum[3], K. D. McKeegan[4], Y. Guan[2], and R. Hervig[5]. [1]Center for Meteorite Studies, ASU, Tempe, AZ 85287, USA. [2]GPS, Caltech, Pasadena, CA, USA. [3]Physics, California State University Fullerton, CA, USA. [4]ESS UCLA, Los Angeles, CA, USA. [5]SESE, ASU, Tempe, AZ, USA.

Introduction: Solar wind elemental abundances are a major Genesis science objective. Spacecraft studies have shown that elements with first ionization potential (FIP) > 9 eV are fractionated relative to those with lower FIP compared with the solar photosphere; however, among elements with FIP < 9eV (which make up most of the terrestrial planets) there is no evidence of fractionation. A major goal of Genesis is to provide a higher precision test of the lack of fractionation for FIP < 9eV.

Method and Results: Accordingly, bulk solar wind analyses for several elements on a variety of Genesis solar-wind collector types are being made by SIMS using the ASU 6f and UCLA 1270 instruments. Fluences are calculated relative to implant standards; relative sensitivity factors (RSFs) are calculated for each set of analyses.

Figure 1 plots Fe and Mg measured in two collector types versus ACE data [1]. Results for some elemental fluences, such as Fe, appear to be consistent across different collector types and techniques. Conversely, results for Mg differ based on collector type even though the solar-wind analytical profiles are clear and multiple standards were made (implanted) simultaneously.

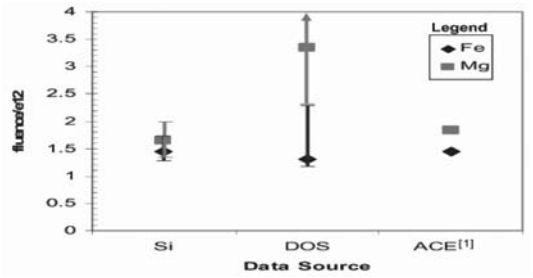

Fig. 1. Average (symbol) and full range (bars) of Genesis solar wind data compared with ACE-derived fluences [1].

We currently have measured fluences for Fe, Mg, Ca, Cr, and Na, but are still investigating possible systematic analytical errors; accordingly, there are no error bars in Fig. 2 below. New standards are currently being generated to see if flight-induced changes (i.e., H-retention; radiation damage) affect the RSFs for the SIMS analyses. In any case, our data show a reasonably close correspondence with photospheric values at this point.

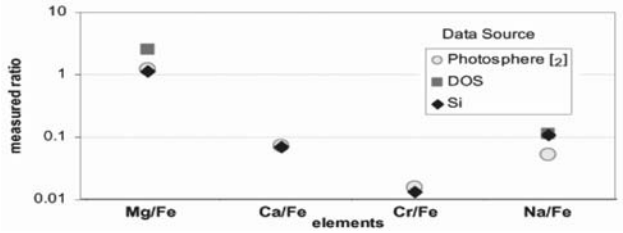

Fig. 2. Comparison of Genesis preliminary measurements from photospheric measurements from [2].

References: [1] Reisenfeld D. et al. ISSI Symposium on the Composition of Matter. Forthcoming. [2] Asplund M. et al. 2004. In *Cosmic abundances as records of stellar evolution and nucleosynthesis,* edited by Bash F. N. and Barnes T. G.

5032

COMPLEX CRATERS ON STARDUST ALUMINUM FOILS: EXPERIMENTAL SIMULATION OF COMET DUST IMPACT BY POROUS AGGREGATE PARTICLES

A. T. Kearsley[1], M. J. Burchell[2], P. J. Wozniakiewicz[1, 3], M. J. Cole[2], G. A. Graham[4], J. Blum[5], and T. Poppe[5]. [1]Natural History Museum, London, SW7 5BD, UK. E-mail: antk@nhm.ac.uk. [2]University of Kent, Canterbury, Kent CT2 7NH, UK. [3]Imperial College of Science, Technology and Medicine, London, SW7 2BP, UK. [4]LLNL, Livermore, CA 94550, USA. [5]Institut für Geophysik und Extraterrestrische Physik, Technische Universität zu Braunschweig, 38106 Braunschweig, Germany.

Introduction: Impact of Wild-2 cometary dust on the aluminum (Al) foils of the Stardust spacecraft created numerous distinctive features [1]. Many are "bowl-shaped" depressions similar to experimental craters from our previous light gas gun shots of mineral grains [2]. However, complex morphology is also common in Stardust impacts, suggesting inhomogeneous internal distribution of mass within impactors [3], like fractal dust aggregates [4, 5]. Our aim has been to recreate complex impact features by shots of novel projectile types, to understand impactor properties that control crater shape, and thence improve interpretation of Wild-2 dust in terms of grain mass and internal structure, especially porosity and density.

Experimental and Analytical Techniques: Buckshot firings onto Al alloy targets were performed at the University of Kent. Porous aggregate projectiles were created by two different methods: 1) from a polydispersive mixture of powdered olivine, Mg orthopyroxene, Ca clinopyroxene, Cr spinel and pyrrhotite, bound by aerosol adhesive droplets; 2) sintered aggregates of 1.5 μm monodispersive silica microspheres [6]. Aggregate particles and impact features were examined by analytical scanning electron microscopy. Stereo-pair images were combined into three dimensional shape models using the Alicona MeX program [7].

Results and Discussion: The shots yielded hundreds of craters. "Bowl-shaped" features of a wide size range were abundant, suggesting impacts by single, dense mineral grains, and implying that many aggregates broke during acceleration and flight. However, large numbers of features were shallow with noncircular outline shape and complex internal structure, many resembling Stardust impacts, albeit of larger size. The mutual interference of depressions in these craters, and in some cases patches of diverse residue composition derived from distinct mineral subgrains, shows clear evidence of synchronous impact by an aggregate, rather than fortuitous crater overlap from discrete particles. The shape is distinct from craters formed by single mineral grains of elongate shape (e.g., acicular needles).

We are now developing mineral aggregates of finer, better-constrained, subgrain sizes, and shall investigate impact of aggregate projectile types on silica aerogel, as well as Al foil.

References: [1] Hörz F. et al. 2006. *Science* 314:1716–1719. [2] Kearsley A. T. et al. 2006. *Meteoritics & Planetary Science* 41:167–180 [3] Kearsley A. T. et al. *Meteoritics & Planetary Science*. Forthcoming. [4] Greenberg J. M. and Gustafson B. Å. S. 1981. *Astronomy & Astrophysics* 93:35–42. [5] Blum J. and Wurm G. 2000. *Icarus* 143.1:138–146. [6] Poppe T. 2003. *Icarus* 164:139–148. [7] Kearsley A. T. et al. 2007. *Meteoritics & Planetary Science* 42:191–210.

5297

COORDINATED CHEMICAL AND ISOTOPIC STUDIES OF IDPs: COMPARISON OF CIRCUMSTELLAR AND SOLAR GEMS GRAINS

L. P. Keller and S. Messenger. Robert M. Walker Laboratory for Space Science, ARES, NASA Johnson Space Center, Houston, TX 7705, USA. E-mail: Lindsay.P.Keller@nasa.gov.

Introduction: Silicate stardust in IDPs and meteorites include forsterite, amorphous silicates, and GEMS grains [1]. Amorphous presolar silicates are much less abundant than expected based on astronomical models [2], possibly destroyed by parent body alteration. A more accurate accounting of presolar silicate mineralogy may be preserved in anhydrous IDPs. Here we present results of coordinated TEM and isotopic analyses of an anhydrous IDP (L2005AL5) that is comprised of crystalline silicates and sulfides, GEMS grains, and equilibrated aggregates embedded in a carbonaceous matrix. Nanometer-scale quantitative compositional maps of all grains in two microtome thin sections were obtained with a JEOL 2500SE. These sections were then subjected to O and N isotopic imaging with the JSC NanoSIMS 50L. Coordinated high-resolution chemical maps and O isotopic compositions were obtained on 11 GEMS grains, 8 crystalline grains, and 6 equilibrated aggregates.

Results: Two GEMS grains had anomalous O isotopic compositions and all of the remaining grains were indistinguishable (±50‰) from solar. The IDP had a bulk $\delta^{15}N$ of +150‰ with hotspots up to +500‰. Grain 1 had a pronounced O isotopic anomaly ($\delta^{17}O = +523 \pm 85‰$; $\delta^{18}O = -100 \pm 37‰$), consistent with this GEMS grain originating from a red giant or AGB star. It is an elongated (0.3 × 0.5 μm) aggregate that is chemically heterogeneous on a 100 nm scale and subgrain element/Si ratios vary by factors of 2 to 3. The bulk composition is sub-solar as is typical for most GEMS grains (Mg/Si = 0.72, Fe/Si = 0.48, S/Si = 0.19, Al/Si = 0.08, Ca/Si = 0.04). The O abundance is stoichiometric, assuming that all Fe is present as metal or sulfide. The grain shows no evidence for zoning or element depletions at the grain rim relative to the core. No relict grains are observed. Grain 2 is a 0.5 μm GEMS grain aggregate of at least 4 morphologically distinct subgrains. It is moderately ^{18}O enriched ($\delta^{18}O = +80 \pm 20‰$), but a sub-region reaches $\delta^{18}O = +145 \pm 30‰$, possibly due to one of the subgrains. The subgrains are compositionally similar but differ in their abundance of metal and sulfide inclusions. The bulk composition is sub-solar except for Mg (Mg/Si = 1.20, Fe/Si = 0.43, S/Si = 0.19, Al/Si = 0.19, Ca/Si = 0.06). No zoning profiles across the aggregate are observed and the O abundance is stoichiometric.

Discussion: The isotopically anomalous GEMS grains bear remarkable resemblance to isotopically solar GEMS grains. Isotopically solar GEMS grains may have formed in the nebula under similar conditions to those that condensed in circumstellar outflows. Alternatively, they may have been isotopically homogenized by extensive irradiation/cycling of material in the ISM [3]. However, the chemical compositions of GEMS grains do not easily fit in with this scenario [4]. The preserved microstructure of the presolar GEMS grains suggests that they were not extensively affected by irradiation or thermal processes.

References: [1] Messenger S. et al. 2007. *Science* 309:737. [2] Kemper F. et al. 2004. *The Astrophysical Journal* 609:826. [3] Bradley J. P. 1999. *Science* 285:1716. [4] Keller L. P. et al. 2005. Abstract #2088. 36th LPSC.

5227

NEUTRON AND GAMMA-RAY PRODUCTION IN MARTIAN SURFACE SOIL AND ROCK

K. J. Kim[1, 2], W. V. Boynton[2], R. C. Reedy[3], and D. M. Drake[4]. [1]Korea Institute of Geoscience and Mineral Resources, Daejeon, Korea. [2]Lunar and Planetary Laboratory, University of Arizona, Tucson, AZ 85721, USA. [3]Institute of Meteoritics, University of New Mexico, Albuquerque, NM 87131, USA. [4]TechSource, Santa Fe, NM 87505, USA.

Introduction: The rock surface abundances on Mars are inferred from orbital data to vary from almost zero to ~30% [1]. The effects of rocks and soil on gamma-ray fluxes were investigated for several cases [2], although only for rocks both much smaller and much larger than neutron-interaction lengths. For this study, we did numerical simulations using a 3-D code for rocks of various sizes in Martian soil.

Calculations: We did the numerical simulations with the Monte Carlo N-Particle eXtended (MCNPX) code using a box model with reflecting walls that has the same atmospheric features and depth profiles as our spherical MCNPX calculations [3]. This model shows the effect of rock and soil mixture without the geometric problems of placing small rocks on the surface of a full-size Mars. We investigated five rock sizes ranging in radii from 5 to 30 cm. The rock is located with its center in the center of the surface, with half of the rock above the ground and half below the ground level. A soil composition with 3% water and a composition similar to the rock for all elements except with much more water and Cl in the soil were used.

Results: *Neutron Flux:* Our results indicated that neutron fluxes in the soil mixture with a 10 cm rock didn't change significantly compared those in pure soil, while those with 20 cm rock did change. This indicates that a 10 cm rock at the surface would not significantly change the capture and inelastic gamma ray fluxes at the surface. The effect of a rock in soil is seen as a decrease of thermal neutron fluxes surround of the rock while the fast neutrons increased. A significantly high neutron flux for neutron energies of 2–35 MeV region near the rock is observed. This implies that the high fast neutron flux would increase the inelastic gamma ray production rate near the rock portion.

Gamma Ray Flux: We are currently investigating which MCNPX libraries can be used to remove interferences of gamma rays with respect to the gamma rays of interest for our study. Major thermal capture and inelastic gamma rays of H, Si, Cl, Fe, and a few other elements will be used.

Conclusions: This study indicated that a rock of radius of 10 cm on Martian surface soil does not significantly affect to the gamma ray fluxes at the surface. However, a rock having a radius of 20 cm would significantly affect the gamma ray flux at the surface due to the neutron fluxes in the rock being different than the surrounding soil. Higher rock abundance in soil will contribute in increase of inelastic gamma ray flux, but in decrease of thermal neutron capture gamma ray flux at the surface. Ratios of such gamma ray fluxes at surface of Mars could provide important indications of the Martian rock abundance.

Acknowledgements: This work was supported by the Mars Odyssey project and the Planning Project of KIGAM.

References: [1] Christensen P. R. 1986. *Icarus* 68:217–238. [2] Squyres S. W. and Evans L. G. 1992. *Journal of Geophysical Research* 97(14):14,701–14,715. [3] Kim K. J. et al. 2007. *Journal of Geophysical Research* 112:E03S09.

5139

ABUNDANT $(Mg,Fe)SiO_3$ GLASS IN SHOCK VEINS IN AN L6 CHONDRITE, NWA 4719

M. Kimura[1], H. Fukuda[1], T. Mikouchi[2], A. Suzuki[3], and E. Ohtani[3]. [1]Ibaraki University, Japan. E-mail: makotoki@mx.ibaraki.ac.jp. [2]Tokyo University, Tokyo, Japan. [3]Tohoku University, Sendai, Japan.

Introduction: High-pressure minerals have been reported in shock melt veins of many chondrites (e.g., [1–3]). Their occurrence indicates shock-induced melting and crystallization under the long duration of high-pressure and temperature conditions (e.g., [2]). Here we report unique high-pressure phase assemblage in an L6 chondrite, NWA 4719.

Petrology and Mineralogy of Shock Veins: NWA 4719 is a newly approved L6 chondrite. It contains well-developed shock veins, which are 0.05 to 1.2 mm in width. The veins mainly comprise two silicate lithologies: 1) coarse-grained rounded to irregular silicate grains (~10 to ~100 μm), and 2) fine-grained (below ~5 μm) silicate aggregate. Coarse-grained lithology mainly consists of olivine and low-Ca pyroxene in composition. Fine-grained lithology is an aggregate mainly comprising olivine and low-Ca pyroxene in composition, mixed with abundant spherules of Fe-Ni metal and troilite.

We identified all silicate minerals both in lithologies as high-pressure polymorphs, ringwoodite, akimotoite and lingunite, by using laser microRaman spectrometer. Majorite is extremely rare in NWA 4719, and this chondrite is characterized by unusually abundant glassy grains in pyroxene composition. Pyroxene grains in composition is mostly glass. Akimotoite is rarely accompanied with pyroxene glass. The fine-grained lithology mainly consists of ringwoodite and pyroxene glass.

Discussion: Pyroxene glass was reported from some heavily shocked chondrites [3–5]. However, these chondrites also contain abundant majorite. Pyroxene glass in NWA 4719 is never associated with majorite. The occurrence in the coarse-grained lithology and identical composition to the host pyroxene suggest that the pyroxene glass was not derived from melt. Such glass was reported as vitrified product from silicate perovskite (e.g., [4]). Our observations are consistent with such origin. Silicate perovskite should form under higher-pressure conditions than majorite (e.g., [3]). The veins in NWA 4719 contain almost exclusively vitrified perovskite, suggesting that after the crystallization of perovskite the shock veins cooled rapidly without crystallization of majorite.

On the other hand, silicate perovskite is completely vitrified at above 477 °C at ambient pressure [6]. Therefore, the post-shock temperature was more than 477 °C. The phase assemblage of NWA 4719 indicates that the veins in it crystallized under higher pressure conditions than veins in most of shocked chondrites.

References: [1] Chen M. et al. 1996. *Science* 271:1570–1573. [2] Ohtani E. et al. 2004. *Earth and Planetary Science Letters* 227:505–515. [3] Xie Z. et al. 2006. *Geochimica et Cosmochimica Acta* 70: 504–515. [4] Chen M. et al. 2004. *Meteoritics & Planetary Science* 39:1797–1808. [5] Tomioka N. and Kimura M. 2003. *Earth and Planetary Science Letters* 208:271–278. [6] Durben D. J. and Wolf G. 1992. *American Mineralogist* 77: 890–893.

5039

SHELL CREEK (ALABAMA) K/T IMPACT SPHERULES—OCCURRENCE AND DIAGENESIS

D. T. King, Jr.[1] and L. W. Petruny[2]. [1]Geology Office, Auburn University, Auburn, Alabama 36849, USA. E-mail: kingdat@auburn.edu. [2]Astra-Terra Research, Auburn, Alabama 36831–3323, USA.

Occurrence: At Shell Creek stratigraphic section, Wilcox County, Alabama, a 35–75 cm thick, Cretaceous-Tertiary (K/T) boundary sand body crops out over an area of ~200 m^2. This sand body consists of a basal impact spherule-bearing, coarse to medium sand and an overlying fine sand with hummocky-type cross-lamination. This K/T boundary sand body probably represents post-impact, shelf sedimentation events involving gravity-driven resedimentation of reworked impact spherule-bearing sands and energetic wave reworking of the impact spherule-bearing, gravity-driven deposits or other subsequently deposited sands. This stratigraphic section represents the most easterly U.S. Gulf Coastal Plain occurrence of abundant impact spherules in a Cretaceous-Tertiary (K/T) boundary sand body [1].

Diagenesis: Most impact spherules from Shell Creek are spherically shaped grains (~1 mm in diameter) that are now hollow, or were hollow prior to secondary calcite filling. Most impact spherules from Shell Creek consist of an outer shell, which is composed of smectitic clays, and an inner region of open space or sparry calcite. Most of these impact spherules still retain vesicles that attest to their former molten condition.

In thin section, the outer walls of some spherules display a laminated structure of alternating light and dark layers. This laminated structure is likely diagenetic (i.e., from devitrification [2]). The laminated wall structure is also typically deformed. The deformation of impact-spherule walls includes concave indentation (plastic deformation) and rim segmentation (brittle breakage). The outer walls of some spherules are not laminated, however, and are essentially all one color or have gradational light to dark shading. Spherules without laminated walls are as likely as those with laminated walls to display hollow and calcite-filled interiors, so it is unclear if there may have been any original compositional difference between spherules with the two wall types.

The outer surfaces of impact spherules commonly show numerous, small indentations that do not appear to be related to plastic deformation. These are interpreted as primary features resulting from vesicular eruption (i.e., bubble popping) on the surface of the grain or in-flight collision with other fine ejecta.

The presence of dark, phyllosilicates in the outer rim of these impact spherules has been noted by [3] in impact spherules from the K/T boundary sands at Moscow Landing, Alabama, and other sites in the Gulf of Mexico region, and by [4] in some Late Archean impact spherules from South Africa. The hollowness, i.e., the absence of most of the original interior of these impact spherules, may be due to dissolution of original glassy cores that did not devitrify like the outer walls [5].

References: [1] King D. T., Jr. and Petruny L. W. GSA-SEPM Special Paper. Forthcoming. [2] Bohor B. F. and Glass B. P. 1995. *Meteoritics* 30: 182–198. [3] Smit J. et al. 1996. GSA Special Paper #307. pp. 151–182. [4] Kohl I. et al. 2006. GSA Special Paper #405. pp. 57–73. [5] Simonson B. M. 2003. *Astrobiology* 3:49–65.

5049

HAGERSVILLE, A NEW CANADIAN IRON METEORITE

S. A. Kissin[1] and R. K. Herd[2]. [1]Department of Geology, Lakehead University, Thunder Bay, Ontario P7B 5E1, Canada. E-mail: sakissin@lakeheadu.ca. [2]Geological Survey of Canada, 601 Booth Street, Ottawa, Ontario K1A 0E8, Canada.

Introduction: While clearing stones from a seeded field on his family farm near the village of Hagersville, Haldimand County, Ontario, Canada (42°58′N, 80°09′W), Mr. Joseph Mahé found a 30 kg iron meteorite in April 1999. The meteorite was shallowly buried in the cultivated field.

Composition: The composition as determined by INAA is: Ni 6.89 wt%, Ge 318 ppm, Ga 75.1 ppm, Ir 2.36 ppm, As 16.9 ppm, Au 1.5 ppm, Co 0.483 wt%, Cr 10 ppm, Cu 125 ppm, Pt 5.9 ppm, Re 260 ppb, Sb 327 ppb, W 1090 ppb. The composition places this meteorite in group IAB.

Petrography: Hagersville is a coarse octahedrite (Og) with very narrow and somewhat discontinuous taenite lamellae and sparse development of net plessite. Abundant rhabdites are present, as well as limited development of lamellar schreibersite. The kamacite contains abundant Neumann lines, and the kamacite itself is polygonalized. The meteorite is extensively weathered on the exterior surface, oxidation products are developed along the surfaces of the lamellae and cracks. Some of the rhabdites are accentuated by oxidation. No remnants of a heat-affected zone were observed.

Discussion: The composition of Hagersville lies in a highly populated area on log Ni versus log element plots for group IAB. Thus, its composition resembles that of a number of group IAB members, especially those of the widely distributed North American meteorites Canyon Diablo and Odessa. In comparison with mean compositions of the latter [1], Hagersville lies within 2σ of the elemental composition of Odessa and within 2σ of all elements except Au and Cu in Canyon Diablo. However, Hagersville differs from Odessa in that the latter contains abundant troilite and troilite-graphite nodules, estimated at one per 12 cm^2 [2], as well as abundant cohenite and graphite in the cliftonite habit. Troilite and troilite-graphite nodules are also abundant in Canyon Diablo, as well as a range of shock features not seen in Hagersville. The similarity in composition of Hagersville to that of Odessa and Canyon Diablo can be attributed to the high population of group IAB irons with this range of compositions.

References: [1] Wasson J. T. Unpublished data. [2] Buchwald V. F. 1974. *Handbook of iron meteorites.*

5231

^{26}Al-^{26}Mg AND ^{53}Mn-^{53}Cr AGE OF A FELDSPATHIC LITHOLOGY IN POLYMICT UREILITES

N. T. Kita[1], I. D. Hutcheon[2], G. R. Huss[3], and C. A. Goodrich[4]. [1]Department of Geology and Geophysics, University of Wisconsin–Madison, Madison, WI, USA. E-mail: noriko@geology.wisc.edu. [2]Lawrence Livermore National Laboratory, Livermore, CA, USA. [3]Hawai‘i Institute of Geophysics and Planetology, University of Hawai‘i at Manoa, Honolulu, HI, USA. [4]Department of Physical Sciences, Kingsborough Community College, Brooklyn, NY, USA.

Introduction: Studies of rare feldspathic clasts in polymict ureilites identified an “albitic lithology” that may represent one of the “missing melts” complementary to monomict ureilites [1–4]. These clasts are characterized by albitic (An 0–25) plagioclase, ferroan calcic pyroxenes, phosphates, ilmenite, silica, and glassy mesostasis rich in FeO, MnO, K_2O, P_2O_5, and TiO_2. Oxygen isotopic compositions of several clasts from this lithology confirm that it is indigenous to the ureilite parent body [5, 6]. SIMS data for glass, pyroxene, and phosphates from one of these clasts in DaG 165 (clast 19) showed a linear correlation on a ^{53}Mn-^{52}Cr evolution diagram with slope $(^{53}Mn/^{55}Mn)_0 = (2.91 \pm 0.16) \times 10^{-6}$, indicating a relative age of 4.5 ± 0.04 Ma prior to angrites and an absolute age of 4.562 Ga [7]. Similar ^{26}Al-^{26}Mg ages were obtained from several albitic clasts from DaG 319 [8]. However, none of these clasts contain both plagioclase and Mn-rich glass. Here we report data from another albitic clast, DaG 319 clast B1, containing plagioclase (An 1–9) in addition to pyroxene, phosphate, and Mn-rich glass, allowing us to compare directly the ^{53}Mn-^{53}Cr and ^{26}Al-^{26}Mg chronometers.

Results: The ^{53}Mn-^{53}Cr analyses of glass in clast B1 were carried out using a Cameca 3f (LLNL). The data show resolvable excess ^{53}Cr up to 90‰ and plot along an isochron with slope $(^{53}Mn/^{55}Mn)_0 \sim 3 \times 10^{-6}$ consistent with data from DaG 165 clast 19 [7]. The Al-Mg analyses of plagioclase, glass, and pyroxene were done in three laboratories: 3f (LLNL), 6f (ASU), and 1270 (GSJ). The ^{27}Al/^{24}Mg ratios of plagioclase were 800–900 with excess ^{26}Mg as high as 2.5‰. The initial ^{26}Al/^{27}Al ratio obtained from an isochron plot is $(3.3 \pm 1.2) \times 10^{-7}$, corresponding to an ^{26}Al age relative to CAI (4.5672 Ga; [9]) of 5.3 (–0.3/+0.5) Ma and an absolute age of 4.562 Ga, exactly matching the Mn-Cr age.

Discussion: The high Al/Mg and Mn/Cr ratios observed among minerals and glass in these feldspathic clasts provide the only high-precision age data for ureilites. A majority of these albitic clasts show $\Delta^{17}O = -1.0$‰, suggesting derivation from deep source regions similar to ferroan ureilites [6]. The single 4.562 Ga age may reflect rapid, fractional extraction of melts on the ureilite parent body [10]. Alternatively, it may represent catastrophic disruption by impact that occurred while the body was still hot [11].

References: [1] Ikeda Y. et al. 2000. *Antarctic Meteorite Research* 13: 177–221. [2] Ikeda Y. and Prinz M. 2001. *Meteoritics & Planetary Science* 36:481–499. [3] Cohen B. A. et al. 2004. *Geochimica et Cosmochimica Acta* 68:4249–4266. [4] Goodrich C. A. et al. 2004. *Chemie der Erde* 64:283–327. [5] Kita N. T. et al. 2004. *Geochimica et Cosmochimica Acta* 68:4213–4235. [6] Kita N. T. et al. 2006. *Meteoritics & Planetary Science* 41:A96. [7] Goodrich C. A. et al. 2002. *Meteoritics & Planetary Science* 37:A54. [8] Kita N. T. et al. 2003. Abstract #1557. 34th Lunar and Planetary Science Conference. [9] Amelin Y. et al. 2002. *Science* 297:1678–1683. [10] Goodrich C. A. et al. *Geochimica et Cosmochimica Acta*. Forthcoming. [11] Kita et al. 2005. *Meteoritics & Planetary Science* 40:A82.

5137

MICRODISTRIBUTION OF OXYGEN ISOTOPES IN CHONDRULES FROM THE LEAST EQUILIBRATED H CHONDRITE

N. T. Kita[1], M. Kimura[2], and L. E. Nyquist[3]. [1]University of Wisconsin-Madison, 1215 W. Dayton, Madison, WI 53706–1692, USA. E-mail: noriko@geology.wisc.edu. [2]Ibaraki University, Mito 310-8512, Japan. [3]NASA Johnson Space Center, Houston, TX 77058–3696, USA.

Introduction: High-precision (sub‰) ion microprobe oxygen isotope analyses of ferromagnesian chondrules from the least equilibrated LL chondrites revealed processes of evaporation and recondensation during their formation as well as variety of oxygen isotope reservoirs contributed to chondrule precursors [1–3]. To compare chondrules from LL and H chondrites, we initiated systematic investigations of oxygen isotopes in chondrules from Y-793408 (H3.2), the least equilibrated H chondrite [4]. This is a part of our collaborative study on petrographic, isotopic and chronological (Mn-Cr and Al-Mg) investigations of ferromagnesian chondrules from the most primitive chondrites.

Samples and Analytical Technique: We prepared two thick polished sections of Y-793408 and selected 48 chondrules to obtain their petrographic texture, mineral and bulk chemical compositions using electron microprobes. Oxygen isotope analyses of olivine and pyroxene were performed with ~15 μm spots using CAMECA 1280 ion microprobe at the University of Wisconsin [3]. The external precision of the analyses were better than 0.4‰ (2SD) for $\delta^{18}O$, $\delta^{17}O$, and $\Delta^{17}O$.

Results and Discussion: Total 22 data were obtained from 4 chondrules (3 type IAB and 1 type IIA) by now. Most data show ^{18}O between +3 to +6‰, roughly parallel to terrestrial mass fractionation (TF) line with $\Delta^{17}O$ ~+0.8‰. So far none of the chondrules show significantly elevated $\Delta^{17}O$ more than +1‰.

Chondrule A1-3 (IAB) has a relict Mg-rich olivine at the center with distinctively lighter oxygen isotope compositions ($\delta^{18}O$ = +2‰, $\delta^{17}O$ = +1‰) compared to the rest of olivine and pyroxene ($\delta^{18}O$ = +5.3‰, $\delta^{17}O$ = +3.6‰). Chondrule A1-5 (IIA) consists of large olivine phenocrysts and shows a small, but detectable variation in $\Delta^{17}O$ from 0 to 1‰. The lowest value was found from Mg-rich core at the periphery of the chondrule, while higher values were from smaller Fe-rich grains. These data show common occurrence of relic grains with more Mg-rich olivine. A large dusty olivine grain in chondrule A1-2 (IAB) shows lighter $\delta^{18}O$ than surrounding pyroxene by ~1‰ on the same mass fractionation line. These data are not in isotopic equilibrium at high temperature and may be explained by relict origin of dusty olivine.

Conclusions: Above results are generally similar to those found in LL 3.0–3.1 chondrites [1], indicating similar reservoirs for chondrules in H and LL chondrites [5–6]. Our preliminary data show higher frequency of relict grains than previous LL3 data [1]. It could be partly due to improved precision to resolve a smaller heterogeneity in oxygen three isotopes, though further analysis is required to address systematic differences.

References: [1] Kita N. T. et al. 2006. Abstract #1496. 37th Lunar and Planetary Science Conference. [2] Kita N. T. et al. 2006. Abstract #1791. 38th Lunar and Planetary Science Conference. [3] Kita N. T. et al. 2007. Abstract #1981. 38th Lunar and Planetary Science Conference. [4] Kimura M. et al. 2002. *Meteoritics & Planetary Science* 37:1417–1434. [5] Clayton R. N. et al. 1991. *Geochimica et Cosmochimica Acta* 55:2317–2337. [6] Bridges J. C. et al. 1999. *Geochimica et Cosmochimica Acta* 63:945–951.

5258

THE THERMAL EVOLUTION OF ASTEROIDS INFERRED FROM Hf-W DATING OF METEORITES

T. Kleine[1], M. Touboul[1], C. Burkhardt[1], B. Bourdon[1], A. Halliday[2], J. Zipfel[3], and A. J. Irving[4]. [1]Institute for Isotope Geochemistry and Mineral Resources, ETH Zürich, Switzerland. E-mail: kleine@erdw.ethz.ch. [2]Department of Earth Sciences, University of Oxford, UK. [3]Forschungsinstitut Senckenberg, Frankfurt, Germany. [4]Department of Earth and Space Sciences, University of Washington, Seattle, WA, USA.

Hf-W chronometry has widely been applied for dating the differentiation of asteroids and terrestrial planets [1], but its potential for dating meteorites and constraining the thermal evolution of asteroids has yet to be explored. Here we present Hf-W isochrons for meteorites that were dated previously using various other chronometers and that derive from parent bodies with relatively well constrained cooling histories. Metal and silicate separates were obtained for several H chondrites and acapulcoites. All metals have Hf/W ~0 but the silicate-rich fractions have Hf/W up to ~50, allowing determination of precise isochrons. We obtained the following ages: ~3 Myr for Ste. Marguerite (H4); ~10 Myr for Kernouvé (H6) and Estacado (H6); ~6 Myr for acapulcoites Dhofar 125 and NWA 2775 (here Myr refers to time after formation of CAIs). These Hf-W ages are older than Pb-Pb ages for phosphates [2, 3] and pyroxenes [4] for the same or similar meteorites, indicating that the Hf-W closure temperature in these samples is higher than the ~780 °C Pb-Pb closure temperature of pyroxenes. Hf-W ages therefore provide essential information on the earliest cooling history of meteorite parent bodies. Our new Hf-W ages combined with previously reported Pb-Pb ages for the same or similar meteorites [2–4] reveal that acapulcoites cooled more rapidly than H6 chondrites but similar to H4 chondrites. This suggests that either the acapulcoite parent body is smaller than the H chondrite parent body or that the burial depth of acapulcoites was shallower. Compared to H6 chondrites, acapulcoites were heated to higher temperatures (as is evident from the formation of FeNi-FeS melts) but cooled more rapidly, indicating that the acapulcoite parent body contained a higher amount of ^{26}Al and hence accreted earlier than the H chondrite parent body. Acapulcoites may derive from a body that accreted as early as the parent bodies of the magmatic irons (<1.5 Myr [5]) but was too small to efficiently retain the heat produced by ^{26}Al decay. Alternatively, the acapulcoite parent body might have accreted later than ~1.5 Myr but before accretion of the H chondrite parent body at ~3 Myr (as derived from the Hf-W age of Ste. Marguerite). The presence of relict chondrules in some acapulcoites suggests that the latter scenario might be more likely. The Hf-W data indicate that the early evolution of asteroids is largely controlled by the time of parent body accretion and hence the amount of ^{26}Al present. This most likely reflects increasing accretion times with increasing distance from the Sun, consistent with the heliocentric zoning of the asteroid belt [6].

References: [1] Kleine T. et al. 2002. *Nature* 418:952–955. [2] Göpel C. et al. 1992. *Meteoritics* 27:226–226. [3] Göpel C. et al. 1994. *Earth and Planetary Science Letters* 121:153–171. [4] Bouvier A. et al. 2007. *Geochimica et Cosmochimica Acta* 71:1583–1604. [5] Kleine T. et al. 2005. *Geochimica et Cosmochimica Acta* 69:5805–5818. [6] Grimm R. E. and McSween H. Y. 1993. *Science* 259:653–655.

5306

SILICON ISOTOPE FRACTIONATION IN CAI-COMPOSITION EVAPORATION EXPERIMENTS

K. B. Knight[1, 2], A. M. Davis[1, 2, 3], N. T. Kita[4], R. A. Mendybaev[1, 2], F. M. Richter[1, 2], and J. W. Valley[4]. [1]Chicago Center for Cosmochemistry, University of Chicago, Chicago, IL, USA. E-mail: kbk@geosci.uchicago.edu. [2]Department of the Geophysical Sciences, University of Chicago, Chicago, IL, USA. [3]Enrico Fermi Institute, The University of Chicago, Chicago, IL 60637, USA. [4]Department of Geology and Geophysics, University of Wisconsin, Madison, WI 53706, USA.

Introduction: Ca-Al-rich inclusions (CAIs), relicts of the earliest condensates of our solar system, contain a unique record of early solar system conditions and processes. Several studies have demonstrated that CAIs likely survived a significant post-condensation heating event [1] prior to incorporation into their host meteorite, causing significant evaporation of the pristine CAIs and alteration of the original isotopic compositions, including depletion of light isotopes of elements such as Mg and Si. Understanding the process and extent of evaporation-driven fractionation in CAI-like systems is of paramount importance for interpretation of these condensates. Following studies quantifying evaporation-driven kinetic fractionation of Mg isotopes in CAI-composition glasses [2, 3], we present complementary Si isotope data obtained from the same residues using an ion microprobe.

Methods: 2.5 mm spheres formed from a uniform initial composition CaO-MgO-Al_2O_3-SiO_2 glass were subjected to a temperature of 1600 °C for varying amounts of time in vacuum. Evaporative mass loss and resultant major element composition was then determined (see [2] for details). Si isotope data from fragments of these residues were obtained using a Cameca IMS 1280 at the University of Wisconsin with a primary beam of Cs^+ focused to a beam diameter of ~10 μm. In contrast to previous Si isotope work using LA-ICP-MS techniques [4], which could determine only ^{29}Si and ^{28}Si, four static Faraday cups were used for simultaneous determinations of ^{28}Si, ^{29}Si, ^{30}Si, and ^{27}Al. The external reproducibility (2σ) is 0.4‰ $\delta^{29}Si$ in and 0.6‰ in $\delta^{30}Si$. Instrumental mass fractionation among residues, however, with their variable major element compositions, is as large as 6‰ in $\delta^{30}Si$. The matrix effect on Si isotopes was calibrated using a set of isotopically unfractionated glasses bracketing the composition range of realized evaporation residues.

Results: Evaporated residues heated to 1600 °C lost between 0 and 90% of their initial Si. Linear Rayleigh fractionation behavior, comparing the log fraction of Si remaining in the evaporation residues with the log ratio of initial and residue $^{29}Si/^{28}Si$, yields a slope (1-α, where α is the kinetic isotope fractionation factor) of 0.0104 ± 0.0004. This is in good agreement with previous Si isotope determinations from 1800 °C evaporation residue data [4], even though the earlier experiments did not make any corrections for matrix effects. It appears that there is not a significant temperature effect on for Si (in contrast to Mg [3]), although further experiments are needed.

References: [1] Richter F. M. et al. 2006. *Meteoritics & Planetary Science* 41:83–93. [2] Richter F. M. et al. 2002. *Geochimica et Cosmochimica Acta* 66:521–540. [3] Richter F. M. et al. *Geochimica et Cosmochimica Acta.* Forthcoming. [4] Janney P. E. et al. 2005. Abstract #2132. 36th Lunar and Planetary Science Conference.

5209

DAUBREELITE AND TROILITE AS A SOURCE OF COMETARY AND MINOR BODY MAGNETISM IN COLD ENVIRONMENT

T. Kohout[1, 2, 3], A. Kosterov[4, 8], M. Jackson[4], L. J. Pesonen[1], G. Kletetschka[3, 5, 7], and M. Lehtinen[6]. [1]Division of Geophysics, University of Helsinki, Finland. E-mail: tomas.kohout@helsinki.fi. [2]Department of Applied Geophysics, Charles University in Prague, Prague, Czech Republic. [3]Institute of Geology, Academy of Sciences of the Czech Republic, Prague, Czech Republic. [4]Institute for Rock Magnetism, University of Minnesota, Minneapolis, MN, USA. [5]Department of Physics, Catholic University of America, Washington, D.C., USA. [6]Geological Museum, University of Helsinki, Finland. [7]GSFC/NASA, Code 691, Greenbelt, MD, USA. [8]Kochi Core Center (KCC), Kochi University, Nankoku City, Kochi, Japan.

Introduction: Various FeNi phases (kamacite, taenite, tetrataenite) are dominant magnetic phases in most chondritic meteorites. In addition, iron-bearing sulfides are detected in meteorites as well as in cometary dust. The low-temperature magnetic properties of the daubreelite ($FeCr_2S_4$), troilite (FeS), and kamacite (FeNi) minerals were investigated. At room temperature daubreelite is paramagnetic and troilite is antiferromagnetic, thus not contributing to remanent nor induced magnetizations. However, at low temperatures magnetic transitions occur, significantly enhancing their magnetic properties.

Daubreelite: Daubreelite is paramagnetic at temperatures higher than its Curie temperature T_c = 150 K. Below T_c daubreelite is ferrimagnetic. The magnetic susceptibility and saturation magnetization of ferrimagnetic daubreelite are approximately 5–10 times lower than those of FeNi. On cooling down through the T_c saturation magnetization of daubreelite sharply increases and reaches maximum of 32 Am^2/kg at 80 K. Below T_c, magnetic susceptibility of daubreelite ranges between 0.5–3.5 10^{-4} m^3/kg reaching maximum value immediately below it.

Troilite: At room temperature troilite is antiferromagnetic. However, at temperature T_m = 60 K, a magnetic transition of uncertain origin occurs, which might be due to a canting of magnetic spins. Below T_m, the saturation magnetization of troilite significantly increases to its maximum value 0.8 Am^2/kg—roughly two orders of magnitude lower than FeNi. Magnetic susceptibility of troilite is low (~4 10^{-7} m^3/kg) with a local maximum around T_m (~1.7 10^{-6} m^3/kg)

Discussion: The magnetization and susceptibility of iron-bearing sulfides, especially daubreelite, is significantly increased in low temperature range. Those minerals can contribute to or even control magnetic properties of bodies in the cold regions of our solar system.

The thermal conditions of the objects in the main asteroid belt are probably above those temperatures. However, the icy trans-Neptunian objects as well as comets containing “magnetic” iron sulfides within the dusty fraction are among candidate objects for recording low-temperature magnetic events. This can be also the case of the comet ^{67}P/Churyumov-Gerasimenko, which will be visited by the Rosetta space probe with the magnetometer on board as well as on the lander. The magnetic properties of iron-bearing sulfides must be considered while interpreting the magnetic observations of such bodies.

5224

EXCESS ARGON IN ASTEROIDAL METEORITES

E. V. Korochantseva[1, 2], M. Trieloff[1], A. I. Buikin[1, 2], J. Hopp[1], and W. H. Schwarz[1]. [1]Institute of Mineralogy, University of Heidelberg, Im Neuenheimer Feld 236, D-69120 Heidelberg, Germany. E-mail: trieloff@min.uni-heidelberg.de. [2]Vernadsky Institute of Russian Academy of Sciences, Moscow, Russia.

^{40}Ar-^{39}Ar dating of meteorites can elucidate the early cooling history of meteorite parent bodies as well as their secondary collisional history [1–9]. In 4.5 Ga old samples, ^{40}Ar is overwhelmingly due to in situ ^{40}K decay, trapped ^{40}Ar is generally unimportant, with ^{40}Ar/^{36}Ar ≤ 1, consistent with primordial production ratios of 10^{-4}, making a trapped component with significant radiogenic ingrowth (^{40}Ar/^{36}Ar >> 1) unlikely. Such an evolved "excess" argon component is furthermore unlikely in meteorites, as these are from small asteroids that effectively degas during heating events, unable of keeping atmospheres of sufficient argon partial pressure to be trapped by host rocks. Nevertheless, we recently detected multiple isochrons in individual L chondrites identifying excess argon, in part of clear extraterrestrial origin [8]. Although a well-known phenomenon for terrestrial samples [10], its occurrence in asteroidal meteorites was not recognized before, most probably as most meteorites 1) have very old 4.5 Ga magmatic ages, 2) lack a clear geological context, and 3) lack clear resolution of trapped from cosmogenic ^{36}Ar to construct proper isochrons. Our results on L chondrites show that during major collisions, degassing asteroids can develop transient "atmospheres," from which evolved argon can be trapped as excess argon component (with 1 ≤ ^{40}Ar/^{36}Ar ≤ 296). Its incorporation occurred most probably fast after collisional induced shock metamorphism, as argon equilibrated on mm (sample) scales, but not cm (meteorite) scales. A major problem for future studies is the unknown siting of excess argon. While for terrestrial samples several identifications of carrier phases of trapped argon interfering with in situ radiogenic argon have succeeded, e.g., impact melt alterations [11], carbonaceous phases [12], ultramafic minerals [13–16], or basalt glasses [17], for extraterrestrial samples hardly clear carrier phase identification is available.

References: [1] McConville P. et al. 1988. *Geochimica et Cosmochimica Acta* 52:2487–2499. [2] Bogard D. D. and Garrison D. H. 2003. *Meteoritics & Planetary Science* 38:669–710. [3] Bogard D. D. et al. 1995. *Geochimica et Cosmochimica Acta* 59:1383–1399. [4] Dixon E. T. et al. 2003. *Meteoritics & Planetary Science* 38:341–355. [5] Trieloff M. et al. 2003. *Nature* 422:502–506. [6] Kunz J. et al. 1995. *Planetary and Space Science* 43:527–543. [7] Korochantseva E. K. et al. 2005. *Meteoritics & Planetary Science* 40:1433–1454. [8] Korochantseva E. V. et al. 2007. *Meteoritics & Planetary Science* 42:113–130. [9] Trieloff M. et al. 2001. *Earth and Planetary Science Letters* 190:267–269. [10] Lanphere M. A. and Dalrymple G. B. 1976. *Earth and Planetary Science Letters* 32:141–148. [11] Trieloff M. et al. 1998. *Meteoritics & Planetary Science* 33:361–372. [12] Trieloff M. et al. 2005. *Geochimica et Cosmochimica Acta* 69:1253–1264. [13] Harrison D. et al. 2003. *Geochemistry Geophysics Geosystems* 4: 2002GC000325. [14] Hopp J. et al. 2004. *Earth and Planetary Science Letters* 219:61–76. [15] Buikin A. I. et al. 2005. *Earth and Planetary Science Letters* 230:143–162. [16] Trieloff M. et al. 1997. *Geochimica et Cosmochimica Acta* 61:5065–5088. [17] Trieloff M. et al. 2003. *Geochimica et Cosmochimica Acta* 67:1229–1245.

5006

SAYH AL UHAYMIR 300—THE MOST MAFIC OF THE FELDSPATHIC LUNAR METEORITES

R. L. Korotev[1], R. Bartoschewitz[2], Th. Kurtz[2], and P. Kurtz[2]. [1]Washington University, St. Louis, Missouri, USA. E-mail: korotev@wustl.edu. [2]Meteorite Laboratory, Gifhorn, Germany.

SaU (Sayh al Uhaymir) 300 is a 153 g lunar meteorite from northern Oman. Originally described a feldspathic regolith breccia [1], it has recently been as classified an feldspathic, crystalline impact-melt breccia [2]. We have analyzed 11 subsamples of the stone with a total mass of 321 mg by instrumental neutron activation analysis (INAA) for some major elements and a variety of trace elements. These data supplement our previously reported data [3].

SaU 300 is compositionally distinct from other nominally feldspathic lunar meteorites. With 7.8% FeO and 18 ppm Sc, it is compositionally more mafic (others range from 3% to 6% FeO). In this regard, SaU 300 is more similar to "mingled" meteorites Yamato-983885 (8.6% FeO), Dhofar 1180 (9.2%), Calcalong Creek (9.7%), and NWA 2995 (9.8%), all of which are regolith or fragmental breccias. Mingled meteorites are richer in Fe and Sc than feldspathic meteorites because the mingled breccias contain mare basalt. However, little or no mare material has been reported in SaU 300 [1, 2, 4]. This observation suggests that SaU 300 is, indeed, the most mafic of the feldspathic lunar meteorites. It is a sample of the lunar highlands, one at the mafic end of range of noritic anorthosites (63 vol% plagioclase calculated from normative concentration of 57% wt%).

Concentrations of incompatible elements in SaU 300 are low (Sm: 1.2 ppm), in contrast to the truly mingled (anorthosite-basalt-KREEP [5]) meteorites mentioned above (2.8–8.6 ppm). Sm/Sc (0.069) is only slightly greater than that of Apollo 16 plutonic anorthositic norite 67513 (0.057) [6], suggesting that SaU 300 is largely uncontaminated by KREEP and does not contain any significant component of near-surface material [7]. This inference is in agreement with the low concentrations of solar-wind gases [8].

As we noted earlier [3], SaU 300 is rich in siderophile elements, presumably from the impactor that formed the melt from which it crystallized. Ir/Au is 3.5, i.e., the same as in H chondrites. A 2.5% component of H chondrite accounts for all of the Ir (19 ppb) Au (5.5 ppb), and 400 ppm of the 440 ppm Ni.

In some respects, SaU 300 resembles NWA 3163 [9], a granulitic breccia that is less mafic (5.9% FeO) and which has remarkably low concentrations of incompatible elements (0.5 ppm Sm). We are unable to find any mixture of NWA 3163 and a reasonable lunar material that accounts for the composition of SaU 300, however.

References: [1] Bartoschewitz et al. 2005. *Meteoritics & Planetary Science* 40:A18. [2] Hudgins J. A. et al. 2007. Abstract #1674. 38th Lunar and Planetary Science Conference. [3] Bartoschewitz et al. 2005. Abstract #1423. 68th Annual Meteoritical Society Meeting. [4] Hsu et al. 2007. 38th Lunar and Planetary Science Conference. Abstract #1149. [5] Korotev R. L. 2005. *Chemie der Erde* 65:297–346. [6] Jolliff B. L. and Haskin L. A. 1995. *Geochimica et Cosmochimica Acta* 59:2345–2374. [7] Korotev R. L. et al. 2006. *Geochimica et Cosmochimica Acta* 70:5935–5956. [8] Bartoschewitz et al. 2005. Abstract #5026. 68th Annual Meteoritical Society Meeting. [9] Irving A. J. et al. 2006. Abstract #1365. 37th Lunar and Planetary Science Conference.

5257

DO WE HAVE A METEORITE FROM THE SOUTH POLE–AITKEN BASIN OF THE MOON?

R. L. Korotev, R. A. Zeigler, and B. L. Jolliff. Washington University in Saint Louis, Saint Louis, MO, USA. E-mail: korotev@wustl.edu.

The South Pole–Aitken (SPA) basin, the largest impact structure in the solar system, encompasses about 5% of the lunar surface ([1] "inner"). Samples from SPA will help us better understand the impact history and crustal evolution of the Moon [2]. The ~50 lunar meteorites probably represent 35–40 source craters. Thus it is likely that 1 or 2 meteorites originate from within the basin. How would we recognize such a meteorite? Data obtained from orbit show the nonmare material of SPA to be more mafic (~10% FeO) than materials of the FHT (Feldspathic Highlands Terrane, 4–5% FeO). SPA material is also richer in Th (1–2 ppm, with a few "hot spots" up to 4 ppm) than the FHT (<1 ppm), but not as rich as the PKT (Procellarum KREEP Terrane) (>4 ppm) [1].

Several lunar meteorites, all breccias, are intermediate to anorthosite and basalt in composition (FeO, Al_2O_3) and richer in Th than mixtures of basalt and anorthosite: NWA 2995 (2 ppm Th), Yamato-983885 (2 ppm), Dhofar 961 (3 ppm), Calcalong Creek (4 ppm), NWA 4472/4485 (7 ppm), and SaU 169 (10 ppm, regolith breccia). SaU 169 and NWA 4472/4485 are likely from the PKT [3, 4]. Of the others, Dhofar 961, an impact-melt breccia [5] with the composition of gabbronorite (18% Al_2O_3, 11% FeO; $Mg' = 63$), has some unusual geochemical properties. Concentrations of incompatible elements are moderately high, e.g., 7 ppm Sm, and would require 10% high-K KREEP [6], if an Apollo breccia. Polymict nonmare materials in the Apollo collection with this level of Sm typically contain 1.2 ppm Eu, and never <1 ppm. Yet Dhofar 961 contains only 0.8 ppm Eu. In essence, the composition of Dhofar 961 does not correspond (as do those of most other "mingled" meteorites [7]) to a mixture of feldspathic material as represented by the feldspathic lunar meteorites, mare basalt, and any form of KREEP as it is known in Apollo samples. Our working hypothesis is that Dhofar 961 derives from ferroan mafic rocks, possibly including basalt, with an intercumulus component that is not KREEP in the additive, polymict sense.

Dhofar 961 may originate from the PKT, but from a point distant from the Apollo samples as no Apollo sample shares its lithophile-element signature. Curiously, Dhofar 961 does share a feature with impact-melt breccias of Apollo 16—high abundance (~1%) of FeNi metal likely derived from an iron meteorite with nonchondritic Ir/Au (1.5) [7, 8]. Alternatively, it may originate from a place where magma-ocean differentiation led to a different flavor of "KREEP"—a place such as the South Pole–Aitken basin. It will be important to obtain a crystallization age of the Dhofar 961 impact-melt component. The stone and its probable pairs, Dhofar 925 and 960, are difficult to obtain, however.

References: [1] Jolliff B. L. et al. 2000. *Journal of Geophysical Research* 105:4197–4216. [2] Pieters C. M. et al. 2001. *Journal of Geophysical Research* 106:28,001–28,022. [3] Gnos E. et al. 2004. *Science* 305:657–659. [4] Korotev R. L. and Zeigler R. A. 2007. Abstract #1340. 28th Lunar and Planetary Science Conference. [5] Jolliff B. L. et al. This issue. [6] Warren P. H. and Wasson J. T. 1979. *Reviews of Geophysics and Space Physics* 17:73–88. [7] Korotev R. L. 2005. *Chemie der Erde* 65:297–346. [8] Korotev R. L. 1994. *Geochimica et Cosmochimica Acta* 58:3931–3969. [9] James O. B. 2002. Abstract #1210. 33rd Lunar and Planetary Science Conference.

5303

PLAGIOCLASE COMPOSITIONS IN EQUILIBRATED ORDINARY CHONDRITES

H. A. Kovach and R. H. Jones. Department of Earth and Planetary Sciences, University of New Mexico, Albuquerque, NM 87131, USA. E-mail: hkovach@unm.edu; rjones@unm.edu.

Introduction: Thermal metamorphism in ordinary chondrites results in progressive equilibration of olivine followed by pyroxene (e.g., [1]). However, little is known about the progression of equilibration of feldspar. Since there are few means to make a quantitative distinction between type 5 and type 6 chondrites, we are investigating the possibility that progressive equilibration of feldspar compositions might provide a means to establish a more detailed measure of the degree of metamorphism.

In type 3 ordinary chondrites, chondrule mesostases have a wide range of compositions [1]. [2] and [3] showed that feldspar is heterogeneous in type 6 OCs. We are investigating the possibility that this heterogeneity is inherited from the chondrules in which individual feldspar grains are located.

We have already analyzed plagioclase in an H6 S2 chondrite, Nazareth (e) [4], and found significant heterogeneity in Ab, Or and FeO. Ab and Or are strongly correlated with each other. X-ray maps show that potassium has a patchy distribution. The heterogeneity in Nazareth (e) does not appear to be related to initial chondrule mesostasis composition. It is possible that plagioclase has not equilibrated as a result of thermal metamorphism, even in a type 6 chondrite. However, based on only this one chondrite, we could not rule out the possibility that heterogeneity was the result of local shock or terrestrial weathering, as Nazareth (e) is weathering grade W3. We have now examined two more chondrites, Oro Grande (H5 S1 W3) and Richardton (H5 S2 W0) in order to try to resolve the reason for heterogeneous plagioclase.

Results: We studied plagioclase in relict chondrules in Oro Grande and Richardton. We obtained several plagioclase analyses within each chondrule by EPMA, using a 5 μm diameter electron beam, and we obtained X-ray maps of selected areas.

Both Oro Grande and Richardton show heterogeneity in plagioclase. Each chondrule shows a similar compositional range: An, Ab, and Or all vary by about 4 mol% within each relict chondrule. Potassium shows significant heterogeneity and a patchy distribution in X-ray maps. However, in these two type 5 chondrites, we see a correlation between Ab and An rather than Ab and Or. FeO and MgO contents of plagioclase in both the type 5 chondrites are comparable to those in Nazareth (e): FeO varies from 0.2 to 2 wt% and MgO is generally <0.1 wt%.

Discussion: Plagioclase compositions in the two type 5 chondrites, with different weathering grades and shock levels, show a significant difference from Nazareth (e), having strongly correlated An and Ab, rather than Ab and Or. Similar plagioclase compositions in both H5 chondrites indicate that neither weathering nor shock is responsible for the heterogeneity in K that we observed in Nazareth (e). It therefore appears that the plagioclase heterogeneity in type 6 chondrites can be attributed to a lack of equilibration during thermal metamorphism. It is possible that we are seeing a progression towards equilibrated plagioclase compositions from type 5 to type 6 chondrites.

References: [1] Brearley A. J. and Jones R. H. 1998. *Planetary materials*, RIMS 36, Ch. 3. [2] Van Schmus W. R. and Ribbe P. H. 1968. *Geochimica et Cosmochimica Acta* 32:1327–1342. [3] Nagahara H. 1980. Proc. NIPR 17:32–49. [4] Kovach H. A. and Jones R. H. 2007. Abstract #1307. 38th LPSC.

5203

HYDRATED METEORITE DISRUPTION TRENDS AS ANALOGS FOR HYDRATED ASTEROIDS

W. J. Kreft[1], M. M. Strait[1], G. J. Flynn[2], and D. D. Durda[3]. [1]Department of Chemistry, Alma College, Alma, MI 48801, USA. E-mail: 08jwkref@alma.edu. [2]Department of Physics, State University of New York, Plattsburgh, NY, USA. [3]Southwest Research Institute.

Introduction: The purpose of our study on asteroids and meteorites is to understand the size distribution of particles after fragmentation from the main body of the asteroid. A careful study of this process will help estimate the composition of the parent body asteroid and also aid us in understanding the origin of interplanetary dust particles [1]. Even though a large fraction of the impacts taking place in the Main Belt are collisions of hydrated bodies, the majority of impact studies have focused on anhydrous targets [2]. This leaves motive to proceed with an investigation of hydrous targets to compare distribution responses to previous results from anhydrous basaltic targets and to look for differences in trends of these differing targets.

Discussion: In this study, meteorites are disrupted using the NASA/Ames vertical gun [3]. A computer program, ImageJ, is used to analyze holes created by the disruption within the chamber to observe the variations in sizes of the fragments. The fragments are collected, sorted by size distributions using sieves, and weighed. The resulting data are displayed in cumulative mass frequency plots to evaluate the size distribution of the fragments [2].

Preliminary results seen in the cumulative mass frequency diagrams show a significant change in slope for the hydrated terrestrial targets, as opposed to the anhydrous ones. The region from 10^{-10} to 10^{-4} grams and from 10^{-1} to 1 grams is similar in all samples. In the hydrous terrestrial targets there is a change to a less negative slope from 10^{-4} to 10^{-1} grams [2]. However, the one hydrous meteorite examined did not show the expected change in slope as observed in the hydrous terrestrial samples. In this work we have disrupted three more hydrous meteorites to determine if the discrepancy is unique to the particular meteorite examined or more general for meteorites.

References: [1] Durda D. D. and Flynn G. J. 1999. *Icarus* 142:46–55. [2] Flynn G. J. et al. 2007. Abstract #1744. 29th Lunar and Planetary Science Conference. [3] Flynn G. J. and Klock W. 1998. Densities and porosities of stone meteorites: Implications for the porosities of asteroids. Abstract #1112. 29th Lunar and Planetary Science Conference.

5270

AN UNUSUAL STREWN FIELD AT THE OTWAY MASSIF, GROSVENOR MOUNTAINS, ANTARCTICA

M. E. Kress[1], G. K. Benedix[2], J. Schutt[3], and R. P. Harvey[3, 4]. [1]Department of Physics & Astronomy, San Jose State University, San Jose, California 95192, USA. E-mail: mkress@science.sjsu.edu. [2]Natural History Museum, London, UK. [3]Antarctic Search for Meteorites (ANSMET). [4]Department of Geological Sciences, Case Western Reserve University.

Introduction: The 2003–04 ANSMET reconnaissance team collected 84 fragments of an unusual strewn field located on a stagnant blue ice field at the Otway Massif, the largest nunatak in the Grosvenor Mountains, Antarctica. This field was originally discovered by ANSMET during the 1985–86 season. This strewn field is typical [1] in that the fragments are found in a narrow ellipse with a long axis of 1.7 km, with the largest fragments at one end. There was a slight dispersion of the fragments perpendicular to the long axis, possibly attributable to a small amount of ice movement since the fall. The field is unusual in that most of the fragments had little or no fusion crust, suggesting either a low-altitude breakup or shattering of the parent body upon impact with blue ice. Either story indicates a relatively short terrestrial lifetime compared to most Antarctic meteorites [2], probably not longer than a few thousand years. There were relatively few fragments whose mass was less than 100 g, most likely due to removal by wind, which is most effective for fragments smaller than about 100 g. Many of the fragments are large enough to rule out substantial post-fall sorting by wind alone [2].

We consider the two possible mechanisms to explain the strewn field and present a model for each: 1) breakup at low altitude, and 2) shatter and scatter upon low-angle impact. Breakup at low altitude entails drag forces on the incoming bolide causing the smaller fragments (with high surface area to volume ratio) to hit the ground first, the classic strewn-field scenario. We will show whether the low velocity required to not form fusion crust is still sufficient to aerodynamically sort the fragments into a 1.7 km long field. In the shatter and scatter model, we will show how a low-angle impact on ice can sort the fragments into a pattern similar to typical strewn fields. Either mechanism indicates that the Otway Massif represents a novel type of strewn field.

These meteorites are mostly classified as L5 chondrites and are known as GRO 03XXX. For more information on the Otway Massif meteorites and strewn field, see the AMLAMP website: http://geology.cwru.edu/~amlamp/BDM/GRO/GRO63/GRO63text.html

Acknowledgements: The 2003–04 ANSMET team members included the authors, and Christopher Cokinos and Erika Eschholtz. ANSMET is funded by grants to R. P. H. from the National Science Foundation and NASA.

References: [1] Norton O. R. 2002. *The Cambridge encyclopedia of meteorites*. Cambridge University Press. pp. 39–42. [2] Harvey R. P. 2003. *Geochemistry* 63:93–147.

5273

THE "SOOT LINE": POLYCYCLIC AROMATIC HYDROCARBONS IN PRIMITIVE CHONDRITES AS TRACERS OF NEBULAR CONDITIONS

M. E. Kress[1], A. G. G. M. Tielens[2], and M. Frenklach[3]. [1]Department of Physics & Astronomy, San Jose State University, San Jose, CA 95192, USA. E-mail: mkress@science.sjsu.edu. [2]Space Science Division, NASA Ames Research Center. [3]Department of Mechanical Engineering, University of California, Berkeley, CA, USA.

Polycyclic aromatic hydrocarbons (PAHs) are strongly bound organic compounds characterized by 6-membered, pi-bonded carbon ring structures. These compounds are observed in almost every phase of the interstellar medium. Observations show that as much as 10% of the carbon in the interstellar medium is bound up in these compounds [1]. A substantial fraction of the carbon in primitive meteorites is bound in aromatic rings as well [2]. PAHs are abundant in carbonaceous chondrites, but they are also found in lower abundance in ordinary chondrites [3].

Meteorites thought to derive from asteroids beyond 2.5 AU contain water of hydration, while those that seem to derive from the inner belt do not. This observation strongly suggests that during the time that the meteorite parent bodies coagulated from gas and fine dust in the solar nebula, the "snow line" was at about 2.5 AU, and this figure is often used in terrestrial planet formation models today.

We apply models for PAH chemical kinetics in sooting flames [4] to nebular conditions. The chemical and physical properties of PAHs are more complex than that of water vapor condensation; however, our model results suggest that there would have been a fairly distinct "soot line" in the solar nebula, analogous to the snow line. We find that, at inner nebular conditions (excess H, C/O ratio < 1, low pressure and T ~1000 K), aromatic rings are relatively stable at T < 900 K and tend to quickly break down at T > 1000 K due to reaction with OH. Their abundances in primitive chondrites likely reflects their abundance in the nebula, during the time period in which meteorites were coagulating. If present, they would condense out at T < a few hundred K. If the nebular gas experienced T > 1000 K, PAHs would be quickly destroyed in the presence of OH. While parent-body temperatures during thermal metamorphism may reach T > 1000 K, they would not have been as quickly destroyed because of the lack of reactants (OH).

Acknowledgements: M. E. K.'s research is supported through a grant to the Virtual Planetary Laboratory (PI: V. Meadows) from the NASA Astrobiology Institute.

References: [1] Allamandola L. J., Tielens A. G. G. M., and Barker J. R. 1985. *The Astrophysical Journal* 290:L25–L28. [2] Cody G. C. and Alexander C. 2005. *Geochimica et Cosmochimica Acta* 69:1085–1097. [3] Clemett S. 1996. Ph.D. thesis, Stanford University. [4] Frenklach M. 2002. *Physical Chemistry Chemical Physics* 4:2028–2037.

5130

A TEST OF THE IMPACT-MASS EXTINCTION HYPOTHESIS AT THE TRIASSIC-JURASSIC BOUNDARY

David A. Kring[1], Wendy S. Wolbach[2], Andrea Patzer[3], and David Goodwin[4]. [1]Lunar and Planetary Institute, 3600 Bay Area Blvd., Houston, TX 77058, USA. E-mail: kring@lpi.usra.edu. [2]Department of Chemistry, DePaul University, Chicago, IL 60614, USA. [3]Abelhain 22, D-26209 Sandkrug, Germany. [4]Department of Geology and Geography, Denison University, Granville, OH 43023, USA.

Introduction: To test the impact-mass extinction hypothesis for the Triassic/Jurassic boundary transition, we located the T/J boundary at two localities using stratigraphic, paleontologic, and carbon isotopic criteria (e.g., [1–2]). One of those sections occurs in Muller Canyon, Nevada, and is a candidate Global Boundary Stratotype Section and Point (GSSP). We examined those strata and bounding strata for shocked quartz and soot.

Sedimentary Lithologies: The T/J boundary occurs within the Muller Canyon Member of the Gabbs Formation. The section is composed of siltstones deposited in a relatively near-shore environment and is variably calcareous. The lower part of this section is composed of decimeter- to meter-thick beds that transition to centimeter- to decimeter-thick beds that are commonly laminated. The boundary is located near this transition and is associated with ~1.8 per mil negative $\delta^{13}C_{org}$ anomaly [2].

Search for Shocked Quartz: 20 bulk samples were disaggregated and processed in ultrasonic baths to float and decant clay particles. Mild acids were used to remove carbonate, leaving silt- to sand-size insoluble residues that were examined for shocked quartz and any other petrologic indicator of impact, using the same techniques applied previously in K/T boundary studies (e.g., [3]). A total of 19,927 grains were examined in the survey. The samples were dominated by quartz, with some feldspar, and minor amounts of other phases. No significant evidence of impact was found, whereas 14 to 27% of grains in K/T boundary residues examined in same way are shocked quartz [3].

Search for Soot: Eight bulk samples were also analyzed for soot. These included a background sample below the boundary, 3 samples immediately below the negative carbon isotope anomaly, 3 samples within the anomaly, and a background sample higher in the section. The same techniques used to isolate soot in K/T boundary samples [4] were applied. No increase over background values was detected in the boundary units, compared to enhancements $>10^3$ seen in K/T boundary sections (e.g., [4]). Indeed, none of the samples had any detectable soot and an upper limit of 4 ppm is calculated.

Conclusions: We were unable to detect a significant quantity of impact debris or one of the possible measures of impact-generated environmental effects. Thus, we are unable to provide any support for the impact-mass extinction hypothesis. This lack of support for the impact-mass extinction hypothesis should not, however, be over-interpreted: it is not proof that an impact did not occur. Additional samples along strike at this locality and additional T/J sections at other localities need to be examined before any firm conclusions can be drawn. It may be prudent, however, to also consider other causes for the mass extinction.

References: [1] Ward P. D. et al. 2004. *Earth and Planetary Science Letters* 224:589–600. [2] Ward P. D. et al. 2007. *Palaeogeography, Palaeoclimatology, Palaeoecology* 244:281–289. [3] Kring D. A. et al. 1994. *Earth and Planetary Science Letters* 128:629–641. [4] Wolbach W. et al. 1988. *Nature* 334:665–669.

5254

RELICT REFRACTORY INCLUSIONS IN MAGNESIUM PORPHYRITIC CHONDRULES FROM THE CH AND CH/CB CARBONACEOUS CHONDRITES

A. N. Krot[1], K. Nagashima[1], G. R. Huss[1], M. Bizzarro[2], F. J. Ciesla[3], and A. A. Ulyanov[4]. [1]HIGP/SOEST, University of Hawai'i at Manoa, USA. E-mail: sasha@higp.hawaii.edu. [2]Geological Inst., Denmark. [3]Carnegie Institution, USA. [4]Moscow State Univ., Russia.

Introduction: It has been suggested that ungrouped carbonaceous chondrite Isheyevo (CH/CB) and possibly other CHs contain multiple generations of chondrules formed by different mechanisms and, possibly, at different times [1]: ferromagnesian and Al-rich porphyritic chondrules formed by melting of solid precursors in the protoplanetary disk, whereas magnesian cryptocrystalline and skeletal chondrules formed in an impact generated plume of melt and gas. Subsequently, we showed that CAIs from Isheyevo and CH chondrites Acfer 182/214 have a bimodal distribution of ^{26}Mg excesses (^{26}Mg*; decay product of ^{26}Al) that appears to correlate with their mineralogy [2]. The majority of the most refractory CAIs (grossite- and hibonite-rich) show either unresolvable or small ^{26}Mg* corresponding to an $(^{26}Al/^{27}Al)_I$ of ~$(5.0 \pm 0.7) \times 10^{-7}$. The less refractory inclusions have nearly the canonical $(^{26}Al/^{27}Al)_I$ of $(4.4 \pm 0.3) \times 10^{-5}$. Both populations of CAIs are characterized by ^{16}O-rich ($\Delta^{17}O < -20‰$) compositions, that probably excludes (i) formation of CAIs from an impact generated plume and (ii) late-stage resetting of Al-Mg systematics of the ^{26}Al-poor CAIs by remelting [2]. We concluded that the ^{26}Al-poor and ^{26}Al-rich populations of the CH CAIs represent samples of at least two generations of refractory inclusions formed before and after injection and homogenization of ^{26}Al in the solar system, respectively. Here we report a discovery of ~30 relict CAIs inside magnesian porphyritic chondrules from these meteorites.

Results and Discussion: These, now relict CAIs formed before the host chondrules, were subsequently mixed with the chondrule precursor materials and melted to various degrees during chondrule formation. About half of the relict CAIs belong to a population of ^{26}Al-poor, very refractory inclusions dominated by grossite and hibonite; other relict CAIs consist mainly of spinel. Grossite and hibonite of the relict CAIs and anorthitic plagioclase of the host chondrules show no evidence for ^{26}Mg*. The only two exceptions are grossite-rich CAIs having small ^{26}Mg* corresponding to the $(^{26}Al/^{27}Al)_I$ of $(1.7 \pm 1.3) \times 10^{-6}$ and $(3.3 \pm 3.0) \times 10^{-7}$. The ^{26}Al-poor grossite-rich and hibonite-rich, igneous CAIs comprise about 50% of all refractory inclusions in the metal-rich chondrites studied [2, 4]; such CAIs, however, are virtually absent in ordinary, enstatite and other carbonaceous chondrite groups. We infer that this isotopically and mineralogically unique population of CAIs was present in the region where magnesian porphyritic chondrules of CH chondrites formed, suggesting that these chondrules formed at a different time or in a different nebular region than chondrules from other chondrite groups. Since most CAIs outside chondrules in CH chondrites show no clear evidence for being affected by the chondrule-forming processes, we infer that either the scale of chondrule-forming event(s) was relatively small and a number of chondrule-forming events in a localized nebular region where these chondrules formed was limited, or chondrule-forming event(s) had little effect on compact objects, like CAIs.

References: [1] Krot A. N. et al. *Chemie der Erde*. Forthcoming. [2] Krot A. N. et al. *The Astrophysical Journal*. Forthcoming. [3] Krot A. N. et al. 2007. Abstract #1888. 38th LPSC. [4] Krot A. N. et al. *Meteoritics & Planetary Science*. Forthcoming.

5131

CHLORINE-RICH CARBONACEOUS COMPOUNDS IN ANOMALOUS CM2 CHONDRITE NORTHWEST AFRICA 3340

S. M Kuehner[1], A. J. Irving[1], D. Rumble III[2], and P. P. Sipiera[3]. [1]Earth & Space Sciences, University of Washington, Seattle, WA, USA. E-mail: kuehner@ess.washington.edu. [2]Geophysical Laboratory, Carnegie Institution, Washington, D.C., USA. [3]Planetary Studies Foundation, Galena, IL, USA.

This very fresh (W0), black, relatively fine-grained, porous stone (12.7 grams) probably is a recent fall judging from its shiny fusion crust (composed of dispersed magnetite and olivine grains + glass). The interior consists of sparse mineral grains, carbon-rich objects, dust-armored chondrules and rare CAI in a heterogeneous, very fine grained, porous matrix composed of bladed Fe-Mg-S-rich phyllosilicates (probably tochinilite-cronstedtite) with some primary calcite pentlandite and diamond. Normally zoned olivine grains (up to 2 mm; range $Fa_{1.5–66}$) are armored by polycrystalline dust, and contain inclusions of Ni-rich troilite, chromite, millerite, kamacite, and taenite. Some carbon-rich objects (up to 50 μm across) are pure graphite, but many are a chlorine-rich organic phase containing ~17 wt% Cl and ~32 wt% C, but no N and little O (Fig. 1). One small spherical CAI is composed of Mg-Al spinel with inclusions of perovskite.

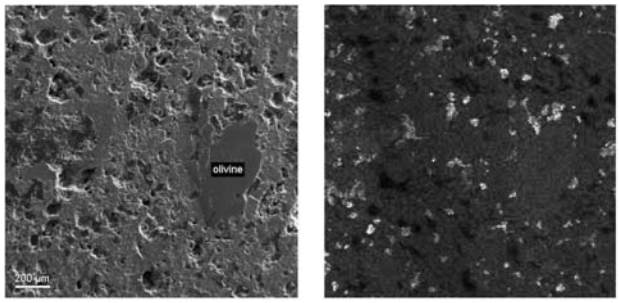

Fig. 1. SEI image of polished face Chlorine X-ray map (bright).

Oxygen Isotopes: Analyses of acid-washed whole samples by laser fluorination gave, respectively, $\delta^{18}O$ = 0.494, 1.166; $\delta^{17}O$ = 6.224, 7.049; $\Delta^{17}O$ = –2.780, –2.542 per mil. These results plot within the field of CM chondrites [1].

Affinities: NWA 3340 appears to be an anomalous CM2 chondrite that contains unusually abundant halogenated carbonaceous compounds. Extractable chlorinated benzoic acids were reported [2] in other CM2 chondrites (Murchison, Orgueil, Murray and Cold Bokkeveld), but we doubt that the Cl-rich phases in NWA 3340 are such compounds. Nevertheless, it appears that various halogen-rich organic compounds (perhaps hydrocarbons and/or oxyacids) must have been present in the early solar nebula prior to accretion of the CM parent body or bodies.

References: [1] Clayton R. N. and Mayeda T. K. 1999. *Geochimica et Cosmochimica Acta* 63:2089–2104; Moriarty G. et al. 2007. Abstract #1289. 38th LPSC. [2] Schöler H. et al. 2005. *Chemosphere* 60:505–1512.

5283

INITIAL INTERPRETATIONS OF GEOCHEMICAL ANALYSES OF ELTANIN IMPACT SPHERULES

Frank T. Kyte[1], Chikako Omura[1], Rainer Gersonde[2], and Gerhard Kuhn[2]. [1]Center for Astrobiology, Institute of Geophysics and Planetary Physics, University of California, Los Angeles, CA 90095–1567, USA. E-mail: kyte@igpp.ucla.edu. [2]Alfred Wegener Institut für Polar- und Meeresforschung, Postfach 120161, D-27515 Bremerhaven, Germany.

Introduction: Eltanin impact deposits record the only known kilometer-size asteroid impact into a deep-ocean (5 km) basin (at 2.5 Ma). Two oceanographic expeditions explored ~80,000 km^2 of the impact region. Locally, meteoritic ejecta (millimeter-size shock-melted asteroid and unmelted meteorites; a low-metal mesosiderite) can be 5–50 kg/m^2. Here we report initial studies of the geochemistry of impact spherules, a trace component in the <500 μm fractions of the ejecta.

Questions: Despite formation by the simple impact of an asteroid into seawater, these spherules have diverse mineralogy, textures, and compositions. What causes this diversity? Some authors have argued that magnesioferrite, which is common in both Eltanin and K/T boundary spherules, reflects formation by atmospheric ablation, as opposed to condensation in a high-temperature impact plume favored by others. Are spherules forming from a relatively uniform impact plume of vapor and liquid or are they derived from mixtures of asteroid minerals (mostly pyroxenes and feldspars) on a millimeter scale, such as from particles spallated from the backside of the projectile? We do find millimeter- to centimeter-size meteorite fragments as 10% of the ejecta. Is there mixing between projectile and target (seawater) components? And once these droplets form, how are they influenced by fractional distillation (by ablation) or condensation (in a plume), or variable degrees of oxidation? This simple impact does not provide simple solutions, as the spherules are also complicated by fractional crystallization by the three minerals found—magnesioferrite, low-Ca pyroxene, and forsteritic olivine—and by variable preservation with common dissolution of olivine and pyroxene.

Results: 170 spherules were sectioned and characterized. Bulk chemical analyses used a grid of ~20, 10 μm microprobe spots. Data have a large compositional range, some of which might be biased by alteration or fractional crystallization, but we are convinced that much of the variability is inherent to the precursor liquid droplets. For example, in a largely glassy spherule formed by accretion of at least five droplets, individual domains have distinct compositions. The clearest trend is a strong correlation between Ca, Al, and Ti across a large range of concentrations. High Ca, Al in some spherules might reflect source components with a high anorthite content, but that does not explain the high Ti. Spherules with the highest Ca, Al, Ti are entirely glass and translucent. The most extreme composition (23% CaO, 37% Al_2O_3, 21% SiO_2) can't be derived by melting anorthite. This trend likely reflects formation of refractory droplets by distillation or early condensation. One of the most interesting and significant elements is Na (first noted by Margolis et al. 1991; *Sci.* 251:1597), because it is not involved in crystallization, and must be derived directly from the seawater target. With Na_2O ranging from 0.2 to 10% and no correlation with other elements, Na is our best measure of projectile-target mixing, but might also be excluded from the highest temperature liquids.

5086

IN-DEPTH STUDIES OF ^{14}C, ^{10}Be, ^{36}Cl, AND ^{26}Al IN THREE LUNAR SOILS AND ONE ROCK: IMPLICATIONS FOR SOLAR-WIND IMPLANTATION

D. Lal[1], A. J. T. Jull[2], L. R. McHargue[2, 3], D. L. Biddulph[2], G. S. Burr[2], and S. Freeman[3]. [1]Scripps Institution of Oceanography, La Jolla, CA 92093–0244, USA. [2]NSF Arizona AMS Facility, The University of Arizona, Tucson, AZ 85721, USA. [3]Scottish Universities Environmental Research Centre, East Kilbride G75 0QU, UK. E-mail: dlal@ucsd.edu.

Introduction: The lunar surface is bombarded with galactic cosmic radiation, and several types of solar radiation: solar wind and more energetic solar particles, including MeV range solar cosmic radiation, all of which have been extensively studied in previous work. We have now extended our previous studies of implanted radioactive ions, ^{14}C and ^{10}Be [1, 2] from solar wind of, and include ^{26}Al and ^{36}Cl in three lunar surface soil samples (10084,1956; 15601,49 and 73221,70), and one rock surface (74275,242). We note that implanted solar ^{10}Be has been studied previously by Nishiizumi and Caffee [3] in a lunar surface soil, 78481 and compared to a buried soil, 78421.

Experimental: We have carried out successive HF etchings of the samples to determine the implanted solar ions from solar wind [2, 3]. In the case of two samples, 10084,1956 and 15601,49, we also separated light and heavy density fractions and analyzed them for the 4 nuclides. The concentrations of the radionuclides ^{14}C, ^{10}Be, and ^{26}Al were determined following standard radiochemical procedures, using the AMS at the Arizona Accelerator Mass Spectrometry Laboratory. The ^{36}Cl measurements were made at the Scottish Universities Environmental Research Centre.

Results: Except in the case of ^{36}Cl, the results for the bulk surface soils show that the first two etches with weak HF (0.12 N) release inappreciable amounts of ^{14}C, ^{10}Be, and ^{26}Al. Appreciable release occurred in the third etch, similar to results found in earlier experiments [1, 2]. The heavy fractions of 10084,1956 and 15601, 49 behave similarly, but the situation is appreciably different for the light fraction of 10084,1956. The differential release pattern is quite different in the case of ^{36}Cl, with an appreciable amount released in the first HF etch in all samples.

Summary: The results for differential release of ^{14}C, ^{10}Be, ^{26}Al, and ^{36}Cl are presented along with their "total" concentrations in the surface soil samples. We also compare the results with those obtained for ^{14}C and ^{10}Be in earlier studies [1–3]. The appreciable release of ^{14}C and ^{10}Be in the case of the light fraction of 10084,1956 is suggestive that the appreciable release observed generally in the third leach might represent implantation of a higher energy component of these nuclides. We interpret those data to mean that the nuclides are implanted to a depth of a few microns in the lunar samples, consistent with "solar energetic particles" [4] or higher-energy solar wind ions [5].

References: [1] Jull A. J. T., Lal D., and Donahue D. J. 1995. *Earth and Planetary Science Letters* 136:693–702. [2] Jull A. J. T. et al. 2000. *Nuclear Instruments and Methods in Physics Research B* 172:867–872. [3] Nishiizumi K. and Caffee M. 2001. *Science* 294:352–354. [4] Benkert J. P. et al. 1993. *Journal of Geophysical Research* 98(E7):13,147–13,162. [5] Wieler R. et al. 2006. *Meteoritics & Planetary Science* 41:A188.

5136

THERMAL EMISSION SPECTROSCOPY OF SYNTHETIC OLIVINES: FAYALITE TO FORSTERITE

M. D. Lane[1] and M. D. Dyar[2]. [1]Planetary Science Institute. USA. E-mail: lane@psi.edu. [2]Mount Holyoke College, USA.

Introduction: Although most terrestrial, mafic igneous rocks have olivine compositions of approximately $Fo_{60–86}$, extraterrestrial olivines such as those from Martian and lunar meteorites, along with other achondrites, have wider compositional ranges of olivine and different mean compositions. Chondritic olivine is mostly forsterite ($Fo_{>90}$; Mg_2SiO_4), although some meteorites contain both forsterite and fayalite (Fe_2SiO_4). In almost all occurrences, olivine compositions are restricted to the solid solution series between forsterite and fayalite, with very little substitution by other cations. It is well known that the changes in chemistry across this binary series are correlated with changes in the unit cell parameters, crystal field spectra, and optical properties (refractive index, 2V, and density). The physical and chemical variations within the olivine series also affect the appearance of their thermal infrared emissivity spectra (2000–240 cm^{-1}; 5–42 μm) that are governed by the vibrations of the constituent molecules.

Samples and Methods: Olivine samples synthesized by Donald Lindsley were used for this thermal emission study. For a comprehensive discussion regarding the sample synthesis technique and their compositions, see [1]. The samples vary in composition from forsterite (Fo_{100}) to fayalite (Fo_0) and include the intermediate compositions $Fo_{89.5}$, Fo_{80}, Fo_{75}, Fo_{70}, Fo_{65}, Fo_{55}, Fo_{50}, Fo_{40}, Fo_{30}, Fo_{20}, and Fo_{10}. Eleven of the 13 samples were very small (<5 mm diameter) and the spot size of the spectrometer approximates the same spot size (or is a bit larger); therefore, it was necessary (except for Fo_{75} that was placed perfectly) to divide the calibrated emissivity spectrum of these samples by an emissivity spectrum of an empty sample cup (a blank) to return a representative mineral spectrum with enhanced spectral contrast. Two samples (Fo_{70} and $Fo_{89.5}$) were larger in diameter (~1 cm; synthesized and pelletized later) and produced clean spectra without having to divide out the background cup. For all 13 samples, sufficient-quality emissivity spectra were acquired to enable spectral trends to be studied and the band emissivity minima to be identified.

Results: Nine bands are present in the spectra of all of the olivine compositions (the forsteritic spectra show an additional four). All nine bands systematically transition to lower wavenumbers (longer wavelengths) with decreasing Mg content (increasing Fe). Previous works (e.g., [2–4]) show this relationship as well, but for transmission IR spectra of Fe-Mg olivines.

Conclusions: Our findings suggest that thermal emissivity spectra systematically change from one end-member to the other in the Mg-Fe olivine system, and that each spectrum is diagnostic of the chemistry of the sample. The emissivity spectra resulting from this study will enable the compositions of unknown Mg-Fe olivines to be identified on celestial bodies or in meteorites.

Acknowledgments: The olivine sample powders were pressed into pellets by Tim Glotch at Caltech.

References: [1] Dyar M. D. et al. *American Mineralogist*. Forthcoming. [2] Duke D. A. and Stephens J. D. 1964. *American Mineralogist* 49:1388–1406. [3] Burns R. G. and Huggins F. E. 1972. *American Mineralogist* 57:967–985. [4] Farmer V. C. 1974. In *The infrared spectra of minerals*. London: Mineralogical Society. pp. 285–303.

5236

A NEW FACILITY FOR THE DETERMINATION OF COSMIC-RAY EXPOSURE AGE IN SMALL EXTRATERRESTRIAL SAMPLES BY USING ^{81}Kr-Kr DATING METHOD

B. Lavielle, E. Gilabert, and B. Thomas. University Bordeaux 1-CNAB–CNRS–Chemin du Solarium, BP 120, 33175 GRADIGNAN Cedex, France. E-mail: lavielle@cenbg.in2p3.fr.

The dating method ^{81}Kr-Kr based on Kr isotopic abundance is considered as one of the most reliable method for measuring the cosmic-ray exposure ages of meteorites (CRE) [1]. This method has the great advantage to not require absolute concentration measurements and also it allows self-correction for shielding by using ^{78}Kr/^{83}Kr for example. In iron meteorites CRE dating is an important tool for studying variations of galactic cosmic rays in the past and complex irradiation histories [2]. The ^{81}Kr abundance is typically 500,000 atoms/g in chondrites [3]. and about 2 to 3 times lower in iron meteorites [4] depending on abundances of the target elements producing Kr in irons (Mo, Ru, Rh). Due to difficulty to resolve ^{81}Br interferences in conventional mass spectrometers even with extremely low background, measurements of such low concentrations normally required large samples of several hundreds mg. A new mass spectrometer has been built at CNAB for measuring very small Kr abundances. This instrument consists of a resonant ionization ion source, a cryogenic sample concentrator and a time-of-flight mass analyzer [5]. It is based on a similar design than the instrument developed at IRIM, Knoxville, University of Tennessee [6, 7] or than the "RELAX" spectrometer operating at Manchester University [8, 9].

We report new measurements of cosmogenic Kr performed in a 60 mg sample of Arlington (IIE) iron meteorite and in a 92 mg sample of Boguslavka (IIA). CRE ages based on ^{81}Kr-Kr have been determined with less than 20,000 atoms of ^{81}Kr and are respectively 163 ± 25 Ma and 56 ± 8 Ma, in good agreement with those previously obtained by using ^{36}Cl-^{36}Ar pair [9]. Several iron meteorite samples are currently under investigation.

Acknowledgements: The CNAB project was financially supported by ANDRA, by the Région Aquitaine (France), by CNRS (GdR FORPRO, Chemistry and SDU-INSU Departments), and by the University Bordeaux 1. We thank particularly N. Thonnard (Institute of Rare Isotope Measurement, Knoxville, University of Tennessee) for his very fruitful collaboration and Jamie Gilmour (SEAES, University of Manchester) for sharing with us his great expertise in the field of RIS-TOF technique.

References: [1] Marti K. 1967. *Physical Review* 18:264. [2] Lavielle B. et al. 1999. *Earth and Planetary Science Letters* 170:93–104. [3] Eugster O. 1988. *Geochimica et Cosmochimica Acta* 52:1649–1662. [4] Lavielle B. et al. 1997. *Meteoritics & Planetary Science* 32:97–107. [5] Lavielle B. et al. *Meteoritics & Planetary Science* 41:A104. [6] Thonnard N. et al. 1987. NIM B29:398–406. [7] Lehmann B. E. et al. 1991. *Applied Geochemistry* 6:419–423. [8] Gilmour J. D. et al. 1991. *Measurement Science and Technology* 2: 589–595. [9] Gilmour J. D. 1994. *Review of Scientific Instruments* 65:617–625. [10] Lavielle B. et al. 1999. *Meteoritics & Planetary Science* 34:A72.

5198

MACRO-CHONDRULES IN GHUBARA L5 CHONDRITE

A.-Y. Lee and B.-G. Choi. Department of Earth Science Education, Seoul National University, Seoul 151-748, South Korea. E-mail: aeryon2@snu.ac.kr.

Introduction: Typical sizes of chondrules in ordinary chondrites are 0.1–3 mm in diameter, however, larger chondrules are not uncommon (e.g., [1, 2]). We examined 3 polished slabs of Ghubara L5 chondrites (total area is about 95 cm^2) and found six chondrules larger than 3 mm in diameter. Here we report petrological characteristics of two of them and the others also will be presented in the meeting. One of them is barred olivine pyroxene chondrule and the other is pyroxene-silica chondrule.

Ghubara L5 Chondrite: Ghubara is the one of the first meteorites found in hot desert of Oman and relatively fresh compared with other desert meteorites [3]. The specimen we observed has chondrules all flattened in the same direction, possibly by impact [4]. Majority of chondrules are similar to those of other ordinary chondrites in size and a few larger chondrules are easily recognized on the surface of polished slabs.

Barred Olivine Pyroxene Macro-Chondrule: Bridges et al. [1] examined 833 ordinary chondrites and found 36 macro-chondrules (>5 mm in diameter). Ruzicka et al. [2] found 10 macro-chondrules from Julesberg (L3) and other 8 ordinary chondrites. Three of them are barred olivine pyroxene chondrule.

The barred olivine pyroxene macro-chondrule in Ghubara has ellipsoidal shape and the size is 3 × 4 mm on the slab. It consists of olivine (Fa_{24}), low-Ca pyroxene (Fs_{20}), and plagioclase (An_{88}) with minor amount of troilite and chromite. The chondrule is entirely surrounded by a thick Fe-Ni metallic rim (~200 μm in thickness). It seems that a barred olivine pyroxene texture is abundant among macro-chondrules.

Pyroxene-Silica Macro-Chondrule: Silica-bearing chondrules and clasts have been previously found in several ordinary chondrites [5, 6]. Brigham et al. [5] divided silica-bearing chondrules and clasts in unequilibrated ordinary chondrites into two types: silica, low-Ca assemblages and silica, fayalite intergrowths. They stated that only the former types are chondrules.

The pyroxene-silica macro-chondrule found in Ghubara also has an ellipsoidal shape and the size is 2.5 × 4 mm. It consists of silica and low-Ca pyroxene (Fs_{20}) overgrown by high-Ca pyroxene (Fs_8, Wo_{43}) along the grain boundaries. It can be divided into silica-rich core and mantle with little silica. Low-Ca pyroxene grains are typically 200 or 300 μm in diameter and the high-Ca pyroxene overgrowth has 10–50 μm in thickness. Silica occurs interstitially and has an irregular and elongated shape (width up to 100 m and as long as 600 μm). Small silica grains are also found in pyroxene and small high-Ca pyroxene grains occurs inside of silica.

References: [1] Bridges J. C. and Hutchison R. 1997. *Meteoritics & Planetary Science* 32:389–394. [2] Ruzicka A. et al. 1998. *Geochimica et Cosmochimica Acta* 62:1419–1442. [3] Grady M. M. 2000. Cambridge University Press. 696 p. [4] Nakamura T. et al. 2000. *Icarus* 146:289–300. [5] Brigham C. A. et al. 1986. *Geochimica et Cosmochimica Acta* 50:1655–1666. [6] Bridges J. C. et al. 1995. *Meteoritics* 30: 715–727.

5034

ELEMENTAL AND Xe ISOTOPIC STRUCTURES IN ENSTATITE METEORITES

Jee-Yon Lee[1], John F. Wacker[2], and Kurt Marti[1]. [1]Department of Chemistry and Biochemistry, University of California San Diego, La Jolla, CA 92093–0317, USA. E-mail: jiyonlee@ucsd.edu. [2]Pacific Northwest National Laboratory, P.O. Box 999, Richland, WA 99352, USA.

Introduction: Enstatite meteorites are known for their highly reduced mineralogy and isotopic systematics of oxygen which agree with those of the Earth and moon [1], which suggest an origin in the inner solar system. Regarding possible present locations in the asteroid belt, Gradie and Tedesco [2] reported that enstatite chondrites are consistent with characteristics of E type asteroids which are located at the inner edge of the belt. Spurný et al. [3] have determined the atmospheric trajectory and orbit of the Neuschwanstein meteorite (EL6) from the photographic records and deduced an orbit which is not compatible for E type asteroids and almost identical to the orbit of H5 Příbram. A Martian interior Xe isotopic structure (Chass-S), a reservoir in the inner solar system, is consistent with solar Xe. Solar-type gas has been observed in only type 3, 4 enstatite chondrites, but the isotopic structures of Xe are poorly known.

Results and Discussion: We report Xe isotopic abundances in clasts and in separates of the Abee enstatite chondrite breccia and compare the isotopic structures to those reported for other enstatite meteorites in order to further constrain the Xe reservoirs in the inner solar system. The Abee-Xe isotopic structures are very uniform in all clasts and are consistent, except for ^{128}Xe and ^{129}Xe, with OC-Xe and also with the Q-Xe signature. Excesses on these two isotopes are due to cosmic ray neutron reactions and extinct ^{129}I, respectively. The trapped Xe isotopic abundances in the Pesyanoe enstatite achondrite, as well as in Ar-rich (subsolar) enstatite chondrites are consistent with variable mixtures of Abee-Xe and of solar-type Xe. A model based on implantation of solar gas in accreting matter was suggested for the origin of the Venus atmosphere [4]. We calculate ratios of retentions of $^4He_{tr}$, $^{20}Ne_{tr}$, and $^{36}Ar_{tr}$ and compare these to "Ar-rich" components in enstatite chondrites [5, 6] at the temperature of 670 K (Mercury), using the IDP and chondrite diffusion data [7, 8]. All "Ar-rich" E chondrites have characteristic ratios $^{36}Ar_{tr}/^{20}Ne_{tr} > 20$ and no evidence for solar ^4He components ($^4He_{tr}/^{20}Ne_{tr} << 0.1$). The loading of solar particles could have occurred either during exposure on surfaces of planetesimals at elevated temperatures or into (differentiated) re-accreting inner solar system materials. The parent objects of enstatite meteorites may have been moved, similar to the case of irons [9], into more stable orbits in the asteroid belt. Support of collisions in the inner solar system and orbit evolutions were reported by Yang et al. [10].

References: [1] Clayton R. N. et al. 1984. Proceedings, 15th Lunar Planet. Sci. Conf. pp. 245–249. [2] Gradie J. and Tedesco E. 1982. *Science* 216:1405–1407. [3] Spurný P. et al. 2003. *Nature* 423:151–153. [4] Wetherill G. W. 1981. *Icarus* 46:70–80. [5] Patzer A. and Schultz L. 2001. *Meteoritics & Planetary Science* 37:947–961. [6] Schultz L. and Franke L. 2002. A Data Collection. MPI, Mainz. [7] Hiyagon H. 1994. *Science* 263:1257–1259. [8] Fechtig H. and Kalbitzer S. 1966. *Potassium-argon dating.* Springer. p. 68. [9] Bottke W. F. et al. 2006. *Nature* 439:821–824. [10] Yang J. et al. 2007. *Nature* 446:888–891.

5042

TITANIUM ISOTOPE HETEROGENEITIES IN THE SOLAR SYSTEM

I. Leya[1], M. Schönbächler[2], U. Wiechert[3], U. Krähenbühl[4], and A. N. Halliday[5]. [1]Physical Institute, University of Bern, Switzerland. E-mail: Ingo.Leya@space.unibe.ch. [2]Department of Earth Sciences & Engineering, Imperial College, London, UK. [3]Institut für Geologische Wissenschaften, Freie Universität Berlin, Germany. [4]Laboratory for Radiochemistry. [5]University of Bern, Switzerland. [5]Department of Earth Sciences, University of Oxford, UK.

Introduction: The solar system, as sampled by meteorites, is relatively homogeneous isotopically, indicating efficient mixing of the material from the precursor molecular cloud. Usually, the preservation of isotopic heterogeneities is attributed to lack of equilibration of presolar grains and/or some refractory condensates with gas and dust of average solar composition. Nucleosynthetic isotope anomalies in bulk chondrites have been measured for O, S, Ti, Cr, Mo, Ru, Ba, Sm, Nd, and some noble gases. However, among these elements, Ti forms one of the most refractory oxides and is therefore well suited for studies of early solar system heterogeneities.

Experimental: Sample preparation, chemical separation, and MC-ICPMS measurements follow the procedure described in [1]. We studied five lunar whole-rock samples and various mineral separates from high-Ti mare basalts, a lunar norite, a forroan anorthosite, and an olivine-normative mare basalt. In addition, we studied bulk samples from four carbonaceous chondrites, three ureilites, two eucrites, one ordinary chondrite, one mesosiderite, and one Martian meteorite. Finally, we analyzed leachates from Allende and mineral separates from Renazzo.

Results: The Ti data for lunar whole-rock samples and mineral separates are, except one, normal within the uncertainties, indicating that Earth and Moon have the same Ti isotope composition. Normal Ti isotope compositions are also observed for the Martian meteorite, the mesosiderite, the ordinary chondrite, the eucrites, and the ureilites, indicating that all these objects (together with Earth and Moon) formed from material with a homogeneous Ti isotope composition. This result is consistent with Zr data, for which no anomalies were found either [2]. However, a variety of authors have reported variations in Cr, Mo, Ba, Sm, and Nd in bulk rock meteorites, although some of the variations are restricted to p-nuclides and some are not yet well defined (e.g., [3–9]). In contrast to the data for ordinary chondrites, eucrites, ureilites, and mesosiderites, the results for whole-rock samples from the carbonaceous chondrites Allende (CV), Orgueil (CI), and Renazzo (CR) clearly indicate that large-scale heterogeneity exists in the Ti isotope composition in the solar system. Since leach experiments and mineral separation have shown that anomalous Ti is not confined in phases in refractory inclusions, we propose scenarios in which presolar grains were not homogeneously distributed in the solar nebula.

References: [1] I. Leya et al. 2007. *International Journal of Mass Spectrometry* 262:247–255. [2] M. Schönbächler et al. 2003. *Earth and Planetary Science Letters* 216:467–481. [3] Shukolyukov A. and Lugmair G. W. 1998. *Science* 282:927–929. [4] Podosek F. A. et al. 1999. Abstract #1307. 30th Lunar and Planetary Science Conference. [5] Podosek F. A. et al. 1997. *Meteoritics & Planetary Science* 32:617–627. [6] Yin Q. Z. et al. 2000. Abstract #1920. 31st Lunar and Planetary Science Conference. [7] Dauphas N. et al. 2002. *The Astrophysical Journal* 565:640–644. [8] Ranen M. C. and Jacobsen S. B. 2006. *Science* 314:809–812. [9] Andreasen R. and Sharma M. 2006. *Science* 314:806–809.

5169

NWA 4518: THE METAL-RICH UNGROUPED ACHONDRITE

C. Lorenz[1], F. Brandstätter[2], I. Franchi[3], and R. Greenwood[3]. [1]Vernadsky Institute of Geochemistry and Analytical Chemistry, Kosygin St. 19, Moscow, 119991, Russia. E-mail: c-lorenz@yandex.ru. [2]Naturhistorisches Museum, Postfach 417, A-1014, Vienna, Austria. [3]PSSRI, Open University, Walton Hall, Milton Keynes MK7 6AA, UK.

Introduction: The NWA 4518 is metamorphosed ultramafic breccia with silicate compositions close to that of HED meteorites. However, the high FeNi metal content and oxygen isotopes composition place NWA 4518 far from known achondrites.

Results: The achondritic rock has a fine- to medium-grained, equigranular texture displaying triple junctions. The main phases are homogeneous olivine $Fo_{68.0}$ (Fe/Mn = 35.6; CaO 0.06; Cr_2O_3 0.04 wt%) (80 vol%), clinopyroxene $En_{44.7}Wo_{42.3}$ (Fe/Mn = 29.4) and orthopyroxene $En_{77.7}Wo_{1.2}$ (Fe/Mn = 42; CaO 0.59; Cr_2O_3 0.12 wt%). The millimeter-size megacrysts of Ol and Px also occur in the rock. The 1 cm crystal of pyroxene $En_{72.1}Wo_{2.3}$ (Fe/Mn = 37.4), contains of 100–200 μm poikilitic inclusions of olivine $Fo_{80.6}$ (Fe/Mn = 38.4), FeNi metal and chromite. The similar smaller megacrysts also were found. Minor phase of meteorite is FeNi metal (2 vol%; 5.7 wt% Ni; Ni/Co = 9.1). It forms angular grains, interconnected by a network of thin metal veinlets. Some of kamacite grains demonstrate weak but distinct heterogenity in Ni and Co. The finest rounded and lamellar inclusions of taenite occur within kamacite. The largest taenite lamellae demonstrate the M-shaped profile of Ni content from the 25 to 14 wt%. The chromite, troilite, and co-existing Cl-apatite and merrilite are rare phases. Chromite (Cr/(Cr + Al) = 0.83; Cr/(Cr + Fe) = 0.71) contains poikilitic inclusions of olivine, pyroxene, FeNi metal (Ni 1.5 wt%) and Ni-bearing sulfides (Ni 3.2–26.5 wt%). Along the veinlets of troilite crosscutting the rock, olivine grains are replaced by fine-grained aggregate of troilite and pyroxene $En_{83.3}Wo_{0.92}$ (Fe/Mn = 19.2). Oxygen isotopes composition of NWA 4518 is $\delta^{17}O = 2.66‰$, $\delta^{18}O = 5.47‰$.

Discussion: The NWA 4518 is a metamorphosed polymict breccia consisting of dunite and orthopyroxenite fragments. The Fe/Mn ratio, CaO and Cr_2O_3 contents of olivine and low-Ca pyroxene are correspond to those of HED [1]. The FeNi inclusions within orthopyroxene megacrysts could have an igneous origin and could indicate the co-crystallization of orthopyroxene, chromite and FeNi metal from the unusual metal-rich melt. The pyroxene megacrysts could be also a source of metal grains occurring in the breccia. The meteorite is depleted in feldspar component that could be a result of silicate fractionation. The opaque veins formed after the breccia joining, could have an impact origin. The oxygen isotopes composition of NWA 4518 is different from that of HED and close to aubrite field. The NWA 4518 probably formed on the parent body that is different from those of known meteorites. Now we continue this study and initialize investigation of a new meteorite, basaltic melt breccia that have exactly the same oxygen isotopes composition as that of NWA 4518, and could be its feldspar-rich complement.

References: [1] Mittlefehldt D. W. et al. 1998. In *Planetary materials*. p. 195. [2] Clayton R. N. and Mayeda T. K. 1996. *Geochimica et Cosmochimica Acta* 60:1999–2018.

5208

SOLAR WIND ARGON FROM GENESIS ALOS REGIME COLLECTORS

J. C. Mabry[1], A. P. Meshik[1], C. M. Hohenberg[1], Y. Marrocchi[1], O. V. Pravdivtseva[1], J. Allton[2], K. McNamara[3], E. Stansbery[3], and D. S. Burnett[4]. [1]Washington University, Physics Department, St. Louis, MO 63130, USA. E-mail: jcmabry@wustl.edu. [2]Lockheed Martin c/o NASA/JSC, Mail Code KT, Houston, TX 77058, USA. [3]NASA/JSC, Mail Code KA, Houston, TX 77058, USA.[4]Geology 100-23, Caltech, Pasadena, CA 91125, USA.

Introduction: Determining solar noble gas isotopic ratios are one piece of the puzzle needed to constrain models of the evolution of terrestrial planets, as well as to understand solar composition and processes. Solar wind (SW) remains the best available source of solar material, even though there is potential for fractionation between true solar values and the solar wind. Here we will focus on SW argon.

In 1974 Cerutti analyzed Apollo SWC foils and found a $^{36}Ar/^{38}Ar$ ratio that could not be resolved from the terrestrial value of 5.3 [1]. But with examination of lunar soils, a difference between solar and terrestrial Ar emerged. Unfortunately, analysis of these soils produced varying results, from 5.48 [2] to 5.80 [3]. With Genesis Aluminum on Sapphire (AloS) samples, we are now able to precisely define the solar wind value and clearly differentiate it from the terrestrial value.

Results: Previously reported Ar data [4] are now confirmed by additional measurements. These measurements were made using samples of bulk SW and the three individual SW flow regimes: interstream SW (low-speed), coronal hole SW (high-speed), and coronal mass ejections (CME). The averages of the isotopic ratio, ^{36}Ar flux, and $^{20}Ne/^{36}Ar$ ratio for each regime are given in the table below. Errors shown for $^{36}Ar/^{38}Ar$ ratios are 1σ statistical errors; for the ^{36}Ar flux and $^{20}Ne/^{36}Ar$ ratios, the numbers in parentheses are uncertainties based on the spread in the measured amounts ^{36}Ar and ^{20}Ne.

Table 1.

Sample	$^{36}Ar/^{38}Ar$	^{36}Ar flux ($10^6/m^2 \cdot s$)	$^{20}Ne/^{36}Ar$
Bulk SW	5.501 ± 0.005	3.81 (0.2)	59 (5)
High-speed	5.502 ± 0.010	2.78 (0.1)	66 (6)
Low-speed	5.508 ± 0.010	3.63 (0.4)	46 (5)
CME	5.467 ± 0.017	3.68 (0.8)	59 (4)
Terr. atm. [5]	5.319 ± 0.008	–	0.524
Terr. atm. [6]	5.305 ± 0.008	–	–

Discussion: These results define the bulk SW $^{36}Ar/^{38}Ar$ ratio to be 5.501 ± 0.005, (with similar precision as the terrestrial value), which is 3.40 ± 0.09% lighter than terrestrial atmospheric Ar. This has implications for atmospheric retention models. Coulomb Drag Theory predicts a small isotopic fractionation between the low- and high- speed SW regimes [7]. Our data restricts this to less than 0.6% for the $^{36}Ar/^{38}Ar$ ratio. Differences between the flow regimes of the $^{20}Ne/^{36}Ar$ ratio suggest elemental SW fractionation, with the low-speed SW ~25% heavier than the other regimes. This probably reflects differences in the efficiency of the FIP effect in the different SW flow regimes.

Acknowledgements: Supported by NASA grants NNJO4HI17G and NAG5-12885.

References: [1] Cerutti H. 1974. Ph.D. thesis. [2] Benkert J. et al. 1993. *Journal of Geophysical Research* 98:13147–13162. [3] Palma R. et al. 2002. *Geochimica et Cosmochimica Acta* 66:2929–2958. [4] Mabry J. et al. 2006. *Meteoritics & Planetary Science* 41:A109. [5] Nier A. 1950. *Physical Review* 77:789–793. [6] Lee J. et al. 2006. *Geochimica et Cosmochimica Acta* 70: 4507–4512. [7] Bodmer R. et al. 1998. *Astronomy & Astrophysics* 337:921–927.

5154

DISTRIBUTION OF Al-Mg MODEL AGES FROM INDIVIDUAL MINERALS IN A SPINEL-BEARING CHONDRULE FROM ALLENDE

K. Makide[1, 2], S. Itoh[2], S. Maruyama[3], M. Yoshitake[4], and H. Yurimoto[2]. [1]HIGP, University of Hawai'i at Manoa. USA. E-mail: makide@higp.hawaii.edu. [2]Hokkaido University, Japan. [3]Okayama University, Japan. [4]Kobe University, Japan.

The timing of formation and thermal processing of chondrules plays an important role in models of early solar system evolution. The inferred uniform distribution of short-lived radionuclide ^{26}Al in the inner solar system [1] makes ^{26}Al-^{26}Mg systematics a powerful relative chronometer of the nebular and early asteroidal processes. Al-Mg isochrons in chondrules are commonly defined by the phases with low Mg contents (glass and anorthite). Although Al-Mg systematics in these phases can be easily disturbed during thermal metamorphism, resulting in Mg-isotope equilibration and lower $(^{26}Al/^{27}Al)_0$ [2–4], a degree of this disturbance is difficult to evaluate quantitatively. In contrast, Mg-isotopic resetting in spinel occurs by Mg-self-diffusion, the speed of which is similar to that of Fe-Mg intradiffusion; the latter can be easily detected in thermally metamorphosed chondrites (petrologic type >3.2) and quantitatively evaluated using compositional profiles [5]. Fe-free regions of spinel crystals must preserve their original Mg-isotopic compositions. Spinel is often a liquidus phase in igneous CAIs [6] and Al-rich chondrules [7] and can be used to date their crystallization age.

Experimental: Mg-isotopic compositions of chondrule spinel were measured with the TiTech Cameca IMS 1270 ion probe by a mono-collector Faraday cup; spot size of primary O^{2-} beam was ~30 μm. Spinel from Russia and augite from Takashima were used as standards for determination of terrestrial isotope ratios of Mg and of the instrumental mass fractionation and the matrix effects. Assuming a reference values for $^{25}Mg/^{24}Mg$ as 0.12663 [8], the $^{26}Mg/^{24}Mg$ are determined as 0.1393611 ± 0.0000099. The deviation in the measured $^{26}Mg/^{24}Mg$ ratio from the reference value was obtained by observed mass fractionation factor under an assumption of linear mass fractionation law: $\Delta^{25}Mg = 0.51622 \times \Delta^{26}Mg$, where $\Delta^{25,26}Mg = [\{(^{25,26}Mg/^{24}Mg)_m/(^{25,26}Mg/^{24}Mg)_{ref}\}-1] \times 1000$. Precision of $^{26}Mg^*$ measurements in spinel is <0.4‰.

Results: The Allende BO chondrule A1-2b-1 (A1) consists of olivine, low-Ca pyroxene, feldspathic mesostasis, and a coarse (200 μm), Fe-free spinel grain. A regression of six measurements from the spinel show $^{26}Mg^*$ corresponding to the initial $^{26}Al/^{27}Al$ ratio of $(1.50 \pm 0.70) \times 10^{-5}$ (forced through the origin). O-isotopic compositions of spinel in A1 reported by [9] is ^{16}O-depleted ($\Delta^{17}O = -7.1 \pm 0.9$‰) relative to those from the Allende CAIs. We infer that spinel crystallized from the host chondrule melt and is not a relict CAI grain. The inferred $(^{26}Al/^{27}Al)_0$ in spinel corresponds to the crystallization time of the host chondrule: ~1.25 My after formation of CAIs with the canonical $(^{26}Al/^{27}Al)_0$ of $\sim 5 \times 10^{-5}$. In contrast, the feldspathic mesostasis in A1 shows no resolvable $^{26}Mg^*$ ($[^{26}Al/^{27}Al]_0 = [1.6 \pm 9.8] \times 10^{-6}$) [9]; this may reflect disturbance of Al-Mg systematics in mesostasis during fluid-assisted thermal metamorphism. Our results indicate that Al-Mg systematics in spinel can be used to constrain crystallization time of chondrules from meteorites experienced thermal metamorphism. It seems plausible that relict spinel grains in chondrules may have preserved $(^{26}Al/^{27}Al)_0$ of their source materials (chondrules of earlier generations or CAIs).

References: [1] Bizzarro M. et al. 2004. *Nature* 431:275. [2] MacPherson G. J. et al. 1995. *Geochimica et Cosmochimica Acta* 30:365. [3] Yurimoto H. et al. 2000. Abstract #1593. 31st LPSC. [4] Huss G. R. et al. 2001. *Meteoritics & Planetary Science* 36:975. [5] Wasson et al. 2001. *Geochimica et Cosmochimica Acta* 65:4539. [6] Stolper E. 1982. *Geochimica et Cosmochimica Acta* 46:2159. [7] Sheng Y. J. et al. 1992. *Geochimica et Cosmochimica Acta* 56:2535. [8] Catanzaro E. et al. 1966. *Journal of Research of the National Institute of Standards and Technology* 70A:453. [9] Maruyama S. et al. 2003. *Geochimica et Cosmochimica Acta* 67:3943.

5109

MAGNESIAN ANORTHOSITIC CLASTS IN LUNAR METEORITES ALHA81005 AND DHO 039: BULK COMPOSITIONS AND REGIONAL SIGNIFICANCE

A. K. Maloy[1] and A. H. Treiman[2]. [1]Rice University, USA. [2]Lunar and Planetary Institute, Houston, TX, USA. E-mail: treiman@lpi.usra.edu.

Introduction: Lunar meteorites Allan Hills A81005 and Dhofar 309 (the former a regolith breccia, the latter a clast-laden impact melt) contain clasts of magnesian anorthositic troctolitic rock with nearly identical chemical compositions. As these meteorites are not source-paired, magnesian anorthositic troctolite may be a widespread rock composition on the lunar farside (Feldspathic Highland Terrane) [1–3].

Methods: EMP and SIMS were used to obtain major and trace element abundances for five magnesian anorthositic clasts. Mineral proportions were calculated from EMP X-ray maps using computer codes for multispectral image analyses [4]. Bulk clast compositions were then calculated from mineral analyses and mineral proportions.

Results: The magnesian anorthositic clasts in ALHA81005 and Dho 309 are chemically similar: Mg′ (molar Mg/[Mg+Fe]) = 81–87, ~5% FeO, ~21–24% Al_2O_3, Eu at ~10 × CI, and other rare earth elements (REEs) at 0.5–2 × CI [5]. Takeda et al. [6] describe similar clasts in Dho 489, which is paired with Dho 309. Ni and Co abundances are low, and Ni/Co = 0.04–0.2 × CI suggest limited chondritic (meteoritic) contributions. Cr_2O_3 abundances are variable, from 0.01 to 0.4%. Clasts in ALHA81005 have more TiO_2 than those in Dho 309 (0.15% versus <0.1%).

Implications: Lunar remote sensing and bulk analyses of lunar meteorites show that the lunar crust must include magnesian, feldspathic, REE-poor lithologies that are not represented in the Apollo collections [1–3]. This material dominates the northern lunar farside—an area called the Feldspathic Highlands Terrane. Lunar Prospector gamma-ray data suggest that the FHT averages ~4.5 wt% FeO, ~28 wt% Al_2O_3, and low abundances of Th (less than 1 ppm) and other highly incompatible elements. The magnesian anorthositic clasts analyzed here are reasonable candidates for this composition, although they contain rather less Al_2O_3. ALHA81005 and Dho 309 are not source-paired (i.e., they did not come from the same locality on the Moon), because they have different pre-terrestrial ages [7, 8]. Thus, it seems reasonable that the magnesian anorthositic compositions of these meteorites' clasts is widespread on the Moon, and may represent a common component of the Moon's Feldspathic Highlands Terrane.

References: [1] Jolliff B. L. et al. 2000. *Journal of Geophysical Research* 105:4197–4216. [2] Gillis J. J. et al. 2004. *Geochimica et Cosmochimica Acta* 68:3791–3805. [3] Korotev R. L. et al. 2003. *Geochimica et Cosmochimica Acta* 67:4895–4923. [4] Maloy A. K. and Treiman A. H. *American Mineralogist*. Forthcoming. [5] Maloy A. K. and Treiman A. H. Forthcoming. [6] Takeda H. et al. 2006. *Earth and Planetary Science Letters* 247:171–184. [7] Eugster O. 2003. *Chemie der Erde* 63:3–30 [8] Nishiizumi K. and Caffee M. W. 2006. *Meteoritics & Planetary Science* 41:A133.

5216

THE POTENTIAL EXISTENCE OF ANALOGUE PLEISTOCENE METEORITE PLACERS IN FORMERLY GLACIATED REGIONS OF RUSSIA WHEN COMPARED TO ANTARCTIC METEORITE PLACERS

A. Mardon[1] and M. Zalcik[2]. [1]Antarctic Institute of Canada, P.O. Box 1223, MPO, Edmonton, Alberta, Canada T5J-2M4. E-mail: amardon@shaw.ca. [2]Noctilucent Cloud Canadian-American Network. E-mail: bluegrama@shaw.ca.

The recovery of over 30,000 meteorites from Antarctic placer zones might have analogue areas for paleo-ice concentration from the last glaciation in areas of northern Russia. In 2005, three meteorites were recovered from Manitoba, Canada. It has been proposed that these were concentrated in the same process as the meteorites that have been recovered in Antarctica. If just one non-Antarctic Pleistocene meteorite place zone was recovered in Russia or Canada, it might yield thousands of separate meteorite samples. Billions of dollars are spent on retrieving nonterrestrial geological samples and meteorites for the time being are still a cost-effective way of collecting geological samples from the inner solar system. With minimal cost, regions and sites could be selected for potential searching for meteorites even if only with public media campaigns to make the populace aware that they might find a piece of either the Moon or Mars in their locale. In-depth topographic analyses in analogue with Antarctic meteorite placer zones might indicate potential areas in the Urals zone, Northern Europe, and North America, together with flow model of Pleistocene paleo-ice sheets could indicate areas where important slow down of ice happened. These areas should be important ancient meteorite trap relicts. The northern hemisphere paleo-ice sheets could have represented a great collectors for extraterrestrial material as well as the Antarctica ice sheet represents the most productive region for the discovery of meteorites on Earth nowadays. Beside being well preserved from the terrestrial weathering processes, meteorites are concentrated in specific regions by ice flow dynamics, according to the "ice-flow model." In this model, the extraterrestrial material is embedded within the ice mass and transported downstream from snow accumulation zones; meteorite traps typically are formed in front of submerged or emerged bedrock obstacles, where the meteorite-bearing ice slows down forming areas of stagnant or slow-moving ice. There, a combination of ice deformation and uplift by the buttressing effect and wind ablation is capable of exhuming and concentrating meteorites trapped in the ice. As a consequence, high ablation rates and low surface velocity is the common characteristic of nearly all meteorite traps. The barrier effect could happen where two ice lobes meet together moving in a opposite way, although the lowest surface velocity are recorded in front of a bedrock barrier (submerged or emerged). During the last glaciation, in the northern hemisphere ice caps similar ice flow condition could have developed. The Urals could have represented a great obstacle to the ice moving southward (or south-westward) in a similar way to the Transantarctic Mountains in Antarctica.

References: [1] Mardon A. A. et al. 2006. Possible Pleistocene meteorite placer deposits on the Canadian prairies similar to Antarctic meteorite placers. *Meteoritics & Planetary Science* 41:A112. [2] Mardon A. A. 1988. The detection of Pleistocene meteorite placer located in North America. *Meteoritics* 23:286. [3] Hildebrand A. R. et al. 2006. A possible meteorite lag deposit after continental glaciation in southeastern Manitoba. *Meteoritics & Planetary Science* 41:A77. [2] Zeoli A. 2007. Personal communication.

5274

Fe ISOTOPIC COMPOSITION OF SUPERNOVA GRAINS

K. K. Marhas, S. Amari, F. Gyngard, and E. Zinner. Laboratory for Space Sciences, Physics Department, Washington University, St. Louis, MO 63130, USA. E-mail: kkmarhas@yahoo.com.

Presolar SiC grains from supernovae (type X) have excesses in ^{57}Fe on the order of ~1000‰ [1]. Two interesting points to be noted along with these excesses are: a) ^{56}Fe/^{54}Fe ratios are normal (within 3σ) for all 36 SiC X grains analyzed, and b) 19 grains with excesses in ^{57}Fe contain Fe-Ni rich subgrains. Out of these 19 grains, 10 were also measured for ^{59}Co. During analysis, ^{59}Co counts from the grains were correlated with the Fe and Ni counts indicating that the subgrains are indeed Fe-Ni-Co subgrains.

The ^{57}Fe enrichment in the SN grains can be explained in four different ways. a) Inner SN zone contributions (Ni zone): The presence of ^{44}Ti and ^{49}V in some supernova grains is explained by contributions from the innermost SN zone [2, 3]. This inner zone is dominated by ^{54}Fe [4]; hence, any contribution from this zone to the formation of SiC should result in very high excesses in ^{54}Fe and huge variations in ^{57}Fe, which is not observed. A mixing calculation from the other zones covers the solar value but is unable to explain the observed high ^{57}Fe anomalies as well as close-to-normal ^{56}Fe/^{54}Fe. b) A neutron-burst model was invoked to explain the Mo and Zr isotopic patterns in X grains [5]. Mixing a very small percentage of n-burst material with solar material might be able to explain the ^{57}Fe enrichments. A way to confirm the contribution from the n-burst region is to obtain evidence for the presence of the radionuclide ^{60}Fe expected to be produced in the n-burst. Unfortunately, due to high Ni/Fe ratios, no ^{60}Ni excess was found within errors. c) The weak s-process is thought to occur in massive stars during core He and/or shell C burning. Calculations [6] indicate excesses in both ^{57}Fe and ^{56}Fe relative to ^{54}Fe. Mixing this material with solar material can explain the anomalies obtained by [1]. d) Presence of the radionuclide ^{57}Co: Another possibility to explain ^{57}Fe excesses is incorporation of radioactive ^{57}Co into SiC and in situ decay. ^{57}Co has a half-life of 272 days, which is very similar to that of ^{49}V, and evidence for it has been detected in X grains [3]. If this explanation is true, the initial ^{57}Co/^{59}Co value inferred from 10 X grains range from 0.01 to 0.75, in agreement with theoretical SN models.

References: [1] Marhas K. K. et al. 2007. Abstract # 2124. 38th Lunar and Planetary Science Conference. [2] Nittler L. R. et al. 1996. *The Astrophysical Journal* 462:L31–L34. [3] Hoppe P. et al. 2002. *The Astrophysical Journal* 576:L61–L72. [4] Rauscher T. et al. 2002. *The Astrophysical Journal* 576:323–348. [5] Meyer B. S. 2000. *The Astrophysical Journal* 540:L49–L52 [6] The L.-S. et al. 2007. *The Astrophysical Journal* 655:1058–1078.

5210

INDIGENOUS AMINO ACIDS PRESENT IN CR PRIMITIVE METEORITES

Z. Martins[1], C. M. O'D. Alexander[2], G. E. Orzechowska[3], M. L. Fogel[4], M. A. Sephton[1], and P. Ehrenfreund[5]. [1]Impacts and Astromaterials Research Centre, Department of Earth Science and Engineering, Imperial College, London, UK. E-mail: z.martins@chem.leidenuniv.nl. [2]Department of Terrestrial Magnetism, Carnegie Institution of Washington, Washington, D.C., USA. [3]JPL, California Institute of Technology, Pasadena, CA, USA. [4]Geophysical Laboratory, Carnegie Institution of Washington, Washington, D.C., USA. [5]Astrobiology Laboratory, Leiden Institute of Chemistry, Leiden, The Netherlands.

Introduction: The CR chondrites are thought to contain the most primitive meteoritic insoluble organic material [1, 2], which closely resembles the insoluble organic matter found in the most primitive interplanetary dust particles (IDPs) [2]. However, their soluble organic inventory has not been extensively studied.

Techniques: We have analyzed the amino acid content of the Antarctic CR2s EET 92042 and GRA 95229, and the CR1 GRO 95577 using high-performance liquid chromatography with UV fluorescence detection (HPLC-FD) and gas chromatography-mass spectrometry (GC-MS). Additionally, compound-specific carbon isotopic measurements for most of the individual amino acids from the EET 92042 and GRA 95229 meteorites were achieved by gas chromatography-combustion-isotope ratio mass spectrometry (GC-C-IRMS).

Results: Our results show that the EET 92042 and GRA 95229 meteorites are among the most amino acid-rich carbonaceous chondrites, with total amino acid concentrations of 180 and 249 ppm, respectively [3]. Racemic enantiomeric ratios, as well as the highly enriched δ^{13}C values [3], indicate that primitive organic matter was preserved in these meteorites. The GRO 95577 meteorite, however, is depleted in amino acids (less than 1 ppm). The variation in amino acid abundances among CRs seems to be related to the degree of aqueous alteration they experienced. The same appears to be true for the CMs [3].

To further investigate the soluble organic inventory of CR chondrites, analysis of the amino acid content of MET 00426 and QUE 99177 is currently being carried out. These are the least altered CR chondrites identified to date, based on their mineralogical characteristics [4]. Our analysis indicates that these two CRs also have high total amino acid abundances and amino acid distributions similar to EET 92042 and GRA 95229.

Conclusions: The Antarctic CR2s EET 92042 and GRA 95229 have the highest amino acid abundances ever detected. This suggests that their soluble organic inventories are more primitive than any other chondrites and, therefore, closer to the original material accreted by chondrites. The analysis of the amino acids present in Antarctic CR meteorites will help to reveal the processes that formed the prebiotic organic material in the early solar system that may ultimately have been delivered to the Earth and other planets.

References: [1] Cody G. D. and Alexander C. M. O'D. 2005. *Geochimica et Cosmochimica Acta* 69:1085–1097. [2] Busemann H. et al. 2006. *Science* 312:727–730. [3] Martins Z. et al. *Meteoritics & Planetary Science*. Forthcoming. [4] Abreu N. M. and Brearley A. J. 2006. Abstract #2395. 37th Lunar and Planetary Science Conference.

5054

SPALLATION AND NEUTRON-CAPTURE PRODUCED COSMOGENIC NUCLIDES IN AUBRITES

J. Masarik[1], K. Nishiizumi[2], and K. C. Welten[2]. [1]Department of Nuclear Physics, Comenius University Bratislava, Slovakia. E-mail: masarik@fmph.uniba.sk. [2]Space Sciences Laboratory, University of California, Berkeley, CA 94720, USA.

Introduction: A purely physical model for the simulation of cosmic-ray-particle interactions with matter was used to investigate the production rates of cosmogenic nuclides in aubrites with radii ranging from 5 to 120 cm. Production rates of spallogenic and neutron-capture produced nuclides were investigated and compared with measured cosmogenic nuclide concentrations to constrain the complex exposure histories of aubrites.

Calculational Model: The numerical simulation of interactions of primary and secondary cosmic-ray particles was done with the LAHET Code System (LCS) [1], which uses MCNP [2] for transport of low-energy neutrons. The investigated objects were spheres with various radii that were divided into spherical layers. We used the spectrum of the galactic-cosmic-ray particles corresponding to solar modulation parameter Φ = 550 MeV and a flux of 4.8 protons/s · cm^2. The statistical errors of the LCS calculated fluxes were 3–5%. The production rates of nuclides were calculated by integrating over energy the product of these fluxes and cross sections for the nuclear reactions making the investigated nuclide. For cross sections of spallogenic products, we relied on the values evaluated by us and tested by earlier calculations (e.g., [3]). Previous calculations of the ^{53}Mn production rate in aubrites showed good agreement with measured ^{53}Mn concentrations in the Norton County aubrite [4]. The production rates of nuclides produced by neutron capture reactions were calculated using the excitation functions from neutron evaluated data files ENDF/B-VI [5], which were previously used for calculating neutron-capture ^{41}Ca in the lunar surface [6]. In our previous work, the calculated production rates of neutron capture ^{41}Ca showed excellent agreement with the measured depth profile of ^{41}Ca in the Apollo 15 drill core [6].

Results and Discussion: The depth profiles depend on the shape of the excitation functions producing a nuclide and the particle spectra. These spectra depend on the shielding of the sample, i.e., its location inside the object, and the object's size. In this work we will compare neutron-capture produced ^{41}Ca and spallation produced ^{10}Be and ^{26}Al measured in various aubrites [7] with calculated production rates to constrain the pre-atmospheric size of these aubrites and depth of the measured samples within these objects. In addition, we will compare measured concentrations of neutron-capture ^{41}Ca, ^{150}Sm, and ^{158}Gd [7, 8] with calculated production rates to constrain the 2π and 4π exposure histories of aubrites.

References: [1] Prael R. E. and Lichtenstein H. 1989. LA-UR-89-3014. [2] Briesmeister J. F. 1993. LA-12625-M. [3] Masarik J. and Reedy R. C. 1994. *Geochimica et Cosmochimica Acta* 58:5307–5317. [4] Englert P. A. J. et al. 1995. *Geochimica et Cosmochimica Acta* 59:825–830. [5] McLane V. E. et al. 1991. BNL-NCS-17541. [6] Nishiizumi K. et al. 1997. *Earth and Planetary Science Letters* 148:545–552. [7] Welten K. C. et al. 2004. *Meteoritics & Planetary Science* 39:A113. [8] Hidaka H. et al. 1999. *Earth and Planetary Science Letters* 173:41–51.

5035

MONITORING COSMIC RAY FLUX VARIATIONS USING ^{129}Xe AND ^{131}Xe IN TROILITE SEPARATES OF IRON METEORITES

K. J. Mathew[1], Jee-Yon Lee, and K. Marti. Department of Chemistry and Biochemistry, University of California, San Diego, CA 92093, USA. [1]Present address: Department of Energy, New Brunswick Laboratory, 9800 S. Cass Avenue, Argonne, IL 60439, USA. E-mails: kattathu.mathew@ch.doe.gov; jiyonlee@ucsd.edu.

Introduction: Calibration of the galactic cosmic ray (GCR) fluxes based on determinations of the abundances of cosmic-ray produced radionuclides of different half-lives, coupled with those of associated stable decay product, in iron meteorites have been suggested [1, 2]. The approach has the limitation that a complexity in the CRE ages of irons due to changes in the geometry during the integral exposure time is not accounted. A reevaluation of the constancy of the GCR flux over the last 1 Ga was presented by [3]. Their inferred average production rate of ^{36}Cl was ~28% lower than the present production rate of this nuclide. However, this study does not constrain the time of increase, nor the possibility of a cyclic variation.

Methodology: A recent flux increase can be calibrated in more detail by a GCR-produced nuclide of appropriate half-life, like ^{129}I with $t_{1/2}$ = 16 Ma, which would monitor cosmic ray flux changes in the past 50 Ma. The ^{129}I-^{129}Xen method [4] uses ^{129}I produced by cosmic rays. However, the cosmic ray produced ^{129}I must be resolved from "extinct" ^{129}I.

CRE ages (T) can be determined from ratios of ^{129}Xe$_n$ and ^{129}I concentrations:

$$F(T) \equiv \frac{\lambda_{129} T}{1 - e^{-\lambda_{129} T}} - 1 = \frac{^{129}\mathrm{Xe}_n}{^{129}\mathrm{I}} \quad (1)$$

where λ_{129} = 4.41 × 10^{-8} a^{-1} is the decay constant of ^{129}I and ^{129}Xe$_n$ represents the n-produced excess concentration.

Results and Discussion: We report the Xe data from a step-wise decomposition, a required procedure for a calibration of excess ^{129}Xe$_n$. Troilite inclusions of iron meteorites are abundant in Te and, therefore, present a suitable mineral phase for the ^{129}I-^{129}Xe chronometry. The ^{129}I-^{129}Xe$_n$ chronology is especially suitable if low-energy secondary neutrons are abundantly produced in the meteorite during its cosmic ray exposure.

We identified the signature of trapped Xe in troilite inclusions as consistent with OC-Xe abundances. Further, a procedure for correcting an interfering radiogenic ^{129}Xe$_r$ component due to the extinct ^{129}I nuclide is developed. GCR secondary neutron reactions on Te provide a system which is independent of shielding, as long as the exposure geometry remains constant, because the fractional isobaric production ratio P(^{129}I)/P$_{129}$ ~1 and is especially suitable for iron meteorites, due to their larger size which provides an environment for developing the GCR secondary neutron component. The ^{129}Xe$_n$ in troilite of Cape York, when coupled to measured ^{129}I concentration, yield a cosmic ray exposure (CRE) age of 82 ± 7 Ma, lower than the preliminary value [5].

References: [1] Voshage H. 1962. *Zeitschrift für Naturforschung* 17A: 422–432. [2] Schaeffer O. A. et al. 1981. *Planetary and Space Science* 29: 1109–1118. [3] Lavielle B. et al. 1999. *Earth and Planetary Science Letters* 170:93–104. [4] Marti K. Abstract #86-06. Workshop on Cosmogenic Nuclides. Lunar and Planetary Institute, Houston. [5] Marti K. et al. 2004. *Meteoritics & Planetary Science* 39:A63.

5138

A TEM, C-XANES, AND NANOSIMS INVESTIGATION OF A FRAGMENT FROM THE STARDUST TRACK ADA

G. Matrajt[1], S. Wirick[2], S. Messenger[3], M. Ito[3], D. Joswiak[1], and D. Brownlee[1]. [1]Department of Astronomy, University of Washington, Seattle, WA 98195, USA. E-mail: matrajt@astro.washington.edu. [2]Department of Physics and Astronomy, State University of New York at Stony Brook, Stony Brook, NY 11794, USA. [3]Johnson Space Center, 2101 NASA Parkway, Houston, TX 77058, USA.

Introduction: We investigated the presence and nature of carbon in fragment #2 from track #26, called Ada. This is a Wild-2 particle ~12 μm in size. Like other fragments in this track, it is composed of multiple nodules of fayalite each surrounded by rims of crystalline SiO_2 (tridymite). The particle was embedded in acrylic and microtomed and sections were subsequently washed with sub-boiling chloroform vapor to dissolve the acrylic, as described in [1]. The sections were first analyzed by TEM to locate and characterize carbonaceous materials. The sections were then analyzed by X-ray absorption near edge structure spectroscopy (XANES) to investigate the bonding state of the carbon. Other sections were analyzed with a NanoSIMS 50L for their C, N, O, and H isotopic compositions.

Results: High-resolution imaging and electron energy loss spectroscopy (EELS) measurements revealed the presence of amorphous carbon in 3 small (<100 nm) regions. In the same area, C, N, and O-XANES measurements revealed the presence of a carbonaceous phase that contains N and O. The O in this phase occurs as a carbonyl (C=O) chemical bond, suggestive of an organic compound. NanoSIMS isotopic images show that the C-rich spot observed with EELS and XANES is ^{15}N-enriched ($\delta^{15}N = 550 \pm 70‰$, 1σ) and D-enriched ($\delta D = 610 \pm 254‰$, 1σ), proving that this organic material is indigenous to Wild-2 and not contamination. The $\delta^{13}C$ of this material is within the range of meteoritic organic matter (–4 ± 19‰). The O isotopes, which show homogeneous distributions (fayalite: $\delta^{17}O = 3.1 \pm 13.9$; $\delta^{18}O = -3.1 \pm 6.7$ and crystalline SiO_2: $\delta^{17}O = 9.0 \pm 12.1$; $\delta^{18}O = -10.4 \pm 5.6$), were also normal.

Discussion: Ada is a Stardust (SD) particle that has carbon concentrated in nanophases <200 nm in size that are found at the periphery of the particle. ^{15}N-enrichments of these C-rich regions are comparable to values found in other SD particles [2], IDPs [3, 4], and carbonaceous chondrites [5, 6]. The carbon is in an organic phase that also contains O. Carbon appears to be less abundant than in IDPs. However, given Ada's mineralogy (similar to OC-type chondrules [7]), composed of fayalite and tridymite, carbonaceous phases are unexpected. Perhaps the C was originally part of a fine-grained matrix that decomposed during impact into the aerogel and the remnants of it are the C-rich nanophases that we found at the edge of the particle.

References: [1] Matrajt G. and Brownlee D. 2006. *Meteoritics & Planetary Science* 41:1715–1720. [2] Matrajt G. et al. *Meteoritics & Planetary Science*. Forthcoming. [3] Floss C. et al. 2004. *Science* 303:1355–1357. [4] Aleon J. et al. 2003. *Geochimica et Cosmochimica Acta* 67:3773–3783. [5] Nakamura-Messenger K. et al. 2006. *Science* 314:1439–1442. [6] Busemann H. et al. 2006. *Science* 312:727–730. [7] Wasson J. and Krot A. 1994. *Earth and Planetary Science Letters* 122:403–416.

5143

ON THE PHYSICAL SEPARATION OF A SMALL FRACTION ENRICHED IN NOBLE GASES FOR NWA 2086 (CV3)

J. Matsuda[1], Y. Matsuo[1], M. Nara[2], and S. Amari[3]. [1]Department of Earth and Space Science, Graduate School of Science, Osaka University, Toyonaka, Osaka 560-0043, Japan. E-mail: matsuda@ess.sci.osaka-u.ac.jp. [2]Laboratory of Chemistry, College of Liberal Arts, Tokyo Medical and Dental University, Chiba 272-0827, Japan. [3]Laboratory for Space Sciences and the Physics Department, Washington University, St. Louis, MO 63130, USA.

Introduction: The fraction that is enriched in the heavy noble gases in meteorites was first obtained by dissolving more than 99 percent of an Allende fragment [1]. This chemical separation procedure can apply to any meteorites from different compositional groups. Matsuda et al. [2] has shown that the fraction that floats on the surface of the water ("floating fraction") during the freeze-thaw disaggregation shows the similar isotopic and elemental abundances to those of the residues prepared using the chemical separation procedure (see also [3, 4]). Advantages of this physical technique include that the major portion of the fragment used for the separation can be saved for other studies.

This physical separation method had previously been applied to two ordinary chondrites (H/L3.2 and L4~6) [5] and Murchison (CM2) [6]. The floating fractions obtained from these chondrites were not enriched in the primordial heavy noble gases compared with the bulk meteorites. To date Allende is the only meteorite that the physical separation method can be successfully applied to. This method was unsuccessful in separating gas-rich fractions even when applied to Murchison, which is a primitive carbonaceous chondrite as Allende, with a different petrologic type (CM2).

To examine whether this physical method is applicable not only to Allende but also to other CV3 chondrites, we applied the method to NWA 2086 (CV3). The shock classification and the weathering grade of NWA 2086 are S1 and W1, respectively.

Results and Discussion: We started from 1.964 g of five chips of NWA 2086. After 300 cycles of the freeze-thaw disaggregation, 0.23 mg of the floating fraction was finally recovered. This yield (0.012%) is smaller than the yield (0.068%) obtained after 216 cycles of Allende [4].

The elemental abundances and the isotopic compositions of noble gases in the floating fraction and the bulk chondrite have been determined with the VG5400 mass spectrometer in Osaka University. The noble gas concentrations in the floating fraction were 3–25 times higher than those in the bulk meteorite, but they were lower than those observed in the Allende floating fractions, where 10–130 times enrichments compared to the bulk meteorite have been achieved [2]. EDX analysis and the Raman spectroscopy of the floating fraction indicate that the floating material of NWA 2086 is mainly carbon. Especially, the Raman spectra of the floating fraction showed only G and D bands of carbon, which made possible to estimate the average in-plane crystallite size. The obtained size for NWA 2086 carbon is slightly larger than that of Allende, but is smaller than that of Murchison.

References: [1] Lewis R. S. et al. 1975. *Science* 190:1251–1262. [2] Matsuda J. et al. 1999. *Meteoritics & Planetary Science* 34:129–136. [3] Zaizen S. et al. 2000. *Antarctic Meteorite Research* 13:100–111. [4] Amari S. et al. 2003. *Geochimica et Cosmochimica Acta* 67:4665–4677. [5] Nishimura C. et al. 2004. *Meteoritics & Planetary Science* 39:A78. [6] Matsuda M. et al. 2006. *Meteoritics & Planetary Science* 41:A115.

5080

A LONG-DURATION AND DIFFUSE COSMIC DUST "VOLCANISM" ROOTED IN THE THERMOSPHERE

M. Maurette and C. Engrand. CSNSM CNRS-Univ Paris Sud, Bat.104, 91405 Orsay-Campus, France. E-mail: maurette@csnsm.in2p3.fr.

Introduction: Since our first paper [1], we constantly attempted to strengthen our scenario "EMMA" (Early MicroMeteorite Accretion). It was initially intended to describe the formation of the Earth's atmosphere through the destruction of a large fraction (about 80–90%) of the incoming micrometeorite flux. We give below a simple outline of this scenario, which was recently improved relying on: i) more accurate measurements of the C, N, and S contents of Antarctic micrometeorites AMMs (cf. [2] and [3]); ii) unweathered AMMs recovered from the ultra-clean snows of central Antarctica (terrestrial grains found in the snow are just the grains that you carry along) [5]; and iii) studies of the Wild-2 dust grains returned by Stardust, which show their striking similarities with AMMs, when one takes into consideration the explosion of hydrous grains throughout the release of the constituent water of their constituent saponite t, which starts around 100 °C [2].

Isotopic and Chemical Composition of an ~1 mg "Puff" of Micrometeoritic Atmosphere: About 500 unmelted AMMs with sizes of about 100 μm were individually analyzed. Our objective was to infer first the isotopic composition of the constituent water of their hydrous silicates (D/H ratio) and their Ne, N, C, and H_2O contents. Just by assuming that these ~500 AMMs get volatilized upon atmospheric entry, they yield a ~1 mg puff of micrometeoritic atmosphere, with a known water D/H ratio, and a chemical composition (i.e., the Ne/N_2, H_2O/Ne, and CO_2/N_2 ratios) just deduced from their average volatile contents. They turned to be astonishingly similar to the corresponding values measured for the $\sim 2 \times 10^{24}$ g mass of the terrestrial atmosphere, which was formed at the latest 4.4 Ga ago.

Preliminary Implications of the Micrometeoritic "Purity" of the Atmosphere: This astonishing purity concerns four elements that were neither formed at the same place nor at the same time, and which show vastly different concentrations in AMMs (i.e., a factor of 10^7 in the case of Ne and H_2O). It implies interesting constraints on the early evolution of the Earth: i) the Moon-forming impact did blow off most of the complex pre-lunar atmosphere and not only 20% of it; ii) the young Earth was mostly degassed at the time of this impact. Then a much simpler and dominant post-lunar micrometeoritic atmosphere could be accreted; and iii) the early greenhouse effect, was probably dominated by this kind of micrometeoritic volcanism "falling from the sky."

References: [1] Maurette M. et al. 2000. *Planetary and Space Science* 48:1117–1137. [2] Maurette M. 2006. In *Comets and the origin and evolution of life,* edited by Thomas P. et al. Berlin: Springer-Verlag. pp. 69–111. [3] Matrajt G. et al. 2003. *Meteoritics & Planetary Science* 38:1585–1600. [4] Engrand C. et al. 2007. Abstract #1668. 38th LPSC. [5] Maurette M., Kurat G., and Engrand C. This issue. [6] Duprat J. et al. *Advances in Space Research.* Forthcoming.

5084

A SURPRISING REAPPRAISAL OF THE DISTRIBUTION OF HEAVY NOBLE GASES IN A "GIANT" UNMELTED MICROMETEORITE FROM GREENLAND

M. Maurette[1] and Ph. Sarda[2]. [1]CSNSM, Bat.104, 91405 Orsay-Campus, France. E-mail: maurette@csnsm.in2p3.fr. [2]Department of Earth Sciences, Bat. 505, 91405 Orsay-Campus, France.

Different SW Irradiation Histories of Micrometeorites and Lunar Dust Grains: Lunar dust grains were exposed for about T_{exp} ~5,000–10,000 yr in SW ions and solar cosmic rays (SCRs). They are still loaded with SW species because they have not been severely eroded by the SW. But micrometeorites (MMs) had much longer T_{exp} ~200,000 yr, and they were flaked off about 60 times through SW-He bursting (see [1], p. 169), thus keeping a much smaller residual amount of SW gases relatively to the more deeply implanted SCRs gases. In 1991, [2] reported on the "complete rare gas study" of a 230 μg fragment (BLII) of the largest (~0.8 mm) unmelted chondritic MMs ever collected by us. BLII might help detecting the dominant type of SCRs during this T_{exp} ~200,000 yr, which integrates about 20,000 solar cycles.

Concentrations of Heavy Noble Gases in BLII: The SCRs' gases would be mostly trapped in the unknown fraction of the top external 10 μm thick layer of BLII, which was exposed to SCRs. We could only rank their concentrations relatively to that of ^{20}Ne. Moreover, the gases released at 750 °C and 1100 °C still look contaminated by terrestrial noble gases. Just for a try, we considered the 1500 °C gas release, which represents about 50% of the total gas release. When the concentrations in cc STP/g are converted into g/g, BLII yields the following scaling: $^{20}Ne/^{36}Ar$ ~0.5; $^{20}Ne/^{84}Kr$ ~12.2; $^{20}Ne/^{132}Xe$ ~5.2 (i.e., a component much "heavier" than that expected from the SW). We next coupled this BLII relative concentrations to the absolute average concentrations of ^{20}Ne ($\sim 1.5 \times 10^{-5}$ cc STP/g) measured in the dominant mass fraction of the micrometeorite mass flux (found in the 100–200 μm size range). This allows estimating the absolute concentration, A(wt%), of all noble gases in this dominant mass fraction.

A Big Surprise! Next, the accretion equation (see p. 96 of [1]) deduced from our scenario EMMA [3] yielded the total amounts (in g) of nobles gases in the atmosphere, which can be compared to the measured values (reported in the adjacent parenthesis): ^{20}Ne: 11.2×10^{16} g (5.8×10^{16} g); ^{36}Ar: 4×10^{17} g (2.2×10^{17} g); ^{84}Kr: 9×10^{15} g (9.7×10^{15} g); ^{132}Xe: 2.2×10^{16} g (5.4×10^{14} g). Unexpectedly, EMMA would well predict the total amounts of all heavy noble gases in the atmosphere, with the exception of the still "missing" xenon. It might be that the dominant SCRs are produced by impulsive flares that are rooted well below the solar chromosphere. They thus sample isotopically heavier material from the Sun interior, before it gets enriched in light elements and/or isotopes during its diffusion to the Sun's surface, where it feeds the "lighter" SW [4]. If this view is correct, then the average $^{20}Ne/^{22}Ne$ ratio of ~11.8 measured for the 100–200 μm size micrometeorites would reflect the Sun interior value, and not that of a mixture of SW and hypothetical "SEPs" component.

References: [1] Maurette M. 2006. *Micrometeorites and the mysteries of our origins.* Berlin: Springer-Verlag. pp. 1–330. [2] Sarda Ph. et al. 1991. 22th Lunar Planet. Scien. Conf. pp. 1165–1166. [3] Maurette M. and Engrand C. 2007. This issue. [4] Manuel O. K. et al. 1983. *Meteoritics* 18: 209–222.

5082

FROM ANTARTICA TO THE STARDUST AEROGEL

M. Maurette[1], G. Kurat[2], and C. Engrand[1]. [1]CSNSM, Bat.104, 91405 Orsay-Campus, France. E-mail: maurette@csnsm.in2p3.fr. [2]University of Vienna, Althanstrasse 14, A-1090, Vienna, Austria.

Introduction: We argued in 1998 [1] that the unmelted chondritic dust recovered from the stratosphere and polar ices and snows (micrometeorites [MMs]) that we and many others analyzed are cometary dust particles. We thus pointed out that cometary dust particles would be similar to MMs, being made of a material related to the CM-type hydrous-carbonaceous chondrites containing refractory phases, kerogen, and being depleted in unbroken chondrules. This "ordinary" dust was formed in the inner solar system and then forwarded to the outer solar system by huge surges of nebular gas [2]. It is timely to compare this "cometary" Antarctica dust to the dust of comet Wild-2 (W2-dust), which was captured in the aerogel of the Stardust mission.

A "Big Surprise": Initially, the name of this mission was selected to summarize the general consensus of 1999 when the mission was launched: comets would be made of interstellar ices and interstellar dust grains. We were impressed by the analytical results obtained by 183 scientists on a 0.2 μg of W2-dust [3]. What is less impressive is the way the data are interpreted and sold as a "big surprise" and/or the "most dramatic early finding" (i.e., relatively to the 1999 consensus). In fact, the W2-dust analyses [4, 5] confirm our earlier deductions because they establish strong similarities with MMs for: i) the abundance of Ca-Al-rich inclusions and presolar grains; ii) the H, C, N, and O isotopic compositions; and iii) the chemical composition of the refractory magnesian silicates and of Fe sulfides.

"Bulbs and Carrots": These similarities imply that hydrous silicates must also be present in the W2-dust, and that they should be dominated by saponite, which is the major hydrous silicate of unmelted MMs. However, the Stardust team repeatedly emphasized that "hydrous silicates are missing" in the W2-dust. The fate of these missing silicates is just pictured in the bulb-shaped aerogel tracks reported many times (e.g., the cover page of [3]). It documents the microscopic explosion of a dust particle containing saponite during its sharp deceleration in the aerogel. Only the most massive and refractory constituent particles can continue traveling to the termini of the tracks. Indeed, saponite contains both OH groups and very labile H_2O, which starts to be released at about 100 °C. Consequently, it should be "instantaneously" released during the pulse heating of the particles and form an explosion bulb in the aerogel—with the result that saponite is now missing. In contrast, "dry" crystalline W2-particles produced the "carrot-shaped" tracks also observed in the aerogel. With these beautiful bulbs, the ultra-clean and cold snow of central Antarctica can be assimilated to a giant inexhaustible cometary dust collector.

References: [1] Maurette M. 1998. In *The molecular origin of life,* edited by Brack A. Cambridge University Press. pp. 147–186. [2] Shu F. et al. 1996. *Science* 271:1545–1552. [3] Brownlee D. et al. 2006. *Science* 314: 1711–1716. [4] Matrajt G. et al. 2003. *Meteoritics & Planetary Science* 38: 1585–1600. [5] Engrand C. et al. 2007. Abstract #1668. 38th LPSC. [6] Duprat J. et al. *Planetary and Space Science.* Forthcoming.

5065

METAMORPHIIC EQUILIBRATION OF UNBRECCIATED EUCRITES

R. G. Mayne and H. Y. McSween, Jr. Department of Earth and Planetary Sciences, University of Tennessee, Knoxville, TN 37996–1410, USA. E-mail: rmayne@utk.edu.

Introduction: The term "equilibrated," when applied to eucrites, generally refers only to the pyroxene quadrilateral compositions [1]. However, in a larger study of the petrology of the unbrecciated eucrites, it was noted that plagioclase compositions measured in so-called equilibrated unbrecciated eucrites are not consistent with this description. Some grains show significant zoning: for example, Chervony Kut plagioclase has an An content that varies by nearly 20% ($An_{75–94}$), despite its equilibrated pyroxene quadrilateral compositions (Mg, Fe, Ca). The minor elements in pyroxenes also show considerable compositional variability, despite equilibration of quadrilateral compositions. It may, therefore, be possible to obtain a better indicator of the degree of equilibration by considering both the major and minor elements of pyroxene as well as zoning within plagioclase.

Methodology: Mineral analyses of pyroxene and plagioclase were made using the electron microprobe. Each sample was assessed for equilibration in three components:

1. The pyroxene quadrilateral compositions were compared to the classification scheme of [1].
2. Ternary plots of Al, Ti, and Cr in pyroxene were made to determine if the minor elements reflected the equilibration trends seen in the quadrilateral.
3. Plagioclase analyses were examined to establish which unbrecciated eucrites exhibited zoning, taken to be a variation of An content by more than 5%.

Samples were ordered with respect to temperature, calculated for each sample using the QUILF two-pyroxene geothermometer [2]. Because these equilibration temperatures were calculated using pyroxene compositions from grains that are exsolved, the resulting output is the exsolution temperature and not that of original crystallization.

Discussion: Nearly all the eucrites studied were equilibrated in terms of their pyroxene quadrilateral compositions. At the highest temperatures, the majority of samples show equilibration in all three components; whereas, at the lowest we see equilibration only in the pyroxene quadrilateral elements. Therefore, as pyroxene equilibration temperature decreases, so does the overall equilibration of the eucrites. The results indicate that the major elements in pyroxene become equilibrated first, followed by plagioclase, and then minor elements in pyroxene. The difference in equilibration between plagioclase compositions and pyroxene major elements is expected as [3] noted that plagioclase in eucrites was more resistant to thermal metamorphism than pyroxene. This is due to slow Si-Al diffusion kinetics in plagioclase compared to Fe-Mg in pyroxenes [3]. Experimental evidence indicates that Al diffusion is very slow in pyroxenes [4], we assume from our results that this also applies to Ti and Cr.

Conclusions: Quantifying these three equilibration indices allows an estimate of the relative degree of metamorphism in eucrites. Results suggest widespread metamorphism on Vesta, as suggested by [5], with most samples showing equilibration in at least major elements in pyroxene.

References: [1] Pun A. and Papike J. J. 1998. *American Mineralogist* 81:1438–1451. [2] Andersen D. J. et al. 1993. *Computers in Geosciences* 19: 1333–1350. [3] O'Neill C. O. and Delaney J. S. 1982. *American Mineralogist* 88:469–472. [4] Freer R. 1982. *Earth and Planetary Science Letters* 58:185–292. [5] Takeda H. and Graham A. L. 1991. *Meteoritics* 26:129–134.

5066

BULK DENSITIES OF METEORITES VIA VISIBLE LIGHT 3-D LASER IMAGING

P. J. A. McCausland[1], C. Samson[2], and A. DesLauriers[3]. [1]Department of Earth Sciences, U. of Western Ontario, London, ON, Canada N6A 5B7. E-mail: pmccausl@uwo.ca. [2]Department of Earth Sciences, Carleton U., Ottawa, Ontario, Canada. [3]Neptec, 302 Legget Drive, Kanata, Ontario, Canada.

Introduction: Bulk density is a fundamental property of meteorites, reflecting processes at work during their formation and subsequent history [1, 2]. Meteorite bulk volume is difficult to measure in a truly nondestructive way. Archimedean methods involving the displacement of a fluid are used [1], employing 40 μm glass beads to avoid sample contamination [3], but this suffers from error due to beads' packing behavior [1, 4]. Infrared 3-D laser imaging is a new nondestructive method for obtaining meteorite volumes [5]. In this study, we assess the performance of a high-resolution visible-light laser digitizer and 3-D modeling software by comparison with meteorite volumes determined via the "glass beads" Archimedean method [3, 4].

Methods: Bulk volume has been measured for five meteorite fragments by the glass beads method [4]. The same fragments were each imaged in 36 orientations at 0.7 m using a 3-D laser digitizer (the laser metrology system [LMS]) and the images were aligned and assembled into a closed 3-D model volume using visualization software (PolyWorks). Spatial and reflective fidelity was tested by the fragments' irregular broken surfaces, fusion crust, cut faces, cracks, large albedo contrasts, and free metal content. Another small fragment was also imaged to test the LMS performance at very small volume.

Discussion: Four of the five fragments return volumes that are 1–5% less than the Archimedean volumes (Table 1). Notably, the best agreement is for Shelbourne and Murchison, which were the "easiest" to assemble into 3-D models, having no cut surfaces or reflective fusion crust. Calculated bulk densities compare well with literature values except for Agoult, which was "difficult," having two cut faces and an extensive fusion crust. Small fragment Nuevo Mercurio gave a bulk density of 3.12 g/cm^3, in excellent agreement with the 3.17 ± 0.04 g/cm^3 determined by the beads method on a 53 g fragment [2]. The laser digitizing method is promising, especially for its application to fragments which are small (~1 cm^3) or friable. More rigorous study is needed, however, to assess and quantify sources of error in the method.

Table 1. Fragment bulk volume obtained by the Archimedean method (beads) and by laser imaging (vLMS); calculated densities (ρLMS) are compared with literature values [1, 2].

		Bulk vol. (cm^3)		Density (g/cm^3)	
Meteorite fragment	Mass (g)	Beads[3, 4]	vLMS	ρLMS	Lit value
NWA 1923 (EUC)	101.97	34.01 ± 0.88	35.59	2.83	(2.86 ± 0.07)
Agoult (EUC)	32.26	10.45 ± 0.12	10.06	3.21	(2.86 ± 0.07)
Shelbourne (L5)	30.39	9.14 ± 0.12	9.03	3.37	(3.35 ± 0.16)
Zagami (SHE)	23.51	8.10 ± 0.36	7.71	3.05	3.07
Murchison (CM2)	10.44	4.52 ± 0.17	4.42	2.36	2.37 ± 0.02
Nuevo Mercurio (H5)	5.37	–	1.72	3.12	3.17 ± 0.04

Acknowledgements: D. Gregory and P. Brown kindly provided these meteorites for this study. D. Labonté, J. Mah, and B. Powaschuk assisted with operating the LMS digitizer. C. S. acknowledges support from an NSERC Discovery Grant.

References: [1] Britt D. T. and Consolmagno G. J. 2003. *Meteoritics & Planetary Science* 38:1161–1180. [2] Wilkison S. L. et al. 2003. *Meteoritics & Planetary Science* 38:1533–1546. [3] Consolmagno S. J. and Britt D. T. 1998. *Meteoritics & Planetary Science* 33:1231–1241. [4] McCausland P. J. A. and Flemming R. L. 2006. Abstract #1574. Lunar and Planet. Sci. XXXVII. [5] Smith D. E. et al. 2006. *Journal of Geophysical Research* 111, doi:10.1029/2005JE002623.

5044

LOW-Ni IVA IRONS DEPLETED IN VOLATILES BY IMPACT REHEATING?

T. J. McCoy[1], C. M. Corrigan[2], J. I. Goldstein[3], J. Yang[3], R. J. Walker[4], R. D. Ash[4], W. F. McDonough[4], and N. L. Chabot[2]. [1]Smithsonian Institution, Washington, D.C. 20560–0119, USA. E-mail: mccoyt@si.edu. [2]Applied Physics Laboratory, Laurel, MD 20723, USA. [3]University of Massachusetts, Amherst, MA 01003, USA. [4]University of Maryland, College Park, MD 20742, USA.

Introduction: Ungrouped iron meteorites may record the processes of condensation, fractional crystallization, oxidation, and impact on a larger set of asteroids than the 13 iron groups. Alternatively, these processes may have acted to produce outliers that have not been previously recognized as from the same asteroidal cores. We have previously [1] discussed EET 83230 as a high-Ni member of group IVA. Here we discuss the meteorites Nedagolla and Santiago Papasquiero (SP) as low-Ni members of group IVA that lost volatile siderophiles via impact reheating.

Results: Several volatile-poor ungrouped irons are similar to group IVA, but more depleted in Ga and Ge. Among these, SP and N'Goureyma fall on the IVA Ir-Ni trend, suggesting a possible link to group IVA. PGE abundances for N'Goureyma refute such a link. In contrast, SP exhibits PGE abundances consistent with a low-Ni IVA iron and similar to Nedagolla, for which such an origin was previously suggested [2].

SP and Nedagolla share a history of impact reheating [3]. Nedagolla exhibits a dendritic structure formed by rapid (0.02 °C/s) cooling from a melt and secondary microstructural features formed by reheating to ~750 °C for several hours [4]. SP lacks a Widmanstätten pattern, instead exhibiting a polycrystalline mass of kamacite ~100 microns in diameter with amoeba-shaped taenite. Structurally, it is similar in many respects to Fuzzy Creek [5] and Babb's Mill (Troost's Iron) [6], both of which were shock-reheated to ~500–600 °C.

Discussion: PGE concentrations and modeling of highly siderophile element abundances for Nedagolla [2] and SP are suggestive of a link to group IVA. Further, they require that, if linked to IVA, these irons formed by crystallization from the core during the first ~20–40% of core solidification [2]. Early crystallization might also explain the P-poor nature of SP.

If SP and Nedagolla crystallized early in the IVA core, why are they so depleted in volatile siderophiles? Impact reheating and remelting, which was common in group IVA, might cause volatile loss. Unlike [7], we suggest that this reheating and volatile loss was a localized process. A clue to volatile loss in Ni-poor IVA irons might be the correlation of cooling rate with Ni concentration, consistent with cooling in an ~300 km, inwardly crystallized core with virtually no silicate mantle [8]. In such a model, low-Ni IVA irons would be nearest the surface, most likely to experience remelting and reheating, and could most easily lose their volatile siderophiles to space. Such a scenario might explain why the low-Ni SP and Nedagolla are highly depleted in Ga and Ge, while the similarly shock-reheated, but deeply buried (even after impact) high-Ni Fuzzy Creek is not.

References: [1] Corrigan C. M. et al. 2005. *Meteoritics & Planetary Science* 40:A34. [2] Walker R. J. et al. 2005. Abstract #1313. 36th LPSC. [3] Buchwald V. F. 1975. *Handbook of iron meteorites*. [4] Miyake G. T. and Goldstein J. I. 1974. *Geochimica et Cosmochimica Acta* 38:747–748. [5] Yang J. et al. 2006. Abstract #1308. 37th LPSC. [6] Yang J. et al. 2007. Abstract #1417. 38th LPSC. [7] Wasson J. T. and Richardson J. W. 2001. *Geochimica et Cosmochimica Acta* 65:951–970. [8] Yang J. et al. 2007. *Nature* 446:888–891.

5321

RAMAN DETECTION OF SHOCK-METAMORPHOSED RUTILE AT BOSUMTWI CRATER

J. F. McHone[1] and M. C. Fries[2]. [1]Arizona State University, Arizona. [2]Carnegie Institution of Washington, Geophysical Laboratory, 5251 Broad Branch Rd. NW, Washington, D.C. 20015, USA. E-mail: m.fries@gl.ciw.edu.

Titanium dioxide II, a presently unnamed pressure polymorph of rutile, has been identified in an archived laboratory sample from Lake Bosumtwi crater in Ghana. During a 1962 western Atlantic expedition, oceanographer Robert Dietz visited Ghana and recovered a suite of suevite-like rocks from along the northern crater rim. An earlier sample supplied by the Geological Survey of Ghana was examined at the USGS in Washington, D.C., [1] and was found to contain lechatelierite and coesite, thus strengthening an impact theory for Bosumtwi crater.

In the late 1980s, unpublished stories [2] describing traces of stishovite in the diamond-bearing gravels of southern Ghana were circulating among skilled exploration mineralogists. Stishovite is widely regarded as a reliable impact-shock indicator mineral, and splits from Robert Dietz's samples were subjected to a (mostly destructive) search process. The whole rocks were crushed, partially dissolved in acids, and finally examined with powder X-ray diffraction techniques. XRD patterns revealed a possible, but not conclusive, stishovite signature; the samples were mostly quartz, rutile, zircon, and graphite. The residual material was bottled and returned to storage.

By the early 2000s, the rapidly developing field of Raman spectroscopy had matured to a useful technique for identifying minute mineral grains. The archived residual powder sample was retrieved and granular splits were examined with a microbeam Raman instrument at Carnegie Institute of Washington's Geophysical Laboratory. As with earlier XRD results, most grains were composed of quartz, rutile, zircon, and graphite. However, under an optical microscope, many subrounded rutile granules 5–12 nm across appeared as aggregates with small, brighter grains adhered to their surface. Larger host masses produced a rutile Raman spectrum with strong bands at wave numbers 440 and 605 cm^{-1}, but the smaller small parasitic grains produced several Raman bands including 172, 284, 313, 341, 356, and 426 cm^{-1}. This Raman pattern is distinct to a shock-metamorphosed polymorph of rutile [3], the orthorhombic alpha PbO_2-structured phase of titanium dioxide (TiO_2-II).

This is the sixth known natural occurrence of TiO_2-II. Previously (see references in [4]) it has been reported in core samples at Ries Crater and Chesapeake Bay impact crater, in ejecta layers of the Australasian microtektite field, and in re-exposed tectonic subduction units in Germany and China. Its recognition at Bosumtwi crater, a well-accepted impact structure, strengthens its possible use as a mineral indicative of impact shock history.

References: [1] Littler et al. 1962. In Astrogeolic Studies Semiannual Progress Report, February 26 to August 26, 1961. USGS Open-File Report. pp. 79–86. [2] Personal communication to J. F. M. [3] El Goresy et al. 2001. A natural shock-induced polymorph of rutile with alpha PbO_2 structure in the Ries crater in Germany. *Earth and Planetary Science Letters* 192:485–495. [4] Jackson et al. 2006. *American Mineralogist* 91:604–608.

5314

COMPARISON OF SYNTHETIC AND NATURAL NAKHLITE PYROXENES: COMPLEXITY OF MINOR ELEMENTS

G. McKay[1], L. Le[2], and T. Mikouchi[3]. [1]Mail Code KR, NASA Johnson Space Center, Houston, TX 77058, USA. [2]ESC Group, NASA Johnson Space Center, Houston, TX 77058, USA. [3]Department of Earth and Planetary Science, University of Tokyo, 7-3-1 Hongo, Tokyo 113-0033, Japan.

Introduction: Zoning in pyroxenes in Martian meteorites contains a rich record of the petrogenesis of these samples. In the clinopyroxene cumulate nakhlite group, major element zoning is generally limited to the outer rims of the pyroxenes. However, minor element zoning, especially of Al, Ti, and Cr, is extensive, complex, and difficult to interpret (e.g., [1–3]). To help mine the rich information about petrogenetic processes from these samples, we have been comparing minor element zoning in synthetic pyroxenes grown under known conditions with zoning observed in natural nakhlite pyroxenes. We have focused on two nakhlites, MIL 03346 (MIL), which is one of the most rapidly cooled nakhlites, and Y-000593 (Y-593), which cooled at a more moderate rate (e.g., [4]).

Experiments and Analyses: The synthetic samples were partially crystallized at oxygen fugacities of IW, IW+1.5, and IW+3.5 (QFM). EPMA analyses were performed on MIL, Y-593, and the three synthetic samples using a single standardization. Standards were repeatedly analyzed during the analytical run. Individual elements were counted for sufficient time to yield 1σ counting statistics of better than ±0.16 wt% for Si and Ca, 0.10% for Fe, .06 for Mg, and .02 for all other elements. All samples were carbon-coated at the same time. These procedures result in minimum bias between samples so that all can be directly compared.

Results: MIL and Y-593 have very different zoning patterns. MIL has limited Al zoning, but Cr varies by ~2x. Y-593 has limited Cr zoning, but Al varies by ~2×. MIL pyroxenes consist of a Cr-depleted central region surrounded by an outer region with Cr content similar to the bulk of Y-593 crystals. Al-rich zones in Y-593 pyroxenes have slightly less Al than bulk MIL pyroxenes. Pyroxenes from both samples have significant and similar octahedrally coordinated Al, as calculated from stoichiometry [5].

Synthetic pyroxenes all have significant sector zoning in Al, Ti, and Cr. Al-rich and Al-poor sectors of the QFM sample have Al contents similar to the Al-rich and Al-poor portions of Y-593. The Al-poor sectors of the IW sample have slightly more Al than the Al-poor portions of Y-593. The IW sample has virtually no octahedrally coordinated Al. The QFM sample has some, but much less than the natural pyroxenes. QFM shows a much smaller range in Ti than both IW and natural pyroxenes, but a larger range in Cr.

Conclusions: The crystallization conditions and/or melt compositions used in our crystallization experiments do not accurately reflect the crystallization of Nakhlite pyroxenes, especially in terms of minor element zoning patterns. The much higher octahedrally coordinated Al in the natural pyroxenes suggests crystallization from a more Al-rich, Si-poor melt and/or crystallization at higher pressure.

References: [1] McKay and Mikouchi. 2005. *Meteoritics & Planetary Science* 40:A100. [2] McKay et al. 2006. *Antarctic Meteorites* 30. p. 61. [3] McKay et al. 2007. Abstract #1721. 38th LPSC. [4] Mikouchi et al. 2006. Abstract #1865. 37th LPSC. [5] Cameron and Papike. 1981. *American Mineralogist* 66:1.

5067

ARE SNC METEORITES FROM THARSIS?

H. Y. McSween[1], N. P. Lang[1], and L. L. Tornabene[2]. [1]Department of Earth and Planetary Sciences, University of Tennessee, Knoxville, TN 37996, USA. E-mail: mcsween@utk.edu. [2]Lunar and Planetary Laboratory, The University of Arizona, Tucson, AZ 85721, USA.

Introduction: Tharsis has long been invoked as a possible source for Martian meteorites [1] because its volcanic activity has extended to recent times, but this hypothesis has been difficult to test by remote sensing due to an obscuring dust cover. However, the distal ends of mapped flows associated with Arsia Mons have a low dust cover index [2]. These lavas may be an especially attractive meteorite source because a rare rayed crater occurs on one of these flows, and rayed craters have characteristics consistent with recent meteorite launch sites [3].

Spectroscopy: Using new mineral spectra, we have been able to accurately deconvolve the laboratory thermal emission spectra of nakhlites and basaltic shergottites and from those data to calculate bulk chemical compositions (method described by [4]). Having demonstrated that this method works, we then compare the compositions of Arsia flows calculated from deconvolved spectra measured by the MGS Thermal Emission Spectrometer (TES) with the analyzed compositions of SNC meteorites. Unfortunately the flows, although relatively free of dust, are partly covered by aeolian sands, as revealed by MRO HiRISE images. Thus we must estimate the degree of sand cover and subtract that proportion of the spectrum measured for a sand-covered by area. The resulting flow spectra are dominated by pyroxenes and plagioclase, as are nakhlites and shergottites, but they have lower spectral contrast and we must also remove alteration phases.

The calculated chemical compositions of the Arsia flows are similar in some respects to SNCs, and they plot near basaltic shergottites and nakhlites on a Ca/Si versus Mg/Si diagram used to classify SNC meteorites. However, the calculated FeO contents of the flows are too low and the Al_2O_3 contents are too high to provide good matches. We have also considered nakhlite and shergottite intercumulus liquid compositions, as well as compositions enriched in cumulus FeTi oxides, which cannot be seen in TES spectra. None of these attempts have produced convincing matches to SNC-like volcanic rocks.

Conclusions: Given the many uncertainties in deconvolving TES spectra from petrologically mixed pixels, we cannot rule out the possibility that SNCs derive from impact sampling of Tharsis flows. But neither can we support this hypothesis with currently available remote sensing data. Further work will attempt to locate sand-free pixels along TES orbital tracks using HiRise imagery, and these pixels might also be targeted by other spacecraft instruments with high spatial resolution. The discovery that even "clean" pixels are dirty in HiRISE images may have profound implications for Mars spectral interpretations.

References: [1] McSween H. Y. 1994. *Meteoritics* 29:757–779. [2] Lang N. P. et al. 2007. Abstract #1718. 38th Lunar and Planetary Science Conference. [3] Tornabene L. L. et al. 2006. *Journal of Geophysical Research* E10006, doi:10.1029/2005JE002600. [4] Wyatt M. B. et al. 2001. *Journal of Geophysical Research* 106:14711–14732.

5023

ATMOSPHERIC DISPERSION OF SMALL IMPACTORS ON MARS: STRENGTH OF THE IMPACTOR

H. J. Melosh and A. S. McEwen. Lunar and Planetary Laboratory, The University of Arizona, Tucson, AZ 85721, USA.

Introduction: In 2006, Malin et al. [1] announced the discovery of 20 small dark areas on the surface of Mars that appeared to the MOC imaging system between 1999 and 2006. The size of the dark areas is on the order of a few km. The HiRISE imager aboard the Mars Reconnaissance Orbiter has imaged nine of these spots, to date. At a resolution of approximately 30 cm/pixel, these dark spots are seen to surround small, fresh-appearing impact craters. With only one exception, the craters form multiple clusters. The largest crater in each cluster ranges from 10 to 25 meters in diameter. If these are primary impactors, as appears most probable, these craters were caused by the impacts of primary objects in the size range of 1 to 3 meters diameter.

Crater Clusters: Only one of the craters imaged by HiRise is single. This crater is about 22 m in diameter and is surrounded by an extensive secondary boulder and crater field extending several km from the primary impact. All of the others form clusters for several to several tens of visible craters that lie within about 100 m of each other. One field contains on the order of 10^3 to 10^4 craters near the limit of resolution that lie mostly within a north-south elongated ellipse measuring about 300 by 500 m. Aside from this ellipse, no obvious signs of uprange-downrange polarity is visible, unlike that seen in terrestrial and Venusian strewn fields, in which the largest crater usually falls downrange of the others due to atmospheric drag [2].

Implications for the Impactors: The theory of atmospheric breakup [3] suggests that a fast-moving meteorite that enters the atmosphere of a planet may be fractured by aerodynamic pressures proportional to $\rho_b v^2$, where ρ_b is the density of the atmosphere at the altitude of breakup and v is the entry velocity. The resulting fragments disperse at a velocity proportional to the entry velocity times the ratio of ρ_b to the projectile density. As the fragments fall atmospheric drag on Earth further sorts the fragments by size, although this seems to have not been important on Mars. The dispersion of the craters observed on suggests breakup at an altitude of about 3 scale heights, implying that the incoming objects possessed strength on the order of 10^4 Pa, substantially less than that of most terrestrial meteors [4]. The widely dispersed field suggests even less strength: indeed models have a difficult time explaining the divergence with even zero strength, unless the impacting object had an unusually low density.

References: [1] Malin M. C., Edgett K. S., Posiolova L. V., McColley S. M., and Noe Dobrea E. Z. 2006. *Science* 314:1573. [2] Passey Q. and Melosh H. J. 1980. *Icarus* 42:211. [3] Melosh H. J. 1981. In *Multi-ring basins,* edited by Schultz P. H. and Merrill R. B. New York: Pergamon. p. 29. [4] Svetsov V. V., Nemtchinov I. V., and Teterev A. V. 1995. *Icarus* 116:131.

5308

PRELIMINARY STUDIES OF Xe AND Kr FROM THE GENESIS POLISHED ALUMINUM COLLECTOR

A. P. Meshik[1], C. M. Hohenberg[1], O. V. Pravdivtseva[1], J. C. Mabry[1], J. H. Allton[2], K. M. McNamara[3], E. K. Stansbery[3], and D. S. Burnett[4]. [1]Washington University, Physics Department, St. Louis, MO 63130, USA. E-mail: am@physics.wustl.edu. [2]Lockheed Martin c/o NASA/Johnson Space Center, Mail Code KT, Houston, TX 770583, USA. [3]NASA/JSC, Mail Code KA, Houston, TX 77058, USA. [4]Geology 100-23, CalTech, Pasadena, CA 91125, USA.

Introduction: Low solar wind (SW) abundances of Xe and Kr require a large collector area to provide measurable quantities of these rare gases. Originally we planned to use large areas of Al on Sapphire (AloS) collectors, but the hard landing of Genesis fractured these collectors, changing our initial plans. The only large, relatively intact, surface exposed to SW was the kidney-shaped polished aluminum T6-6061 alloy (AlK) designed to serve as a thermal shield rather than a SW collector. Here we describe what has been done and the problems remaining to be solved for optimized Xe and Kr abundances and isotopic compositions from the AlK.

Experimental: A laser extraction technique was developed for the AlK with controlled depth resolution using 7 ns-pulsed (30Hz) UV laser (266 nm). Longer focal length (100 mm) optics and a deeper cell were needed for acceptable laser extraction from the distorted surface of the post-impact AlK collector. A large area (~10 cm^2) is needed to recover enough Kr and Xe for reasonably precise measurement. A sliding shutter with a narrow slit was installed in the cell to protect the sapphire viewport from deposition of some of the Al sputtered during raster of these large areas. Noblesse, our new 8-multiplier mass spectrometer, was designed for Kr and Xe measurements and, prior to this, it has only been exposed to atmospheric noble gases.

Results: Diffusion losses from the aluminum alloy heat shield are much greater than from the AloS collectors. AlK has apparently lost ~35% of SW-He and ~15% of SW-Ne [1], but this trend suggests that the AlK retained most of its Kr and Xe. Blanks for Kr and Xe remain a problem due to the complex design including a linear-motion feedthrough for the shutter and the long raster times required for the areas extracted. Electropolishing of all internal surfaces, two-week bake (with AlK samples included) at 215 °C, and extensive exercising of moveable parts to reduce gas release in flexing have allowed us to reduce Xe blanks to about 1×10^{-15} c^3 $STP^{132}Xe$, equivalent to that contained in ~2 cm^2 of this collector. However, the first attempt to study the AlK revealed a new problem—an unknown contaminant released from AlK that was not completely removed by gettering. Nevertheless, both the observed $^{84}Kr/^{132}Xe$ ratio of ~16 and the lighter than atmospheric Xe composition suggest a mixture of ~1 part SW-Xe and ~3 parts atmospheric Xe, about 3 times more than expected from blanks. Work is underway to discover the contaminant and develop a more efficient cleaning protocol for heavy noble gases released from AlK Genesis collector. We will report data from areas large enough for reasonably precise Kr and Xe once proper gettering is established.

Acknowledgements: Supported by NASA grant NNJ04HI17G.

References: [1] Meshik A., Marrocchi Y., and Hohenberg C. et al. 2006. *Meteoritics & Planetary Science* 41:A121.

5215

LIBNUCNET: A TOOL FOR UNDERSTANDING NUCLEOSYNTHESIS

B. S. Meyer and D. C. Adams. Department of Physics and Astronomy, Clemson University, Clemson, SC 29634–0978, USA. E-mail: mbradle@clemson.edu.

Introduction: With recent advances, the sciences of nucleosynthesis and meteoritics have become increasingly intertwined (e.g., [1]). This is true in particular for the study of presolar grains (e.g., [2]) and the study of extinct radioactivities in primitive meteorites (e.g., [3]). Such intergrowth of the two sciences is calling for increased sophistication on the part of practitioners in either field regarding the details of the other.

Libnucnet: In order to help facilitate an understanding of nucleosynthesis by the broadest possible community, we are releasing libnucnet, our code module for computing yields from nuclear reaction networks. Libnucnet is free software written in the C programming language. It is available at http://www.webnucleo.org/home/modules/libnucnet.

Libnucnet is built on top of other freely available and well-tested code modules-libgdome and gsl (the GNU Scientific Library). We provide tutorials and over twenty code examples that demonstrate how to download, install, and use libnucnet.

The API: While one goal of our release of libnucnet is to allow students and professionals to gain a better appreciation of nucleosynthesis theory by running their own calculations, another is to provide a useful module for modelers to incorporate into their own codes. The libnucnet application programming interface (API) is straightforward to use and is documented online at the webnucleo.org web site. Libnucnet's flexibility and capacity to handle multiple excited states within a single nuclear species and multiple physical zones in an astrophysical model should make it an excellent choice for many applications.

References: [1] Meyer B. S. and Zinner E. 2007. In *Meteorites and the early solar system II*. p. 69. [2] Clayton D. D. and Nittler L. R. 2004. *Annual Review of Astronomy and Astrophysics* 42:39–78. [3] Sahijpal S. and Soni P. 2006. *Meteoritics & Planetary Science* 41:953–976.

5312

SERIAL IMPACTS OR RANDOM ALIGNMENT? MONTE CARLO SIMULATIONS OF THREE 38th PARALLEL IMPACT STRUCTURES

Xin Miao[1], K. R. Evans[1], and J. R. Morrow[2]. [1]Department of Geog., Geol., and Planning, Missouri St. University, Springfield, MO 65897, USA. E-mail: xinmiao@missouristate.edu. [2]Department of Geol. Sci., San Diego St. University, San Diego, CA 92182–1020, USA.

Introduction: The 38th parallel structures across Kansas, Missouri, and Illinois alternately have been regarded as crypto-explosive structures [1, 2] and serial impacts [3]. Decaturville and Crooked Creek are accepted impact structures [4]. The recovery of abundant shocked quartz grains from breccias associated with the Weaubleau structure makes it a third viable impact structure along this trend. Currently, we regard other structures as having uncertain affinities. Nevertheless, the three known impact structures are aligned and stratigraphic age constraints cannot exclude the possibility that they are temporally related as products of serial impact. We used Monte Carlo simulations to test the hypothesis that these three impacts were unrelated temporally and aligned randomly across the 200 km distance that separates them.

Model Parameters and Simulations: Of the 174 currently accepted terrestrial impacts, most have been found on land [4]. Many are small, and others are double impacts, so model values of 200 and 300 incidents assume that some impacts remain undiscovered. The model also assumes a rectangular surface area of 148,939,100 km^2 (12,204 × 12,204 km) to represent the present-day land area with an additional 200 km buffer to avoid edge effects. Tectonism (i.e., subduction, sea-floor spreading, mountain building, and reconfiguration of landmasses) was not addressed.

Monte Carlo simulations were programmed in MatLab. A series of 10,000 random impact simulations were completed for 20 runs using various parameter combinations to estimate the standard deviation of N_{event}. A search algorithm identified clusters of three or more impacts within 100, 200, or 300 km radius, and the routine further identified those aligned in one cluster, allowing for angular discordance up to ±2°. These parameters are conservatively estimated, and they can be used to generate an upper limit of the probability for random narrowly aligned impacts.

Results and Discussion: With 100 km radius and 200 impacts, N_{event} were only 6.6 ± 2.5 for 10,000 simulations. N_{event} increased to 25.3 ± 3.4 with 300 impacts. Thus, random alignment within 100 km radius is highly improbable with $P < 0.003$. This model returned a probability an order of magnitude lower than those derived by Rampino and Volk [3]. Their equation assumed that third and subsequent impacts must align with the first two that constituted a linear trend. Suppose the length D is 200 km and a zone of width w is 5 km, the probability of the third crater falling along this strip is about 0.03. However, our results also indicated that the probability would increase dramatically when the search radius became larger. With 200 impacts, N_{event} was 124.8 ± 10.9 when radius was 200 km, and 668.1 ± 34.7 when radius was 300 km. With 300 impacts, N_{event} was 439.8 ± 17.3 when radius was 200 km and 2315.0 ± 57.9 when radius was 300 km. Therefore, based on simulations and our current knowledge of impact rates, it is highly unlikely that the 38th parallel structures resulted from random, temporally unrelated impact events.

References: [1] Snyder F. G. and Gerdemann P. E. 1965. *American Journal of Science* 263:465–493. [2] Luczaj J. 1998. *Geology* 26:295–298. [3] Rampino M. H. and Volk T. 1996. *Geophysical Research Letters* 23:49–52. [4] Earth Impact Database. 2007. http://www.unb.ca/passc/ImpactDatabase/. Accessed 10 May, 2007.

5193

PETROLOGY AND MINERALOGY OF GRV 021710, A NEW CR CHONDRITE FROM ANTARCTICA

B. Miao[1, 2], Y. Lin[2], and D. Wang[3]. [1]Department of Resources and Environment Engineering, Guilin University of Technology, Guilin 541004, China. E-mail: miaobk@hotmail.com. [2]State Key Laboratory of Lithospheric Evolution, Institute of Geology and Geophysics, CAS, P.O. Box 9825, Beijing 100029, China. [3]Key Laboratory of Isotope Geochronology and Geochemistry, Guangzhou Institute of Geochemistry, CAS, Guangzhou 510640, China.

Introduction: Since 1998, nearly 10,000 meteorites have been collected from Grove Mountains, East Antarctica [1]. Of more than 600 classified meteorites, only one is a CR chondrite (GRV 021710) [2]. Here, we report the petrology and mineralogy of GRV 021710, and discuss its petrogenesis.

Results: GRV 021710 (442.6 g) is very fresh and has a complete fusion crust. It is composed of chondrules, Fe,Ni metal, and fine-grained matrix. The chondrules have sharp boundaries, and are generally 0.5–2 mm in diameter, with a few up to 4 mm. Except for a FeO-rich chondrule (type II), others are FeO-poor (type I). Most of the chondrules are Fe,Ni metal–rich and multilayered. Sizes of the Fe,Ni metal appear to increase from the periphery to the center of the chondrules. In addition, there are some large nodules of metal (0.3–0.5 mm in diameter). Only one CAI (380 × 680 μm) was found on the polished thin section studied in this work. It is a fluffy type A consisting mainly of spinel and melilite with thin diopside rims. The matrix (35 vol%) contains abundant phyllosilicates and less magnetite.

Most olivines are FeO-poor ($Fa_{1.4 \pm 0.6}$) and contain <0.53 wt% MnO and 0.16–0.80 wt% Cr_2O_3. Other grains of olivines in the type II chondrule contain much higher FeO, and they are compositionally zoned with Fa content increasing from $Fa_{23.9}$ at the cores to $Fa_{35.6}$ at the rims. Low-Ca pyroxenes ($Fs_{1.2 \pm 0.7}$) are also FeO-poor. The metal grains in one chondrule and a few grains in matrix are analyzed. The metal grains in the outer area of the chondrule and in the matrix have lower Ni contents (4.55–5.45 wt%) than those in the central area of the chondrule (8.77–8.69 wt%). Other minor elements of metallic Fe-Ni are Co (0.18–0.83 wt%, 0.3), Cr (<0.45 wt%), and P (0.19–0.43 wt%).

Discussion: GRV 021710 shares major petrographic properties with other CR chondrites, including FeO-poor silicates, high metal content, and multilayered type I chondrules [3]. Hence, we classify it as a new member of CR chondrites. On the other hand, it has a lower abundance of the fine-grained matrix, and the average size of chondrules is slightly larger in comparison with typical CR chondrites, e.g., Renazzo and Al Rais [4]. Though the multilayered texture of some large type I chondrules and compositional variation of Fe,Ni metal in CR chondrites may be related to multiple thermal events [5], the genetic relationship between chondrules and metal is unclear. A detailed study of metallic Fe,Ni in GRV 021710 is in process.

Acknowledgements: This work is supported by the National Natural Science Foundation of China (Grants #40673055 and #40473037).

References: [1] Lin Y. et al. 2006. *Meteoritics & Planetary Science* 41: A107. [2] Russell S. S. et al. 2005. *Meteoritics & Planetary Science* 40: A201–A263. [3] Ichikawa O. and Kojima H. 1997. *Antarctic Meteorites* 22. pp. 61–63. [4] Weisberg M. K. et al. 1993. *Geochimica et Cosmochimica Acta* 57:1567–1586. [5] Wasson J. T. and Rubin A. E. 2007. Abstract #2312. Lunar and Planetary Institute Conference.

5294

THEORETICAL CRYSTALLIZATION OF A REDUCED SHERGOTTITE: APPLYING MELTS TO Y-980459

T. Mikouchi and E. Koizumi. Department of Earth and Planetary Science, University of Tokyo, Hongo, Bunkyo-ku, Tokyo 113-0033, Japan. E-mail: mikouchi@eps.s.u-tokyo.ac.jp.

Introduction: Recent oxygen fugacity measurements of shergottite Martian meteorites subdivided them into "reduced" and "oxidized" subgroups, which are also closely related to their distinct isotopic abundances [1]. The reduced subgroup shows a more primitive nature compared to the oxidized one. Y-980459 (Y98) has the most mafic bulk composition among the reduced shergottites and is possibly a melt rock [2]. The texture and mineralogy of Y98 shows that it cooled at ~5 °C/h [2]. In contrast, Dar al Gani 476 (DaG 476) is considered to be a cumulate rock [3] in spite of a similar bulk composition to Y98. Dhofar 019 (Dho 019) has a slightly more ferroan bulk composition than these two [4]. In this study, we used the MELTS program to calculate major element melt and mineral compositions starting from a Y98 bulk composition ($\log fO_2$ = IW + 1) with/without fractionation to explore formation history of DaG 476 and Dho 019.

Results and Discussion: As previous studies showed, liquidus temperature of the Y98 melt is about 1440 °C and olivine (Fo_{86}) immediately appears at 1430 °C, and is close to the olivine core composition in Y98 [2]. When the temperature drops to 1250 °C without fractionation, olivine is Fo_{75} and pyroxene is $En_{76}Wo_3$. These compositions are close to their core compositions in DaG 476. Because they are extensively zoned in DaG 476, we suggest that two-stage cooling history could produce DaG 476, that is, cooling of Y98 melt in equilibrium at first down to 1250 °C, and then fast cooling to crystallize the groundmass. The estimated cooling rate for DaG 476 (0.03–5 °C/h) [3] probably records second-stage rapid cooling. Therefore, there is a possibility that both Y98 and DaG 476 came from the same melt. When we fractionate solid phases from Y98 melt, the residual melt is close to the Dhofar 019 bulk composition at 1350 °C. The melt is then close to the QUE 94201 bulk composition at 1160 °C as suggested by [5]. QUE 94201 would rapidly crystallize from this (or related) melt without accumulation. When we cool the fractionated Y98 melt at 1350 °C down to 1185 °C without fractionation, pyroxene, and olivine compositions ($En_{64}Wo_7$ and Fo_{67}, respectively) are similar to cores of those in Dho 019 [4]. Thus, Dho 019 could also originate from Y98 (or related) melt.

Conclusion: Y98 and DaG 476 may stand as a representative parent melt of reduced shergottites. This composition is also important because it is similar to a partial melt composition of the Martian mantle at 1500 °C [6].

References: [1] Herd C. D. K. 2003. *Meteoritics & Planetary Science* 38:1793–1805. [2] Mikouchi T. et al. 2004. *Antarctic Meteorite Research* 17: 13–34. [3] Mikouchi T. et al. 2001. *Meteoritics & Planetary Science* 36:531–548. [4] Taylor L. A. et al. 2002. *Meteoritics & Planetary Science* 37:1107–1128. [5] Symes S. et al. 2006. Abstract #2043. 37th Lunar and Planetary Science Conference. [6] Bertka C. M. and Holloway J. R. 1994. *Contributions to Mineralogy and Petrology* 115:313–322.

5290

Y-000027, Y-000047, AND Y-000097: MORE FRAGMENTS OF THE LHERZOLITIC SHERGOTTITE BLOCK

T. Mikouchi and T. Kurihara. Department of Earth and Planetary Science, University of Tokyo, Hongo, Bunkyo-ku, Tokyo 113-0033, JAPAN, E-mail: mikouchi@eps.s.u-tokyo.ac.jp.

Introduction: All the known lherzolitic shergottites are considered a launch pair because of their similar petrology and mineralogy with identical crystallization and exposure ages. In spite of these similarities, each sample is slightly different from one another in mineral chemistry, probably due to different degrees of re-equilibration (e.g., [1]). Recently, three new lherzolitic shergottites, Y-000027, Y-000047, and Y-000097, were identified in the Yamato 00 Antarctic meteorite collection [2]. We report their mineralogy and petrology to confirm their pairing [2] and compare them with other lherzolitic shergottites.

Petrography and Mineral Chemistry: All samples show two distinct textures, poikilitic and nonpoikilitic. In poikilitic areas, large pyroxene oikocrysts (~8 mm, $En_{77}Fs_{21}Wo_2$-$En_{67}Fs_{22}Wo_{11}$ and $En_{54}Fs_{16}Wo_{30}$-$En_{48}Fs_{14}Wo_{38}$) enclose rounded olivine grains (usually ~0.5 mm, $Fa_{24–31}$) and euhedral chromites (~0.2 mm). Olivine grains located near the edges of pyroxene oikocrysts have more Fe-rich compositions as compared with those near oikocryst centers. In nonpoikilitic areas, olivine ($Fa_{30–33}$), maskelynite ($An_{59}Ab_{40}Or_1$-$An_{47}Ab_{50}Or_3$), and pyroxene ($En_{54}Fs_{16}Wo_{30}$-$En_{48}Fs_{14}Wo_{38}$ and $En_{67}Fs_{27}Wo_6$-$En_{60}Fs_{25}Wo_{15}$) are major constituent phases with minor amounts of merrillite and opaque minerals (mainly chromite with rims of ulvöspinel-rich component). Olivine grains in nonpoikilitic areas are usually ~1 mm, while pyroxene and maskelynite are smaller. Shock metamorphism is severe in all sections as the presence of a striking wide shock melt vein (~1.5 mm wide) in Y-000027.

Discussion and Conclusion: The identical mineralogy and petrology of three samples confirmed that they are paired meteorites. The mineralogy and inferred crystallization history of Y 00 shergottites are also generally similar to those of previously known lherzolitic shergottites [1]. Olivines in ALH 77005 and GRV 99027 show a tight compositional distribution ($Fa_{24–30}$), but those in LEW 88516 and Y-793605 have wider compositional distributions and are more Fe-rich. NWA 1950 ($Fa_{23–32}$) is intermediate between ALH 77005-GRV 99027 and LEW 88516-Y-793605. These observations suggest that ALH 77005 and GRV 99027 experienced larger degrees of re-equilibration than LEW 88516 and Y-793605 [1]. Y 00 olivine composition is similar to NWA 1950 and Y-793605-LEW 88516 olivines, but different from any of them. Thus, Y 00 shergottites are probably not paired with Y-793605. The presence of merrillite in Y 00 is also distinct from Y-793605, which lacks merrillite. However, it is likely that three Y 00 lherzolites are another fragments of the lherzolitic shergottite block on Mars.

References: [1] Mikouchi T. 2005. *Meteoritics & Planetary Science* 40:1621–1634. [2] Misawa K. et al. 2006. *Antarctic Meteorites* 30. pp. 63–64.

5277

EXPERIMENTS ON NEW, GEOPHYSICALLY CONSTRAINED MARTIAN MANTLE COMPOSITIONS

M. E. Minitti[1], Y. Fei[2], and C. M. Bertka[3]. [1]Center for Meteorite Studies, School of Earth and Space Exploration, Arizona State University, USA. E-mail: minitti@asu.edu. [2]Geophysical Laboratory, Carnegie Institution of Washington, USA. [3]Directorate for Science and Policy Programs, AAAS.

Introduction: Many studies have sought to link Martian meteorite lithologies to melts from the Martian mantle (e.g., [1–3]). Most of these studies have met with limited success, with the most realistic linkages offered by melts derived from Martian magma ocean cumulates (e.g., [3]). Martian mantle melting studies commonly employ unique Martian mantle compositions in order to strengthen the connection between the Martian meteorites and melts derived from these mantles. For this study, we utilize two new Martian mantle compositions that, for the first time, are consistent with geophysical parameters (e.g., moment of inertia, crustal thickness [4]) and geochemical parameters provided by the Martian meteorites. With these new mantle compositions, we seek not only to create Martian meteorite lithologies, but the global basaltic (and basaltic andesite) lithologies detected by the Thermal Emission Spectrometer (TES). The first new composition represents a mixture of CM and L chondrite compositions in a ratio of ~45:55, respectively. The second composition is a mixture of H and L chondrite compositions in a ratio of ~33:67, respectively. Both compositions are SiO_2-enriched and have higher proportions of modal orthopyroxene than the Martian mantle of [5] and have Mg#s between those of [3] and [5].

Experimental: We created the two mantle compositions above by mixing silicate, carbonate, and phosphate powders. The oxidation state of powders was set at one log unit below the iron-wüstite (IW) oxygen buffer in an Ar-H_2 gas mixing furnace. The powders were then packed into graphite crucibles with caps which were in turn sealed in Pt tubes. Two Pt tubes, one containing the CM+L mixture and the other containing the H+L mixture, were loaded into a single 0.5″ piston cylinder assembly. Running both compositions at the same time ensures they see identical conditions at each P-T step and it halves the number of experiments necessary to complete phase diagrams for both compositions. Our initial experiments have been conducted at 20 kbar (~150 km in the Martian mantle) and 1300–1400 °C in a non-end-loaded piston cylinder apparatus in the Depths of the Earth laboratory at Arizona State University. Experiment durations fell between 21–70 hours. We will explore greater pressures (e.g., 40 kbar; ~300 km in the Martian mantle) in later experiments.

Preliminary Results: Each experimental product contains large (10–50 μm), euhedral crystals and analyzable pools of melt. The 1300 °C experiments fell very close to the solidi of both compositions, with <5% melt present in the experimental products. Future analyses will establish the exact compositions of the olivines, pyroxenes, aluminous phase(s), and melts present in the experimental products. Comparison between the experimental melt, Martian meteorite and TES lithology compositions will test the ability of the new mantles to yield known Martian lithologies.

References: [1] Bertka C. M. and Holloway J. R. 1988. Proceedings, 18th Lunar and Planetary Science Conference. pp. 723–739. [2] Longhi J. et al. 1992. In *Mars*. pp. 184–208. [3] Agee C. B. and Draper D. S. 2004. *Earth and Planetary Science Letters* 224:415–429. [4] Bertka C. M. and Fei Y. 1998. *Earth and Planetary Science Letters* 157:79–88. [5] Dreibus G. and Wänke H. 1985. *Meteoritics* 20:367–382.

5228

U-Pb AGES OF NWA 856 BADDELEYITE

K. Misawa and A. Yamaguchi. Antarctic Meteorite Research Center, National Institute of Polar Research, Tokyo 173-8515, Japan. E-mail: misawa@nipr.ac.jp.

Introduction: Bouvier et al. [1] have argued that crystallization ages of shergottites were old (~4.0 Ga), and suggested that most radiometric ages of shergottites were reset recently (i.e., ~180 Ma) by acidic aqueous solutions percolating throughout the Martian surface. To test this old age interpretation, we have undertaken in situ U-Th-Pb isotope analysis for baddeleyite (ZrO_2) in shergottites using an ion microprobe. Shergottites contain baddeleyite which crystallized from a late-stage melt, incorporated a certain amount of uranium into its crystal structure with negligible common lead, and is considered to be stable during acid leaching process at the Martian surface. Thus, this mineral is especially suitable for U-Pb geochronology of shergottites.

Samples and Analytical Techniques: Polished sections of basaltic shergottites, NWA 856 and Zagami, were examined by an EPMA (JEOL JXA 8200) at the NIPR. Baddeleyite was identified by mapping of approximate zirconium concentrations, using the Lα peak, with the EPMA. Many of the baddeleyite grains found in basaltic shergottites were too small for ion probe analysis (<5 μm in size). Standard baddeleyites, Phalaborwa (2060 Ma [2]) from South Africa and FC1 (1099 Ma [3]) from the Duluth Complex, Minnesota, were used as references. In situ U-Th-Pb isotope analysis was carried out using the NIPR SHRIMP II similar to the method described in [4].

Results and Discussion: Thorium/uranium ratios of baddeleyite were small (<<0.1), thus common lead was monitored using a ^{208}Pb signal and assumed to be the same isotopic compositions as that of modern terrestrial lead [5]. Because all baddeleyite grains examined were small (~10 μm in size) and the primary O^- beam may have overlapped in grain boundaries, the common lead correction sometimes exceeded 50%. Nevertheless, we have obtained an averaged $^{206}Pb/^{238}U$ age of 186 ± 12 Ma for NWA 856 baddeleyite.

Our preliminary results are consistent with the previous Sm-Nd age of ~170 Ma for NWA 856 ([6] and unpublished data) as well as the minimum $^{206}Pb/^{238}U$ ages of baddeleyite in Zagami and NWA 3171 [7], but do not support the unique insight into 4.0 Ga crystallization ages for shergottites claimed by the Lyon group [1]. Although shergottites experienced intense shock metamorphism (≥~25 GPa [8]), shock effects on U-Th-Pb isotope systems of baddeleyite must be small compared to those of plagioclase and pyroxene. Thus, the obtained young ages appear to represent crystallization of Martian surface lava flow.

References: [1] Bouvier A. et al. 2005. *Earth and Planetary Science Letters* 240:221–233. [2] Heaman L. M. and LeCheminant A. N. 1993. *Chemical Geology* 110:95–126. [3] Paces J. B. and Miller J. M. 1993. *Journal of Geophysical Research* 98:13997–14013. [4] Misawa K. et al. 2005. *Geochimica et Cosmochimica Acta* 69:5847–5861. [5] Stacey J. S. and Kramers J. D. 1975. *Earth and Planetary Science Letters* 26:207–221. [6] Brandon A. et al. 2004. Abstract #1931. 35th Lunar and Planetary Science Conference. [7] Herd C. D. K. et al. 2007. Abstract #1664. 38th Lunar and Planetary Science Conference. [8] Fritz J. et al. 2005. *Meteoritics & Planetary Science* 40:1393–1411.

5280

PETROLOGY AND GEOCHEMISTRY OF NEW UREILITES AND UREILITE GENESIS

D. W. Mittlefehldt[1], J. S. Herrin[2], and H. Downes[3]. [1]NASA/Johnson Space Center. E-mail: david.w.mittlefehldt@nasa.gov. [2]ESCG Jacobs, USA. [3]University of London, UK.

Ureilites are C-bearing, basalt-depleted olivine+pyroxene achondrites from a differentiated asteroid. The group is heterogeneous, exhibiting ranges in O isotopic composition, Fe/Mg, Fe/Mn, pyx/ol, siderophile and lithophile trace element content, and C content and isotopic composition [1]. Some of these characteristics are nebular in origin; others were strongly overprinted by asteroidal igneous processes. The consensus view is that most ureilites are melt residues, but some are partial cumulates or have interacted with a melt [1, 2]. An "unroofing" event occurred while the parent asteroid was hot that froze in mineral core compositions and resulted in FeO reduction at olivine grain margins. We have studied several new ureilites, but will focus here on two anomalous stones: LAR 04315 and NWA 1241.

LAR 04315 is texturally unusual. It contains olivine with angular subdomains, and low-Ca pyroxene riddled with wormy inclusions of metal+troilite, graphite, and possibly other phases, and irregular inclusions of high-Ca pyroxene. Reduction occurred along olivine grain margins and internal fractures, but not along subdomain boundaries. Although texturally odd, LAR 04351 is a typical ureilite in mineral and bulk composition. The olivine is $Fo_{80.8}$ and falls on the ureilite Fe/Mn-Fe/Mg trend. Its olivine composition falls within the range of the majority of ureilites, and it is typical of these ureilites in bulk rock lithophile and siderophile element contents.

NWA 1241 has been classified as a monomict ureilite bearing suessite ($[Fe,Ni]_3Si$) [3], but our sample does not support this. We obtained two chips of distinct material. Lithology A is an unbrecciated ureilite containing magnesian olivine ($Fo_{89.1}$) only a trace of fine-grained metal, and no suessite. It is coarse-grained with part having typical ureilite texture, and part consisting of large (1–2 mm) low-Ca pyroxene grains poikilitically enclosing olivine. Lithology B is highly weathered, contains $Fo_{82.5}$ olivine and abundant metal, much of it as medium-grained (up to 0.1 mm) suessite. Lithology B is medium grained and appears to have a typical ureilite texture, but because of the abundance of opaque phases and plucked grains, the texture is obscured. Lithology B is the material previously described [3]. Both lithology A and B fall on the ureilite Fe/Mn-Fe/Mg olivine trend. We had sufficient material only of lithology A for bulk analysis. It is typical of the magnesian group of ureilites in lithophile and siderophile elements. Although classified as a monomict ureilite, NWA 1241 is certainly dimict, and could be polymict.

Suessite previously has been documented only from polymict ureilites in uncertain textural context. Its occurrence in unbrecciated lithology B may allow for definition of the formation mechanism of this reduced phase. We do not concur with the suggestion that it is the product of the late reduction event [3]; it is too coarse-grained and abundant in lithology B compared to the metal typically formed by this event. Yet at this time it does not seem possible that Si^0 could have formed in equilibrium with FeO-bearing silicates of lithology B.

References: [1] Mittlefehldt D. W. et al. 1998. Reviews in Mineralogy 36. Chapter 4. [2] Goodrich C. A. et al. 2001. *Geochimica et Cosmochimica Acta* 65:621. [3] Ikeda Y. 2006. *Antarctic Meteorites* 30. p. 28.

5018

ASEM OBSERVATION OF IMPACT SPHERULES WITH CARBON, Fe, AND Ni AT THE P/T AND K/T GEOLOGICAL BOUNDARIES

Y. Miura. Inst. Earth Planet. Material Sciences, Graduate School of Science & Engineering, Yamaguchi University, Yoshida 1677-1, Yamaguchi, 753-8512, Japan. E-mail: yasmiura@yamaguchi-u.ac.jp.

Introduction: There are no direct observation of meteoritic elements of iron-group elements (Fe, Ni) and separated carbon (with minor calcium) elements for spherules on geological boundary. The purpose of this paper is to show impact evidences on P/T (Permian/Triassic) and K/T (Cretaceous/Tertiary) spherules with Fe, Ni, and C elements from field-emission analytical scanning electron microscopy (FE-ASEM) operated by the author [1–5].

FE-ASEM Observation of Carbon with Fe, Ni, Co in Spherules at the K/T and P/T Boundaries: Carbon-rich grains with iron-group elements (Fe, Ni) by impact on limestone rocks has been obtained at the sample of K/T and P/T geological boundaries in Spain and Meishan, China, by in situ observation as aggregates of spherules with Fe-Ni-Si-C (in 10 μm size).

Various Changes of Carbon in the P/T and K/T Spherules: The K/T spherule show mixtures of Fe-S-Si, Fe-Si-Ni, and C-Fe-Ca systems in composition which are main sources from target rocks and meteorite projectiles. Multiple aggregates of several sizes of spherules indicate vaporization of impact event. In fact, sample of large spherules (600 μm in size) contain smaller spherules (10 μm in size) with two types of minor grains (1 μm and 100 nm in size), which are direct evidences of impact vaporization from meteorite and target rocks at the K/T geological boundary. Carbon grains can be found at the K/T sample by the FE-ASEM observation. The P/T spherule from Meishan, China, show also mixtures of Fe-S-Si, Fe-Si-Ni, and C-Fe-Ca systems in composition which are main sources from target rocks and meteorite projectiles. Multiple aggregates of several sizes of spherules are also found a sample of large spherules (700 μm in size) containing smaller spherules (7 μm in size) with two types of minor grains (1 μm and 200 nm in size), where carbon grains (98%) can be found at the P/T sample by the FE-ASEM observation. Theses irregular and anomalous compositional aggregates can be found at spherules of two geological boundaries.

Application to Events at Several Major Geological Boundaries: The above results on spherules can be applied to elucidate causes of five geological boundaries with mass extinction based on various impacts among atmosphere, ocean, and rocks [5].

Summary: Spherules of P/T and K/T geological boundaries are irregular mixtures of 3 sizes (10 μm, 1 μm, and 100 nm in sizes) with composition found in target rocks and meteorites which are evidence of impact vaporization caused by a collision of an asteroid with target rocks.

References: [1] Miura Y. 2006. Abstract #2441. 37th LPSC. [2] Miura Y. 2006. ICEM 2006 Symposium Abstract Papers Volume. Yamaguchi, Japan: Yamaguchi University. pp. 102–103, 112–113. [3] Miura Y. 2007. LPI Contribution #1338. Abstract #1277. [4] Miura Y. 2006. *Antarctic Meteorites* 29 (NIPR) 30:69–74. [5] Miura Y. 2007. *Antarctic Meteorites* 30 (NIPR).

5017

DETAILED ASEM ANALYSES OF CARBON-BEARING IMPACT MATERIALS AT THE BARRINGER METEORITE CRATER IN THE USA

Y. Miura. Inst. Earth Planet. Material Sciences, Graduate School of Science and Engineering, Yamaguchi University, Yoshida 1677-1, Yamaguchi, 753-8512, Japan. E-mail: yasmiura@yamaguchi-u.ac.jp.

Introduction: Carbon-bearing materials of the Barringer meteorite crater, Arizona, USA, have been reported by X-ray diffraction (XRD) and analyzed scanning electron microscopy (ASEM) without carbon EDX data in 1993 [1]. The purpose of this paper is to elucidate carbon distribution and formation process of the same sample in 1993 with field-emission ASEM with carbon EDX detection (JEOL7000F) operated by author [2–4].

Large Carbon Materials with Iron and without Oxygen: Large blocks of carbon-bearing (99%) materials with about 10 cm in width are mixed with 1) Fe-Ni with carbon in the vein, 2) calcium-rich carbonate, and 3) silica-rich oxides in the rim. Minor elements of Ca and Si are from target rocks around the crater (but little oxygen), though Ca and Si-rich grains in the rim have enough oxygen. Complicated mixtures of FeNi-rich grains with and without carbon and oxygen are found at FeNi-rich grains of kamacite composition in the vein with much carbon but little oxygen. Contents of carbon and oxygen are largely changed at these FeNi-rich grains.

Different Feature of Carbon-Rich Grains: Carbon shapes of Barringer crater blocks are varied from irregular to polyhedral shapes with filled core or curved carbon texture. Carbon-rich (99.9%) grains have trace amounts of Fe and Ni. Curved feature of carbon-rich (91.7%) grains contains much Fe, Ni, and oxygen contents. These irregular and mixed features of carbon-rich grains indicate formation of rapid reaction during the Barringer cratering. In-site observation by the FE-ASEM shows detailed feature of carbon-rich grains with irregular wormy-like texture due to vaporization during impact.

Content of Carbon: Carbon contents of carbon-rich grains are varied from 99.9% to 91.7%, with CaO (1.5% to 2.1%) and SiO_2 (2.2% to 2.5%), where carbon with calcium elements can be explained from target rock of limestone around the crater.

Summary: 1) Rapid-mixture of carbon-rich and Fe-Ni-rich grains are found by the FE-ASEM images of the Barringer crater, Arizona, USA. 2) Content of carbon and oxygen of mixed grains can be explained as formation of impact on terrestrial surface. 3) Irregular and wormy texture and Ca content of carbon-rich grains indicates vapor growth of impact event from target rocks.

References: [1] Miura Y., Noma Y., and Iancu G. 1993. *Meteoritics* 28: 402. [2] Miura Y. 2007. LPI Contribution #1338. Abstract #1277. [3] Miura Y. 2007. *Antarctic Meteorites* 30. Tokyo: NIPR.

5020

THE STUDY OF FINE-GRAINED INTERSTICE FILLING MATERIALS IN CHONDRULE AND THE FINE-GRAINED RIM WITHIN COLD BOKKEVELD CHONDRITE BY FIB-TEM/STEM

M. Miyahara[1], S. Uehara[2], E. Ohtani[1], T. Nagase[1], and R. Kitagawa[3]. [1]Institute of Mineralogy, Petrology and Economic Geology, Graduate School of Science, Tohoku University, Sendai 980-8578, Japan. [2]Department of Earth and Planetary Sciences, Faculty of Science, 33, Kyushu University, Hakozaki, 6-10-1, Fukuoka 812-8581, Japan. [3]Graduate School of Science, Hiroshima University, 1-3-1 Kagamiyama, Higashi-Hiroshima, Hiroshima 739-8526, Japan. E-mail: miyahara@ganko.tohoku.ac.jp.

Introduction: Some chondrules in carbonaceous chondrites are covered with a fine-grained rim (FGR). Although some chondrules contain a fine-grained interstice filling material (FGIFM), few investigations have been conducted on the FGIFM [1]. It is possible that the formation of the FGIFM and FGR are related to each other. In this study, the FGIFM and FGR within the Cold Bokkeveld CM chondrite were extracted by a focused ion beam (FIB) system and characterized by TEM/STEM subsequent to XRD, Raman spectroscopy, and EMPA.

Results: A relatively large chondrule in the Cold Bokkeveld CM chondrite was selected for a FIB-TEM/STEM work. The FIB-TEM/STEM analyses revealed that the FGIFM consisted mainly of amorphous phase, iron sulfate hydrate, and Fe-serpentine. A part of the chondrule is altered while maintaining its original shape, and abundant amorphous phase materials are observed in the FGIFM. The pseudomorph in the FGIFM is surrounded by an assemblage of tubular iron sulfate hydrate and platy Fe-serpentine. The iron sulfate hydrate appears to be the alteration product of iron (-nickel) sulfide. On the other hand, the FGR consists of amorphous phase material and iron (-nickel) sulfide. The texture of the FGR is definitely different from that of the FGIFM. The FGR is homogeneous and consists mainly of amorphous phase clusters and iron (-nickel) sulfide. Iron sulfate hydrate and Fe-serpentine, which are commonly observed in the FGIFM, cannot be identified in the FGR.

Discussion: The textures, mineral paragenesis, and chemical composition of the FGIFM in chondrules and the FGR covering the chondrules in the Cold Bokkeveld CM chondrite differ from each other. This suggests that the alteration of chondrules to form the FGIFM and the formation of the FGR occurred separately. The FGIFM consists of amorphous phase material, iron sulfate hydrate, and Fe-serpentine. These are the alteration products of enstatite, metallic iron, and iron (-nickel) sulfide by an acidic aqueous solution, whereas the FGR consists of amorphous phase material and iron (-nickel) sulfide. Evidence for alteration by an acidic aqueous solution was not found in the FGR. The sedimentary structure of the FGR implies that it was formed by the accretion scenario proposed by [2].

References: [1] Hanowski N. P. and Brearley A. J. 2001. *Geochimica et Cosmochimica Acta* 65:495–518. [2] Metzler K., Bischoff A., and Stöffler D. 1992. *Geochimica et Cosmochimica Acta* 56:2873–2897.

5146

MID-INFRARED SPECTRA OF ACHONDRITES: SEARCH FOR DIFFERENTIATED MATERIAL IN CIRCUMSTELLAR DUST

A. Morlok[1, 2], C. Koike[3], M. Anand[4], K. Tomeoka[1], and M. M. Grady[4]. [1]Department of Earth and Planetary Sciences, Kobe University, Nada, Kobe 657-8501, Japan. E-mail: morlok70@kobe-u.ac.jp. [2]The Natural History Museum, Cromwell Road, SW7 5BD, London, UK. [3]Kyoto Pharmaceutical University, Yamashina, Kyoto 607-8412, Japan. [4]The Open University, Walton Hall, Milton Keynes MK7 6AA, UK.

Introduction: Infrared observations of dust in the debris disks of evolving young stars give us the opportunity to infer the mineralogical composition of materials forming in those locations (e.g., [1]). Assuming that similar evolution of materials took place in other solar systems, differentiated bodies are expected to form in several million years after their birth. To find evidence of such material, we started a systematical mid- and far-infrared study of achondritic meteorites, of which the first results are presented here.

Techniques: Mass absorption coefficients were obtained from KBr pellets mixed with sample material in a wavelength range from 2.5 to 25 μm.

Results: Millbillillie (eucrite) shows strong bands at 9.43, 10.37, 11.22, 15.91, and 19.87 μm, reflecting the mixture of pyroxene and plagioclase. Another eucrite, Pasamonte, has generally similar but much weaker features. Bilanga (diogenite) exhibits typical strong pyroxene bands at 9.43, 10.63, 11.45, and 19.87 m.

The olivine-rich ureilite Sahara 99201 shows the strongest bands at 9.97, 11.15, and 19.35 μm, with weaker broad bands at 16.46 and 23.36 μm. Dhofar 125 (acapulcoite), which is dominated by pyroxene and olivine with minor feldspar, has features at 9.31, 9.93, 11.18, and 19.35 μm. Peña Blanca Springs (aubrite), dominated by enstatite, plagioclase and olivine, has a complex spectrum with the strongest features at 9.28, 10.63, 11.65, and 19.28 μm. Nova 003 (brachinite) shows typical olivine bands at 10.15, 11.27, and 19.72 μm.

Discussion: The results of our measurements allow us to compare the IR spectra of the meteorites with those of astronomical objects. We found that the ureilite spectrum shows good similarity to the SPITZER spectra of dust material in the debris disk around the 16 my old star HD 113766 [2]. An earlier study did also show similarity of the spectrum of the Hajmah (a) ureilite to that of another young star, HD 179218 [4]. Ureilites show a wide range of shock effects of pressures up to 100 GPa (e.g., [3]). Thus, the spectral similarities would suggest that impact processing was taking place in the debris disk stage of those young stars. Nova 003 (brachinite) also shows good similarity to the same astronomical spectra except some shift in band position.

We also found that the spectra of Pasamonte (eucrite) and Dhofar 125 (acapulcoite) show some similarity to those of HR 7012 [2] and HD 104237, respectively. These young stars could also already be in the debris disk stage.

Acknowledgements: Many thanks to Addi Bischoff (Muenster) and C. Smith (London) for providing the samples, C. Chen (NOAO) for the spectra of HD 113766 and HR 7012, and Roy van Boekel (Heidelberg) for that of HD 104237.

References: [1] Lisse et al. 2007. *The Astrophysical Journal* 658:584–592. [2] Chen et al. 2006. *The Astrophysical Journal Supplement* 166:351–377. [3] Papike et al. 1999. *Planetary materials.* pp. 4–83. [4] Morlok et al. 2006. Abstract #1519. 37th LPSC.

5214

THE EFFECT OF LINE COOLING IN CHONDRULE-FORMING SHOCKS

M. A. Morris[1], S. J. Desch[1], and F. J. Ciesla[2]. [1]School of Earth and Space Exploration, Arizona State University, USA. E-mail: melissa.a.morris@asu.edu. [2]Department of Terrestrial Magnetism, Carnegie Institution of Washington, USA.

Introduction: Chondrule formation is a long-standing problem in meteoritics, but passage through nebular shocks satisfies nearly all the experimental constraints on chondrule formation [1–4]. An unresolved issue is how effectively gas-phase CO and H_2O molecules can cool the gas and chondrules following the passage of the shock. [2] and [3] neglected this effect, treating the gas as optically thick to these "line photons," and finding chondrule cooling rates <100 K/h. [1] assumed vibrational and rotational photons from CO, and rotational photons from H_2O, escaped the shocked gas as if it were always optically thin, finding cooling rates >1000 K/h. Here we estimate the magnitude of the cooling by line photons without assuming the post-shock gas is optically thick or thin.

Updated Cooling Rates: We have used the SCAN-H_2O database [5] of 1.2 million lines (rotational plus vibrational) of the H_2O molecule to recalculate the cooling rate. This database contains four times as many lines as that used by [6]. We have also used more exact escape probabilities [7] than used by [6], and we have included absorption by dust grains. We find (in the absence of dust) that cooling rates are enhanced by about 30% over those calculated using the cooling rates of [6], and the emission is effectively optically thin much further past the shock front. This would cool the gas and the chondrules below 1000 K in only 100 s. The high water-to-gas ratios consistent with the high oxygen fugacities inferred for the chondrule-forming region [8] would increase the cooling even more. This enhanced cooling is attributable solely to vibrational line photons from H_2O. We estimate that rotational line photons can cool the post-shock gas by only 4 K before it becomes optically thick to these photons. The total cooling from CO line photons we estimate as <72 K. The coolants assumed by [1] are insignificant, but vibrational line photons from H_2O are very effective coolants.

Water-to-Dust Ratio: Because vibrational line photons from H_2O so effectively cool the gas, high oxygen fugacities [8] would seem incompatible with cooling rates <100 K/h, but we find that dust significantly reduces the photon escape probabilities and the cooling rates. Dust grains (overall opacity 5 cm^2/g) absorb the line photons that would have escaped and cool the gas. Five minutes and 300 km past the shock front, when T = 1500 K, almost all line photons are absorbed by dust and cooling plummets from >10,000 to ~100 K/h. Cooling rates <100 K/h are compatible with H_2O/H_2 ratios hundreds of times solar, provided the dust-to-water ratio remains near solar. This suggests that elevated oxygen fugacities in the chondrule forming region are due to concentrations of dust and water ice combined.

References: [1] Iida A., Nakamoto T., Susa H., and Nakagawa Y. 2001. *Icarus* 153:430. [2] Desch S. J. and Connolly H. C. 2002. *Meteoritics & Planetary Science* 37:183–207. [3] Ciesla F. J. and Hood L. L. 2002. *Icarus* 158:281. [4] Desch S. J., Ciesla F. J., Hood L. L., and Nakamoto T. 2005. In *Chondrites and the protoplanetary disk*. ASP Conference Series 341. p. 849. [5] Jorgensen U. G., Jensen P., Sorenson G. O., and Aringerl B. 2001. *Astronomy & Astrophysics* 372:249. [6] Neufeld D. A. and Kaufman M. J. 1993. *The Astrophysical Journal* 418:263. [7] Hummer D. G. and Rybicki G. B. 1982. *The Astrophysical Journal* 254:767. [8] Fedkin A. V. and Grossman L. 2007. Abstract #2014. 38th LPSC.

5237

PRELIMINARY SHOCKED-QUARTZ PETROGRAPHY, UPPER WEAUBLEAU BRECCIA, MISSOURI, USA

J. R. Morrow[1] and K. R. Evans[2]. [1]Department of Geol. Sciences, San Diego State University, San Diego, CA 92182, USA. E-mail: jmorrow@geology.sdsu.edu. [2]Department of Geography, Geology, and Planning, Missouri State University, Springfield, MO 65804, USA.

Introduction: The Weaubleau structure, an ~18 km diameter circular anomaly in southwestern Missouri, is among the most well preserved of the 38th parallel structures spanning the North American Midcontinent [1, 2]. Recent and ongoing work provides strong structural, stratigraphic, petrographic, and biostratigraphic evidence that the Weaubleau structure resulted from a marine bolide impact event during the late Osagean to early Meramecian (mid-Mississippian) interval [1–4]. In the ~9 km diameter central portion of the structure, a distinct polymict unit forms the upper part of the informal "Weaubleau Breccia," which includes a variety of breccia types across the structure. The upper polymict unit, interpreted to be an impact crater-filling resurge breccia, contains lithic clasts, fossils, and grains sourced from pre-event Lower Mississippian, Lower Ordovician, and Precambrian crystalline target units [1–4].

Quartz Occurrence: Insoluble residues of formic and hydrochloric acid-dissolved bulk samples from resurge breccia outcrops along Missouri Highway 13, which runs through the east-central part of the structure, yielded abundant loose siliciclastic sand and gravel grains. A petrographic microscope point-count of 1400 grains in the 100–500 μm fraction identified 55 vol% monocrystalline quartz, 23 vol% chert and polycrystalline quartz, 12 vol% radial-fibrous quartz of probable diagenetic origin, 1 vol% feldspar, and 9 vol% quartz with pervasive mosaic extinction and common planar microstructures (PMs).

Evidence of Shock Metamorphism: The PMs in quartz include 1) about 60 freq% planar fractures (PFs) or cleavage occurring in multiple sets of open, parallel, flat to curviplanar forms aligned with distinct orientations; and 2) about 40 freq% short, closed, and partly decorated multiple sets of parallel planes that closely match previously documented shock-induced planar deformation features (PDFs) in quartz from other proven impact craters [5]. The PDFs are ~1–3 μm wide, are spaced ~1.5–5 μm apart, are characterized by discrete crystallographic orientations, and occur in multiple sets with up to 5 sets per grain. About 10 vol% of the PM-bearing quartz grains show reduced birefringence, based on qualitative comparison with the highest order interference colors present in the same sample. Preliminary universal stage microscope indexing of the PMs show that c(0001) crystallographic orientations are most frequent, although $\omega\{10\bar{1}3\}$, $\pi\{10\bar{1}2\}$, $\xi\{11\bar{2}2\}$, $(r/z)\{10\bar{1}1\}$, and other higher index planes are present. The common occurrence of altered quartz containing well-preserved PMs, which strongly resemble shock-induced PFs and PDFs, provides further robust evidence that the Weaubleau structure resulted from a major bolide impact event.

References: [1] Evans K. R. et al. 2003. *Assoc. Missouri Geol. Field Trip Guidebook.* pp. 1–31. [2] Evans K. R. et al. 2003. Abstract #4111. LPI Contribution 1167. [3] Evans K. R. et al. 2005. *Meteoritics & Planetary Science* 40:A45. [4] Miller J. F. et al. 2006. *Geological Society of America Abstracts with Programs* 38(7):184. [5] French B. M. 1998. LPI Contribution 954. 120 p.

5009

PETROGRAPHY OF SHOCKED-QUARTZ SAND IN SLUMPBACK BRECCIA, CENTRAL WETUMPKA IMPACT STRUCTURE, ALABAMA

J. R. Morrow[1] and D. T. King, Jr.[2] [1]Geological Sciences, San Diego State University, San Diego, California 92182, USA. E-mail: jmorrow@geology.sdsu.edu. [2]Geology Office, Auburn University, Auburn, AL 36849, USA.

Description: The Late Cretaceous, shallow-marine Wetumpka impact event excavated into an ~120 m thick Upper Cretaceous sequence of siliciclastic, argillaceous, and marly sediments disconformably overlying gently south-dipping, pre-Cretaceous schists and gneisses of the Appalachian piedmont [1]. Roadcuts near the crater center expose slumpback deposits including chaotic polymict megabreccia and breccia composed of metamorphic blocks, comminuted metamorphic- and sedimentary-clast lithic gravel, sand grains, and argillaceous matrix. Point-count and universal stage analyses of 250–1000 μm quartz sand from the breccia matrix showed 69 vol% monocrystalline quartz, 12 vol% polycrystalline quartz, 5 vol% quartz with sweeping, undulatory extinction, and 14 vol% quartz with planar microstructures (PMs) and mosaic extinction. About 90 vol% of the quartz grains showed rounded edges, indicating that they were sourced from the upper, sedimentary part of the target. Virtually all quartz grains with PMs also display a mosaic extinction pattern of patchy, blocky, and sharply divided crystal subdomains. This pattern is distinguished from the broad, sweeping, undulatory extinction noted in non-PM bearing grains, which is interpreted as the result of normal burial metamorphism.

The common quartz PMs, which match those from other proven impact structures [2–4], include both "P1" and "P2" types (cf. [4]). P1 planes are planar fractures (PFs) or cleavage occurring in multiple sets of open, parallel, flat to curviplanar forms aligned with distinct crystallographic orientations. They show 2–4 sets per grain, are ~3–5 μm wide, are ~10–50 μm or more apart, comprise 76 freq% of the PMs, cross most or all of the grain, and display planes equivalent to c(0001), $(r/z)\{10\bar{1}1\}$, $\xi\{11\bar{2}2\}$, and $m\{10\bar{1}0\}/a\{11\bar{2}0\}$ crystallographic orientations. P2 planes, which strongly resemble closed and partly decorated planar deformation features (PDFs), comprise 24 freq% of the PMs, are about 1–3 μm wide, and are spaced <10 μm apart. The P2 sets are often developed off of or crosscut by through-going P1 planes, resulting in "ladder" or "feather" structures (cf. [4]). The P2 planes include c(0001), $\omega\{10\bar{1}3\}$, $\pi\{10\bar{1}2\}$, $(r/z)\{10\bar{1}1\}$, and $\xi\{11\bar{2}2\}$ orientations. Such other shock-metamorphic indicators as reduced birefringence, diaplectic glass, or melt were not noted.

Discussion: The poorly consolidated, saturated, and porous upper target layers at Wetumpka probably played a critical role in the resulting greater abundance of P1 sets relative to P2 sets, as well as in the crystallographic orientations of these sets. The quartz PM development and the presence of both low- and high-index sets give evidence of the predicted heterogeneous distribution and impedance of shock energy through the target. Further, these target properties may have also hindered development of such other expected shock products as diaplectic glass and melt.

References: [1] King D. T., Jr. et al. 2006. *Meteoritics & Planetary Science* 41:1625–1631. [2] French B. M. et al. 1997. *Geochimica et Cosmochimica Acta* 61:873–904. [3] French B. M. 1998. LPI Contribution #954. 120 p. [4] French B. M. et al. 2004. *GSA Bulletin* 116:200–218.

5230

ADSORPTION OF WATER GAS ON TO GRAINS IN THE ACCRETION DISK AS A SOURCE OF INNER SOLAR SYSTEM WATER: DIRECT EVIDENCE FROM MONTE CARLO SIMULATION

K. Muralidharan[1], P. A. Deymier[1], M. Stimpfl[2], M. J. Drake[2], and N. H. de Leeuw[3]. [1]Department of Material Science and Engineering, The University of Arizona, Tucson, AZ, USA. [2]Lunar and Planetary Laboratory, The University of Arizona, Tucson, AZ, USA. [3]Department of Chemistry, University College London, UK.

Introduction: The origin of water in the inner solar system is not yet well understood. Because of the co-existence of water and small solid particulates in the accretion disk from which our planetary system formed, we propose that adsorption of water onto the surfaces/pores of olivine could play an important role in the delivery of water to the rocky planets. To this end, our group has been involved in studying the interaction between water gas and olivine surfaces by means of atomistic simulation, looking at the effect of orientation of the surfaces [1], chemical composition [2], mode of adsorption, and surface defects [3] on the heat of adsorption. Static atomistic simulations, such as the energy minimization technique employed by [1], cannot provide direct quantitative estimates on the extent of water surface coverage as a function of temperature. However, the heat of adsorption computed for these systems is high enough to support the speculation that water could be retained on olivine surfaces at temperatures and at p_{H2O} consistent with those of the accretion disk [3, 4]. In order to obtain direct estimates of the amount of water that can be stored on olivine surfaces one needs take into account the effect of temperature and time, which can be achieved by applying the methods of kinetic Monte Carlo (kMC) simulation.

Method: The system under investigation consisted of a box containing water molecules at a p_{H2O} consistent with that of the accretion disk [5], and a surface grid with the spacing of 1 μm representing the selected olivine surface. At each grid node the energy of interaction between the surface and the water molecule was chosen to be equal to the heat of adsorption at the same coordinates, as determined by [1] for {100}, and using unpublished data provided by one us (Stimpfl) for {110}. Using this information in conjunction with the kMC procedure we estimated the rate of adsorption/desorption of water as a function of position on the {100} and {110} olivine surfaces, from which we obtained the extent of transient and equilibrium water coverage on the selected olivine surfaces, over a relevant range of temperature and p_{H2O}.

Results: Our preliminary kMC investigation shows that: 1) water is retained on the surfaces at high temperature which implies that adsorption of gaseous water onto dust grains can start from the early stages of accretion, and 2) that the total amount of water retained on these surfaces can account for a considerable part of the Earth's water budget. These results support our previous inferences using the data from static simulations.

References: [1] Stimpfl M. et al. 2006. *Journal of Crystal Growth* 294: 83–95. [2] Stimpfl M. et al. 2006. Abstract #1771. Goldsmith Conference. [3] Stimpfl M. et al. 2007. Abstract #1183. 38th Lunar and Planetary Science Conference. [4] De Leeuw N. H. et al. 2006. *Meteoritics & Planetary Science* 41:A45. [5] Lodders K. 2003. *The Astrophysical Journal* 591:1220–1247.

5012

NITROGEN IN SAYH AL UHAYMIR 290

S. V. S. Murty[1], R. R. Mahajan[1], and R. Bartoschewitz[2]. [1]Physical Research Laboratory, Ahmedabad, India. [2]Meteorite Laboratory, Lehmweg 53, D-38518 Gifhorn, Germany.

Introduction: SaU 290 has been initially classified as an anomalous E chondrite, but later reclassified as CH3, based on petrology, chemistry, and O isotopes [1, 2]. Light noble gases (He, Ne) in SaU 290 are dominated by solar component, while trapped Ar, Kr, and Xe are similar to E-chondritic component [2, 3]. CH chondrites can be easily recognized by their characteristic heavy $\delta^{15}N$ value of ~1000‰, as in the cases of ALH 85085 [4], Acfer 182 [5], and PAC 91467 [6]. Here we report nitrogen results for a bulk sample of SaU 290.

Experimental: Gas extraction has been carried out by step-wise heating, by combustion up to 1000 °C and by pyrolysis subsequently at 1200 °C and 1600 °C. Nitrogen and noble gases have been analyzed by standard procedures [7]. Cosmic-ray exposure age of 1.2 Ma, derived from ^{21}Ne is in agreement with the reported value [2], but trapped gas amounts are lower in our sample by factors of 1.6(^{22}Ne), 2.3(^{36}Ar), 7.3(^{84}Kr), and 4.2(^{132}Xe) respectively, as compared to [2]. This difference could be partly due to the heterogeneous distribution of trapped noble gas carriers in SaU 290 and partly due to contamination, as a result of desert weathering, particularly in the case of heavy noble gases, as has been discussed [2].

Nitrogen: Nitrogen data for SaU 290 are being reported for the first time. A total N (117 ppm) with $\delta^{15}N$ (914‰) is present. As cosmogenic contribution will be negligible, due to large N content and low exposure age, this value directly represents the trapped N signature, which falls in the range found in other CH meteorites [4–6]. About 95% N with $\delta^{15}N$ of 921‰, ~98% C (monitored as CO_2 released during combustion), but only 22% ^{36}Ar are released up to 800 °C, clearly showing that the principal carriers of N and heavy noble gases are different. Beyond 800 °C, the $\delta^{15}N$ started to slide toward lighter value and reached the lowest observed value (400‰) at the melting step of 1600 °C.

Discussion: Based on combustion temperature and C/N ratio, at least four N components have been identified in CH chondrites [5], with two low temperature components [950‰ (250–350 °C), 500‰ (400–525 °C)] and two high temperature components with >1000‰. Based on microprobe studies, four carriers of isotopically heavy N have been identified, two associated with carbon-silicate aggregates, one with Si rich Fe-Ni metal and one with hydrated matrix [6]. Though it is difficult to compare with the data of Acfer 182 [5] due to different temperature stepping used, the data of SaU 290 clearly suggests the presence of an N component with $\delta^{15}N < 400$‰, hosted in non carbonaceous phase and having high release temperature (>1200 °C). This decrease in $\delta^{15}N$ at high temperature is not an artifact of terrestrial contamination, as any such contamination, if present, is expected to be prominent at lower temperatures, as also attested by heavy noble gases in the present data and [2]. Light nitrogen carriers, such as nanodiamonds with $\delta^{15}N = -110$‰ [8] and TiN with $\delta^{15}N = -359$ ‰ [9] have been identified in Acfer 182 and Isheyevo, respectively.

References: [1] Bartoschewitz R. et al. 2005. *Meteoritics & Planetary Science* 40:A18. [2] Park J. et al. 2005. *Antarctic Meteorites* 29. pp. 69–70. [3] Park J. et al. 2005. Abstract #1632. 36th LPSC. [4] Grady M. M. and Pillinger C. T. 1990. *Earth and Planetary Science Letters* 97:29–40. [5] Grady M. M. and Pillinger C. T. 1993. *Earth and Planetary Science Letters* 116:165–180. [6] Sugiura N. and Zashu S. 2001. *Meteoritics & Planetary Science* 36:515–524. [7] Rai V. K. et al. 2003. *Geochimica et Cosmochimica Acta* 67:2213–2237. [8] Grady M. M. et al. 1995. *Earth and Planetary Science Letters* 136:677–692. [9] Meibom A. et al. 2007. *The Astrophysical Journal* 656:L33–L36.

5013

NWA 1500: IS IT A UREILITE?

S. V. S. Murty[1], R. R. Mahajan[1], and R. Bartoschewitz[2]. [1]Physical Research Laboratory, Ahmedabad, India. [2]Meteorite Laboratory, Lehmweg 53, D-38518 Gifhorn, Germany.

Introduction: NWA 1500 has been initially classified as an ureilite and was discussed as a possible member of the still-missing basaltic ureilites [1]. However, its low C content [2], occurrence of plagioclase [3], and oxygen isotopic composition [4] suggest that NWA 1500 could be a primitive achondrite. Refined O-isotope data in fact show that NWA 1500 plots in the field of brachinites [4]. We have investigated noble gases and nitrogen in NWA 1500 to verify its ureilite affinity.

Experimental: We have planned our stepwise heating gas extraction protocol, assuming NWA 1500 to be a ureilite, combustion up to 1000 °C to release gases from carbon phases and subsequent pyrolysis at 1200 and 1600 °C, by following standard procedures [5]. There was no detectable CO_2 (as monitored by convectron gauge) during combustion steps, clearly establishing its very low C content, unlike typical ureilites, but similar to low carbon ureilite FRO 90054 [6].

Noble Gases: A cosmic ray exposure age of 9.4 Ma has been obtained from cosmogenic ^{21}Ne and ^{38}Ar. Trapped gas amounts (^{36}Ar = 6.1 $\times 10^{-8}$ ccSTP/g, ^{36}Ar/^{132}Xe = 249 and ^{84}Kr/^{132}Xe = 1.26) are very low compared to ureilites [7]. The isotopic ratios ^{40}Ar/^{36}Ar = 12.2 and ^{129}Xe/^{132}Xe = 1.13 are much above typical ureilites, having values of <1 and 1.03, respectively [7]. If all the radiogenic ^{40}Ar produced during 4.5 Ga has been completely retained, a K content of 6.1 ppm can be inferred. The noble gas elemental ratios indicate that they have not been significantly affected by terrestrial weathering, a feature typical of hot desert meteorites. It has been found that ureilites from hot deserts are not prone to terrestrial noble gas contamination, their carriers being resistant carbon phases [8].

Nitrogen: We determined an N content of 3.6 ppm with δ^{15}N of 10.8‰, with peak release at 1000 °C (1.45 ppm N; 2.2‰), but with no accompanying CO_2 release. Nitrogen in bulk monomict ureilites range between 6 to 55 ppm (δ^{15}N [‰] –2 to –70), with different polymorphs of C being the major carrier phases of N [5]. NWA 1500 is almost free of C and hence the silicate phase is the most likely carrier of N. A sharp jump in δ^{15}N to 102‰ (with 97 ppb N) has been observed at the melting step due to release of cosmogenic nitrogen. Correction for the cosmogenic contribution, leads to the composition of the trapped N to be 2.9‰.

Discussion: In a plot of ^{36}Ar/^{132}Xe versus ^{84}Kr/^{132}Xe (not shown here), NWA 1500 falls in the field of brachinites and away from ureilite field. There is no N data available for winonaites, brachinites, or silicate inclusions of IAB irons for comparison. From the high temperature release data of N for the nonmagnetic acid residue of Four Corners IAB iron [9], the inferred δ^{15}N (cosmogenic corrected) for silicate is light, unlike NWA 1500. Comparison of NWA 1500 data with those of winonaites and brachinites for oxygen isotopes [4], noble gas elemental and ^{129}Xe/^{132}Xe ratios [10, 11] suggest that it is closer to brachinites.

References: [1] Bartoschewitz R et al. 2003. *Meteoritics & Planetary Science* 38:A64. [2] Mittlefehldt D. W. and Hudon P. 2004. *Meteoritics & Planetary Science* 39:A69. [3] Goodrich C. A. et al. 2006. *Meteoritics & Planetary Science* 41:925–952. [4] Greenwood R.C. et al. 2007. Abstract #2163. 38th LPSC. [5] Rai V. K. et al. 2003a. *Geochimica et Cosmochimica Acta* 67:2213–2237. [6] Rai V. K. et al. 2002. *Meteoritics & Planetary Science* 37:A120. [7] Rai V. K. et al. 2003b. *Geochimica et Cosmochimica Acta* 67:4435–4456. [8] Murty S. V. S. and Rai V. K. 2006. *Meteoritics & Planetary Science* 42:A211. [9] Franchi I. A. et al. 1993. *Geochimica et Cosmochimica Acta* 57:3105–3121. [10] Benedix G. K. et al. 1998. *Geochimica et Cosmochimica Acta* 62:2535–2553. [11] Patzer A. et al. 2003. *Meteoritics & Planetary Science* 38:1485–1497.

5184

KINETICS OF CONDENSATION AND GROWTH OF SILICATE AND METAL DUSTS, AND ITS IMPLICATION TO CHEMICAL HETEROGENEITY IN THE PROTOSOLAR DISC

H. Nagahara[1] and K. Ozawa. [1]Department of Earth and Planetary Sci., The University of Tokyo, Hongo, Tokyo 113-0033, Japan. E-mail: hiroko@eps.s.u-tokyo.ac.

Introduction: Formation and evolution of silicates and metal dusts control the distribution of dusts in the solar nebula, and further control the nature of planetesimals that finally evolved to planets. Because the dusts grains were formed through condensation and growth in the solar nebula, kinetic behavior of the two phases and accompanied chemical fractionation are the fundamental processes that govern the chemical heterogeneity of the nebula. We have investigated dust growth by using a kinetic dust growth model, and show how silicate and metal grains grow and chemically fractionate.

Kinetic Condensation: Kinetic condensation experiments were carried at a fixed temperature under various degrees of supersaturation (S) [1]. The experiments along with new experiments at smaller S give the condensation coefficients of unity regardless of S. The lower limit for Fe condensation is $S \sim 10$. It is worth noting that metallic iron condensed on the surface of Al_2O_3 almost without kinetic barrier due to surface tension.

Growth of Metal/Silicate: A kinetic condensation model that describes nucleation and growth with chemistry of gas and dusts was developed by modifying a model by [2]. The parameters are cooling time scale of the gas (τ) and total pressure. The bulk composition of the gas is fixed to CI. If we do not consider heterogeneous condensation, the phases appear are forsterite, enstatite, SiO_2 that does not appear in equilibrium and Fe, although the relative abundances, condensation temperature, and grain size distribution change with τ. On the contrary, forsterite condensed earlier is mantled by metallic iron if heterogeneous condensation is taken into consideration, which prevents formation of enstatite through a reaction between forsterite and gas. Then, the gas becomes supersaturated in SiO_2, which resulted in condensation of SiO_2. The size distribution of grains is strongly dependent on τ; it is in the order or nm at τ in the order of hours (chondrule formation time scale), whereas the size is in the order of mm to m at τ in the order of 10^5 years (nebular evolution time scale or longer).

Nebular Heterogeneity: It has been known that the accretion velocity of grains is largest for the size in the order of m, whereas it is smaller for smaller or larger grains in an accretion disc. Combining the chemical growth calculated in the present study and physical movement of the grains, metal grains in slowly cooled regions become large, which are lost by selective accretion to the young sun. Rapidly cooled regions were unfractionated.

References: [1] Ikeda Y. et al. 2007. 38th LPSC. [2] Kozasa T. and Hasegawa H. 1987. *Progress of Theoretical Physics* 77:1402–1401.

5291

ALUMINUM-MAGNESIUM ISOTOPE SYSTEMATICS OF CHONDRULES FROM CR CHONDRITES

K. Nagashima[1], A. N. Krot[1], and M. Chaussidon[2]. [1]University of Hawai'i at Manoa, USA. E-mail: kazu@higp.hawaii.edu. [2]CRPG/CNRS, France.

Introduction: The inferred uniform distribution of the short-lived radionuclide ^{26}Al in the inner solar system [1, 2] makes it one of the best chronometer for dating the earliest processes in the solar nebula, including CAI and chondrule formation. The ^{26}Al-^{26}Mg systematics in chondrules from primitive ordinary, CO3.0, and Acfer 094 (ungrouped) chondrites suggest contemporaneous formation of chondrules from ordinary and CO chondrites that started ~1 Myr after formation of CAIs with ^{26}Al/^{27}Al of ~5×10^{-5} and lasted for ~2 Myr [3–7]. To constrain age and duration of chondrule formation, we study ^{26}Al-^{26}Mg systematics of Al-rich, type I, and type II chondrules in CRs, which are mineralogically pristine and retained their primary nebular signatures [8]. Although it has been previously shown that there is a Pb-isotopic age difference between chondrules in CRs and CAIs in CVs [9], resolvable ^{26}Mg excess (^{26}Mg*) was reported only in 1 out of 11 CR chondrules studied [10].

Experimental: Mg-isotopic compositions were measured in two type I, two type II, and three Al-rich chondrules from EET 92042, EET 92147, GRA 95229, and NWA 721 using the UH Cameca IMS 1280 SIMS. We also analyzed a type C CAI #10 from El Djouf 001 that appears to have experienced melting during chondrule formation [11]. Mg isotopes and ^{27}Al were measured with a monocollector EM and FC, respectively. The mass-resolving power was set to ~3800. ^{26}Mg* was calculated assuming a linear mass-fractionation law. Most measurements were done in plagioclase. Relative sensitivity factor for plagioclase was calculated based on the measurements on Miyakejima plagioclase.

Results and Discussion: Two Al-rich and one type II chondrules, and type C CAI show resolvable ^{26}Mg* corresponding to $(^{26}\text{Al}/^{27}\text{Al})_0$ ratio of $(6.2 \pm 0.8) \times 10^{-6}$ and $(0.95 \pm 0.3) \times 10^{-6}$, $(2.2 \pm 1.4) \times 10^{-6}$, and $(1.4 \pm 0.9) \times 10^{-6}$, respectively (all data are fitted through the origin). The remaining chondrules have no resolvable ^{26}Mg*: $(^{26}\text{Al}/^{27}\text{Al})_0 < 3 \times 10^{-6}$. The inferred $(^{26}\text{Al}/^{27}\text{Al})_0$ ratios in the CR chondrules correspond to an age difference of ~2–4 Myr after CAIs with the canonical ^{26}Al/^{27}Al ratio, consistent with an age difference inferred from Pb-Pb isotope systematics [9]. Most of the CR chondrules analyzed so far, however, appear to have formed 3–4 My after CAIs. The CR chondrule ages are systematically lower than those from primitive ordinary and CO3.0 chondrites [3–7], indicating that formation of the majority of CR chondrules postdated the formation of most chondrules in ordinary and CO chondrites and lasted for ~2 Myr. The inferred $(^{26}\text{Al}/^{27}\text{Al})_0$ in type C CAI #10 and 2 Al-rich chondrules (Fig. 1) showing O-isotope heterogeneity due to the presence of CAI relict grains [11] suggest that some CAIs were recycled late, during CR chondrule formation.

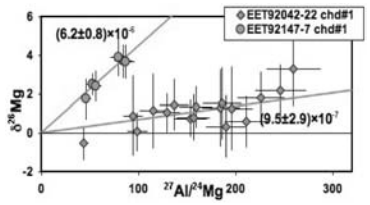

Fig. 1.

References: [1] Bizzarro et al. 2004. *Nature* 431:275. [2] Thrane et al. 2006. *The Astrophysical Journal* 646:159. [3] Kita et al. 2000. *Geochimica et Cosmochimica Acta* 64:3913. [4] Huss et al. 2001. *Meteoritics & Planetary Science* 36:975. [5] Kunihiro et al. 2004. *Geochimica et Cosmochimica Acta* 68:2947. [6] Kurahashi et al. 2004. #1476. 35th LPSC. [7] Sugiura and Krot. *Meteoritics & Planetary Science*. Forthcoming. [8] Krot et al. 2002. *Meteoritics & Planetary Science* 39:1931. [9] Amelin et al. 2002. *Science* 297:1678. [10] Marhas et al. 2000. *Meteoritics & Planetary Science* 35: A102. [11] Krot et al. 2005. *The Astrophysical Journal* 622:1333.

5278

HYDROTHERMAL ALTERATION EXPERIMENTS ON ANHYDROUS COMETARY IDPs

K. Nakamura-Messenger[1, 2], S. Messenger[1], S. J. Clemett[1, 2], and L. P. Keller[1]. [1]Robert M Walker Laboratory for Space Science, ARES, NASA Johnson Space Center, Houston, Texas 77058, USA. E-mail: keiko.nakamura-1@nasa.gov. [2]ESCG, NASA/JSC Houston, TX, USA.

Introduction: Although hydrated interplanetary dust particles (IDPs) bear some similarities to carbonaceous chondrites, some are distinguished by high carbon contents (bulk C ~3-6X CI) [1]. Thomas et al. [2] suggested that carbon-rich hydrated particles may have been derived from aqueously altered anhydrous cometary materials. Spectroscopic features of hydrated silicates and carbonate were reported from the Deep Impact mission, suggesting that some comets contain aqueously altered materials [3]. Anhydrous (CP) IDPs are good candidates for the original precursor of C-rich hydrated IDPs. To evaluate this cometary aqueous alteration hypothesis, we carried out a systematic series of hydrothermal alteration experiments on CP IDPs. We have previously shown that such experiments are feasible [4]. Here we have broadened the parameters of our experiments to determine how these materials behave when exposed to different thermal and aqueous environments.

Methods: Individual cluster CP IDPs were embedded in epoxy and 70 nm thick sections were obtained by ultramicrotomy then transferred to C-coated Cu or Au grids. The sample grids were immersed in aqueous solutions (pH 7–14), and heated at 25~150 °C for 12 to 96 hours. The sections were observed before and after the hydrothermal experiments by transmission electron microscopy (TEM) for precise mineralogical and crystallographic studies of individual phases.

Results: After 12 h in 25 °C pH 13 solution, GEMS grains were altered, showing wavy layered structures. These materials were poorly crystalline and rapidly degraded in the electron beam, such that diffraction and lattice fringe data could not be acquired. Their chemical compositions remained unchanged. After 24 h in 100 °C pH 12, enstatite grains were also altered. Chemically and crystallographically, the enstatite appears to have transformed into serpentine. After 24 h in 100 °C pH 13, the sample completely transformed into Fe, Mg-rich fibrous layer silicate, probably smectite.

Discussion: These parameters are well-matched with previous predictions based on computer modeling (e.g., [5]). We reported unusual IDPs whose mineralogical and isotopic characteristics are mostly typical of anhydrous cometary CP IDPs but also contained minor hydrated phases (hybrid IDPs) [6]. The hybrid IDPs have very primitive characteristics which are normally associated with anhydrous IDPs. The hybrid IDPs contain up to 10% of the phyllosilicate smectite, indicating of non-optimal conditions for aqueous alteration such as improper pH, minimal fluid, or low-T. Hybrid IDP like material was produced in 12 h in 25 °C pH 13 solution, which is probably the minimum condition to initiate aqueous alteration reactions in cometary materials.

References: [1] Keller L. P. et al. 1993. 24th LPSC. p. 785. [2] Thomas et al. 1995. *Meteoritics* 27:296. [3] Lisse C. et al. 2006. *Science* 313:635. [4] Nakamura K. et al. 2005. *Meteoritics & Planetary Science* 40:A110. [5] Brearley A. J. 2006. In *Meteorites and the early solar system* II. p. 584. [6] Nakamura K. et al. 2005. Abstract #1824. 36th LPSC.

5093

HEAVILY FRACTIONATED NOBLE GASES IN AN ACID RESIDUE FROM THE KLE 98300 EH3 CHONDRITE

D. Nakashima[1, 2], U. Ott[2], A. El Goresy[3], and T. Nakamura[4]. [1]Laboratory for Earthquake Chemistry, University of Tokyo, Tokyo, Japan. E-mail: naka@eqchem.s.u-tokyo.ac.jp. [2]Max-Planck-Institut für Chemie, Mainz, Germany. [3]Bayerisches Geoinstitut, Universität Bayreuth, Bayreuth, Germany. [4]Department of Earth and Planetary Sciences, Kyushu University, Fukuoka, Japan.

E3 chondrites are known to show characteristic signatures of noble gases, i.e., sub-Q gases ($^{36}Ar/^{132}Xe = 37 \pm 18$; [1]), which are believed to be products of elemental fractionation of Q gases ($^{36}Ar/^{132}Xe = 50–100$; [2]). However, isotopic compositions and host phases of sub-Q gases are still unknown. If sub-Q gases are fractionated Q gases, sub-Q gases should be contained in HF/HCl residues, similar to the case of Q gases [3]. In this study, we analyzed noble gases in a HF/HCl residue of the KLE 98300 EH3 chondrite, which is suspected to contain sub-Q gases [4].

The $^{36}Ar_{trapped}/^{84}Kr/^{132}Xe$ ratios are 10.3/0.3/1, which are below the Q-range and even lower than sub-Q elemental ratios. Xe isotopic ratios are almost identical to those of Xe-Q [3]. The same is true for Kr isotopic ratios. Thus, heavy noble gases in an acid residue of KLE 98300 are isotopically Q-like but are elementally fractionated relative to Q gases, suggesting that the acid residue contains fractionated Q gases, which may be sub-Q gases.

Assuming that the acid residue of KLE 98300 had contained Q noble gases with typical elemental ratios ($^{36}Ar/^{84}Kr/^{132}Xe = 76/0.8/1$; [2]) and that fractionation of the Q gases occurred on the parent body, there are two possible explanations: thermal metamorphism and shock heating. Although elemental ratios reflect thermal metamorphism [2], Q gas elemental ratios of highly equilibrated ordinary chondrites such as type 6 are still in the Q-range [5]. Shock recovery experiments showed that shock heating induces Q gas depletion but does not change Q gas elemental ratios [6]. Thus, such parent body processes are not responsible for the highly fractionated Q gases in KLE 98300. Therefore, it is considered more likely that Q gases in KLE 98300 had already been fractionated before accretion to the parent body. This is consistent with the suggestion of [1].

In summary, we found elementally fractionated Q gases in a HF/HCl residue of the KLE 98300 EH3 chondrite. Since the elemental ratios can not be explained by parent body processes, fractionation processes prior to the accretion to the parent body should be considered.

Acknowledgements: We thank C. Sudek for technical support during HF/HCl treatments of meteorite samples.

References: [1] Patzer A. and Schultz L. 2002. *Meteoritics & Planetary Science* 37:601–612. [2] Busemann H. et al. 2000. *Meteoritics & Planetary Science* 35:949–973. [3] Lewis R. S. et al. 1975. *Science* 190: 1251–1262. [4] Nakashima D. et al. 2006. Abstract #1119. 37th Lunar and Planetary Science Conference. [5] Alaerts L. et al. 1979. *Geochimica et Cosmochimica Acta* 43:1399–1415. [6] Nakamura T. et al. 1997. Abstract #1416. 28th Lunar and Planetary Science Conference.

5096

CHEMICAL AND ISOTOPIC SIGNATURES DURING HYDROUS ALTERATION OF INSOLUBLE ORGANIC MATTER FROM CM CHONDRITES

H. Naraoka and Y. Oba. Department of Earth Sciences, Okayama University, Japan. E-mail: naraoka@cc.okayama-u.ac.jp.

Introduction: Carbonaceous chondrites contain a high-molecular and solvent-insoluble organic matter (IOM) as the most abundant component for carbon species. This macromolecular IOM is consisted mainly of aromatic hydrocarbon structure with minor aliphatic carbon as well as heteroelements (N, O, S). Using several IOM purified from the Murchison and Antarctic CM chondrites, we have revealed a wide variation of H/C ratio, indicating various degrees of thermal alteration [1]. The high H/C (0.62 by atomic) IOM of the Murchsion meteorite yielded abundant acetic acid (~400 ppm) during hydrous pyrolysis, being an important abiotic process to generate acetic acid [2]. In this study, we have examined chemical and isotopic changes of the resulting Murchison IOM after hydrous pyrolysis, and discussed the $\delta^{13}C$ and δD distribution of IOM from Antarctic CM chondrites with respect to their alteration.

Experimental: The Murchison IOM was subjected to hydrous pyrolysis at 270 °C, 300 °C, and 330 °C for 72 hours in a degassed sealed tube. The D value of water used in this study (−75‰ relative to SMOW) is similar to that of bulk water in Murchison (~−88‰) [3]. The $\delta^{13}C$ and δD values of the resulting IOM residue were determined using an isotope ratio mass spectrometer in on-line mode coupled with an elemental analyzer and a high-temperature pyrolyzer, respectively.

Results and Discussion: With increasing temperature, the H/C ratio of the Murchison IOM decreased down to 0.31 due to preferential loss of H to C. Furthermore, the bulk δD value decreased significantly from +986‰ (original) to +307‰ (270 °C) and +25‰ (330 °C), indicating that the hydrogen of IOM can be readily exchangeable with environmental water under hydrothermal condition. The $\delta^{13}C$ (relative to PDB) of the Murchison IOM became larger by a few ‰ from −13.0‰ (original) to −16.1‰ (330 °C) during the hydrous pyrolysis.

The chemical and isotopic signatures of the Murchison IOM after hydrous pyrolysis are compared to $\delta^{13}C$ and δD values of Antarctic CM meteorites. The thermally altered CM chondrites such as B-7904 and A-881280 show relatively small H/C ratio (0.15–0.29) with $\delta^{13}C$ of −13.9 to −15.1‰ and δD of +432 to +450‰, suggesting a potential evolution of IOM during hydrothermal activity on the meteorite parent body. Although the chemical signature of Y-793321 and A-881334 (H/C = 0.34–0.36) implies the similar thermal evolution as that of B-7904 and A-881280, the $\delta^{13}C$ signature is distinctive (−7.6 to −9.0‰), possibly due to different origins.

References: [1] Naraoka H. et al. 2004. *Meteoritics & Planetary Science* 39:401–406. [2] Oba Y. and Naraoka H. 2006. *Meteoritics & Planetary Science* 41:1175–1181. [3] Robert F. 2002. *Planetary and Space Science* 50:1227–1234.

5307

EVIDENCE FOR AN IMPACT STRUCTURE IN THE SANGRE DE CRISTO MOUNTAINS NEAR SANTA FE, NEW MEXICO

H. E. Newsom[1], W. E. Elston[1], B. A. Cohen[1], E. L. Tegtmeier[1], M. T. Petersen[1], A. S. Read[2], and T. H. McElvain[3]. [1]Department of Earth and Planetary Sciences, University of New Mexico, MSC03-2050, Albuquerque, NM, 87131, USA. E-mail: newsom@unm.edu. [2]New Mexico Bureau of Geology, NM Tech, 801 Leroy Place, Socorro, NM 87801–4796, USA. [3]111 Lovato Lane, Santa Fe, NM 87505, USA.

Introduction: Shatter cones discovered in 2005 in road cuts on NM 475 in the Sangre de Cristo Mountains equal those of Sudbury and Vredefort in centimeter to meter size. Breccias in Proterozoic crystalline basement and fault blocks of Mississippian-Pennsylvanian carbonates are now being examined to determine whether their distribution is compatible with development stages observed in other large impact structures including: 1) Excavation stage—ejecta blanket, fall-back breccia, in situ breccias of crater wall and floor. 2) Breccia dikes and pseudotachylites injected into the crater wall and floor, subsequent to the shock wave responsible for shatter cones. 3) Landslide blocks and megabreccias (clasts >1 m) from collapse of the crater wall during the enlargement stage.

As NM 475 rises into the mountain, it passes into deeper structural levels. Breccias encountered are tentatively interpreted a progressing from crater wall to floor to subfloor. Distances to key exposures are in miles, tentative interpretations in italics:

0.0 Santa Fe, intersection of NM 475 and NM 590.

4.1 Curve. *Allochthonous km-size carbonate blocks carried by a crater-collapse debris avalanche:* Blanket of matrix-supported megabreccia, with clasts of Proterozoic crystal-line rocks, separates brecciated in situ Proterozoic from Paleozoic carbonates. This zone is bleached within 10 m of the contact, as seen across the valley as well. Near foot of next ridge north, a megabreccia tongue penetrates basal carbonates. It incorporates carbonate clasts with millimeter-wide fractures, injected by granite grains with multiple fracture sets in quartz. Preliminary optical examination of these fractures (which need to be confirmed by other methods) suggest that these are PDFs.

4.3 Cross bridge. *Collapse megabreccia:* Elongated (max 10+ m) steeply dipping brecciated granite clasts and meter-size clasts of sheared mafic schist. Similar megabreccias occur along I-25, 20 km south of this location.

Down creek 50 m: *Breccia dike injected from above, in a fluidized medium:* Breccia wall, angular decimeter granite clasts supported by comminuted granite matrix; sparse rounded decimeter-to-meter clasts of mafic schist in accretionary envelopes.

5.9 *Subfloor:* Shatter cones in autochthonous granite and schist, best developed in granite.

Conclusions: In view of the complex tectonic history of the region, the significance of various breccias remains uncertain. However, the presence of PDFs (if confirmed) and shatter cones indicates that impact played a role. The maximum age of the event is Mississippian, actual age and extent of the structure are undetermined. Accumulating field evidence suggests that this could be a substantial structure with regional implications.

5286

TITANIUM ISOTOPIC COMPOSITIONS OF RARE PRESOLAR SIC GRAIN TYPES FROM MURCHISON

A. N. Nguyen[1], L. R. Nittler[1], C. M. O'D. Alexander[1], and P. Hoppe[2]. [1]Department of Terrestrial Magnetism, Carnegie Institution of Washington, Washington, D.C., USA. E-mail: nguyen@dtm.ciw.edu. [2]Max-Planck-Institut fur Chemie, Kosmochemie, P.O. Box 3060, D-55020 Mainz, Germany.

Introduction: The different types of presolar SiC grains form in distinct stellar sources. Mainstream SiC from low-mass C-rich asymptotic giant branch (AGB) stars make up the large majority of all presolar SiC grains, and thus have been the most widely studied [1]. The rare grain types Y and Z are believed to originate from lower-than-solar metallicity AGB stars [2, 3] whereas X grains condense in type II supernovae [4] and A+B grains could form in J-type carbon stars [5]. These group classifications are based on the grains' C, N, and Si isotopic compositions. Titanium isotopic ratios are affected by Galactic chemical evolution, but also by neutron capture nucleosynthesis in AGB stars. Only about 250 presolar SiC grains have been analyzed for their Ti isotopic compositions, again with most being mainstream grains [3–10]. In this study, we focus on obtaining Ti isotopic compositions of rare type presolar SiC grains.

Experimental: We selected presolar SiC grains from Murchison residues that were previously analyzed for their C and Si isotopes in the Carnegie IMS 6f. For five A+B grains, the Al and Mg isotopes had also been measured in the Mainz NanoSIMS. We measured the 5 Ti isotopes, ^{28}Si, and ^{52}Cr simultaneously in the Carnegie NanoSIMS 50L. The ^{52}Cr was measured to correct for interference from ^{50}Cr. A total of 70 grains were analyzed (27 A+B, 22 Y, 9 Z, 3 X, and 9 mainstream), with most being 1 μm or less in size following the previous isotopic measurements.

Results: The Ti isotopic compositions of the SiC grains of all types fall in the ranges that have been seen in previous work [3–10]. For the A+B grains, the ^{46,47,49,50}Ti/^{48}Ti ratios form a positive correlation with δ^{29}Si and overlap the trend seen in mainstream SiC, though the slope is a bit more shallow. The Z grains exhibit the lowest ^{46,47,49}Ti/^{48}Ti ratios, which are correlated with low δ^{29}Si. The trend displayed between these ratios is an extension of the trend seen for mainstream SiC grains [6, 9, 11], consistent with an origin in lower-than-solar metallicity AGB stars. These grains show excesses of ^{50}Ti (and ^{30}Si) due to n-capture, which is expected to be more prominent in lower metallicity stars. The Y grains also show excesses in ^{50}Ti due to s-process contributions. While in some grains the Ti appears to be in solid solution, others clearly contain internal TiC grains, indicated by wide variations in Ti count rates during a measurement. It will be constructive to determine whether certain grain types contain more internal TiC than others.

References: [1] Hoppe P. and Ott U. 1997. In *Astrophysical implications of the laboratory study of presolar material.* pp. 27–58. New York: AIP. [2] Hoppe P. et al. 1997. *The Astrophysical Journal* 487:L101–L104. [3] Amari S. et al. 2001. *The Astrophysical Journal* 546:463–483. [4] Nittler L. R. et al. 1996. *The Astrophysical Journal* 462:L31–L34. [5] Amari S. et al. 2001. *The Astrophysical Journal* 559:248–266. [6] Alexander C. M. O'D. and Nittler L. R. 1999. *The Astrophysical Journal* 519:222–235. [7] Gyngard F. et al. 2006. *Meteoritics & Planetary Science* 41:A71. [8] Hoppe P. et al. 1994. *The Astrophysical Journal* 430:870–890. [9] Huss G. R. and Smith J. B. *Meteoritics & Planetary Science.* Forthcoming. [10] Zinner E. et al. *Geochimica et Cosmochimica Acta*. Forthcoming. [11] Lugaro M. et al. 1999. *The Astrophysical Journal* 527: 369–394.

5281

COSMOGENIC IRON-60 IN IRON METEORITES: MEASUREMENTS BY LOW-LEVEL COUNTING

K. Nishiizumi[1] and M. Honda[2]. [1]Space Sciences Laboratory, University of California, Berkeley, CA 94720–7450, USA. E-mail: kuni@ssl.berkeley.edu. [2]Department of Chemistry, Nihon University, Setagaya-ku, Tokyo, Japan.

Introduction: ^{60}Fe with a half-life of 1.5 Myr is produced from ^{62}Ni and ^{64}Ni by cosmic rays. The production rate of ^{60}Fe in meteorites is far lower than for other cosmogenic nuclides such as ^{10}Be, ^{26}Al, ^{36}Cl, or ^{53}Mn because of the low isotopic abundance of ^{62}Ni (3.63%) and ^{64}Ni (0.93%). Previous measurements of ^{60}Fe in meteorites have been very limited due to the low specific activity of the nuclide in addition to its low concentration. Since the first ^{60}Fe measurement in the Odessa iron meteorite [1], only a few results have been published based on accelerator mass spectrometry (AMS) measurements [2, 3]. Even with the high sensitivity of AMS, ^{60}Fe measurements are very difficult due to the low isotopic ratio measured, ~10^{-14} ^{60}Fe/Fe. In this work, ^{60}Fe in iron meteorites was measured using low level counting methods.

Sample and Methods: 2.37 kg of Odessa (IAB, 7.25% Ni) [1], 0.74 kg of Bogou (IAB, 7.15% Ni), 1.5 kg of Carbo (IID, 10.02% Ni), 1.5 kg of Grant (IIIAB, 9.24% Ni), 0.5 kg of Williamstown (Kenton County, IIIAB, 7.38% Ni), and 0.5 kg of Aroos (Yardymly, IICD, 6.71% Ni) were dissolved and Fe fractions from each iron meteorite were separated in 1958–1963. ^{60}Fe β-decays to ^{60}Co ($t_{1/2}$ = 5.27 yr). In 1980, we extracted Co from each Fe fraction using a series of isopropyl ether solvent extractions and anion ion exchange columns. The activity of ^{60}Co in the Fe solutions was near secular equilibrium with ^{60}Fe by 17–20 yr after separation of the Fe fraction. First, the milked ^{60}Co was measured using a well-type Ge detector. Then we measured the ^{60}Co in 3 samples by β–γ coincidence using a gas-flow GM counter and a 3" well type NaI(Tl) detector equipped with an anti-coincidence guard counter.

Results and Discussion: We found 0.16 ± 0.06 dpm ^{60}Fe/kgFe (2.0 ± 0.7 dpm ^{60}Fe/kgNi) for Odessa, 0.26 ± 0.09 (2.5 ± 0.8) for Grant, 0.33 ± 0.26 (4.2 ± 3.3) for Bogou, and 0.20 ± 0.08 (1.8 ± 0.7) for Carbo using Ge detector measurements. ^{60}Co measurements for Aroos and Williamstown are indistinguishable from the blank. The β–γ coincidence technique reduced uncertainties but required more than a 2-month counting period for each sample. As we expected, the dpm ^{60}Fe/kgNi is well correlated with the observed ^{53}Mn concentration for each iron meteorite. Goel and Honda [1] found an ^{60}Fe specific activity of 0.9 ± 0.2 dpm/kg Fe in Odessa, a factor of 6 higher than this work. On the other hand, ^{60}Fe measurements by AMS [2] gave about a factor 2 lower than this work. It has been 27 years, 5 half-lives of ^{60}Co, since the last Co extraction from these 6 iron meteorite solutions. It would be possible to extract Co from the iron solutions and to measure ^{60}Co again. The counting time would be 2–3 weeks per sample for ±10% uncertainty using the present high-sensitivity Ge detector system. Aliquots of the Fe solution, an amount of <10^{-5} of the solution, could be used for AMS measurement of ^{60}Fe to allow comparison of the two determination methods. On the other hand, the low-level counting method used in this work is not applicable for new meteorite samples.

Acknowledgments: We thank the U.S. Natural History Museum and E. L. Fireman for providing meteorite samples. This work was supported by NASA grants.

References: [1] Goel P. and Honda M. 1965. *Journal of Geophysical Research* 70:747–748. [2] Knie K. et al. 1999. *Meteoritics & Planetary Science* 34:729–734. [3] Kutschera W. 1986. *Nuclear Instruments and Methods in Physics Research B* 17:377–384.

5188

COSMOGENIC RADIONUCLIDES IN GLASS SPHERULES FROM THE SOUTH POLE WATER WELL IN ANTARCTICA

K. Nishiizumi[1], M. W. Caffee[2], and S. Taylor[3]. [1]Space Sciences Laboratory, University of California, Berkeley, CA 94720–7450, USA. E-mail: kuni@ssl.berkeley.edu. [2]Department of Physics, Purdue University, West Lafayette, IN 47907, USA. [3]CRREL, Department of the Army, Hanover, NH 03755, USA.

Introduction: Micrometeorites in the size range 0.1–1 mm, originally extracted magnetically from deep-sea sediments [1] have been collected from ice in Greenland and Antarctica (e.g., [2, 3]). Most cosmochemical analyses were made on iron or silicate spherules from deep-sea sediments. Glass spherules are rare in deep sea sediments [4] but common in polar ice deposits and they have not been proven to be extraterrestrial. Their major elemental compositions and the presence of Fe-Ni beads in about 10% of the glass spherules suggest that they might be extraterrestrial, however, the most unambiguous means of identifying this material as extraterrestrial materials is the detection of cosmogenic nuclides.

Sample Description and Analysis: Three glass spherules (SP18-4, 18-5, and 19-2) were collected from the South Pole water well, Antarctica, and have a depositional age between 1100 and 1500 A.D. [3]. SP18-4 (470 μm in diameter) was green-yellow glass, SP18-5 (430 μm) was dark brown to black opaque glass, and SP19-2 (720 μm) was brown glass and had many bubbles (<10 μm in diameter) in it. Quantitative elemental analysis for a polished surface of each spherule was performed using EPMA with a spot size of 30 μm diameter beam. After weighing, the individual samples were dissolved and Be and Al were isolated for AMS measurements [5]. The ^{10}Be and ^{26}Al concentrations were determined at the Lawrence Livermore National Laboratory (LLNL) AMS facility [6] and are shown in Table 1.

Discussion: Cosmogenic nuclide concentrations clearly indicate all glass spherules are extraterrestrial in origin. ^{26}Al concentrations in the spherules are higher than those produced by galactic cosmic rays and indicate the production by solar cosmic rays as small bodies in space. Using on ^{10}Be, ^{26}Al, target elemental concentrations, and calculated production rates [7], we estimate the exposure condition of each spherule. SP18-4 and 19-2 were exposed to cosmic rays for more than 3 Myr and had radii of 1–2 cm before atmospheric entry. The exposure age of SP18-5 was ~0.3 Myr and its pre-atmospheric radius was ≤7 mm. However, the classification of original materials is still unknown.

Table 1. Chemical composition (wt%) and cosmogenic nuclide concentrations (dpm/kg) of glass spherules.

	O	Mg	Al	Si	Ca	Mn	Fe	^{10}Be	^{26}Al
SP18-4	45	20.0	1.67	24.3	1.27	0.29	7.7	16.1 ± 0.7	134 ± 5
SP18-5	44	18.7	1.54	22.2	1.80	0.69	11.0	1.2 ± 0.4	72 ± 7
SP19-2	42	16.8	–	21.2	5.33		14.5	13.4 ± 0.4	80 ± 3

Acknowledgments: This work was supported by NASA and NSF grants. Part of this work was performed under the auspices the DOE by UC-LLNL under contract W-7405-Eng-48.

References: [1] Brownlee D. E. 1981. In *The sea 7*, edited by Emiliani C. pp. 733–762. [2] Maurette M. et al. 1991. *Nature* 351:44–47. [3] Taylor S. et al. 1998. *Nature* 392:899–903. [4] Nagasawa H. et al. 1979. *Geochimica et Cosmochimica Acta* 43:267–272. [5] Nishiizumi K. et al. 1991. *Earth and Planetary Science Letters* 104:315–324. [6] Davis J. C. et al. 1990. *Nuclear Instruments and Methods in Physics Research B* 52:269–272. [7] Reedy R. C. 1990. 21st Lunar and Planetary Science Conference. pp. 1001–1002.

5179

PALEOMAGNETISM OF BASALTS FROM LONAR IMPACT CRATER

I. Nishioka[1], M. Funaki[2], and K. Venkata Rao[3]. [1]The Graduate University for Advanced Studies, Kanagawa 240-0193, Japan. E-mail: nishioka@nipr.ac.jp. [2]National Institute of Polar Research, Tokyo 173-8515, Japan. [3]Geological Survey of India, Nagpur 440006, India.

Introduction: Magnetic anomaly studies of Martian and lunar surfaces demonstrated the presences of demagnetized areas around the large impact structures [1–2]. Strong stress waves were estimated to be responsible for parts of the demagnetization. To investigate effects of impact crater formation in natural remanent magnetization of surrounding rocks, we studied paleomagnetism of Lonar impact crater in Maharashtra state, central India.

Lonar is a bowl-shaped simple crater with a rim-to-rim diameter of 1.8 km. The crater was entirely formed in Deccan basalt flows. At least five lava flows can be recognized on the inner wall of the crater. Eight to ten cores were collected from the uppermost flows at eight sites, the lower flows at ten sites, and outside of the rim at seven sites. Alternating field and thermal stepwise demagnetizations were performed on these samples. The outward tilting of the basalt flows due to the uplifted rim were corrected to constrain timing of remanence acquisition.

Results: As earlier studies have demonstrated, two paleomagnetic directions were isolated for basalts from the inner walls [3–4]. The soft component was erased until 10–20 mT while the hard component decayed linearly to the origin of orthogonal plot.

The hard component, which is probably primary remanence of the Deccan basalt, passed the positive fold test. The overall mean direction for the uppermost flows after the tilt correction ($D = 125°$, $I = 41°$, $a95 = 4°$) was similar to that of the outside sites ($D = 126°$, $I = 38°$, $a95 = 3°$). The directions of the soft component were near parallel to the present earth field in this area. In contrast to the hard component, Fisher's precision parameter decreased after the tilt correction. This decrease yields the negative fold test for both upper and lower flows.

Discussions: The hard component was restored to the pre-impact direction after the tilt correction. The pre-existing magnetization of the uppermost flow remained stable within the rocks through the impact event. More scattered directions of the hard component for the lower flows might be explained by the large secular variation of the geomagnetic field at that time [5]. In contrast to the hard component, the low-coercivity part of the magnetization was acquired after the uplift of the rim. Shock remanence is expected to be acquired in the early stage of impact cratering process before any tectonic movements [4]. The soft component of the basalt from Lonar is, thus, likely viscous or chemical remanent magnetization.

References: [1] Mohit P. S. and Arkani-Hamed J. 2004. *Icarus* 168: 305–317. [2] Halekas J. S. et al. 2002. *Geophysical Research Letters* 29: 1645. [3] Poornachandra Rao G. V. S. and Bhalla M. S. 1984. *Geophysical Journal of the Royal Astronomical Society* 77:847–862. [4] Cisowski S. M. and Fuller M. 1978. *Journal of Geophysical Research* 83:3441–3458. [5] Vandamme D. et al. 1991. *Reviews in Geophysics* 29:159–190.

5156

HYDROTHERMAL EXPERIMENTS OF ENSTATITE WITH Fe AND SiO_2: EVALUATION OF EFFECTS OF METAL AND GLASS ON AQUEOUS ALTERATION OF CHONDRULES IN CV AND CR CHONDRITES

I. Ohnishi and K. Tomeoka. Graduate School of Science, Kobe University, Nada, Kobe 657-8501, Japan. E-mail: ichiro@kobe-u.ac.jp.

Introduction: Carbonaceous chondrites of types 1–3 contain various amounts of hydrous phyllosilicates. The phyllosilicates differ among the different types of chondrite [1–3]; e.g., saponite forms in CV chondrites, whereas serpentine forms in CR chondrites. Our recent hydrothermal alteration experiments of enstatite [4] suggested that the differences in phyllosilicate mineralogy mainly resulted from different pH of aqueous solution.

Some CV chondrites and most CR chondrites show evidence of limited degree of aqueous alteration (e.g., [1–3]). Previous studies (e.g., [1–3]) showed that mesostasis glass, Fe-Ni metal, and enstatite in chondrules in those chondrites were more preferentially involved in aqueous alteration than other major constituents. This raises the possibility that the reactions of these phases at an early stage of alteration gave some influence on alteration conditions, thus on alteration products.

In order to test this possibility, we conducted hydrothermal experiments of the three different sets of powdered starting materials: 1) orthoenstatite (OEN) and Fe metal (9/1 in weight ratio); 2) OEN and Fe metal (5/5); and 3) OEN and SiO_2 (9/1). Each set of starting materials was reacted with aqueous solutions of pH 12 (0.01-N NaOH), 13 (0.1-N NaOH), and 14 (1-N NaOH) at 300 °C for 168 h (see [4] for experimental details). The recovered samples were studied using XRD, SEM, and TEM.

Results: *Experiment 1 (OEN/Fe = 9/1)*: At pH 12, small XRD peaks of serpentine are detected. At pH 13 and 14, XRD peaks of not only serpentine but also saponite are found.

Experiment 2 (OEN/Fe = 5/5): At pH 12 and 13, large XRD peaks of only serpentine are detected. At pH 14, large XRD peaks of both serpentine and saponite are detected. Under the same pH conditions, intensities of serpentine peaks are larger than those in the products of experiments 1.

Experiment 3 (OEN/SiO_2 = 9/1): At all pHs (12, 13, and 14), XRD peaks of saponite are detected, and their intensities increase with increasing pH. No serpentine peaks are found.

Discussion: The results of our experiments showed that aqueous alteration of enstatite depends on not only pH but also Fe and SiO_2 contents of the solutions. In the Fe-bearing systems, there are two tendencies: 1) the proportion of serpentine and saponite increases with decreasing pH, and 2) the amounts of serpentine increase with increasing Fe contents. In the SiO_2-bearing system, only saponite forms and the amounts of saponite increase with increasing pH. These results suggest that, in CR chondrites, enstatite was altered under low alkaline conditions, and the dissolution of Fe-Ni metal facilitated the formation of serpentine. In CV chondrites, enstatite was altered under more alkaline conditions, and the dissolution of SiO_2 glass facilitated the formation of saponite.

References: [1] Tomeoka K. and Buseck P. R. 1990. *Geochimica et Cosmochimica Acta* 54:1745–1754. [2] Keller L. P. and Buseck P. R. 1990. *Geochimica et Cosmochimica Acta* 54:2113–2120. [3] Weisberg M. K. et al. 1993. *Geochimica et Cosmochimica Acta* 57:1567–1586. [4] Ohnishi I. and Tomeoka K. 2007. *Meteoritics & Planetary Science* 42:49–61.

5110

IMPACT-MELT GENERATION AT METEOR CRATER, ARIZONA: IMPLICATIONS FOR IMPACTS INTO VOLATILE-RICH TARGET ROCKS

G. R. Osinski[1], T. E. Bunch[2], and J. Wittke[2]. [1]Canadian Space Agency, 6767 Route de l'Aeroport, Saint-Hubert, QC, J3Y 8Y9, Canada. E-mail: gordon.osinski@space.gc.ca. [2]Geology Department, Bilby Research Center, Northern Arizona University, Flagstaff, AZ, USA.

Introduction: Impact melting is one of the most characteristic features of meteorite impact events. It is known that target lithology, in particular the effect of volatiles, plays an important role in determining the amount of melt generated and the characteristics of impact melt–bearing impactites. Here we present the results of our ongoing investigations of the generation of impact melts at Meteor Crater, Arizona.

Impact melts at Meteor Crater: Meteor Crater was formed ~50 ka by the impact of an ~40 m diameter iron projectile into a target sequence of interbedded dolomite and sandstone, with subordinate limestone and siltstone [1]. Recent studies have yielded important information about the generation of impact melt at Meteor Crater. Hörz et al. [2] provided the first detailed study of the ballistically dispersed melt particles and placed constraints on the stratigraphic extent of the melt zone. Melosh and Collins [3] suggested that Meteor Crater formed by a low-velocity impact event. Our studies have documented the presence of carbonate-derived melts [4] and impact melt–bearing breccias [5] at Meteor Crater for the first time.

Results: Here we show that siliceous dolomite, limestone, and carbonate-bearing sandstones underwent shock melting during the formation of Meteor Crater. The initial product was a SiO_2-poor, CaO-MgO-CO_2-rich dolomitic melt that crystallized Ca-rich clinopyroxene, Mg-rich olivine, Mg-rich orthopyroxene, calcite, and minor dolomite. The residual melt quenched to a glass with exceptional CO_2 contents (up to 40 wt%). Spherules of calcite and the skeletal habit of the silicate crystallites attest to rapid quenching of the melt.

Discussion and Conclusions: We have shown that carbonates underwent melting at Meteor Crater, in addition to other sedimentary lithologies as previously noted [6]. This work adds to a growing body of evidence showing that impact melting is common during impacts into volatile-rich targets (see [6] for a review). Questions still remain, however, such as why silicate phases derived from the melting of sedimentary rocks are common at Meteor Crater, when at larger craters (e.g., Ries and Haughton), carbonate melt phases predominate.

Acknowledgements: The primary author (G. R. O.) is extremely grateful to the Barringer Family Fund for Meteorite Impact Research for funding this research and to the Barringer Crater Company for access to the site.

References: [1] Shoemaker E. M. 1963. In *The Moon, meteorites and comets*, by Middlehurst B. M. and Kuiper G. P. University of Chicago Press. pp. 301–336. [2] Hörz F. et al. 2002. *Meteoritics & Planetary Science* 37: 501–531. [3] Melosh H. J. and Collins G. S. 2005. *Nature* 434:157. [4] Osinski G. R. et al. 2003. *Meteoritics & Planetary Science* 38:A42. [5] Osinski G. R. et al. 2006. Abstract #1005. 37th Lunar & Planetary Science Conference. [6] Osinski G. R. et al. In *The sedimentary record of meteorite impacts*, by Evans K. et al. Geological Society of America Special Paper. Boulder, Colorado: Geological Society of America. Forthcoming.

5036

INJECTION OF SUPERNOVA DUST GRAINS INTO PROTOPLANETARY DISKS

N. Ouellette[1], S. J. Desch, and J. J. Hester[2]. [1]Department of Physics, Arizona State University, Tempe, AZ, USA. E-mail: Nicolas.Ouellette@asu.edu. [2]School of Earth and Space, Arizona State University, Tempe, AZ, USA.

Introduction: The presence of live ^{60}Fe in the early solar system, with an abundance inferred from meteorites to be $^{60}Fe/^{56}Fe \approx 3–7 \times 10^{-7}$ [1, 2], places it near a stellar nucleosynthetic source at the time of its formation. Non-stellar sources of short-lived radionuclides (SLRs) are not predicted to supply this level of ^{60}Fe [3]. The most plausible source is a nearby core-collapse supernova, as these explosions of massive stars are naturally associated with star-forming regions, and it is likely that the Sun formed in such an environment [4, 5]. Low-mass stars and their protoplanetary disks are typically found ~0.2 pc from massive stars (e.g., [6]). It is likely the solar nebula received many SLRs, including ^{60}Fe, when a massive star exploded a few tenths of a parsec away.

Dust Injection: Numerical hydrodynamics simulations have shown that a disk at least 0.1 pc from a supernova will survive the shock with very little mass loss [7]. However, most of the ejecta are deflected around the disk, and only about 1% of the gas intercepted by the disk is injected. This would be insufficient to account for meteoritic abundances if SLRs like ^{60}Fe remained in the gas phase, but of course all known SLRs are refractory and would have condensed into dust grains within a few years of the supernova explosion [8]. Supernova dust grains larger than 0.1 microns follow trajectories decoupled from the gaseous ejecta. They are not deflected around the disk, but are instead injected very efficiently [9].

Injection Efficiency: We take gas velocities from [7] and calculate the trajectories of supernova dust grains entrained in the ejecta as they cross the bow shock and approach the disk, accounting for gas drag and gravitational forces. We simultaneously calculate their temperatures assuming radiative cooling balances frictional heating. We consider grains approaching the disk with a variety of impact parameters and determine whether they are deflected around the disk, are injected into it but burn up (exceed 1500 K), or penetrate the disk intact. We find that >70% of grains larger than 0.1 microns are injected (95% for 1 micron grains), but most grains smaller than this are deflected.

SLR Abundances: Supernova grains are typically 0.01–10 microns in size, with almost all mass found in large grains that are injected efficiently [10]. If the solar nebula sat 0.2 pc from the supernova of a 25 $M_\odot$ progenitor (using results of [11]), with radius 30 AU and mass 0.01 $M_\odot$, a 90% injection efficiency would result in the disk having $^{60}Fe/^{56}Fe \approx 3.7 \times 10^{-7}$. Other SLRs, including ^{26}Al, ^{41}Ca, ^{36}Cl, and ^{53}Mn, would also be injected in sufficient quantities to explain the meteoritic abundances.

References: [1] Tachibana S. and Huss G. 2003. *The Astrophysical Journal* 588:L41. [2] Mostefaoui S. et al. 2004. *New Astronomy Reviews* 48: 155. [3] Wadhwa M. et al. 2007. In *Protostars and planets V.* p. 831. [4] Hester J. et al. 2004. *Science* 304:1116. [5] Hester J. J. and Desch S. J. 2005. In *Chondrites and the protoplanetary disk* 107. [6] McCaughrean M. J. and O'Dell C. R. 1996. *AJ* 111:1977. [7] Ouellette N. et al. *The Astrophysical Journal*. Forthcoming. [8] Colgan S. W. J. et al. 2004. *The Astrophysical Journal* 427:874. [9] Ouellette et al. 2005. In *Chondrites and the protoplanetary disk* 527. [10] Amari S. et al. 1994 *Geochimica et Cosmochimica Acta* 58:459. [11] Woosley S. E. and Weaver T. 1995. *The Astrophysical Journal* 101:181.

5037

COMPARATIVE STUDY OF NEAR- AND FAR-SIDE LUNAR SOILS: TOWARD THE UNDERSTANDING EARLY EVOLUTION OF THE EARTH AND THE MOON

M. Ozima[1], Q. Z. Yin[2], F. A. Podosek[3], and Y. N. Miura[4]. [1]U. of Tokyo, Japan. E-mail: EZZ03651@nifty.ne.jp. [2]UC Davis, CA, USA. [3]Washington University, St. Louis, USA. [4]ERI, University of Tokyo, Tokyo, Japan.

Because of the almost total lack of geological record on the Earth for the time before 4 Ga, the Earth history during this period is still enigmatic. We propose that a comparative study of far- and near-side lunar soil would shed new light on this dark age of the Earth history as well as on the Earth-Moon system dynamic evolution.

Due to a strong dynamic coupling between the Earth and the Moon, theories have concluded that the Earth has been facing only to the near-side of the Moon since the formation of the Earth-Moon system, and that due to tidal energy dissipation, the Moon has been receding from the Earth (e.g., [1]). Therefore, we infer that there may have been substantial interaction between the Earth through the atmosphere and the near-side lunar surface, especially in ancient time, whereas the far-side has remained essentially intact to the terrestrial atmospheric influence. We suggest that the comparison of the far-side and near-side surface samples would impose crucial constraints on the evolution of the Earth and the Moon such as those listed below.

1. When Did the Geomagnetic Field (GMF) First Appear? Ozima et al. [2] suggested that terrestrial atmospheric components such as N and light noble gases could be transported from the Earth's atmosphere to the Moon, if the Earth was nonmagnetic. Therefore, the search for these terrestrial components in lunar soil would constrain the time for the first appearance of the geomagnetic field.

2. Have the Day Length and Earth-Moon Distance Changed in Geological Time? If the Moon has been receding from the Earth, the day length of the Earth should also have changed. Theoretical conclusions on these fundamental problems can be empirically constrained from the comparison of terrestrial volatile components between the near and far side lunar soils, and from the examination of vertical section of the nearside soils.

3. When Did the Biotic Oxygen Atmosphere Form? Ozima et al. [3] suggested that oxygen fractionated in the upper atmosphere might be responsible to the exotic oxygen observed in lunar metal by Ireland et al. [4]. The oldest record of this specific terrestrial oxygen would constrain the initiation of the biotic Earth atmosphere.

References: [1] Murray C. D. and Dermott S. F. 1999. *Solar system dynamics*. Cambridge: Cambridge U. Press. [2] Ozima M. et al. 2005. *Nature* 436:655–659. [3] Ozima M. et al. 2007. Abstract #1129. 32nd LPSC. [4] Ireland T. R. et al. 2006. *Nature* 440:775–778.

5206

ORIGIN OF BOUNDARY CLINOPYROXENES BETWEEN SPINEL AND MELILITE IN TYPE B1 CAIs

J. M. Paque[1], H. A. Ishii[2], A. Toppani[2, 3], J. R. Beckett[1], J. P. Bradley[2], D. S. Burnett[1], N. Teslich[2], and W. Moberlychan[2]. [1]Div. Geol. & Planet. Science, Caltech, Pasadena, CA 91125, USA. E-mail: julie@paque.com. [2]Inst. Geophys. Planet. Phys., LLNL, Livermore, CA 94557, USA. [3]Centre de Spect. Nucleaire et de Spect. de Masse, Batiments 104, 91405, Orsay Campus, France.

Introduction: Small (<5 μm) boundary clinopyroxenes (b-cpx) on spinel (sp) inclusions in melilite (mel) are ubiquitous in the type B1 CAIs. B-cpx on sp in high-Åk mel in the core of the inclusion could be explained by crystallization, either initial or during remelting. However, b-cpx on sp inclusions in low-Åk mantle mel are not readily explained in this way because mantle mel crystallized and incorporated b-cpx long before the appearance of clinopyroxene (cpx) in the crystallization sequence. To further constrain the crystallization and/or alteration processes, and to test the hypothesis that b-cpx were formed from melt inclusions, we examined the sp/mel interface of four sp in Leoville and Allende CAIs using FIB/TEM.

Results: FIB/TEM shows only cpx as a boundary phase between sp and mel in Allende TS-34, but Leoville 3537-2 interface regions are more complex with glass (gl), calcite, perovskite (pv), and cpx in variable amounts. In general, mel is essentially unaltered in Leoville and noticeably altered in Allende CAIs, but it is the Leoville sp/mel boundaries that show evidence for alteration, whereas those for Allende do not.

Glass, probably hydrated, is found on both Leoville sp boundaries. These are unlikely to be quenched residual gl because there is no high Åk mel associated with the cpx and the compositions are incompatible with late stage CAI melts. They may reflect a previously unrecognized pre-terrestrial alteration event localized to the sp/mel boundaries. The alteration products were later converted to gl by a (mild?) shock which preferentially heated and melted the porous, possibly hydrated, alteration phases. A jagged, presumably corrosion, texture for the glass/mel interfaces supports this interpretation.

Discussion: B-cpx from the core are compositionally similar to coarse-grained cpx and although they may be relict relative to the most recent melting event, they likely share a common origin with the larger grains. A unique origin for b-cpx in the mantle of type B1s is required due to the anomaly of an apparent late-stage crystal being included in an early crystallizing phase. A possible clue is that type A inclusions have sp boundary pv analogous to the sp b-cpx in type B1 inclusions, and that these sometimes have a rind of cpx, interpreted by [1] as a reaction between pv and melt. Occasional pv is found in and on type B1 sp, and since pv does not occur in the crystallization of bulk type B1s, these must be regarded as relict grains [2]. Once in contact with a melt, the relict pv dissolved indirectly and often completely, reacting with the melt to form cpx. The cpx would also be unstable during initial phases of crystallization, and the texture of the b-cpx is consistent with partial resorption.

References: [1] El Goresy A. et al. 2002. *Geochimica et Cosmochimica Acta* 66:1459. [2] Connolly H. C. and D. S. Burnett. 1999. *Meteoritics & Planetary Science* 32:829.

5015

^{39}Ar-^{40}Ar "AGE" OF BASALTIC SHERGOTTITE NWA 3171

Jisun Park* and Donald D. Bogard. ARES, NASA-JSC, Houston, TX 77058, USA. *NASA Postdoctoral Fellow. E-mail: jisun.park@nasa.gov.

Northwest Africa 3171 is a 506 g, relatively fresh-appearing basaltic shergottite with similarities to Zagami and Shergotty, but not obviously paired with any of the other known African basaltic shergottites [1, 2]. Its exposure age has the range of 2.5–3.1 Myr [3], similar to those of Zagami and Shergotty [4]. We made ^{39}Ar-^{40}Ar analyses of a "plagioclase" (now shock-converted to maskelynite) separate and of a glass hand-picked from a vein connected to shock melt pockets. Plagioclase was separated using its low magnetic susceptibility and then heavy liquid with density of <2.85 g/cm^3.

The ^{39}Ar-^{40}Ar age spectrum of NWA 3171 plag displays a rise in age over 20–100% of the ^{39}Ar release, from 0.24 to 0.27 Gyr. The first 20% of the ^{39}Ar release involves terrestrial weathering products characterized by adsorbed terrestrial Ar and likely terrestrial K contamination. Over the last 80% of the ^{39}Ar release, constant values of the ^{36}Ar/^{37}Ar ratio indicate that essentially all ^{36}Ar released is cosmogenic. An isochron plot (^{40}Ar/^{36}Ar versus ^{39}Ar/^{36}Ar) of these data (R^2 = 0.996) has a slope corresponding to an age of 225 ± 4 Myr. Essentially the same age is obtained whether we use total ^{36}Ar or correct for trapped ^{36}Ar. A radiometric formation age for NWA 3171 has not yet been reported. However, the Ar-Ar age spectrum of NWA 3171 closely resembles that of Zagami, and the Arrhenius diffusion plots of ^{39}Ar for the two shergottites also are similar. Thus, the "true" age of NWA 3171 may be similar to the Zagami age (177 ± 3 Myr; [5]). This implies NWA contains an extra component of ^{40}Ar, not accompanied by significant trapped ^{36}Ar, an inference that we have made for Zagami as well (Bogard and Park, this issue). We suggest this excess ^{40}Ar was inherited from the basaltic melt.

The ^{39}Ar-^{40}Ar age spectrum for the glass inclusion is very different and shows apparent Ar-Ar ages ranging between 0.3 and 1.9 Gyr. Variations in the ^{36}Ar/^{37}Ar ratios indicate release of trapped ^{36}Ar throughout most of the extraction. An isochron plot of ^{36}Ar/^{40}Ar versus ^{39}Ar/^{40}Ar suggests the release of terrestrial Ar in the first ~30% of the ^{39}Ar release, and high K/Ca ratios in these extractions also suggest terrestrial weathering. We used trapped ^{36}Ar in the isochron by subtracting a cosmogenic $^{36}Ar_{cos}$ component obtained from average data reported for Zagami and Shergotty whole rock [4, 6–8]. Measured ^{36}Ar/^{37}Ar ratios were used to apportion this $^{36}Ar_{cos}$ over individual releases. The temperature extraction data of 780–1160 °C (corresponding to ~37%–93% of the ^{39}Ar release) define a mixing line between a radiogenic component and Martian atmospheric Ar with ^{40}Ar/^{36}Ar 1800, consistent with previously reported values for Martian atmospheric Ar [9]. Like other impact glasses in shergottites, NWA 3171 glass contains Martian atmosphere incorporated at the time of impact formation, and does not directly yield a formation age.

References: [1] Irving A. J. et al. 2005. *Meteoritics & Planetary Science* 39:A49. [2] Meyer C. 2004. *The Mars meteorite compendium*. http://www-curator.jsc.nasa.gov/antmet/mmc/XXXII_NWA3171.pdf. [3] Nishiizumi and Caffee. 2006. *Meteoritics & Planetary Science* 69:A133. [4] Eugster et al. 1997. *Geochimica et Cosmochimica Acta* 61:2749–2757. [5] Nyquist et al. 2001. *Space Science Reviews* 96:105–164. [6] Park J. 2005. Ph.D. thesis, Univ. of Tokyo. [7] Schwenzer et al. 2007. *Meteoritics & Planetary Science* 42:387–412. [8] Terribilini et al. 1998. *Meteoritics & Planetary Science* 33:677–684. [9] Bogard and Garrison. 1999. *Meteoritics & Planetary Science* 34:451.

5248

STELLAR COMPANIONS AND THE EARLY STAGES OF PLANET FORMATION

I. Pascucci and D. Apai. Steward Observatory, The University of Arizona, Tucson, AZ, USA. E-mail: pascucci@as.arizona.edu.

Introduction: Two-thirds of the G stars in the solar neighborhood are members of multiple-star systems [1] and several of them are found to harbor giant planets [2]. Similarly, young low-mass pre-main sequence stars are very frequently found in multiple systems, most commonly in binaries [3]. This suggests that planet formation around a single star such as our Sun may be atypical and urges us to explore the effect of stellar companions on this process. We tackle this question from an observational point of view. Because meteoritic evidence from our solar system as well as numerical simulations of grain agglomeration suggest short time scales for the formation of planetesimals [4], it is crucial to know how stellar companion(s) affect the dust processing in the first few million years.

Method: We selected two statistically significant samples of young coeval disks around single and multiple stars that have been observed with the Spitzer Space Telescope. From the strength and shape of the 10 micron silicate emission feature, we infer the degree of grain growth and crystallinity in the upper layer of the selected disks. We use the slope of the mid-infrared continuum as a proxy for dust settling.

Results: Our study shows that stellar companions at projected separations larger than 10 AU do not appreciably affect the initial dust processing. Hence the first steps of planet formation are not influenced by the presence of a star at tens of AU. We discuss our results in the context of other studies investigating later stages of planet formation in multiple systems.

References: [1] Duquennoy A. and Mayor M. 1991. *Astronomy & Astrophysics* 248:485–524. [2] Desidera S. and Barbieri M. 2007. *Astronomy & Astrophysics* 462:345–353. [3] Duchene G. et al. 2007. In *Protostars and planets V*. p. 379. [4] Beckwith S. et al. 2000. In *Protostars and planets IV*. p. 533.

5242

EXPERIMENTAL AND PETROLOGIC STUDIES OF SCHREIBERSITE CORROSION

M. A. Pasek[1] and V. D. Pasek[2]. [1]Steward Observatory, The University of Arizona, Tucson, AZ, USA. E-mail: mpasek@lpl.arizona.edu. [2]Lunar and Planetary Laboratory, The University of Arizona, Tucson, AZ, USA.

Introduction: Schreibersite, $(Fe,Ni)_3P$, is a common meteoritic mineral. Phosphorus in schreibersite is reduced relative to orthophosphate, PO_4^{3-}, the stable oxidation state on the surface of the Earth. Consequently, P in schreibersite is oxidized by water and atmospheric O_2. The only known mineral associated with the oxidation of schreibersite is cassidyite, $Ca_2(Ni,Mg)(PO_4)_2 \times 2H_2O$, a poorly studied mineral associated with the Wolf Creek meteorite [1]. Since nearly all P on the surface of the Earth is orthophosphate, schreibersite corrosion products may serve as an indicator of extraterrestrial impacts.

Samples and Methods: Schreibersite corrosion was studied by a series of experiments in which ~1 g of a synthetic iron phosphide (Fe_3P) powder or ~7 g samples of the Seymchan or Canyon Diablo meteorites were oxidized in water at 25 °C for 1 day to 1 month. Oxidation took place both under air and under an inert Ar atmosphere to elucidate the effects of O_2. The aqueous corrosion products were analyzed by ^{31}P NMR, EPR, and MS techniques [2, 3].

NWA 4194 is a weathered enstatite meteorite with 20–200 μm grains of schreibersite surrounded by P-rich rust. A section of NWA 4194 was analyzed by EMPA (Sx50), with a focus on P chemistry in the rust.

Results and Discussion: Schreibersite corrodes to phosphite (HPO_3^{2-}), orthophosphate (HPO_4^{2-}), hypophosphate ($HP_2O_6^{3-}$), and pyrophosphate ($HP_2O_7^{4-}$) in aqueous solution. The oxidation state of P in these compounds ranges from 3+ to 5+, and their formation proceeds by a free radical pathway [3].

Schreibersite in NWA 4194 is surrounded by a hydrous Fe, Ni, Ca, P-rich oxide. The oxide is highly heterogeneous, and is enriched in P relative to Fe and Ni. Ca was introduced from the terrestrial environment during weathering. The O:P ratio is ~3:1 ($R^2 = 0.883$), which may indicate that the P is reduced relative to orthophosphate.

These heterogeneous phases are incompletely characterized, but may represent a new group of reduced P minerals. If so, these minerals would demonstrate the formation of reduced P oxides on Earth. Since reduced P compounds are derived almost exclusively from extraterrestrial sources and crustal P is uniformly orthophosphate, detection of phosphite or hypophosphate in soil or rock samples may serve as an indicator of ancient meteorite impacts or meteoritic flux.

Finally, schreibersite was a highly reactive source of P on the early Earth and may have primed the environment with reduced P compounds, which react with organics to form phosphorylated compounds, enabling the origin of life. Several species of bacteria can use reduced P as their sole P source [4], which may be an ancient genetic indicator of the environment of the early Earth.

References: [1] White J. S. et al. 1967. *American Mineralogist* 52: 1190–1197. [2] Pasek M. A. and Lauretta D. S. 2005. *Astrobiology* 5:515–535. [3] Pasek M. A. et al. 2007. *Geochimica et Cosmochimica Acta* 71: 1721–1736. [4] Kononova S. V. and Nesmeyanova M. A. 2002. *Biochemistry (Moscow)* 67:220–233.

5178

IMPACT-MELT BRECCIA FROM DHALA IMPACT STRUCTURE, BUNDELKHAND CRATON, CENTRAL INDIA

J. K. Pati[1], V. Srivastava[1], A. C. Shukla[1], W. U. Reimold[2], and C. Koeberl[3]. [1]Department of Earth and Planetary Sciences, Nehru Science Centre, University of Allahabad, Allahabad-211 002, India. E-mail: jkpati@yahoo.co.in. [2]Museum for Natural History (Mineralogy), Humboldt University Berlin, Invalidenstrasse 43, D-10115 Berlin, Germany. E-mail: uwe.reimold@museum.hu-berlin.de. [3]Department of Geological Sciences, University of Vienna, Althanstrasse 14, A-1090, Vienna, Austria. E-mail: christian.koeberl@univie.ac.at.

The Dhala structure (25°17′59.7″N, 78°8′3.1″E) with a rim-rim diameter of about 15 km is a complex impact structure of likely Proterozoic age [1–3]. The host rocks are predominantly granitoids (~2.5 Ga) that are overlain by sediments of the 1.6 Ga Vindhyan Supergroup. Seven patchy outcrops of melt breccia occur between 1.93 km NW of Dhala village and 1.02 km SW of Maniar village (78°2′18″E, 25°2′42″N) over a length of nearly 6 km in a semi-circular pattern. These outcrops were earlier considered as "Mohar felsic volcanics occur as linear bodies" [4]. These exposures represent melt breccia and are the only lithounit in the structure containing shock-metamorphosed mineral and rock clasts. The exposed outcrops range in width from 7 to 169 m and length from 15 to 446 m. The total exposed area of all 7 outcrops is 0.07 km^2. The melt breccia is reddish/range in color and composed of lithic and mineral clasts set in a devitrified, fine-grained matrix composed of mainly feldspar spherulites and a submicroscopic groundmass. Numerous ovoid- to droplet-shaped vesicles mostly filled with either quartz or quartz-calcite have diameters up to 6 cm. Partly digested granitoid and quartz clasts constitute the major clast fraction. The clasts range in size from 1 mm to 20 cm. The clast proportion varies from 10 to 35 vol%. The clasts are subangular to subrounded in shape and show random orientation. The flow lines in the melt breccia also show varied orientations. The rock and mineral clasts within the melt breccia contain diagnostic shock metamorphic features, such as multiple sets of planar deformation features (up to 5 sets of PDFs per grain) in quartz and feldspar, ballen-textured quartz [5], and checkerboard feldspar, as well as various thermal alteration textures that are typically found in clasts of initially superheated impact melt. Most PDFs are of the decorated type; many shocked quartz grains appear toasted. The percentage of shocked quartz and feldspar grains in the impact melt breccia is variable (7–67 vol%). A zircon crystal with shock-induced planar fractures was also noted. The present findings suggest that the melt breccia is indeed of impact origin; the array of melt breccia outcrops possibly represents the remnants of a voluminous impact melt sheet.

References: [1] Pati J. K. 2005. *Meteoritics & Planetary Science* 40: A121. [2] Pati J. K. et al. 2006. *Meteoritics & Planetary Science* 41:A121. [3] Pati J. K. and Reimold W. U. 2007. *Journal of Earth Systems Science* 116(2):81–98. [4] Srivastava S. K. and Nambiar K. V. 2003. *Geological Survey of India Records* 136:52–54. [5] Pati J. K. et al. 2006. 1st International Conference on Impact Cratering in the Solar System, ESTEC, Noordwijk, The Netherlands. pp. 169–170.

5090

RESOLUTION OF SMALL-SCALE STRUCTURAL DIFFERENCES IN THE CR CHONDRITE MACROMOLECULAR MATERIAL

V. K. Pearson[1], G. H. Morgan[1], D. Turner[1], M. Perronnet[2], and I. Gilmour[1]. [1]PSSRI, The Open University, Walton Hall, Milton Keynes, MK7 6A, UK. E-mail: v.k.pearson@open.ac.uk. [2]NASA Johnson Space Center, 2101 NASA Road One, Houston, TX 77058–3696, USA.

Introduction: Recent work on the organic material in CR chondrites [1, 2] has provided insights into the alteration of the CR macromolecule during parent body processing. The organic inventory of these meteorites, the distribution and abundance of species, reflects the pre-terrestrial processes evidenced by complementary geochemical and mineralogical evidence [3].

We have previously illustrated that meteoritic macromolecular material can be thermally degraded during pyrolysis into its constituent species [1, 4, 5 and references therein]. We have conducted a survey of CR chondrites using Pyrolysis-4D GCxGC-TOFMS as previously demonstrated by [6, 7]. This technique is superior to previous py-GCMS methods as it can separate eluting compounds according to molecular weight and polarity, allowing the identification of compounds present at low abundance that would previously have been unidentifiable.

The application of this technique enables the identification of organic species at low abundances that have been unseen in previous studies. Identification of these trace components and their comparison between samples of the CR group can provide insights into CR chondrite parent body processing.

Methodology and Samples: 11 CR chondrites have been analyzed using py-GCxGC-TOFMS. This technique employs two serial columns of different polarities for two dimensional separation (molecular weight and polarity) and subsequent rapid detection by TOFMS. Experimental conditions are as described in [7]. Samples analyzed cover a spectrum of alteration, and include falls, Antarctic finds, and desert finds.

Results and Discussion: The resolving capabilities of the 4D GCxGC-TOFMS system [6, 7] lead to the identification of several components at low abundance that have been unresolved by conventional techniques plus aromatic species, e.g., 1–4-ring PAHs that are regularly identified in chondritic meteorites. The low-abundance organics, however, reveal subtle differences in macromolecular structure that have been previously indistinguishable, and indicate the true structural diversity of primitive organic material. We present a comparison of the trace components across the CR chondrite group to ascertain whether these differences are related to pre-terrestrial nebula or parent body processes, terrestrial weathering in varied environments or contamination.

References: [1] Pearson V. K. et al. 2006. *Meteoritics & Planetary Science* 41:1291–1303. [2] Wang Y. et al. 2005. *Geochimica et Cosmochimica Acta* 69:3711–3721. [3] Krot A. 2002. *Meteoritics & Planetary Science* 37:1451–1490. [4] Sephton M. A. et al. 2002. *Natural Product Reports* 19:1–22. [5] Gilmour I. 2004. In Treatise on Geochemistry, vol. 1, edited by Davis A. M. pp. 269–290. [6] Watson J. et al. 2005. Abstract #1842. 36th Lunar and Planetary Science Conference. [7] Pearson V. K. et al. 2007. Abstract #1338. 38th Lunar and Planetary Science Conference.

5295

NITROGEN, CARBON, AND HYDROGEN ISOTOPES IN THE METAL OF THE NWA 1814 CB CHONDRITE

C. Perron and S. Mostefaoui. Laboratoire d'Etude de la Matière Extraterrestre, MNHN and CNRS, 75005 Paris, France.

Introduction: CB chondrites are rare and peculiar meteorites. They have been attributed different origins, but none of these has yet provided a clear explanation for one of their most remarkable characteristics: their high enrichment in ^{15}N. We have started measuring the isotopic composition of nitrogen, along with those of carbon and hydrogen in metal grains of the NWA 1814 meteorite, with a threefold motivation: 1) confirm that NWA 1814 is indeed a CB chondrite (no N isotope analysis has been performed up to now on this meteorite); 2) study a metal that seems more evolved than that of other CB_as, having large areas of tetrataenite, and numerous inclusions of daubréelite, schreibersite, and carbide [1]; and 3) take advantage of the high spatial resolution of the NanoSIMS ion probe to try to precisely locate the nitrogen carriers.

Experimental: Isotopic composition measurement and imaging were carried out on a polished mount of NWA 1814 with the MNHN NanoSIMS in the multicollection mode, using a Cs^+ primary ion beam. C^- and CN^- ions were collected in the same session, H^- in a subsequent session. For all three elements, we used a terrestrial kerogen of known isotopic compositions as a standard.

Results: As expected, N is more concentrated in tetrataenite than in kamacite (by about a factor of 3), while the reverse is true for C. The highest N concentrations are found in μm-size spots associated with sulfide and carbide. The most N-rich spots are also C-rich but not so much as carbides. They seem to lie at grain boundaries. They contribute only a small fraction of the total N in metal. The N isotopic composition is anomalous, within the CB range. N is isotopically homogeneous in neighboring phases (i.e., kamacite, tetrataenite, sulfide, carbide, N-rich spots) within each imaged area of metal grains. $\delta^{15}N$ varies from grain to grain (from ~150 ‰ to ~900‰). Variations also seem to exist between different regions within a given (cm-size) metal grain, but we have data for only 3 grains and clearly need more measurements to assess these variations. The carbon isotopic composition is about normal, with $\delta^{13}C$ ~−35 ‰. Hydrogen is apparently light, with δD ~−700‰, which agrees with analyses of Bencubbin metal [2]. However, we cannot exclude that this low value is a matrix effect, as our kerogen standard may not be well adapted to the analysis of H in metal.

Conclusion: N isotopic compositions confirm that NWA 1814 is a CB chondrite. A thermal event, probably that responsible for the metal microstructures, allowed N to partition between adjacent phases in the metal, and isotopically equilibrate locally, but not between different metal grains. We have to establish whether this occurred in the parent body, or prior to accretion.

References: [1] Perron C. and Leroux H. 2004. *Meteoritics & Planetary Science* 39:A82. [2] Aléon J. et al. 2004. Abstract #1645. 35th Lunar and Planetary Science Conference.

5062

THE ORIGIN OF BROWN OLIVINE IN MARTIAN DUNITE NWA 2737

C. M. Pieters[1], R. L. Klima[1], T. Hiroi[1], M. D. Dyar[2], M. D. Lane[3], A. H. Treiman[4], S. K. Noble[5], J. M. Sunshine[6], and J. L. Bishop[7]. [1]Brown University, USA. E-mail: Carle_Pieters@brown.edu. [2]Mt. Holyoke College, USA. [3]Planetary Science Institute, Tucson, AZ, USA. [4]Lunar and Planetary Institute, USA. [5]Johnson Space Center, USA. [6]Univ. Md., USA. [7]SETI.

The Northwest Africa (NWA) 2737 meteorite is the second Martian meteorite has been identified that is composed primarily of heavily shocked dunite. This meteorite has several similarities to the Chassigny dunite cumulate, but the olivine is more Mg rich and, most notably, is very dark and visually brown [1, 2]. Carefully coordinated analyses of NWA 2737 whole rock and olivine separates were undertaken using visible and near-infrared reflectance, mid-infrared emission and reflectance, and Mössbauer spectroscopic studies of the same samples along with detailed petrography, chemistry, and SEM and TEM analyses [3]. Mid-infrared spectra of this sample indicate that the olivine is fully crystalline and that its molecular structure remains intact. Near-infrared spectra of NWA 2737 olivine are compared with those of Chassigny and San Carlos in the figure below. The unusual color and spectral properties that extend from the visible through the near-infrared part of the spectrum are shown to be due to nanophase metallic iron particles ($npFe^0$) dispersed throughout the olivine during a major shock event on Mars. Although a minor amount of Fe^{3+} is present, it cannot account for the well-documented unusual optical properties of Martian meteorite NWA 2737. Apparently unique to the Martian environment, this "brown" olivine exhibits spectral properties that can potentially be used to remotely explore the P-T history of surface geology in addition to surface composition.

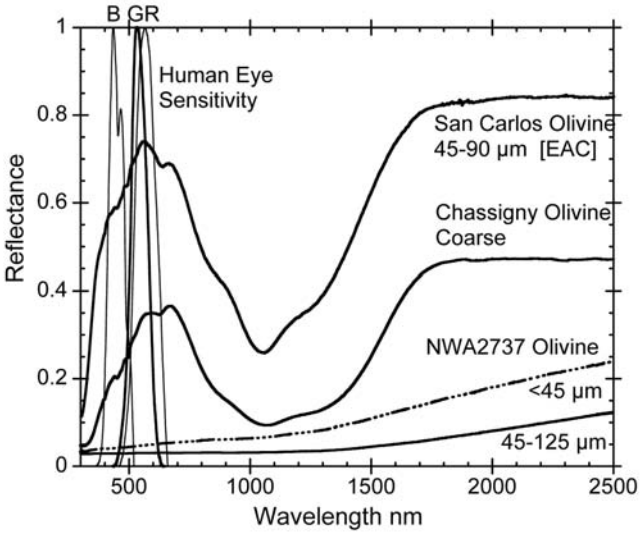

Fig. 1. Reflectance spectra of two size fractions of NWA 2737 olivine compared to coarse-grained Chassigny and San Carlos olivine. The low albedo and distinct "red" sloped continuum of NWA 2737 is due to a small amount of $npFe^0$ that is pervasive throughout the olivine.

Acknowledgements: Support from the Mars Fundamental Research Program is greatly appreciated.

References: [1] Beck et al. 2006. *Geochimica et Cosmochimica Acta* 70:2127–2139. [2] Treiman et al. 2007. *Journal of Geophysical Research* 112, doi:10.1029/2006JE002777. [3] Pieters et al. *Journal of Geophysical Research*. Forthcoming.

5074

HARVEY NININGER'S 1948 PETITION TO NATIONALIZE METEOR CRATER

H. Plotkin[1] and R. S. Clarke, Jr.[2] [1]Department of Philosophy, Talbot College, University of Western Ontario, London, Ontario, Canada N6A 3K7. E-mail: hplotkin@rogers.com. [2]Smithsonian Institution, National Museum of Natural History, MRC 119, Department of Mineral Sciences, P.O. Box 37012, Washington, D.C. 20013–7012, USA.

At the June 1948 meeting of the American Astronomical Society, Harvey Nininger petitioned to pass a motion in support of nationalizing Meteor Crater. Speaking to the motion, he argued that the mining efforts of the Barringers, who held title to the crater, were leading to mutilation of the crater rim and removal of meteoritical material without proper documentation. Nininger then went on to make the unauthorized—and false—claim that the Barringers would be receptive to a fair purchase offer for the crater.

Only one person—Lincoln LaPaz—spoke against the motion, and it passed on a near unanimous vote, with only four persons voting against it: LaPaz, Frederick Leonard, Clyde Tombaugh, and one unidentified individual. The Barringers, who had not been given advance notice of the petition and were not present at the meeting, felt ambushed. They quickly notified Nininger that his rights to exploration and research at the crater were being terminated, and soon thereafter they gave exclusive rights to his arch-rival, LaPaz.

Intrigued by a letter that Dorrit Hoffleit wrote to Gene Shoemaker, we joined her in puzzling over what lay behind Nininger's curious and self-defeating behavior. Based on a close reading of the voluminous Nininger correspondence, we conclude that it was rooted primarily in his complex relationships with Leonard and LaPaz, and his fervent desire to establish a national institute for meteoritical research with them.

But Nininger's falling-out with Leonard and his vicious cat-and-dog fight with LaPaz brought his proposed institute plan to an end, and forced him to act on his own. In 1946 he established his American Meteorite Museum on Route 66, some five miles from the crater. He hoped to move his museum to the crater itself, but knew that was not possible, as the Tremaines, whose Bar-T-Bar cattle ranch owned the land surrounding the crater, had plans of their own for establishing a tourist center there.

Running out of options, Nininger wondered what would happen if the crater was acquired by a federal agency and made into a public park, with an accompanying tourist center and museum. With characteristic élan, he could picture himself at the head of such a facility—in essence the administrator of the crater—with a secure salary and adequate space to exhibit his meteorite collection. In the hope that he could bring such a favorable prospect to fruition, Nininger self-assuredly—if naively—presented his petition to the American Astronomical Society to nationalize Meteor Crater.

But Nininger's plan did not work. The Barringers forcefully rebutted the allegations in his petition and made it clear they had no intention of relinquishing their title to the crater. They argued that any nationalization of the crater would end scientific exploration there, simply leading to its sterile preservation. They considered themselves as stewards of the crater, who were acting as trustees for the advancement of scientific knowledge. As of now, four generations of Barringers have provided ample proof of the wisdom, success, and generosity of their stewardship.

5043

POSTIMPACT BIOTIC RECOVERY INSIDE THE LATE EOCENE CHESAPEAKE BAY SUBMARINE IMPACT CRATER

C. Wylie Poag. U.S. Geological Survey, USA. E-mail:wpoag@usgs.gov.

Introduction: Eight continuously cored boreholes drilled inside the Chesapeake Bay impact crater provide an unusual opportunity to analyze the biotic transition following a large submarine impact [1]. I have focused mainly on sedimentology and microfossils, especially benthic foraminifera, to interpret the paleoenvironmental changes that mark that transition. The results indicate that the transition interval is not uniformly expressed at all sites.

Results: The postimpact paleoenvironmental record can be divided into a succession of five steps. Step 1 is represented by ~3 cm of silty clay recovered at a single site, which contains evidence of microspherules [2]. No indigenous microfossils are present in this interval, but reworked older specimens (Late Cretaceous to middle Eocene) are common. Step 2 is represented at 6 sites by 14–139 cm of multidirectional, cross-laminated, silty quartz sand. The microfossil assemblage resembles that of the Step 1 interval. Step 3 is represented at 4 sites by 18–22 cm of horizontal, parallel, silt, and clay laminae. Sparse reworked foraminifera (no indigenous species) characterize this interval. Step 4 is represented at 4 sites by 18 cm–20 m of microfossil-rich marine clay, which contains abundant indigenous mollusks, ostracodes, foraminifera, bolboformids, radiolarians, calcareous nannofossils, and dinoflagellates [3], including >50 species of benthic foraminifera. The foraminiferal assemblage is further distinguished by a prominent group of siliceous agglutinated species. Step 5 is represented at all sites by continued deposition of microfossil-rich marine clay (12–48 m), but without the siliceous foraminifera. The top of the transition interval is represented by a species acme among the calcareous benthic foraminifera.

Interpretation: Step 1 represents fallout debris derived directly from the impact. The sediments of Step 2 accumulated as a series of small debris flows and turbidites, presumably stirred up by postimpact storms. Step 3 represents a dead zone, which supported no indigenous benthic organisms. Step 4 represents the initial re-occupation of the crater basin by a diverse community of marine microorganisms. Paleodepth is estimated to have been ~300 m. The siliceous foraminiferal assemblage, however, indicates that sea-floor environments were still abnormal, perhaps unusually warm and saline due to remnant impact effects. Step 5 represents a full return to normal marine conditions, but bottom waters were depleted in dissolved oxygen and enriched in organic detritus.

The fallout and turbidite deposition (Steps 1 and 2) were essentially instantaneous, and represent the last vestiges of direct influence by the impact. The dead zone (Step 3) represents tranquil, yet hostile, bottom conditions, which lasted ~1–3 kyr following the impact. The siliceous foraminiferal assemblage (Step 4) lasted ~27 kyr in the outer part of the crater, but as long as ~350 kyr near the center of the crater. Complete biotic recovery, represented by a peak in the number of calcareous benthic foraminiferal species during Step 5, was achieved in ~30 kyr near the outer rim, but not until ~500 kyr postimpact near the crater center.

References: [1] Poag C. W. et al. 2004. Springer-Verlag. 522 p. With CD-ROM. [2] Poag C. W. and Norris R. D. 2005. U.S. Geological Survey Professional Paper #1688. pp. F1–F57. [3] Edwards L. E. et al. 2005. U.S. Geological Survey Professional Paper #1688. pp. H1–H67.

5264

STRUCTURAL CRATER RIM ANALYSIS AT METEOR CRATER

M. Poelchau[1], T. Kenkmann[1], and D. A. Kring[2]. [1]Museum für Naturkunde, Berlin, Germany. E-mail: michael.poelchau@museum.hu-berlin.de. E-mail: thomas.kenkmann@museum.hu-berlin.de. [2]Center for Advanced Space Studies, LPI, Houston, Texas, USA. E-mail: kring@lpi.usra.edu.

Introduction: Meteor Crater, located in Arizona, USA, shows obvious morphological deviations from a circular crater shape. Its square shape has been interpreted to be a consequence of a regional joint system that runs diagonally to the square [1, 2]. The crater rim was re-examined to determine if there are further deviations from circularity and any preferential directions in the orientation of bedding that might reveal the direction of impact. In particular, detailed measurements of strike-dip were collected around the entire crater rim as a function of GPS data.

Results: Analysis of the strike and dip of bedding in the rim shows that the data reflect the general morphology of the crater rim. Stereo plots reveal differences between the (roughly) N-S-trending segments, which display a greater amount of axial rotation, and the E-W-trending segments. This implies an axis of bilateral symmetry with a NNW-SSE orientation, which might be an indicator for a direction of impact.

We also applied a new method of analysis that displays geographic data in an azimuthal reference scheme relative to the crater center. The strike of rock layers in the rim is then examined for deviations from a concentric or circular orientation with regards to the crater center. The majority of deviations in our data set coincide with the rough square shape of the rim, in particular at the western and eastern flank. The most proximal part of the ejecta, defining the overturned flap of the crater rim, was also measured and shows more chaotic behavior that has less relation to crater rim morphology, which is in part due to the sparse distribution of appropriate outcrops.

Geographic coordinates and altitude were measured of the boundary between the Kaibab and Moenkopi formations, exposed in the top portion of the rim, in order to create a three-dimensional model. This originally subhorizontal surface has been uplifted and overturned to varying degrees during the impact. Strongest uplift occurred in the four corners of the crater, especially in the SE, where even the lower Coconino Formation is well exposed over a 300 m long segment. It is possible that the horizontal momentum of an obliquely striking impactor could exhibit preferential force downrange and extrude a larger block of the crater wall relative to the rest of the crater. An impactor traveling to the SE would contradict Shoemaker, who suggests the impactor was moving to the NNW [3], but no consensus has been reached on this matter so far.

Acknowledgements: We would like to thank D. F. G. for funding this project (KE 732-11/1).

References: [1] Shoemaker E. M. 1960. Structure of the Earth's crust and deformation of rocks. Rept. 18. pp. 418–434. [2] Roddy D. J. 1978. Proceedings, 9th Lunar Planet. Sci. Conf. pp. 3891–3930. [3] Roddy D. J. and Shoemaker E. M. 1995. *Meteoritics* 30:567.

5022

NEWLY DISCOVERED ANDA-TYPE INDOCHINITES FROM THAILAND AND CHINA

H. Povenmire. Florida Institute of Technology, 215 Osage Drive, Indian Harbour Beach, FL 32937, USA. E-mail: katiehal1@yahoo.com.

A prominent area where the Philippinite tektites are found is the Pangasinan Province (119°55′E, 16°16′N) The Anda-type tektites are regarded as a subdivision of the Pangasinan tektites. These tektites have peculiar surface features that resemble imprints of seashells or even rodent teeth marks. Until recently, this is the only area where these tektites have been found.

Recently, Clyde Barnhart closely examined approximately 800 kg of Thailand indochinites. Among other findings, one spectacular and several other less profound Anda-type tektites were found. This specimen is a splash form dumbbell with a weight of 67.9 gm and dimensions of 77 × 26 × 24 mm. The depth of the Anda-type surface features vary from 0.3–1.8 mm.

More recently, similar Anda-type tektites have been found on the Khorat Plateau between Khon Kaen and Nakhon Ratchathani in NE Thailand. One specimen weighed 74.4 g.

In February 2006, this researcher was made aware of a large, banana-shaped Anda-type tektite from Guangdong Province, China (110°54′E, 29°34′N). It weighed approximately 67.0 g and had dimensions of 77 × 27 × 23 mm. It was heavily water worn but still contained 29 areas of deep Anda-type etchings.

This led me to examine bags of unsorted tektites from Yunnan Province, China (100°06′E, 25°45′N). In this there were found 10 waterworn, but excellent specimens. Most of these were in the 10–20 g range and of different shapes. The distance between these sites was more than 2400 km.

The scientific importance of these findings is that the Anda-type surface features are not unique to the Island of Anda. Most of these tektites seem to have been in a marine environment, which may have been a factor in the unique surface features.

References: [1] Beyer H. O. 1962. Philippine Tektites Museum and Institute of Archaeology Quezon City Manila, vol. I, plate no. 25. [2] O'Keefe J. A., editor. 1963. *Tektites*. Chicago, Illinois: University of Chicago Press. p. 36. [3] O'Keefe J. A. 1976. *Tektites and their origin*. New York: Elsevier p. 5, plate 7E. [4] Povenmire H. 2003. *Tektites: A cosmic enigma*. Cocoa Beach, FL: Blue Note Publishing. [5] Povenmire H. and Barnhart C. 2004. Newly discovered Anda-type and stretched Indochinites from Thailand. *Meteoritics & Planetary Science* 39:A87. [6] Lehrman N. 2006. Personal communication.

5317

I-Xe SYSTEM IN MAGNETITES SEPARATED FROM CO CHONDRITES OF DIFFERENT PETROLOGIC TYPE

O. V. Pravdivtseva, C. M. Hohenberg, and A. P. Meshik. McDonnell Center for the Space Sciences and Physics Department, Washington University, CB 1105, Saint Louis, MO 63130, USA. E-mail: olga@wuphys.wustl.edu.

Magnetites are one of the first alteration products formed in carbonaceous chondrites and thus provide insight for the onset and duration of aqueous alteration in different types of carbonaceous chondrites, as well as among different petrologic types within the same chondrite group.

In our previous work [1], in preparation for this extended study of magnetites from different types of carbonaceous chondrites, we investigated the possibility of iodine contamination during the chemical separation in LiCl, first applied by Herzog et al. [2]. Contamination by halogens can compromise the I-Xe system in magnetite, creating apparently younger ages if it roughly correlates with radiogenic ^{129}Xe. Two pure magnetite samples from Orgueil were separated using LiCl, one prior to irradiation, the other separated after the irradiation and thus free of chemically introduced iodine-derived ^{128}Xe. The I-Xe ages of both of these pure Orgueil magnetites were consistent with each other within the experimental uncertainties (about 3 Ma older than our earlier I-Xe age for the Orgueil highly magnetic fraction [3]), confirming that LiCl processing prior to irradiation does not compromise the I-Xe isochron.

Here we present first results for CO chondrites. Following the procedure of Herzog et al. we separated magnetites from 10 CO chondrites—Colony (3.0), Kainzas (3.1), Felix (3.2), Ornans (3.3), Yamato-82050,115 (3.3), Lance (3.4), Allan Hills A77003, 117 (3.5), Yamato-82094,110 (3.5), Yamato-790992,80 (3.5), Warrenton (3.6)—almost completely covering the range of petrologic types (from 3.0 to 3.7 [4, 5]). SEM analyses confirmed samples to be iron oxides with small amounts of Ni present. Aliquots of these magnetite separates have been saved for future more detailed studies of the individual morphologies. The samples were irradiated in the Missouri University Research Reactor (MURR) with Shallowater (4563.2 ± 0.6 Ma [6]), as the absolute age and irradiation standard.

The I-Xe system has been studied in Colony (3.0) and Kainzas (3.1). Kainzas did not contain any radiogenic ^{129}Xe but small amounts of ^{128}Xe were present at temperature steps lower than 1250 °C, consistent with minor iodine contamination due to the chemical separation, and similar to that observed in our earlier work on Orgueil [1]. The I-Xe system in Colony magnetite closed 6.1 ± 3.1 Ma after Shallowater (4,563.2 ± 0.6 Ma [6]), ~8 Ma later than in Orgueil CI magnetite [1]. I-Xe measurements in other CO chondrites are in progress and the revealed history, alteration or solid-state diffusion can then be addressed.

Acknowledgements: This work is supported by NASA grant #NNG06GE84G.

References: [1] Pravdivtseva et al. 2003. Abstract #1863. 34th Lunar and Planetary Science Conference. [2] Herzog G. F. et al. 1973. *Science* 180: 489–491. [3] Hohenberg C. M. et al. 2000. *Geochimica et Cosmochimica Acta* 64:4257–4262. [4] McSween H. Y., Jr. 1977. *Geochimica et Cosmochimica Acta* 41:479–491. [5] Scott E. R. D. and Jones R. H. 1990. *Geochimica et Cosmochimica Acta* 54:2485–2502. [6] Gilmour J. D. et al. 2006. *Meteoritics & Planetary Science* 41:19–31.

5320

TUNGSTEN AND NICKEL ISOTOPES IN TWO ENSTATITE ACHONDRITES: ITQIY AND ZAKŁODZIE

G. Quitté[1] and B. Zanda[2]. [1]Laboratoire des Sciences de la Terre, ENS Lyon, France. E-mail: Ghylaine.Quitte@ens-lyon.fr. [2]Muséum National d'Histoire Naturelle, Paris, France.

Introduction: Itqiy and Zakłodzie are two enstatite meteorites with an achondritic texture. They formed under reducing conditions and are metal-rich. Various data suggest that they formed by loss of a partial melt but their high metal content is difficult to reconcile with this scenario. They may also be impact melts formed on enstatite chondritic parent bodies. The goal of the present study is three-fold: 1) to test the above hypotheses for the formation of enstatite achondrites, 2) to better understand their early evolution and their link with each other and with enstatite chondrites, and 3) to bring constraints on the first stages of metal segregation in the early solar system.

Samples and Technique: Itqiy is essentially composed of low-Ca pyroxene and kamacite. Zakłodzie shows similar features to Itqiy in terms of mineralogy and chemistry, but it contains a considerable amount of plagioclase and significantly less metal, and the noble gas data for both meteorites are very different [1]. Zakłodzie is more weathered than Itqiy but has a much shorter terrestrial exposure age [1]. After crushing of an Itqiy piece, 3 mineral phases were separated with a hand magnet: a magnetic fraction (metal), a slightly magnetic fraction (metal + sulfures), and a nonmagnetic fraction (silicates). The samples were digested and tungsten was then extracted with a two-step ion-exchange procedure. The elution fraction containing Ni was dried and further purified on ion-exchange resins. Finally, W and Ni isotope compositions were measured using a MC-ICPMS at ENS Lyon.

Results: All three fractions have the same Ni isotopic composition as the terrestrial standard; there is neither an excess nor a deficit in ^{60}Ni and the other ratios are normal as well. As far as W isotopes are concerned, metal is characterized by a small deficit of about half an epsilon unit, silicates have the isotopic composition of the standard and the third fraction is slightly enriched in radiogenic ^{182}W. Further analyses are in progress to confirm these preliminary data.

Discussion and Outlook: The absence of any Ni isotopic anomaly in Itqiy indicates that this meteorite formed late, when all ^{60}Fe had already decayed. Note however that the ^{60}Fe-^{60}Ni system may not be a suitable ubiquitous chronometer for early events in the solar system [2] so that Ni-isotopic data in enstatite achondrites possibly provide no chronological informations. For W, the suprachondritic isotopic composition of metal means that it is of secondary origin and formed by reduction from a radiogenic source. Noble gas data suggest that Itqiy experienced a recent thermal event [1]. Our new isotopic data are not inconsistent with such an event, but put constraints on the peak temperature: it must have been lower than 800–900 °C as the Hf-W system has not been fully re-equilibrated. Tungsten and Ni isotopic analyses of Zakłodzie are in progress and should provide complementary informations as both meteorites most likely originate from different parent bodies.

References: [1] Patzer A. et al. 2002. *Meteoritics & Planetary Science* 37:823–833. [2] Quitté G. 2007. Abstract #1900. 38th Lunar and Planetary Science Conference.

5077

SPECTRAL CALIBRATION OF ORTHOPYROXENE-CLINOPYROXENE MIXTURES: IMPLICATIONS FOR INTERPRETING ASTEROID SPECTRA

V. Reddy[1], E. A. Cloutis, M. A. Craig, and M. J. Gaffey. [1]Department of ESSP, University of North Dakota, Grand Forks, USA. E-mail: Vishnu.kanupuru@und.nodak.edu.

Introduction: Pyroxenes are one of the most important and abundant minerals on inner solar system bodies. They have been spectrally detected on surfaces of terrestrial planets, the Moon, and asteroids. Depending on their petrogenesis, pyroxenes can substitute a wide range of cations in their crystal structure [1]. Accurate quantification and identification of the abundances and chemistries of these cations from telescopic spectral data can help constrain the conditions under which the target object formed [2]. To accomplish this task, lab spectral studies of pyroxenes are necessary. Here we present results of near-IR spectral calibration of linear mixing experiments of two ortho- (OPX) and clinopyroxene (CPX) mixtures. The intent of this calibration study is to help interpret asteroid spectra.

Methodology: Absolute reflectance spectra (0.35–2.5 μm) of two OPX (PYX032-$Fs_{41.5}$ $Wo_{3.6}$, PYX023-$Fs_{9.4}$ $Wo_{1.3}$) and two CPX (PYX017-$Fs_{8.1}$ $Wo_{44.4}$, PYX005-$Fs_{9.9}$ $Wo_{49.1}$) in two particle size ranges (<45 μm and 90–180 μm) at 10 and 20 wt% intervals, respectively, were obtained at University of Winnipeg Planetary Spectrometer Facility. Spectral parameters (band centers and band area ratio [BAR]) were calculated using SpecPR.

Results: Spectral parameters of the mixtures were plotted to identify any trends either as a function of mineral abundance or particle size. Plotting band I center versus BAR of both the mixtures (PYX032+017 and PYX023+005) showed two different trends. The band I center and BAR for PYX032+017 mixture displayed a linear increase in BAR and decrease in band I center with increasing OPX content for both particle sizes. However, the trend line for PYX023+005 mixture does not show a linear relationship between band I center and BAR. This discrepancy between the band parameters of the two OPX+CPX mixtures is primarily due to the type of CPX.

Due to low Fe content, type A CPX do not display a band II and type B CPX show a very weak feature. Both CPX used in this experiment were type B, but the depth of band II varied with PYX017 showing a ~10% deep feature and PYX005 showing a ~3% feature. The weaker PYX005 band II significantly reduced the BAR of the PYX023+005 mixture and the band I versus BAR trend line is very similar to that of olivine-OPX mixture from [4]. The weak band II in PYX005 essentially behaves like olivine (which has only band I) spectrally in the mixture. A mixture of type A CPX and OPX would also be spectrally similar to an olivine-OPX mixture. This has significant implications for interpreting asteroid spectra and care should be taken to distinguish between olivine and CPX in a mixture as it could lead to entirely different petrologic interpretations.

Acknowledgments: V. R. thanks L. Stewart, K. McCormack, and L. Kaletzke for their help with sample preparation. This research is supported by NASA NEOO Grant NNG04GI17G and GSA Shoemaker Impact Cratering Award.

References: [1] Schade U. et al. 2004. *Icarus* 168:80–92. [2] Papike J. J. 1996. *American Mineralogist* 81:525–544. [3] Cloutis E. A. and Gaffey M. J. 1991. *Journal of Geophysical Research* 96:22,809–22,826. [4] Cloutis E. A. et al. 1986. *Journal of Geophysical Research* 91:11,641–11,653.

5141

IMPROVING THE CALCULATIONS OF PRODUCTION RATES OF COSMOGENIC NUCLIDES

R. C. Reedy. Institute of Meteoritics, MSC03-2050, University of New Mexico, Albuquerque, NM 87131, USA.

Introduction: With the measurements of the abundances of cosmogenic nuclides in solar system matter continually getting more accurate and precise, there is a need for the best possible production rates to interpret those results. Early predictions of production rates were varied but limited [1]. Since about 1990, the use of advanced Monte Carlo codes for the production and transport of nuclear particles has been a major improvement in calculating production rates [2–6]. Much work has been done with such calculations and on improving them. However, more work to improve such calculations is needed. Important parts of such modern calculations are the inputs to the calculation of particle fluxes, especially the nature of the target and the irradiating particles, and the cross sections for the proton- and neutron-induced reactions making the product nuclide.

Nuclear Reaction Cross Sections: There has been much work done to get good cross sections for the production of cosmogenic nuclides. Cross sections for protons making most of these nuclides are now in good shape [7]. However, neutrons usually dominate the production of cosmogenic nuclides, and work is being done to measure neutron cross sections [8, 9] Some work on adjusting neutron cross sections will also have to be done with measurements with well-characterized extraterrestrial samples (like Knyahinya or the Apollo 15 deep drill core) or with laboratory-irradiated samples to extend such cross section measurements, similar to what was done earlier [5].

Improved Calculated Particle Spectra: The effects of bulk composition were studied earlier [3], and work is being done on other details in calculating the fluxes of nuclear particles in objects of interest. Earlier work only considered large slabs (2π irradiations) or spheres for omnidirectional (4π) irradiations. Details on the shape of an object probably are important [4], but more work is needed on quantifying these effects of shape. The exact nature of the particles incident on the object is important. The shape of the flux of galactic cosmic ray (GCR) particles as a function of energy [10] affects such calculations. Earlier works ignored incident alpha particles [3–5], but their inclusion does impact the results of the calculations [6]. The cases where the details of spectral shapes and the inclusion of alpha particles are most important need to be determined.

Acknowledgements: Work support by NASA's Cosmochemistry Program.

References: [1] Reedy R. C. 1987. *Nuclear Instruments & Methods B* 29:251–261. [2] Reedy R. C. 2000. *Nuclear Instruments & Methods B* 172: 782–785. [3] Masarik J. and Reedy R. C. 1994. *Geochimica et Cosmochimica Acta* 58:5307–5317. [4] Kim K. J. et al. 2005. *Meteoritics & Planetary Science* 40:A80. [5] Leya I. et al. 2000. *Meteoritics & Planetary Science* 35: 259–286. [6] McKinney G. W. et al. 2006. *Journal of Geophysical Research* 111, doi:10.1029/2005je002551. [7] Reedy R. C. 2007. Abstract #1192. 38th Lunar and Planetary Science Conference. [8] Sisterson J. M. 2007. Abstract #1667. 38th Lunar and Planetary Science Conference. [9] Sisterson J. M. 2007. This issue. [10] Masarik J. and Reedy R. C. 2007. Abstract #1193. 38th Lunar and Planetary Science Conference.

5142

ELEMENTAL MAPPING OF THE MOON WITH THE SELENE GAMMA-RAY SPECTROMETER

R. C. Reedy[1], N. Hasebe[2], E. Shibamura[3], T. Miyachi[2], T. Takashima[4], M.-N. Kobayashi[5], O. Okudaira[2], N. Yamashita[2], S. Kobayashi[2], Y. Karouji[2], M. Hareyama[2], O. Gasnault[6], S. Maurice[6], and C. d'Uston[6]. [1]Inst. of Meteoritics, University of New Mexico, Albuquerque, NM 87131, USA. [2]Research Inst. for Sci. & Eng., Waseda University, 3-4-1, Okubo, Shinjuku, Tokyo, 169-8555, Japan. [3]College of Health Science, Saitama Prefectural University, 820, Sannomiya, Koshigaya, Saitama, 343-8540, Japan. [4]Inst. of Space and Astronautical Science, Japan Aerospace Exploration Agency, 3-1-1 Yoshinodai, Sagamihara, Kanagawa, 229-8510, Japan. [5]Nippon Medical School, Kosugicho, Nakaharaku, Kawasaki 211-0063 Japan. [6]Centre d'Etude Spatiale des Rayonnements, B. P. 44346, 31028 Toulouse, France.

Introduction: Elemental maps of the Moon from gamma-ray spectrometers (GRS) orbiting the Moon have been very important in understanding the origin and evolution of the Moon and its present state [1]. Previous GRS missions to the Moon have only mapped a few elements. Better elemental maps and maps of more elements are needed. Gamma-ray and other instruments on upcoming lunar missions such as the Indian Chandrayaan-1 and the Japanese SELENE will provide such elemental maps. Gamma rays are the best probes of many elements in the Moon [2]. The advanced GRS experiment on SELENE will map many elements and is described here.

The SELENE Gamma-Ray Spectrometer: Previous lunar gamma-ray spectrometers were scintillators with poor energy resolution. The GRS on SELENE will have a large germanium detector with excellent energy resolution, similar to the Mars Odyssey GRS [3]. The spectra on previous lunar GRS experiments only had a few dozen peaks, while over 300 peaks have been observed at Mars [3]. The SELENE GRS will be mechanically cooled and surrounded by bismuth germanate (BGO) and plastic scintillators to reduce backgrounds [4–5]. Only 4 elements, K, Ti, Fe, and Th, were mapped by previous lunar GRS missions; SELENE will produce better maps of these key elements. SELENE will also map other important elements, including O, Mg, Al, Si, Ca, U, and H [5].

Lunar Science with GRS Results: The results from the SELENE GRS for many elements will allow global studies of the composition of lunar terranes such as highlands, maria, KREEP, and large basins like South Pole–Aitken [6]. Having many elements will allow variations in a mare or terrane to be studied. Results for U will help understand this major lunar heat source and the evolution of lunar refractory elements. The direct detection of H by its gamma ray will determine its three-dimensional distribution on the Moon, especially near the poles.

Acknowledgements: Work mainly supported by JAXA.

References: [1] Arnold J. R. et al. 2005. *Meteoritics & Planetary Science* 40:A17. [2] Reedy R. C. 1978. Proceedings, 9th Lunar and Planetary Science Conference. pp. 2961–2984. [3] Evans L. G. et al. 2007. *Journal of Geophysical Research* 112, doi:10.1029/2005JE002657. [4] Kobayashi M. et al. 2002. *Advances in Space Research* 30:1927–1931. [5] Hasebe N. et al. *Earth Planets & Space*. Forthcoming. [6] Jolliff B. L. et al. 2000. *Journal of Geophysical Research* 105:4197–4216.

5195

HIGH-PRESSURE, TEMPERATURE EXPERIMENTAL CONSTRAINTS ON VOLATILE, SIDEROPHILE ELEMENT DEPLETIONS (CD, IN) IN MANTLES

K. Righter. Mail Code KT, NASA-JSC, Houston, TX 77058, USA. E-mail: kevin.righter-1@nasa.gov.

Introduction: The Earth and other differentiated bodies are depleted in volatile elements [1]. This is commonly attributed to condensation processes, whereby these bodies accrete from materials that were already depleted. Although this may be true in general, a complete understanding remains elusive for many elements [2, 3]. Additionally, many of the volatile elements are also siderophile in low-pressure conditions [4], demonstrating that a specific mantle concentration could be caused by volatility or core formation. Experimental studies in the last decade have shown that the concentrations of many siderophile elements in the Earth's mantle can be explained by high pressure and temperature core formation processes [5], but little is known about many of the volatile siderophile elements. As a result, studies of Cd and In are being initiated to determine if these elements are lithophile or siderophile at conditions proposed for early magma oceans on Earth and other bodies.

Experiments and Analyses: Experiments have been carried out at 1 GPa and 1650 °C, using a piston cylinder apparatus. Basaltic starting material containing wt% levels of CdO and In was encapsulated in MgO with Fe metal. Equilibration of the metal-silicate mixture results in liquid silicate and liquid metal, which upon quench were analyzed at NASA-JSC.

Results: Silicate liquids are MgO-rich (~20 wt%) and FeO-bearing (~8 wt%), similar to that expected for a magma ocean. Metallic liquids are Fe-rich (~80 wt%) with smaller amounts of Cd, In, P, and Pd. Metal-silicate partition coefficients, D(M/S) (where D = wt% element in metal/wt% element in silicate), measured were: D(Cd) = 1.9; D(In) = 1.7; and D(P) = 6.3.

Discussion: A recent study has highlighted an In depletion for the terrestrial mantle that is smaller than expected based on other elements (such as Cd) along the volatility trend as originally defined [2]. However, the new experimental results reported here do not reveal a major difference between D(In) and D(Cd) at high PT conditions. Instead the difference in depletion may be due to two aspects of the behavior of Cd and In: a) In is mildly compatible in clinopyroxene [2] and some high-pressure silicates [6], b) In is lithophile in metal-silicate systems at high PT conditions. Whether In and Cd depletions are due to volatility, late veneer additions, or high-PT core formation will be evaluated with more experimental data. However, high-PT core formation is an alternative to origin from a late veneer (e.g., [7, 8]), and consistent with two other volatile siderophile elements—Ga and Sb [9, 10].

References: [1] Allegre C. J. et al. 2001. *Earth and Planetary Science Letters* 185:49–69. [2] G. Witt-Eickschen et al. 2007. Abstract #1536. 38th Lunar Planet. Sci. Conf. [3] Van Westrenen W. and Murthy V. R. 2006. LPI Workshop on Early Planetary Differentiation, December 2006. [4] Capobianco C. J. et al. 1999. *Geochimica et Cosmochimica Acta* 63: 2667–2677. [5] Righter K. 2003. *Annual Reviews of Earth and Planetary Science* 31:135–174. [6] Suzuki T. and Akaogi M. 1998. AGU Geophysical Monograph 101. pp. 261–270. [7] Yi W. et al. 2000. *Journal of Geophysical Research* 105:18,927–18,948. [8] O'Neill H. St. C. 1991. *Geochimica et Cosmochimica Acta* 55:1135–1157. [9] Righter K. and Drake M. J. 2000. *Geochimica et Cosmochimica Acta* 64:3581–3597. [10] Righter K. et al. 2004. *Meteoritics & Planetary Science* 39:A89.

5318

WESTON

M. C. Robson. John J. McCarthy Observatory, New Milford, Connecticut 06776, USA. E-mail: Monty.Robson@mccarthyobservatory.org.

Introduction: As the bicentennial of the historically significant Weston fall approaches, it is clear that the event still commands considerable interest. Professor Richard Binzel's opening comments in the latest and greatest anthology on meteoritics, *Meteorites and the early solar system II*, attest to this continuing fascination [1]. Binzel begins his foreword to the volume with the infamous quote concerning Weston and attributed to Thomas Jefferson: "I would sooner believe Yankee professors would lie than stones would fall from the heavens."

Weston was the first well-documented meteorite fall in the Americas and it happened just as science accepted that stones do fall from the sky. The meteoroid's impact with Earth's atmosphere and its subsequent fragmentation brought an abrupt end to the tranquility of morning twilight in western Connecticut on December 14, 1807. Shock waves rattled homes seventy kilometers north of ground zero, where fragments fell on a populace that, for the most part, had never heard of stones falling from heaven.

The author's ongoing research on Weston began two years ago at the Weston Public Library. The colorful library director provided a copy of the Silliman-Kingsley report [2] to me. I thanked her and had turned to depart when Jane Atkinson said, "But you know, none of it landed in Weston." The Yankee professors, Benjamin Silliman and James Kingsley from Yale College, conducted an in situ investigation of the fall area and wrote three versions of their report [2–4]. The Silliman-Kingsley reports are the main primary sources for my research.

Conclusions: Much in Weston literature is incorrect. The Weston meteor was observed at 06:00 equivalent Eastern Standard Time, not at the almost unanimously given 6:30 A.M. of modern literature. The nearest fragment fell 7 kilometers from the position given in the Meteoritical Society database [5]. The mass recovered was a small fraction of that shown in the Catalogue of Meteorites [6]. A likely source of the Jefferson quote has been found.

References: [1] Binzel R. P. 2006. Foreword. In *Meteorites and the early solar system II*, edited by Lauretta D. S. and McSween H. Y., Jr. The Univ. of Arizona. [2] Silliman B. and Kingsley J. L. 1809. *Transactions of the American Philosophical Society* 6:323–345. [3] Silliman B. and Kingsley J. L. 1807. Letter. New Haven: Connecticut Herald, December 29, 1807. [4] Silliman B. and Kingsley J. L. 1810. An account of the meteor. *Memoirs, Connecticut Academy of Arts and Sciences* 1:141–161. [5] The Meteoritical Bulletin. 2007. http://tin.er.usgs.gov/meteor/metbull.php?code=24249. Accessed May 14, 2007. [6] Natural History Museum. 2007. The catalogue of meteorites. http://internt.nmh.ac.uk/jdsml/research-curation/projects/metcat/detail.dsml?Key=W760. Accessed May 14, 2007.

Additional Information: If you have any questions regarding this paper, please telephone Monty Robson at (860) 354-1595 or e-mail at Monty.Robson@mccarthyobservatory.org or mcrobson@charter.net.

5002

LOS MELLIZOS STRUCTURE: A POSSIBLE NEW 15 KM WIDE IMPACT CRATER IN THE DESEADO PLATEAU, SANTA CRUZ PROVINCE, ARGENTINA

M. C. L. Rocca. Mendoza 2779-16A, Ciudad de Buenos Aires, Argentina, (1428DKU). E-mail: maxrocca2006@hotmail.com.

Introduction: Los Mellizos structure is a large circular depression in the hilly plateau named Meseta del Deseado, Santa Cruz Province, Argentina, South America. (42°20′S, 70°00′W).

This giant structure was studied in detail by the author by the examination of Landsat satellite color images and aerial photos at Instituto Geografico Militar (IGM) of Buenos Aires city.

The crater forms a circular basin with a rim-to-rim diameter of 15 kilometers.

The rim consists of a circular ring of low hills. This circular feature has also a clear difference in its color (light orange to pink) when compared with the color of the surrounding area (brown). Rocks exposed in the surrounding areas are darker than the rocks exposed in the circular structure.

The crater seems to be eroded to the point that only in a few places does the present edge of the rim correspond to the original lip of the crater. Radial faults are present in this structure.

In the north, a small river flows around the circular rim of the structure and another small river crosses the whole structure from the SW to NE.

A central peak is apparently exposed and is visible in the radar images of the German's DLR X-SAR ql-10028 La Española and ql-10029 Cerro Cojudo Blanco.

At present, the geology of this entire area is not know in much detail.

The surroundings of the structure are made up of volcanic formations from the Middle Jurassic age (170–140 Ma) Chon Aike Formation [1–3].

Rocks exposed there are rhyolitic ignimbrites, piroclastic rocks and tuffs.

This structure is quite old and quite eroded and it is similar to the El'gygytgyn impact structure, Russia.

It could represent a new example of an impact structure formed in siliceous volcanics.

If confirmed as a new impact crater then it would represent the largest impact structure located in continental Argentina.

Age is estimated as Mesozoic.

Further research on this site is in progress.

Acknowledgements: This work was funded by the Planetary Society, Pasadena, CA, USA.

References: [1] Barrio de R., Panza J. L., and Nullo F. E. 1999. *Anales SEGEMAR* 29:511–527. In Spanish. [2] Panza J. L. and Cobos J. C. 2001. *Boletin SEGEMAR* 296:1–81. In Spanish. [3] Panza J. L. and Haller M. J. 2002. Relatorio XV Congreso Geologico Argentino, I:89–101. In Spanish.

5053

SAMPLING ASTEROID SURFACES USING MAGNETS

P. Rochette[1], J. Gattacceca[1], and M. Gounelle[2]. [1]CEREGE CNRS University of Aix-Marseille, France. E-mail: rochette@cerege.fr. [2]MHNH, Paris, France.

Sampling material of the regolith of a small asteroid appears to be a tricky task, as demonstrated by the Hayabusa mission. This is due to the very low gravity that makes both landing and mechanical sampling (as done on the Moon and Mars) insecure. An alternative concept is put forward here, using the magnetic force created by a small permanent magnet. Our database of meteorite magnetic susceptibility χ demonstrates that all chondrites except R type have magnetic susceptibility $\log\chi > 3.5$ (χ in 10^{-9} m^3kg^{-1}) [1], which is the value for most magnetic terrestrial basalts. This value also corresponds to the threshold for marked attraction of material by a rare earth magnet. Most carbonaceous chondrites (except some CM and oxidized CV) have $\log\chi > 4$, up to 5.5. This roughly corresponds to a content of magnetic minerals (FeNi metal or magnetite, more rarely pyrrhotite) in the 1–40% range. To illustrate the magnetic sampling concept we used a terrestrial basalt regolith from the McMurdo Island in Antarctica, as an analog of a chondritic asteroid regolith. This material has a $\log\chi = 3.8$ (i.e., in the lower range for C chondrites) angular grain shape and a wide granulometry spectrum. We dropped a 7 g rare earth magnet onto the spread basaltic material and lifted it. Six grams of material were collected by the magnet, with granulometry similar to the one of the starting material. Similar experiments on chondrite powders are ongoing.

The sampling scheme can be summarized as followed: one magnet is stored in a volume devoted to sample collection and is deployed below the spacecraft when touchdown or low-altitude flight is programmed. Deployment can be done by a semi-rigid fine string of up to a few meters in length. This length ensures that the magnet touches the ground and more or less plows into the regolith during the touchdown or low-altitude flight. This concept has the great advantage of allowing sampling with a simple rebound of the probe onto the surface or a flight at very low altitude with non-zero lateral velocity. Indeed, attraction of the particles is instantaneous and does not require that the magnet be immobile with respect to the regolith at any time. Once the spacecraft has started increasing its distance from the ground, the string will be rolled on a wheel by a small motor to allow the magnet, together with attached particles to come back into is lodging, which will be included into the re-entry module. This system ensure a rather low mass and volume of the whole sampling system, with respect to the sample mass. Moreover, contamination of the sample is minimal compared with sampling scheme using impactor, fluid injection or adhesive organics. Will the sampling be representative of the bulk material, made at 80 to 99% of nonmagnetic particles? Indeed the magnet operates some fractioning, as demonstrated in our experience: the extract has a $\log\chi = 4.2$, i.e., 3 times more magnetic than the starting material. However, we expect that the fine grain size of magnetic grains in chondrites will minimize this fractioning.

References: [1] Rochette P. et al. 2006. *Meteoritics & Planetary Science* 41:A152.

5052

MAGNETIC CLASSIFICATION OF ACHONDRITES

P. Rochette[1], J. Gattacceca[1], L. Sagnotti[2], L. Folco[3] G. Consolmagno[4], and M. Denise[5]. [1]CEREGE CNRS Aix-Marseille University, France. E-mail: rochette@cerege.fr. [2]INGV Roma, Italy. [3]Museo Nazionale Antartide, Siena, Italy. [4]Specola Vaticana, Vatican City. [5]MNHN Paris, France.

Low-field magnetic susceptibility (χ) provides a rapid and non-destructive way to classify ordinary chondrites into the LL, L, and H groups, based on non-overlapping range of metal amount [1]. Most non-ordinary chondrites groups also show a narrow range of χ values, except C2, CM, and CV [2]. The total number of achondrite specimens currently in our database is 641; these are from 221 different meteorites, after tentative pairing of hot and cold desert ones. The use of magnetic susceptibility measurement as a classification tool in achondrites is not as straightforward as in the case of chondrites that show well-defined value both at the scale of the individual meteorite and of the meteorite group. All achondrites, except unbrecciated ureilites, show significantly larger dispersion at the meteorite scale, with respect to chondrites. We infer that this is typical of magmatic processes, which produce larger heterogeneities in modal mineralogy at the centimeter scale, compared to the accretionary processes in chondrites. The dispersion observed in ureilites at the meteorite scale, smaller than in any chondrite group, suggests an original petrogenetic process responsible for the metal distribution, postdating magmatic processes. One can distinguish low and high magnetic subgroups in lunar (non-regolith and regolith material, respectively) and Martian meteorites (pyrrhotite- and magnetite-bearing, respectively [3]). On average the achondrites groups can be ranked as shown below according to increasing susceptibility (in 10^{-9} m^3/kg). However, in most of the groups can be found one or two anomalous meteorites that can be one order of magnitude less or more magnetic than the average (computed excluding the anomalies).

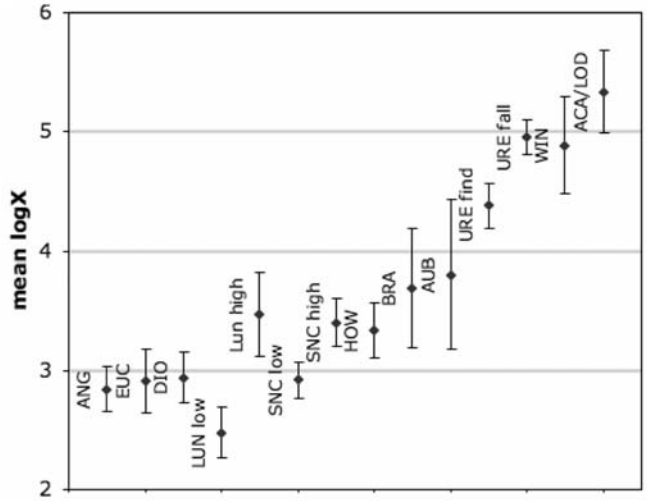

Fig. 1.

References: [1] Rochette P. et al. 2003. *Meteoritics & Planetary Science* 38:251–268. [2] Rochette P. et al. 2006. *Meteoritics & Planetary Science* 41:A152. [3] Rochette P. et al. 2005. *Meteoritics & Planetary Science* 40:529–540.

5055

TRENDS IN THE METEORITE FLUX SINCE 1800: HISTORIC VERSUS ASTRONOMIC MODULATIONS

P. Rochette[1], N. Thouveny[1], J. Gattacceca[1], and L. Folco[2]. [1]CEREGE CNRS University of Aix-Marseille, France. E-mail: rochette@cerege.fr. [2]Museo Nazionale dell'Antartide, Università di Siena, Italy.

Meteorites are systematically studied as they provide a unique record of the composition and history of the solar system. The way they are transferred from their parent bodies (mostly asteroids) controls the intensity and composition of the flux arriving on Earth. Making inferences on the bulk composition of the asteroid belt depends on the transfer efficiency versus asteroid family. Another key issue is the stability through time of the meteorite flux: is what we collect now on Earth an equilibrium state or a snapshot of a variable flux? The existence of meteorite flux variability in the past has been invoked from the yearly time scale [1] to the several Myr time scale [2, 3], as well as at the 1–100 kyr time scale based on comparison between Antarctic and fall collections [4, 5]. Some evidences were also put forward for the last two centuries [6–8].

To tackle these issues, we propose an analysis of the meteorite falls recorded through historical time. We restricted our study to meteorite falls that have been properly documented, with recovered material that has been classified according to the admitted procedure, and with some material still curated. This avoids counting doubtful meteorites. Here we show that the fluctuations in meteorite fall rate through the last two centuries cannot be ascribed solely to human factors and random noise. In particular a sudden change in the meteorite fall number and composition (with lower proportions of H and L) is observed around 1930. Moreover, significant periodicities appear based on spectral analysis, mostly in the 3–5 yr range and at 17 yr, as well as in the 8–12 yr range.

Given the short time scale involved, the processes responsible for these fluctuations should affect meteoroids already in a near-Earth crossing orbit. Much remains to be clarified to provide a mechanical interpretative framework for our observations. At this preliminary stage, one may already point out that the observed short-term fluctuations in meteorite fall rate and composition imply that the meteorite input over the last two centuries is a quite limited and accidental sampling of the asteroid belt general population. We also predict that large changes in compositional proportions at a longer time scale are to be expected [2–5].

References: [1] Halliday I. and Griffin A. A. 1982. *Meteoritics* 17:31–47. [2] Heck P. R et al. 2004. *Nature* 430:323–325. [3] Farley et al. 2006. *Nature* 439:295–297. [4] Harvey R. P. and Cassidy W. A. 1989. *Meteoritics* 24:9–14. [5] Cassidy W. A. 2003. *Meteorites, ice and Antarctica: A personal account*. Cambridge University Press. [6] Hughes D. W. 1981. *Meteoritics* 16:269–281. [7] Treiman A. H. 1993. *Meteoritics* 28:246–252. [8] Lipschutz et al. 1996. *Planetary and Space Science* 45:517–523.

5190

COMBINED MICRO-IR AND MICRO-RAMAN ANALYSES OF COMET 81P/WILD-2 PARTICLES COLLECTED BY STARDUST

A. Rotundi[1], G. A. Baratta[2], J. Borg[3], J. R. Brucato[4], H. Busemann[5, 6], L. Colangeli[4], L. D'Hendecourt[3], Z. Djouadi[3], G. Ferrini[7], I. A. Franchi[6], M. Fries[8], F. Grossemy[3], L. P. Keller[9], V. Mennella[4], K. Nakamura[10], L. R. Nittler[5], M. E. Palumbo[2], S. A. Sandford[11], A. Steele[8], and B. Wopenka[12]. [1]Dip. Sci. Applicate, Univ. di Napoli "Parthenope," Italy. E-mail: rotundi@uniparthenope.it. [2]INAF-Oss. Astr. di Catania, Italy. [3]Inst. d'Astrophysique Spatiale, Univ. Paris-Sud, Orsay-Cedex, France. [4]INAF-Oss. Astr. di Capodimonte, Napoli, Italy. [5]DTM, Carnegie Inst., Washington, D.C., USA. [6]PSSRI, Open Univ., Milton Keynes, UK. [7]Novaetech s.r.l., Città della Scienza, Napoli, Italy. [8]GL, Carnegie Inst., Washington, D.C., USA. [9]NASA-JSC, Houston TX, USA. [10]Jacobs Sverdrup, Eng. Sci. Contract Group, Houston, TX, USA. [11]Astroph. Branch, NASA-Ames Res. Cent., Moffett Field CA, USA. [12]Washington Univ., St. Louis, MO 63130, USA.

The Stardust mission captured particles from comet 81P/Wild-2 and returned them to Earth. A preliminary examination (PE) was performed on grains extracted from tracks formed by the impact of the grains into the aerogel using different analytical techniques [1]. We present here a portion of the PE data that focused on spectroscopic analyses [2].

We report micro-infrared, micro-Raman, and field emission scanning electron microscope analyses of 16 Stardust particles. From mid-IR spectra of six of these particles we infer the CH2/CH3 ratio in the analyzed comet 81P/Wild-2 organics to be ~5–10. This is greater than the values seen in organics in the diffuse interstellar medium lines of sight (2.2), indicating the presence of longer or less-branched aliphatic chains. Values of the same order of magnitude are observed in interplanetary dust particles (IDPs), suggesting some of them are of cometary origin. The Raman spectra are dominated by condensed aromatic hydrocarbons (or "disordered carbonaceous material"), and occasionally also aliphatics are seen. The D and G Raman parameters span a range similar to that observed in IDPs and in most primitive meteorites. Both the IR and Raman data imply the presence of a very labile carbonaceous component. In addition, hydrated silicates may be present in two particles, one of which may also contain carbonates. The latter findings still need to be confirmed with other techniques. In some cases the analyses rendered difficult to interpret because of the presence of compressed aerogel mixed with the grains.

Conclusions: The analyzed grains 1) are rich in complex organic compounds; 2) are compositionally and structurally heterogeneous, even within the same track, suggesting that cometary particles consist of a mixture of subgrains of various sizes and compositions, in accordance to other PE results [1]; 3) contain carriers of a unique labile component, testifying to the primitive character of the organics stored in this comet for 4.56 Ga; and 4) may show some aqueous alteration. The heterogeneity, "primitive" carbons and materials with low degrees of oxidation, suggest that the material survived collection relatively unscathed.

References: [1] *Science*. 2006. 314:1711–1739. [2] Rotundi A. et al. *Meteoritics & Planetary Science*. Forthcoming.

5124

DIVERSE CM CLASTS IN OC REGOLITH BRECCIAS: DERIVATION OF CM PROJECTILES FROM THE DISRUPTED PARENT BODY OF 298 BAPTISTINA

Alan E. Rubin[1] and William F. Bottke[2]. [1]Institute of Geophysics, Univ. California, Los Angeles, CA 90095, USA. [2]Southwest Research Institute, 1050 Walnut St., Boulder, CO 80302, USA.

CM2 chondrites are the largest carbonaceous-chondrite group; CM2 clasts are the most common exotic clasts in OC and HED breccias. Because numerous exotic clasts were strongly shocked when they accreted to their hosts, it is remarkable that many CM2 clasts are hydrated and relatively unshocked. We studied three CM clasts in shock-stage-S3 H-chondrite regolith breccias: AB3 and AB8 in Abbott and PV3 in Plainview [1]. AB3 (shock-stage S3, subtype 2.3 ± 0.1) contains some altered chondrules and ~35 vol% PCP. A few spinel- and diopside-rich CAIs occur. AB8 (S3, subtype 2.1) is yellow-green. It contains abundant phyllosilicate and ~30 vol% PCP; pyrrhotite, pentlandite, and Ca carbonate (ringed by Mn-bearing carbonate) are present. About 90% of chondrule phenocrysts have been altered. PV3 (S3) consists of a 2250 × 1600 μm clast and a 10–500 μm thick rim. The interior contains pyrrhotite, pentlandite, and minor Ca carbonate (ringed by complex carbonate). Olivine grains in the clast are cut by thin sulfide veins; there is also a 10 × 400 μm magnetite-sulfide vein. Olivine has a sharp peak at Fa 0–1. Phyllosilicates and PCP are absent. Two spinel-rich CAIs occur. The PV3 rim consists of fine-grained silicate material containing silicate and sulfide grains; some silicate grains have numerous sulfide blebs. The rim texturally resembles a clast-laden impact-melt breccia. Olivine in the rim is bimodal (with subequal peaks at Fa 1 and 18), indicating mixing of material from the Plainview host (Fa 17–18) and the PV3 interior (Fa 0–1). AB3 and AB8 accreted to the H regolith at low velocities and were not strongly shocked. PV3 was shocked and heated during accretion; phyllosilicates were dehydrated. Olivine crystal lattices healed during annealing. All three clasts were later shocked to S3 along with their hosts.

We postulate that the CM clasts came from the Baptistina asteroid family (BAF) that formed by the disruption ~160 Ma ago of a ~170 km C-type asteroid in the innermost main belt [2]; for Baptistina, a = 2.264 AU. Insights from meteorite delivery models suggest that the BAF is the source of most CM chondrites [3]. The swarm of fragments produced by this event may explain the steep population of fresh 0.2–0.6 km craters found on the nearby asteroid Gaspra [2]. If true, the same BAF bombardment should have affected the OC and HED meteorite precursors, which presumably resided near the BAF because i) OC and HEDs dominate fall statistics and ii) the main dynamical source for most meteorites is the nearby ν_6 resonance [4]. A very small fraction of BAF fragments should have obtained similar orbits to those of the OC and HED precursors. These meteoroids would have had high collision probabilities and low impact velocities; clasts AB3 and AB8 may represent CM projectiles with this dynamical history. A larger fraction of BAF fragments would have achieved different orbital angles than OC and HED precursors and collided at high relative velocities; PV3 may have formed in this manner.

References: [1] Fodor R. V. and Keil K. 1976. *Geochimica et Cosmochimica Acta* 40:177–189. [2] Bottke W. F. et al. 2007. Abstract #2165. 38th Lunar and Planetary Science Conference. [3] Bottke W. F., Vokrouhlický D., and Nesvorný D. *Nature*. Forthcoming. [4] Bottke W. F. et al. 2006. *Nature* 439:821–824.

5094

SOURCE(S) OF THE EXTINCT SHORT-LIVED NUCLIDES: A MASSIVE STAR VERSUS X-WIND IRRADIATION

S. Sahijpal and G. Gupta. Department of Physics, Panjab University, Chandigarh, India. E-mail: sandeep@pu.ac.in.

Introduction: Based on the X-ray flare data of protostars [1, 2] and the X-wind irradiation scenario [3], a numerical code has been developed to infer the irradiation yields of the short-lived nuclides [4]. Several refinements have been made to the code in the present work. The 0.25 R_x wide reconnection ring is now divided into twenty concentric annular zones compared to the five zones [4]. This increases the simulation resolution, hence the reliability by reducing the discreteness. Several additional reaction cross sections for the production of ^{7}Be, ^{10}Be, and ^{36}Cl have been included. The normalized differential mass spectrum for the irradiation yields of the short-lived nuclides for an ensemble of protoCAIs for a specific set of simulation parameters is presented in Fig. 1. We have performed the sensitivity analysis of the various simulation parameters on the irradiation yields.

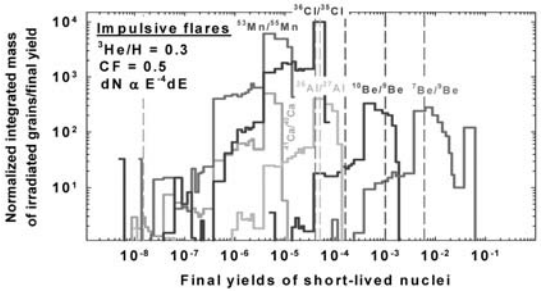

Fig. 1. Normalized differential mass spectra of the final yields of the short-lived nuclides for the core-mantle ensemble (core sizes in the range: 500 μm–13 mm) of grains at the end of a simulation. The dashed vertical lines represent the various empirical estimates of the short-lived nuclides.

Results: The production of some of the short-lived nuclides is feasible with an appropriate choice of the simulation parameters. These parameters have to be fine-tuned to obtain the desirable yields of some of the short-lived nuclides, with a disparity still remaining in the other nuclides. The physico-chemical processes have to operate in a specific manner to obtain the canonical value of ^{26}Al/^{27}Al. A spread by a factor of two in (^{26}Al/^{27}Al)peak yield is inferred in the case of the simulation presented in Fig. 1.

Discussion: Based on the detailed analysis of the X-wind irradiation scenario ([4] and the present work), it is quite likely that the major contributor of ^{26}Al to the early solar system was either a stellar source or local irradiation of nebular gas by superflares with $L_x > 10^{32}$ ergs s^{-1} [4]. The former seems to be more plausible in the absence of any reliable observations of the superflares [2]. It is quite likely that a massive (≥30 $M_\odot$) star, evolving through Wolf-Rayet phase followed by supernova Ib/c, produced ^{26}Al and ^{60}Fe [5, 6]. Even though, the IMF is dominated by ≥25 $M_\odot$ stars, the ≥30 $M_\odot$ stars (e.g., θ^1 Ori. C in ONC) evolve faster and would lead in triggering the star formation within a molecular cloud [5]. The injected ^{26}Al and ^{60}Fe would provide the heat for the differentiation of planetesimals within the initial 10 Ma [7].

Acknowledgements: This work is supported by a PLANEX(ISRO) grant.

References: [1] Feigelson E. D. et al. 2002. *The Astrophysical Journal* 572:335–349. [2] Wolk S. J. et al. 2005. *The Astrophysical Journal* 160:423–449. [3] Shu F. H. et al. 2001. *The Astrophysical Journal* 548:1029–1050. [4] Sahijpal S. and Soni P. *Meteoritics & Planetary Science*. Forthcoming. [5] Sahijpal S. & Soni P. 2006. *Meteoritics & Planetary Science*. 41:953–976. [6] Limongi M. and Chieffi A. 2006. *The Astrophysical Journal* 647:483–500. [7] Sahijpal S. et al. *Meteoritics & Planetary Science*. Forthcoming.

5149

ORIGIN OF ^{17,18}O-RICH MATERIALS FROM ACFER 094

N. Sakamoto[1], Y. Seto[1], S. Itoh[1], K. Kuramoto[2], K. Fujino[1], K. Nagashima[3], A. N. Krot[3], and H. Yurimoto[1]. [1]Department of Natural History Sciences, Hokkaido University, Sapporo 060-0810, Japan. E-mail: naoya@ep.sci.hokudai.ac.jp. [2]Department of Cosmosciences, Hokkaido University, Sapporo 060-0810, Japan. [3]Hawai'i Institute of Geophysics and Planetology, School of Ocean and Earth Science and Technology, University of Hawai'i at Manoa, Honolulu, HI 96822, USA.

Introduction: The mass-independent fractionation of oxygen isotopes in our solar system is generally considered to result from mixing of isotopically distinct nebular reservoirs [1]. Recently unique Fe-O-S bearing material, called new-PCP, is extremely enriched in heavy oxygen isotopes of ^{17}O and ^{18}O of +180‰ relative to the Earth's ocean [2]. We examine continued oxygen isotope studies and thermodynamic calculations in order to consider the forming condition of new-PCP.

Results: Based on the unique chemical composition of new-PCP, hundreds grains of new-PCP were identified in an Acfer 094 polished thin section using FE-SEM-EDS. Four grains from them were selected to determine oxygen isotopic compositions and the heterogeneity within grain by isotopography [3]. All analyzed grains are significantly enriched in ^{17}O and ^{18}O relative to SMOW (~180‰) as much as previously reported in the new-PCP [2].

Thermodynamic calculation of the Fe-O-S system has been carried out for sulfurization and oxidation of Fe-metal and troilite. The calculation shows oxidation of troilite or metal would occur below 360 K independent on total pressure under a constant P_{H2O}/P_{H2} ratio of ~5×10^{-4}; a characteristic value for a gas of solar composition [4]. If the P_{H2O}/P_{H2} ratio increases, formation of new-PCP occurs at higher temperature. An experimental result supports the co-existence of magnetite and FeS with water below 373 K [5].

Discussion: Because the water vapor (H_2O) is the major oxidant in the solar nebula, the oxygen isotopic composition of the new-PCP corresponds to that of nebular water. The sublimation temperature of water ice is below 200 K even in the several-fold H_2O-enriched nebula. Therefore, the new-PCP was formed in the inner solar nebula before that oxygen isotopic equilibrium had not been achieved. Alternatively, the new-PCP was formed in the Acfer 094 parent body before that oxygen isotope exchange was not experienced between water and matrix silicates. These forming conditions are consistent with the lack of mineralogical and petrographical evidence of aqueous alteration of Acfer 094 [6].

References: [1] Clayton R. N. 1993. *Annual Review of Earth and Planetary Sciences* 21:115–149. [2] Sakamoto N. et al. 2007. Abstract #1644. 38th Lunar and Planetary Science Conference. [3] Yurimoto H. et al. 2003. *Applied Surface Science* 203-204:793–797. [4] Krot A. N. et al. 2000. In *Protostars and planets IV.* pp. 1019–1054. [5] Herndon J. M. et al. 1975. *Nature* 253:516–518. [6] Greshake A. 1997. *Geochimica et Cosmochimica Acta* 61:437–452.

5201

ORIGIN OF CHONDRULES: A PLANETARY CONNECTION

I. S. Sanders. Department of Geology, Trinity College, Dublin, Ireland.

Chondrules, those frozen droplets of partly crystallized silicate melt that occur in abundance in chondritic meteorites, obviously cooled in space, i.e., in the solar nebula, but we do not know where and how they became molten. Robert Hutchison convinced me 15 years ago, using arguments revisited in [1], that chondrules were not made by the melting of small, preformed clumps of dust, but originated instead in large bodies, planetesimals or protoplanets, either by impact melting or, as I prefer, by the splashing of bodies that were already molten [2].

The ubiquity of molten bodies in the solar nebula during its first two million years is widely accepted today. Tungsten isotope ratios imply that iron cores were molten within <1 Myr of CAIs [3], and ^{26}Al is now known to have been potent enough to have maintained near-total meltdown in bodies >30 km in radius for that first 2 Myr period [2]. Collisions involving the molten bodies were inevitable and would have launched enormous numbers of molten droplets back into the disk, to re-accrete later as chondrules. Importantly, chondritic parent bodies >30 km in radius can only have accreted after about 2 Myr, when the heat source had waned sufficiently, otherwise they, too, would have melted. Measured Al-Mg chondrule ages in all classes of meteorite cluster between 1.5 and 2.5 Myr, in remarkably good agreement with this scenario.

The formation of chondrules by splashing can be reconciled with many observations [2]. The process is consistent with the chondrules' primitive chemistry (reflecting near-total meltdown), with their restricted range of "peak" temperatures (presumably buffered by convection), and with the efficiency with which they were evidently made. Settling of olivine prior to splashing may account for the correlation of chondrule Si/Mg with age. Settling of iron prior to splashing would explain depletion of Fe, Co, and Ni in the L and LL chondrites.

The post-impact plume of chondrules might provide just the kind of "nebular" setting that has been inferred for chondrule origins. Its ephemeral nature in a cold ambient setting is consistent with the admixture of presolar grains in chondrites. It would provide an appropriately high "dust-to-gas" ratio for liquid droplets and compound chondrules. Large blobs of liquid would make megachondrules. Mutual thermal radiation would retard cooling rates. Solid bits of ejected crust would account for "clast chondrules" and "planetary fragments." Unmelted dust grains engulfed by droplets would be described as "relict." Hot re-accretion could explain chondrules that indent one another. Lost volatiles might condense locally, re-accrete with matrix dust, and account for back-diffusion into chondrules and for the complementary relationship between chondrules and matrix in some chondrites.

Impacts after 2 Myr also led to chondrule formation. An impact at 4.5 Myr almost certainly generated chondrules in the CB meteorites, and crystalline lunar spherules are really impact-generated chondrules. Impacts have also been implicated in very early volatile loss, prior to chondrite accretion [4, 5]. It is probably no longer appropriate, or even wise, to imagine the solar nebular in the absence of colliding planetary bodies.

References: [1] Hutchison R., Bridges J. C., and Gilmour J. D. 2005. In *Chondrites and the protoplanetary disk*. San Francisco: Astronomical Society of the Pacific. pp. 933–950. [2] Sanders I. S. and Taylor G. J. 2005. In *Chondrites and the protoplanetary disk*. San Francisco: Astronomical Society of the Pacific. pp. 915–932. [3] Kleine T. et al. 2005. *Geochimica et Cosmochimica Acta* 69:5805–5818. [4] Asphaug E. et. al. 2006. *Nature* 439: 155–160. [5] Bland P. A. and Benedix G. K. 2006. *Meteoritics & Planetary Science* 41:A22.

5046

"FIXING" INTERSTELLAR AND PROTOSOLAR D AND ^{15}N ENRICHMENTS INTO METEORITIC MATERIALS

S. A. Sandford. Astrophysics Branch, NASA-Ames Research Center, Moffett Field, CA 94035, USA.

Introduction: The presence of isotopic anomalies in the form of enrichments of D and ^{15}N in meteorites, IDPs, and now cometary samples from comet 81P/Wild-2, are thought to be due to molecular species (or products of molecular species) formed in the interstellar medium and/or protosolar nebula [1–3]. This contention is supported by various astrochemical models of these environments and by observation of rotational lines of specific gas phase molecular species in dense interstellar clouds that show enrichments of D and ^{15}N [1, 4–7]. However, the isotopically enriched molecules seen in the interstellar medium to date are simple, volatile species, molecules that clearly are not the carriers of the anomalies seen in meteoritic materials. This suggests that there must be physical and chemical processes in the interstellar medium and/or protostellar nebulae that "fix" the anomalies seen in small species into more robust materials.

Discussion: The "fixing" of D and ^{15}N anomalies could occur in several ways. First, processes could occur whereby the volatile enriched species seen in astronomical observations are converted into more complex refractory materials capable of surviving in meteoritic parent bodies. If this processing occurs in the interstellar medium, the meteoritic carriers would be bona fide interstellar molecules. If the processing occurs in the protosolar nebula, the carriers will have an interstellar heritage, but their identities will be more reflective of protosolar or parent body conditions.

Alternatively, the same processes that produce isotopic enrichments of D and ^{15}N in small, volatile species in the interstellar medium may also enrich larger and more complex species that so far remain undetected because these species do not lend themselves to detection by radio techniques (for example, they have no strong rotational lines or are refractory materials that condense onto grains where they produce no rotational lines at all). Depending on the species and protosolar conditions, this class of materials could also survive intact into meteorite parent bodies, i.e., represent bona fide interstellar species, or could be further processed in the protosolar nebula and parent body.

If is, of course, possible (even likely) that all of these combinations of processing occur. I will discuss some of the processes whereby D and ^{15}N enrichments are thought to occur in the interstellar medium and summarize the molecular "fingerprints" these different processes are expected to leave on the resulting carriers. I will also discuss means by which it may be possible to determine whether the same anomalies seen in simple molecules in the interstellar medium are also carried by more complex species as well.

References: [1] Sandford S. A., Bernstein M. P., and Dworkin J. P. 2001. *Meteoritics & Planetary Science* 36:1117–1133. [2] Messenger S. 2000. *Nature* 404:968–971. [3] McKeegan K. D. et al. 2006. *Science* 314: 1724–1728. [4] Langer W. D. and Graedel T. E. 1989. *The Astrophysical Journal* 69:241–269. [5] Rodgers S. D. and Charnley S. B. 2004. *Monthly Notices of the Royal Astronomical Society* 352:600–604. [6] Jacq T., Walmsley C. M., Henkel C., Baudry A., Mauersberger R., and Jewell P. R. 1990. *Astronomy & Astrophysics* 228: 447–470. [7] Roueff E., Lis D. C., Van Der Tak F. F. S., Gerin M., and Goldsmith P. F. 2005. *Astronomy & Astrophysics* 438:585–598.

5316

XRD AS A TOOL TO CONSTRAIN OLIVINE COMPOSITION: APPLICATIONS TO H AND L CHONDRITES

T. J. Schepker and A. Ruzicka. Cascadia Meteorite Laboratory, Department of Geology, Portland State University, Portland, OR 97207, USA. E-mail: tomschepker@hotmail.com.

Introduction: Recent work by Bland et al. [1] and Menzies et al. [2] has sought to quantify modal abundance of chondrites using X-ray diffraction (XRD). This work utilized complex techniques involving a specialized X-ray detector (position sensitive detector or PSD) that enabled simultaneous X-ray detection from 0–120° 2θ [1]. Olivine with different Fa contents appears to have slightly different XRD peak positions [3]. However, it is difficult to ascertain the exact relationship between Fa content and peak position using existing databases alone, as the data were not obtained with the same instruments or under the same conditions. We performed experiments on equilibrated (type 4–6) H and L chondrites to evaluate whether conventional XRD techniques using the same instrument and scanning conditions can be used to reliably infer olivine Fa content, and thereby to classify chondrites, as an alternative to the more time-consuming and expensive electron microprobe (EMP) technique.

Methods: Sample material was prepared by grinding with an agate rock grinder, and samples were sieved to less than 30 μm particle size. Powder specimens were scanned using default continuous settings on Portland State University's Phillips X'pert 3040 X-ray diffractor, using a 15 mm mask with scan settings of 0.5 seconds per 0.02° 2θ between 5–90° 2θ. Co Kα radiation and a side loading, open top specimen holder were utilized for all scans. The Phillips X'pert Graphics and Identify software (version 1.2d) was then employed for normal peak fitting analysis for all minerals expected in an ordinary chondrite. Three olivine peaks showing relatively little overlap with other phases were selected for further detailed analysis, to determine whether exact centroid position varied with average Fa content in olivine as determined by previous EMP analysis. Nineteen scans were performed under these conditions on a variety of H 4–6 and L 4–6 ordinary chondrites. We made multiple scans of the meteorites to obtain an estimate of the internal precision.

Results: We report a good correlation between peak position and Fa composition for the olivine peak located at ~79.2–79.5° 2θ. For this peak, we determined a correlation line with r^2 of ~0.85, or ~0.89 if one apparently spurious data point is omitted. We observed no overlap in peak position between L and H type ordinary chondrites. Therefore, we can differentiate between the two types based on XRD data alone. Moreover, internal precision (~0.013° 2θ) is found to be small compared to the difference in average peak position between H and L chondrites (~0.16° 2θ). For equilibrated H- and L-type ordinary chondrites, we can obtain Fa composition to ±1 mol% at 95% confidence utilizing XRD. Thus, our results suggest that conventional XRD can be used to relatively quickly constrain olivine compositions in ordinary chondrites and possibly in other types of samples.

References: [1] Bland P. A. et al. 2004. *Meteoritics & Planetary Science* 39:3–16. [2] Menzies O. N. et al. 2005. *Meteoritics & Planetary Science* 40:1023–1042. [3] Deer W. A. et al. 1966. *An introduction to rock forming minerals.*

5001

HIGHLY SIDEROPHILE ELEMENTS IN EARTH AND MARS

G. Schmidt. Institute of Nuclear Chemistry, University of Mainz, Germany. E-mail: gerhard.schmidt@uni-mainz.de.

The relative abundances of highly siderophile elements (HSE: Os, Ir, Ru, Pt, Rh, Pd) in the Earth's primitive upper mantle (PUM) and the continental upper crust (UCC) is a key issue for understanding the origin and the influence of impactors on the chemical composition of planets. Over the past twelve years we have measured the HSE in many mantle suites of the Earth by neutron activation. Estimates of Rh/Ir, Ru/Ir, Pd/Ir, and Pt/Os derived from PUM indicates modestly suprachondritic compositions [1]. The Os, Ir, Ru, Pt, and Pd pattern on PUM perfectly match the IVA iron meteorite Charlotte recently measured by Walker et al. [2]. The question raises if HSE in PUM are added to the accreting Earth by a late bombardment of iron meteorites or some unsampled inner solar system materials more highly fractionated than enstatite chondrites?

The HSE and Ni systematics of the UCC closely resemble IIIAB iron meteorites (many impact craters on Earth are produced by this type of iron meteorite projectile, e.g., [3] and references therein), pallasites, and the evolved suite of Martian meteorites (Fig. 1), possibly representing the elemental pattern of the Martian crust [4]. Probably the Martian crust and the Earth crust preserve an imprint of the same materials. In fact, the first meteorite of any type ever identified on another planet by NASA's Mars Exploration Rover Opportunity was an iron meteorite. Calculations show that a projectile with a radius of ≤54 km would yield the abundances of HSE and Ni in the UCC.

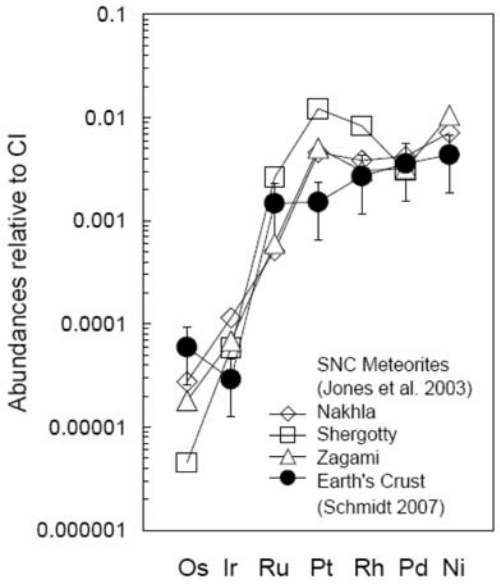

Fig. 1.

References: [1] Schmidt G. 2004. *Meteoritics & Planetary Science* 39: 1995–2007. [2] Walker R. J. et al. 2005. Abstract #1313. 36th LPSC. [3] Schmidt G. et al. 1997. *Geochimica et Cosmochimica Acta* 61:2977. [4] Jones J. H. et al. 2003. *Chemical Geology* 196:21–41.

5244

SULFIDE-RICH ASSEMBLAGES IN CR TYPE II CHONDRULES FORMED BY HIGH-TEMPERATURE GAS-SOLID REACTION

D. L. Schrader[1], D. S. Lauretta[1], and H. C. Connolly, Jr.[1, 2, 3]. [1]The University of Arizona, Lunar and Planetary Laboratory, Tucson, AZ 85721, USA. E-mail: schrader@lpl.arizona.edu. [2]Department of Physical Sciences, Kingsborough College of the City, University of New York, 2001 Oriental Blvd., Brooklyn, NY 10023, USA. [3]Department of Earth and Planetary Sciences, AMNH Central Park West, New York, NY 10024, USA.

Introduction: Type II chondrules in the CR chondrite MAC 87320 (MAC) contain complex sulfide-rich assemblages [1, 2]. These assemblages contain rounded and elongated Ni-rich Fe,Ni-metal (avg = 29.8 wt% Ni), rounded phosphates, and Ni-rich troilite (avg = 0.7 wt% Ni). These assemblages are morphologically and compositionally similar to the products of experimental gas-solid oxidation-sulfidation of an Fe-based alloy above the Fe-FeS eutectic (988 °C) [3]. This similarity suggests that these sulfide-rich assemblages formed above the Fe-FeS eutectic by rapid gas-solid reactions in a region of enhanced fS_2 and fO_2, compared to canonical [4].

Procedure: The experimental, analytical, and observational techniques are described in [2, 3]. Time scales for sulfidation were estimated using experimentally determined kinetic data and the morphology of each assemblage. The volume and surface area were determined by measuring the average radii of each assemblage; their shape was approximated to be spherical. Volume percents of each phase were assumed to be equal to the surface area exposed in thin section. The size and mass of the starting metal was estimated assuming that all Fe and Ni was originally present as an alloy. Experimentally determined linear rate constants for H_2S gas molecule adsorption on Fe alloys were used to estimate the formation times of the assemblages in MAC.

Discussion: The similarity between sulfide-rich assemblages in type II chondrules of the CR chondrite MAC and experimental gas-solid reaction products suggests a gas-solid formation process for these assemblages. Formation times of these assemblages were estimated using our experimentally determined linear rate constants [3] and assuming similar formation conditions as the experiments (1000 °C, 1 atm, enhanced fS_2 and fO_2). The reaction kinetics are rapid and each assemblage corroded in ~1 second. Lauretta et al. [5] suggest some troilite in meteorites resulted from flash heating and rapid cooling in a region of S-rich gas in contact with chondrule metal, during or after chondrule formation. Our experiments support this hypothesis and suggest that sulfide-rich assemblages in MAC type II chondrules formed during flash heating at temperatures above the Fe-FeS eutectic from a gas-solid reaction in a region of enhanced fS_2.

References: [1] Connolly H. C. et al. 2003. Abstract #1770. 34th Lunar and Planetary Science Conference. [2] Schrader D. L. et al. 2007. Abstract #1368. 38th Lunar and Planetary Science Conference. [3] Schrader D. L. et al. 2006. Abstract #2256. 37th Lunar and Planetary Science Conference. [4] Ebel D. S. and Grossman L. 2000. *Geochimica et Cosmochimica Acta* 64: 339–366. [5] Lauretta D. S. et al. 2001. *Geochimica et Cosmochimica Acta* 65:1337–1353.

5151

CHEMICAL COMPOSITION AND Lu-Hf AGE OF THE LUNAR MARE BASALT METEORITE KALAHARI 009

T. Schulz[1, 2, 3], A. K. Sokol[3, 4], H. Palme[1], G. Weckwerth[1], C. Münker[2, 3], and A. Bischoff[4]. [1]Institut für Geologie und Mineralogie, Universität zu Köln, Zülpicherstr. 49b, D-50674, Köln, Germany. [2]Mineralogisch-Petrologisches Institut, Universität Bonn Poppelsdorfer Schloss, 53115 Bonn, Germany. [3]Zentrallabor für Geochronologie, Institut für Mineralogie, Universität Münster, Corrensstr. 24, D-48149 Münster, Germany. [4]Institut für Planetologie, Wilhelm-Klemm-Str. 10, D-48149 Münster, Germany.

Introduction: Kalahari 009 is a lunar mare basalt breccia consisting of fragments of basaltic lithologies embedded in a fine-grained matrix [1]. Based on its mineralogy, this meteorite can be classified as a VLT mare basalt. Compared to other mare basalts Kalahari 009 has an unusual young Ar-Ar age of ~1.7 Ga [2]. In order to place this meteorite in the context of lunar magmatism, we analyzed selected major and trace elements on whole-rock powders using XRF and INAA. Additionally we obtained a Lu-Hf isochron age on whole-rock, ilmenite, and pyroxene separates.

Results: The chemical composition of Kalahari 009 is given in the table. The Lu-Hf isochron yields an age of ~4.2 Ga.

Table 1. Chemical composition of Kalahari 009.

Major	(wt%)	Trace	(ppm)	Trace	(ppm)
SiO_2	46.04	P	227	Er	<9
TiO_2	0.67	Sc	45	Tm	<0.3
Cr_2O_3	0.36	V	143	Yb	1.6
Al_2O_3	12.70	Co	23.3	Lu	0.3
FeO	18.50	Ni	<20	Hf	0.7
MnO	0.23	Ga	1.0	Ta	0.1
MgO	7.88	As	0.4	W	0.3
CaO	11.17	La	0.94	Re	0.03
Na_2O	0.44	Ce	3.7	Ir	<0.004
K_2O	0.19	Nd	3.4	Th	0.10
		Sm	0.74	U	0.14
Total	98.18	Eu	0.4		
		Gd	2.0		
Fe/Mn	79.7	Tb	0.2		
Mg/Cr	19.3	Dy	4.0		
		Ho	0.36		

Discussion: Fe/Mn and Mg/Cr ratios of Kalahari 009 are similar to other lunar mare basalts and the TiO_2 content is one of the lowest among all basaltic lunar meteorites. Kalahari 009 has a flat chondrite-normalized REE pattern, similar to that observed in NEA-003 [3], but unlike that observed in all other mare basalts. Therefore these two meteorites probably sample a common but so far unidentified lunar reservoir.

The Lu-Hf age is similar to ages of other very-low Ti basalts but is significantly older than the Ar-Ar age [2]. Such a young Ar-Ar age is also observed for NEA-003 [3]. We propose that the Lu-Hf age most likely dates crystallization, whereas the Ar-Ar ages record probably an impact related degassing event.

References: [1] Sokol A. K. and Bischoff A. 2005. *Meteoritics & Planetary Science* 40:A177–A184. [2] Fernandes V. A. et al. 2007. Abstract #1611. 38th Lunar and Planetary Science Conference. [3] Haloda et al. 2006. Abstract #2269. 37th Lunar and Planetary Science Conference.

5058

REVISING THE K DECAY CONSTANT

W. H. Schwarz and M. Trieloff. Institute of Mineralogy, University of Heidelberg, Im Neuenheimer Feld 236, D-69120 Heidelberg, Germany. E-mail: wschwarz@min.uni-heidelberg.de.

The accuracy of current K-Ar age calculations is limited by the uncertainties of the ^{40}K decay constants [1, 2]. Critical values to calculate K-Ar or Ar-Ar ages are: 1) the total decay constant of ^{40}K ($5.543 \cdot 10^{-10}$ a^{-1}, evaluated by data compilation of [3]), 2) the ^{40}K/K ratio of 0.01167% [4], and 3) the branching ratio of 10.48/89.52 of the dual decay to ^{40}Ar and ^{40}Ca [1, 3]. These values can be revised by precise determination of systematic offsets of Ar-Ar and U/Pb ages of minerals from a variety of rocks of different geological age (e.g., [5, 6]), particular very old rocks like meteorites are useful [7]. However, many meteorite classes are seriously disturbed by secondary ^{40}Ar loss (HEDs, L chondrites, e.g., [8–10]), and only few retained ^{40}Ar since primordial cooling, e.g., certain R and H chondrites [7, 11]. Using the H chondrite parent body cooling history [7, 12], the age offset of U/Pb and Ar-Ar ages for ~4.5 Ga old rocks is ~30 Ma [7, 13], significantly smaller than 1% as noted in [5] or [6]. A biotite from the Great Dyke Intrusion in Zimbabwe (~2.5 Ga old) yields an age offset of ~20 Ma, while Ar-Ar ages of pseudotachylites from the ~2.0 Ga old Vredefort impact structure [14] yield a difference of ~17 Ma (recalculated for a new NL25 standard age of 2557 ± 4 Ma). These new data lead to a decay constant of $\sim 5.520 \cdot 10^{-10}$ a^{-1}, only a little smaller than that defined by [1]; this result will not change including data from other laboratories (e.g., [5, 6]). It is slightly different from a result obtained by direct detection ($5.554 \cdot 10^{-10}$ a^{-1} [15, 16]), but different ^{40}K/K and branching ratios were used for these calculations. Geochronological data alone do not give clear evidence whether the branching ratio or the ^{40}K/K ratio is wrong by about 1%. If the ^{40}K/K ratio of 0.01167% is taken as correct, the decay constant to ^{40}Ar would be $\sim 0.575 \cdot 10^{-10}$ a^{-1}, corresponding to a branching ratio of ~10.42/89.58.

References: [1] Steiger and Jäger. 1977. *Earth and Planetary Science Letters* 36:359–362. [2] Begemann F. et al. 2001. *Geochimica et Cosmochimica Acta* 65:111–121. [3] Beckinsale and Gale. 1969. *Earth and Planetary Science Letters* 6:289–294. [4] Garner et al. 1975. *Journal of Research of the National Institute of Standards and Technology A*, 79:713–725. [5] Kwon et al. 2002. *Mathematical Geology* 34:457–474. [6] Krumrei et al. 2006. *Chemical Geology* 227:258–273. [7] Trieloff M. et al. 2003. *Nature* 422:502–506. [8] Korochantseva E. V. et al. 2007. *Meteoritics & Planetary Science* 42:113–130. [9] Korochantseva E. V. et al. 2005. *Meteoritics & Planetary Science* 40:1433–1454. [10] Kunz J. et al. 1995. *Planetary and Space Science* 43:527–543. [11] Buikin A. I. et al. 2006. *Meteoritics & Planetary Science* 41:A30. [12] Schwarz W. H. and Trieloff M. 2006. *Meteoritics & Planetary Science* 41:A161. [13] Trieloff M. et al. 2001. *Earth and Planetary Science Letters* 190:267–269. [14] Trieloff M. et al. 1998. *Meteoritics & Planetary Science* 33:361–372. [15] Malonda and Carles. 2002. *Applied Radiation and Isotopes* 56:153–156. [16] Kossert and Günther. 2004. *Applied Radiation and Isotopes* 60:459–464.

5030

WEATHERING EL HAMMAMI (H5) IN THE LABORATORY—PETROGRAPHY AND NOBLE GASES

S. P. Schwenzer[1, 2], U. Billmeier[1], K. Schmale[3], A. Bischoff[3], and U. Ott[1]. [1]Max-Planck-Institut für Chemie, J.-J. Becherweg 27, D-55128 Mainz, Germany. [2]Present address: Lunar and Planetary Institute, 3600 Bay Area Boulevard, Houston, TX 77058–1113, USA. E-mail: schwenzer@lpi.usra.edu. [3]Institut für Planetologie, Wilhelm-Klemm-Str. 10, D-48149 Münster, Germany.

Introduction: As many meteorites are finds, it is important to characterize the influence of weathering on the meteorites' features. For this study the ordinary chondrite El Hammami (H5, shock stage 2, [1]) was used. Small pieces of this meteorite were exposed to a set of conditions evolving over substrates in the laboratory for more than two years after which petrographical [2] and noble gas investigations were carried out.

Experimental and Petrography: A sample of El Hammami was cut into cubes of 0.5 cm edge length. Containers were filled with different substrates (mixtures of carbonates, quartz, and NaCl, as well as a desert soil sample) upon which a bag containing the meteorite sample was placed and covered with substrate. The containers were then filled with distilled water. After 3 and 27 months samples were removed for petrographical investigations. After 27 months the pH of the solutions varied between 6.5 and 8.9. The samples showed weathering grade W1 (after [3]). In a second experiment samples were weathered within a quartz substrate (pH of the solution ~5) for 5 months. These samples showed much more extensive weathering.

Noble Gases: An untreated sample of El Hammami and two laboratory weathered samples—from the containers with soil from the desert of Hammada el Hamra and a limestone substrate—were measured for noble gases.

El Hammami Original: In an untreated piece of El Hammami, we found $1443 * 10^{-8}$ ccSPP/g ^{4}He, which is ~20% higher than in [4]. Our abundance of $39.4 * 10^{-8}$ ccSTP/g ^{3}He is about 10% higher than in [4]. The amount of cosmogenic ^{21}Ne is $10.2*10^{-8}$ ccSTP/g. Amounts of ^{36,38,40}Ar in [4] are only about 62–65% of what we found: 3.18, 2.53, and 8230 ($*10^{-8}$ ccSTP/g). ^{84}Kr and ^{132}Xe are 1.01 and $1.11*10^{-10}$ ccSTP/g, respectively.

Laboratory Weathered Samples: ^{3}He is slightly depleted in the sample from the limestone substrate, whereas ^{4}He and ^{20,21,22}Ne show enrichments in both laboratory treated samples. ^{36,38,40}Ar are depleted in both laboratory weathered samples. ^{84}Kr and ^{132}Xe are enriched by factors of ~3 and 1.6, respectively. The change in Xe isotopic composition is consistent and indicates a contribution of ~40–50% of adsorbed air.

Conclusions: Although our noble gas data set is not complete, some explanations are possible. Depletion/enrichment of isotopes can be traced back to weathering of possible carrier phases. For the cosmogenic nuclides some of the variations can be explained by weathering of the metal phase—consistent with what is observed in the thin sections. Heavy noble gases, mainly Kr and Xe, are adsorbed as can also be seen in the degassing patterns. A more complete data set will be presented at the conference.

Acknowledgements: We thank Niels Hoppe for parts of the data reduction.

References: [1] Grossmann J. N. 1998. *Meteoritics & Planetary Science* 33:A222. [2] Schmale K. 2006. Bachelor's thesis, University of Münster. [3] Wlotzka F. 1993. *Meteoritics & Planetary Science* 28:460. [4] Schultz L. and Franke L. 2004. *Meteoritics & Planetary Science* 39: 1889–1890.

5187

MARTIAN METEORITE NAKHLA: NOBLE GASES IN BULK, MINERAL SEPARATES AND ETCHED BULK

S. P. Schwenzer[1, 2], M. Colindres[1], U. Billmeier[1], S. Herrmann[1], and U. Ott[1]. [1]Max-Planck-Institut für Chemie, J.-J. Becherweg 27, D-55128 Mainz, Germany. [2]Present address: Lunar and Planetary Institute, 3600 Bay Area Boulevard, Houston, Texas 77058–1113, USA. E-mail: schwenzer@lpi.usra.edu.

Introduction: The Martian meteorite Nakhla belongs to the sub-group of nakhlites. It is an igneous rock composed of augite (80.8 ± 4.3%), olivine (10.8 ± 4.7%), and mesostasis (8.4 ± 2.1) [1]. Regarding noble gases, several studies exist (e.g., [2–8], and also references in [9]), but there still is discussion about the mechanism of incorporation and the siting. Our study provides a set of five noble gases obtained on a same sample split of Nakhla and mineral separates (pyroxene, olivine, and mesostasis) as well as data from an etched Nakhla sample.

Bulk and Etched: Comparing the untreated bulk sample with the etched sample (see [2] for details) shows that etching—together with 15% of the mass—removes 38% of ^{3,4}He, 33% of ^{20}Ne, 30% of ^{21}Ne, 32% of ^{22}Ne, 26% of ^{36}Ar, 29% of ^{38}Ar, and 37% of ^{40}Ar, but the sample gained ^{84}Kr (factor of 18) and ^{132}Xe (factor of 22). This shows that the etched part is the carrier of the isotopes lost, and that adsorption causes severe gain in ^{84}Kr and ^{132}Xe. The effect is large enough to reduce the Martian atmospheric signature in ^{129}Xe/^{132}Xe of the bulk sample (1.52) to the air ratio (0.98). Excess ^{129}Xe* in the sum of the etched sample is completely masked by the high amount of air. In the (1000 + 1200) °C step of bulk and etched sample ^{129}Xe* is 2.0 and 0.40$^{*}10^{-12}$ ccSTP/g, respectively.

Bulk and Mineral Separates: Mass balance calculations on the basis of the petrographic data [1] show that for ^{3}He and ^{20,21,22}Ne the amounts calculated from the separates fit the measured bulk value. In contrast, ^{4}He, ^{36,38,40}Ar, and ^{132}Xe are higher in bulk than what we calculate from the sums of the mineral separates. The Martian atmospheric high ^{129}Xe/^{132}Xe ratio is seen in all separates. It is—in the (1000 + 1200) °C steps—accompanied by very low ^{84}Kr/^{132}Xe ratios (olivine: 0.6, mesostasis: 2.5).

Conclusions: Treatment with 6 N HCl affects the noble gas budget. Not only up to 38% loss of some isotopes occurs, but also incorporation of air compromises krypton and xenon. The effect is not observed in 0.3 N HNO_3 [8] and has also not been observed in earlier analyses of different splits of the etched material [2]. From these observations and our study of mineral separates we conclude that Kr and Xe in a first step may have been incorporated into the rock due to the iddingsite formation. An impact shock event redistributed parts of it—together with other isotopes such as ^{4}He—into neighboring phases. As a result of the weak shock it resides near grain boundaries in the case of the nakhlites and is removed by HCl etching. Fractionated air adsorbs onto these etched surfaces [10].

Acknowledgements: We thank Jörg Fritz for the mineral separation and Niels Hoppe for parts of the data reduction.

References: [1] Treiman A. H. 2005. *Chemie der Erde* 65:203–270. [2] Ott U. et al. 1988. *Meteoritics* 23:295–296. [3] Ott U. 1988. *Geochimica et Cosmochimica Acta* 52:1937–1948. [4] Murty S. V. S. et al. 1999. *Meteoritics & Planetary Science* 34:A84–85. [5] Mathew K. J. and Marti K. 2002. *Earth and Planetary Science Letters* 199:2–20. [6] Bart G. D. et al. 2001. Abstract #1363. 32nd LPSC. [7] Gilmour J. D. et al. 1999. *Earth and Planetary Science Letters* 166:139–147. [8] Gilmour J. D. et al. 2001. *Geochimica et Cosmochimica Acta* 65:343–354. [9] Schwenzer S. P. and Ott U. 2006. Abstract #1614. 37th LPSC. [10] Herrmann S. et al. 2006. *Meteoritics & Planetary Science* 41:A75.

5033

CHARACTERIZATION OF Fe-Ni-BEARING METEORITES BY SYNCHROTRON X-RAY DIFFRACTION

R. B. Scorzelli[1], R. R de Avillez[2], M. Duttine[1], and P. Munayco[1]. [1]Centro Brasileiro de Pesquisas Físicas, Rua Xavier Sigaud, 150-22290-180 Rio de Janeiro, RJ, Brazil. [2]Departamento de Ciência dos Materiais e Metalurgia, Pontifícia Universidade Católica, Rua Marquês de São Vicente, 225-2453-900, Rio de Janeiro, RJ, Brazil.

Fe-Ni-bearing meteorites contain very unique minerals due to their formation at very slow cooling rates. Some of these minerals have similar lattice parameters, only differing in the formation of superlattice patterns or in their composition. This differentiation is hard to achieve with conventional X-ray diffraction equipment and commonly used exposure times. In particular, the co-existence of the ordered Fe-Ni phase, tetrataenite (L_{10}) with disordered paramagnetic Fe-rich phase, antitaenite, previously proposed based on Mössbauer evidence [1], but never unambiguously observed by a diffraction method.

This paper reports the results of synchrotron X-ray diffraction investigation of iron meteorites carried out at the Laboratório Nacional de Luz Sincrotron (Campinas, Brazil). The goniometer was used in Bragg-Brentano geometry, with divergence and scattering slits (1.5 mm) and a 1 mm wide receiving slit. The X-ray wavelength was chosen to be 0.174565 nm (7102.5 ± 2.5 eV), a value which is near the minimum scattering power of Fe, to increase the scattering power difference between iron and nickel. The LaB6 NIST standard (660a) was used to check the angular position and to evaluate the instrumental profile. X-ray diffraction data were analyzed using the TOPAS 3.0 Rietveld program [2] and the fundamental parameters approach.

The results for the Santa Catharina meteorite confirmed for the first time the presence of a disordered face centered cubic phase (FCC), space group Fm-3m, with stoichiometry $Fe_{0.6665}Ni_{0.3335}$ and lattice parameter of 0.3588 nm. This phase agrees with the previously proposed paramagnetic antitaenite [1]. The other two Fe-Ni phases were an ordered phase and iron-deficient tetrataenite ($Fe_{0.4356}Ni_{0.5644}$) and a disordered phase, face centered cubic, with almost the same composition as the ordered phase ($Fe_{0.4385}Ni_{0.5615}$). The relative amounts of these phases are 44.6 wt% tetrataenite, 48.9 wt% antitaenite and 6.5 wt% disordered FCC phase. Results for other meteorites will also be reported.

References: [1] Rancourt D. G. and Scorzelli R. B. 1995. *Journal of Magnetism and Magnetic Materials* 150:30–36. [2] TOPAS 3.0 Technical Reference Manual. 2005. Bruker AXS, Karlsruhe.

5144

UNDERSTANDING DIVERSE SHOCK AND BRECCIATION HISTORIES OF BASALTIC AND OTHER METEORITES

Edward R. D. Scott[1] and William F. Bottke[2]. [1]HIGP, University of Hawai'i at Manoa, Honolulu, HI 96822, USA. E-mail: escott@hawaii.edu. [2]Southwest Research Institute. 1050 Walnut Street, Suite 400, Boulder, CO 80302, USA.

Introduction: Two major types of meteoritic basalts, eucrites and angrites, have remarkably different textures. Eucrites are mostly breccias, commonly shocked and metamorphosed. By contrast, the 8 angrites are unbrecciated, unshocked and largely unmetamorphosed [1]. Ordinary chondrites and aubrites, like eucrites, are commonly brecciated, shocked, and metamorphosed, whereas acapulcoite, lodranite, brachinite and CO3 chondrite breccias and shocked samples are rare. What caused this textural dichotomy?

Parent Bodies of Large Meteorite Groups: Many large meteorite groups are linked to families in the inner asteroid belt that formed <2 Ga (e.g., the CM, L, and HED meteorites are connected by a collisional cascade to the Baptistina, Flora, and Vesta families [2, 3]). These families are not only dynamically favored to produce meteorites but they also possess an enormous reservoir of fragments, such that collisions on family members tend to produce many more meteoroids than smaller asteroid groups residing in the same region of space.

Dating Shock and Breccia Formation: The surface area of family asteroids >3 km across can be 100× greater than that of the original body, implying that impact processing is more efficient on small bodies. However, several features suggest that some breccias/shocked rocks formed on large bodies [4–7]. Given that asteroidal regolith breccias are consolidated at much greater depths than lunar regolith breccias [8], and that family-forming events cause mixing between material near the parent body's exterior and fragments from the interior, many shocked/brecciated rocks in a meteorite group should be a combination of old/new material. Accordingly, these rocks are telling us about i) life on the parent body, ii) deformation and mixing during the family-forming event, and iii) subsequent impacts on the meteorite-precursor bodies.

Discussion: There are few angrites so the lack of breccias could be a fluke (i.e., perhaps their precursor just happened to be coherent). But it could also mean that they do not come from a traditional family-forming event. We propose that the angrite parent body was Ceres-sized or larger (cf. [10, 11]) and experienced a "hit-and-run" collision with a protoplanet [12]. An ~10 km body produced by this event was then dynamically embedded in the main belt 4.5 Ga [13]. We argue that the small size of the precursor limited the amount of shocked/brecciated rocks it could retain, so that its disruption mainly produced coherent rocks.

References: [1] Mittlefehldt D. W. et al. 2002. *Meteoritics & Planetary Science* 37:345-369. [2] Bottke W. F. et al. *Nature.* Forthcoming. [3] Nesvorny D. et al. *Icarus.* Forthcoming. [4] Bogard D. D. 1995. *Meteoritics* 30:244–268. [5] Keil K. 1982. LPI Tech. Report 82-02, pp. 65–83. [6] Korochantseva E. V. et al. 2007. *Meteoritics & Planetary Science* 42: 113–130. [7] Hohenberg C. M. et al. 1990. *Geochimica et Cosmochimica Acta* 54: 2133–2140. [8] Bischoff A. et al. 2006. In *Meteorites and the early solar system II*, pp. 679–712. The Univ. Arizona Press. [9] Wilson L. and Keil K. 1991. *Earth and Planetary Science Letters* 104:505–512. [10] Irving A. J. et al. 2006. *Eos* 87:P51E–1245. [11] Busemann H. et al. 2006. *Geochimica et Cosmochimica Acta* 70:5403–5425. [12] Asphaug E. et al. 2006. *Nature* 439:155–160. [13] Bottke W. F. et al. 2006. *Nature* 439:821–824.

5168

X-RAY DIFFRACTION AND TRANSMISSION ELECTRON MICROSCOPIC STUDIES OF NEW-PCP FROM ACFER 094 CARBONACEOUS CHONDRITE

Y. Seto, N. Sakamoto, K. Fujino, and H. Yurimoto. Department of Natural History Sci., Hokkaido University, Sapporo 060-0810, Japan.

Introduction: Recently, a unique Fe-O-S bearing material called new-PCP (poorly characterized phase) has been found from matrix of an ungrouped carbonaceous chondrite Acfer 094 [1]. The new-PCP has extremely enriched in heavy oxygen isotopes of $\delta^{17}O$ and $\delta^{18}O$ of +180‰ relative to SMOW. The extremely heavy oxygen-isotopic composition may represent of early solar system water and of ^{16}O-poor reservoir of the solar system [2]. However, the chemical compositions of the grain have not corresponded to any minerals reported. Here we conducted Synchrotron-radiation X-ray diffraction (SRXRD) and transmission electron microscopic (TEM) studies of the new-PCP to clarify the mineralogy.

Experimental: A new-PCP grain of 20 × 7 × 5 μm^3 in size in a polished thin section of Acfer 094 was selected for this study. Two specimens were extracted from this grain by focused ion beam technique using SIINT-SMI3050TB system. A block of 10 × 7 × 4 μm^3 and a thin film of 8 μm × 4 μm × 50 nm were prepared for SRXRD and TEM studies, respectively. The SRXRD measurements were carried out in BL13A, Photon Factory, KEK, Japan. Angle dispersive XRD pattern of monochromatized 0.42621 Å beam was collected using a flat imaging plate (IP, Rigaku R-Axis4). An exposure time of over 10 hours was needed to obtain a clear diffraction pattern. Three types of TEM were used in this study: JEOL JEM-2010 for microstructural observations and electron diffraction analysis, HITACHI HD2000+EDAX Genesis (STEM+EDS) for nano-resolution elemental map analysis, and JEOL JEM-2001F+Gatan GIF Tridiem for electron loss spectroscopy (EELS), microstructural observations and electron diffraction analysis. Accelerating voltage of TEM studies were all 200 kV.

Results and Discussion: The SRXRD pattern shows clear Debye-Scherrer rings indicating that the new-PCP is an aggregate of small crystals consisting of magnetite Fe_3O_4 (*Fd3m*, a = 8.3870[5] Å) and pentlandite $(Fe,Ni)_9S_8$ (*Fm3m*, a = 10.156[2] Å). A TEM study shows that the aggregate consists of 100–300 nm fuzzy grains. An STEM-EDX mapping shows that the fuzzy structure in the grain corresponds to an intergrowth of magnetite and pentlandite with vermiculate texture. The intergrown magnetite is 10–30 nm wide and 100–200 nm long. The interstices of magnetite are filled with pentlandite. The electron diffraction patterns of magnetite show that the main spots are arranged in the manner of face-centered cubic symmetry indicating magnetite. There are weak extra spots between the main spots, indicating three-fold superstructure along all axes. The periodicity corresponding to the superstructure also appears in the high-resolution TEM image. On the other hand, electron diffractions from pentlandite are weak. Because SRXRD shows clear diffraction peaks of pentlandite, the pentlandite might be decomposed by the high-energy electron radiation.

These observations support that new-PCP is a decomposed material from Fe-Ni metal and Fe-Ni sulfide by oxidization and sulfurization in low temperature [2].

References: [1] Sakamoto N. et al. 2007. Abstract #1644. 38th Lunar and Planetary Science Conference. [2] Sakamoto N. et al. 2007. This issue.

5021

CHAOS DOWNUNDER: THE SHOEMAKERS' PIONEERING SEARCH FOR AUSTRALIAN CRATERS

C. S. Shoemaker[1], J. F. McHone[2], and F. A. Macdonald[3]. [1]U.S. Geological Survey, Flagstaff, Arizona 86001, USA. E-mail: cshoemaker@usgs.gov. [2]Arizona State University, USA. [3]Harvard University, USA.

From 1984 to 1997, Gene and Carolyn Shoemaker spent 12 field seasons in remote reaches of Australia. They were studying an area of planetary science that melds astronomy and geology, the chaos of collision. Impact cratering is fundamental throughout our solar system; Gene wished to evaluate populations and fluxes of Earth-crossing asteroids and comets through a telescopic search for these bodies and a geologic study of impact sites here on Earth. Newly discovered asteroids and comets, data previously established on lunar craters, and recognition of impact craters and debris layers on Earth allowed a reassessment of our bombardment history. Australia's stable and ancient land surface, its aridity, and its low relief make it a perfect place to preserve a geologic record of planetary impacts. Together the Shoemakers, with occasional help from others, explored the Outback, studying known impact structures and finding new ones. About ten were known when they first arrived, but ultimately they visited close to twenty, mapping geology, gravity, and magnetics in detail, and collecting meteorites and tektites—anything not previously done.

The Shoemakers' studies in Australia bordered on primitive in comparison with today's techniques. Circular features for investigation were identified with early Landsat spacecraft images, topographic maps, conversation and letters, and even road maps with labeled meteorite craters. When possible, aerial photography of specific areas and regional maps with written geology reports were obtained. Sometimes there were no photos nor topographic maps. In this situation they used a rod, staff, and alidade on a tripod. The Global Positioning System (GPS) was not available in the early years, so they often used a theodolite and triangulated from stars to obtain their exact location. Notebooks were used to keep records, as computers could easily suffer from the dust in their fieldwork. A satellite phone became available in their last two years, but seldom were they in touch with the rest of the world. Routine orbital images were in the future, as were Web sites where they could be viewed. Today's electronic devices were not available to the Shoemakers. They traveled thousands of Outback kilometers in a Toyota Hilux trayback. Fuel drums, camping supplies, food and water, professional library and materials, extra tools and tires, and emergency equipment all were loaded in back. They might not see another person for weeks at a time but shared the outdoors with kangaroos and wallabies, dingoes, camels, and a beautiful assortment of Australian birds. Adventures and misadventures were the norm as the Shoemakers crossed and re-crossed the Outback, working their way on small dirt tracks, or no tracks, to reach their crater destination; every day brought something new.

During most years when they made their trips, crater funding was not readily available; only a handful of scientists were seriously studying impacts. The Shoemakers wanted to show their colleagues the many different Australian craters. Their desire came to fruition with the Meteoritical Society's 1990 meeting in Perth, and its crater expedition field trip. Some 50 international participants visited 9 remotely located sites. This adventure helped lay the foundation for future exploration and today more than thirty confirmed and suspected sites [1] are known Downunder.

References: [1] *Australian Journal of Earth Science* 52(4/5). Shoemaker Memorial Issue on the Australian Impact Record, 2005.

5071

REFRACTORY INCLUSIONS IN AN UNUSUAL CARBONACEOUS CHONDRITE, NWA 1465

S. B. Simon[1], L. Grossman[1, 2], and M. Langstaff[1]. [1]Department of Geophysical Sci., 5734 S. Ellis Ave., USA. [2]The Enrico Fermi Institute, The University of Chicago, Chicago, IL 60637, USA. E-mail: sbs8@uchicago.edu.

Introduction: NWA 1465 is classified as an anomalous CV3 [1]. It is petrologically similar to the reduced subgroup of CV3s but its bulk oxygen isotopic composition plots on the CR line [2]. We investigated the refractory inclusion population found in a polished thin section of the meteorite. The section, made from the fragment shown in [2] and provided by S. Kambach, a collector, has a 6 mm long zone rich in blue refractory inclusions visible to the naked eye. This area alone contains over 20 inclusions, and we have identified 120 CAIs, from ~30 to ~600 μm across, in 120 mm^2 of the section. Except for four small, completely rimmed CAIs, all are unrimmed or partially rimmed fragments. The meteorite exhibits a foliation like that of Leoville.

Observations: Eighty-one of the inclusion fragments we found are melilite-rich; 14 of these contain hibonite. As in the reduced CV3s and the CRs, melilite is virtually unaltered, but unlike CRs, no grossite-bearing inclusions are present. The most common (32 of 120) of the 16 assemblages in the NWA inclusion fragments is melilite (mel)-spinel (sp), followed by sp-pyroxene (23); mel-sp-perovskite (pv) (18); mel-sp-anorthite (11); and, notably, 7 mel-sp-pv-hibonite (hib)-fassaite (fass) inclusions, in which the latter three Ti-rich phases are commonly intimately intergrown, and some of the fass reaches the most Ti-rich (~21 wt% TiO_2 + Ti_2O_3), MgO-poor (~2 wt%) compositions that we are aware of. It has $^{27}Al/^{24}Mg$ as high as 17, Al/Si > 1, and Ti^{3+}/Ti_{tot} mostly ~0.55 to ~0.75, coexisting with mel ($Åk_5$). In one of these samples fass has 1–2 wt% Sc_2O_3. Hibonite occurs as small, Ti-rich (7–9 wt% TiO_2) laths enclosed in gehlenitic mel. Ti-rich fass also occurs in some mel-rich, hib-free inclusions, both between mel grains and poikilitically enclosing mel ($Åk_{5–10}$). The other fass occurrence is a 100 × 200 μm sp-poor clast in an otherwise sp-, hib-, mel-rich inclusion fragment. In a unique inclusion, melt (now glass) with 80–85 wt% SiO_2 invaded a sp-mel ($Åk_{70–75}$)-diopside assemblage. Twelve mel-rich fragments contain interstitial anorthite that appears to be primary.

Discussion: A few of the inclusion fragments may have been derived from type Bs but most are consistent with derivation from compact type As (CTAs), albeit atypical ones. Some unusual or unique assemblages found: 1) fassaite in contact with hibonite and perovskite. In such occurrences, fassaite probably exhibits the maximum extent of Ti substitution that can occur in meteoritic pyroxene. Some of the fass compositions found in the present study are unlike those seen in either typical types A or B inclusions. The closest compositions to these were found in one grain in a rare, hib-bearing CTA from Allende [3], but even these are poorer in total Ti oxides by ≥3 wt% than the most Ti-rich composition in NWA 1465. The present fass represents the most extreme degree of crystal-liquid fractionation so far seen in a CTA. 2) Primary anorthite with mel + sp but no fass. 3) SiO_2-rich glass in contact with mel. This object is puzzling, as the SiO_2-rich liquid should have either evaporated away or reacted with mel to form diopside, which is not present at the contact.

References: [1] Russell S. et al. 2004. *Meteoritics & Planetary Science* 39:A215. [2] Greshake A. et al. 2003. Abstract #1560. 34th Lunar and Planetary Sci. Conf. [3] Simon S. B. et al. 2001. *Meteoritics & Planetary Science* 36:331.

5119

ORIGIN OF THE MARTIAN SATELLITES PHOBOS AND DEIMOS

S. Fred Singer. University of Virginia/SEPP, USA. E-mail: singer@sepp.org.

Introduction: The origin of the Martian satellites presents a puzzle of long standing. Conventional hypotheses either violate physical laws or have difficulty accounting for the observed orbits. Both satellites have near-circular and near-equatorial orbits. Phobos' orbit has been observed to shrink (since its discovery in 1877), indicating the influence of tidal perturbations. Extrapolating their orbits backward in time yields nearly identical circular orbits at the synchronous limit, followed by parabolic orbits suggesting capture [1]. But there is no obvious mechanism for energy dissipation to capture of these small bodies; nor should such capture yield equatorial orbits.

Contemporaneous formation with the planet Mars is contradicted by dynamics. The obliquity of Mars' axis, about 25°, indicates formation by stochastic impacts of large planetesimals, at least in the last stages of Mars accumulation. But the equatorial orbits of the satellites would require that the obliquity of Mars changed quasi-adiabatically, i.e., very slowly compared to the orbital periods of the moons. This suggests that Mars acquired the moons only after its formation was completed, but it leaves the mechanism uncertain.

With capture and contemporaneous formation both unlikely, we propose a third possibility: Capture of a large Mars-Moon, during or shortly after the formation of the planet, with Phobos and Deimos as its surviving remnants. Arguments are given in favor of such a hypothesis and illustrative examples are shown.

Arguments for a Capture Origin:

1. Capture of a large body is dynamically easier, since the greater tidal friction is likely to dissipate sufficient kinetic energy to turn an initially hyperbolic orbit into a bound elliptic orbit.
2. A large Mars-Moon (M-M) would change the angular momentum of Mars in the capture process. Analogous to the Earth-Moon case, our calculations show that M-M's initial orbit would be inclined and even retrograde, but its final orbit would be prograde, near-equatorial, and at the synchronous limit.
3. Capture of M-M from a retrograde orbit would reduce the angular momentum of Mars, dissipate kinetic energy of rotation, and contribute internal heat energy required for melting the planet.
4. The close passage of the Mars-Moon within the Roche limit would have fractured it. Tidal friction would soon drive the largest pieces into Mars, with the smallest pieces remaining as Phobos and Deimos. Phobos is spiraling into Mars now and will disappear in a few million years; but Deimos, beyond the synchronous orbit limit, will survive against tidal friction.
5. The present orbit of Phobos makes it likely that more massive fragments existed in the past and have spiraled into Mars because of by tidal perturbation—lifetime being inversely proportional to mass. ("If the dinosaurs had had better telescopes, they would have observed them.")
6. The present orbit of Deimos, just beyond the synchronous limit, provides an important clue about its origin.
7. There are no ready alternatives to explain the origin of the Martian moons.

References: [1] S. F. Singer. 1968. *Geophysical Journal of the Royal Astronomical Society* 15:205–226. Origin of the Moon by Capture. In *The Moon*, edited by Hartmann W. et al. 1986. Houston: LPI. pp. 471–485.

5108

STATUS OF CROSS SECTION MEASUREMENTS FOR NEUTRON-INDUCED REACTIONS NEEDED TO UNDERSTAND COSMIC RAY INTERACTIONS

J. M. Sisterson. Francis H. Burr Proton Therapy Center, Massachusetts General Hospital, 30 Fruit Street, Boston, MA 02114, USA. E-mail: jsisterson@partners.org.

Good cross section measurements for both proton- and neutron-induced reactions are essential input to theoretical models used to analyze the cosmogenic nuclide archives in meteorites, lunar rocks, or the Earth's surface. Secondary neutrons produced in primary cosmic-ray (mostly protons) interactions contribute significantly to these archives, particularly at depth in an object. Most relevant cross sections for proton-induced reactions are well measured but there are only a few cross section measurements for neutron-induced reactions at energies >30 MeV.

Two adjunct techniques are used to measure the needed cross sections for neutron-induced reactions. Quasi-monoenergetic neutrons (70–155 MeV) are used at iThemba LABS, South Africa, and this technique will be adapted for planned measurements using 200, 300, and 400 MeV neutrons at the Research Center for Nuclear Physics, Osaka, Japan, by K. Nishiizumi et al. in October 2007 [1]. White neutron beams with energies from ~0.1–750 MeV are used to measure energy integrated (average) cross sections [2–4] at the Los Alamos Neutron Science Center, Los Alamos (LANSCE). Completed irradiations at iTL and LANSCE are listed in Table 1. Relatively short-lived radionuclides are measured in these targets using gamma ray spectroscopy. The radionuclides or stable isotopes produced will be measured using accelerator mass spectrometry or mass spectrometry.

Table 1. Targets irradiated/ to produce this cosmogenic nuclide.

Nuclide	At LANSCE	At iTL
^{22}Na	SiO_2, Si, Al, Mg	SiO_2, Si, Al
^{14}C	SiO_2, Si, Al	SiO_2
^{41}Ca	$CaCO_3$, Fe, Ni	$CaCO_3$, Fe, Ni
^{36}Cl	KNO_3, $CaCO_3$, Fe, Ni	K_2CO_3, $CaCO_3$, Fe, Ni
^{26}Al	Si, Al	Si, Al
^{10}Be	SiO_2	SiO_2
^{53}Mn	$CaCO_3$, Fe, Ni	$CaCO_3$, Fe, Ni
^{21}Ne	SiO_2, Mg, Al, Si	

At LANSCE, two different energy spectra are used in the average cross section measurements. Two or six inches of polyethylene placed well upstream remove almost all neutrons with energies <0.1 MeV and varying amounts of neutrons with higher energies. Thus one spectrum was harder than the other and the dependence of the cross section value for a particular reaction on the energy spectrum could be investigated. For these particular neutron spectra, all the measured cross sections for the same reaction agreed within at most a factor of two.

Even though the average cross section measured does depend on the exact nature of the neutron energy spectrum, this study shows that these average cross sections are useful indicators of the range of values that a particular cross section might assume at high energies.

References: [1] Nishiizumi K. 2007. Personal communication. [2] Sisterson J. M. and Ullmann J. 2005. *Nuclear Instruments and Methods in Physics Research B* 234:419–432. [3] Sisterson J. M. et al. 2005. *Nuclear Instruments and Methods in Physics Research B* 240:617–624. [4] Sisterson J. M. and Chadwick M. B. 2006. *Nuclear Instruments and Methods in Physics Research B* 245:371–378.

5284

TIME VARIABILITY OF THE INNER DUST ZONE IN PRE-MAIN SEQUENCE DISK SYSTEMS

M. L. Sitko[1, 2], W. J. Carpenter[1], R. L. Kimes[1], J. L. Wilde[1], D. K. Lynch[3], R. W. Russell[3], R. J. Rudy[2], S. M. Mazuk[3], C. C. Venturini[3], R. C. Puetter[4], C. A. Grady[5, 6], S. M. Brafford[7], and R. B. Perry[8]. [1]Department of Physics, University of Cincinnati, Cincinnati OH 45221, USA. E-mail: sitkoml@ucmail.uc.edu. [2]Space Science Institute, 4750 Walnut St., Suite 205, Boulder, CO 80301, USA. [3]The Aerospace Corporation, Los Angeles, CA 90009, USA. [4]Center for Astrophysics and Space Science, University of California, San Diego, CA 92093, USA. [5]Eureka Scientific, Inc., Oakland, CA 94602, USA. [6]Exoplanets and Stellar Astrophysics Laboratory, Code 667, Goddard Space Flight Center, Greenbelt, MD 20771, USA. [7]1368 Gumbert Dr., Amelia, OH 45102, USA. [8]NASA Langley Research Center, Hampton, VA 23681, USA.

Introduction: The dust sublimation zone is the region of pre-main sequence (PMS) disks where dust grains most easily anneal, sublime, and condense out of the gas. Because of this, it is a location where crystalline material may be produced and redistributed throughout the rest of the disk. A 10-year program to monitor the thermal emission of the grains located in this region indicates that it can undergo large changes in emitted flux. Here, we report the nature of those changes, and the implications for the production of larger crystalline grains.

Observations: The bulk of the observations were carried out with the Aerospace Corporation's Broadband Array Spectrograph (BASS) on NASA's Infrared Telescope Facility (IRTF) between 1996 and 2006. BASS detects light in the 2.9–13.5 micron wavelength range, with a wavelength-dependent spectral resolution of 30–125. Additional spectra from 0.4–2.5 microns, at a spectral resolution of 1000, were also obtained on a few occasions using The Aerospace Corporation's Visible and Near-Infrared Imaging Spectrograph (VNIRIS).

Results: Changes in the thermal emission between 3 and 13.5 microns were observed in a number of PMS disk systems, such as HD 31648 and HD 163296. This emission is consistent with it being produced at the location of the disk where, with increasing distance from the star, there is a transition from a disk of gas to one of gas+dust. The variability requires changes in the amount of exposure to radiation this zone receives from the star. In a third object, DG Tau, the outbursts were accompanied by increased emission on the 10 micron silicate band on one occasion, while on another occasion it was in absorption. This requires lofting of the material above the disk into the line of sight.

Discussion: Cyclic variations in the heating of the dust sublimation zone will lead to the annealing of large grains, the sublimation of smaller grains, followed by recondensation as the zone enters a cooling phase. Lofting of dust above the disk plane and outward acceleration by stellar winds and radiation pressure can redistribute the processed material to cooler regions of the disk. This processing is consistent with the detection of the preferential concentration of large crystalline grains in the inner few AU of PMS disks [1].

References: [1] Van Boekel R. et al. 2004. *Nature* 432:479–482.

5153

ACHONDRITIC FRAGMENTS IN ORDINARY CHONDRITE BRECCIAS

A. K. Sokol[1, 2], K. Mezger[2], M. Chaussidon[3], and A. Bischoff[1]. [1]Institut für Planetologie, Wilhelm-Klemm-Str. 10, 48149 Münster, Germany. E-mail: sokola@uni-muenster.de. [2]Institut für Mineralogie, Corrensstr. 24, 48149 Münster, Germany. [3]CRPG-CNRS, Vandoeuvre-lès-Nancy, France.

Introduction: The chondrite regolith breccia Adzhi-Bogdo (LL3–6) contains several lithic fragments with igneous textures which are best described as akali-granitoids [1]. In the breccia Study Butte (H3–6), one igneous-textured fragment with an andesitic bulk composition was observed [2]. Since these fragments most likely formed by melting and magmatic differentiation on a parent body, their occurrence indicates mixing of achondritic fragments with chondritic components. Al-Mg isotope data for these igneous-textured clasts reveal no evidence for radiogenic ^{26}Mg and indicate that the formation of these igneous clasts, the incorporation into the parent body regolith, and the lithification must have occurred late, after almost all ^{26}Al had decayed [3].

To determine whether the fragments formed on their present parent bodies or whether they represent fragments of an achondritic projectile, oxygen isotope ratios were measured.

Results: In situ measurements of plagioclase, quartz, and pyroxene in the fragments are presented in Fig. 1. All fragments fall in the range of ordinary chondrites.

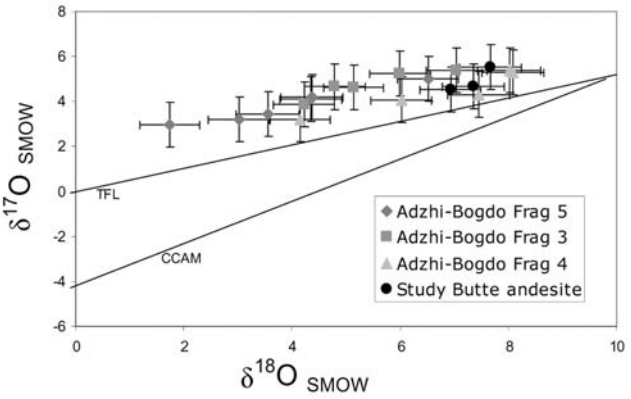

Fig. 1.

Discussion: The results imply that the fragments derive from an ordinary chondrite precursor or formed on a parent body within the same oxygen isotope region of the solar nebula as ordinary chondrites. Thus, the granitic fragments may have formed on the same parent body as the surrounding host-rock material. The andesite data falls in the range of LL chondrite although its host rock is a H3–6 chondrite. Inclusions of ordinary chondrites within other ordinary chondrites have been described by Bischoff et al. [5]. The present results may indicate that melt formation and extreme differentiation on ordinary chondrite bodies occurred in the early stage of solar system formation. The relatively large range in $\delta^{18}O$ within the clasts is mass dependent and may show isotope fractionation on the parent body during the differentiation process.

References: [1] Bischoff A. et al. 1993. *Meteoritics* 28:570–578. [2] Fredriksson K. et al. 1989. *Zeitschrift für Naturforschung* 44a:945–962. [3] Sokol A. K. et al. *Meteoritics & Planetary Science*. Forthcoming. [5] Bischoff et al. 2006. In *Meteorites and the early solar system II*, edited by D. S. Lauretta and H. Y. McSween, Jr. Tucson: The University of Arizona. pp. 679–712.

5197

CENTRAL UPLIFT STRUCTURE REVEALED BY DEEP DRILLING AT MANICOUAGAN

J. G. Spray and L. M. Thompson. Planetary and Space Science Centre, University of New Brunswick, 2 Bailey Drive, Fredericton, New Brunswick E3B 5A3, Canada. E-mail: jgs@unb.ca.

Introduction: Over the last decade, an intensive mineral exploration program on the main island of the 100 km in diameter Manicouagan impact structure of Quebec has resulted in the production of over 17 km of drill core, of which ~10 km are now held at the Planetary and Space Science Centre, University of New Brunswick. Critically, several of these holes are more than 1.5 km in length. This provides an unprecedented window into the third dimension of a complex impact structure, with Manicouagan now ranking as one of the most comprehensively drilled craters on Earth. (Most of the core from the more extensively drilled Popigai crater in Siberia has been effectively lost [1]. Moreover, this crater was drilled to relatively shallow depths.) Coupled with renewed field activities, we are able to determine the structure of the central uplift at Manicouagan, which forms a topographic high rising above the impact melt sheet. Here we report initial results based on field work, drill core geology, and melt sheet geochemistry.

Central Uplift Structure: The central uplift forms a 22 km long, 19 km wide horseshoe-shaped topographic high (incomplete ring), which rises above the melt sheet to its highest point in the north (Mont de Babel), with the open end of the horseshoe occurring to the south. The horseshoe consists of a series of fault-bounded blocks, which comprise anorthositic, charnockitic, and metagabbroic lithologies of the ~1 Ga Grenville target terrain. These rocks are variably shocked. Maskelynite is common in the anorthosites. Drilling reveals that the center of the horseshoe exhibits marked footwall relief beneath the melt sheet in the form of a fault-bounded, 1 km wide, 7 km long graben that extends south of Mont de Babel, which is up to 1.4 km deep.

Impact Melt Sheet Thickness and Compositional Trends: The impact melt sheet at Manicouagan is well exposed in coastal sections and certain inland locations. Previous work indicated that the impact melt sheet is currently no thicker than ~300 m [2, 3]. The recent drilling evidence shows that the melt sheet is, in places, more than 1 km thick, far in excess of previously suggested values. Preliminary interpretation of the geochemistry of over 60 samples indicates that the deeper levels of the graben may have facilitated differentiation, in contrast to the <500 m thick main mass sections, which are more homogeneous. The thickest section of melt sheet exhibits two geochemical units: 1) an upper layer characterized by relatively high SiO_2 and K_2O (~500 m), and 2) a lower layer with relatively low SiO_2 and K_2O and higher CaO, MgO, and FeO (~900 m), the basal 400 m of which is increasingly clast-bearing. The fact that the thick melt section has undergone differentiation, in contrast to sections beyond the central horseshoe uplift, indicates that the graben formed prior to melt crystallization. This means that faulting was syn- to immediately post-impact and that the structure of the central region at Manicouagan is controlled by large-displacement fault systems.

References: [1] Whitehead J., Grieve R. A. F., and Spray J. G. 2002. *Meteoritics & Planetary Science* 37:623–647. [2] Currie K. L. 1972. Geological Survey of Canada, Department of Energy, Mines and Resources, Bulletin 198. 153 p. [3] R. J. Floran et al. 1978. *Journal of Geophysical Research* 83:2737–2759.

5126

HIGH-PRECISION ND ISOTOPIC MEASUREMENTS USING ISOPROBE-T THERMAL IONIZATION MASS SPECTROMETER

G. Srinivasan and A. Das. Department of Geology, University of Toronto, Toronto, ON M5S 3B1, Canada. E-mail: srini@geology.utoronto.ca.

Introduction: The Isoprobe-T Mass Spectrometer at the University of Toronto is a newly funded thermal ionization mass spectrometer for isotopic studies in planetary sciences by Canada Foundation for Innovation. This instrument is currently being established for high-precision measurements of Nd isotopic composition. The present study utilized the multi-collector detection system, which consists of nine movable detectors (Faraday cups), three on low-mass side of the beam axis designated [L3], [L2], and [Ax] (the latter capable of being positioned on the axis), and six on the high-mass side designated [H1] to [H6]. The Nd isotopic measurements were carried out in the 4 sequence multi-dynamic mode in order to minimize measurement uncertainties due to variations in relative detector efficiencies. Nd with 7 isotopes is measured as a metal in a triple filament geometry using zone refined Re filaments. Nearly ~750 nanograms of Nd were loaded on the outer filament following the procedure described in [1, 2]. A typical ^{142}Nd beam of 4 volts was obtained on a 10^{11} ohm resistor. A typical measurement consists of 400 cycles and each cycle consists of 4 sequences. The measurement time for each baseline corrected sequence is 10 seconds.

We measured Nd isotopic composition of Caltech Beta standard [3] and a Alfa Aesar ICPMS Nd standard solution (Lot #012312A, Stock #14431). The results of measurements are quoted with respect to the Nd isotopic average values obtained for this set of measurements for the nNdβ standard [2, 3].

Table 1. Nd isotopic composition of nNdβ [3].

^{142}Nd	μ^{142}	μ^{143}	μ^{145}	μ^{148}	μ^{150}
5.8	−1.2 ± 4.0	−4.5 ± 4.0	−12.0 ± 4.0	−10.0 ± 8.0	−39.9 ± 10.0
1.3	10.3 ± 12.0	−9.7 ± 10.0	−7.1 ± 8.0	0.6 ± 28.0	2.2 ± 36.0
5.4	−0.5 ± 10.0	7.6 ± 6.0	12.9 ± 4.0	26.7 ± 16.0	24.0 ± 20.0
5.9	−3.9 ± 4.0	−0.4 ± 4.0	0.8 ± 6.0	15.1 ± 8.0	32.0 ± 10.0
5.5	−5.0 ± 4.0	−2.0 ± 2.0	6.7 ± 2.0	7.0 ± 6.0	33.5 ± 10.0
6.3	−2.2 ± 2.0	2.8 ± 2.0	3.6 ± 2.0	−7.0 ± .0	−41.6 ± 8.0
4.7	5.9 ± 4.0	7.0 ± 2.0	0.0 ± 2.0	−7.5 ± 8.0	−3.0 ± 10.0

The ^{142}Nd values are the measured signal strength in volts. The isotopic ratios are reported as variations in parts per million with respect to the average values obtained for these analyses. Errors reported in the table are 2σ(mean). Fractionation factor is with respect to $^{146}Nd/^{144}Nd$ ratio. The mean values obtained from nNdβ standard are reported $^{142}Nd/^{144}Nd = 1.141844 \pm 0.000006$; $^{143}Nd/^{144}Nd = 0.511890 \pm 0.000003$; $^{145}Nd/^{144}Nd = 0.348404 \pm 0.000003$; $^{148}Nd/^{144}Nd = 0.241569 \pm 0.000003$; $^{150}Nd/^{144}Nd = 0.236506 \pm 0.000008$ (1σ). The μ^{150} values were also measured only once in each cycle. From these preliminary measurements we demonstrate that Nd isotopic measurements for all isotopes excluding 148 and 150 have an external reproducibility of better than 15 ppm.

References: [1] Sharma M., Papanastassiou D., and Wasserburg G. J. 1996. *Geochimica et Cosmochimica Acta* 60:2037–2047. [2] Sharma M. and Chen C. 2004. *Precambrian Research* 135:315–329. [3] Wasserburg G. J. et al. 1981. *Geochimica et Cosmochimica Acta* 45:2311–2323.

5061

PRESOLAR Fe OXIDE FROM THE ACFER 094 CARBONACEOUS CHONDRITE

F. J. Stadermann, M. Bose, and C. Floss. Laboratory for Space Sciences and Physics Department, Washington University, St. Louis, MO 63130, USA. E-mail: fjs@wustl.edu.

Introduction: Acfer 094 is one of the most primitive carbonaceous chondrites and contains high abundances of presolar silicate grains (e.g., [1, 2]). However, little is known about the compositions of many of these grains. We are carrying out combined NanoSIMS and Auger Nanoprobe analyses of size-separated fractions of Acfer 094 silicate matrix material [3] to investigate the elemental and isotopic compositions of both silicate and oxide grains. We have identified presolar grains from Acfer 094 on the basis of their O-isotopic compositions and determined their elemental compositions [4]. Here we discuss a unique grain, 34C-10, that consists essentially only of Fe and O.

Experimental: After the presolar grains were located using NanoSIMS O-isotopic imaging, the sample mount was moved to the new PHI 700 Auger Nanoprobe at Washington University for in situ elemental measurements. Complete elemental spectra were obtained to determine compositions and high-resolution elemental maps were acquired for selected grains (cf. [4]).

Results: 34C-10 is a group 4 grain [5] that has normal $^{17}O/^{16}O$, but is enriched in ^{18}O ($^{17}O/^{16}O = 4.12 \pm 0.14 \times 10^{-4}$; $^{18}O/^{16}O = 2.68 \pm 0.04 \times 10^{-3}$). The grain is about 400 nm across with a roughly triangular shape, and appears to be an aggregate of several subgrains. Point spectra, as well as elemental maps, show that only Fe and O are present; small amounts of Mg were seen in some spectra, but no Si, Al, or Ca were detected. In order to evaluate the relative proportions of Fe and O, we compared the Auger spectra obtained on the grain with those from a magnetite standard. The results show that 34C-10 has a higher ratio of Fe to O than magnetite and is compositionally similar to wüstite (FeO).

Discussion: To our knowledge, this is the first observation of a presolar Fe-oxide grain. Wüstite and periclase (MgO) form the solid solution series magnesiowüstite ($Mg_xFe_{1-x}O$). Thermodynamic calculations show that magnesiowüstite can condense under nonequilibrium conditions and should be present in the outflows of O-rich AGB stars [6]. Moreover, this phase, specifically $Mg_{0.1}Fe_{0.9}O$, has been proposed as the carrier of the 19.5 μm emission feature observed in certain low-mass-loss AGB stars [7]. Group 4 grains have enigmatic origins with possible sources including formation in supernovae or high metallicity AGB stars. Fe isotopic measurements will be carried out to provide additional constraints on the origin of this grain.

Acknowledgements: We thank A. Nguyen for preparation of the Acfer 094 silicate grain separates.

References: [1] Nguyen A. et al. 2007. *The Astrophysical Journal* 656: 1223–1240. [2] Vollmer C. et al. 2006. Abstract #1284. 37th Lunar and Planetary Science Conference. [3] Nguyen A. 2006. Ph.D. thesis, Washington University. 194 p. [4] Bose M. et al. 2007. This issue. [5] Nittler L. et al. 1997. *The Astrophysical Journal* 483:475–495. [6] Ferrarotti A. S. and Gail H.-P. 2003. *Astronomy & Astrophysics* 398:1029–1039. [7] Posch Th. et al. 2002. *Astronomy & Astrophysics* 393:L7–L10.

5100

ELEMENTAL COMPOSITION OF COMET 81P/WILD-2 DERIVED FROM STARDUST SAMPLES

T. Stephan. Institut für Planetologie, Wilhelm-Klemm-Str. 10, 48149 Münster, Germany. E-mail: stephan@uni-muenster.de.

Introduction: Determining the elemental composition of 81P/Wild-2 is one of the prime objectives of analyzing cometary dust returned by the Stardust mission [1]. Samples were collected by two capture media, silica aerogel and Al foils. While aerogel was meant for sampling the cometary dust almost intact, on Al foils, impacting cometary dust particles formed hypervelocity craters with residual cometary matter [2].

First results on elemental composition were recently reported by [3], mainly focusing on data from entire particle tracks and data from Al foil craters. In the present study, the elemental compositions of various samples investigated during the preliminary examination phase are discussed comparatively to extract a comprehensive data set from various sources, and from there, conclusions are drawn on the Wild-2 nucleus composition.

The Available Data Set: For the present comparison, data obtained by three different techniques were used: 1) synchrotron-based X-ray microprobe analysis (SXRM) of entire particle tracks [3], 2) scanning electron microscopy using energy-dispersive X-ray analysis (SEM-EDX) of cometary residues associated with impact features on Al foils [3], and 3) time-of-flight secondary ion mass spectrometry (TOF-SIMS) of particles extracted from aerogel [4], of residual cometary matter in aerogel tracks [3, 5], as well as of impact residues on Al foils [3, 6].

Results: Figure 1 shows geometric mean values of element ratios from samples captured by aerogel and from impact residues on Al foils. Besides an enrichment of some volatile elements like Li, Cu, K, Ga, and Na that might be attributed to contamination of the capture media, most elements show within a factor of two abundances close to average solar system (CI) composition (Fig. 1). However, for impact residues on Al foils, a slight trend of increasing depletion with increasing volatility was observed (dotted line in Fig. 1), maybe indicative for a slight element fractionation during impact, while for samples captured by aerogel, no such trend is visible, except for a general depletion in S.

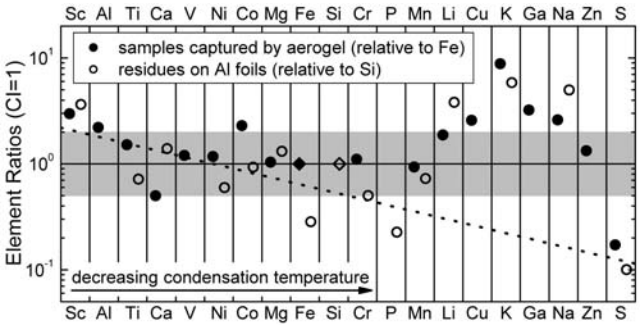

Fig. 1. Geometric mean values of element ratios normalized to CI chondritic element ratios.

Conclusions: Besides deviations that can be explained by the capture process, Wild-2 dust shows a rather CI-like composition.

References: [1] Brownlee D. et al. 2006. *Science* 314:1711–1716. [2] Hörz F. et al. 2006. *Science* 314:1716–1719. [3] Flynn G. J. et al. 2006. *Science* 314:1731–1735. [4] Stephan T. et al. *Meteoritics & Planetary Science*. Forthcoming. [5] Stephan T. et al. 2007. *Meteoritics & Planetary Science*. Forthcoming. [6] Leitner J. et al. 2007. *Meteoritics & Planetary Science*. Forthcoming.

5262

NEW RESULTS FOR TERRESTRIAL ANALOG MEASUREMENTS FOR METEORITIC POROSITY STUDIES

M. M. Strait[1], D. P. Wignarajah[2], and G. J. Consolmagno[2, 3]. [1]Alma College, Alma, MI 48801, USA. E-mail: straitm@alma.edu. [2]Fordham University, Bronx, NY 10458, USA, and American Museum of Natural History, New York, NY 10024, USA. [3]Specola Vaticana, Vatican City.

Introduction: We have been studying porosity for a number of years to understand the physical makeup of primitive solar system materials [1]. The porosity of most meteorites is extraordinarily uniform, with a 95% confidence range of about 7 + 2% [2]. To validate these measurements and to contrast the differences in porosity in these materials with rocks that have not experienced the processes that occur as a rock moves from an asteroid to the surface of the Earth, here we evaluate a set of terrestrial rocks with a range of porosities, an updated version of a terrestrial sample evaluation presented earlier [3].

Results: Porosity has been measured using a helium pycnometry/glass bead method [4], in which volumes measured by He infiltrated into the pore space of the sample are contrasted with volumes displaced with tiny glass beads, and an imaging method, in which backscattered SEM images of thin sections are evaluated by counting pixels within visible pore spaces [5].

In meteorite samples the two methods agree, but some discrepancies led us to look more closely at the nature of porosity in general. We have acquired a suite of terrestrial samples and measured the porosity using both methods. Thin sections were made of one portion of a specimen for each rock type; the remaining portion was used directly for the pycnometry measurements. Although statistically (F-test and t-test) the results from both methods are the same at a 1% level of significance, a visual examination shows some discrepancy between the porosity measurements.

Unlike meteorites where the scatter was fairly even around a one-to-one correlation line, in the terrestrial samples the hand sample measurements were consistently high. The discrepant meteorite samples, primarily carbonaceous chondrites, average about 20% high compared with hand samples' porosity. The terrestrial samples average about 300% high for the hand samples, ranging up to 1100% high. The high porosity samples, primarily sedimentary rocks, correlate fairly well between the two methods, but mid to low porosity samples, igneous and metamorphic rocks, are consistently lower using the thin section measurements.

Thin section measurements miss vugs, holes, and large cracks, while pycnometry cannot measure pore space that is not accessible to the He. The problem seems to be less severe in the meteorites, especially ordinary chondrites, because the samples are more compact (from impacts, etc.) and a network of shock-induced cracks provides a connected pathway for the He. However, clearly in both sets there is a level of porosity accessible to the He that cannot be seen in the imaging technique because of resolution limitations. More work needs to be done to determine the nature and location of porosity in rock samples and determining the presence of macro-, mid-level, and microscale forms.

References: [1] Strait M. M. and Consolmagno G. J. 2004. *Meteoritics & Planetary Science* 39:A100. [2] Strait M. M. and Consolmagno G. J. 2005. Abstract #2073. 36th Lunar and Planetary Science Conference. [3] Strait M. M. and Consolmagno G. J. 2006. *Meteoritics & Planetary Science* 41: 5171. [4] Britt D. T. and Consolmagno G. J. 2003. *Meteoritics & Planetary Science* 38:1161–1180. [5] Strait M. M. et al. 1996. 27th Lunar and Planetary Science Conference. pp. 1285–1286.

5328

ISOTOPIC FRACTIONATION OF IRON DURING KINETIC EVAPORATION OF METALLIC IRON

S. Tachibana, H. Nagahara, K. Ozawa, and M. Yamada. Department of Earth and Planetary Science, The University of Tokyo, Japan. E-mail: tachi@eps.s.u-tokyo.ac.jp.

Kinetic evaporation of condensed materials at low pressures plays important roles in chemical and isotopic fractionations in planetary materials. Preferential evaporation of lighter isotopes leads to enrichment of heavier isotopes in a residual phase. Enrichments of heavier isotopes of Mg and Si in some CAIs [1] may have been caused by kinetic evaporation. A kinetic fractionation factor (α) between two isotopes during evaporation is usually predicted to be the square root of the inverse mass ratio of the two isotopes. However, α for evaporation of silicate melts or forsterite are known to be closer to unity than the predicted value (e.g., [2–6]), i.e., less fractionation than predicted. On the other hand, of iron during evaporation of molten FeO was found to be consistent with the predicted value [7, 8].

In this study, we carried out evaporation experiments of metallic iron, one of the major constituents in planetary materials, in a vacuum to determine α for iron during evaporation of metallic iron. Evaporation experiments of metallic iron were performed in a vacuum furnace at ~1550 K and ~1450 K for 18 and 85 hours, respectively. The isotopic fractionation during evaporation of solid is controlled by diffusion of isotopes in residual solids with forming isotopic zoning profiles [3]. The isotopic zoning profile reaches a steady state eventually and remains unchanged for further evaporation. The heating durations in present experiments were set to be long enough for diffusion-controlled isotopic fractionation to reach the steady state based on evaporation rates and diffusion rates of iron [9].

The surface isotopic composition of evaporation residue at the steady state is determined only by α [3]. The surface isotopic compositions of iron (^{54}Fe, ^{56}Fe, and ^{57}Fe) were thus analyzed for evaporation residues using ion microprobe (Cameca IMS 6f, installed at Dept. Earth Planet. Sci., Univ. Tokyo) to determine α. The surface isotopic compositions of evaporation residues were mass-dependently enriched in heavier isotopes. The obtained α was almost the same as the square root of the inverse mass ratio of the two isotopes, which is consistent with evaporation of iron from FeO melt but inconsistent with evaporation of silicate materials. This may be attributed to surface atomistic processes for evaporation, the details of which are unclear at present.

References: [1] Clayton R. N. et al. 1988. *Philosophical Transactions of the Royal Society A* 325:483–501. [2] Davis A. M. et al. 1990. *Nature* 347: 655–658. [3] Wang J. et al. 1999. *Geochimica et Cosmochimica Acta* 63:953–966. [4] Wang J. et al. 2001. *Geochimica et Cosmochimica Acta* 65:479–494. [5] Richter F. M. et al. 2002. *Geochimica et Cosmochimica Acta* 66:521–540. [6] Yamada M. et al. 2006. *Planetary and Space Science* 54:1096–1106. [7] Wang J. et al. 1994. 25th Lunar and Planetary Science Conference. pp. 1459–1460. [8] Dauphas N. et al. 2004. *Analytical Chemistry* 76:5855–5863. [9] Tachibana S. et al. 2002. *Meteoritics & Planetary Science* 37:A138.

5158

ANISOTROPIC EVAPORATION OF FORSTERITE IN PROTOPLANETARY DISCS AND ITS EFFECT ON INFRARED SPECTRA

A. Takigawa, M. Yokoyama, S. Tachibana, H. Nagahara, and K. Ozawa. Department of Earth and Planetary Science, The University of Tokyo, Japan. E-mail: takigawa@eps.s.u-tokyo.ac.jp.

Introduction: Astronomical observations have revealed the presence of crystalline forsterite (Mg_2SiO_4) in protoplanetary discs based on spectrum energy distributions (SED) (e.g., [1]). Crystalline forsterite evaporates when it is transported to high-temperature regions in discs. Forsterite is expected to evaporate anisotropically in the presence of hydrogen gas, the dominant gas species in a protoplanetary disc, as well as in vacuum [2, 3]. The SED of the protoplanetary discs is expected to change with anisotropic evaporation of forsterite.

To investigate the evaporation anisotropy of forsterite in hydrogen gas, we conducted evaporation experiments of forsterite in H_2 gas. The results are compared with model calculation on the IR spectrum [4] for different shapes of forsterite.

Experiments: Evaporation experiments were conducted in a stainless-steel vacuum chamber with a tungsten mesh heater. Samples (single crystal forsterite cut into 1 × 3 × 4 mm size parallelepipeds) were heated at 1535 °C and 1657 °C for various durations. Pressure of hydrogen gas in the chamber during experiments was kept at 10^{-2} to 10 Pa by controlling a flow rate of hydrogen gas. Vacuum experiments were also carried out for comparison. Evaporation rates along three crystallographic axes were calculated from the weight losses and the original shapes of three starting materials.

Results and Discussion: Evaporation rates of forsterite along different crystallographic orientations (*Va*, *Vb*, *Vc*) are much faster than those in vacuum and increase with increasing hydrogen pressure (linearly with $(P_{H2})^{\sim 0.5}$), which is consistent with previous experiments [5].

Forsterite evaporates anisotropically in hydrogen gas as expected, but the degree of anisotropy at 1535 °C seems to be different from that in vacuum. The ratio of evaporation rates along different crystallographic orientations change with P_{H2}. *Vc*/*Va* becomes farther from unity with increasing hydrogen pressure, while *Vb*/*Vc* becomes closer to unity.

Implication to Infrared Spectroscopy: The experimentally obtained evaporation anisotropy in hydrogen gas is used to calculate the change of shape of spherical forsterite at 1535 °C, which is further applied to calculate the infrared spectra. The spectra shows observable change in peak positions and relative strength of absorption bands in the range of mid- to far-IR, and will be able to resolve the shape effect from temperature and composition effect, which further suggests the formation environment of the forsterite grains.

References: [1] Van Boekel R. et al. 2004. *Nature* 432:479–482. [2] Ozawa K. et al. 1996. 27th Lunar and Planetary Science Conference. pp. 989–990. [3] Yamada M. et al. 2006. *Planetary Space Science* 54:1096. [4] Sogawa H. et al. 2006. *Astronomy & Astrophysics* 451:357–361. [5] Kuroda D. and Hashimoto A. 2006. *Antarctic Meteorite Research* 15: 152–164.

5300

CORRELATED STUDY OF Lu-Hf AND REE IN LUNAR ZIRCONS, WITH IMPLICATIONS FOR THE DIFFERENTIATION AGE OF KREEP

D. J. Taylor, K. D. McKeegan, and T. M. Harrison. Department of Earth and Space Sciences & IGPP, UCLA, Los Angeles, CA, 90095, USA. E-mail: dtaylor@ess.ucla.edu.

Introduction: A coupled U-Pb–^{176}Lu-^{176}Hf isotope study of lunar zircons from the KREEP-rich Apollo 14 landing site has yielded a highly unradiogenic $^{176}Hf/^{177}Hf$ signature, as previously reported in [1], for which a two-stage model age of 4.515 ± 0.015 Ga for the source region can be obtained. The lunar zircons analyzed in this study were isolated from an Apollo 14 soil (14163) and saw cuttings saved during processing of three Apollo 14 polymict breccias (14304, 14305, 14321). Because these zircons were not found in association with specific mineral clasts, it is impossible to know with certainty the source rocks for each zircon. However, a clearly defined negative trend seen in the age versus $\varepsilon_{Hf(T)}$ diagram indicates the existence of a strongly ITE-enriched source region, the most likely candidate for which is urKREEP. An extensive study of REE, Y, U, and Th abundances along with Ti crystallization temperatures and O isotopes (using the CAMECA 1270 ion microprobe at UCLA) has been undertaken in parallel with the Lu-Hf study to further characterize the zircons and obtain further clues to the nature of the source region. This abstracts reports the results of the REE study.

Results: The REE patterns of 68 lunar zircons all show a negative Eu anomaly (average Eu/Eu* = ~0.02) and absent or very small positive Ce anomaly (average Ce/Ce* = ~1.1) indicating crystallization in reducing conditions.

The composition of a liquid in equilibrium with the lunar zircons were calculated using zircon-melt partition coefficients as determined by [2] assuming power law dependence of partition coefficients with ionic radius. The results show a chondrite-normalized downward-sloping pattern characteristic of the KREEP component [3], although the absolute abundances are less (average Lu is ~10 times chondritic, compared to 200 times chondritic for KREEP). The mean La/Lu ratio of the calculated liquid (La/Lu ~3) is also consistent with KREEP (La/Lu = 2.28).

Discussion: As discussed by [2] and [4], there are difficulties associated with selection of an appropriate zircon-liquid distribution coefficient and the above-reported results can change, depending on what is chosen. However, the negative $\varepsilon_{Hf(T)}$ evidence for a strongly depleted source region (Lu/Hf = 0.68 times chondritic) parental to the zircons, coupled with the KREEP-like REE composition obtained using the "best" partition coefficients, strengthens the assertion that the Lu-Hf closure age of 4.515 ± 0.015 Ga can be viewed as the closure age of KREEP. As the KREEP source region is considered to be the last residuum of the global lunar magma ocean, dating its formation is akin to establishing the duration of the lunar magma ocean, and implies that primary differentiation of the Moon was complete within 60 million years of the formation of refractory meteorite inclusions.

References: [1] D. J. Taylor, McKeegan K. D., Harrison T. M., and McCulloch M. 2007. Abstract #1338. 38th Lunar and Planetary Science Conference. [2] Hinton R. W. and Upton B. G. J. 1991. *Geochimica et Cosmochimica Acta* 55:3287–3302. [3] Warren P. H. 1989. Workshop on Moon in Transition: Apollo 14, KREEP, and Evolved Lunar Rocks. 149. [4] Snyder G. A., Taylor L. A., and Crozaz G. 1993. *Geochimica et Cosmochimica Acta* 57:1143–1149.

5319

RE-EVALUATION OF THE "LIFE ON MARS" HYPOTHESIS: ORIGIN OF CARBONATE-MAGNETITE ASSEMBLAGES IN MARTIAN METEORITE ALH 84001

K. L. Thomas-Keprta[1], S. J. Clemett[1], D. S. McKay[2], E. K. Gibson[2], S. J. Wentworth[1], and FEI Corporation[3]. [1]ESCG at NASA/Johnson Space Center, Houston, TX 77058, USA. E-mail: kthomas@ems.jsc.nasa.gov. [2]KR, ARES, NASA/Johnson Space Center, Houston, TX 7705, USA. [3]FEI Company, Hillsboro, OR 97124, USA.

The Mars meteorite ALH 84001 is a sample of the ancient Martian surface with a crystallization age of 4.5 Ga. Internal cracks and fissures within this meteorite preserve evidence of early Martian hydrothermal activity in the form of carbonate disks which are dated at 3.9 Ga. The mechanism(s) through which these disks formed has been a subject of considerable debate ever since the suggestion that biological processes could, in part, be responsible [1]. Subsequently, a number of alternative, purely inorganic mechanisms have been advocated (e.g., [2–4]) which all involve partial thermal decomposition of carbonate. It has become clear that a prerequisite to critically evaluating these hypotheses is that a far more detailed characterization of the physical and chemical properties of the carbonate disks and their associated mineral phases must first be achieved. Here we present the most detailed and comprehensive TEM analyses of ALH 84001 carbonate disks yet obtained. The results indicate that these carbonates exhibit a subtle complexity that is difficult to reconcile with any of the current "simple purely inorganic processes."

Electron transparent sections from a complete carbonate disk were extracted in situ from an ALH 84001 fracture surface using focused ion beam techniques. These were compared with ultramicrotome sections of Roxbury siderite (which is compositionally similar to ALH 84001 carbonate) that were heated under a range of heating regimes ranging from 10^{8}–10^{-2} K s^{-1} to simulate the inorganic thermal decomposition scenarios discussed above.

Independent of the heating rate, the decomposition of Roxbury siderite always produced iron oxides with significant incorporation of Mg(II) and Mn(II) cations. This implies that the chemically pure magnetite crystals embedded within ALH 84001 carbonate is not a consequence of the thermal decomposition of Fe-rich carbonate. In the absence of any alternative, viable hypothesis, we propose that a substantial fraction of the magnetites in ALH 84001 carbonate must have originated independent of the carbonate and were subsequently deposited by allochthonous mechanisms.

References: [1] McKay et al. 1996. *Science* 273:924. [2] Brearley 2003. *Meteoritics & Planetary Science* 38:849. [3] Treiman. 2003. *Astrobiology* 3:369. [4] Golden et al. 2004. *American Mineralogist* 89:439.

5092

STATIC AMORPHIZATION OF PLAGIOCLASE: COMPARISON TO THE FORMATION PRESSURE OF DIAPLECTIC GLASS IN SHOCK EXPERIMENTS

N. Tomioka[1], A. Kunikata[1], H. Kondo[1], T. Nagai[2], T. Narita[3], and T. Yamanaka[3]. [1]Department of Earth and Planetary Sciences and Center for Planetary Science, Kobe University, Kobe 657-8501, Japan. E-mail: nao@kobe-u.ac.jp. [2]Department of Earth Sciences, Hokkaido University, Sapporo 060-0810, Japan. [3]Department of Earth and Space Science, Osaka University, Toyonaka 560-0043, Japan.

Introduction: In heavily shocked stony meteorites, plagioclase in host rock has transformed into glass, called maskelynite, in a solid-state reaction. The formation pressure of maskelynite has been estimated based on dynamic high-pressure experiments [1]. However, duration of pressure in laboratory shock experiments is significantly smaller (10^{-6} s) than that in meteorite parent bodies (100 s) estimated by the mineralogy of shock-induced melt veins [2, 3]. Therefore, there is a possibility that shock pressures of heavily shocked meteorites could be overestimated due to kinetic effect of amorphization. In this study, amorphization pressures of plagioclases were investigated based on static high-pressure experiments using a diamond anvil cell (DAC).

Experimental Methods: Fine-grained powder (~5–30 μm) of natural plagioclases were compressed at 20, 27, 33, 37, 49 GPa (Ab_{99}), 31, 34, 35 GPa (Ab_{89}) and 25, 31 GPa (Ab_4), respectively, at room temperature by DAC, and were kept at elevated pressures for 30 minutes. Recovered specimens were examined by laser Raman spectroscopy and transmission electron microscopy.

Results and Discussion: In the Ab_{99} samples compressed up to 33 GPa, characteristic Raman peaks (~290, 480, 510 cm^{-1}) of plagioclase were observed, but these peaks were not observed in the samples compressed at 37 and 49 GPa. Among the samples of Ab_{89} plagioclase, Raman peaks of plagioclase were observed only in the sample compressed at 31 GPa. In TEM observations of the samples (Ab_{99}, 37 GPa; Ab_{89}, 35 GPa) that did not show any Raman peaks of plagioclase, all of the grains in these samples showed diffuse scattering in electron diffraction that suggest an amorphous nature. Meanwhile, in the Ab_{99} sample compressed at 33 GPa that showed very weak Raman peak of plagioclase, a part of the grains shows powder diffraction rings from extremely fine grains. In the Ab_4 samples (25, 31 GPa) examined only by TEM, all of the grains are amorphous. The present results revealed that amorphizations of Ab_{99}, Ab_{89}, and Ab_4 plagioclases are completed at pressures below 37, 34, and 25 GPa, respectively. The amorphization pressure increases with increasing albite component. It is consistent with the amorphization pressure of experimentally shocked plagioclase that increases with increasing albite component [4, 5]. The pressures are slightly higher (<3 GPa) but no significant difference from those in the present static high-pressure experiments. Static compression experiments under high temperature are further required to estimate exact amorphization pressures of plagioclases in natural impact on the parent bodies of meteorites.

References: [1] Stöffler D. et al. 1991. *Geochimica et Cosmochimica Acta* 55:3845–3867. [2] Xie et al. 2001. *European Journal of Mineralogy* 13: 1177–1190. [3] Ohtani et al. 2004. *Earth and Planetary Science Letters* 227: 505–515. [4] Ostertag R. 1983. *Journal of Geophysical Research* 88:364–376. [5] Stöffler D. et al. 1986. *Geochimica et Cosmochimica Acta* 50:889–903.

5057

THE FORMATION OF PLANETESIMALS AND DISSIPATION OF THE EARLY SOLAR NEBULA

M. Trieloff. Institute of Mineralogy, University of Heidelberg, Im Neuenheimer Feld 236, D-69120 Heidelberg, Germany. E-mail: trieloff@min.uni-heidelberg.de.

Protoplanetary disks with fine dust surround their host stars ~3–6 Ma [1], which constrains the time scales of planetesimal formation. Formation of asteroid-size planetesimals in the early solar system occurred similarly fast, within a few Ma (e.g., [2–4]). Hence, planetary precursors were present within "normal" disk lifetimes before dissipation. However, it is not yet clear if full-size terrestrial planets formed with or without disk gas. For Jupiter, rapid accretion of a massive ice-rock core and gas acquisition from the disk is evident. However, Earth and Mars needed 33 Ma and 13 Ma for complete core formation and accretion, as modeled by Hf-W ages [5], i.e., significantly longer than the formation of Jupiter and asteroids, or estimated disk lifetimes [1]. Neon isotopes are a powerful tool to constrain the timing of terrestrial planet accretion and disk dissipation [6–11], as small accreting components (dust or planetesimals) would be subject to ion implantation of solar wind neon after disk dissipation. Recent studies using advanced high precision neon isotope measurements [12–15] demonstrate that Earth's precursor components acquired solar neon as solar wind-implanted ions ("Ne-B"), similar to carbonaceous chondrite [16] or Rumuruti parent bodies. For the latter, thermochronological modeling suggests very early brecciation and irradiation [17–19]. Several irradiation scenarios are possible: 1) disk gas dissipation 3–4 Ma after CAIs in the inner solar system, possibly triggered by photoevaporation of the disk, 2) irradiation of planetesimals with high orbital inclinations before disk gas dispersal, and 3) late accretion of fine, irradiated dust to Earth, e.g., before or after the collision of Theja and proto-Earth that formed the Moon [20, 21].

References: [1] Haisch K. E. et al. 2001. *The Astrophysical Journal* 553:L153–L156. [2] Amelin Y., Krot A. N., et al. 2002. *Science* 297:1678. [3] Trieloff M., Jessberger E. K., et al. 2003. *Nature* 422:502–503. [4] Kleine T., Mezger C., et al. 2004. *Geochimica et Cosmochimica Acta* 68:2935. [5] Kleine T., Münker C., et al. 2002. *Nature* 418:952. [6] Honda M. et al. 1991. *Nature* 349:149. [7] Trieloff M., Kunz J., et al. 2000. *Science* 288:1036–1038. [8] Trieloff M. et al. 2001. *Science* 291:2269a. [9] Trieloff M. and Kunz J. 2005. *Physics of the Earth and Planetary Interiors* 148:13–38. [10] Harrison D. et al. 2003. *Geochemistry Geophysics Geosystems* 4, no. 2002GC000325. [11] Trieloff M. 2002. *Geochimica et Cosmochimica Acta* 66:A784. [12] Hopp J. et al. 2004. *Earth and Planetary Science Letters* 219: 61–76. [13] Buikin A. I. et al. *Earth and Planetary Science Letters* 230:143–162. [14] Hopp J. and Trieloff M. 2005. *Earth and Planetary Science Letters* 240:573–588. [15] Ballentine C. J., Marty B., et al. 2005. *Nature* 433:33. [16] Goswami J. N. and Lal D. 1979. *Icarus* 10:510. [17] Trieloff M. et al. 1998. *Meteoritics & Planetary Science* 33:361–372. [18] Trieloff M. et al. 2001. *Earth and Planetary Science Letters* 190:267–269. [19] Buikin A. I. et al. 2006. *Meteoritics & Planetary Science* 41:A30. [20] Tolstikhin I. and Hofmann A. W. 2005. *Physics of the Earth and Planetary Interiors* 148:109–130. [21] Schwarz W. H. et al. 2005. *Contributions to Mineralogy and Petrology* 149:675–684.

5219

THERMOCHRONOLOGY OF ALH 84001 REVISITED

M. Trieloff. Institute of Mineralogy, University of Heidelberg, Im Neuenheimer Feld 236, D-69120 Heidelberg, Germany. E-mail: trieloff@min.uni-heidelberg.de.

The history of Mars can be constrained by radioisotope chronometry of Martian meteorites (e.g., [1–4]). Among them, ALH 84001 is the only rock with a high magmatic age (Sm-Nd) of 4.4–4.5 Ga [1]. Hence, disturbances or reset of its radiochronometric systems are sensitive to almost the entire history of the planet. The ^{40}Ar-^{39}Ar age was interpreted to record part of the heavy meteorite bombardment in the early solar system about 4 Ga ago [2, 3], and Ar retention properties were used to infer paleotemperatures for most of Martian history <0 °C, precluding large-scale activities of liquid water on Mars since 4 Ga ago [4]. These interpretations crucially depend on the inferred Ar diffusion parameters of the K-carrier phase maskelynite—a high-pressure transformation of plagioclase—and that it formed 4 Ga ago. Here I compare ^{40}Ar-^{39}Ar dating and Ar diffusion of ALH 84001 maskelynite and experimentally shocked plagioclase (22, 34, and 45 GPa [5]). The results show i) the release pattern and Ar diffusion parameters of maskelynite are dominated by a complex multidomain systematics, different from plagioclase or basalt glass [6, 7]; ii) assuming an alternative scenario—that maskelynite was formed when the meteorite was ejected into space [1]—implies that the diffusion parameters of plagioclase (not maskelynite) are relevant to determine partial ^{40}Ar loss of ALH 84001; iii) modeling the ALH 84001 age spectrum [3], taking into account ^{39}Ar recoil effects [8, 9], yields significantly higher ^{40}Ar loss than assumed by [4]; and iv) shock experiments show that plagioclase loses about 20% of radiogenic ^{40}Ar, almost independently on shock pressures of 22, 34, and 45 GPa [5], somewhat different from previous results [10]. If maskelynite indeed formed late upon ejection from Mars, this implies that the pre-shock ^{40}Ar-^{39}Ar age of ALH 84001 could be 4.4–4.5 Ga, and that the K-Ar system did not record a 4 Ga event. The 20% ^{40}Ar loss is ascribed to shock-wave effects and represents a partial advance in disentangling effects of shock from local post-shock heating, allowing better identification of influences on the K-Ar system during impact metamorphism, e.g., a) total reset of impact-melt rocks [8], b) impact-melt rocks that are not completely reset, e.g., L chondrite melts [11, 12], or c) rocks that lost ^{40}Ar without strong shock, i.e., probably recorded a heating effect due to impact-melt sheets (like HEDs; [13–15]).

References: [1] Nyquist L. E. et al. 2001. *Space Science Reviews* 96: 105–164. [2] Ash R. D. et al. 1996. *Nature* 380:57. [3] Bogard D. D. and Garrison G. H. 1999. *Meteoritics & Planetary Science* 34:451–473. [4] Shuster D. L. and Weiss B. P. 2005. *Science* 309:594–597. [5] Trieloff M. et al. 1994. *Meteoritics* 29:541. [6] Trieloff M. et al. 2003. *Geochimica et Cosmochimica Acta* 67:1229–1245. [7] Harrison D. et al. 2003. *Geochemistry Geophysics Geosystems* 4, no. 2002GC000325. [8] Trieloff M. et al. 1998. *Meteoritics & Planetary Science* 33:361–372. [9] Trieloff M. et al. 2005. *Geochimica et Cosmochimica Acta* 69:1253–1264. [10] Jessberger E. K. and Ostertag R. 1982. *Geochimica et Cosmochimica Acta* 46:1465–1471. [11] Bogard D. D. et al. 1995. *Geochimica et Cosmochimica Acta* 59:1383–1399. [12] Korochantseva E. V. et al. 2007. *Meteoritics & Planetary Science* 42:113–130. [13] Bogard D. D. and Garrison D. H. 2003. *Meteoritics & Planetary Science* 38:669–710. [14] Kunz J. et al. 1995. *Planetary and Space Science* 43:527–543. [15] Korochantseva E. K. et al. 2005. *Meteoritics & Planetary Science* 40:1433–1454.

5059

THE EARLY THERMAL HISTORY OF THE LL CHONDRITE PARENT BODY

M. Trieloff[1] and E. K. Jessberger[2]. [1]Institute of Mineralogy, University of Heidelberg, Im Neuenheimer Feld 236, D-69120 Heidelberg, Germany. E-mail: trieloff@min.uni-heidelberg.de. [2]Institute of Planetology, University of Münster, Wilhelm-Klemm-Str. 10, D-48149 Münster, Germany.

Meteorite thermal histories as recorded by ^{40}Ar-^{39}Ar thermochronometry allow us detailed insight into the accretion, cooling, and collisional events of small asteroidal parent bodies in the solar system [1–12]. Meteorite parent bodies seem to have formed within the first 4–5 Ma after CAIs, and experienced heating by ^{26}Al decay. This lead to metamorphism of ordinary chondrites that cooled in a layered parent body, as demonstrated by inverse correlations of cooling rate and petrologic types of a suite of unshocked H chondrites [5, 13]. During cooling the parent body surface was repeatedly affected by smaller impacts [12], but not collisionally restructured, e.g., ureilite, mesosiderite, and possibly IAB iron parent bodies [13, 3].

The parent body cooling history is not yet clarified for other ordinary chondrite parent bodies. For the LL chondrites, previous data suggested an early major impact at ~4.2 Ga [4, 14, 15]. Using previously published data from the Heidelberg laboratory [15, 16], new ^{40}Ar-^{39}Ar data of the LL chondrite Ensisheim, re-analyses of Uden and Trebbin WR, and other sources [1, 4, 6, 7], taking into account age spectra modeling of fine-grained samples disturbed by ^{39}Ar recoil [17, 18], and correcting for a –30 Ma bias to adjust U-Pb and K-Ar age scales [5, 10], we outline the LL chondrite parent body history as follows: a 4.2 (±0.05) Ga event, most probably a major impact, is seen in a number of meteorites of varying petrologic type (Ensisheim, Uden, Trebbin, Bhola, Krähenberg light, MIL 99301). LL chondrites older than 4.3 Ga show an inverse correlation of petrologic type and ^{40}Ar-^{39}Ar age, with LL3 being 4.53 ± 0.03 Ga, LL5 ranging between 4.53 ± 0.02 (Olivenza) and 4.42 ± 0.02 Ga (ALH 78109), and LL6 ranging between 4.45 ± 0.03 and 4.35 ± 0.02 Ga (Trebbin F), one LL7 (ALH 84027) with 4.38 ± 0.02 Ga, as expected for an onion-shell layered body. Final conclusions, however, should wait until complete cooling histories are available for these samples.

References: [1] Turner G. et al. 1978. Proceedings, 9th Lunar Planet. Sci. Conf. pp. 989–1025. [2] Bogard D. D. and Garrison D. H. 2003. *Meteoritics & Planetary Science* 38:669–710. [3] Bogard D. D. et al. 2005. *Meteoritics & Planetary Science* 40:207–224. [4] Dixon E. T. et al. 2004. *Geochimica et Cosmochimica Acta* 40:3779–3790. [5] Trieloff M. et al. 2003. *Nature* 422:502–506. [6] Takigami Y. and Kaneoka I. 1987. Proceedings, 11th Symp. Ant Met. p. 133. [7] Kaneoka I. 1980. Proceedings, 5th Symp. Ant Met. p. 117. [8] Kunz J. et al. 1995. *Planetary and Space Science* 43:527–543. [9] Korochantseva E. V. et al. 2007. *Meteoritics & Planetary Science* 42:113–130. [10] Trieloff M. et al. 2001. *Earth and Planetary Science Letters* 190:267–269. [11] Korochantseva E. K. et al. 2005. *Meteoritics & Planetary Science* 40:1433–1454. [12] Schwarz W. H. and Trieloff M. 2006. *Meteoritics & Planetary Science* 41:A161. [13] Göpel et al. 1994. *Earth and Planetary Science Letters* 121:153–171. [14] Keil K. et al. 1994. *Planetary and Space Science* 42:1109–1122. [15] Trieloff M. et al. 1994. *Meteoritics* 29:541. [16]Trieloff M. et al. 1989. *Meteoritics* 24:332. [17] Trieloff M. et al. 1998. *Meteoritics & Planetary Science* 33:361–372. [18] Trieloff M. et al. 2005. *Geochimica et Cosmochimica Acta* 69:1253–1264.

5221

^{40}Ar-^{39}Ar AGES OF AUSTRALASIAN TEKTITES

M. Trieloff[1], K. Bollinger[1], J. Kunz[1], and E. K. Jessberger[2]. [1]Institute of Mineralogy, University of Heidelberg, Im Neuenheimer Feld 236, D-69120 Heidelberg, Germany. E-mail: trieloff@min.uni-heidelberg.de. [2]Institute of Planetology, University of Münster, Wilhelm-Klemm-Str. 10, D-48149 Münster, Germany.

The origin of Australasian tektites [1, 2] was frequently associated with age paradoxes, e.g., multiple impacts not only separated in space [2] but also time [3]. We performed ^{40}Ar-^{39}Ar of Australasian tektites covering the whole area of this largest tektite strewn field. We show that step-heating age spectra of individual samples yield concordant and precise ^{40}Ar-^{39}Ar plateau ages, if large specimens are dated and if corrections for excess ^{40}Ar are applied. Excess argon can be either distinguished by discrimination of low- and high-temperature extractions of saddle-shaped [4] age spectra (e.g., in a javanite or thailandite) or—in the case of our australite samples—by careful isochron analysis that yields an intercept slightly different from air with ^{40}Ar/^{36}Ar = 307 ± 5 (although we cannot definitely exclude mass fractionated argon, as in [5]). Mean plateau ages of four Asian tektites are 784 ± 9 ka, for four australites 790 ± 16 ka, the age difference is insignificant. Hence, we infer a single tektite forming event 786 ± 13 ka ago for the Australasian strewn field (incl. age monitor HD-B1 uncertainty), improving a previously reported age of 760 ± 50 ka [5]. Our results and previous studies [6, 7] demonstrate the presence of disturbances by excess argon, e.g., in the flanges of button-flanged australites, but also their cores [7]. Excess argon may also have caused apparently older ages of australites reported previously [3]. Our results are in line with recent reports that even (partial glassy) impact melts (e.g., L-chondritic [8, 9] or terrestrial [10]), or glasses from other geologic settings [11, 12] contain characteristic amounts of excess argon. A more rigorous evaluation of trapping sites of excess argon is highly desirable not only for impact melts, but also for ultramafic rocks [13–16], to elucidate various argon components (radiogenic, atmospheric, mantle) e.g., in SNC meteorites.

References: [1] Koeberl C. 1990. *Tectonophysics* 171:405–422. [2] Wasson J. T. 1991. *Earth and Planetary Science Letters* 102:95–109. [3] Storzer D. et al. 1984. *Meteoritics* 19:317. [4] Lanphere M. A. and Dalrymple G. B. 1976. *Earth and Planetary Science Letters* 32:141–148. [5] Trieloff M. et al. 2005. *Geochimica et Cosmochimica Acta* 69:1253–1264. [6] Izett G. A. and Obradovich J. D. 1992. 23rd Lun. Planet. Sci. Conf. pp. 593–594. [7] McDougall I. and Lovering J. F. 1969. *Geochimica et Cosmochimica Acta* 33:1057–1070. [8] Bogard D. D. et al. 1995. *Geochimica et Cosmochimica Acta* 59:1383–1399. [9] Korochantseva E. V. et al. 2007. *Meteoritics & Planetary Science* 42:113–130. [10] Trieloff M. et al. 1998. *Meteoritics & Planetary Science* 33:361–372. [11] Harrison D. et al. 2003. *Geochemistry Geophysics Geosystems* 4, no. 2002GC000325. [12] Trieloff M. et al. 2003. *Geochimica et Cosmochimica Acta* 67:1229–1245. [13] Hopp J. et al. 2004. *Earth and Planetary Science Letters* 219:61–76. [14] Buikin A. I. et al. 2005. *Earth and Planetary Science Letters* 230:143–162. [15] Trieloff M. et al. 1997. *Geochimica et Cosmochimica Acta* 61: 5065–5088. [16] Hopp J. and Trieloff M. 2005. *Earth and Planetary Science Letters* 240:573–588.

5225

NOBLE GAS CHRONOLOGY OF RUMURUTI

M. Trieloff[1], D. Nakashima[2, 3], and U. Ott[3]. [1]Institute of Mineralogy, University of Heidelberg, Im Neuenheimer Feld 236, D-69120 Heidelberg, Germany. E-mail: trieloff@min.uni-heidelberg.de. [2]Laboratory for Earthquake Chemistry, University of Tokyo, Hongo, Bunkyo-Ku, Tokyo 113-0033, Japan. [3]Max-Planck-Institut für Chemie, Mainz, Germany.

R chondrites frequently display disturbed ^{40}Ar-^{39}Ar age spectra, which impedes the evaluation of the early chronology of the Rumuruti parent body [1, 2]. In an ongoing initiative to constrain the history of meteorite parent bodies [3–6], we applied thermochronological modeling [7, 8] to ^{40}Ar-^{39}Ar age spectra of three Rumuruti lithologies that differ in petrologic type (types 3, 3.8, 5/6). The age spectra show partial plateaus and interfering disturbances (^{40}Ar loss, ^{39}Ar recoil) that decrease with increasing grain size. A well-defined age plateau of 4.53 ± 0.01 Ga was obtained for the coarse-grained type 5/6 lithology. The age corrected for the bias imposed by obsolete K decay constants [3, 9] is 4.56 Ga. This implies rapid cooling of equilibrated rocks from the interior R-chondrite parent body—similar to fast-cooled H4 chondrites [3]—and requires very early impact-induced parent body restructuring and breccia formation. In fact, most R chondrites are light/dark structured regolith breccias consisting of highly recrystallized fragments as well as unequilibrated lithologies and contain solar wind–implanted rare gases [10].

We furthermore analyzed Rumuruti noble gases by step-heating. Solar He and Ne are released at comparably high temperatures of 800 °C and fractionated, suggesting significant loss of solar wind–implanted gases. If this thermal event was stronger than post 4.56 Ga events recorded by the ^{40}Ar-^{39}Ar thermochronometer, solar-wind implantation and loss must have occurred before, i.e., within a few Ma after accretion, consistent with early irradiation records suggested for terrestrial precursor planetesimals [11–17]. By means of diffusion calculations we will discuss if thermal mobilization and secondary ^{40}Ar loss detected in the age spectra could have been sufficient to cause loss of solar wind He and Ne—admitting late solar wind incorporation—or if solar noble gas loss requires a strong thermal event that would have caused significantly higher losses of radiogenic ^{40}Ar than observed—favoring very early irradiation.

References: [1] Schulze H. et al. 1994. *Meteoritics & Planetary Science* 29:275–286. [2] Dixon E. T. et al. 2003. *Meteoritics & Planetary Science* 38:341–355. [3] Trieloff M. et al. 2003. *Nature* 422:502–506. [4] Korochantseva E. V. et al. 2007. *Meteoritics & Planetary Science* 42:113–130. [5] Kunz J. et al. 1995. *Planetary and Space Science* 43:527–543. [6] Korochantseva E. K. et al. 2005. *Meteoritics & Planetary Science* 40: 1433–1454. [7] Trieloff M. et al. 1998. *Meteoritics & Planetary Science* 33: 361–372. [8] Trieloff M. et al. 1994. *South African Journal of Geology* 97: 365–384. [9] Trieloff M. et al. 2001. *Earth and Planetary Science Letters* 190:267–269. [10] Weber H. W. and Schultz L. 2001. Abstract #1500. 32nd LPSC. [11] Trieloff M. et al. 2000. *Science* 288:1036–1038. [12] Trieloff M. et al. 2001. *Science* 291:2269a. [13] Harrison D. et al. 2003. *Geochemistry Geophysics Geosystems* 4, no. 2002GC000325. [14] Hopp J. et al. 2004. *Earth and Planetary Science Letters* 219:61–76. [15] Buikin A. I. et al. *Earth and Planetary Science Letters* 230:143–162. [16] Trieloff M. and Kunz J. 2005. *Physics of the Earth and Planetary Interiors* 148:13–38. [17] Hopp J. and Trieloff M. 2005. *Earth and Planetary Science Letters* 240:573–588.

5166

THREE-DIMENSIONAL STRUCTURES OF MICROMETEORITES AND MODEL DUST PARTICLES: POROSITIES AND FRACTAL DIMENSIONS

A. Tsuchiyama[1], T. Okazaki[1], K. Murata[1], K. Wada[2], H. Kimura[2], T. Noguchi[3], T. Nakamura[4], T. Nakano[5], and K. Uesugi[6]. [1]Department of Earth and Space Science, Graduate School of Science, Osaka University, Japan. E-mail: akira@ess.sci.osaka-u.ac.jp. [2]Hokkaido University, Japan. [3]Ibaraki University, Japan. [4]Kyushu University, Japan. [5]AIST/JSC. [6]JASRI/SPring-8.

Introduction: Examination of Stardust samples shows that anhydrous IDPs are consistent with the cometary origin although the conclusion has not been definitive [1]. Some micrometeorites (MMs) collected from Antarctic ice or snow are similar to anhydrous IDPs [2] and are considered to have a cometary origin. Thus, such porous cosmic dust should be the most primitive materials in the solar system that can be obtained on the Earth. In the present study, we examine 3-D structures of Antarctic MMs and compare them with model particles of interplanetary dust, especially on their porosities and fractal dimensions.

Experiments and Image Analysis: Thirty-nine MMs collected from Antarctic snow by NIPR were examined. The 3-D structures were obtained by SR-microtomography [3] at BL20XU or BL47XU of SPring-8 (10 keV, 0.5 μm voxel size). Pores were easily recognized in the CT slices. Most of them are connected to the exterior in 3-D (open pores) and closed pores are rare. To estimate porosities including open pores, p, we have developed a new method to extract open pores by virtually wrapping a MM particle with a cloth. Fractal dimensions of MMs, F_D, were also obtained using box-counting method.

Model Dust Particles: In the solar system formation scenario, submicron solid particles are aggregated into large particles and planetesimals are made from these aggregates. Ballistic cluster-cluster aggregates (BCCA) and ballistic particle-cluster aggregates (BPCA) are considered as the elemental aggregates. The 3-D shape features (open porosities p and fractal dimensions F_D) were also obtained by the same method and compared with the MMs results. Aggregates of two BCCAs by collision were obtained in simulation (collision velocity: 0.385–17.4 m/s) [4] and also compared with the MMs.

Results and Discussion: The MM textures are divided into three groups: 1) porous, 2) nonporous, and 3) others (e.g., a large solid grain with a small amount of fine materials). For group (1), open porosities (8–41%) have negative correlation with closed porosity (3.3–0.1%), indicating that highly porous MMs have highly connected pores. For groups (1) and (2), fractal dimension decreases with increasing open porosity (F_D = 2.9–2.5, p = 2–41%). BCCA (F_D = 1.79, p = 78%), aggregates of BCCAs by collision (F_D = 2.2–2.5, p = 56–83%), and the porous and nonporous MMs have a single trend, but BPCA (F_D = 2.53, p = 44%) deviates from this trend. This may indicate some genetic relation between the BCCA and porous MMs although MMs should have experienced more complex processes than simple aggregation by collision.

References: [1] Zolensky et al. 2006. *Science* 314:1735–1739. [2] Nakamura et al. 2005. *Meteoritics & Planetary Science* 40:A110. [3] Uesugi K. et al. 2001. *Nuclear Instruments & Methods in Physics Research A* 467/468:853–856. [4] Wada et al. 2007. *The Astrophysical Journal* 661:320–333.

5056

CUMULUS ORIGIN OF OLIVINE MEGACRYSTS IN YAMATO-980459?

T. Usui[1], H. Y. McSween, Jr.,[1], and C. Floss[2]. [1]Department of Earth and Planetary Sciences, University of Tennessee, USA. E-mail: tusui@utk.edu. [2]Laboratory for Space Sciences and Physics Department, Washington University, USA.

Primitive melts provide critical information on their mantle source regions, but most Martian meteorites have been fractionated. An olivine-phyric shergottite, Yamato-980459 (Y98), is interpreted to represent a primary melt, because its olivine megacrysts have magnesian cores (Fo84) that appear to be in equilibrium with the Y98 whole-rock composition based on Fe-Mg partitioning (e.g., [1]). However, CSD plots for Y98 olivines show a size gap [1, 2], suggesting a cumulus origin. Since melting experiments were recently performed using the Y98 whole-rock composition to infer the thermal structure and volatile contents of the Martian mantle, this interpretation should be scrutinized.

Y98 is characterized by magnesian olivine megacrysts, and pyroxenes with orthopyroxene cores mantled by pigeonite and augite. Here we report major, minor, and trace element compositions of Y98 olivines and compare them with results from melting experiments [3, 4] and thermodynamic calculations [5, 6]. Cores of the olivine megacrysts have major and minor element contents identical to those of the most magnesian olivines from the experiments, but they differ slightly from those of thermodynamic calculations. This is probably because the Y98 whole-rock composition lies outside the range of liquids used to calibrate these models. The megacryst cores (Fo80–85) exhibit minor and trace element (Mn-Ni-Co-Cr-V) characteristics distinct from other olivines (megacryst rims and groundmass olivines, Fo < 80), implying that the megacryst cores crystallized under more reduced and higher-temperature conditions. We also found some reversely zoned pyroxenes that have augite cores (low-Mg#) mantled by orthopyroxene (high-Mg#), although they are uncommon. The augite cores have distinctly LREE-enriched patterns relative to the other pyroxenes. The calculated REE pattern of a melt in equilibrium with the augite cores is not consistent with Y98 or other depleted shergottites, but is consistent with the enriched shergottites.

Considering the CSD patterns of Y98 olivines, we propose that the olivine megacrysts are cumulus grains which probably formed in a feeder conduit by continuous melt replenishment, and the melt compositions are indistinguishable from the Y98 whole rock. The magma replenishments may have produced a fractionated mush that assimilated crust, resulting in the formation of the LREE-enriched augite cores. The final magma pulse entrained these cumulus olivines and pyroxenes and then crystallized groundmass olivines and pyroxenes. Although Y98 contains small amounts of cumulus materials (<~6 vol%), we conclude that the Y98 whole-rock composition can be used to represent a Martian primary melt composition.

References: [1] Greshake A. et al. 2004. *Geochimica et Cosmochimica Acta* 68:2359–2377. [2] Lentz R. and McSween H. Y., Jr. 2005. *Antarctic Meteorite Research* 18:66–82. [3] Musselwhite D. S. et al. 2006. *Meteoritics & Planetary Science* 41:1271–1290. [4] Draper D. S. 2007. Abstract #1447. 38th Lunar and Planetary Science Conference. [5] Toplis M. J. 2005. *Contributions to Mineralogy and Petrology* 149:22–39. [6] Libourel G. 1999. *Contributions to Mineralogy and Petrology* 136:63–80.

5099

Fe-BEARING MINERALS IN WEATHERED ORDINARY CHONDRITES FROM THE ATACAMA DESERT

M. Valenzuela[3], P. Munayco[1], Y. A. Abdu[2], R. B. Scorzelli[1], E. dos Santos[1], and D. Morata[3]. [1]Centro Brasileiro de Pesquisas Físicas, Rua Xavier Sigaud 150, 22290-180 Rio de Janeiro, Brazil. [2]Department of Geological Sciences, University of Manitoba, Winnipeg, Manitoba R3T 2N2, Canada. [3]Universidad de Chile, Plaza Ercilla 803, Santiago, Chile.

Here we report the results of ^{57}Fe Mössbauer spectroscopy, involving equilibrated weathered ordinary chondrites (OC) collected in the Atacama Desert, northern Chile, that include the three chemical groups (H, L, and LL). The present ^{57}Fe Mössbauer results obtained at room temperature (RT) and at liquid helium temperature (4.2 K) on 15 OC samples precise the quantity and nature of all the Fe-bearing phases recognized in previous RT ^{57}Fe Mössbauer works [1, 2].

The degree of weathering in ordinary chondrites can be quantitatively measured using Mössbauer spectroscopy to determine the proportions of the Fe-bearing phases occurring mainly as Fe^0 in the Fe-Ni metal, Fe^{2+} in the ferromagnesian silicates and troilite, and Fe^{3+} in the terrestrial alteration products. In newly fallen equilibrated OC, the amounts of Fe0 (kamacite and taenite) and Fe^{2+} (olivine, pyroxene, and troilite) are known within narrow limits. Thus, the abundance of oxidized iron in weathered chondrites can be related to specific starting compositions and to the level of terrestrial weathering [3, 4].

The RT spectra exhibit a complex mixture of magnetic, paramagnetic, and superparamagnetic phases for all samples. They can be fitted with two Fe^{2+} doublets associated with the presence of olivine and pyroxene, and a third doublet attributed to paramagnetic and/or superparamagnetic Fe^{3+} oxyhydroxides (small-particle goethite, akaganeite, and lepidocrocite) identified only through low-temperature measurements. A magnetic sextet, with a broad distribution of hyperfine fields, due to large-particle goethite is also included in the fitting together with magnetic components associated with Fe-Ni metal, troilite, hematite, and magnetite.

The spectra collected at 4.2 K allow the identification and quantification of almost all the phases present in the sample. These spectra are composed of troilite, goethite, magnetite, hematite, Fe-Ni (kamacite and taenite) and an additional magnetic component (B_{hf} = 48–49T) identified as akaganeite, present at RT as Fe^{3+} doublet. The olivine and pyroxene components show magnetic relaxation effects in all low-temperature spectra and are fitted using the spheric relaxation model of the Normos program.

The Mössbauer spectral areas of Fe^{3+} components indicates that the oxidation level of the studied Atacama OC range from ~15% to ~75%. The analysis of the ferric oxidation of the primary phases derived from the Mössbauer results shows that Fe-Ni metal and troilite as well as the ferromagnesian silicates appear to be affected by oxidation. Further, the rate of weathering of the ferromagnesian silicates is found to be nearly the same, indicating that both olivine and pyroxene are equally susceptible to oxidation.

References: [1] Valenzuela et al. 2006. *Meteoritics & Planetary Science* 41:A179. [2] Valenzuela et al. *Hyperfine Interactions*. Forthcoming. [3] Bland et al. 2002. *Hyperfine Interactions* 142:481–494. [4] Bland et al. 1996. *Geochimica et Cosmochimica Acta* 60:2053–2059.

5234

MONT DIEU IRON METEORITE: PETROGRAPHY AND GEOCHEMISTRY

N. Van den Borre[1, 4], H. Goethals[2], J. Hertogen[3], and Ph. Claeys[4]. [1]Department of Geology and Soil Sciences, Ghent University, B-9000 Ghent, Belgium. E-mail: niejls@gmail.com. [2]Royal Belgian Institute of Natural Sciences, B-1000 Brussels, Belgium. [3]Geo-institute, Katholieke Universiteit Leuven, B-3001 Leuven, Belgium. [4]Department of Geology, Vrije Universiteit Brussels, B-1050 Brussels, Belgium.

An ~450 kg fragment of the Mont-Dieu iron meteorite was recently acquired by the Museum of the Royal Belgian Institute of Natural Sciences. A large fragment in a good state of preservation is dedicated to scientific research. This piece shows much less rust damage than the ones present in the collection of the Musée National d'Histoire Naturelle in Paris [1]. The metal phase shows Widmanstätten structure and is composed essentially of kamacite, with fine lines of Ni-rich taenite, and locally troilite associated with schreibersite. Its chemical composition is for the major elements in wt%: Fe: 92.1, Ni: 7.6, and Co: 0.3 and for trace elements in ppm: Cu: 212, Ga: 24.5, Ge: 73.5, Ir: 7.7, Rh: 2.1, Pd: 4.2, Os: 10.4, Pt: 20, Au: 1.0. Locally, the Mont Dieu meteorite is characterized by the common presence of silicate inclusions. The bulk composition of these silicate inclusions appears chondritic. They are composed of olivine (~SiO_2: 39.7 wt%; FeO: 15.8 wt%, MgO: 43.2, MnO: 0.4 wt%), pyroxene (~SiO_2: 60.0 wt%; FeO: 9.3 wt%, MgO: 31.2, MnO: 0.4, CaO: 0.9, Al_2O_3: 0.2, TiO_2: 0.1) and plagioclase (~SiO_2: 64.6 wt%; Al_2O_3: 21.1, Na_2O: 9.3, K_2O: 0.9, FeO: 0.8, CaO: 2.7), along with phases of chromite, troilite, schreibersite, and metal. These results agree with the previously proposed classification of Mont Dieu as fine octahedrite IIE iron meteorite [1, 2].

References: [1] Grossman. 1997. *Meteoritics & Planetary Science* 31: A159–166. [2] Desrousseaux et al. 1996. *Meteoritics & Planetary Science* 31:A36.

5292

HRTEM ANALYSES OF STARDUST SAMPLES AND THEIR COMPARISON WITH TOF-SIMS RESULTS

C. H. van der Bogert[1], U. Golla-Schindler[2], and T. Stephan[1]. [1]Institut für Planetologie, Wilhelm-Klemm-Str. 10, 48149 Münster, Germany. E-mail: vanderbogert@uni-muenster.de. [2]Institut für Mineralogie, Corrensstr. 24, 48149 Münster, Germany.

Introduction: Recent analyses of Stardust samples reveal that there are a wide variety of unexpected and seemingly unusual minerals found in the samples collected from comet 81P/Wild-2 [1, 2]. In addition, a wide range of olivine (Fo_4–Fo_{100}) and pyroxene (En_{52}–En_{100}) compositions are observed in the samples (e.g., [1]). Indeed, it was unexpected to discover such a broad range of compositions and exotic refractory minerals, including CAI-like particles, suggesting that comets may incorporate materials from a greater cross section of the early protoplanetary disk than previously thought, thus requiring significant large-scale mixing [1, 2]. No confirmed carbonates or phyllosilicates have been found thus far, which indicates that Wild-2 may not have been affected by aqueous alteration [1, 3].

As the multi-approach analysis of Stardust cometary samples continues, we now have the opportunity to compare different types of data collected from individual cometary grains. One advantage of this approach is that we can correlate elemental analyses with high sensitivity by time-of-flight secondary ion mass spectrometry (TOF-SIMS) with elemental and mineralogical analyses of very high spatial resolution by high-resolution transmission electron microscopy (HRTEM). As a result, it is possible to gain greater insight into the nature of Wild-2 materials.

Sample C2004,1,44,4,5,#47: So far in this study, one sample has been characterized by both TEM and TOF-SIMS techniques. This sample is similar to some other samples already characterized by TEM methods (e.g., [1, 3]). It is approximately 9 × 20 μm in size and is composed of a variety of different mineral grains, intermingled with vesicular glass, which mainly consists of melted aerogel. Iron sulfide and metal grains, which are all smaller than 100 nm, are randomly distributed throughout the melted aerogel and correspond to the generally homogeneous distribution of S- and Ni-rich pixels as seen in TOF-SIMS secondary ion images [4].

At one end of the sample are several dark (electron-opaque) mineral grains, the largest of which measures 1.6 × 0.5 μm and is composed of a subhedral core with darker surrounding material. This grain exhibits very high Ca content along with O and some C, as seen with both EDX [this work] and TOF-SIMS [4] analyses. Several smaller grains having the same elemental composition surround the larger grain. One small tabular grain is possibly a Ca, Fe silicate. Many of the grains exhibit well-defined diffraction patterns and resolvable lattice patterns using HRTEM imaging, which will help to specifically identify these phases. In particular, it is possible that some of the grains are carbonates, but further analyses are needed to answer this important question.

Further results from additional particles analyzed using both HRTEM and TOF-SIMS techniques will be presented.

References: [1] Zolensky M. et al. 2007. *Science* 314:1735–1739. [2] Brownlee D. et al. 2007. *Science* 314:1711–1716. [3] Mikouchi T. et al. 2007. Abstract #1946. 38th Lunar and Planetary Science Conference. [4] Stephan T. et al. *Meteoritics & Planetary Science.* Forthcoming.

5196

SEYMCHAN: A MAIN GROUP PALLASITE—NOT AN IRON METEORITE

D. van Niekerk[1], R. C. Greenwood[2], I. A. Franchi[2], E. R. D. Scott[1], and K. Keil[1]. [1]Hawai'i Institute of Geophysics and Planetology, University of Hawai'i, Manoa, Honolulu HI, 96822, USA. E-mail: dionysos@higp.hawaii.edu. [2]PSSRI, The Open University, Milton Keynes, MK7 6AA, UK.

Seymchan was initially classified as a group IIE iron meteorite [1], but was subsequently reclassified as ungrouped [2]. The iron, which was discovered in 1967, consists of two pieces totaling ~351 kg [3]. A recent (2004) expedition [4] to the same locality has led to the discovery of more meteorite masses. Reports suggest that 20% of the recent finds are pallasitic (or partly pallasitic), while the rest are irons [4]. The recent finds are poorly documented, but photographs of cut slabs attest to the heterogeneous nature of both metal:olivine (metal veins up to tens of centimeters versus zones dominated by olivine) and olivine-fragment size (centimeter-to-millimeter size). Glorieta Mountain and Brenham also contain large olivine-free metal regions. Neutron activation analysis of the pallasite metal (Table 1) reveals that it is identical to the iron meteorite, thus confirming that its occurrence in the same locality is not coincidence and that they are related. The composition of the metal groups Seymchan with the Main Group, but the high Ir indicates that it is anomalous (PMG-am). The metal composition of Brenham and Glorieta Mountain are not closely associated with Seymchan, although they are also classified as PMG-am.

Table 1. INAA data for Seymchan [5].

	Iron (1984)	Iron (1985)	Pallasite
Cr (μg/g)	24	31	13
Co (mg/g)	5.28	5.26	5.33
Ni (mg/g)	92.8	93.3	95.1
Cu (μg/g)	121	152	140
Ga (μg/g)	24.8	26.3	25.6
As (μg/g)	18.6	18.8	18.2
W (μg/g)	0.52	0.34	0.52
Ir (μg/g)	0.662	0.694	0.676
Au (μg/g)	2.007	2.115	2.132

Electron microprobe analyses and scanning electron microscopy of two thick sections (each ~500 mm^2) indicates that the pallasite-textured portion of Seymchan is mostly unweathered, and composed of FeNi metal, olivine, troilite, chromite, schreibersite, and whitlockite. The metal is dominated by low-Ni kamacite, while rims of central plessite regions contain up to 37% Ni. Olivine ($Fa_{11.3}$) is well rounded, and infiltrated by minor troilite along grain boundaries and fractures. Schreibersite is mostly found in contact with olivine, and whitlockite is also a minor phase. Chromite was completely absent in one section, while dominating the second. Oxygen isotope measurements on olivine grains from Seymchan gave the following results (n = 2): $\delta^{17}O$ = 1.209‰; $\delta^{18}O$ = 2.660‰; $\delta^{17}O^*$ = –0.186‰. This value falls within the field of Main Group pallasites measured by [6].

Acknowledgements: We thank Dr. J. Wasson for contributing his data (pallasite metal was provided by Dr. M. A. Nazarov).

References: [1] Scott E. R. D. and Wasson J. T. 1976. *Geochimica et Cosmochimica Acta* 40:103–115. [2] Wasson J. T. and Wang J. 1986. *Geochimica et Cosmochimica Acta* 50:725–732. [3] Krinov E. L. 1968. The Meteoritical Bulletin, No. 43. [4] Nazarov M. A. 2007. Personal communication. [5] Wasson J. T. 2007. Personal communication. [6] Greenwood et al. 2006. *Science* 313:1763.

5112

GLASS INCLUSIONS IN ALLENDE (CV3) OLIVINE: HEATING EXPERIMENTS

M. E. Varela[1], R. Clocchiatti[2], and G. Kurat[3]. [1]Complejo Astronómico El Leoncito (CASLEO), Av. España 1512 sur, J5402DSP, San Juan, Argentina. E-mail: evarela@casleo.gov.ar. [2]Laboratoire Pierre Süe, CEA, CNRS, CEN Saclay, F-91191 France. [3]Department of Lithospheric Sciences, University of Vienna, Althanstrasse 14, 1090 Vienna, Austria.

Introduction: Glass inclusions represent small volumes of liquids enclosed by a host mineral during its growth. Heating experiments on glass inclusions allow reversing the post-entrapment processes that occurred inside the inclusions during cooling. These experiments—performed on glassy and glass-bearing inclusions in olivine—enable us to obtain information regarding the conditions prevailing during host formation, either in terrestrial or extraterrestrial rocks (e.g., [1–5]). Here we report on the heating experiments performed with glass inclusions in olivine of the CV3 Allende chondrite.

Methods and Results: Heating experiments were performed in a Pt-Pt90Rh10 heating stage at 1 bar pressure in a hot He atmosphere as oxygen getter [6]. The oxygen fugacity is estimated to have been between 10^{-9} and 10^{-10} atm at 1200 °C corresponding, approximately, to the equilibrium of a mixture of Ar-H_2 (1% H_2). Quenching times were less than 1 s. The system was calibrated at the melting point of Au (1063 °C). Runs were performed with a gradual increase rate of temperatures until the final temperature of 1100 °C, 1250 °C, and 1450 °C, respectively. The final temperatures were held during 2 h (with exception of a second run at 1250 °C which was held during 24 h) after which a rapid quench (less than 1 s to about 500 °C) preserved the final conditions.

The major variations observed in the chemical composition of the heated glass inclusions is an increase of the FeO and MgO contents, with values up to 9 wt% and 19.4 wt%, respectively, as compared with the unheated glasses due to dissolution of the host olivine in the melt. However, glasses seem not to have reached equilibrium with their host showing Kd(Fe/Mg) (olivine/liquid) values ranging from 0.14 to 0.4. Interesting is the content of Na_2O in the heated glass inclusions that covers the same range as those in the unheated glasses, with exception of two glass inclusions that were heated to a final temperature of 1450 °C and the glass from the mesostasis (Fig. 1), which apparently lost Na at that high T.

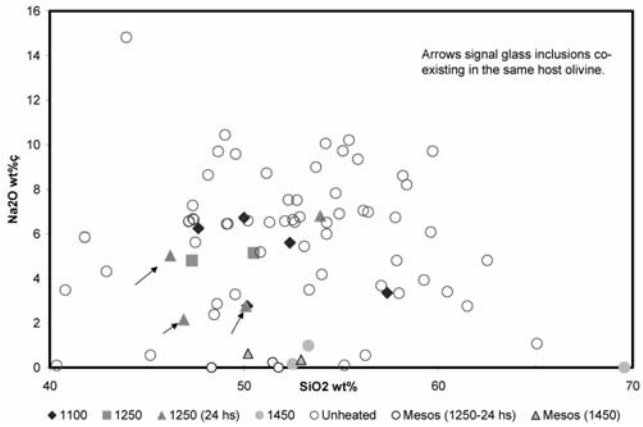

Fig. 1.

References: [1] Sobolev et al. 1976. *Institute of Geology and Geophysics,* Siberian Division of the USSR Academy of Sciences 5:146–149. [2] Clocchiatti R. and Massare D. 1985. *Contributions to Mineralogy and Petrology* 89:193–204. [3] Fuchs et al. 1973. *Smithsonian Contributions to the Earth Sciences* 10:38. [4] Sobolev A. 1996. *Petrology* 4:228–239. [5] Varela et al. 2000. *Meteoritics & Planetary Science* 35:3–52. [6] Zapunny et al. 1989. *Geochemica International* 26:120–128.

5226

SULFIDE-METAL TEXTURAL RELATIONS IN AN EXTENSIVELY MELTED STARDUST GRAIN FROM COMET 81P/WILD-2

M. A. Velbel[1] and R. P. Harvey[2]. [1]Department of Geological Sciences, Michigan State University, East Lansing, MI 48824–1115, USA. E-mail: velbel@msu.edu. [2]Case Western Reserve University, Cleveland, OH 44106–7216, USA.

This paper describes the (TEM-scale) petrography of sulfides and metals in one large and almost completely melted Stardust fragment. The sample described here represents an opportunity to examine in detail petrographic relationships of minerals in the Fe-Ni-S system that co-exist in a single fragment, but that are in many ways representative of the same minerals in a broad range of Stardust grains examined to date [1].

Rounded objects (beads) are very common and widely distributed in this sample as in many other samples [1], ranging in diameter from tens of nanometers or smaller to slightly more than 100 nm. TEM images show both concentrically layered (two-phase) spherical beads and hollow spherical shells strongly resembling the outer shells of the concentrically layered beads. EDS mapping reveals that the cores of concentrically layered spherical objects are dominated by Fe, whereas S appears to be preferentially concentrated in the outer layers of layered spherical beads. SAED patterns indicate FeS (troilite) in some, Fe,Ni metal (taenite) in others. Hollow shells appear identical to shells around cores; cores may have been separated from some shells during ultramicrotomy.

Deviations from simple spherical geometry, although relatively uncommon as a fraction of all occurrences, are especially informative. In some beads with cores and distinct shells of largely uniform thickness, the cores are not spherical. This core morphology suggests that some bead/droplet precursors were not completely melted during particle capture; equant but initially angular grains become rounded (beginning with rounding of edges and corners) if mass- or heat-transfer is rate-determining during dissolution or melting [3]. Compound beads consisting of pairs of Fe-Ni-rich cores connected by bridging material consisting of Fe-S-rich material suggest that the core material separated in a not fully molten state, and that this compound droplet was still in translational (and possibly rotational) motion while the shell material was in a liquid state (still fully molten).

FeS in this Stardust sample is polygenetic. Much FeS in this sample occurs as the outer shells of beads (solidified sulfide/metal droplets), indicating that much stoichiometric FeS in this Stardust particle is thoroughly melted and extensively modified. FeS occurs as unmelted angular-subhedral grains and incompletely melted non-spherical cores of beads (primary cometary FeS; [1]) and as shells/envelopes around rounded Ni-bearing (completely melted) metal and/or (residual primary?) pentlandite cores (secondary, capture-produced FeS). Pentlandite similarly occurs as both a primary preserved precapture mineral (occurring as isolated angular crystals), and as part of partially or completely melted (rounded) grains. The presence of primary Ni-bearing sulfides (pentlandite) and the widespread occurrence of Fe,Ni metal (taenite) cores in most Fe-Ni-S beads formed by melting suggests that Stardust projectile particles contained Ni-bearing sulfides.

References: [1] Zolensky M. E. et al. 2006. *Science* 314:1735–1739. [2] Hörz F. et al. 2006. *Science* 314:1716–1719. [3] Velbel M. A. 2004. *Journal of Geoscience Education* 52:52–59.

5177

WHOLE-ROCK OXYGEN ISOTOPE COMPOSITIONS ARE UNRELATED TO DEGREE OF AQUEOUS ALTERATION IN CM2 CHONDRITES

M. A. Velbel[1], E. K. Tonui[2], and M. E. Zolensky[3]. [1]Department of Geological Sciences, Michigan State University, East Lansing, MI 48824–1115, USA. E-mail: velbel@msu.edu. [2]Department of Earth and Space Sciences, UCLA, Los Angeles, CA, USA. [3]Astromaterials Research & Exploration Science Office, NASA Johnson Space Center, USA.

Introduction: This paper re-examines published whole-rock oxygen isotope data for CM2 chondrites [1], including nine non-Antarctic falls and 25 Antarctic finds, and revisits previously published relationships between whole-rock oxygen isotope compositions and aqueous alteration of CM chondrites [2].

Oxygen Isotope Compositions of Antarctic CM2 Finds: Antarctic CM2 finds and non-Antarctic CM2 falls plot on the same mixing line (slope 0.70) on an oxygen three-isotope plot [1]. If oxygen isotopes of Antarctic CM2 finds were affected by terrestrial weathering, then 1) their pre-weathering compositions would have plotted off the mixing line, and 2) the composition of each Antarctic find would have been shifted from its pre-terrestrial composition, along a line with a slope corresponding to mass-dependent fractionation, to its present composition on the mixing line. Furthermore, this would had to have happened for each Antarctic CM2 on the mixing line, by precisely and only the amount required to move each sample's plot from its pre-terrestrial composition to its measured composition. A simpler scenario is that 1) Antarctic CM2s plot (like their counterpart non-Antarctic CM2 falls) on the mixing line before arrival in Earth's environment, and 2) the oxygen isotope compositions of Antarctic CM2 chondrites [1] are their pre-terrestrial compositions, unmodified by terrestrial weathering.

Oxygen Isotope Composition and Degree of Aqueous Alteration: Non-Antarctic CM2 falls Murray and Murchison, and Antarctic CM2 finds QUE 93005 and ALH 83100, all have nearly identical oxygen isotope compositions [1]. Murchison and Murray are two of the least altered CM2 chondrites known [2]; ALH 83100 [3] and QUE 93005 [4–6] are among the most altered CM2s known. The wide range in degree of alteration exhibited by four CM2 chondrites [2–6] with nearly identical oxygen isotope compositions [1] suggests that oxygen isotopes do not reflect the degree of aqueous alteration of these CM2 chondrites.

Conclusions: Distribution of oxygen isotope compositions of Antarctic CM2 finds and non-Antarctic CM2 falls along the same preterrestrial mixing line on an oxygen three-isotope plot suggests similar (pre-terrestrial) controls on oxygen isotope compositions of both non-Antarctic CM2 falls and Antarctic CM2 finds. Whole-rock oxygen isotope compositions of CM2 chondrites do not reflect mass-dependent effects of pre-terrestrial aqueous alteration, and therefore are not related to other previously suggested measures of aqueous alteration [2].

References: [1] Clayton R. L. and Mayeda T. K. 1999. *Geochimica et Cosmochimica Acta* 63:2089–2104. [2] Browning L. B. et al. 1996. *Geochimica et Cosmochimica Acta* 60:2621–2633. [3] Zolensky M. E. et al. 1997. *Geochimica et Cosmochimica Acta* 61:5099–5115. [4] Rubin A. E. et al. 2007. *Geochimica et Cosmochimica Acta* 71:2361–2382. [5] Velbel M. A. et al. 2005. Abstract #1840. 36th Lunar and Planetary Science Conference. [6] Velbel M. A. et al. 2005. *Meteoritics & Planetary Science* 40: A161.

5172

MICRODENTICLES: AQUEOUS CORROSION TEXTURES ON WEATHERED CHAIN SILICATES AS TERRESTRIAL ANALOGS OF PYROXENE ALTERATION IN MARS METEORITES

M. A. Velbel[1], S. J. Wentworth[2], K. L. Thomas-Keprta[2], A. R. Donatelle[1], and D. S. McKay[3]. [1]Department of Geological Sciences, Michigan State University, East Lansing, MI 48824–1115, USA. E-mail: velbel@msu.edu. [2]ESCG, Mail Code JE23, Johnson Space Center, Houston, TX 77058, USA. [3]Astrobiology Group, NASA-JSC, Houston, TX 77058, USA.

Denticulated margins (also known in older literature as "sawtooth," "cockscomb," or "hacksaw" terminations) are a common feature of pyroxenes and amphiboles, visible in transmitted-light microscopy of grain mounts and thin sections, and by electron microscopy. Denticles are remnants of undissolved material that formerly constituted the walls between elongate etch pits (the characteristic aqueous-dissolution form of chain-silicate minerals) [1], and occur where a grain boundary, transmineral fracture, or dislocation array transects the crystal at a high angle to the z-axis [1]. Denticles occur widely in terrestrial near-surface materials that have experienced low-temperature aqueous alteration, including chemically weathered regoliths, soils in a variety of climatic and geomorphic settings, sediments, and sedimentary rocks [1–5]. Ranges of dissolution forms and dimensions (commonly tens of microns in length) are identical on both pyroxenes and amphiboles in these materials [1–4]. Denticles are much less common on surfaces of chain-silicates altered by aqueous solutions at higher temperatures.

Microdenticles (with lengths in the micron-submicron range rather than tens of microns) are developed on the lateral surfaces of larger "classic" denticles on various naturally weathered amphiboles and pyroxenes from weathered regoliths at several terrestrial localities. Microdenticles share the shape and orientation of the larger, more typical denticles, suggesting similar crystallographic controls on the corrosion process. However, because the elongate pointed forms are on surfaces closer in orientation to prism faces than to (001) termini of the chain silicate crystals, these arrays of microdenticles more closely resemble a surface covered with imbricate pointed scales than a sawtooth margin. The arrays of imbricate microdenticles are formed by aqueous alteration during weathering of chain-silicates; they are later-stage corrosion forms on already corroded surfaces of chain-silicate minerals that show larger-scale evidence of typical weathering [1, 4].

The scaly, imbricate microdenticles on terrestrial chain-silicates are demonstrably formed by low-temperature aqueous alteration (weathering). Furthermore, they are similar in size, shape, and distribution to microdenticles on pyroxenes in several Mars meteorites [5, 6]. These similarities support previous proposals of a low-temperature aqueous origin of microdenticles and related corrosion textures in Mars meteorites [5, 6].

References: [1] Velbel M. A. 2007. In *Heavy minerals in use.* Developments in Sedimentology, vol. 58, edited by Mange M. and Wright D. pp. 113–150. [2] Mikesell et al. 2004. *Quaternary Research* 62:162–171. [3] Schaetzl et al. 2006. *Physical Geography* 27:170–188. [4] Velbel M. A. 1989. *Clays and Clay Minerals* 37:515–524. [5] Wentworth et al. 2005. *Icarus* 174: 382–395. [6] Wentworth et al. 1998. 29th Lunar and Planetary Science Conference. pp. 1793–1794.

5301

DEPTH PROFILING OF GENESIS SOLAR WIND COLLECTORS WITH LASER POST-IONIZATION SNMS

I. V. Veryovkin[1], C. E. Tripa[1], M. R. Savina[1], M. J. Pellin[1], and D. S. Burnett[2]. [1]Materials Science Division, Argonne National Laboratory, Argonne, IL 60439, USA. E-mail: verigo@anl.gov. [2]Division of Geological and Planetary Sciences, California Institute of Technology, Pasadena, CA 91125, USA.

The samples returned to Earth by the Genesis mission of NASA's Discovery Program contain a record of the elemental and isotopic abundances of the solar wind. This record is implanted in the near-surface region of the sample collectors allowing the solar wind material to be distinguished from terrestrial contamination, which occurred due to the abrupt landing of the Genesis spacecraft. At Argonne National Laboratory, we have recently developed a new laser post-ionization secondary neutral mass spectrometer (LPI–SNMS) called SARISA, which is capable of accurate measurements of ultra-trace concentrations of many metallic elements implanted in Genesis solar wind collectors. In this work, we will report results of our measurements of abundances of Mg in two types of such collectors, silicon and diamond-like carbon (film on silicon). These depth profiling measurements were conducted in resonance-enhanced multi-photon ionization (REMPI) regime, in two-color scheme with two Ti-sapphire post-ionization lasers tuned to 285.30 nm and 375.66 nm wavelengths, with the repetition rate of 1 kHz.

To make our analyses quantitative, we used two specially prepared standard reference samples, made from exactly the same materials as the flown Genesis collectors and implanted with a known fluence of 43 keV Mg ions: 2×10^{13} at/cm^2 in diamond-like carbon and 1.1×10^{13} at/cm^2 in silicon. The ^{25}Mg isotope was significantly enhanced in these reference samples in order to help distinguish the implant from any terrestrial surface contamination (where ^{24}Mg has the highest abundance). The measurements of these standards allowed us to characterize the actual efficiency and detection limits of the new SARISA instrument: the useful yield of the instrument peaked at about 20% with a mass resolution of ~2000 and detection limits corresponded to <50 parts per trillion.

We measured concentration versus depth profiles for Mg in solar wind collectors (Si and diamond-like carbon, respectively) and compared them to Mg implant standards. One apparent feature of the solar wind implants was that maximums of their profiles were broad, with apparent diffusion of the implanted atoms towards the surface. Since the Genesis solar wind collectors were subjected in space to intense bombardment by protons and alpha-particles, and solar light heated them to the temperature of ~200 °C for nearly 2 years, this feature can be explained by radiation-enhanced thermal diffusion processes. The total fluences of Mg in solar wind determined from our measurements were: $(2.74 \pm 0.20) \times 10^{12}$ and $(2.46 \pm 0.20) \times 10^{12}$ at/cm^2 for Si and diamond-like carbon collectors, respectively (at 2σ error level). More detailed studies of diffusion processes in these collectors are needed to determine in what extent this minor discrepancy in fluences is caused by losses of the collected material due to processes of diffusion and surface sputtering by solar wind.

Acknowledgements: This work is supported by the U.S. Department of Energy, BES-Materials Sciences, under Contract W-31-109-ENG-38 and by NASA under Work Orders W-19,895 and W-10,091.

5293

EVIDENCE FOR YOUNG JAROSITE PRECIPITATION ON MARS

E. P. Vicenzi[1], M. Fries[2], A. Fahey[3], D. Rost[1, 5], J. P. Greenwood[4], and A. Steele[2]. [1]Department of Mineral Sciences, Smithsonian Institution, Washington, D.C. 20560, USA. E-mail: vicenzie@si.edu. [2]Carnegie Institution of Washington, Washington, D.C., USA. [3]National Institute of Standards and Technology, Gaithersburg, MD, USA. [4]Wesleyan University, Middletown, CT, USA. [5]The Manchester University, Manchester, UK.

Introduction: In recent years both orbital- and ground-based missions have returned data consistent with sulfate mineralization at, or near, the surface of Mars at multiple locations [1–3]. Detailed analysis of the stratigraphy of Burns Cliff at Endurance crater has been interpreted to represent a binary mixture of altered basalt and jarosite-rich sediment deposited some billions of years ago [4, 5]. Because jarosite is stable only under low pH conditions, it is an important environmental indicator mineral. Additionally, the large fraction of structural water in jarosite makes it an ideal target for indirect analysis of the Martian paleo-hydrosphere. We have extended our examination of sulfate alteration in Miller Range 03346 to include veinlet material adjacent to the fusion crust (hereafter FC) of the meteorite.

Methods: An uncoated thin section of MIL 03346 containing fusion crust was examined using a variable pressure FE-SEM, VP X-ray spectral imaging, and Raman imaging. A carbon film was applied prior to magnetic sector negative secondary ion mass spectrometry for hydrogen isotope analysis.

Results: *Electron and Elemental Imagery:* Backscattered electron images reveal at least one vein that truncates the fusion crust, indicating that some aqueous alteration took place in Antarctica. However, the preponderance of secondary mineralization appears metamorphosed by atmospheric heating during descent to Earth. In some cases straight-walled veinlets wither to irregular lens within tens of micrometers of the FC. In other cases, subspherical voids occur between alteration veinlets and the FC. Anhydrite fills some veinlets near the FC, a phase not yet identified within the interior of the meteorite. Finally, sulfate alteration is observed to crosscut silicate alteration veinlets.

Raman Spectroscopy: Scanning vibrational spectroscopy has revealed jarosite-filled veins adjacent to the FC. It is impossible to unambiguously determine if the FC cuts the jarosite as voids occupy the volume between the FC and the jarosite-filled portion of the vein.

Hydrogen Isotopes: Ion microprobe analyses to determine the D/H ratio conducted on jarosite within the interior of MIL 03346 are nonterrestrial and range from 2498 ± 480‰ to 2956 ± 955‰ using both spot analysis and imaging raster modes.

Discussion: On the basis of their nonterrestrial hydrogen isotope ratios, in addition to microtextural information, jarosite in MIL 03346 is clearly Martian in origin. Because the crystallization age of the meteorite is ~1.3 Ga [6], jarosite precipitation must be Amazonian in age, and therefore significantly younger than the earlier (Hesperian) global sulfate mineralization event. The preterrestrial jarosite additionally confirms that older silicate veinlets in MIL 03346 also precipitated beneath Mars.

References: [1] Gendrin A. 2005 et al. *Science* 307:1587. [2] Klingelhöfer G. et al. 2004. *Science* 306:1740. [3] Rieder R. et al. 2004. *Science* 306:1746. [4] Squyres S. W. et al. 2006. *Science* 313:1403. [5] Bibring J.-P. et al. 2006. *Science* 312:400. [6] Shih C.-Y. et al. 2006. 37th Lunar and Planetary Science Conference.

5041

DENSE WATER INCLUSIONS IN FUSED K-Na FELDSPAR GLASSES FROM POPIGAI

S. A. Vishnevsky, N. A. Gibsher, and L. N. Pospelova. Inst. of Geol. & Mineralogy, Novosibirsk, Russia. E-mail: svish@uiggm.nsc.ru.

Introduction: Dense water inclusions were reported earlier in lechatelierite and high-silica glasses from the Popigai suevites and impact fluidizites [1, 2]. The inclusions were trapped at high (0.8–3.3 GPa) residual shock pressures which lasted up to 12 s in time by the action of water buffer [3, 4]. Below are the results of first cryometric and other studies of water inclusions in fused K-Na feldspar glasses from the Popigai megabreccia.

Observations: The glasses are clear, well-outlined schlieren disseminated in tagamite matrix. Following to microprobe data, they have the next composition (in wt%): SiO_2 64.25–65.23, TiO_2 0.03–0.05, Al_2O_3 18.78–19.06, FeO 0.02–0.04, CaO 0.38–0.81, Na_2O 4.44–5.35, K_2O 5.17–7.28, P_2O_5 0.02–0.12, totals 94.6–96.54. The totals are indicative for volatiles. The glasses are saturated with co-genetic fluid inclusions of various phase composition at 20 °C: gaseous (G), gas+liquid with various proportions between (G+L) and entirely liquid (L) ones (see Fig. 1). Following to cryometry, the liquid phase of the inclusions is a water of low to moderate salinity (8.3–13.5 wt% in NaCl-equivalent).

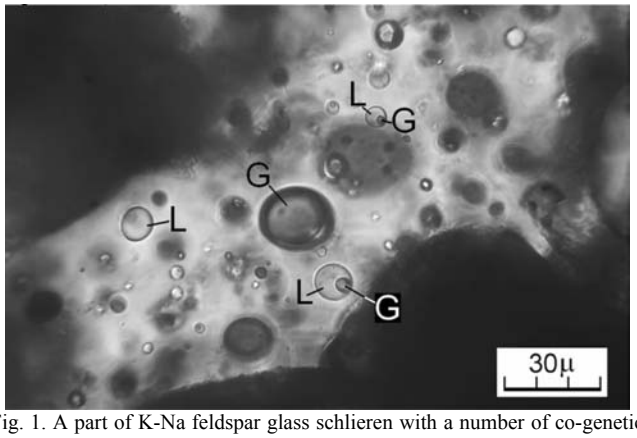

Fig. 1. A part of K-Na feldspar glass schlieren with a number of co-genetic water inclusions of various densities (G, G+L, L).

Interpretation: The solidification temperatures for the glasses studied can range from ~1200 °C ("dry" melting of the feldspars at stage III of shock metamorphism [5]) to ~700 °C ("wet" melting of the feldspars, see mineralogical reference books). So, following to phase diagram of water after [6], the trapping pressure for dense, 0.5–1 g/cm^3, water fluid inclusions in the glasses can range from ~0.2–0.5 GPa (700 °C) to 1.5–2.6 GPa (1200 °C). Any lithostatic variant of such high trapping pressures is excluded, and the data observed are indicative for the action of water buffer delaying the shock pressure release in the Popigai impactites.

References: [1] Vishnevsky S. A. et al. 2005. Abstract #1145. 36th Lunar & Planetary Science Conference. [2] Vishnevsky S. A. et al. 2006. *Russian Geology & Geophysics* 47:711–730. [3] Vishnevsky S. A. and Gibsher N. A. 2006. *Doklady Earth Sciences* 409:981–984. [4] Vishnevsky S. A. et al. 2006. Abstract #1268. 37th Lunar & Planetary Science Conference. [5] Engelhardt W. and Stöffler D. 1968. *Shock metamorphism of natural materials*. Baltimore: Mono Book Corp. pp. 159–168. [6] Juza J. et al. 1986. Proceedings, 10th Internat. Conf. on Properties of Steam. pp. 106–116.

5218

COSMOGENIC NUCLIDES IN IAB IRONS—EXPOSURE AGES AND NOBLE GAS PRODUCTION IN METAL-SHIELDED SILICATES

N. Vogel, I. Leya, and K. Ammon. Institute of Physics, University of Berne, Switzerland. E-mail: nvogel@space.unibe.ch.

Introduction: Cosmogenic nuclides are produced by interactions of cosmic rays with meteoritic target elements. While production rates are well known for most major elements in stony and iron meteorites, those for silicates embedded in metal are scarce due to the difficulty of modeling the influence of the bulk chemical composition on the cosmogenic nuclide production (matrix effect [1]). While large matrix effects have been calculated for the production of ^{21}Ne from Mg (up to 100% higher production compared to chondrites because of larger amounts of secondary neutrons due to high Fe-Ni contents) (e.g., [2]), also distinctly lower ones have been estimated, e.g., for the Chinguetti stony iron [3]. We compare exposure ages deduced from cosmogenic He, Ne, and Ar from the metal and silicate phases of Landes and Ocotillo using literature production rates to test their validity and better constrain the influence of bulk chemistry on cosmogenic nuclide production in IAB irons.

Exposure Ages and Matrix Effects: For exposure age calculation we used ^{21}Ne and ^{38}Ar production rates from [2] and slightly adjusted ^{3}He rates from [4], both taking into account matrix effects. Metal ^{38}Ar ages are most robust with respect to target chemistry and are 160 and 500 Ma for Landes and Ocotillo (both ±15%). They agree well with metal ^{3}He and ^{21}Ne ages and silicate ^{38}Ar ages. Silicate ^{21}Ne and in particular ^{3}He ages are distinctly higher than the metal ages. Presuming identical exposure ages for metal and silicates, the ^{21}Ne production rates, and thus the matrix effects, would need to be even higher than the ones given in [2]. This is in contrast to the results from a "Berne Plot" (^{3}He/^{21}He versus ^{22}Ne/^{21}Ne): the silicate data points of Landes and Ocotillo lie well off the modeled data field adjusted to IAB silicate chemistry, which can be explained by matrix effects of ~15% (assuming only minor effects for ^{3}He).

Conclusions and Outlook: Argon-38 exposure ages for Landes and Ocotillo metal phases are ~160 Ma and ~500 Ma, respectively. The production rates of [2] and [4] yield consistent metal ^{3}He, ^{21}Ne, and ^{38}Ar ages for Landes and Ocotillo. Applying ^{3}He and ^{21}Ne production rates to our silicate inclusions yields distinctly higher ages than those of the metal phases, independent from the silicate chemistry used. This is in contrast to the rather low matrix effects suggested from silicate ^{3}He/^{21}Ne ratios. Therefore, we plan to remodel those production rates including matrix, shielding, and meteoroid size effects. If the discrepancy remains, pre-irradiation of the silicate inclusions needs to be considered. Therefore, the IAB iron meteorite Caddo County with a cosmic-ray exposure age of only ~5 Ma [5] will be included in the study. We also plan to determine ^{36}Cl-^{36}Ar exposure ages, which are largely independent from the above effects and will thus serve as absolute ages, against which the noble gas production rates can be calibrated.

References: [1] Begemann F. and Schultz L. 1988. 19th Lunar and Planetary Science Conference. pp. 51–52. [2] Masarik J. and Reedy R. C. 1994. *Geochimica et Cosmochimica Acta* 58:5307–5317. [3] Welten K. C. et al. 2001. *Meteoritics & Planetary Science* 36:939–946. [4] Leya I. et al. 2004. *Meteoritics & Planetary Science* 39:367–386. [5] Takeda H. et al. 2000. *Geochimica et Cosmochimica Acta* 64:1311–1327.

5107

AUGER ANALYSIS OF PRESOLAR SILICATES IN ACFER 094 AND THE DISCOVERY OF A PRESOLAR CAI

C. Vollmer[1], F. J. Stadermann[2], M. Bose[2], C. Floss[2], P. Hoppe[1], and F. E. Brenker[3]. [1]Max Planck Institute for Chemistry, D-55020 Mainz, Germany. E-mail: cvollmer@mpch-mainz.mpg.de. [2]Laboratory for Space Sciences, Washington University, St. Louis, MO 63130, USA. [3]Geoscience Institute/ Mineralogy, JWG-University, D-60054 Frankfurt, Germany.

Introduction: Mineralogical characterization of presolar silicates is an analytical challenge due to their small size (usually <0.5 μm) and surrounding "normal" silicates. However, such investigations are crucial in understanding formation histories of these grains (e.g., [1]). Transmission electron microscopy (TEM) is typically the method of choice, but preparation of electron transparent lamellae from meteoritic grains is a difficult and time-consuming task (e.g., [2]). Auger spectroscopy provides a promising analytical alternative: elemental information of sub-μm size grains can be obtained with ~10–20 nm resolution without elaborate sample preparation [3]. Here we report on Auger spectroscopy results of presolar silicates in Acfer 094.

Methods: Presolar silicates were identified by NanoSIMS oxygen isotope mapping at MPI for Chemistry in Mainz [4]. Auger analysis was performed at the newly installed Washington University PHI 700 Scanning Auger Nanoprobe. Up to now, only qualitative results are discussed. Elemental abundance estimates are based on relative peak heights, but calibration of sensitivity factors is in progress.

Results: Nine of 31 presolar silicates are Mg-rich, 4 have similar Mg+Fe peak heights, and 12 are dominated by Fe. Whereas the spectra of the Mg-rich silicates are usually very pure, those of the Fe-rich silicates appear more complex with Ca, Al, or S present in some cases. Surprisingly, 5 grains contain only Si and O with little or no Fe. One 650 × 500 nm^2 size grain comprises at least 3 different Ca-Al-rich minerals: it can thus be regarded as the first discovered presolar CAI.

Discussion: Equilibrium condensation theory predicts Mg-rich silicates to condense (e.g., [5]) and about a third of the silicates analyzed here are of such a type. Si-rich grains probably formed in the ejecta of RGB/AGB stars with Mg/Si < 1, an abundance ratio that is observed in ~10% of all stars [5]. Alternatively, this might be a secondary effect as Mg is preferentially removed during interstellar passage [6]. TEM analysis of two Si-rich presolar silicates [2, 7] revealed a similar chemistry (up to 80 mol% SiO_2) though no sputtering features like particle tracks are reported there. Fe-rich presolar silicates could have condensed under nonequilibrium conditions, but this heterogeneity may also be due to secondary alteration (e.g., [7]) or sample contamination. Comparison of O isotopes of the presolar CAI with model calculations suggests that it condensed in the ejecta of a ~1.5 $M_\odot$ red giant with lower-than-solar metallicity. Mineralogical determination of the different subphases is not possible at this moment, but will be the topic of a future TEM analysis.

References: [1] Messenger S. et al. 2005. *Science* 309:737–741. [2] Vollmer et al. 2007. Abstract #1262. 38th LPSC. [3] Stadermann F. J. et al. 2006. Abstract #1663. 37th LPSC. [4] Vollmer et al. 2006. Abstract #1284. 37th LPSC. [5] Ferrarotti A. S. and Gail H.-P. 2001. *Astronomy & Astrophysics* 371:133–151. [6] Bradley J. P. 1994. *Science* 265:925–929. [7] Nguyen A. N. et al. 2007. *The Astrophysical Journal* 656: 1223–1240.

5160

REVISITING THE ELEMENTAL COMPOSITION OF THE ENSTATITE CHONDRITES

J. Wade[1], C. L. Smith[2], S. James[2], A. Verchovsky[1], and M. M. Grady[1, 2]. [1]PSSRI, The Open University, Walton Hall, Milton Keynes, MK6 7AA, UK. E-mail: j.wade@open.ac.uk. [2]Department of Mineralogy, The Natural History Museum, Cromwell Road, London, SW7 5BD, UK. E-mail: c.l.smith @nhm.ac.uk.

Introduction: Enstatite chondrites have often been cited as model precursors for the Earth, based primarily upon stable isotope considerations [1, 2]. On the other hand, it has proven difficult to reconcile their bulk elemental abundances with those of the Earth.

In order to explore any compositional link that the enstatite meteorites may have with other planetary bodies, a good understanding of the range of their compositions is required. Previous work has used a variety of methods to examine the minor and trace element composition of these materials, with individual work often focusing upon either a restricted range of elements and/ or a restricted number of meteorite samples. In addition, the highly reduced nature of the meteorites and the chemical reactivity of some of the meteorite components implies that only samples from falls should be considered for analysis. This, inevitably, makes drawing any conclusions from their bulk compositions somewhat difficult.

Here we present data from a comprehensive range of EH and EL falls, using a quadrupole ICP-MS technique for minor and trace element analysis, together with ICP-AES for the major and minor elements. The aim is to provide an internally consistent data set of compositions for a wide range of elements. In addition, we also present high-resolution C, N, and noble gas isotopic analysis of the bulk materials. Both data sets should allow better constraints to be placed upon both the models of enstatite chondrite formation, and their genetic relationship with other planetary bodies.

References: [1] Javoy M. 1995. The integral enstatite chondrite model of the Earth. *Geophysical Research Letters* 22:2219–2222. [2] Newton J. et al. 2000. The oxygen isotope record in enstatite meteorites. *Meteoritics* 35: 689–698.

5211

A LASER PROBE $^{40}Ar/^{39}Ar$ INVESTIGATION OF TWO MARTIAN LHERZOLITIC BASALTIC SHERGOTTITES

E. L. Walton[1], S. P. Kelley[2], and C. D. K. Herd[1]. [1]Department of Earth & Atmospheric Sciences, University of Alberta, Canada. E-mail: ewalton@ualberta.ca. [2]Department of Earth Sciences, The Open University, Milton Keynes, UK.

Introduction: We report argon isotope analyses of two different Martian shergottites: NWA 1950 and ALH 77005. The results are discussed in the context of the recently rekindled debate surrounding the age of shergottite meteorites (e.g., [1]). A survey of shock generated melts in the thick sections analyzed in this study is given by [2]. Localized melts are a minor component of NWA 1950 (1.8 vol%) compared to the relative abundance in ALH 77005 (up to 30 vol%); the latter exhibits extensive shock melt networks, interconnected melt pockets and highly vesiculated plagioclase glass.

Samples, Methods, and Results: A total of 49 extractions were obtained using an SPI 25W 1090 nm fiber laser focused through a Leica petrological microscope resulting in ~70 μm melt pits. Corrections for mass spectrometer discrimination, irradiation interferences, and cosmogenic ^{36}Ar concentrations have been applied to all argon data following extraction. The coarse size (mm) of minerals and melt pockets in the studied meteorites enabled clean argon extractions (i.e., fusion of a single phase).

NWA 1950: A plot of $^{40}Ar/^{36}Ar$ versus $^{39}Ar/^{36}Ar$ yields a range of apparent ages for igneous minerals (552–2246 Ma), and an isochron age of 382 ± 36 Ma, derived from 11 of the lowest points. Argon extractions from a large melt pocket are well distinguished from those of the minerals, exhibiting $^{40}Ar/^{36}Ar$ ratios in the range 1260–1488, yielding apparent ages of 3303–6920 Ma. Assuming ejection from the same area of the Martian subsurface [3], the radiometric ages obtained by Rb-Sr and Sm-Nd for ALH 77005 (185 ± 11 Ma and 173 ± 6 Ma; [4]) can be used for comparison with ages obtained in this study for NWA 1950.

ALH 77005: Argon isotope data is scattered on a plot of $^{40}Ar/^{36}Ar$ versus $^{39}Ar/^{36}Ar$ and does not yield an isochron. Melt pockets have high $^{40}Ar/^{36}Ar$ ratios (1600–2000), while unmelted igneous minerals possess low $^{40}Ar/^{36}Ar$ ratios (~300); olivine containing melt vein networks form a mixing array between the two. Apparent ages for individual laser spot extractions are 373–8108 Ma.

Discussion: The data appear to shed light upon the debate over the crystallization ages of shergottites. The equilibration shock pressure of NWA 1950 (~35 GPa) is less than that of ALH 77005 (>45 GPa; [5]) which experienced a post-shock temperature increase of 800 ± 200 K [5]; NWA 1950 yields younger and more reproducible ages. Although some excess argon is present in the igneous minerals of NWA 1950, apparent and isochron ages approach Rb-Sr and Sm-NdG ages. As in earlier analyses, high ages are focused in shock-melted pockets and not in the unmelted minerals. In contrast, the highly shocked and melted ALH 77005 exhibits ages ranging up to, and older than, our solar system. These observations are consistent with young crystallization ages for shergottite meteorites. Based on our careful study of microstructures associated with shock, the best explanation for apparently old Ar-Ar ages is incorporation of atmospheric argon during impact on the Martian surface.

References: [1] Bouvier A. et al. 2005. *Earth and Planetary Science Letters* 240:221–223. [2] Walton E. L. and Herd C. D. K. 2007. *Meteoritics & Planetary Science* 42:63–80. [3] Gillet Ph. et al. 2005. *Meteoritics & Planetary Science* 40:1175–1184. [4] Borg L. E. et al. 2002. *Geochimica et Cosmochimica Acta* 66:2037–2053. [5] Fritz J. et al. 2005. *Meteoritics & Planetary Science* 40:1393–1411.

5176

NANOSIMS MEASUREMENTS OF SOLAR WIND Mg, Fe, AND Cr FLUENCES

J. Wang[1], L. R. Nittler,[1] and D. S. Burnett[2]. [1]Department of Terrestrial Magnetism, Carnegie Institution of Washington, Washington, D.C. 20015, USA. E-mail: jwang@dtm.ciw.edu. [2]Geological and Planetary Sciences, Caltech, Pasadena, CA 91125, USA.

Introduction: The chemical composition of the Sun provides the reference standard for a wide variety of astronomical, cosmochemical, and geochemical studies. To better determine the solar composition, the Genesis spacecraft collected solar wind at the L1 point in the space for 27 months prior to returning samples to Earth in September 2004. Prior ion probe analyses of Genesis samples have found discrepant results for the Mg and Fe solar wind fluences from different collector materials [1]. We report measurements of Mg, Fe, and Cr depth profiles in Genesis diamond-like C sample 60062 using the Carnegie Institution Cameca NanoSIMS 50L ion microprobe. Our results for Mg and Fe are similar to previous analyses of the same sample using different instruments.

Experimental: The very high primary beam density of the NanoSIMS allows smaller craters to be analyzed compared to the IMS 6f and IMS 1270 ion probes used for previous work. For this study, a 4 nA –16kV O^- primary beam of about 2 μm in diameter was rastered at 25 × 25 μm^2 on the sample surface with positive secondary ions extracted from the central 25% of the rastered area. Masses ^{12}C, ^{24}Mg, ^{25}Mg, ^{52}Cr, ^{54}Fe, and ^{56}Fe were measured simultaneously to a depth of about 500 nm from the surface. ^{25}Mg and ^{54}Fe implanted standards were measured before, after, and in between sample analyses to quantify relative fluences. Since no Cr implant standard was available at the time of our analyses, we used the relative sensitivity factors in diamond reported by [2] to quantify Cr fluences. We analyzed 10 craters with one showing abnormally low ^{12}C count rates and thus excluded. One crater showed significant surface contamination of Fe and no Fe data could be deduced.

Results: We found an Mg fluence of $4.33 \pm 0.26 \times 10^{12}$ cm^{-2} and an Fe fluence of $2.39 \pm 0.15 \times 10^{12}$ cm^{-2} for sample 60062. These are in good agreement with previous measurement of the same samples by IMS 6f [1]. As seen before, the fluences derived from diamond-like C are higher than those from Si collectors; an explanation for this discrepancy is still lacking but the results from Si are preferred. Based on three ^{52}Cr depth profiles, we estimated a Cr fluence of 2.2×10^{11} cm^{-2}. This value is about seven times higher than that found in Si by [1]. However, surface contamination for this sample is apparently a contributing factor. The $^{25}Mg/^{24}Mg$ ratios derived from the profiles are slightly elevated (by up to ~10%) compared to the terrestrial value, probably indicating a large contribution of MgH to the ^{25}Mg signal in the flight sample. Further measurements at higher mass resolution will provide more accurate isotopic abundances. Analyses of additional elements and collector materials also will be conducted to get more accurate data of the solar wind composition and to understand differences between different collector materials.

Acknowledgements: This work is supported by NASA grant NNX07AG19G.

References: [1] Burnett D. S. et al. 2007. Abstract #1843. 38th Lunar and Planetary Science Conference. [2] Wilson R. G. 1997. *International Journal of Mass Spectrometry and Ion Processes* 143:43–49.

5313

SEM-PETROGRAPHY OF OSTENSIBLY ANCIENT NORTH RAY CRATER LUNAR IMPACT-MELT ROCKS

P. H. Warren[1], D. J. Taylor[2], S. de Leuw[1, 2], M. Cosarinsky[2], B. E. Schmidt[2], K. Dyl[2], and E. Spengler[2]. [1]Institute of Geophysics and Planetary Physics, University of California, Los Angeles, CA 90095, USA. [2]Department of Earth & Space Sciences, University of California, Los Angeles, CA 90095, USA.

Lunar polymict impactite samples have yielded ages that strongly cluster near 3.9 Ga, especially for impact-melt breccias. This curiously unimodal age spectrum clearly indicates that the rate of cratering (i.e., collisions between the Moon and asteroids and comets) was vastly higher ~3.9 billion years ago than it has been over the last 85% of solar system history. The bombardment history before 3.9 Ga, however, has been controversial. The relative scarcity of ages >3.9 Ga has led many to infer a spike in the global lunar cratering rate at ~3.9 Ga, i.e., the lunar "cataclysm" hypothesis [1]. Do the clustered ~3.9 Ga ages reflect a bump or inflection on a basically monotonic decline in the late-accretionary impact rate, or a large-factor and global spike?

The age of the Nectaris basin is key. On photogeologic-stratigraphic grounds, Nectaris is clearly older than Imbrium and Serenitatis; and two-thirds of the Moon's still-recognizable basins appear even older than Nectaris [2]. Impact-melt breccias (IMBs) of Nectaris origin are presumably present among the Apollo 16 samples. Ar ages for Ap-16 IMBs largely cluster from 3.87–3.92 Ga, and 3.90–3.92 Ga is often assumed to be the age of Nectaris (e.g., [1, 2]). However, there are reasons to doubt the proposed linkage between these common Ap-16 IMBs and Nectaris. Compared to the Ap-16 site, the Nectaris region is greatly depleted in incompatible elements; the ~3.9 Ga age IMBs are incompatible-rich [3]. The typical siderophile-element pattern of the ~3.9 Ga age IMBs features the same distinctively high Au/Ir typical of Ap-14, Ap-15, and Ap-17 IMBs, albeit the regoliths at these sites contain very minor debris from Nectaris in comparison to Imbrium and Serenitatis (to accept the cataclysm hypothesis, must we also assume a uniform source of impactor asteroids?).

A more direct challenge to the proposed ~3.9 Ga age for Nectaris stems from ~15 Ar ages reported for small rocks from the two Ap-16 North Ray crater sampling stations. We have used SEM and *e*-probe techniques to better constrain the impact-melting, brecciation, and thermal evolution of 12 such rocklets with reported age (after correction to modern decay constants) ≥4.03 Ga. Previous petrographic descriptions of these samples have ranged from brief [4] to both brief and nonspecific [5, 6], and none have utilized SEM. Some of these pre-4.03 Ga North Ray crater rocks are plausibly interpreted as true pre-"cataclysm" impact products; most are (at least individually) dubious. As an example of the utility of SEM, we readily noted that most of the "feldspathic fragment-laden" IMBs [6] contain reverse-zoned plagioclase relicts, with very sharp boundaries between the Ab-rich core and the rim. The scale of these rims is consistent within each IMB, and affords a constraint on the degree to which CaAl-NaSi interdiffusion (vastly slower than Ar diffusion) managed to equilibrate the relict feldspars with the melt-derived groundmass.

References: [1] Tera F. et al. 1973. 9th Lunar and Planetary Science Conference. [2] Wilhelms D. E. 1987. The Geologic History of the Moon. USGS Prof. Paper #1348. 302 p. [3] Warren P. H. 2003. Abstract #4129. Third International Conference on Large Meteorite Impacts. [4] Delano J. W. and Bence A. E. 1977. 8th Lunar Science Conference. [5] Mauer P. et al. 1978. *Geochimica et Cosmochimica Acta* 42:1687–1720. [6] James O. B. 1981. *PLPSC* 12:209–233.

5259

ISOTOPIC EVIDENCE OF TEKTITE FORMATION FROM LOESS

John T. Wasson[1] and Klaus Mezger[2]. [1]Univ. California, Los Angeles, CA 90095–1567, USA. E-mail: jtwasson@ucla.edu. [2]Univ. Münster, DE-48149, Münster, Germany.

Introduction: Tektites are a special class of impact product. They are essentially free of unmelted grains, they contain ^{10}Be at levels expected in local soils [1], and the layered tektites appear have formed by the flow of a melt sheet [2]. To account for the ^{10}Be and the efficient melting, Wasson [2] suggested that tektites formed by in situ melting of loess, perhaps by a Tunguska-like aerial burst. From a region in NE Thailand we collected tektites, soil, and basalts; in this region all tektites are layered.

The Australasian tektites are the youngest (0.8 Ma) and most abundant. Loess is deposited over much of the continents during glaciations. Because Australasian tektites were formed 4 ka after glacial maximum 20.2 when ice volumes were still high [3], loess deposits should have been present. Loess is expected to show minor compositional variations (e.g., in Sr and Nd isotopic compositions) associated with local sources and differences in the degrees of weathering. Although current soils are associated with a more recent glaciation, sources and spatial distributions were probably similar.

Results and Discussion: We determined Sr and Nd isotopic compositions for 9 tektites from locations ranging from the Ban Song (14.51 N, 104.97 E) to Ban Huai Sai (14.89 N, 105.46 E), a distance of about 67 km. We also analyzed four basalts (emplaced about 1 Ma ago) from a small area close to Ban Song and three soils from different parts of the field area. Soils from the plains were highly weathered with high contents of coarse quartz; those from a sloping location at the NE end of the field included fine fragments of pyroxene and plagioclase.

The ranges in Sr and Nd isotopic compositions in the tektites are small. The ^{143}Nd/^{144}Nd ratios are 0.51206 within a sampling uncertainty (1σ) of about 0.00001. The ^{87}Sr/^{86}Sr ratios show a resolvable range across the field ranging from about 0.7203 at Ban Song to 0.7182 at Huai Sai. Sampling uncertainties (1σ) appear to be about 0.0003.

The four basalts had uniform ^{87}Sr/^{86}Sr ratios of 0.70376 and ^{143}Nd/^{144}Nd ratios of 0.51287. Because the 87/86 ratios are far lower than those in the nearby Ban Song tektites, it is clear that there is no basaltic component resolvable in the tektites.

Soil 87/86 ratios range from 0.7126 (most weathered) to 0.7171 (least weathered). It is possible that, prior to weathering in the latter sample, the Sr ratio was similar to that in local tektites. Because we obtained only one 143/144 ratio, 0.51223 in the least weathered soil, we cannot assess Nd weathering trends.

In summary, the uniform Nd and the small variations in Sr are consistent with the origin of the tektites from loess. The Sr variations are not the result of contamination by recent basalts. They may result from soil weathering, but because the opposite geographic trend is observed in our soils, other sources must also be investigated. A carbonate component similar to that in N. Chinese loess (87/86 ~0.710; [4]) might also be present.

References: [1] Ma P. et al. 2004 *Geochimica et Cosmochimica Acta* 68:3883. [2] Wasson J. T. 2003. *Astrobiology* 3:163. [3] Wasson J. T. and Heins W A. 1993. *Journal of Geophysical Research* 98:3043. [4] Jahn B.-M. et al. 2001. *Chemical Geology* 178:71.

5255

MATRIX COMPOSITIONS IN CR CHONDRITES

John T. Wasson and Alan E. Rubin. Univ. California, Los Angeles, CA 90095–1567, USA. E-mail: jtwasson@ucla.edu.

Introduction and Experimental: The origin of the nebular fine fraction is poorly understood. Some have proposed that it preserves the record of presolar materials [1], others that it is largely the product of evaporation and recondensation in the solar nebula [2]. These end models lead to different expectations: uniform compositions for presolar fines, variable compositions for recycled fines.

Because CR chondrites are relatively primitive (no thermal metamorphism, minor aqueous alteration), have large chondrules and have large amounts (~30 vol%) of matrix, they are well-suited to provide important clues about the formation and evolution of the nebular fine fraction at the CR location. We used the electron microprobe (with a 3 μm beam) to make BSE images and to determine the concentrations of 10 elements in 9 rectangular matrix patches ranging from 45 to 60 μm on a side (grids of 6 × 6, 7 × 7, or 8 × 8 points) in the well-preserved CR chondrite LAP 02342. An advantage of this approach compared to broad-beam analysis is that we could develop compositional criteria for eliminating anomalous points (e.g., those with excessive amounts of a mineral phase or low totals). The fraction of points discarded was typically ~20%. We do not discuss data for two patches where we discarded ~50% of the points. We confirmed that the data are reproducible by analyzing grids on the same patches on separate days. Even easily volatilized elements such as K showed the same (relatively high) contents in duplicate runs. In two patches about half the points had high Ca and low totals implying secondary carbonates; it appears that Ca mobilization occurred at an early stage of aqueous alteration.

Results and Discussion: Of special interest was the S content of the matrix. In CR chondrites the fraction of S associated with chondrules (interior or exterior) is low [3]. We measured 3.4 mg/g S in the matrix, and estimate that this accounts for 80% of the S in the whole rock.

Even though we have discarded anomalous points, we find that matrix compositions tend to vary from one patch to the next. For some elements and ratios the means are resolvable at confidence limits >95%. We observed differences in S/Fe ratios and in Mg/Si ratios. The simplest model to explain these variations is that the fine nebular fraction was clumpy, and that each parcel had a unique history. We observe these variations on scales of millimeters within the meteorite, even in areas adjacent to the same chondrule. This suggests that bulk compositional differences occur on a small (centimeter to meter) scale in the solar nebula. This interpretation is consistent with production of fines together with chondrules in small events, but inconsistent with fines preserving a history of the nebula that predates chondrule formation. The compositional variations may reflect a clumpiness in the distribution of phases vaporized during small-scale chondrule-forming events.

References: [1] Alexander C. 2005. *Meteoritics & Planetary Science* 40:943. [2] Wasson J. T. and Trigo-Rodríguez J. M. 2005. Abstract #3043. 36th Lunar and Planetary Science Conference. [3] Weisberg M. et al. 1993 *Geochimica et Cosmochimica Acta* 57:1567.

5288

PETROLOGY OF MATRIX IN THE SEMARKONA ORDINARY CHONDRITE

M. K. Weisberg[1, 2], D. S. Ebel[2], and H. C. Connolly Jr.[1] [1]Department of Physical Sciences, Kingsborough College, City University of New York, Brooklyn, NY 11235, USA. E-mail: mweisberg@kbcc.cuny.edu. [2]Department of Earth and Planetary Sciences, American Museum of Natural History, New York, NY 10024, USA.

Introduction: The origin of chondrite matrix, its constituents, and its relationship to chondrules and refractory-rich inclusions are poorly understood. Early work showed ordinary chondrite matrix to be a complex mixture of olivine, pyroxene, and feldspathic components (e.g., [1]). Mn-rich forsterite (LIME olivine) has been identified in the matrix of Semarkona [2]. We are particularly interested in Mn-rich forsterite because it is a ubiquitous component of many primitive materials including matrix, amoeboid olivine aggregates (AOAs), interplanetary dust particles (IDPs), and comet samples [2–4]. However, its morphology, textural setting, and associated phases are not well documented. These issues led us to initiate a study of the matrix in primitive meteorites. Here we present the preliminary results of our petrologic survey of matrix in Semarkona, the least equilibrated ordinary chondrite. Our goals are to survey and characterize the material interstitial to the chondrules and fragments in a thin section of Semarkona, and decipher the origins of matrix constituents.

Results: We focused on regions between two or more sharply bound, adjacent chondrules. The matrix is a mixture of components that include 1) isolated mineral grains, 2) fluffy (porous) fine-grained (<1 μm) aggregates, 3) fragments with igneous textures, and 4) rare microchondrules. Some of the fragments have textures that suggest that they are chondrule fragments. The isolated grains are dominantly olivine but include low-Ca pyroxene. Olivine morphologies include irregularly shaped, euhedral, tabular, and lath-shaped crystals. The 13 olivine grains that were analyzed show a wide compositional range from Fa_{1-39}, with (wt%) 0.1–1.2 MnO and 0.1–0.5 Cr_2O_3. Included are two low-iron, Mn-enriched (LIME) olivine grains, having (wt%) MnO and FeO, respectively, of 1.0 and 3.0 in one grain and 0.6 and 1.0 in the other. Na occurs in small (50 μm) fragments that are intergrowths of olivine, high-Ca pyroxene, and a material with 76.1 SiO_2, 7.6 Al_2O_3, and 6.1 Na_2O. The microchondrules are 50 μm in size and contain olivine phenocrysts in a glassy mesostasis.

Discussion and Conclusions: The matrix of Semarkona is a highly unequilibrated mixture of solar system materials, both primitive and processed. Presolar grains are also present (e.g., [5]). Some of the matrix has suffered hydrothermal alteration [6], but much of it appears to be pristine. We are currently working to characterize and decipher the origins of matrix materials. Some of the matrix material, such as Mn-rich (LIME) olivine, has been interpreted to be a nebular condensate (e.g., [2]). The occurrence of this primitive material in chondrites, IDPs, and comet samples suggests a close relationship between the silicates that accreted to form asteroids and comets.

References: [1] Scott E. R. D. et al. 1984. *Geochimica et Cosmochimica Acta* 48:1741–1757. [2] Klöck W. et al. 1989. *Nature* 339: 126–128. [3] Weisberg M. K. et al. 2004. *Meteoritics & Planetary Science* 39:1741–1753. [4] Zolensky M. E. et al. 2006. *Science* 314:1735–1739. [5] Huss G. R. and Lewis R. S. 1999. *Geochimica et Cosmochimica Acta* 59: 115–160. [6] Hutchison R. et al. 1987. *Geochimica et Cosmochimica Acta* 51:1875–1882.

5282

THE COMPLEX EXPOSURE HISTORY OF FRO 97013, A UREILITE WITH A VERY SHORT TRANSFER TIME FROM PARENT BODY TO EARTH

K. C. Welten[1], L. Franke[2], U. Ott[2], M. W. Caffee[3], and K. Nishiizumi[1]. [1]Space Sciences Laboratory, University of California, Berkeley, CA 94720, USA. E-mail: kcwelten@berkeley.edu. [2]MPI für Chemie, Postfach 3060, 55020 Mainz, Germany. [3]PRIME Laboratory, Purdue University, West Lafayette, IN 47907, USA.

Introduction: Based on cosmogenic radionuclides in 11 small Antarctic ureilites from the Frontier Mountain stranding area, we previously proposed that 9 of these represent a small and heterogeneous ureilite shower, while two others (FRO 97013 and 01030) represent two independent falls [1]. The low ^{10}Be and ^{26}Al concentrations in FRO 97013 suggested that this meteorite either has a cosmic-ray exposure (CRE) age of ~1 Myr or was exposed under very high shielding conditions [1]. The purpose of this work is to constrain the CRE history of FRO 97013, FRO 01030, and the FRO ureilite shower.

Experimental: We measured noble gases in FRO 97013, 01030, and the paired ureilites FRO 90036/90054 as described previously [1]. We determined the cosmogenic ^{3}He, ^{21}Ne, and ^{22}Ne components and used the chemical compositions determined in [1] to calculate the noble gas production rates, using equations proposed in [2]. In addition to previous measurements of cosmogenic ^{10}Be, ^{26}Al, and ^{41}Ca [1], we also measured ^{36}Cl in these ureilites.

Results and Discussion: Cosmogenic ^{3}He and ^{21}Ne in FRO 90036/ 90054 yield an average CRE age of 8.7 ± 1.0 Myr, while FRO 01030 shows an age of 4.7 ± 1.2 Myr. These ages are consistent with the concentrations of ^{10}Be and ^{26}Al, which indicate near-saturation levels [1]. However, the low ^{10}Be and ^{26}Al concentrations and low cosmogenic ^{22}Ne/^{21}Ne ratio (~1.05) in FRO 97013 all indicate that its CRE history was dominated by 2π irradiation at a depth of ~150 g/cm^2 on the ureilite precursor body (UPB) rather than by 4π irradiation as a small object in space. In addition, the low ^{26}Al/^{10}Be ratio of ~2.2 constrains the 4π irradiation time to <0.1 Myr. In this scenario, the elevated ^{41}Ca concentration of 30 dpm/kg [Fe] must also be a remnant of the first-stage irradiation, yielding a significant contribution of neutron-capture ^{41}Ca, which is only produced at high shielding. Based on a first-stage irradiation depth of ~150 g/cm^2 on the UPB, a second stage of <0.1 Myr as a small object, and neutron-capture ^{41}Ca depth profiles for 2π irradiation [3], the ^{41}Ca concentration yields a terrestrial age of ~125 kyr. This CRE scenario suggests that the FRO 97013 precursor body is (or was) in a favorable location to deliver collisional fragments to Earth. In addition, we note that the ejection age of ~0.2 Myr for FRO 97013 coincides with one of the main peaks in the CRE age distribution of CM2 chondrites [4, 5]. Although the range of CRE ages of ureilites (0.1–50 Myr) is similar to that of ordinary chondrites and HED meteorites, this work corroborates the trend that >60% of the ureilites have CRE ages <10 Myr [6].

Acknowledgments: We thank L. Folco for providing the ureilite samples. This work was supported by NASA grant NNG-06GF22G.

References: [1] Welten K. C. et al. 2006. Abstract #2391. 37th Lunar and Planetary Science Conference. [2] Eugster O. 1988. *Geochimica et Cosmochimica Acta* 52:1649–1662. [3] Nishiizumi K. et al. 1997. *Earth and Planetary Science Letters* 148:545–552. [4] Nishiizumi K. et al. 1993. 24th Lunar and Planetary Science Conference. pp. 1085–1086. [5] Nishiizumi K. and Caffee M. W. 2002. *Meteoritics & Planetary Science* 37:A109. [6] Rai V. K. et al. 2003. *Geochimica et Cosmochimica Acta* 67:4435–4456.

5304

CONSTRAINING THE COMPLEX EXPOSURE HISTORY OF JIDDAT AL HARASIS 073, A LARGE L6 CHONDRITE SHOWER FROM OMAN

K. C. Welten[1], L. Huber[2], M. W. Caffee[3], K. Nishiizumi[1], and I. Leya[2]. [1]Space Sciences Laboratory, University of California, Berkeley, CA 94720, USA. E-mail: kcwelten@berkeley.edu. [2]Physikalisches Institut, University of Bern, Switzerland. [3]PRIME Laboratory, Purdue University, West Lafayette, IN 47907, USA.

Introduction: While complex cosmic-ray exposure (CRE) histories are rare among small- to medium-size chondrites, more than 50% of the large (meter-size) chondrites show complex histories. In 2002, a large L6 chondrite strewn field, Jiddat al Harasis (JaH) 073, was discovered in Oman [1]. This well-documented strewn field covers an area of ~60 km^2 and contains ~3400 fragments with a total mass of ~600 kg. Based on the factor of ~10 variation in ^{21}Ne [2] and up to 50% variation in ^{26}Al/^{10}Be ratios [3], we proposed a complex exposure history with a second stage of <1 Myr. To constrain the CRE history in more detail, we now present a combined data set of cosmogenic radionuclides and noble gases in nine strewn-field fragments and the main mass (~52 kg).

Experimental Methods: We measured concentrations and isotopic compositions of He, Ne, and Ar in 29 aliquots of 16 different samples, including 7 samples of the main mass. For cosmogenic radionuclide analyses we first removed terrestrial weathering products by leaching with 6N HCl and then measured ^{10}Be, ^{26}Al, and ^{41}Ca in 10 samples. Concentrations of ^{10}Be and ^{26}Al were measured at PRIME Laboratory [4], those of ^{41}Ca at LLNL [5].

Results and Discussion: Since the radionuclide data indicate a first-stage exposure >5 Myr on the parent body, followed by a second exposure of 0.5–1.0 Myr as a large object in space [3], the factor of 10 variation in ^{21}Ne mainly reflects differences in shielding depth on the parent body. Based on model calculations for 2π irradiation [6], we estimate that the most and least shielded samples (#592 and #664, respectively) were vertically ~125 cm apart. From the concentrations of neutron-capture 41Ca and neutron-capture depth profiles [7], we estimate that #592 and #664 were 5 and 20 cm, respectively, from the pre-atmospheric surface. We thus calculate a pre-atmospheric diameter of ≥150 cm.

All JaH 073 samples show elevated ^{36}Ar/^{38}Ar ratios due to the presence of trapped atmospheric Ar and "neutron-capture" ^{36}Ar (from radioactive decay of neutron-capture produced ^{36}Cl). To determine the contribution of neutron-capture ^{36}Ar, we assumed a constant cosmogenic ^{21}Ne/^{38}Ar ratio of 9, which takes into account that 10–15% of the cosmogenic ^{38}Ar was lost during oxidation of the metal [7, 8]. We thus derive neutron-capture ^{36}Ar contents (in 10^{-8} cm^3 STP/g) of <0.1 to 1.6. The profile of neutron-capture ^{36}Ar versus ^{21}Ne constrains the burial depth of JaH 073 to ~20 cm and the first-stage CRE age of JaH 073 to ~65 Myr assuming 2π exposure.

Acknowledgments: We thank B. Hofmann for providing the JaH 073 samples. This work was supported by a NASA grant.

References: [1] Gnos E. et al. 2003. *Meteoritics & Planetary Science* 38:A31. [2] Huber L. et al. 2006. Abstract #1628. 37th Lunar and Planetary Science Conference. [3] Welten K. C. et al. 2006. *Meteoritics & Planetary Science* 41:A187. [4] Sharma P. et al. 2000. *Nuclear Instruments and Methods in Physics Research B* 172:112–123. [5] Davis J. et al. 1990. *Nuclear Instruments and Methods in Physics Research B* 52:269–272. [6] Leya I. et al. 2001. *Meteoritics & Planetary Science* 36:1547–1561. [7] Welten K. C. et al. 2001. *Meteoritics & Planetary Science* 36:301–317. [8] Welten K. C. et al. 2003. *Meteoritics & Planetary Science* 38:157–173.

5302

SYNCHROTRON-BASED ORGANICS AND MINERALOGICAL SURVEY OF THREE STARDUST TRACKS

A. J. Westphal[1], S. Bajt[2], A. L. Butterworth[1], S. Fakra[3], Z. Gainsforth[1], M. A. Marcus[3], M. C. Martin[3], C. J. Snead[1], and T. Tyliszczak[3]. [1]SSL, UC Berkeley, USA. E-mail: westphal@ssl.berkeley.edu. [2]Lawrence Livermore National Laboratory, USA. [3]Lawrence Berkeley Laboratory.

Introduction: Wild-2 particles captured in the Stardust cometary dust collector exhibit remarkable diversity between and within individual particle tracks in aerogel. Several particles studied during the Stardust preliminary examination are, so far, unique in the collection [1]. There is an urgent need to survey particles in tracks and to target specific particles for extraction and destructive analysis. Here we describe an in aerogel survey at the Advanced Light Source (LBNL) of three tracks using synchrotron-based Fourier transform infrared spectroscopy (FTIR), microbeam X-ray fluorescence (μXRF), X-ray absorption near-edge spectroscopy (μXANES), X-ray diffraction (XRD), and scanning transmission X-ray microscopy (STXM).

Sample Preparation: We extracted three tracks from aerogel tile 38 in aerogel keystones [2], and initially mounted them on polysilicon micropickleforks. These tracks, named Chiquita (103), Siria (104), and Hebe (105) were ~300, ~1300, and ~2400 μm long, respectively. After FTIR and initial XRF mapping (below), 50 μm thick wafers were taken from near the tops of Siria and Hebe for subsequent STXM work. The remainders of the keystones were flattened onto 6 μm thick polypropylene film [2].

FTIR: FTIR mapping of keystones was done in transmission mode using FTIR 1.4.3. These keystones showed no evidence of the "labile organics" reported for other Stardust tracks [3].

X-Ray Microbeam Analysis: We made detailed XRF maps of tracks in the flattened keystones on ALS μXAS 10.3.2 for major elements with Z > 16. We did XANES and XRD analysis on hot spots in Ca, Cr, Mn, Fe, and Ni.

STXM: We mapped wafers from the mouths of Siria and Hebe for Mg and Al at ALS STXM 11.0.2 at 125 nm resolution, and on selected regions did Mg K-, Al K-, and Fe L-edge XANES mapping at 25 nm resolution. We also did CNO-XANES at ALS STXM 5.3.2 on the Siria wafer.

Track Surveys: The two terminal particles of Chiquita were consistent with Fe metal and a sulfide. Numerous small Mn-rich particles were found in the bulb. The terminal particle of Siria is a Cr-, Mn-rich mineral with a Fe-XANES spectrum consistent with orthopyroxene. The Siria wafer contained tens of Mg-rich particles up to 1 μm diameter in 6 distinct regions. From O-XANES we measured a density of 25 ± 1 mg cm^3 for the background aerogel, rising to 43 mg cm^3 in the track wall. More than 50% of the analyzed Fe hot-spots in Hebe were consistent with sulfides, but other identified phases were glass, metal, and olivine. Hebe shows a strong longitudinal gradient in Ni/Fe. Particle heterogeneity was evident: Mg-K XANES imaging revealed a 400 nm olivine within several Fe-rich spots in a 2 μm region. All three tracks were poor in Ca-bearing minerals. One particle in Hebe was K-rich, and several others were elevated in Se. We find strong heterogeneity between tracks, within tracks and within particles.

Acknowledgments: This work was partially supported by the U.S. DOE at LLNL under contract no. W-7405-Eng-48.

References: [1] Zolensky M. E et al. 2006. *Science* 314:1735. [2] Westphal A J. et al. 2004. *Meteoritics & Planetary Science* 39:1375. [3] Sandford S. et al. 2006. *Science* 314:1720.

5115

SIMULATING THE ORGANIC AND VOLATILE CONTRIBUTIONS TO PLANETARY SURFACES AND ATMOSPHERES FROM EXTRATERRESTRIAL DUST

R. C. Wilson, V. K. Pearson, D. C. Turner, G. H. Morgan, I. A. Franchi, I. P. Wright, and I. Gilmour. Planetary and Space Sciences Research Institute, Open University, Milton Keynes, UK. E-mail: r.c.wilson@open.ac.uk.

Introduction: Extraterrestrial dust particles (EDPs) experience aerodynamic breaking upon atmospheric entry, subjecting particles to flash heating. At the predicted entry heating temperatures [1], EDP volatiles and organics will be evaporated [2, 3] and deposited into the Earth's atmosphere [4, 5] and surface, thus contributing to the global inventory of organic species.

Detailed analysis of meteoritic organics has been hindered by the lack of sensitivity of conventional GC-MS methods. Py-GCxGC-TOFMS is well suited to extraterrestrial sample analysis as very small samples can be pyrolyzed (<1 mg). The GCxGC system can separate species that co-elute on a conventional GC-MS while the TOFMS allows increased sensitivity across the whole mass range. This approach has been used to simulate the flash-heating event experienced by EDPs upon atmospheric entry, and to identify the nature of vaporized species.

Experimental Techniques: Samples were flash heated using a Pyrola 2000 Filament Pulse Pyrolyser (Pyrolab, Sweden), as described previously [6], at temperatures comparable to those modeled by Love and Brownlee (1991). Offline flash heating was repeated until 10 mg of each residue was collected for evolved gas analysis. Additional pyrolysis experiments were repeated online coupled to a Pegasus 4D GCxGC-TOFMS (LECO, Corporation), allowing characterization of volatile-organic and high molecular weight organic components evaporated during simulations.

Results: We have been able to successfully identify, and in part quantify, volatiles and organics released during these simulations. Liberated organics include a range of aliphatic and aromatic species [6]. In particular, aliphatic and aromatic alcohols, carboxylic acids, nitrogen containing compounds (amino acid derivatives, amines, amides, nitriles and nitrogen and sulfur-nitrogen heterocycles and their derivatives), and 1–4 ringed PAHs and their associated alkylated species.

We have applied organic maturity parameters including the methyl naphthalene ratio, which displays a marked change with increasing flash-heating temperature. Such ratios are regarded as indicators of thermal instability in organic-rich geological samples and can be applied here to determine the extent of organic alteration through flash heating.

References: [1] Love S. G. and Brownlee D. E. 1991. *Icarus* 89:26–43. [2] Rodante F. 1992. *Thermochimica Acta* 200:47–60. [3] Anders E. 1989. *Nature* 342:255–257. [4] Matrajt G. et al. 2003. *Meteoritics & Planetary Science* 38:1585–1600. [5] Glavin D. P. et al. 2004. *Advances in Space Research* 33:106–113. [6] Wilson R. C. et al. 2007. Abstract #1799. 38th LPSC.

5246

CLASSIFICATION OF SECONDARY REDUCTION TEXTURES IN UREILITES

J. H. Wittke[1], T. E. Bunch[1], and C. A. Goodrich[2]. [1]Department of Geology, Northern Arizona University, Flagstaff, Arizona 86011, USA. E-mail: james.wittke@nau.edu. [2]Department of Physical Sciences, Kingsborough Community College, 2001 Oriental Boulevard, Brooklyn, New York 11235, USA.

Introduction: Ureilites are primitive achondrites dominated by olivine and pigeonite, with minor augite, orthopyroxene, graphite, sulfide, and metal [1]. After classifying several dozen ureilites, we observed a pattern of increased reduction of olivine and to a lesser extent, pyroxenes, with concomitant loss of graphite and increased degree of hardness. From these observations, we have developed a new classifying element useful in distinguishing various types of ureilites.

Methodology: We recognize four stages of reduction based upon the volume ratio of graphite to reduction rim metal, and the thickness of the reduction rims on olivine. Those ureilites that have unreacted graphite and very lightly reduced silicates are assigned lowest reduction grade, R1. Ureilites where no graphite remains and olivine rims are heavily reduced with over 50 vol% of grain mass affected, are assigned highest grade, R4.

Table 1.

	R1	R2	R3	R4
Graphite/metal (vol%)	>10	10–1	<0.5	0
Rim thickness of reduced olivine (mm)	<15	15–50	50–150	>50 vol% of olivine
Degree of hardness	Soft	Med	Hard	Extreme
Carbides and diamonds	None	None	Carbides	Diamonds and carbides

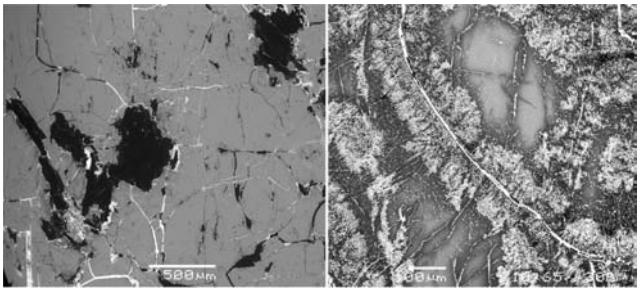

Fig. 1. Backscattered electron images. Left: NWA 1834; grade R1 with large patches of graphite. Right: NWA 2376; grade R4 extensively reduced with no residual graphite.

Interpretation: Secondary reduction rims on olivine in ureilites are commonly agreed to result from a sudden drop in pressure (hence carbon-controlled fO_2) and temperature, most likely to due to impact excavation during parent body break up [1–3]. The factors that might lead to such varying degrees of this reduction in observed samples are not clear (there is, for example, no correlation with core Fo, hence no apparent correlation with original depth), but may be related to the size of the fragment in which each sample was embedded during this event [3]. The correlation of diamond occurrence with other indications of increased reduction suggests a role for shock, although in general we do not observe any correlation with other shock features.

References: [1] Mittlefehldt D. W. et al. 1998. Reviews in Mineralogy 36. pp. 4-1–4-195. [2] Warren P. H. and Huber H. 2006. *Meteoritics & Planetary Science* 41:835–849. [3] Goodrich C. A. et al. 2004. *Chemie der Erde* 64:283–327.

5249

MELT SPHERULES FROM PETER'S POND, CAROLINA BAY, SOUTH CAROLINA

J. H. Wittke[1], T. E. Bunch[1], A. West[2], and R. S. Harris[3]. [1]Department of Geology, Northern Arizona University, Flagstaff, Arizona 86011, USA. E-mail: james.wittke@nau.edu. [2]GeoScience Consulting, Dewey, AZ, 86327, USA. [3]Geological Sciences, Brown University, Providence, Rhode Island 02912, USA.

Introduction: Very high-temperature melt products from Peter's Pond (Carolina Bay) near Blacksville SC consist of highly vesiculated ropy melts and three types of glassy spherules, ≥700 mm in diameter. These melt products (MPs) include welded glassy spherules, thermally processed clay clasts, and partially melted clays. Mullite- and corundum-bearing glasses and spherules occur in contact with clay balls that appear to have experienced low-grade thermal alteration.

Mineralogy: Observations of clay-melt interfaces with mullite or corundum-rich glassy enclaves indicate that the melt glasses in these MPs are derived from clays enriched in kaolinite with smaller amounts of iron oxides and illite. MPs with a mullite-glass core are partly rimmed by partially dissolved kaolinite clay balls; mullite needles penetrate the clay-glass interface. In addition, the melt interface has quench crystals of aluminous hematite set in Fe-poor and Fe-rich glasses. Mullite, corundum, and an aluminosilicate phase are common in the refractory spherules. Impactites and shards also contain "black clay clasts" enriched in carbonaceous matter that display a considerable range of thermal decomposition in concert with increased vesiculation and vitrification of the clay host. The interface between mullite-rich glass and a thermally decomposed black clay clast is decorated by iron silicide (Fe_3Si or gupeiite) spherules.

Petrology: Host glass compositions are remarkably uniform as are the compositions of Al-rich phases. Mullite-bearing spherules are the most common type and typically contain a few corundum crystals. Al-hematite-bearing spherules are less common, and spherules with both mullite and Al-hematite are least common. The iron silicide spherules probably formed by reduction of FeO in the glass during the thermal breakdown of carbonaceous matter in the black clay. The occurrence of mullite and Fe_3Si indicates formation by a very high-energy mechanism in a reducing environment unknown under natural conditions with the exceptions of lightning strikes [1] and impact craters [2]. In addition to the very high temperature and reduced phases described above, 10–20 μm-size Fe_3C spheres (cohenite) with tiny inclusions of Fe phosphide (steadite), containing up to 1.10 wt% Ni and 0.78 wt% Co, are found in the reduction zones of spherules and shards within 10s of microns of highly oxidized Al-hematite. Neither cohenite nor steadite are naturally occurring terrestrial minerals and are only found in meteorites and gray cast iron. In addition, magnetic fractions extracted from the same, disturbed deposit within the Peter's Pond rim and along an old railroad cut, were analyzed by INAA. These samples contain 15 ± 7 ppb of Ir, 395 ± 40 ppm of Ni, and 574 ± 57 ppm of Cr.

Conclusions: The mineralogy observed in these MPs indicates very high temperatures consistent with formation in an impact plume, e.g., ejecta from the Chesapeake Bay impact event, or from a very unusual industrial process.

References: [1] Sheffer A. A. et al. 2003. Abstract #1467. 34th LPSC. [2] Hoffman V. et al. 2005. *Meteoritics & Planetary Science* 40:A69.

5111

HIGHLY VOLATILE TRACE ELEMENT DISPOSITION IN CARBONACEOUS CHONDRITES

S. F. Wolf. Department of Chemistry, Indiana State University, Terre Haute, IN 47809–5901, USA. E-mail: wolf@indstate.edu.

Introduction: We are investigating the efficacy of selective, stepwise chemical dissolution of homogenized bulk meteorites with comprehensive elemental analysis of leachates in providing information regarding host phase identity and disposition of the highly volatile trace elements (HVTEs) in carbonaceous chondrites. Initial experiments revealed that >90% of the HVTEs Cd, Bi, Tl and In in Allende (CV3) and Murchison (CM2) were released by 9 M HOAc and 4 M HNO_3 [1]. However, these fractions also contained >80% of the major/minor mineral constituent elements Fe, Mg, Mn, Ni, and alkalis, thus precluding specific phase identification and HVTE disposition. In order to achieve greater chemical and spatial selectivity we have further modified our procedure to decrease dissolution rate in order to test the hypothesis that the HVTEs are preferentially sited in or on high surface area/volume ratio material. Additionally, we included Orgueil (CI1) in our second suite of tests in order to provide contrasting information for a carbonaceous chondrite possessing a different thermal and aqueous alteration history.

Methods: Our modified partial dissolution procedure includes an initial twelve 24 h treatments with increasingly aggressive reagents: H_2O (25 °C), H_2O (80 °C), 0.09 M HOAc, 0.9 M HOAc, 9 M HOAc (x3), 0.4 M HNO_3, 4 M HNO_3 (x3), and 6 M HCl. All subsequent treatments, analyses and calculations are as reported in [1].

Results: Measured releases of major/minor elements are consistent with dissolution of a complex mixture of phases. As expected, dissolution rates are generally inversely proportional to petrographic type (CI1 > CM2 > CV3). This trend is most apparent for highly soluble alkali elements. Releases of Na, K, and Rb are highly correlated with each other for each meteorite type. Interestingly, this trend is not followed by the most thermally volatile alkali Cs whose release patterns suggest siting in a more varied distribution of chemical environments in all three meteorites. Fractional release patterns show multiple S-containing phases with different abundances in each meteorite. Orgueil and Murchison contain a water-soluble S-component (most likely sulfate). HOAc-soluble, HNO_3-soluble, and HNO_3/HCl-soluble S-containing phases with different relative abundances were also observed. HVTE releases patterns are remarkably similar for all three meteorites. When only Allende is considered (putatively the least altered) data show Mg/Fe and Mn/Fe release ratios consistent with congruent dissolution olivine by HOAc and HNO_3 with an abundance agreeing with Bland et al. [3]. Correlation between releases of HVTEs, some moderately VTEs, and a 0.09–0.9 M HOAc-soluble S-rich phase preceding olivine dissolution indicates a volatile-rich material. These results are consistent with the presence of a high surface area/volume ratio material. This material is enriched 30× bulk HVTE content and contains ~10% of the HVTE inventory. While these results are suggestive of the presence of volatile-rich primary nebular condensate, redistribution of HVTEs and VTEs by secondary processes cannot be precluded by these results alone.

References: [1] Wolf S. F. 2005. *Meteoritics & Planetary Science* 41: A190. [2] Podosek F. A. et al. 1997. *Meteoritics & Planetary Science* 32: 617–627. [3] Bland P. A. et al. 2004. *Meteoritics & Planetary Science* 39: 3–16.

5048

A NEW SAMPLE PREPARATION METHOD THAT IS IDEAL FOR THE RAMAN ANALYSIS OF STARDUST, IDPS, AND OTHER SAMPLES THAT CONTAIN DISORDERED CARBONACOUS MATERIAL

B. Wopenka[1], G. Matrajt[2], D. Joswiak[2], and D. Brownlee[2]. [1]Department of Earth and Planetary Sciences, Washington University, St. Louis, MO 63130, USA. E-mail: bwopenka@wustl.edu. [2]Department of Astronomy, University of Washington, Box 351580, Seattle, WA 98195, USA.

Despite many limitations, Raman spectroscopy continues to be a very powerful and promising technique to learn more about the nature of the organic (i.e., carbon-dominated) compounds in Stardust particles (SD) and IDPs. However, several analytical aspects need to be kept in mind: 1) graphite and other sp2-bonded carbonaceous materials (CM) are highly absorbing for visible excitation wavelengths, and the laser beam will be totally absorbed in the uppermost ~100 nm of the surface layer of the sample. For samples that contain CMs, even in minor concentrations, Raman spectroscopy will always be a surface technique and samples containing CM do not need to be thicker than 100 nm; 2) structurally disordered, chemically impure, sp2-bonded CM with small crystallite size and high porosity has a very low thermal conductivity that potentially can cause in situ heating of the sample under the laser beam and the resulting in situ expansion of the C-C bond will cause a peak down-shift and misinterpretations. Thus, in addition to using the lowest possible power density of laser excitation, it is desirable to put the sample on a substrate with high thermal conductivity that can function as a heat sink.

Keeping the above in mind, we developed a sample preparation technique that is ideal for the Raman analysis of SD and IDPs. This technique is based on the study of microtomed slices of the particle rather than the study of a whole particle that is crushed or pressed in a substrate, as was used in most past Raman studies of IDPs and SD [1–5]. The microtomed slices (80 nm thick) are deposited over Ni-grids (to avoid sample heating), followed by removal of the acrylic embedding medium using chloroform [6]. The advantages of this technique are: 1) it allows to make Raman analyses in well photo-documented slices of parallel samples (or even the very same 80 nm thick sample) that are also analyzed with TEM, NanoSIMS, and C-XANES techniques; 2) in addition to getting information on the "primitiveness" of the CM by comparing the parameters for the D and G bands to other extraterrestrial materials [5], it is possible to detect and identify silicates and other minerals in SD and IDPs. Using this new sample preparation technique we analyzed and compared three different samples: "Febo" (SD), W7154 (IDP), and Murchison. We found them to be very similar in terms of CM primitiveness. In addition we showed that Raman can be very complementary to TEM given that we could confirm via Raman the presence of pyrrhotite in SD "Febo," and discovered remnants of phyllosilicates in both Murchison and the IDP.

References: [1] Wopenka B. 1988. *Earth and Planetary Science Letters* 88:221–231. [2] Muñoz-Caro G. M. et al. 2006. *Astronomy & Astrophysics* 459:147–159. [3] Quirico E. et al. 2005. *Planetary and Space Science* 53:1443–1448. [4] Sandford S. A. et al. 2006. *Science* 314:1720–1724. [5] Rotundi A. et al. *Meteoritics & Planetary Science*. Forthcoming. [6] Matrajt G. and Brownlee D. E. 2006. *Meteoritics & Planetary Science* 41: 1715–1720.

5199

ANALYSIS OF RESIDUES RESULTING FROM IMPACTS INTO ALUMINIUM 1145 FOIL: EXPERIMENTS TO FACILITATE STARDUST CRATER ANALYSES

P. J. Wozniakiewicz[1], A. T. Kearsley[1], M. J. Burchell[2], N. J. Foster[2], M. J. Cole[2], P. A. Bland[1, 3], and S. S. Russell[1]. [1]IARC, Natural History Museum, London, SW7 5BD, UK E-mail: p.wozniakiewicz@nhm.ac.uk. [2]University of Kent, Canterbury, Kent CT2 7NH, UK. [3]IARC, Imperial College London, South Kensington Campus, London, SW7 2AZ, UK.

Introduction: Return of the Stardust cargo and the ensuing preliminary examination (PE) revealed the successful capture of many particles in both the aerogel and foil of its collector [1]. While originally primarily intended as a means of securing the aerogel in place, the value of foils as an informative collection medium was quickly realized [2]. Fully exploiting this unique opportunity requires that we understand the impact process occurring on these foils; and in particular, whether it is possible to distinguish the most important minerals expected within cometary materials, and to establish how their compositions may have been modified during capture. Following preliminary analysis of diverse mineral residues prior to the return of Stardust [3, 4], we now focus our investigation to include a suite of olivines from Mg-endmember forsterite through to Fe-endmember fayalite, and two sulfides, both identified as important components of Stardust materials analyzed so far [5].

Experimental Methodology: For this study, a series of light-gas gun shots were conducted at the University of Kent, firing important cometary minerals into Stardust foils. The six olivine powder samples were of synthetic origin, with compositions of Fo_{100}, Fo_{80}, Fo_{60}, Fo_{40}, Fo_{20}, and Fo_{0}. Powdered sulfides, pyrrhotite and pentlandite, were prepared from grains carefully extracted from terrestrial ore minerals. The powders were fired as single component buckshots [6]. Residues on the crater wall of 5 craters attributable to each projectile composition were then analyzed by SEM EDX at the Natural History Museum. X-ray count rates for the major elements of each mineral were then plotted against data from a sample of the original projectiles.

Results and Discussion: We find that for the olivines, whilst clearly distinct in composition from one another in both projectile and residue form, residues exhibit an increased Mg count rate relative to Si and Fe. The change may be attributable partly to geometrical affects of the analysis technique, but we also suspect some preferential loss to vapor of the more volatile Si and Fe. This will be investigated further by analytical transmission electron microscopy. Residues from the sulfide minerals exhibit variable loss in S relative to Fe and Ni, as was seen in analyses taken from aerogel-trapped particles in Stardust [5], suggesting that low S is due to capture, and is not an indication of original diverse nonstoichiometric composition. Our results suggest the task of deciphering original chemistry from fine-grained and melted Stardust residues is not an easy one.

References: [1] Brownlee D. E. et al. 2006. *Science* 314:1711–1716. [2] Tsou et al. 2003. *Journal of Geophysical Research* 108, doi:10.1029/2003JE002109. [3] Wozniakiewicz P. et al. 2006. *Meteoritics & Planetary Science* 41:A190. [4] Kearsley A. T. et al. 2006. *Meteoritics & Planetary Science* 42:191–210. [5] Zolensky M. E. et al. 2006. *Science* 314:1735–1739. [6] Burchell M. J. et al. 1999. *Measurement Science and Technology* 10:41–50.

5260

THE INTRIGUING METEORITE WIS 91600 AS OBSERVED FROM AN ORGANIC PERSPECTIVE

H. Yabuta, C. M. O'D. Alexander, M. L. Fogel, and G. D. Cody. Carnegie Institution of Washington, USA. E-mail: hyabuta@ciw.edu.

Introduction: The meteorite WIS 91600 has been identified as an ungrouped carbonaceous chondrite C2 with a reflectance spectrum consistent with D- or T-type asteroidal precursor [1]. The mineralogy of this chondrite differs from CM chondrites [2], but is similar to Tagish Lake and some with Orgueil in regards to the types of hydrated matrix phases present [1].

Given these physical and mineralogical characteristics, it is worth comparing the chemical features of insoluble organic matter (IOM) in WIS 91600 with those of the other carbonaceous chondrites to aid interpretation of the origin and chemical history of this unusual meteorite. We report elemental, isotopic, and structural characteristics of the IOM from WIS 91600.

Experimental: IOM from WIS 91600 and the other carbonaceous chondrites were prepared by demineralization of the bulk meteorites using a CsF-HF technique [3] followed by desulfurization in air, rinsing (with HCl, Milli-Q water, and dioxane), and drying. Elemental and isotopic compositions of the IOM were measured by elemental analyzer (C and N) or thermal conversion elemental analyzer (H and O) coupled with isotope mass spectrometry. Chemical structures of the IOM were analyzed by solid-state ^{13}C NMR and pyrolysis-GC-MS, respectively.

Results and Discussion: Elemental and isotopic analyses [4]: H/C ratio of the IOM from WIS 91600 was 0.41, which was similar to that (0.42) of the mildly-heated CM, Yamato (Y-) 793321. The value was between that from Tagish Lake (0.33) and those of the nonheated CM (0.6–0.7). δ^{13}C of WIS 91600 IOM (–11.19‰) was also similar to that of heated CM, PCA 91008 (–11.38‰). Its δD (349‰) was at the similar level of those of PCA 91008 (243‰) and Tagish Lake (596‰).

^{13}C NMR: The NMR spectrum of WIS 91600 IOM is dominated by aromatic carbon, similarly to that of the heated CM Y-793321 [5], laboratory-heated Murray [6], and Tagish Lake [7]. The variable contact time behavior of WIS 91600, however, differs significantly from that of Tagish Lake, CMs, CRs, and a CI [3], but is similar to that of at least partially heated CV chondrites (e.g., Vigarano).

Pyrolysis-GC-MS: The pyrolysis yield from WIS 91600 IOM was low and the molecular distribution was very simple, which was similarly observed in IOMs from heated chondrites and Tagish Lake. This is completely distinct from the pyrolytic behavior of most of CM, CI, and CR chondrites [8].

Integrating these results, we conclude that WIS 91600 IOM reveals a history that includes mild heating and/or chemical oxidation. Further multilateral investigations including chemical degradation, carbon-XANES, and Raman would be necessary.

References: [1] Hiroi T. et al. 2005. Abstract #1564. 36th Lunar and Planetary Science Conference. [2] Brearley A. J. 2004. Abstract #1358. 35th Lunar and Planetary Science Conference. [3] Cody et al. 2002. *Geochimica et Cosmochimica Acta* 66:1851–1865. [4] Alexander C. M. O'D. et al. *Geochimica et Cosmochimica Acta*. Forthcoming. [5] Yabuta H. et al. 2005. *Meteoritics & Planetary Science* 40:779–787. [6] Yabuta H. et al. 2007a. *Meteoritics & Planetary Science* 42:37–48. [7] Cody and Alexander. 2005. *Geochimica et Cosmochimica Acta* 69:1085–1097. [8] Yabuta H. et al. 2007b. Abstract #2304. 38th Lunar & Planetary Science Conference.

5200

HIGHLY METAMORPHOSED EUCRITES, A-87272 AND DaG 945: RESIDUES AFTER CRUSTAL PARTIAL MELTING

A. Yamaguchi[1, 2], J.-A. Barrat[1], N. Shirai[3], C. Okamoto[3, 4], T. Setoyanagi[3], and M. Ebihara[2, 3]. [1]UBO-IUEM, Place Nicolas Copernic, 29280 Plouzané Cedex, France. [2]National Institute of Polar Research, Tokyo 173-8515, Japan. [3]Department of Chemistry, Tokyo Metropolitan University, Hachioji, Tokyo 192-0397, Japan. [4]Graduate School of Environmental Studies, Nagoya University, Furocho, Nagoya 464-8601, Japan.

Introduction: Eucrites are pigeonite-plagioclase basalts and gabbro, possibly derived from the Vestan crust. Basaltic eucrites exhibit varying degrees of metamorphism [1–3]. Most of eucrites were metamorphosed under the solidus, but some of them were reheated above the solidus temperatures. Basaltic eucrites are classified into two compositional series; main group-Nuevo Laredo trend and Stannern trend (e.g., [4]). Stannern trend eucrites have similar major element compositions to the main group, but have more elevated concentrations of incompatible elements. It is difficult to explain petrogenetic origin of the two series from a single magmatic body. Recently, Barrat et al. [5] suggested that the origin Stannern trend eucrites can be explained by contamination of crustal partial melts into main group eucritic magmas. The model is consistent with the presence of partially melted eucrites [3]. We studied mineralogy and chemistry of two partially melted eucrites, A-87272 and DaG 945.

Results and Discussion: A-87272 and DaG 945 are coarse-grained eucrites mainly composed of pigeonite and plagioclase and minor minerals. Pyroxenes and plagioclase compositions are typical ranges of basaltic eucrites [1]. Pyroxenes in both eucrites have remnant Ca-zoning, and pigeonite in A-87272 is partially inverted into orthopyroxene (i.e., type 7). Plagioclase in A-87272 shows partial equilibration whereas that in DaG 945 preserves original igneous zoning. These mineralogical features are consistent with those of metamorphosed eucrites. However, spinel is extremely enriched in Ti, and silica minerals occur as large grains or laths. Thus, these eucrites experienced high temperature metamorphism which caused partial melting [5].

The chondrite-normalized REEs of A-87272 and DaG 945 have LREE depletions (La/Yb_{CI} = 0.80 and 0.53, respectively) with a positive Eu anomaly. These patterns are rather similar to those of cumulate eucrites. However, mineralogical data (e.g., high FeO/MgO ratios of pyroxenes) rule out the cumulate origin. Another possibility includes undersampling of Ca phosphates. However, this seems unlikely considering that we analyzed aliquots of large homogenized powder (~2–3 g). We suggest that the unusual REE patterns resulted from partial melting with the extraction of partial melts.

The presence of both residual eucrites and Stannern trend eucrites can be explained by the crustal partial melting model [4]. The source of secondary reheating may include impact processes, internal heating (e.g., from magma ocean), local intrusions, which overprint global crustal metamorphism [1, 4, 5]. We suggest that the formation of eucrite crust is more complex processes than previously proposed.

References: [1] Takeda H. and Graham A. L. 1991. *Meteoritics* 26: 129–134. [2] Yamaguchi A. et al. 1996. *Icarus* 124:97–112. [3] Yamaguchi A. et al. 2001. *Geochimica et Cosmochimica Acta* 65:3577–3599. [4] Warren P. H. and Jerde E. 1987. *Geochimica et Cosmochimica Acta* 51:713–725. [5] Barrat J. A. et al. 2007. *Meteoritics & Planetary Science*. This issue.

5117

RELATIONSHIP OF MAIN-GROUP PALLASITES AND IIIAB IRON METEORITES

J. Yang[1], C. Hung[1], J. I. Goldstein[1], and E. R. D. Scott[2]. [1]Department of Mechanical and Industrial Engineering, University of Massachusetts, Amherst, MA 01003, USA. E-mail: jiyang@ecs.umass.edu. [2]Hawai'i Institute of Geophysics and Planetology, University of Hawai'i at Manoa, Honolulu, HI 96822, USA.

Introduction: Pallasites are conventionally thought to come from core-mantle boundaries of differentiated asteroids. Based on the chemical elemental distribution pattern and oxygen isotopes, it was proposed that the main group (MG) pallasites come from the same parent body as the IIIAB irons [1]. However, this relationship has been challenged [2, 3]. Here we report new data on cloudy zone particle size and relative cooling rates of MG pallasites and IIIAB irons.

Results: We measured the sizes of high-Ni particles bordering the tetrataenite rim after careful polishing and etching of a selection of MG pallasites and IIIAB irons. The sizes of the high-Ni particles in 10 MG pallasites vary from 105 to 188 nm and in 8 IIIAB irons from 47 to 71 nm. The sizes of the high-Ni particles are not correlated with Ni content in the MG pallasites but correlate directly with Ni content in the IIIAB irons.

Discussion: *Cooling Rates:* Using the proportionality between the high-Ni particle size and the metallographic cooling rate [4], the cloudy zone cooling rates in the IIIAB irons vary by a factor of ~2.7. They are also consistent with the variation of the measured metallographic cooling rates with Ni content [2]. For the MG pallasites, the inferred cooling rates vary by a factor of ~4. This range exceeds the 1 uncertainty (10–20%) and indicates that MG pallasites did not cool at the same radius in the pallasite parent body.

Link between Pallasites and Irons: The measured particle sizes in MG pallasites suggest that these meteorites cooled ~2.5 to 25 times slower than the IIIAB irons. This precludes formation of MG pallasites at the core-mantle boundary of the IIIAB parent body. It also suggests that MG pallasites and IIIAB irons come from separate bodies. If the MG pallasites are from a single body, there must have been a significant thermal gradient across the pallasite zone. Pallasites could come from parent bodies that are not related to any iron meteorite parent body [3]. The formation of pallasites appears to require violent mixing of molten metal from a core with mantle olivine [3, 5], possibly due to a hit-and-run impact between differentiated protoplanets [6].

References: [1] Wasson J. T. and Choi B.-G. 2003. *Geochimica et Cosmochimica Acta* 67:3079–3096. [2] Yang J. and Goldstein J. I. 2006. *Geochimica et Cosmochimica Acta* 70:3197–3215. [3] Scott E. R. D. 2007. Abstract #2284. 38th Lunar and Planetary Science Conference. [4] Yang J. et al. 2007. *Nature* 446:888–891. [5] Greenwood R. C. 2006. *Science* 313: 1763–1765. [6] Asphaug E. et al. 2006. *Nature* 439:155–160.

5202

PLANETARY WAVES AS A TRANSPORT MEDIUM OF EUROPEAN NOCTILUCENT CLOUDS AFTER THE TUNGUSKA EVENT OF 1908

M. Zalcik[1] and A. A. Mardon[2]. [1]Noctilucent Cloud Canadian—American Network. E-mail: bluegrama@shaw.ca. [2]Antarctic Institute of Canada, P.O. Box 1223, MPO, Edmonton, Alberta, Canada T5J-2M4. E-mail: amardon@shaw.ca.

Following the Tunguska explosion of June 30, 1908, the source of which was likely a massive stony meteorite, noctilucent clouds (NLC) were reported in Europe, and it has been suggested that these NLC were a direct result of increased meteoric nuclei introduced by the impacting body [1]. It has been pointed out the significance of planetary waves as a transport mechanism for atmospheric conditions favorable for NLC formation. Since these waves are known to move from east to west [2], the formation of NLC in Europe could have very well been due to planetary wave transport of attendant atmospheric physical conditions, if not the meteoric nuclei as well, from the site of the Tunguska impact much farther east in Asia. This might be the mechanism for the transport of NLC phenomena around the world in progressive times. NLCs in the Americas might even have the same time delay.

Conclusions: An in-depth analysis of dates when NLC were seen in Europe, or anywhere else for that matter, may shed light on the type of planetary wave responsible, be it a 2-day, 4-day, or 5-day wave.

References: [1] Turco R. P., Toon O. B., Whitten R. C., Keesee R. G., and Hollenback D. 1982. *Planetary and Space Science* 30:1147–1181. [2] Dalin P. 2007. Personal communication.

5155

COMPOSITION AND ORIGIN OF MATRIX IN CARBONACEOUS CHONDRITES

B. Zanda[1, 2] and R. H. Hewins[1, 2]. [1]Muséum national d'Histoire naturelle, 61 rue Buffon, Paris, France. E-mail: zanda@mnhn.fr. [2]Department of Geological Sciences, Rutgers University, 610 Taylor Rd., Piscataway, NJ, USA.

Introduction and Method: In [1] we showed that refractory inclusions, chondrules, and matrix all contributed to the oxygen isotopic budget of chondrites and estimated the composition associated with each of these petrographic components at the time of chondrite formation. The present isotopic composition of chondrites can, in turn, be used to estimate their make up of petrographic components. Here we compare the chemical composition of carbonaceous chondrites (CC) with their abundances of matrix derived from their oxygen isotopic composition.

Results: Figure 1 displays a correlation between the bulk concentrations [C] and [H_2O+] in CC and their vol% matrix. A similar, but less tight ($R^2 = 0.65$) correlation also exists for S. The regression lines do not intercept the x axis at 0 vol% matrix but around 40 vol% for H_2O+ and C and 20 vol% for S.

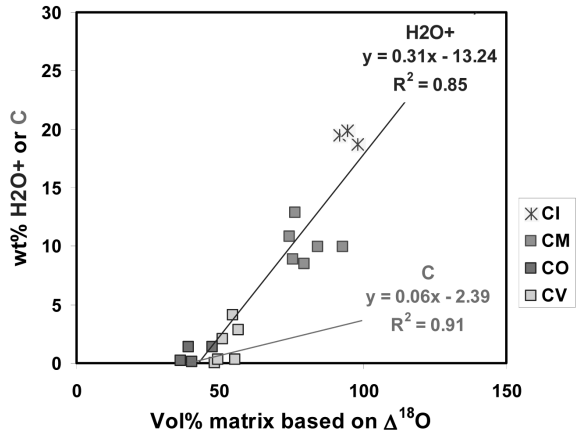

Fig. 1. Correlation of bulk [C] and [H_2O+] with vol% matrix in CC (individual points not shown for [C]). $\Delta^{18}O = \delta^{18}O - \delta^{17}O = 0.0673$ vol% matrix + 1.0 (after [1]).

Discussion: Structural water, organics, and S in CC are all within the matrix. C and H_2O+ correlate together ($R^2 = 0.81$) and are likely to share a common origin. C, H_2O+, and S-bearing phases originated together with the other matrix constituents or contaminated the matrix in fixed proportions. A fraction only of the matrix however contained them. From the intercept of the correlations with the x-axis, we calculate that volumes of matrix equal to 65% and 30% of the chondrule volume respectively contained no H_2O+ (nor C), and no S. We infer that accretionary rims around chondrules were originally layered: the inner layer (thick ~1/10 of the chondrule radius) contained none of these volatile elements while a second layer (of the same thickness) contained S but no C or water ice. Outer layers and/or matrix contained all these elements. As these layers all share a common oxygen isotopic and bulk chemical composition (except for volatiles), we argue that they were formed successively in the nebula, possibly by fractional condensation.

References: [1] Zanda B. et al. 2006. *Earth and Planetary Science Letters* 248:650–660.

5289

FIB-TEM STUDY OF A WARK-LOVERING RIM IN AN ALLENDE TYPE-A CAI

T. J. Zega[1], M. Cosarinsky[2], R. M. Stroud[1], and K. D. McKeegan[2]. [1]Materials Science and Technology Division, Naval Research Laboratory, Washington, D.C. 20375, USA. E-mail: tzega@nrl.navy.mil. [2]Department of Earth and Space Sciences, UCLA, Los Angeles, CA 90095–1567, USA.

Introduction: Wark-Lovering rims (WLRs) occur around many of the calcium- and aluminum-rich inclusions (CAIs) in chondritic meteorites, consist of micron-thick layers of silicates and oxides, and are believed to have formed either by flash heating [1] or condensation [2]. Isotopic analysis has shown that WLR phases in a type-A CAI in the Allende CV chondrite (TS#25) yield well-correlated isochrons in an Al-Mg evolution diagrams, which imply formation 1.3×10^5 years after the CAI interior [3]. We have initiated a correlated structure-isotope study of WLRs and CAIs to gain insight into their petrogenesis. Here we present results from a transmission electron microscope (TEM) analysis of a WLR in the Allende CV3 chondrite.

Methods: A 20 × 1 × 1 μm strap of Pt was deposited across part of the WLR surrounding a type-A CAI in the Allende CV chondrite (TS25F1). We used an FEI Nova 600 focused-ion-beam scanning-electron microscope (FIB-SEM) to create and extract, in situ, an electron-transparent cross section of the WLR for TEM analysis [4]. The FIB section was studied using a JEOL 2200FS TEM equipped with bright- and dark-field STEM detectors, an in-column energy filter, and energy-dispersive spectrometer.

Results and Discussion: The WLR consist of three layers: an innermost layer of spinel intergrown with hibonite blades and minor perovskite; an intermediate layer of melilite, pervasively replaced by anorthite; and an outermost layer of Ti-Al-rich pyroxene grading outward to Al-diopside. Bright- and dark-field imaging and selected-area electron-diffraction patterns show that the WLRs consist of a complex mixture of polycrystalline material. Most material is coarse-grained (μm) and exhibits subhedral texture. However, some grains, e.g., melilite, contain partially developed faces that form triple junctions with surrounding material. Inclusions were observed in several grains, and occur both in and between the melilite and anorthite. Grossular and sodalite have also been identified within the WLR.

These results, in addition to the Mg isotopic data, are difficult to reconcile with condensation models. The coarse-grained microstructure, triple junctions, and inclusions are suggestive of solidification from a melt. Thus, the formation of this WLR is more consistent with flash heating of a refractory precursor material, subsequent reaction with the ambient gas (possibly either nebular gas or that produced by vaporization of CAI material), and diffusion of light Mg into the rim producing a gradient in δ^{25}Mg values from the pyroxene toward the spinel layer [3]. The occurrence of grossular and sodalite, however, are suggestive of later-stage metasomatism [5].

References: [1] Wark D. and Boynton W. V. 2001 *Meteoritics & Planetary Science* 36:1135–1166. [2] Simon J. I. et al. 2005. *Earth and Planetary Science Letters* 238:272–283. [3] Cosarinsky M. et al. 2005. *Meteoritics & Planetary Science* 40:A34. [4] Zega T. J. et al. *Meteoritics & Planetary Science*. Forthcoming. [5] Krot A. et al. 1995. *Meteoritics & Planetary Science* 30:748–775.

5051

SILICA-BEARING OBJECTS IN THE CH CHONDRITE SaU 290

Aicheng Zhang[1], Weibiao Hsu[1], and Rainer Bartoschewitz[2]. [1]Laboratory for Astrochemistry and Planetary Sciences, Purple Mountain Observatory, Nanjing 210008, China. E-mail: aczhang@pmo.ac.cn. [2]Bartoschewitz Meteorite Laboratory, Lehmweg 53, D-38518 Gifhorn, Germany.

Introduction: Silica-bearing objects (SBO) are rare but appear widely in chondrites as chondrules or fragments [1–4]. They are usually depleted in refractory elements such as Ca, Al, and Ti. SBOs are thought to have formed in a fractionated nebular gas [2]. They provide important information about processes in the early solar nebula. Here, we report seven SBOs found in the CH chondrite SaU 290.

Petrography and Mineralogy: In one thin section of SaU 290, seven SBOs were observed. They are rounded or irregular and range in size from 70 to 230 μm. Silica appears as rounded or elongated grains (3 to ~20 μm) in SBOs. They are either enclosed by feldspathic glass or by Mn-rich pyroxene grains. Silica grains also appear as blebs at the edges of chondrules (both types I and II). Mn-rich pyroxene occurs only in four SBOs. It appears as lath-shaped grains intergrown with low-Ca pyroxene or in feldspathic glass. Both Mn-rich and Mn-poor pyroxene grains could be present in a given SBO.

Large silica grains (~20 μm) in SaU 290 have a near pure SiO_2 composition. Analyses of small grains (<5 μm) yield minor amounts of Al_2O_3, CaO, and other elements (Fe and Mg), which are probably due to beam overlap. Pyroxene shows a large chemical variation from enstatite to diopside or to hypersthene (14.43–36.69 wt% MgO, 0.44–28.97 wt% FeO, and 0.12–20.86 wt% CaO). MnO is low (<0.5 wt%) in enstatite and hypersthene but is high (up to 8.45 wt%) in most diopside grains [2]. Mn-rich pyroxene also contains a relatively high content of Cr_2O_3 (1.33–3.14 wt%). Olivine grains are predominant forsterite ($Fo_{97–98}$). Glass is generally feldspathic with various amounts of SiO_2 (60.64–79.57 wt%), Al_2O_3 (4.75–20.84 wt%), CaO (0.43–11.93 wt%), Na_2O (0–3.63 wt%), and K_2O (0.01–1.57 wt%).

Discussion: SBOs in SaU 290 are generally similar to those of other CH chondrites (Acfer 182 and 207) [2], CR chondrites [3], and ordinary chondrites [4]. They usually contain a silica portion and a silicate portion. Pure Fe metal grains are absent in SBOs, excluding the formation of silica by reduction of ferrous pyroxene. Some pyroxene grains in SBOs of SaU 290 contain very high MnO content. Mn enrichment is an indication of fractional condensation in a nebular gas by removing of olivine and pyroxene [2]. Consequently, pyroxene incorporates Mn during crystallization from a melt. The partition coefficient of Mn between pyroxene and melt is very high. The KD values are between 30 and 34 for high-Ca and between 25 and 71 for low-Ca pyroxene [5, 6]. The calculated apparent pyroxene-melt KD(Mn) value for SaU 290 is between 8 and 54. Coexisting of both Mn-rich and Mn-poor pyroxene within the same SBO suggests that either Mn-rich pyroxene crystallized earlier than Mn-poor pyroxene or they formed during separate processes.

References: [1] Bischoff A. et al. 1993. *Geochimica et Cosmochimica Acta* 57:2631–2648. [2] Hezel D. C. et al. 2003. *Meteoritics & Planetary Science* 38:1199–1215. [3] Krot A. N. et al. 2004. *Meteoritics & Planetary Science* 38:1931–1955. [4] Brigham C. A. et al. 1986. *Geochimica et Cosmochimica Acta* 50:1655–1666. [5] Ewart A. and Griffin W. L. 1994. *Chemical Geology* 117:251–284. [6] Mahood G. and Hildreth W. 1983. *Geochimica et Cosmochimica Acta* 47:11–30.

5240

50 YEARS OF THE METEORITICAL BULLETIN

J. Zipfel[1], J. N. Grossman[2], and H. Connolly[3]. [1]Senckenberg, 60325 Frankfurt, Germany. E-mail: jzipfel@senckenberg.de. [2]USGS, 954 National Center, Reston, VA 20192, USA. [3]Kingsborough College of CUNY, Brooklyn, NY 11235, USA; Lunar and Planetary Laboratory, University of Arizona, Tucson, AZ 85745, USA.

Introduction: The Meteoritical Bulletin (MB) announces new meteorite finds and falls from all over the world. What started with a single entry in 1957 [1] has become a huge data compilation with hundreds of new meteorites listed every year, e.g., a total of 1560 newly listed meteorites already in 2007 [2]. The first edition of the MB was edited by E. L. Krinov, printed by the Committee on Meteorites of the Academy of Sciences of the former USSR and distributed via mail. Publishing such a Bulletin was decided during the September meeting of the Permanent Commission on Meteorites at the International Geological Congress in Mexico in 1956. It was established with a goal of disseminating information on new falls and finds to members of the commission, scientific institutions and individual researchers.

History: E. L. Krinov from the Academy of Science in Moscow was editor from 1957 through 1970 for the MB, No. 1–49. Interestingly enough, the first preliminary report of a meteorite fall on a Soviet ship in the Arabian Sea published in the MB, No. 1, turned out to describe a piece of coal after detailed investigation. The observed sound phenomena were caused by defects in the electrical circuit [3]. Earlier issues were incorporated in the *Catalogue of meteorites* edited by M. H. Hey in 1966 and published by the British Museum for Natural History [4]. Issues published between 1966 and 1969 were reprinted in Meteoritics in 1970 [5]. Starting in 1970, the MB was published in *Meteoritics* (1970–1995) and *Meteoritics & Planetary Science* (since 1996), the journals of the Meteoritical Society. This was intended to bring the information to the attention of a larger audience. Krinov was followed by a number of editors: R. Clarke (1971–1976), A. Graham (1978–1990), F. Wlotzka (1990–1995), J. Grossman (1994–2001), S. Russell (2002–2005) and H. Connolly (since 2006). With the huge number of desert meteorite recoveries the work load became too large for a single editor and associated editors were appointed. Since 2001 the number of associated editors increased from one to currently five.

Nomenclature Committee: The Nomenclature Committee (NC) of the Meteoritical Society is intimately linked to the MB. The editor of the MB is an ex officio member of the NC. Each new meteorite name has to be accepted by the NC prior to its publication in the MB. The NC was only founded in 1973 on suggestion by V. Buchwald and J. Wasson [6] because of a need for unique names in order to avoid confusion in the literature.

Conclusions: The MB has become an important and integral part of the Meteoritical Society. Both scientists and collectors benefit equally from the gathering of geographic and classification data of new meteorites and their documentation. Electronic databases, such as the Meteoritical Bulletin database and MetBase, are essential tools and mostly rely on these data.

References: [1] Krinov E. L. 1957. The Meteoritical Bulletin, No. 1, Academy of Sciences, Moscow. [2] Connolly H. et al. 2007. *Meteoritics & Planetary Science* 42:413–466. [3] Krinov E. L. 1957. The Meteoritical Bulletin, No. 3. Academy of Sciences, Moscow. [4] Hey M. H. 1966. *Catalogue of meteorites,* 3rd ed. London: British Museum. [5] The Meteoritical Bulletin, Nos. 36–48. 1970. *Meteoritics* 5:85–109. [6] Buchwald V. F. and Wasson J. T. 1972. *Meteoritics* 7:17–22.

5147

Fe-Ni SULFIDES IN CHONDRITES REVEALED

Michael Zolensky[1], Kazumasa Ohsumi[1], GeorgAnn Robinson[2], Glenn Morgan[3], Kenji Hagiya[4], and Takashi Mikouchi[5]. [1]NASA Johnson Space Center, Houston, TX 77058, USA. E-mail: michael.e.zolensky@nasa.gov. [2]Jacobs Sverdrup, Houston, TX 77058, USA. [3]Jacobs Engineering, Houston, TX 77058, USA. [4]University of Hyogo, Hyogo 678-1297, Japan. [5]Tokyo University, Tokyo 113-0033, Japan.

What Fe-Ni sulfides are present in carbonaceous chondrites, chondritic IDPs, and Wild-2 samples? What do the presence of specific sulfide minerals, with specific well-defined crystal structures, tell us about the physical conditions on asteroids and comets? The sulfides in chondritic materials are known to include troilite, pyrrhotite, pentlandite, and a poorly characterized Fe-Ni sulfide intermediate in composition between the latter phases [1, 2]. Many studies have mapped out the phase relations in the Fe-Ni-S system, with up to 4 wt% Ni, and the most common minerals here are the pyrrhotites, which basically take the NiAs structure. Below 308 °C the simple hexagonal NiAs structure is complicated by the appearance of ordered Fe vacancies which result in a confusing number of lower symmetry superstructures [3]. In addition, there also exist numerous incommensurate pyrrhotite superstructures [4]. These pyrrhotites have specific, fairly well-determined upper temperature stability fields. Although some experimental work (and the resultant phase diagrams) suggest that these phases should not be stable to room temperature we have identified many of them at room temperature in chondritic IDPs by SXRD [5]. In addition, for Fe-sulfides formed below 75 °C, smythite, rather than pyrrhotite, is stable. Thus we can use the pyrrhotites and smythite as cosmothermometers for chondrite sulfide formation if we can determine the exact structures of numerous Fe-sulfides (with minor Ni).

In the past decade we have made numerous attempts to determine the crystal structures of chondrite sulfides by synchrotron X-ray diffraction (SXRD), but with only a few exceptions we have found them to be apparently amorphous by this technique. This has always been rather perplexing since these sulfides frequently exhibit euhedral crystal morphologies. This is in clear contrast to the situation for IDPs where we frequently were successful in our crystal structure analyses [5]. We were beginning to conclude that the chondrite sulfides had generally been rendered amorphous by shock. However, we have learned that practically all of our chondrite thin sections have very thin amorphous surfaces, a common polishing side effect of which we were unaware. The IDPs we examined never showed this effect because we prepared those samples by ultramicrotomy, which obviously does not render the surface amorphous. We have begun to remove these coatings, and explore the crystal structures of the sulfides by a combination of electron backscattered diffraction (EBSD) and SXRD, beginning with Orgueil and Kaidun CM1. The apparently "amorphous pyrrhotite" in Kaidun CM1 is actually crystalline smythite (a low temperature sulfide). Orgueil contains predominantly various pyrrhotites, whose exact crystal structures we are now exploring by SXRF.

References: [1] Vaughan and Craig. 1978. *Mineral chemistry of metal sulfides*. Cambridge University Press. p. 493. [2] Zolensky and Thomas. 1995. *Geochimica et Cosmochimica Acta* 59:4707–4712. [3] Sack and Ebel. 2006. In Reviews in Mineralogy and Geochemistry, vol. 61. [4] Nakazawa and Morimoto. 1971. *Materials Research Bulletin* 6:345–358. [5] Ohsumi, Hagiya, and Zolensky. 2002. Lunar and Planetary Science XXXIII.

5040

EVALUATION OF PRESSURE DURING AQUEOUS ALTERATION AND METAMORPHISM OF ASTEROIDS

M. Yu. Zolotov[1], M. V. Mironenko[2], and M. L. Krieg[1]. [1]School of Earth and Space Exploration, Arizona State University, Tempe, AZ 85287–1404, USA. E-mail: zolotov@asu.edu. [2]Vernadsky Institute of Geochemistry and Analytical Chemistry, Russian Academy of Sciences, Moscow, 119991, Russia.

Alteration of asteroids during the first 10–15 Ma could have caused increase in pressure (*P*) and destruction of some bodies [1, 2]. Production of H_2 through oxidation of Fe, P, C, S, Ni, and Si by H_2O and its separation into the gas phase was likely to be the major reason for rising *P*. Production of gases, increasing temperature (*T*) and evaporation of aqueous solution led to increase in *P*. On the other hand, elevated porosity and permeability, dissolution, chemical consumption, condensation (H_2O gas), diffusion and escape of gases reduced *P* buildup and could have caused *P* to decrease. We modeled alteration of chondrites with thermochemical equilibrium and mass balance calculations in closed isochoric-isothermal systems [3] in order to evaluate the effects of degree of alteration, water/rock mass ratio (*W/R*), porosity, rock composition, and *T* on pressure in specific zones inside asteroids.

Results show that *P* can potentially reach several hundred bars and is proportional to the amount of aqueously altered rock (degree of alteration). Maximum pressures are observed at the aqueous to metamorphic transition. Complete consumption of aqueous solution is followed by decrease in *P*, which could be accounted for by H_2 use via reduction of previously formed phases. If occurred, further metamorphism causes minor variations in *P* owing to the interplay of dehydration and redox reactions. Dehydration releases H_2O(g) and increases porosity. In redox processes, H_2O(g) and H_2(g) are consumed due to oxidation and reduction, respectively. Lower porosities lead to higher *P* over the course of aqueous and metamorphic processes. At each degree of alteration, highest *P* values correspond to water/altered rock ratio (local *W/R*) of ~0.2. That *W/R* value also represents the aqueous to metamorphic transition. At lower *W/R* ratios, H_2 production and *P* are limited by the amount of water; at higher *W/R*, they are limited by the amount of rock and affected by H_2 dissolution in water.

We evaluated specific *T*-*W/R*-porosity-alteration progress conditions at which explosive destruction of typical asteroids can occur at $P > 10^2$ bar [1, 2]. For example, at 100 °C and original porosity of 50%, that *P* can be achieved at bulk *W/R* of 0.1–1 and at the degree of alteration above ~0.2. Lower original porosity and/or higher *T* can cause destructions of asteroids at earlier stages of aqueous alteration. At the metamorphic stage, destructions are less likely.

Finally, abundances of oxidized minerals in chondrites (e.g., [4]) were used to evaluate the amount of H_2 produced and corresponding upper limits for *P* in localized regions of their parent bodies. For CM2 chondrites, ~6 moles H_2 per kg of water-free rock, 20 °C and 50–20% porosity lead to *P* of 0.7–1.8 kbar. For CI chondrites (~3.5 moles H_2, 150 °C, 50–20% porosity) maximum *P* is 0.6–1.5 kbar. These estimations demonstrate the need for H_2 removal via diffusion into peripheral asteroidal zones and escape, consistent with oxidizing nature of CM2 and CI chondrites.

References: [1] Grimm R. E. and McSween H. Y., Jr. 1989. *Icarus* 82: 244–280. [2] Wilson L. et al. 1999. *Meteoritics & Planetary Science* 34:541–557. [3] Mironenko M. V. and Zolotov M. Yu. 2005. Abstract #2207. 36th Lunar and Planetary Science Conference. [4] Bland P. A. et al. 2004. *Meteoritics & Planetary Science* 39:3–16.